



Wind Tunnel Tests of Parabolic Trough Solar Collectors

March 2001–August 2003

N. Hosoya and J.A. Peterka

Cermak Peterka Petersen, Inc.

Fort Collins, Colorado

R.C. Gee

Solargenix Energy, LLC

Raleigh, North Carolina

D. Kearney

Kearney & Associates

Vashon, Washington

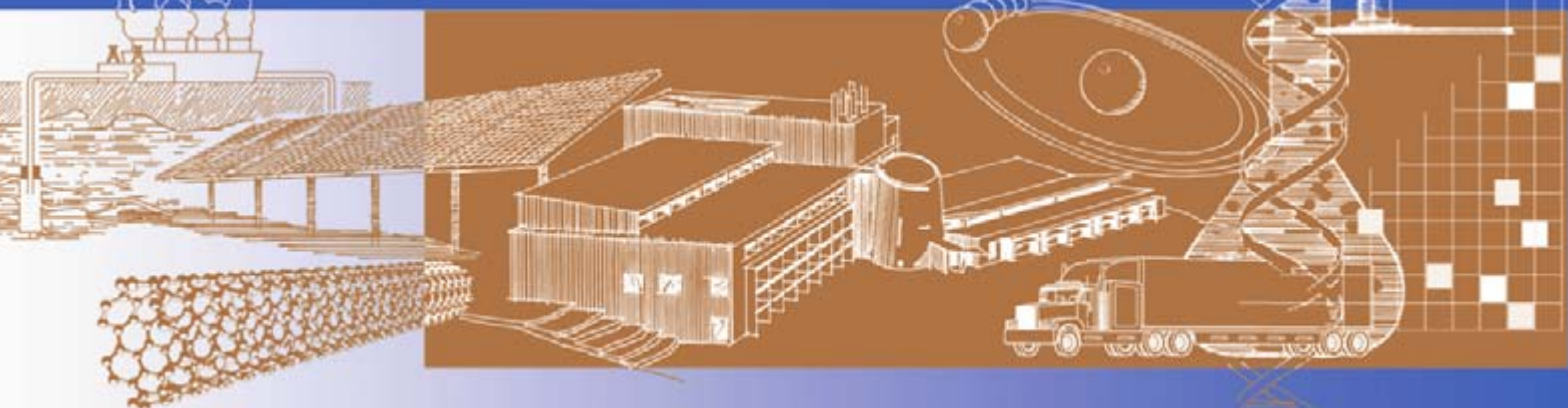
Subcontract Report

NREL/SR-550-32282

May 2008



NREL is operated by Midwest Research Institute • Battelle Contract No. DE-AC36-99-GO10337



Wind Tunnel Tests of Parabolic Trough Solar Collectors

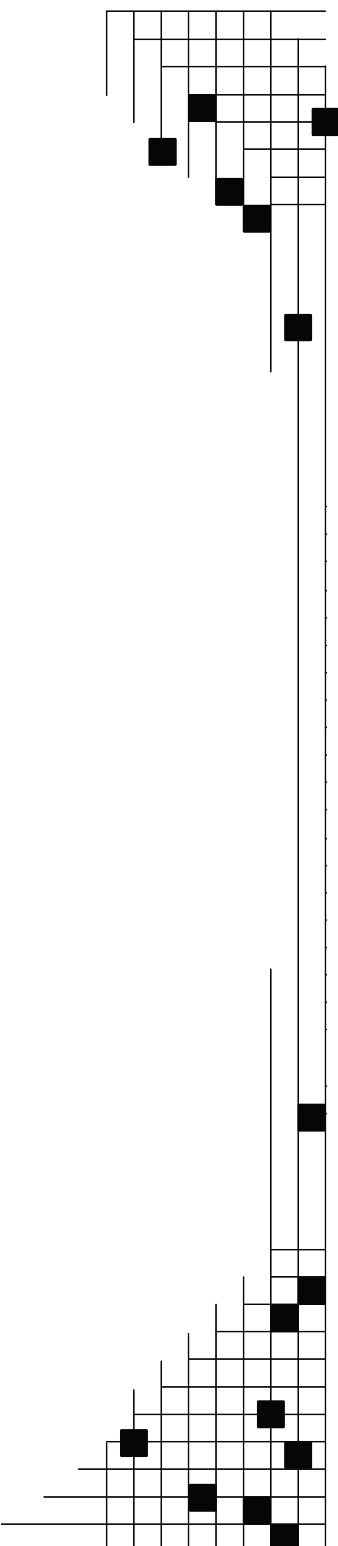
March 2001–August 2003

N. Hosoya and J.A. Peterka
Cermak Peterka Petersen, Inc.
Fort Collins, Colorado

R.C. Gee
Solargenix Energy, LLC
Raleigh, North Carolina

D. Kearney
Kearney & Associates
Vashon, Washington

Subcontract Report
NREL/SR-550-32282
May 2008



NREL Technical Monitor: Mary Jane Hale
Prepared under Subcontract No. NAA-2-32439-01

National Renewable Energy Laboratory
1617 Cole Boulevard, Golden, Colorado 80401-3393
303-275-3000 • www.nrel.gov

Operated for the U.S. Department of Energy
Office of Energy Efficiency and Renewable Energy
by Midwest Research Institute • Battelle

Contract No. DE-AC36-99-GO10337

**This publication was reproduced from the best available copy
Submitted by the subcontractor and received no editorial review at NREL**

NOTICE

This report was prepared as an account of work sponsored by an agency of the United States government. Neither the United States government nor any agency thereof, nor any of their employees, makes any warranty, express or implied, or assumes any legal liability or responsibility for the accuracy, completeness, or usefulness of any information, apparatus, product, or process disclosed, or represents that its use would not infringe privately owned rights. Reference herein to any specific commercial product, process, or service by trade name, trademark, manufacturer, or otherwise does not necessarily constitute or imply its endorsement, recommendation, or favoring by the United States government or any agency thereof. The views and opinions of authors expressed herein do not necessarily state or reflect those of the United States government or any agency thereof.

Available electronically at <http://www.osti.gov/bridge>

Available for a processing fee to U.S. Department of Energy
and its contractors, in paper, from:

U.S. Department of Energy
Office of Scientific and Technical Information
P.O. Box 62
Oak Ridge, TN 37831-0062
phone: 865.576.8401
fax: 865.576.5728
email: <mailto:reports@adonis.osti.gov>

Available for sale to the public, in paper, from:

U.S. Department of Commerce
National Technical Information Service
5285 Port Royal Road
Springfield, VA 22161
phone: 800.553.6847
fax: 703.605.6900
email: orders@ntis.fedworld.gov
online ordering: <http://www.ntis.gov/ordering.htm>



Printed on paper containing at least 50% wastepaper, including 20% postconsumer waste

TABLE OF CONTENTS

1.	INTRODUCTION	1
1.1	Background and Scope of Parabolic Trough Wind Tunnel Test Program	1
1.2	Wind Load Issues.....	2
2.	TEST SETUP AND PROCEDURES	3
2.1	Boundary Layer Simulation Technique	3
2.2	Wind-Tunnel Models.....	4
2.2.1	Balance Model for Lift and Drag Force Measurements	5
2.2.2	Balance Model for Pitching Moment Measurements	7
2.2.3	Pressure Model.....	8
2.2.4	Non-Instrumented Solar Collector Models.....	12
2.3	Instrumentation	12
2.3.1	Signal Conditioner for High-Frequency Force and Moment Balances	12
2.3.2	CPP Multi-Pressure Measurement System	13
2.4	Test Configurations and Matrix	13
2.5	Test Procedures	25
2.6	Accuracy and Uncertainty of Test Results.....	26
3.	ANALYSIS METHODS	29
3.1	Definition of Test Parameters	29
3.1.1	Orientation of Solar Collector.....	29
3.1.2	Load Coefficients.....	30
3.1.3	Consideration for Load Cases for Structural Strength Design.....	31
3.2	Particular Treatment of Pressure Data	32
3.2.1	Integration of Distributed Local Pressures	32
3.2.2	Instantaneous Pressure Distributions	33
3.2.3	Interpolation of Point Pressures	34
4.	RESULTS AND DISCUSSION	38
4.1	Boundary Layer Simulation.....	38
4.2	Effects of Reynolds Number and Turbulence Intensity.....	39
4.3	Isolated Solar Collector.....	41
4.3.1	Test Results.....	41
4.3.2	Flow Visualization.....	46
4.4	Exterior Solar Collectors in Array Field.....	49
4.4.1	General Observations.....	49
4.4.2	Effects of Wind Protective Fence Barrier and Torque Tube	63
4.5	Interior Solar Collectors in Array Field	70
4.5.1	General Observations.....	70
4.5.2	Effects of Torque Tube	92
4.6	Loads on Deep Interior Solar Collectors	93
4.7	Wind Characteristics Within Array Field	100
4.8	Summary of Design Load Cases and Combinations.....	103
4.8.1	Structural Strength Design Loads	103
4.8.2	Local Peak Differential Design Pressures.....	105
4.8.3	Instantaneous Differential Pressures.....	111
4.8.4	Example Calculations of Design Loads	120

4.9	Adjustment to Pressure Test Data.....	123
4.9.1	Adjustment Factor.....	123
4.9.2	Effectiveness of the Adjustment Factors to Pressure Data	126
5.	CONCLUDING REMARKS.....	132
6.	REFERENCES	133
7.	APPENDICES	1
7.1	APPENDIX A - VALIDITY OF FULL-SCALE PREDICTION.....	A1
7.2	APPENDIX B - LIST OF OVERALL LOAD DATA.....	B1
7.3	APPENDIX C - WIND CHARACTERISTICS SIMULATED IN A WIND TUNNEL.....	C1
7.4	APPENDIX D - INSTANTANEOUS DIFFERENTIAL PRESSURE CONTOURS FOR SELECTED TEST CONFIGURATIONS	D1
7.5	APPENDIX E - TIME SERIES OF LOCAL PRESSURES.....	E1

LIST OF FIGURES

Figure 2-1 CPP aerodynamic wind tunnel	4
Figure 2-2 Wind tunnel setup	5
Figure 2-3 Lift and drag force balance model	6
Figure 2-4 Lift and drag force balance model assembly.....	6
Figure 2-5 Photograph of Pitching Moment Balance Model.....	7
Figure 2-6 Pitching Moment Balance Model Assembly.....	8
Figure 2-7 Pressure model	9
Figure 2-8 Pressure model assembly	10
Figure 2-9 Coordinates of pressure taps	11
Figure 2-10 Collector field model.....	12
Figure 2-11a Test configurations for array field study, exterior field	15
Figure 2-12 Test matrix	17
Figure 2-13 Test Configurations for Phase 4	22
Figure 2-14 Test Configurations for Deep Interior Tests, (a) Yaw = 0 degrees	23
Figure 2-15 Photograph of Test Setup for Configuration I8	25
Figure 2-16a Typical statistical variation of mean load.....	26
Figure 3-1 Definition of coordinate system and key dimensions	30
Figure 3-2 Tributary areas assigned for differential pressure taps	33
Figure 3-3 Interpolation of point pressures.....	34
Figure 3-4 Example of mirror panel arrangement for interpolation of differential pressures.....	36
Figure 4-1 Turbulent boundary layer simulated in wind tunnel	39
Figure 4-2 Sensitivity of load coefficients to Reynolds Number	40
Figure 4-3 Effects of turbulence intensity on horizontal force	41
Figure 4-4a Loads on isolated solar collector with and without torque tube, balance study.....	42
Figure 4-5a Comparisons of balance and pressure results for isolated collector, without torque tube	45
Figure 4-6 Flow around isolated solar collector	48
Figure 4-7 Loads on exterior collector for Configuration B1, collector in Row 1 at Module Position 4 (from edge), yaw = 0 degrees	50
Figure 4-8a Loads on exterior collector for Configuration B3 Collector in Row 1 at Module Position 1 (at edge), yaw = 0 degrees.....	51
Figure 4-9a Loads on exterior collector for Configuration B4, collector in Row 2 at Module Position 1 (at edge), yaw = 0 degrees.....	53
Figure 4-10a Loads on exterior collector for Configuration B5, collector in Row 3 at Module Position 1 (at edge), yaw = 0 degrees.....	55
Figure 4-11 Pitching Moment of Exterior Collector (a) Configuration B1, Yaw = 0 degrees	57
Figure 4-12a Effect of row position along edge of array field, yaw = 0 degrees	61
Figure 4-13 General flow patterns within array field	63
Figure 4-14a Loads on exterior collector with protective fence for Configuration D3, collector in Row 1 at Module Position 1 (at edge), yaw = 0 degrees	64
Figure 4-15 Effect of wind protective fence	66

Figure 4-16	Effect of torque tube on collector in array field, Configurations B1 and E1, collector in Row 1 at Module Position 4 (from edge), yaw = 0 degrees	67
Figure 4-17	Effect of torque tube on collector in array field, Configurations B3 and E3, collector in Row 1 at Module Position 1 (at edge), yaw = 0 degrees	68
Figure 4-18	Effect of torque tube on collector in array field, Configurations B4 and E4, collector in Row 2 at Module Position 1 (at edge), yaw = 0	69
Figure 4-19a	Loads on interior collector for Configuration C1, collector in Row 2 at Module Position 4 (from edge), yaw = - 30 degrees.....	71
Figure 4-20a	Loads on interior collector for Configuration C3, collector in Row 3 at Module Position 4 (from edge), yaw = - 30 degrees.....	74
Figure 4-21a	Loads on interior collector for Configuration C5, collector in Row 5 at Module Position 4 (from edge), yaw = - 30 degrees.....	77
Figure 4-22	Effect of row position at interior of array field, yaw = 0 degrees.....	80
Figure 4-23	Pitching Moment of Interior Collector (a) Configuration C2, Yaw = 0 degrees	81
Figure 4-24	Wind flow within interior of array field.....	82
Figure 4-25a	Loads on interior collector for Configuration C2, collector in Row 2 at Module Position 2 (from edge), yaw = - 30 degrees.....	83
Figure 4-26a	Loads on interior collector for Configuration C4, collector in Row 3 at Module Position 2 (from edge), yaw = - 30 degrees.....	86
Figure 4-27a	Loads on interior collector for Configuration C6, collector in Row 5 at Module Position 2 (from edge), yaw = - 30 degrees.....	89
Figure 4-28	Effect of torque tube on collector in array field, Configurations C5 and F5, yaw = 0 degrees	92
Figure 4-29	Effect of Row Position for Collectors at 4 th Column, Yaw = 0 degrees	94
Figure 4-30	Effect of Row Position for Collectors at 4 th Column, Yaw = 30 degrees	96
Figure 4-31	Effect of Row Position for Collectors at 8 th Column, Yaw = 0 degrees	97
Figure 4-32	Effect of Row Position for Collectors at 8 th Column, Yaw = 30 degrees	98
Figure 4-33	Effect of Row Position for Collectors at 12 th Column, Yaw = 30 degrees	99
Figure 4-34	Mean Velocity and Turbulent Profiles Within Array Field (a) Pitch = 0 deg.....	101
Figure 4-35a	Local peak differential pressure distribution, field exterior	106
Figure 4-36	Vortex flow forming from corner of collector	111
Figure 4-37a	Instantaneous differential pressure distribution with the largest local peak, yaw = - 30 degrees	112
Figure 4-38a	Instantaneous differential pressure distribution with	116
Figure 4-39	Comparison of Previous Balance and Pressure Data, (a) Horizontal Force Component.....	123
Figure 4-40	Comparison of Balance and Adjusted Pressure Data,.....	127
Figure 4-41	Comparison of Balance and Adjusted Pressure Data.....	130
Figure 4-42	Comparison of Balance and Adjusted Pressure Data.....	131

LIST OF TABLES

Table 2-1	Test Configurations	14
Table 2-2	Estimated Uncertainty Associated with Mean Load Measurement	28
Table 3-1	Influence Factors for Interpolation of Differential Pressures	37
Table 4-1	Summary of Load Cases and Load Combinations	104
Table 4-2	Summary of Peak Local Differential Pressures.....	110
Table 4-3	Selected Summary of Instantaneous Differential Distribution with the Largest Local Peak.....	115
Table 4-4	Differential Pressure Distributions Resulting in.....	119
Table 4-5	Design Pressure Conversion Factors for Different Mean Recurrence Intervals.....	122
Table 4-6	Adjustment Factors to Be Applied to Previous Pressure Data	126

LIST OF SYMBOLS

C_{fx}	Horizontal force coefficient
C_{fz}	Vertical force coefficient
C_{my}	Pitching moment coefficient
C_p	Pressure coefficient
C_{dp}	Differential pressure coefficient
f_x	Horizontal force
f_z	Vertical force
m_y	Pitching moment
p	Pressure
Δp	Differential pressure
H	Top height of solar collector
H_c	Height of collector pivot
L	Horizontal length of solar collector
W	Aperture width
n	Mean velocity profile power law exponent
p_s	Static pressure in wind tunnel at reference height z_{ref}
q	Reference dynamic pressure
U	Local mean velocity
U_{Hc}	Velocity at height of collector pivot
U_R	Reference velocity ($= U_{Hc}$)
x, y	Horizontal coordinates
z	Vertical coordinate
ν	Kinematic viscosity of approach flow
ρ	Density of approach flow
$\sigma_u(z)$	Standard deviation of $() = ()'_{rms}$
$()_{max}$	Maximum value during data record
$()_{min}$	Minimum value during data record
$()_{mean}$	Mean value during data record
$()_{rms}$	Root mean square about the mean

1. INTRODUCTION

1.1 Background and Scope of Parabolic Trough Wind Tunnel Test Program

Wind load estimates for parabolic trough solar collectors have relied largely on wind tunnel tests sponsored by Sandia National Laboratories in the late 1970s and early 1980s, specifically Peterka et al. (1980, 1992) and Randall et al. (1980, 1982). These tests involved wind-tunnel measurements in a boundary-layer wind tunnel at Colorado State University (CSU) performed by current principals of Cermak Peterka Petersen, Inc. (CPP). The reports provided mean wind load coefficients for an isolated parabolic trough collector and for a collector within an array field. The wind loads were measured using a force balance to determine overall mean load. No assessment for dynamically fluctuating load or peak load was made. Further, the measurements did not include the distribution of local pressures across the face of the collector. Measurements of these missing elements are the primary contributions of this current study. The wind-tunnel data presented in this report was, in part, designed to augment these missing load components that are of significance for designers of solar collectors. The study also includes examination of wind loads on collectors located deep inside an array field for the purpose of extending design load data as a function of position.

The focus of the current study was the wind loads on a 26-ft (7.9-m) section of parabolic trough collector with an aperture of 16.4 ft (5 m), supported with a minimum distance of collector to ground of 1.2 ft (0.35 m). Two versions of the instrumented collector models were used for the wind-tunnel study: One was a model installed on a high frequency force balance to measure overall fluctuating loads; the other was a pressure-tapped model primarily designed to obtain the distribution of the pressure loads across the face of the collector at 30 discrete local points, but also to measure overall loads on the collectors. The collector was first studied as an isolated unit to obtain baseline loading. The collector was then studied at a variety of locations in a collector field. The effects of a porous fence at the edge of the field were included in some tests, because available documents on other collectors have shown beneficial shielding with protective fences of about 50% solidity. Test configurations and procedures for the study presented here are described in Section 2.



This report also presents investigative test results related to the effect of Reynolds Number on aerodynamic load coefficients of the solar collector since the curved surface of the parabolic collector could potentially cause the measured load coefficients to be dependent on Reynolds number (specifically affected by the test wind speed). The effect of turbulence intensity in the approach flow was similarly of concern. Sandia Laboratories Report SAND 92-7009 (see Peterka and Derickson, 1992) demonstrated a sensitivity to turbulence intensity for heliostats (see Figures

2 and 3 of that report). Whether or not a similar phenomenon occurs for parabolic trough collectors needed to be resolved. A series of wind-tunnel tests on an isolated collector were conducted to examine and identify these effects. The tests showed, as described in detail in Section 4.2, that the load coefficients of the solar collector were essentially independent of Reynolds number in a range realized in the wind tunnel, probably due to sufficiently high level of turbulence over the height of the collector modeled in a surface boundary layer flow. The effect of the turbulence was found to be insignificant as long as the turbulent approach flow was simulated properly in the wind tunnel.

The initial series of tests examined wind loads on interior solar collectors as deep as the 5th row from the windward edge of the array field, where considerable reduction of wind loads was realized. However, a possibility existed that the loads would continue to decrease further downwind, leading to potential cost reduction in the trough structures by optimization of the design. Subsequent tests investigated this issue by measurements of loads deep interior of the array field, extending to the 20th row downwind. A rigid pressure model, described in Section 2, was used to measure distributions of local pressures from which overall lateral and vertical forces and pitching moment were computed by integration of pressures. It was hoped that variation of these load components could be conveniently fitted to analytical models to calculate desired loads for an arbitrary distance into a field. This is discussed fully in Section 4.

1.2 Wind Load Issues

Most building codes are based on the concept of quasi-steady loads. That is, the peak load is assumed to result from the same flow mechanisms as for the mean flow, so that the peak load is just the mean load times the square of the gust factor for the wind gust under study. For example, the national wind load standard ASCE 7-98 (ASCE 2000) or the model building code IBC (International Building Code) 2000 (International Code Council, Inc., 2000) would predict the gust factor in wind to be 1.53 for a peak gust in an open country environment. For a structure that has a quasi-steady wind load, the peak load due to a peak gust would be $1.53^2 = 2.34$ times the mean load. Prior to this report, only mean coefficients had been measured for parabolic troughs [Peterka et al. (1980)], requiring that peak loads be calculated using mean coefficients applied at the peak gust speeds (equivalent to uniformly applying the 2.34 multiplicative factor to the mean load). However, many types of wind loads do not obey the quasi-steady approximation, and it is for this reason that peak loads have been measured in this current study. For cases where these peak coefficients are available, they can be used directly to produce the appropriate peak load. Example calculations are included in section 4.7.4 to illustrate this point.

The validity of boundary-layer wind tunnel testing for wind loads on structures is based on similarity arguments (see Cermak, 1971, 1975, and 1976) and on model-to-full-scale test comparisons for models tested at scales of about 1:200 to 1:500. For models at larger scales, for example 1:45 as used in the current study, there are fewer model/full scale comparisons (the few that have been completed are for buildings, and agreement has been good). The writers are unaware of any comprehensive full-scale wind-load tests on solar collectors that have been carried out in a turbulent wind, which would provide a basis for model/full-scale test comparison. Ultimately, the acceptability of boundary-layer wind-tunnel tests for solar collectors should be based on model-to-full-scale tests. More discussion of this issue is contained in Appendix A.

2. TEST SETUP AND PROCEDURES

Modeling of the aerodynamic loading on a structure requires special consideration of flow conditions to obtain similitude between the model and the prototype. A detailed discussion of the similarity requirements and their wind-tunnel implementation can be found in Cermak (1971, 1975, 1976). In general, the requirements are that the model and prototype be geometrically similar, that the approach mean velocity at the model building site have a vertical profile shape similar to the full-scale flow, and that the Reynolds Number for the model and prototype be equal.

These criteria are satisfied by constructing a scale model of the structure and its surroundings and by performing the tests in a wind tunnel specifically designed to model atmospheric boundary-layer flows. Reynolds Number similarity requires that the quantity UD/v (the ratio of flow inertia force to viscous force) be similar for model and prototype. Since v , the kinematic viscosity of air, is identical for both, Reynolds Numbers cannot be made equal with a reasonable wind velocity, for such a velocity would introduce unacceptable compressibility effects. However, for sufficiently high Reynolds Numbers ($>2 \times 10^4$) the pressure coefficient at any location on a blunt, sharp-edged body becomes independent of the Reynolds Number. Thus, an exact equality of the Reynolds Number is no longer required for similarity. On the other hand, the pressure coefficient on a streamlined body, such as a circular cylinder, is known to vary over the wide range of the Reynolds number typically encountered at full ($10^6 - 10^7$) and model (5×10^4) scales.

For streamlined bodies such as a circular cylinder or a sphere, on the other hand, it is known that the load coefficients are highly dependent on the Reynolds Number above the typical range of the Reynolds Number for wind-tunnel models. The main geometric features of the solar collectors consisted of reflective concentrator panels assembled in a thin parabolic shape; therefore, a possible Reynolds Number effect that would invalidate the model test was addressed. A series of preliminary tests as described in Section 4.2 indicated that the necessary Reynolds Number independence for the aerodynamic performance of the parabolic solar collectors could be adequately achieved in a wind tunnel. All model tests reported herein were performed at a sufficiently high velocity to maintain the independence of Reynolds Number. That is, the model Reynolds number was sufficiently high such that the measured pressure and load coefficients were essentially independent of the Reynolds number. As such the wind-tunnel data presented in this report are directly applicable to full-scale parabolic solar collectors.

2.1 Boundary Layer Simulation Technique

The wind-tunnel test was performed in the boundary-layer wind tunnel in the Wind Engineering Laboratory of CPP (Figure 2-1). This closed-circuit wind tunnel had a 68-ft-long test section covered with roughness elements to reproduce at model scale the atmospheric wind characteristics required for the model test. Some of these wind characteristics pertaining to wind load are explained in Appendix C. The wind tunnel had a flexible roof, adjustable in height, to maintain a zero pressure gradient along the test section and to minimize blockage effects.

The wind-tunnel floor upstream from the modeled area was covered with roughness elements constructed from 0.75-in. cubes. Spires and a low barrier were installed in the test section entrance to provide a thicker boundary layer than would otherwise be available, permitting a somewhat larger scale model. The spires, barrier, and roughness were designed to provide a modeled atmospheric boundary layer approximately 4 ft thick and a mean velocity power law exponent and turbulence structure in the modeled atmospheric boundary layer similar to that expected in open country. Figure 2-2 is a photograph of the test section of the wind tunnel as

modeled. The approach wind established for the model test is explained more fully in Section 4.1.

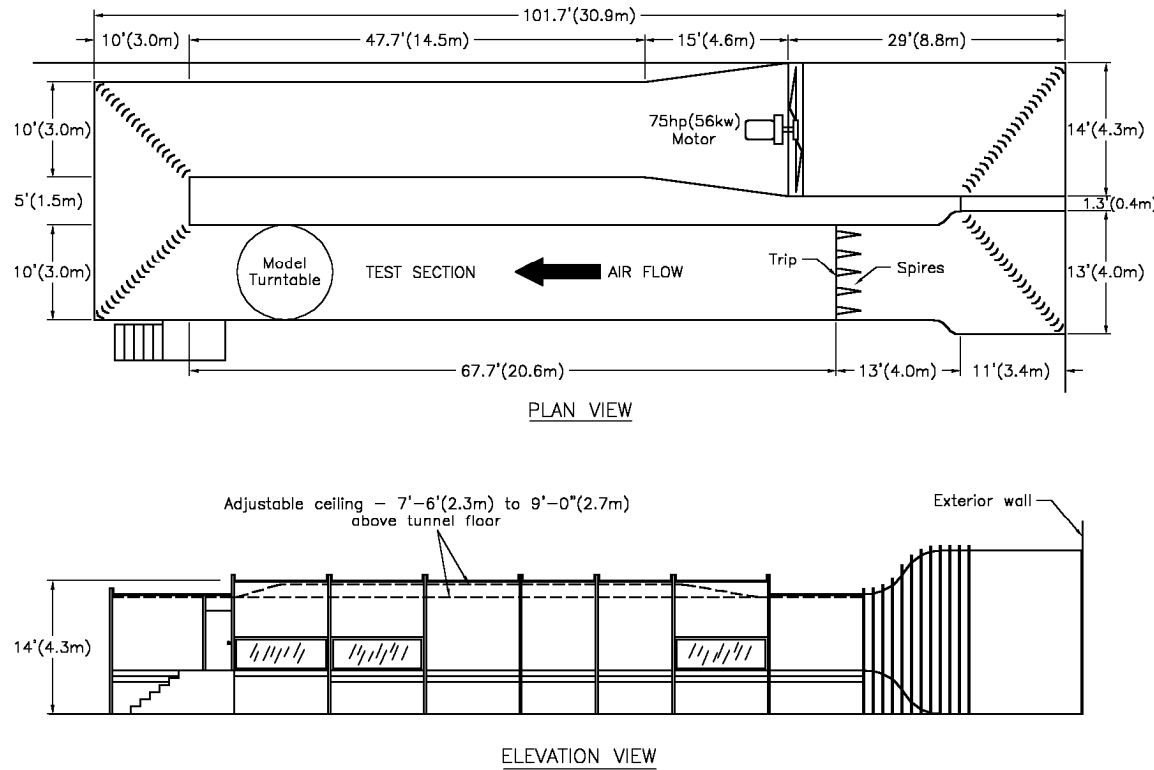


Figure 2-1 CPP aerodynamic wind tunnel

2.2 Wind-Tunnel Models

Four types of wind-tunnel models of a parabolic trough solar collector were constructed for this wind-tunnel study. They were (1) a light-weight model for measuring lift and drag dynamic wind loads using a high-frequency force balance, (2) a light-weight model instrumented with a set of strain gages for direct measurement of pitching moment, (3) a rigid plastic model instrumented with pressure taps for measuring pressure distribution over the surface of the collector concentrator component, and (4), in the array field studies, a number of non-instrumented dummy mock-ups surrounding the instrumented model. The instrumented models and the mock-ups were constructed at a scale of 1:45 based on the set of dimensions consistent with the Solargenix Energy parabolic trough. These overall dimensions are identical to those of the LS-2 collector (Cohen, 1999) and are expected to result in non-dimensional load data applicable over a range of modest variations in parabolic trough configurations. The thickness and rear side details of the concentrator component compared to an actual collector were not viewed as critical aspects of the wind test model configuration, with the possible exception of a torque tube, which is discussed later in this report. In the following sections, the wind-tunnel models and construction technique are described.



Figure 2-2 Wind tunnel setup

2.2.1 Balance Model for Lift and Drag Force Measurements

Both balance models¹ consisted of all key features of a parabolic trough solar collector, including a main parabolic concentrator module, support pylons, and the receiver and collector support pedestals. The main concentrator component was made of solid plastic, molded using stereo lithography apparatus (SLA) technology. The concentrator model was 1/8 in. thick at the chord center and tapered to 1/16 in. thick at the top and bottom edges. The thickness was varied to maintain stiffness near the location where the concentrator was fastened as well as to obtain lightness in weight.

The model used for lift and drag measurements consisted of a pair of aluminum arms glued to either side of the concentrator component, which was then attached to an aluminum pedestal with setscrews for support and to permit the concentrator to rotate a full 360 degrees about the designated center of rotation. The arms also held a replica of the receiver made of a 1/16-in. OD brass pipe and a removable torque tube replica at the back center of the concentrator module. A 5/16-in. OD brass tube was used to model the torque tube for selected test runs. The aluminum pedestals, or pylons, were slightly oversized for the model, compared to the actual support pylons, in order to obtain sufficient rigidity required for measuring accurate dynamic wind loading.

The entire solar collector model was mounted on a high-frequency force balance consisting of sets of strain-gage transducers, designed by CPP that measured horizontal force. The force balance was coupled by FUTEK load cells, Model L2357, with a rated capacity of 2 lbs. to measure the vertical force.

¹ A balance model is also referred to as a dynamic model since it is designed to measure fluctuating wind load as well as mean load.

A photograph of this balance model is given in Figure 2-3, and the assembly is illustrated in Figure 2-4.

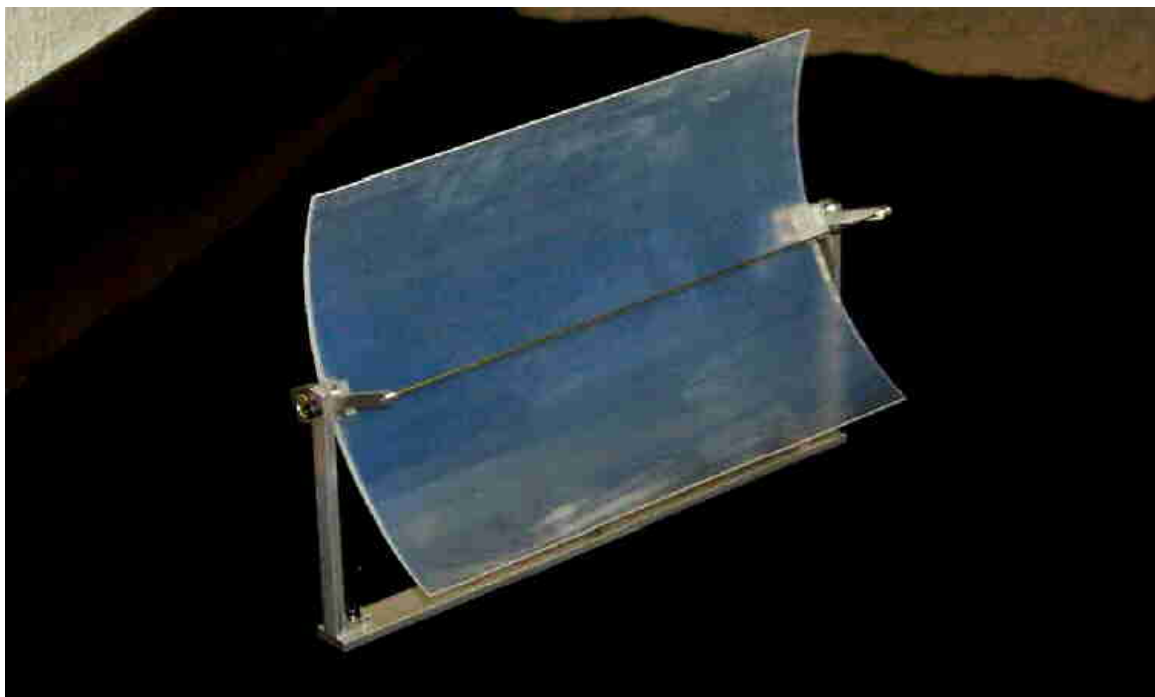


Figure 2-3 Lift and drag force balance model

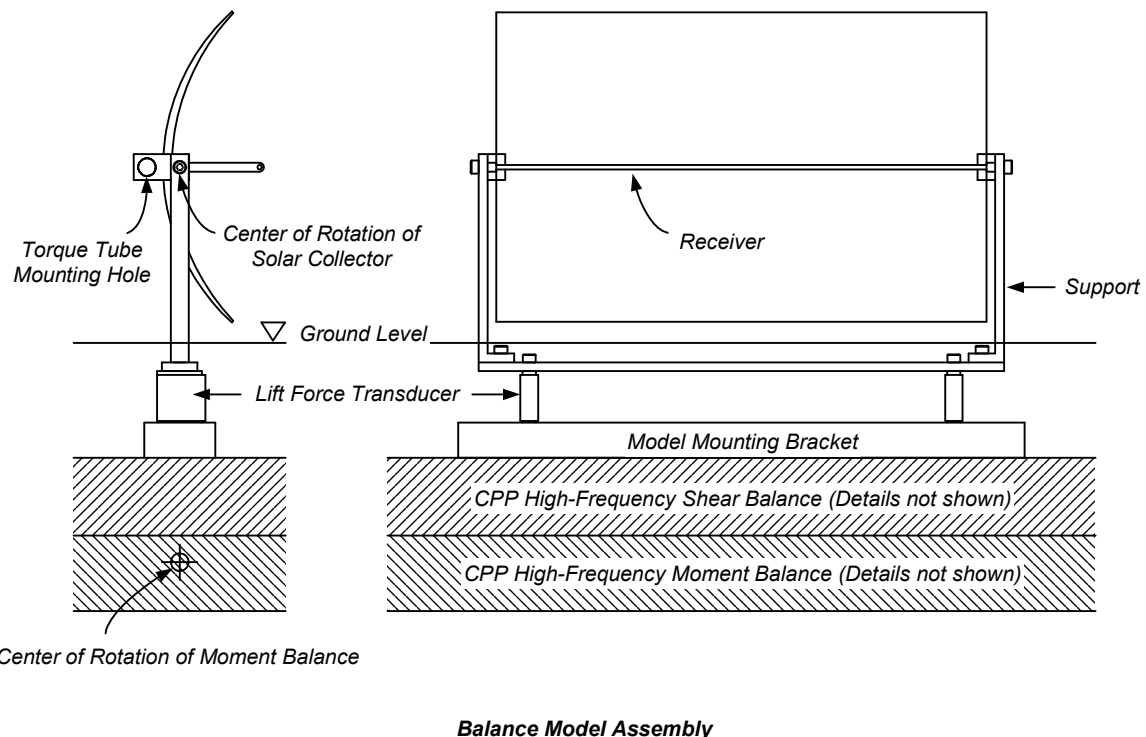


Figure 2-4 Lift and drag force balance model assembly

2.2.2 Balance Model for Pitching Moment Measurements

The pitching moment balance model consisted of the parabolic module described above mounted on a miniature torque transducer designed and built specifically for this purpose. The torque transducer was made of an aluminum tube, and cantilevered out from a rigid aluminum reaction post. The transducer was instrumented with 4 strain gages wired into a conventional Wheatstone bridge circuit for direct measurement of torsion about the principle axis of the tube. The parabolic module was mounted at the open end of the transducer, matching the pivot center, for delivering overall pitching moment directly to the torque transducer.

The torque transducer was essentially a thin-wall aluminum tube. It measured 1 inch in length and 0.5 inch in OD with a wall thickness of 1/16 inch. These dimensions, particularly the wall thickness, were selected to obtain adequate sensitivity in the anticipated range of pitching moment while maintaining required stiffness for measurement of the wind load fluctuations. At the expected maximum load, the new transducer was designed to yield 2 μ -strains in the primary shear direction.

A photograph of the balance model is given in Figure 2-5, and the assembly is illustrated in Figure 2-6.

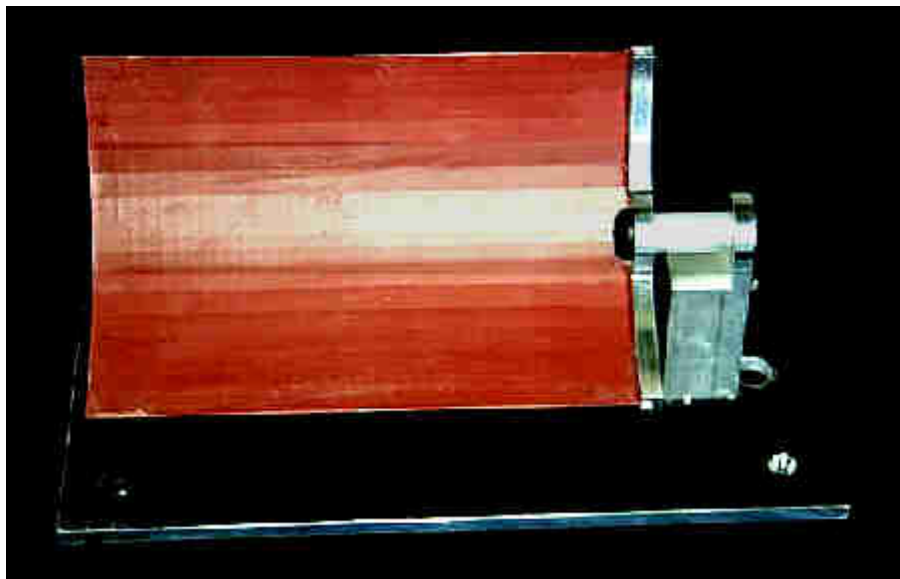


Figure 2-5 Photograph of Pitching Moment Balance Model

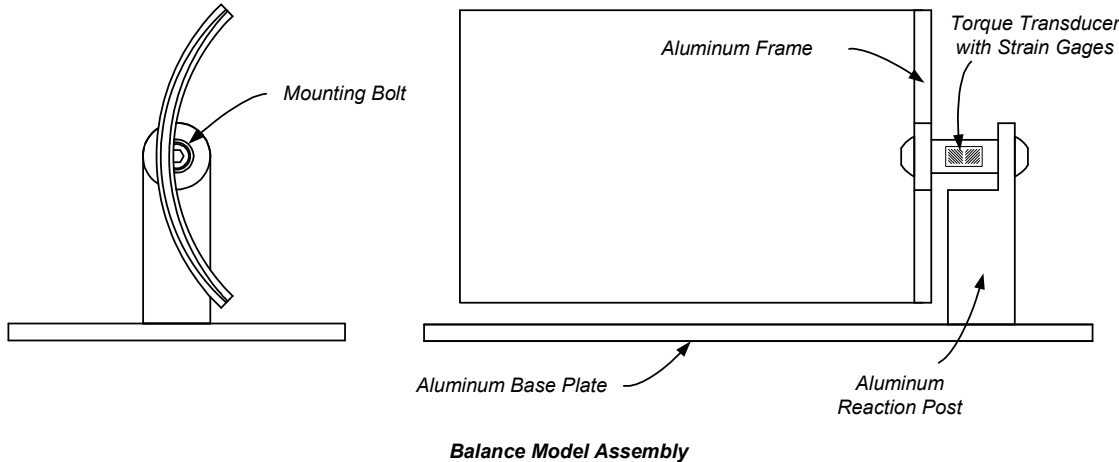


Figure 2-6 Pitching Moment Balance Model Assembly

2.2.3 Pressure Model

A pressure model was designed to measure the distribution of local pressures on the front and back surfaces of the collector concentrator module. The model was made of a 1/5-in. plastic with a total of 60 pressure taps pre-installed using the SLA technique. Thirty pressure taps were dedicated to measure pressures on the front surface, with thirty corresponding taps on the back surface. The pressure taps were laid out so that differential pressures across the collector concentrator could be numerically obtained by pairing the pressure taps on the front surface with the corresponding taps on the back surface. The pressure taps were 1/32-in. diameter, and pressures sensed at these taps were routed to the sides of the model where plastic tubes directed the pressure input to transducers mounted underneath the turntable.

Pressures over the concentrator modules can vary in space and time, because of spatial and temporal variation in approach velocity (turbulence), the bluff geometry of the solar collector, and the wide range of the operational conditions. Surrounding solar collectors and wind barriers also affect the pressure distributions. The variation of pressures near the corners and edges of the solar collector can be very large. To capture the large pressure gradient anticipated, several pressure taps were placed near the extreme corners and edges of the model. It should be noted that the number of the pressure taps incorporated in the model is probably the physical upper limit without overly distorting its geometry.

The concentrator component of the pressure model had overall dimensions identical to those of the balance model counterpart except for somewhat larger thickness to accommodate the pressure taps. The other model components including the support legs, arms, and receiver were constructed similarly, if not identically, to those for the balance model. Figure 2-7 shows a photograph of the pressure model, and the pressure tap locations are schematically shown in Figure 2-8.

The exact locations of the pressure taps are given in Figure 2-9 using the local coordinate system projected on the vertical plane.

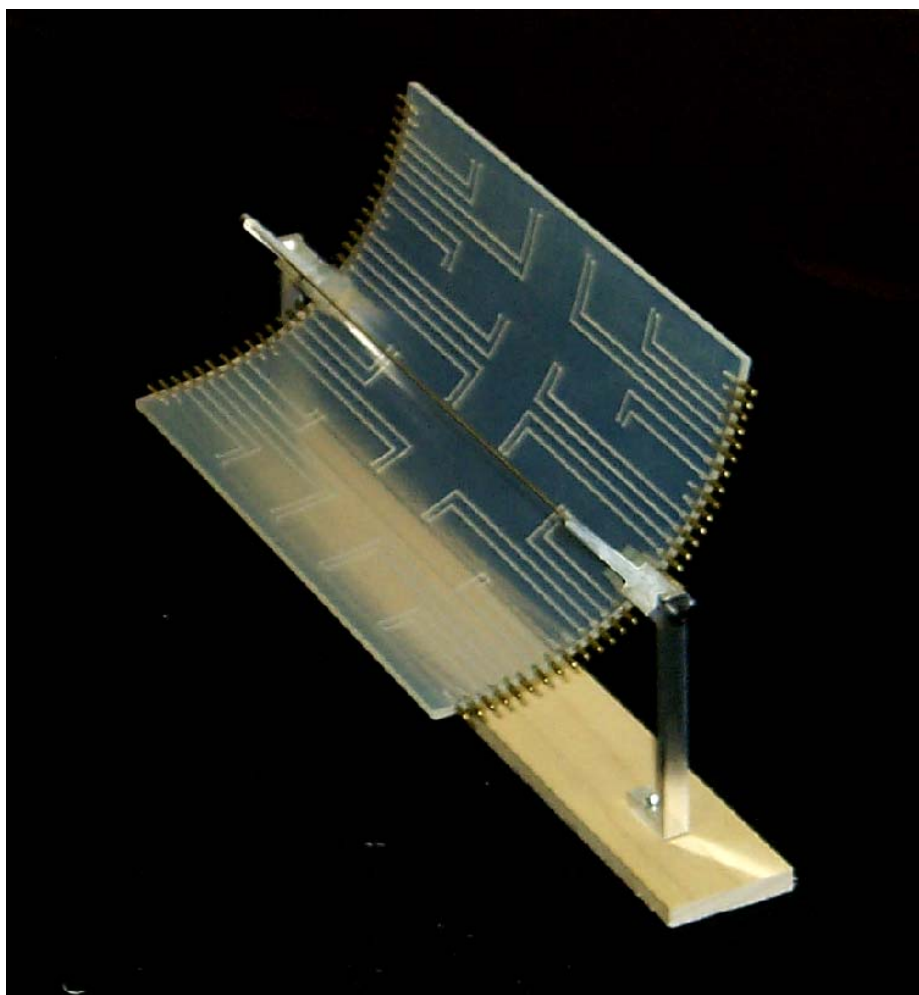
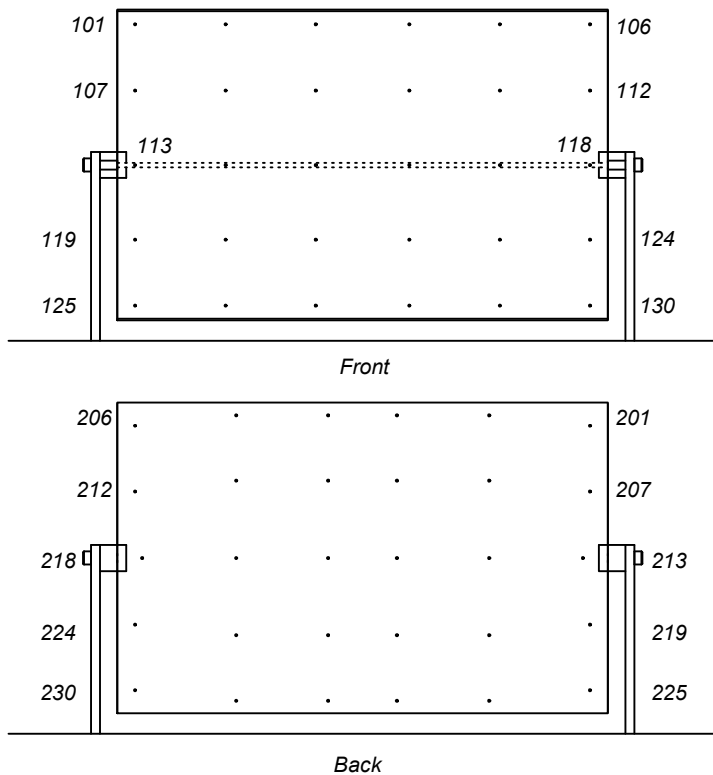
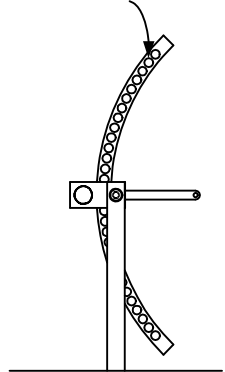


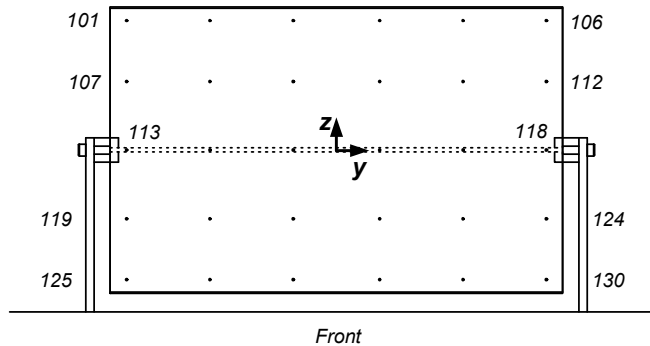
Figure 2-7 Pressure model

Pressure Tap Access Holes



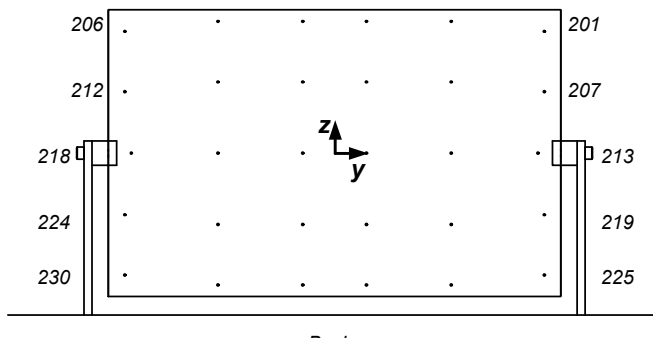
Pressure Model Assembly and Pressure Tap Numbers

Figure 2-8 Pressure model assembly



Front

Tap	y, ft	z, ft												
101	-12.05	7.46	107	-12.05	3.95	113	-12.05	0.00	119	-12.05	-3.95	125	-12.05	-7.46
102	-7.26	7.46	108	-7.26	3.95	114	-7.26	0.00	120	-7.26	-3.95	126	-7.26	-7.46
103	-2.48	7.46	109	-2.48	3.95	115	-2.48	0.00	121	-2.48	-3.95	127	-2.48	-7.46
104	2.48	7.46	110	2.48	3.95	116	2.48	0.00	122	2.48	-3.95	128	2.48	-7.46
105	7.26	7.46	111	7.26	3.95	117	7.26	0.00	123	7.26	-3.95	129	7.26	-7.46
106	12.05	7.46	112	12.05	3.95	118	12.05	0.00	124	12.05	-3.95	130	12.05	-7.46



Back

Tap	y, ft	z, ft												
201	12.05	7.02	207	12.05	3.54	213	11.67	0.00	219	12.05	-3.54	225	12.05	-7.02
202	6.70	7.58	208	6.70	4.10	214	6.70	0.00	220	6.70	-4.10	226	6.70	-7.58
203	1.83	7.58	209	1.83	4.10	215	1.83	0.00	221	1.83	-4.10	227	1.83	-7.58
204	-1.83	7.58	210	-1.83	4.10	216	-1.83	0.00	222	-1.83	-4.10	228	-1.83	-7.58
205	-6.70	7.58	211	-6.70	4.10	217	-6.70	0.00	223	-6.70	-4.10	229	-6.70	-7.58
206	-12.05	7.02	212	-12.05	3.54	218	-11.67	0.00	224	-12.05	-3.54	230	-12.05	-7.02

Figure 2-9 Coordinates of pressure taps

2.2.4 Non-Instrumented Solar Collector Models

The test program called for multi-configuration wind-tunnel tests on solar collectors at different locations within an array of collectors. To model a field of solar collectors, a number of non-instrumented collector models were constructed, which would surround the instrumented model. The non-instrumented models, also referred to as dummy mockups, were made with readily available PVC pipes with a 6-in. OD cut in proper size. Several dummy units were attached to a long aluminum shaft supported horizontally by specially made brackets to allow rotation of the collectors about the pitch axis.

For the array field study, the solar collector models were laid out in rows with a spacing equivalent to 2.8 times the collector aperture. A typical arrangement of the non-instrumented solar collectors in a field is shown in Figure 2-10.



Figure 2-10 Collector field model

2.3 Instrumentation

2.3.1 Signal Conditioner for High-Frequency Force and Moment Balances

The data acquisition system for the balance tests included Honeywell Accudata amplifier/signal conditioners and IO Tech elliptic low-pass filters from which the output DC signals were fed into a Metrabyte analog-to-digital converter (ADC) with +/-10 volt input range at a 12-bit resolution. The force and moment balances were statically calibrated prior to the wind-tunnel tests to obtain calibration factors for conversion of the voltage output to loads in engineering units. These force

and moment balance systems, with the collector model mounted, had inherent natural frequencies of higher than 40 and 80 Hz, respectively, and were sufficient for measurement of dynamic loads.

2.3.2 CPP Multi-Pressure Measurement System

Pressure data on the solar collector were acquired using the CPP multi-pressure system (MPS). The system features simultaneous signal samples from 512 individual pressure transducers at a maximum design rate of 500 samples per second per channel. When fully configured, the MPS would consist of four 16-channel analog-to-digital converters with a 16-bit resolution and eight 64-channel multiplexers, both manufactured by IO Tech, connected to an IEEE488 controller onboard a desktop personal computer. For the present wind-tunnel study requiring 60 pressure taps on the model, the system was configured with a single 16-bit ADC and a multiplexer for a total capacity of 64 data channels. The differential pressure transducers used were Data Instruments Model XPC with a full-scale range of +/-0.14 psid (differential pressure) combined with a signal amplifier that provided a gain of 50.

The wind pressure at the model exterior was transmitted to the pressure transducer using a two-segment plastic tube. The plastic tube consisted of a 13-in. (1/32-in. ID) section and a 36-in. (1/16 in. ID) section joined together with a small brass coupler. The inherent frequency response characteristics of the tube system were measured before the pressure tests so that a compensation digital filter could be designed. The response correction filter was then incorporated in the data acquisition software and applied to the measured pressure signals during the data collection.

2.4 Test Configurations and Matrix

A multi-phase test program was initially designed in coordination with Solargenix Energy and was refined as the wind-tunnel study progressed in order to optimize the overall test program. The test program essentially consisted of four Phases. Phase 1 conducted tests on an isolated solar collector with a wide range of the yaw and pitch angles of the concentrator module. The yaw angle defined the azimuth of the collector relative to approach wind, and the pitch angles defined the tilt with respect to the vertical plane. These angular parameters are fully explained later in Section 3.1. The effects of the Reynolds Number and incident turbulence were also studied in this phase. Phase 2 of the program investigated wind loads on the solar collectors around the edge of a simulated array field, referred to herein as the exterior solar collectors. For several collector positions, the effect of wind protective barriers was also examined. Phase 3 tests were conducted on the collector at various positions within the array field, the interior solar collectors. In all these test phases, the balance and pressure data acquisition techniques were used as necessary to determine wind loads for the solar collector. Phase 4 tests included direct measurement of the pitching moment using a light-weight balance model especially designed for those tests, as well as the test series using pressure measurements to examine the influence of deep interior locations on forces and pitching moments.

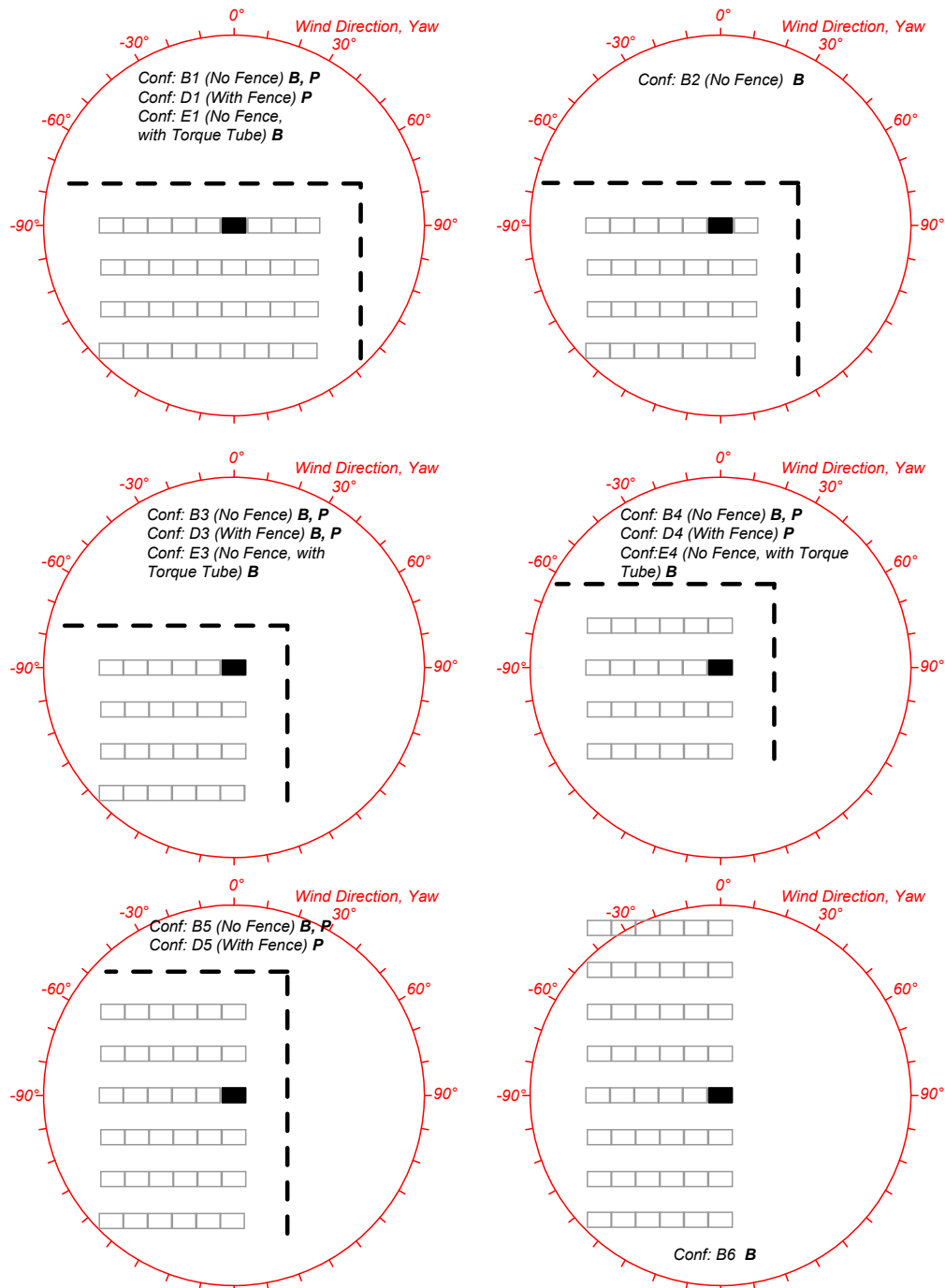
Series of wind-tunnel tests were grouped according to physical test configuration and were given configuration identifications for ease of data management. Table 2-1 summarizes the designated test configuration.

Phases 2 and 3: For the exterior and interior field studies, Figure 2-11a and Figure 2-11b concisely illustrate various test configurations. The side notes indicate the type of the data acquisition method: **B** for the balance technique and **P** for the pressure technique. These configuration IDs, for example A1 or C5, are frequently referred throughout this report for sake of convenience.

The ranges of the yaw and pitch angles varied depending on the test configurations. Figure 2-12 gives the combinations of these angles tested for different test configurations in the form of test matrices.

Table 2-1 Test Configurations

Conf.	Description
A1	Single Collector in Nominal Roughness.
A2	Single Collector With Torque Tube in Nominal Roughness.
A3	Single Collector in Bare Floor.
A4	Single Collector in Smooth Roughness.
A5	Single Collector in Rough Roughness.
Bx	Collector at Edge of Field. x = Position ID.
Cx	Collector at Interior of Field. x = Position ID.
Dx	Collector at Edge of Field With Protective Fence. x = Position ID.
Ex	Collector at Edge of Field With Torque Tube. x = Position ID.
Fx	Collector at Interior of Field with Torque Tube. x = Position ID.



Side notes "B" and "P" indicate the completed test configuration by Balance Measurement and Pressure Measurement, respectively.

Figure 2-11a Test configurations for array field study, exterior field

be used directly for the present solar collector data because (1) the ASCE wind speeds are given as a 3-second gust speed rather than a mean speed adopted for the wind-tunnel test, and (2) the ASCE wind speeds are referenced at an elevation of 33 ft rather than the collector pivot height of 9.35 ft. Thus, conversion of the ASCE wind speeds is necessary using the procedures explained in ASCE 7-98. Conversion of a 50-year wind load is also explained in ASCE 7-98 for different mean recurrence intervals and is presented here.

Conversion of ASCE Basic Wind Speed

Consider a solar collector site in California for which ASCE 7-98 (Figure 6-1) gives the basic wind speed of $V = 85$ mph. Using Figure C6-1, the corresponding hourly mean wind speed at 33 ft, U_{33} , is obtained as

$$U_{33} = V / 1.53 = 85 / 1.53 = 55.6 \text{ mph hourly mean.}$$

Using values implied by Table 6-4 of ASCE 7-98, the mean wind speed at the collector pivot height, U_{hc} , is given as

The hourly mean wind speed of 46.4 mph is the design wind speed for the solar collectors in California.

Design Wind Loads

Based on the design wind speed, the corresponding design pressure, q , is calculated by

$$q = \frac{1}{2} \rho U_{hc}^2 = 0.00256(46.4)^2 = 5.51 \text{ psf.}$$

Here, the constant 0.00256 is conveniently used to obtain the reference pressure in psf from the wind speed in mph. As an example, we wish to determine the 50-year peak design loads on the innermost-shielded solar collectors (Configuration C5) when that collector is oriented at a -60 degree pitch angle (a downward-facing stow position). We note from Table 4.1 that the largest peak vertical force, Load Case 3, is produced at this -60 degree pitch angle, at a yaw angle of 0 degrees, so this orientation is of special interest to designers. Table 4.1 shows the peak C_{fz} is 2.754 and the corresponding C_{fx} value is 1.404, and the C_{my} value is 0.107. Using equations (4.5) – (4.7):

$$\text{Horizontal Force } f_x = qLW C_{fx} = (5.51)(25.97)(16.40)(1.404) = 3,295 \text{ lbs}$$

$$\text{Vertical Force, } f_z = qLW C_{fz} = (5.51)(25.97)(16.40)(2.754) = 6,463 \text{ lbs}$$

$$\text{Pitching Moment, } m_y = qLW^2 C_{my} = (5.51)(25.97)(16.40)^2(0.107) = 4,118 \text{ lb-ft.}$$

Note that these loads are to be applied simultaneously to the structure because the wind-tunnel results were obtained as a concurrent load combination from the time series data for which the vertical force was maximized.

Comparison to Design Loads Determined by Quasi-Steady Assumption

As pointed out in Section 1.2, the traditional approach to obtaining the structural design loads on solar collectors has been based on the quasi-steady assumption. With this technique, the measured mean load is scaled to follow the gust wind speed to provide the equivalent peak load. The scale factor is known as the gust load factor, and ASCE 7-98 or the model building code IBC

Isolated Solar Collector - Balance and Pressure Studies

Yaw	Pitch																							
	-180	-165	-150	-135	-120	-105	-90	-75	-60	-45	-30	-15	0	15	30	45	60	75	90	105	120	135	150	165
0.0			X*	X*	X*	X*	X*	X*	X*	X*	X*	X*	X*	X*	X*	X*	X*	X*	X*	X*	X*	X*	X*	X*
30.0			X	X	X	X	X	X	X	X	X	X	X	X	X	X	X	X	X	X	X	X	X	
60.0			X	X	X	X	X	X	X	X	X	X	X	X	X	X	X	X	X	X	X	X	X	
90.0																								
120.0			X	X	X	X	X	X	X	X	X	X	X	X	X	X	X	X	X	X	X	X	X	
150.0			X	X	X	X	X	X	X	X	X	X	X	X	X	X	X	X	X	X	X	X	X	
180.0			X*	X*	X*	X*	X*	X*	X*	X*	X*	X*	X*	X*	X*	X*	X*	X*	X*	X*	X*	X*	X*	
-150.0																								
-120.0																								
-90.0																								
-60.0																								
-30.0																								

Note:

X* = With and Without Torque Tube.

For Configurations A3, A4, A5, Yaw = 0, and Pitch = 0, -90.

Exterior Solar Collector - Balance Study

Yaw	Pitch																							
	-180	-165	-150	-135	-120	-105	-90	-75	-60	-45	-30	-15	0	15	30	45	60	75	90	105	120	135	150	165
0.0	X*	X*	X*	X*	X*	X*	X*	X*	X*	X*	X*	X*	X*	X*	X*	X*	X*	X*	X*	X*	X*	X*	X*	X*
30.0	X	X	X	X	X	X	X	X	X	X	X	X	X	X	X	X	X	X	X	X	X	X	X	X
60.0	X	X	X	X	X	X	X	X	X	X	X	X	X	X	X	X	X	X	X	X	X	X	X	X
90.0																								
120.0																								
150.0																								
180.0																								
-150.0																								
-120.0																								
-90.0																								
-60.0																								
-30.0	X	X	X	X	X	X	X	X	X	X	X	X	X	X	X	X	X	X	X	X	X	X	X	

Note:

X* = With and Without Torque Tube.

Figure 2-12 Test matrix

Exterior Solar Collector with Fence - Balance Study

Pitch		-180	-165	-150	-135	-120	-105	-90	-75	-60	-45	-30	-15	0	15	30	45	60	75	90	105	120	135	150	165	180
Yaw		X	X	X	X	X	X	X	X	X	X	X	X	X	X	X	X	X	X	X	X	X	X	X	X	
0.0		X	X	X	X	X	X	X	X	X	X	X	X	X	X	X	X	X	X	X	X	X	X	X	X	
30.0		X	X	X	X	X	X	X	X	X	X	X	X	X	X	X	X	X	X	X	X	X	X	X	X	
45.0		X	X	X	X	X	X	X	X	X	X	X	X	X	X	X	X	X	X	X	X	X	X	X	X	
90.0																										
120.0																										
150.0																										
180.0																										
-150.0																										
-120.0																										
-90.0																										
-60.0																										
-30.0		X	X	X	X	X	X	X	X	X	X	X	X	X	X	X	X	X	X	X	X	X	X	X	X	

Interior Solar Collector - Balance Study

Pitch		-180	-165	-150	-135	-120	-105	-90	-75	-60	-45	-30	-15	0	15	30	45	60	75	90	105	120	135	150	165	180
Yaw		X*	X*	X*	X*	X*	X*	X*	X*	X*	X*	X*	X*	X*	X*	X*	X*	X*	X*	X*	X*	X*	X*	X*	X*	
0.0		X*	X*	X*	X*	X*	X*	X*	X*	X*	X*	X*	X*	X*	X*	X*	X*	X*	X*	X*	X*	X*	X*	X*	X*	
30.0		X	X	X	X	X	X	X	X	X	X	X	X	X	X	X	X	X	X	X	X	X	X	X	X	
60.0																										
90.0																										
120.0																										
150.0																										
180.0																										
-150.0																										
-120.0																										
-90.0																										
-60.0																										
-30.0		X	X	X	X	X	X	X	X	X	X	X	X	X	X	X	X	X	X	X	X	X	X	X	X	

Note:

X* = With and Without Torque Tube.

Figure 2-12 (continued) Test matrix

Exterior Solar Collector - Pressure Study

Pitch		-180	-165	-150	-135	-120	-105	-90	-75	-60	-45	-30	-15	0	15	30	45	60	75	90	105	120	135	150	165	180
Yaw		X	X	X	X	X	X	X	X	X	X	X	X	X	X	X	X	X	X	X	X	X	X	X	X	
0.0	X	X	X	X	X	X	X	X	X	X	X	X	X	X	X	X	X	X	X	X	X	X	X	X	X	
30.0	X	X	X	X	X	X	X	X	X	X	X	X	X	X	X	X	X	X	X	X	X	X	X	X	X	
45.0	X	X	X	X	X	X	X	X	X	X	X	X	X	X	X	X	X	X	X	X	X	X	X	X	X	
90.0																										
120.0																										
150.0																										
180.0																										
-150.0																										
-120.0																										
-90.0																										
-60.0																										
-30.0	X	X	X	X	X	X	X	X	X	X	X	X	X	X	X	X	X	X	X	X	X	X	X	X	X	

Exterior Solar Collector with Fence - Pressure Study

Pitch		-180	-165	-150	-135	-120	-105	-90	-75	-60	-45	-30	-15	0	15	30	45	60	75	90	105	120	135	150	165	180
Yaw		X	X	X	X	X	X	X	X	X	X	X	X	X	X	X	X	X	X	X	X	X	X	X	X	
0.0	X	X	X	X	X	X	X	X	X	X	X	X	X	X	X	X	X	X	X	X	X	X	X	X	X	
30.0	X	X	X	X	X	X	X	X	X	X	X	X	X	X	X	X	X	X	X	X	X	X	X	X	X	
45.0	X	X	X	X	X	X	X	X	X	X	X	X	X	X	X	X	X	X	X	X	X	X	X	X	X	
90.0																										
120.0																										
150.0																										
180.0																										
-150.0																										
-120.0																										
-90.0																										
-60.0																										
-30.0	X	X	X	X	X	X	X	X	X	X	X	X	X	X	X	X	X	X	X	X	X	X	X	X	X	

Figure 2-12 (continued) Test matrix

Interior Solar Collector - Pressure Study

		Pitch																								
		Yaw																								
Pitch	Yaw	-180	-165	-150	-135	-120	-105	-90	-75	-60	-45	-30	-15	0	15	30	45	60	75	90	105	120	135	150	165	180
0.0	X*	X*	X*	X*	X*	X*	X*	X*	X*	X*	X*	X*	X*	X*	X*	X*	X*	X*	X*	X*	X*	X*	X*	X*	X*	
30.0	X*	X*	X*	X*	X*	X*	X*	X*	X*	X*	X*	X*	X*	X*	X*	X*	X*	X*	X*	X*	X*	X*	X*	X*	X*	
60.0																										
90.0																										
120.0																										
150.0																										
180.0																										
-150.0																										
-120.0																										
-90.0																										
-60.0																										
-30.0	X*	X*	X*	X*	X*	X*	X*	X*	X*	X*	X*	X*	X*	X*	X*	X*	X*	X*	X*	X*	X*	X*	X*	X*		

Note:

X* = With and Without Torque Tube.

Figure 2-12 (continued) Test matrix

Phase 4: Figure 2-13 illustrates the configurations of the solar collectors tested for the additional pitching moment tests. These test configurations had been investigated in the Phase 2 and 3 tests, and were repeated here for comparison purposes. The selection of the configurations was based largely on the test results from the earlier Phase that exhibited significant pitching moments. For all the indicated configurations, the tests were conducted for a full rotation of the pitch angle at intervals of 15 degrees. (Refer to Figure 2-10 and Figure 2-13 that show the test setup for Configuration C5 at a yaw angle of -30 degrees.)

The test configurations for the deep interior tests are shown in Figure 2-14. The pressure distribution over the collector concentrator was measured on the unit at the 5th, 10th, 15th and 20th rows from the upwind edge of the array field for the yaw angle of 0 degrees (Figure 2-14(a)). Two column positions, 4th and 8th from the open side edge, were also tested at this yaw angle. At a yaw angle of 30 degrees (Figure 2-14(b)), the row positions of 5th, 10th and 15th, and the column positions of 4th, 8th and 12th were tested. A limited set of pitch angles were of interest, including -15, -60, 0, 75 and 105 degrees, at which the Phase 3 wind-tunnel study showed relatively large integrated wind loads. Note that Configurations I2 and I3 are nearly identical. To optimize the test program, Configuration I3 was eliminated from the test plan. In this report, the test results obtained for Configuration I2 also substitute for those referring to Configuration I3 for convenience. A photograph of one of the test setups, Configuration I8, is given in Figure 2-15.

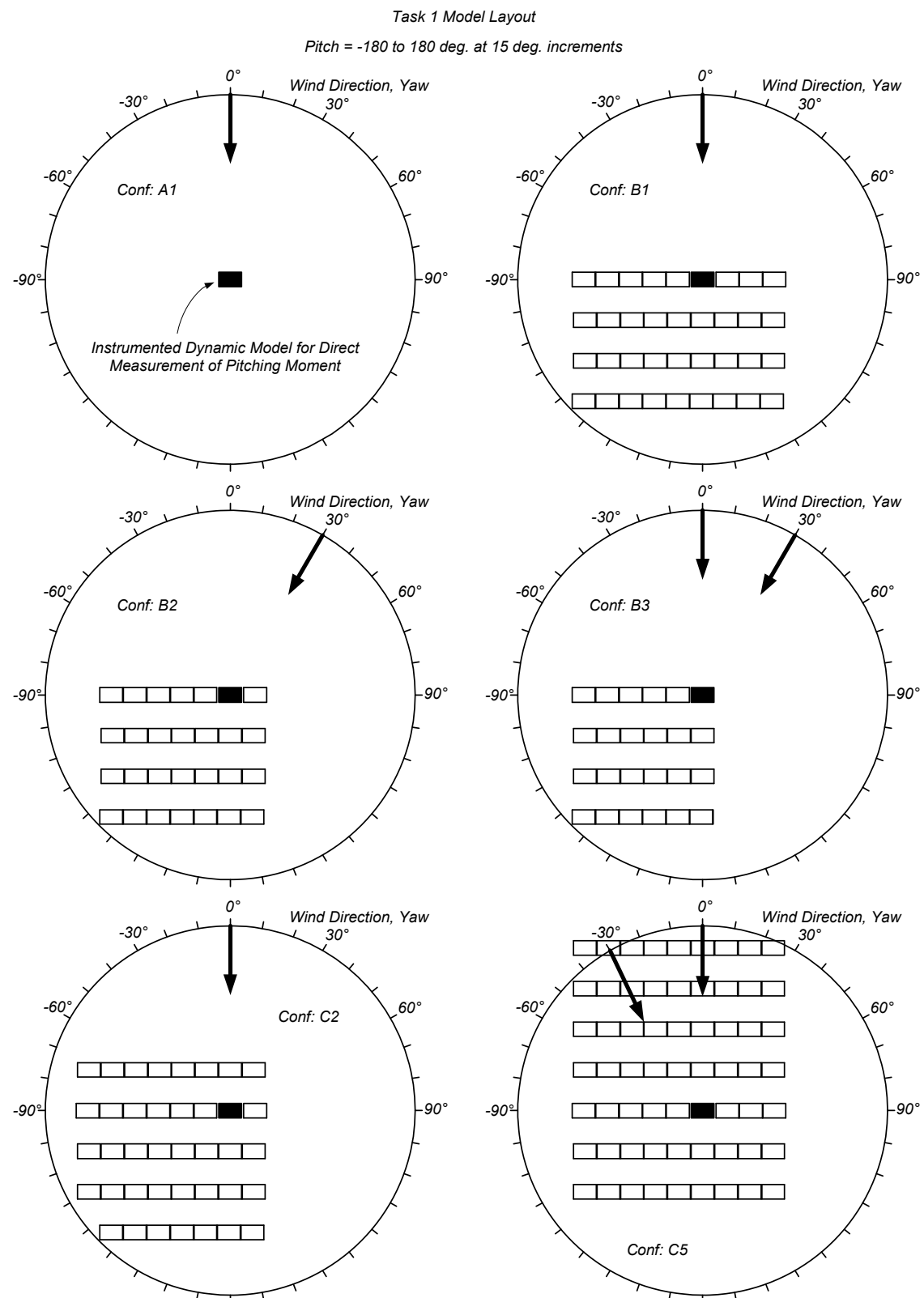


Figure 2-13 Test Configurations for Phase 4

Task 2 Model Layout for Yaw = 0 deg.

Pitch = -15, -60, 0, 75, and 105 deg.

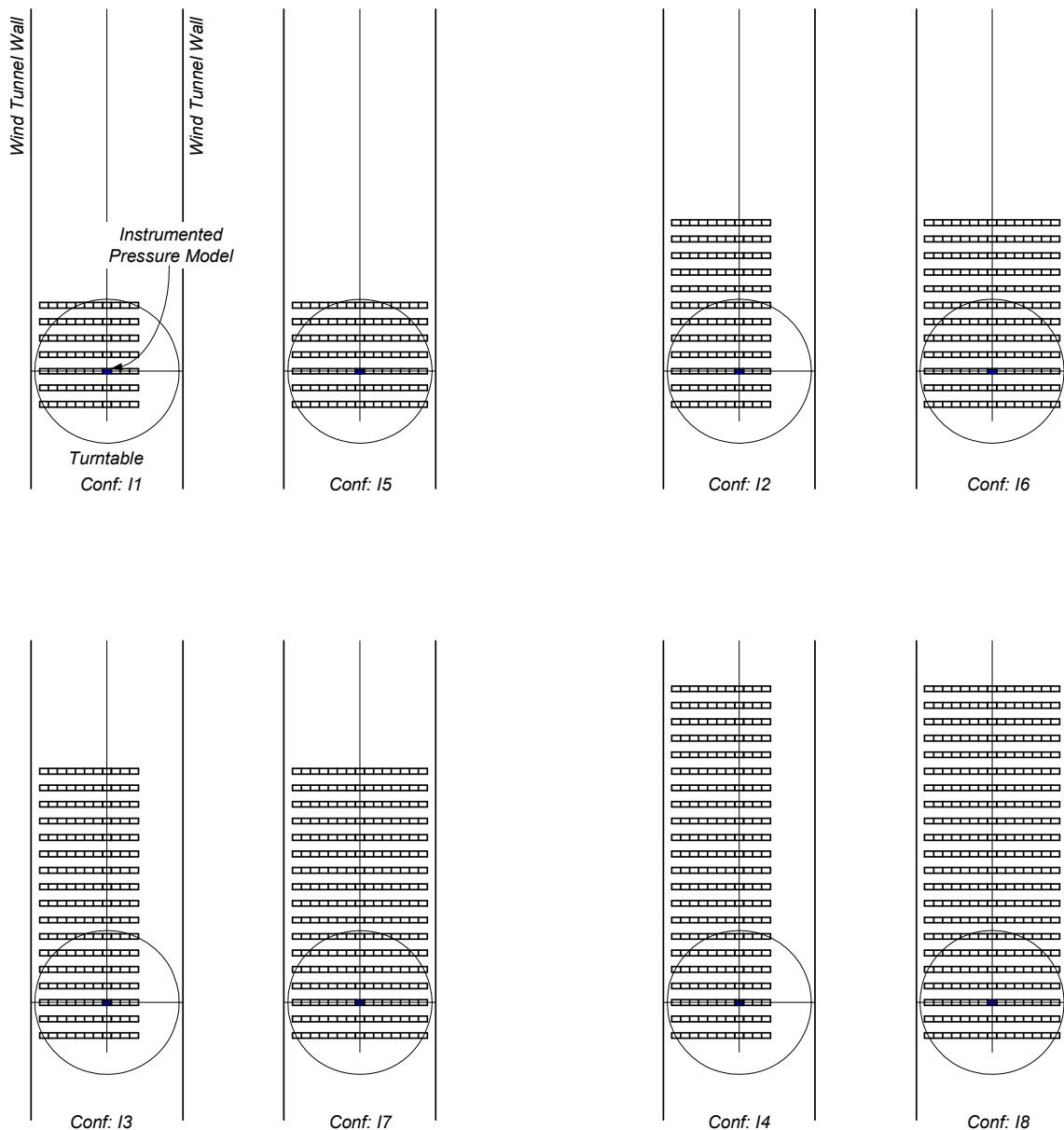
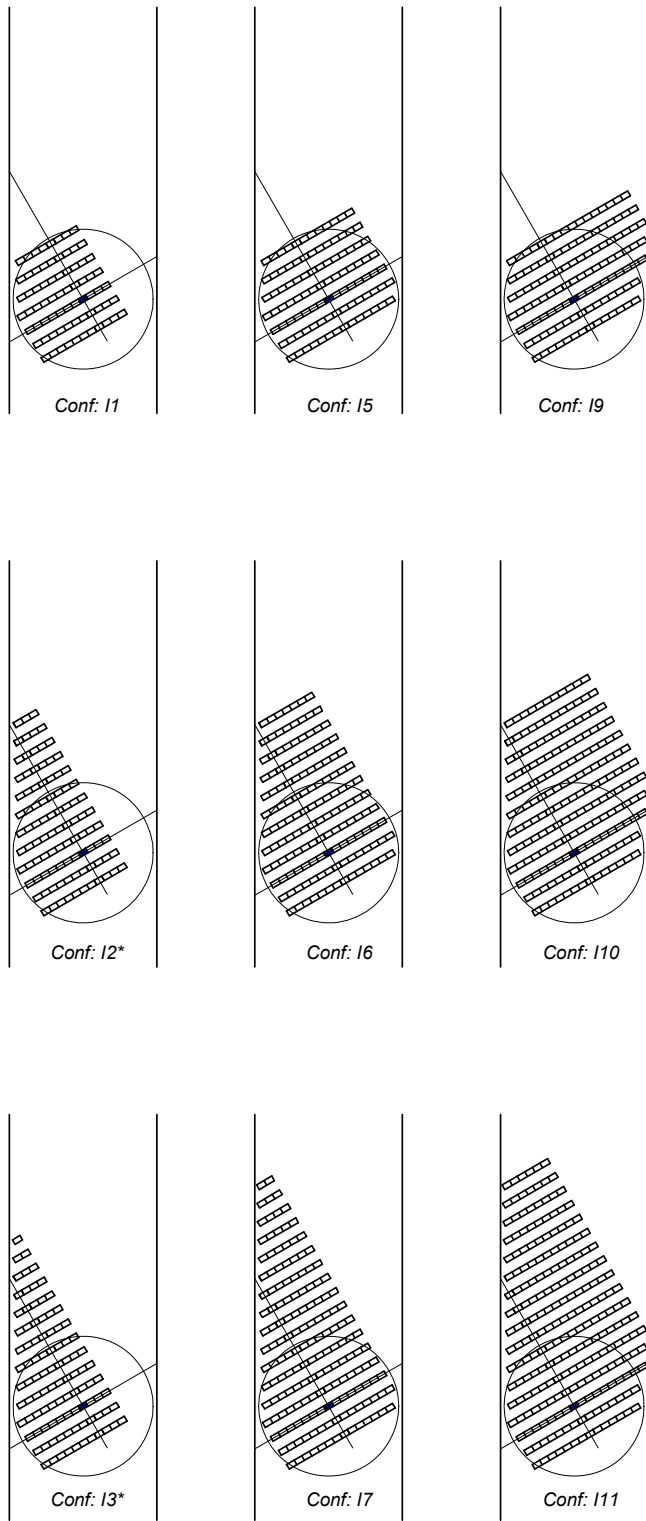


Figure 2-14 Test Configurations for Deep Interior Tests, (a) Yaw = 0 degrees

Task 2 Model Layout for Yaw = 30 deg.

Pitch = -15, -60, 0, 75, and 105 deg.



Note: Configurations I2 and I3 are nearly identical. The test results for Conf. I2 substitute Conf. I3.

Figure 2-14 Test Configurations for Deep Interior Tests, (b) Yaw = 30 degrees



Figure 2-15 Photograph of Test Setup for Configuration I8

2.5 Test Procedures

Each test series for a chosen collector configuration involved sequential adjustment of the yaw and pitch angles. The yaw angle was set simply by rotating the turntable on which the wind-tunnel models were mounted. For the pitch angle adjustment, a set of jigs were made so that the angle could be set consistently by aligning the top and bottom edges of the collector against the jig.

Once these angles were set, the data acquisition proceeded as follows. First, with the wind tunnel turned off, the outputs from all the transducer channels (load transducers for the balance tests and the pressure transducers for the pressure tests) were recorded as zero measurement. The wind tunnel was then turned on while monitoring the mean approach wind speed at the height of the collector pivot. When the mean wind speed stabilized at the nominal test speed of approximately 20-25 feet per second (fps), the data acquisition initiated. The transducer outputs were measured and the zero readings were subtracted to obtain net response level in time series for permanent storage in a disk file.

For each test, the data collection process was repeated several times to minimize the statistical errors that occur when measuring random signals. The rate of data sampling differed between the balance and pressure measurement because of the different frequency bandwidths of interest for a particular measurement technique. The balance data were measured at a rate of 250 samples per second for about 8-16 seconds with 4-8 repetitions, depending on the particular test, and the pressure data at a rate of 500 samples per second for 16 seconds with 4 repetitions. The total duration of the data samples was 64 seconds for both balance and pressure measurements. Note that the test results presented in this report were obtained as ensemble averages over all the repetitions performed for a run.

2.6 Accuracy and Uncertainty of Test Results

Complete analysis of accuracy and uncertainty associated with load measurements performed with a wind tunnel is no trivial matter. It would require, in general, sophisticated statistical investigation on random processes as well as characterization of instruments used. Although an extensive effort might be prudent in many engineering practices, this section limits the analysis to two readily identifiable sources of uncertainties: (1) the statistical variation of the measured mean loads and (2) the performance of the instruments.

Because fluctuations of wind loads are random in nature, determination of their true mean and root mean square (standard deviation) theoretically requires infinitely long measurement duration. Although this is not possible, acceptable estimates of these quantities can be obtained by cumulating the statistical results over several repeated measurements of reasonable length. As an example, Figure 2-16a illustrates the variation of the mean loads measured by the force balance on an isolated solar collector over repeated tests. The data were taken for 16 extended measurements (compared to the nominal 8), and the overall means were assumed to represent the true values. All the load components asymptotically converge to the assumed true means as the number of measurements increases. Figure 2-16b shows a similar plot for a typical pressure measurement in a wind tunnel.

The load measurement instrument consisted of the force and pressure transducers, signal conditioner, and analog-to-digital converter. This equipment can be a source of measurement uncertainty because of, for example, non-linear response, instability, and limited resolution. A careful calibration of the instrument revealed the response characteristics and the possible worst error in the measured loads.

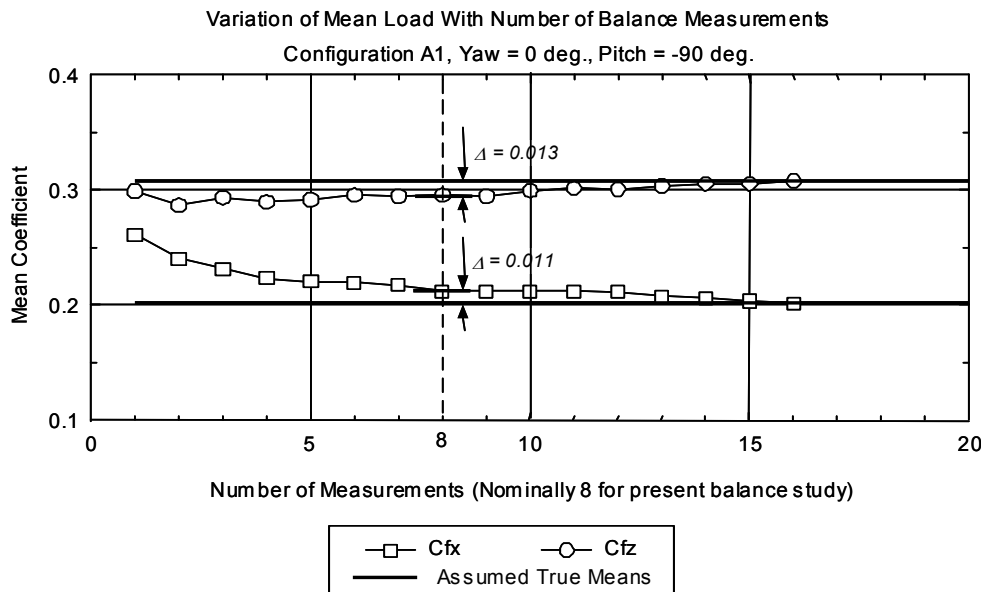


Figure 2-16a Typical statistical variation of mean load measurement, balance study²

² Figure 2-16a,b show how long the measurement should be to obtain a statistically accurate mean estimate. To do this, multiple measurements were repeated, each measurement with the equal sample duration, and the means were computed from individual measurements. What is plotted in these Figures is the cumulative means with the increasing number of sample blocks. That is, the first (left-most) point represents the mean computed from the first sample block only. The

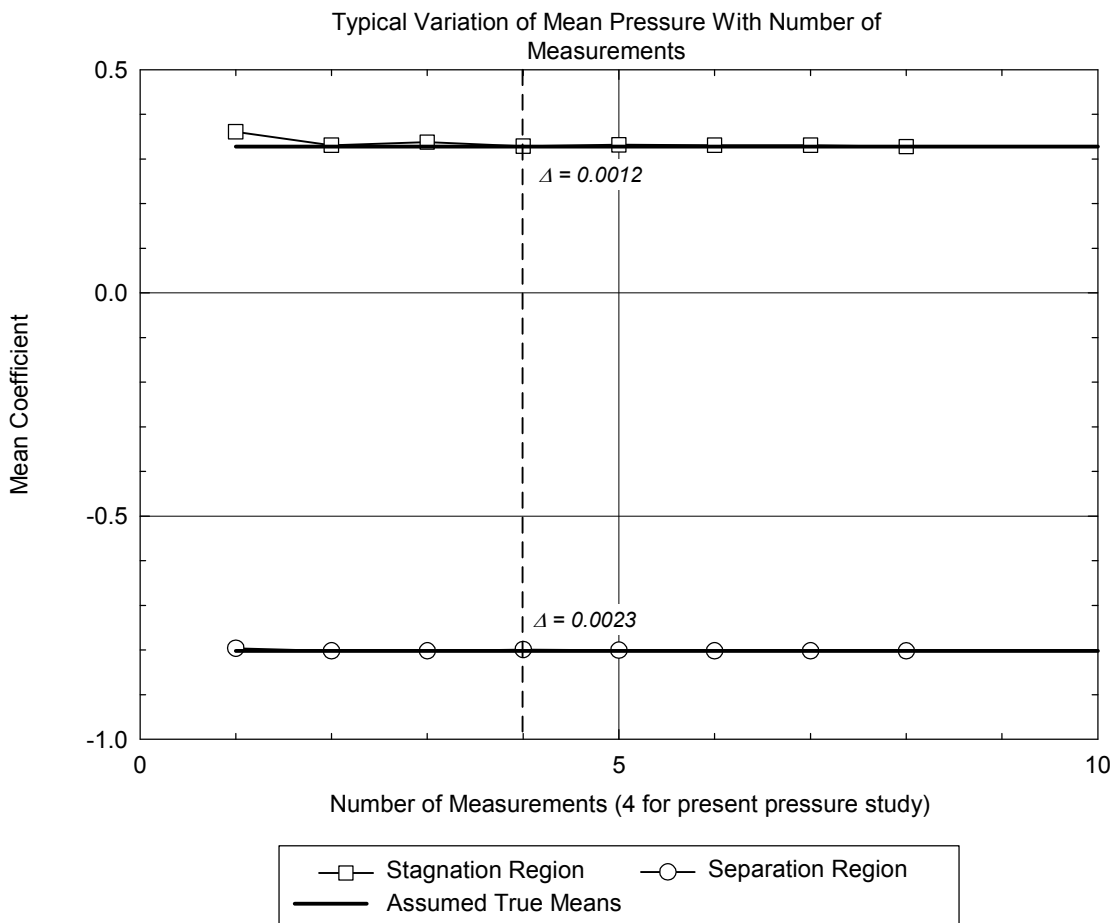


Figure 2-16b Typical statistical variation of mean load measurement, pressure study

Table 2-2 summarizes the uncertainties in the mean load measurement caused by the above two sources and the combined effect. Note that the total errors were simply obtained as an algebraic summation of the errors due to these two sources of uncertainty disregarding any statistical

second point was computed as an average of the means from the first and second sample blocks, effectively increasing the total sample duration. The third point is the average of the first three sample blocks, and so forth. Obviously, the mean from the single sample block alone (the first point in the graph) has the largest uncertainty and deviates from the true mean the largest. Its effect remains in the succeeding points, although should be gradually diminishing, because the first mean is repeatedly used to compute the overall cumulative means. This is why the plot tends to approach the true mean from its either side dictated by the inaccuracy of the very first mean estimate. To be more precise, the y-axis of the graph should have been labeled "Cumulative Mean Coefficient."

Alternatively, we could have taken several measurements, each with different sample durations. If you plot the individual means from these measurements as a function of the sample duration, you would see that the mean fluctuates about the true mean with decreasing variation.

correlation; they reflect the worst case. In average, it is reasonable to assume that the actual level of uncertainty would be somewhat smaller than what is indicated. If these possible errors are directly related to the largest measured mean overall loads, the uncertainties can be estimated as 3% for the force and moment components for the balance study. For the pressure study, the uncertainty of about 6% would result for all the load components. The instrument uncertainty (denoted as Source 2) shown in Table 2-2 was estimated as a combination of the worst cases that could occur for each of the contributing load transducers, resulting in the higher level of uncertainty.

Table 2-2 Estimated Uncertainty Associated with Mean Load Measurement

	Overall Load Component			Pressure Component				
	f_x	f_z	m_y	p^+	p^-	f_x	f_z	m_y
Due to Source (1)	0.011	0.013	0.0042	0.0012	0.0023	0.0025	0.0035	0.00052
Due to Source (2)	0.0053 lbs.	0.0094 lbs.	0.0061 lb-in.	0.044 psf	0.044 psf	0.013 lbs.	0.018 lbs.	0.012 lb-in.
Equivalent load coef.	0.050	0.090	0.013	0.087	0.087	0.12	0.17	0.026
Total	0.061	0.103	0.017	0.088	0.089	0.13	0.18	0.026

Source (1) Statistical variation of random signal.

Source (2) Characteristics of instrumentation. The worst possible errors observed during static calibration are indicated.

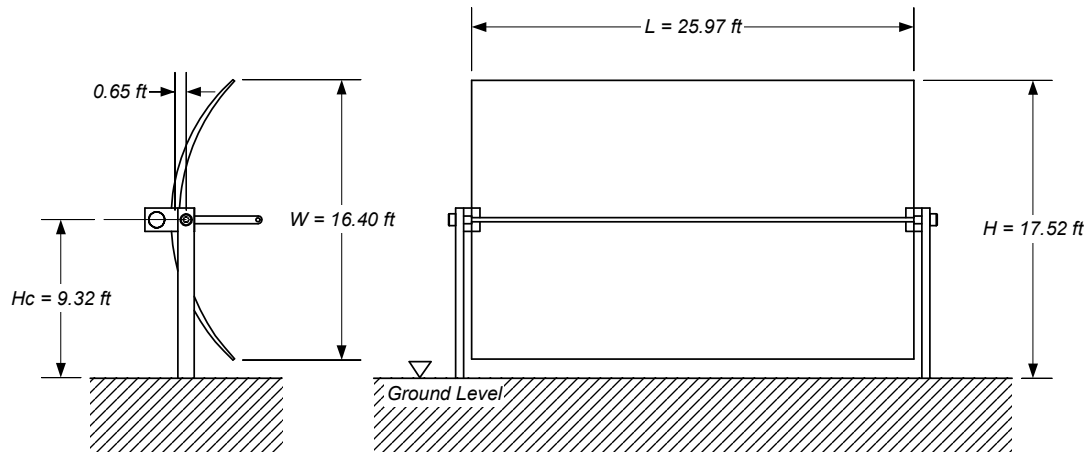
3. ANALYSIS METHODS

The chief objective of the present wind-tunnel study was to determine wind loads on parabolic trough solar collectors that would provide guidelines for design. The wind load effects of interest for the present study included the overall lateral force, vertical force, pitching moment about the collector pivot axis, and pressure distributions over the concentrator surface. It is common practice to present the wind loads measured in a wind tunnel in the form of load coefficients directly applicable to full-scale structures through use of consistent scaling parameters. This section describes the definition of the relevant test parameters and basic techniques involved in the data analysis.

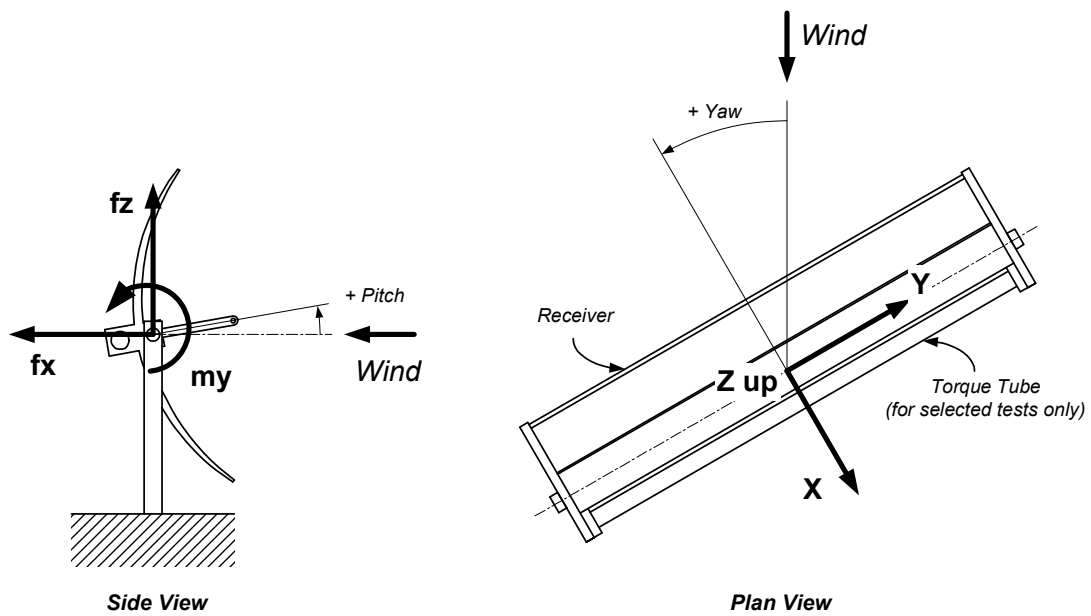
3.1 Definition of Test Parameters

3.1.1 Orientation of Solar Collector

Parabolic trough solar collectors are typically designed to follow the apparent motion of the sun by rotating about a one dimensional axis throughout the day. Because of this, wind loads exerted on the drive mechanism vary depending on the tilt angle of the collector, herein called the pitch angle. In addition, the incident angle of the approach wind relative to the span of the solar collector, or the yaw angle, causes the wind loads to vary. Thus, the orientation of the solar collector, defined by the pitch and yaw angles is an important factor for evaluating the aerodynamic performance and structural design criteria of the collector. Figure 3-1 schematically shows the definition of the pitch and yaw angles established for the current wind-tunnel study, as well as that of the overall loads and several characteristic dimensions of the solar collector. It should be noted that the two modes of operation for the solar collectors can be conveniently distinguished by the sign of the pitch angle. That is, the positive and negative pitch angles imply the normal operation and stow modes, respectively.



Key Dimensions



Definition of Coordinate System

Figure 3-1 Definition of coordinate system and key dimensions

3.1.2 Load Coefficients

Wind load effects are characterized in terms of non-dimensional coefficients. The definitions of the load coefficients are:

Horizontal Force, f_x

$$Cf_x = \frac{f_x}{qLW} \quad (3.1)$$

Vertical Force, f_z

$$Cf_z = \frac{f_z}{qLW} \quad (3.2)$$

Pitching Moment, m_y

$$Cm_y = \frac{m_y}{qLW^2} \quad (3.3)$$

where f_x , f_z , and m_y are the aerodynamic loads (Figure 3-1), L is the span-wise length, and W is the aperture width of the collector. The quantity, q , is the mean reference dynamic pressure measured at the pivot height of the solar collector, H_c , as given by

$$q = \frac{1}{2} \rho U^2 \quad (3.4)$$

Here U is the mean wind speed at the pivot height, and ρ is the density of air. Similarly, the pressure coefficient is expressed by

$$Cp = \frac{p}{q} \quad (3.5)$$

where p is the local pressure relative to the undisturbed ambient static pressure. Because the collector is essentially a curved thin plate composed of a number of reflective concentrator panels, the net pressure between the opposing surfaces is of significance for the design load of the collector structure. The net pressure, or the differential pressure coefficient, Cdp , is defined herein as

$$Cdp = \frac{p_f - p_b}{q} \quad (3.6)$$

where p_f and p_b are the pressures on the front (reflective) side and the back side, respectively.

3.1.3 Consideration for Load Cases for Structural Strength Design

In general, parabolic trough solar collectors are either tracking the sun (normal operation) or assume a stationary downward-facing attitude called the “stow” position (at night or during cloudy or very windy periods). During sunny periods with moderate and low winds, the solar collectors are in the normal operation mode, with the parabolic reflector rotated toward the sun. Wind loads on the solar collectors during normal operation are a concern because deformation of the parabolic trough reflector surface can cause a loss of efficiency. During strong winds, where the structural strength might be a concern, the solar collectors are typically rotated to the “stow” mode with the concentrators facing down to limit wind loads and to prevent the reflective surface from being damaged. Sufficient data were obtained in the wind-tunnel testing to provide load data for structural analysis in both operating modes.

Within a field of solar collectors, the largest wind loads experienced by an individual collector module will vary depending on its position and the presence of a protective barrier. Application of the design loads appropriate for the exterior collector modules throughout the entire field would result in over-design for most of the interior units, which in fact constitute the majority of the field collector modules. On the other hand, use of the interior design loads on the exterior collector modules can expose those modules to higher risk of structural failure. To provide

practical design criteria, different design load cases were determined separately for the exterior collector modules with and without a protective fence, various locations of interior modules, and in particular the collector module denoted as Configuration C5 (Figure 2-13), which was considered to be most representative for a large array field as a whole.

The load cases were derived as the loading condition that would maximize the individual overall load components in either the positive or negative direction. Each load case specified the peak load for one component as primary and the simultaneous point-in-time load values for the other two as extracted from the integrated pressure or balance time series data. For the structural strength design, applying the combination of all three load components is appropriate.

3.2 Particular Treatment of Pressure Data

While the balance tests were suited for measurement of overall loads on the solar collector, determination of the detailed load distribution required the pressure tests. The tests were performed to measure instantaneous distribution of local pressures over the collector module at a total of 60 locations. The results of the pressure tests were intended to allow finite element analysis, wherein wind forces imparted to the surfaces of a parabolic trough concentrator can be used to determine the developed stresses and deformations of the concentrator (e.g., support structure, parabolic-shaped mirrors, etc.). To serve this need, a number of unique pressure distributions were determined based on several relevant load conditions. The analysis method for obtaining these pressure distributions is described in Section 3.2.2. In addition, the overall loads were computed by integrating the distribution of the measured local pressures for comparison with the directly measured loads by the balance technique. The procedure is explained in this section.

3.2.1 Integration of Distributed Local Pressures

Distribution of point pressures and differential pressures can be integrated over the parabolic concentrator surface to numerically determine the total loads on the parabolic trough solar collector. The resulting loads should approximate reasonably those measured directly using the force balance. Some discrepancy can be expected because the measured pressure distribution is discrete and the integration is, therefore, piecewise, whereas the total loads measured by the balance are, in principle, the result of true integration of continuously distributed pressures. In addition, the balance loads include the contribution due to not only the concentrator module itself, but also other secondary structural elements such as the pylon supports and the receiver. Nevertheless, the comparison of the pressure and balance total loads is useful in confirming the validity and consistency of the test results in general and is discussed in Section 4. Here we explain the technique used in the current study to determine the integral loads from the pressure distribution data.

Because the pressure distribution measured on the pressure model is discrete, the integration is actually a weighted summation of point pressures:

$$Q = \sum_{i=1}^N w_i p_i. \quad (3.14)$$

Here Q is the load effect of interest, p_i is the surface pressure (or differential pressure at the tap location i), and N is the number of pressure taps. The quantity w_i is the weight factor assigned at the pressure tap location i . If, for example, the load effect to be obtained is force, the weight factor typically represents the tributary area associated with the pressure tap. The weight factors for calculation of the forces and pitching moment for all the pitch angles tested in the study are tabulated in a spreadsheet file on the CD-ROM provided to NREL as backup to this report (also see Appendix E).

Figure 3-2 shows the tributary areas defined for the solar collector, as well as the differential pressure taps with the identification numbers. The boundaries indicated by dashed lines were established to divide the distance between two adjacent pressure taps in half. The choice of the tributary areas is somewhat arbitrary, as long as each of these areas is exclusively assigned to a particular tap, and the individual tributary areas collectively account for the entire exposed area exerting the wind load. The pressure is usually assumed to be uniform within the tributary area. For calculations of the horizontal and vertical forces, the effective tributary areas projected on the vertical and horizontal planes, respectively, were computed for different pitch angles, taking into account the curvature of the concentrator. This was necessary to resolve the pressure load acting perpendicular to the concentrator surface into the respective force components. The resulting effective tributary areas were the weight factors that appear in Equation 3.14. For the pitching moment, the weight factors used were a combination of the tributary area and the effective distance about the axis of rotation.

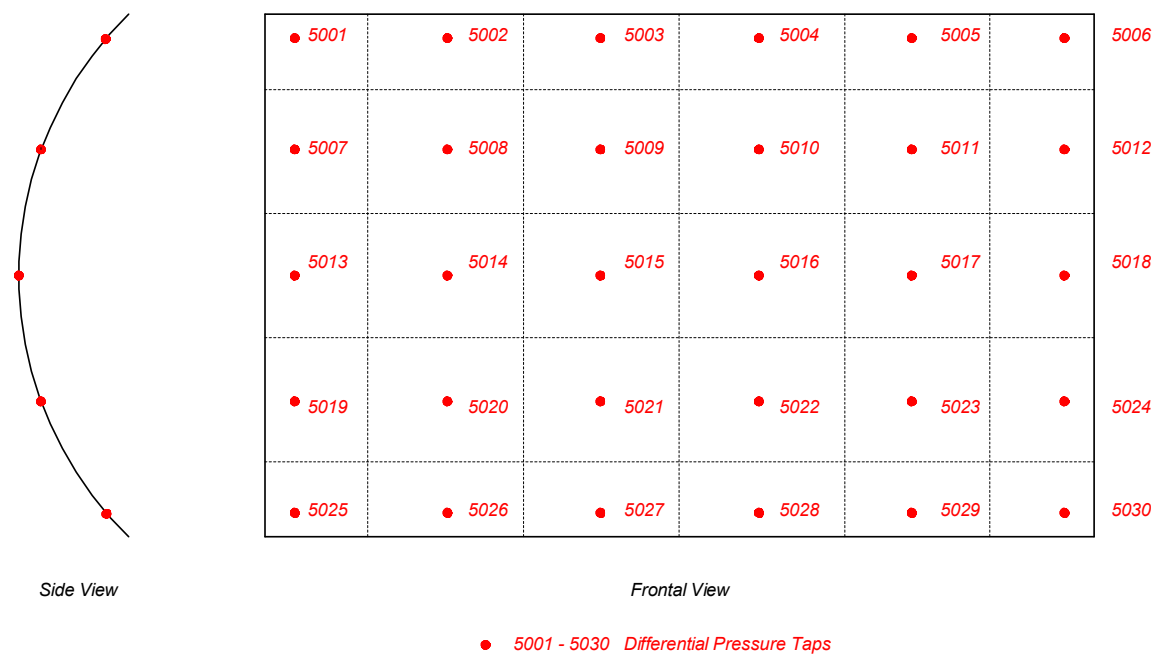


Figure 3-2 Tributary areas assigned for differential pressure taps

3.2.2 Instantaneous Pressure Distributions

Simultaneous measurement of the pressure at all the tap locations permits realization of pressure distributions at any given instant in time. In this wind-tunnel study, several conditions relevant to structural design were identified in order to extract specific sets of pressure distributions from the time series data stored in computer disk files. The extracted pressure distribution can be regarded as a *snapshot* of pressure pattern occurring when a specified condition is met. One of the conditions for the snapshot analysis was the occurrence of the peak local differential pressure at any tap location. In this case, the time series of the differential pressures were computed for each tap location shown in Figure 3-2, and the instantaneous pressure distribution was recorded when the largest local differential pressure occurred regardless of the tap location. The other conditions were associated with the occurrence of the integrated loads, described in the preceding section, exceeding a specified level, for example, the 80th percentile from minimum to maximum peaks.

A number of snapshot pressure distributions were taken from different test configurations, and some of the results are presented in sections 4.8.2 and 4.8.3.

3.2.3 Interpolation of Point Pressures

In order to apply the measured differential pressure distribution to the individual reflector panels on the solar collector, spatial interpolation of these pressures may be necessary. This is because the pressure tap layout on the wind-tunnel model does not necessarily coincide with that of the reflector panels of the actual solar collector. This section provides a simple technique for interpolating point pressures by a superposition of measured pressures in the vicinity of the desired application point on the reflector panel. That is,

$$p_i = \sum_{j=1}^m \psi_j p_j, \quad (3.15)$$

$$\sum_{j=1}^n \psi_j = 1. \quad (3.16)$$

In this case, p_j is the pressure measured at the pressure tap j , ψ_j is the influence factor associated with the pressure tap, and m is the number of pressure taps contributing to the reflector panel. Selection of the influence factors ψ_j can be based on a common technique used in the finite element analysis for obtaining an interior solution within a two-dimensional element. To illustrate this, Figure 3-3 shows a case where the nodal point of the reflector panel is surrounded by four pressure taps.

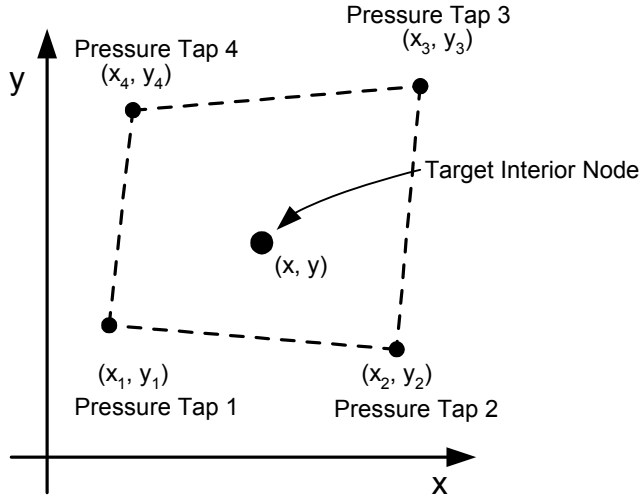


Figure 3-3 Interpolation of point pressures

In this example, the influence factors for each pressure tap location can be assumed to take the following form based on the Pascal's triangle:

$$\psi_j = a_j + b_j x + c_j y + d_j xy \quad (3.17)$$

in which a_j , b_j , c_j , and d_j are the constants to be determined. The x and y are the coordinates of the point at which the interpolated pressure is determined. For the solar collector, these

coordinates are measured over the curved concentrator surface. Consider, for now, the influence factor for the first pressure tap, so that $j = 1$. The above equation becomes

$$\psi_1(x, y) = a_1 + b_1x + c_1y + d_1xy. \quad (3.18)$$

By imposing the following boundary conditions

$$\psi_1(x_1, y_1) = 1, \text{ and } \psi_1(x_2, y_2) = \psi_1(x_3, y_3) = \psi_1(x_4, y_4) = 0, \quad (3.19)$$

a system of simultaneous equations are obtained. In a matrix form,

$$\begin{vmatrix} 1 & x_1 & y_1 & x_1y_1 \\ 1 & x_2 & y_2 & x_2y_2 \\ 1 & x_3 & y_3 & x_3y_3 \\ 1 & x_4 & y_4 & x_4y_4 \end{vmatrix} \begin{Bmatrix} a_1 \\ b_1 \\ c_1 \\ d_1 \end{Bmatrix} = \begin{Bmatrix} 1 \\ 0 \\ 0 \\ 0 \end{Bmatrix}. \quad (3.20)$$

By solving these equations for the constants a_1 , b_1 , c_1 , and d_1 , the influence factor for the first pressure tap is established as a function of arbitrary coordinates, x and y , as given in Equation 3.18. The actual numerical value of the influence factor is then calculated by evaluating Equation 3.18 at the concentrator nodal point with the obtained constants. The remaining influence factors can be determined similarly by repeating the above exercise for the other three pressure tap locations.

Note that the above influence factors are identical to the *shape*, or *interpolation function* derived for a linear quadrilateral element often used in the finite element analysis. Similarly, the influence factors for two contributing pressure taps and three contributing pressure taps are analogous to interpolation functions for line and triangular elements. The description and derivation of these interpolation functions can be found in the literature on the finite element methods, such as the reference by Huebner *et al.* (1995), and are omitted in this report.

As a practical example, consider a solar collector composed of twenty reflector panels of equal size (Figure 3-4). Using the technique explained above, Table 3-1 summarizes the influence factors by which the differential pressures are interpolated at the centroid of each reflector panel.

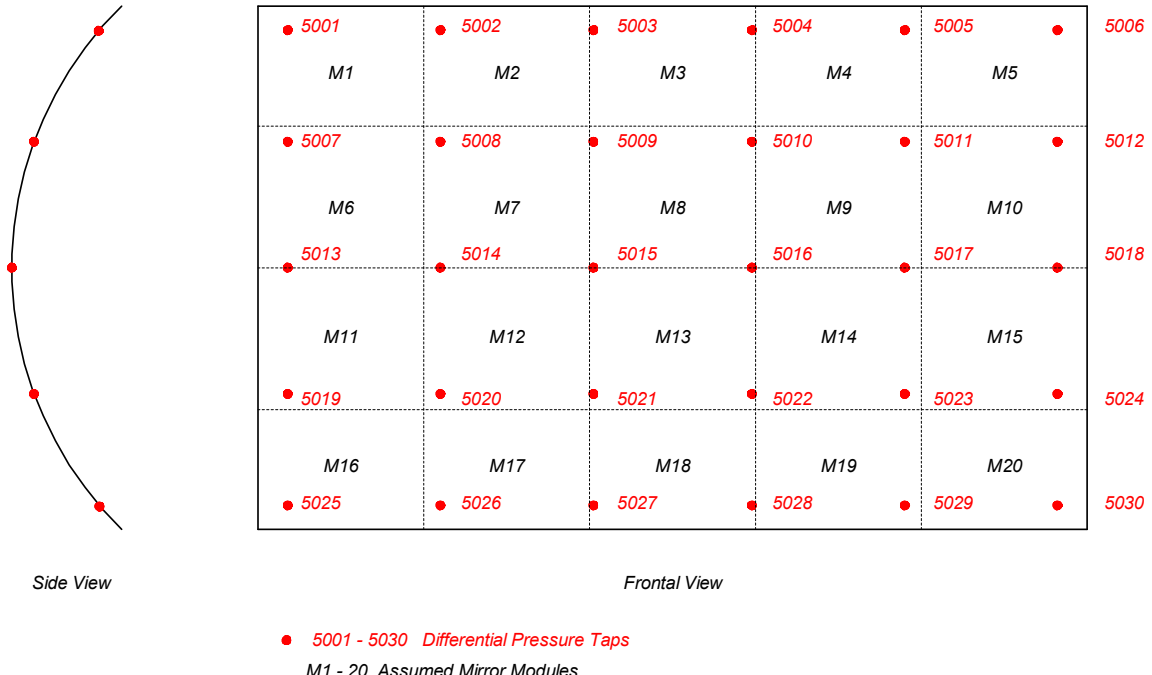


Figure 3-4 Example of reflector panel arrangement for interpolation of differential pressures

Table 3-1 Influence Factors for Interpolation of Differential Pressures

Tap	Mirror 1	Mirror 2	Mirror 3	Mirror 4	Mirror 5	Mirror 6	Mirror 7	Mirror 8	Mirror 9	Mirror 10
5001	0.4516	0.0000	0.0000	0.0000	0.0000	0.0000	0.0000	0.0000	0.0000	0.0000
5002	0.2403	0.3923	0.0000	0.0000	0.0000	0.0000	0.0000	0.0000	0.0000	0.0000
5003	0.0000	0.2996	0.3446	0.0000	0.0000	0.0000	0.0000	0.0000	0.0000	0.0000
5004	0.0000	0.0000	0.3474	0.2990	0.0000	0.0000	0.0000	0.0000	0.0000	0.0000
5005	0.0000	0.0000	0.0000	0.3929	0.2403	0.0000	0.0000	0.0000	0.0000	0.0000
5006	0.0000	0.0000	0.0000	0.0000	0.4516	0.0000	0.0000	0.0000	0.0000	0.0000
5007	0.2011	0.0000	0.0000	0.0000	0.0000	0.3709	0.0000	0.0000	0.0000	0.0000
5008	0.1070	0.1747	0.0000	0.0000	0.0000	0.1973	0.3222	0.0000	0.0000	0.0000
5009	0.0000	0.1334	0.1534	0.0000	0.0000	0.0000	0.2461	0.2830	0.0000	0.0000
5010	0.0000	0.0000	0.1547	0.1331	0.0000	0.0000	0.0000	0.2853	0.2456	0.0000
5011	0.0000	0.0000	0.0000	0.1749	0.1070	0.0000	0.0000	0.0000	0.3227	0.1973
5012	0.0000	0.0000	0.0000	0.0000	0.2011	0.0000	0.0000	0.0000	0.0000	0.3709
5013	0.0000	0.0000	0.0000	0.0000	0.0000	0.2818	0.0000	0.0000	0.0000	0.0000
5014	0.0000	0.0000	0.0000	0.0000	0.0000	0.1499	0.2448	0.0000	0.0000	0.0000
5015	0.0000	0.0000	0.0000	0.0000	0.0000	0.0000	0.1870	0.2150	0.0000	0.0000
5016	0.0000	0.0000	0.0000	0.0000	0.0000	0.0000	0.0000	0.2168	0.1866	0.0000
5017	0.0000	0.0000	0.0000	0.0000	0.0000	0.0000	0.0000	0.0000	0.2452	0.1499
5018	0.0000	0.0000	0.0000	0.0000	0.0000	0.0000	0.0000	0.0000	0.0000	0.2818
5019	0.0000	0.0000	0.0000	0.0000	0.0000	0.0000	0.0000	0.0000	0.0000	0.0000
5020	0.0000	0.0000	0.0000	0.0000	0.0000	0.0000	0.0000	0.0000	0.0000	0.0000
5021	0.0000	0.0000	0.0000	0.0000	0.0000	0.0000	0.0000	0.0000	0.0000	0.0000
5022	0.0000	0.0000	0.0000	0.0000	0.0000	0.0000	0.0000	0.0000	0.0000	0.0000
5023	0.0000	0.0000	0.0000	0.0000	0.0000	0.0000	0.0000	0.0000	0.0000	0.0000
5024	0.0000	0.0000	0.0000	0.0000	0.0000	0.0000	0.0000	0.0000	0.0000	0.0000
5025	0.0000	0.0000	0.0000	0.0000	0.0000	0.0000	0.0000	0.0000	0.0000	0.0000
5026	0.0000	0.0000	0.0000	0.0000	0.0000	0.0000	0.0000	0.0000	0.0000	0.0000
5027	0.0000	0.0000	0.0000	0.0000	0.0000	0.0000	0.0000	0.0000	0.0000	0.0000
5028	0.0000	0.0000	0.0000	0.0000	0.0000	0.0000	0.0000	0.0000	0.0000	0.0000
5029	0.0000	0.0000	0.0000	0.0000	0.0000	0.0000	0.0000	0.0000	0.0000	0.0000
5030	0.0000	0.0000	0.0000	0.0000	0.0000	0.0000	0.0000	0.0000	0.0000	0.0000

Tap	Mirror 11	Mirror 12	Mirror 13	Mirror 14	Mirror 15	Mirror 16	Mirror 17	Mirror 18	Mirror 19	Mirror 20
5001	0.0000	0.0000	0.0000	0.0000	0.0000	0.0000	0.0000	0.0000	0.0000	0.0000
5002	0.0000	0.0000	0.0000	0.0000	0.0000	0.0000	0.0000	0.0000	0.0000	0.0000
5003	0.0000	0.0000	0.0000	0.0000	0.0000	0.0000	0.0000	0.0000	0.0000	0.0000
5004	0.0000	0.0000	0.0000	0.0000	0.0000	0.0000	0.0000	0.0000	0.0000	0.0000
5005	0.0000	0.0000	0.0000	0.0000	0.0000	0.0000	0.0000	0.0000	0.0000	0.0000
5006	0.0000	0.0000	0.0000	0.0000	0.0000	0.0000	0.0000	0.0000	0.0000	0.0000
5007	0.0000	0.0000	0.0000	0.0000	0.0000	0.0000	0.0000	0.0000	0.0000	0.0000
5008	0.0000	0.0000	0.0000	0.0000	0.0000	0.0000	0.0000	0.0000	0.0000	0.0000
5009	0.0000	0.0000	0.0000	0.0000	0.0000	0.0000	0.0000	0.0000	0.0000	0.0000
5010	0.0000	0.0000	0.0000	0.0000	0.0000	0.0000	0.0000	0.0000	0.0000	0.0000
5011	0.0000	0.0000	0.0000	0.0000	0.0000	0.0000	0.0000	0.0000	0.0000	0.0000
5012	0.0000	0.0000	0.0000	0.0000	0.0000	0.0000	0.0000	0.0000	0.0000	0.0000
5013	0.2818	0.0000	0.0000	0.0000	0.0000	0.0000	0.0000	0.0000	0.0000	0.0000
5014	0.1499	0.2448	0.0000	0.0000	0.0000	0.0000	0.0000	0.0000	0.0000	0.0000
5015	0.0000	0.1870	0.2150	0.0000	0.0000	0.0000	0.0000	0.0000	0.0000	0.0000
5016	0.0000	0.0000	0.2168	0.1866	0.0000	0.0000	0.0000	0.0000	0.0000	0.0000
5017	0.0000	0.0000	0.0000	0.2452	0.1499	0.0000	0.0000	0.0000	0.0000	0.0000
5018	0.0000	0.0000	0.0000	0.0000	0.2818	0.0000	0.0000	0.0000	0.0000	0.0000
5019	0.3709	0.0000	0.0000	0.0000	0.0000	0.2011	0.0000	0.0000	0.0000	0.0000
5020	0.1973	0.3222	0.0000	0.0000	0.0000	0.1070	0.1747	0.0000	0.0000	0.0000
5021	0.0000	0.2461	0.2830	0.0000	0.0000	0.0000	0.1334	0.1534	0.0000	0.0000
5022	0.0000	0.0000	0.2853	0.2456	0.0000	0.0000	0.0000	0.1547	0.1331	0.0000
5023	0.0000	0.0000	0.0000	0.3227	0.1973	0.0000	0.0000	0.0000	0.1749	0.1070
5024	0.0000	0.0000	0.0000	0.0000	0.3709	0.0000	0.0000	0.0000	0.0000	0.2011
5025	0.0000	0.0000	0.0000	0.0000	0.0000	0.4516	0.0000	0.0000	0.0000	0.0000
5026	0.0000	0.0000	0.0000	0.0000	0.0000	0.2403	0.3923	0.0000	0.0000	0.0000
5027	0.0000	0.0000	0.0000	0.0000	0.0000	0.0000	0.2996	0.3446	0.0000	0.0000
5028	0.0000	0.0000	0.0000	0.0000	0.0000	0.0000	0.0000	0.3474	0.2990	0.0000
5029	0.0000	0.0000	0.0000	0.0000	0.0000	0.0000	0.0000	0.0000	0.3929	0.2403
5030	0.0000	0.0000	0.0000	0.0000	0.0000	0.0000	0.0000	0.0000	0.0000	0.4517

4. RESULTS AND DISCUSSION

Extensive wind-tunnel tests were conducted that involved measurements of overall loads on the solar collectors using a high-frequency force balance and determination of detailed pressure distributions on the collector concentrator. A number of test configurations were examined for different positions of the solar collector within a collector field for various combinations of yaw and pitch angles, as well as for a few cases with an isolated solar collector. Because of the continuous interest by Solarenix and CPP in creating a comprehensive database, the total number of test runs well exceeded that originally proposed. It is not the intent of this section to present all of the test results in detail, but rather to present a review of the most important findings. The force and moment coefficient results of the overall loads obtained from the balance measurements and by the integration of pressure distributions are tabulated in Appendix B for all the tests conducted. In addition, the time series data of the measured pressure distributions for all test configurations, described in Appendix E, have been recorded on a set of CD-ROMs that provide backup data to this report.

Significant test conditions and results on the integrated overall loads on the isolated and field solar collectors are presented in Sections 4.1 through 4.7 for a variety of test configurations. Sections 4.8 and 4.9 give the summary of the structural design loads and the detailed differential pressure distributions over the concentrator that can be used for the structural analysis of a parabolic trough collector. In addition, the use of these wind-tunnel test results for the structural design is demonstrated in Section 4.8. The turbulent boundary layer simulated in the wind tunnel is described in the next section.

4.1 Boundary Layer Simulation

One of the most important prerequisites for load measurements in a wind tunnel is modeling of an atmospheric boundary layer at the scale of the model. Several key characteristics of the boundary layer are described in detail in Appendix C. In general, the vertical profiles of mean wind speed and turbulence intensity are of particular significance for simulating wind loads. A representative size of turbulent eddies, commonly denoted as a turbulence integral scale, also plays a role depending on its relation to typical dimensions of a wind-tunnel model. The importance of exact boundary layer simulation, however, tends to diminish for a structure surrounded by significant objects that can dictate the local wind characteristics, such as a solar collector within a field consisting of many adjacent units.

Figure 4-1 shows the mean wind velocity and turbulence intensity profiles simulated for the current study. As seen, the modeled boundary layer profiles compare well with those suggested by the well-recognized literature for winds over an open country exposure. It should be noted that the designated model scale (1:45) was much larger than that for which the CPP wind tunnel was primarily designed (1:200 to 1:500). For this reason, a series of wind measurements were conducted before the load measurements to obtain the appropriate boundary layer flow. The integral scale of turbulence was also measured at the height of the collector pivot point and was equivalent to about 70 ft at full scale. The suggested empirical values for an open country boundary layer flow vary greatly, for example, 390 ft (Counihan 1975) and 150 ft (Engineering Science Data Unit [ESDU] 1975). Although the simulated turbulence length scale was smaller than those cited, it was considered acceptable because it is widely understood that the effect of the length scale is generally insignificant if it is larger than the typical structure size.

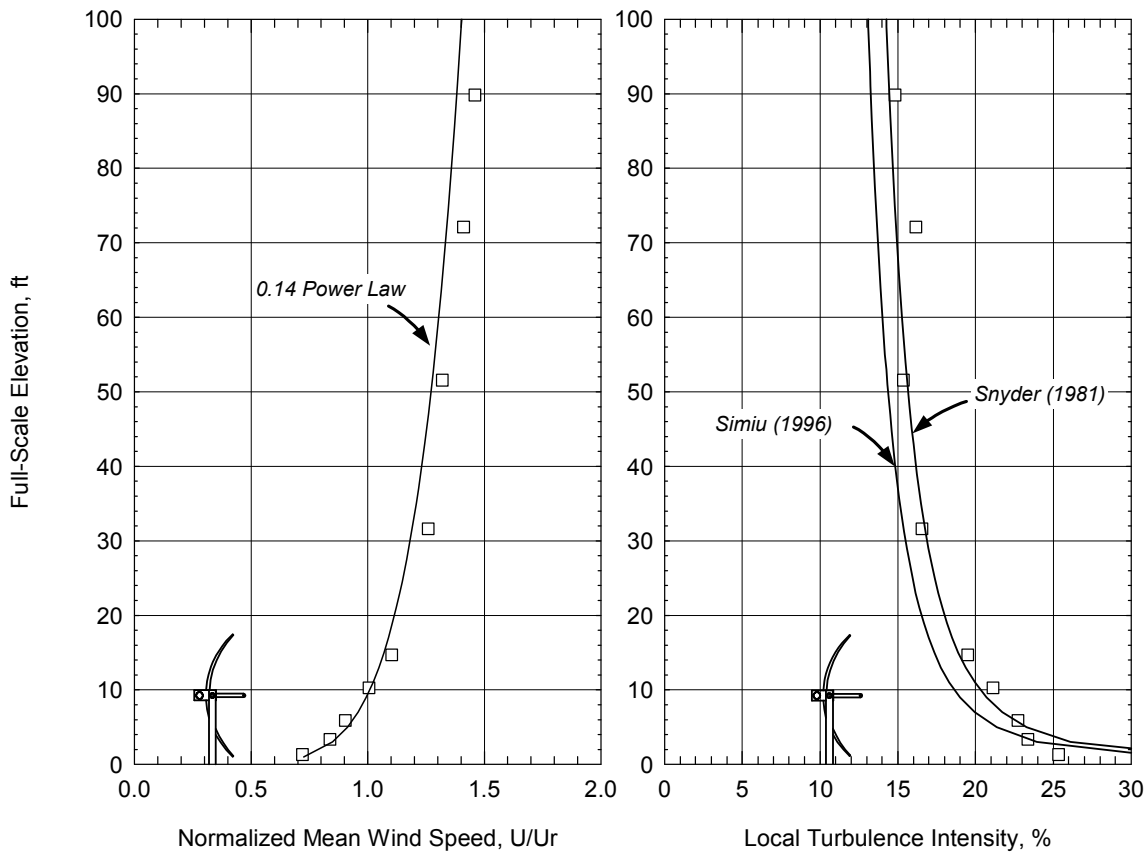


Figure 4-1 Turbulent boundary layer simulated in wind tunnel

Wind profile measurements were made using a single hot-film anemometer mounted on a computer-controlled vertical traverse and oriented horizontally transverse to the flow. The instrument was a TSI, Inc., constant-temperature anemometer (Model 1053b) with a 0.002-in.-diameter platinum-film sensing element.

As described in Section 3.1, the wind loads presented in this report have been normalized using the characteristic dimensions of the solar collector and the mean dynamic pressure of approach wind at the collector pivot height. In determining the dynamic pressure, a Pitot static tube was used in the wind tunnel. For most of the tests, the measurement was made directly at the pivot height of the collector at some point upwind of the array field. For the deep interior array tests in Phase 4, however, it was not possible to measure the dynamic pressure at the same location due to the significantly expanded size of the array field. Instead, the dynamic pressure was measured well above the collector field (3 ft at model scale and 135 ft at full scale) where the influence of the array was negligible, and the corresponding dynamic pressure at the collector pivot height was determined using the approach velocity profile for normalizing the wind loads on the collector.

4.2 Effects of Reynolds Number and Turbulence Intensity

One of the most essential considerations for load measurements in a wind tunnel is sensitivity of the load coefficients with the Reynolds Number. This is because wind tunnel tests cannot exactly simulate the high Reynolds typically encountered for full-scale structures. The mismatch is of

particular concern for streamlined or curved shape structures because the load coefficients can be highly dependent on the Reynolds Number. A series of preliminary tests were conducted to test the sensitivity of the wind load coefficients to the Reynolds Numbers.

Figure 4-2 shows the mean load coefficients at a pitch angle of -60 degrees with different Reynolds Numbers. The model Reynolds Numbers were calculated using the mean wind speed at the collector pivot height and the aperture width as the reference quantities. As the figure indicates, the load coefficients are nearly invariant of the Reynolds Number for the range tested.

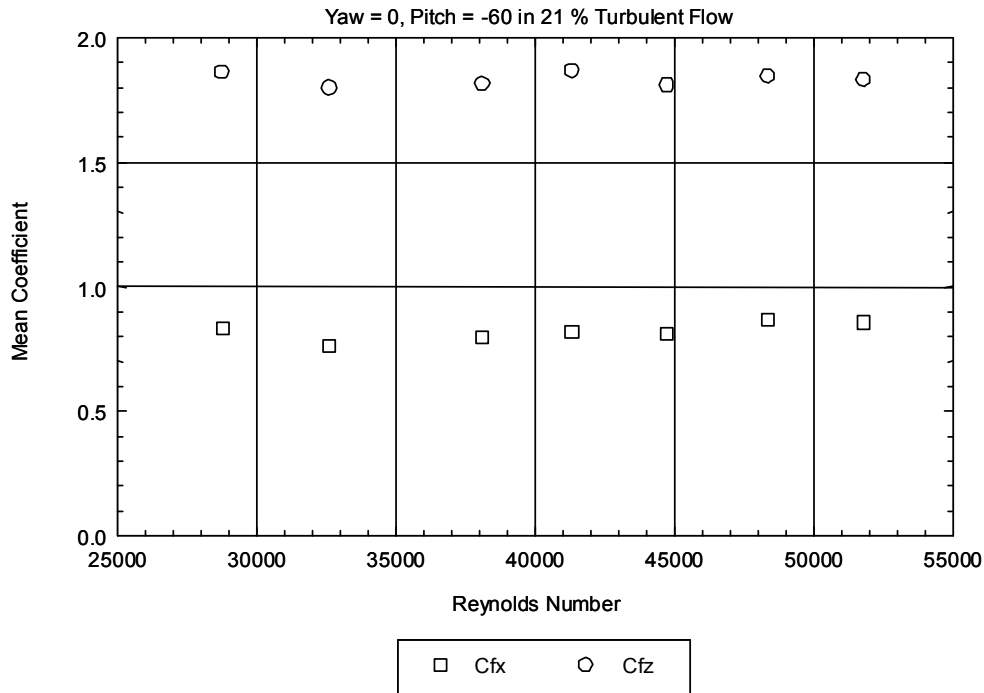


Figure 4-2 Sensitivity of load coefficients to Reynolds Number

Proper modeling of turbulence intensity is also important because it affects the fluctuations of the load, as well as the mean load to some extent. Figure 4-3 shows the effect of turbulence intensity on the mean horizontal load at a pitch angle of 0 degrees for a range of Reynolds Numbers. The load coefficients are similar for all turbulence intensities simulated when the Reynolds Number exceeds 46,000. In this particular test, the small variations at the lower Reynolds Numbers are probably due to poor signal-to-noise ratio or initial drift of the data acquisition instrument, rather than the aerodynamic behavior of the solar collector. The disparity of the load coefficients for different turbulence intensities is nominal, considering a slight variation of the velocity profiles to obtain the different turbulence levels over the height of the solar collector. The effect of the turbulence intensity is properly accounted for in the current study because the simulated turbulent boundary layer is representative of a terrain exposure encountered in open country exposure as intended. All data tests in this study, other than those shown in the above figures, were run at the typical Reynolds Number of 50,000 in the turbulent boundary layer with 21% turbulence intensity at the pivot height of 9.3 ft.

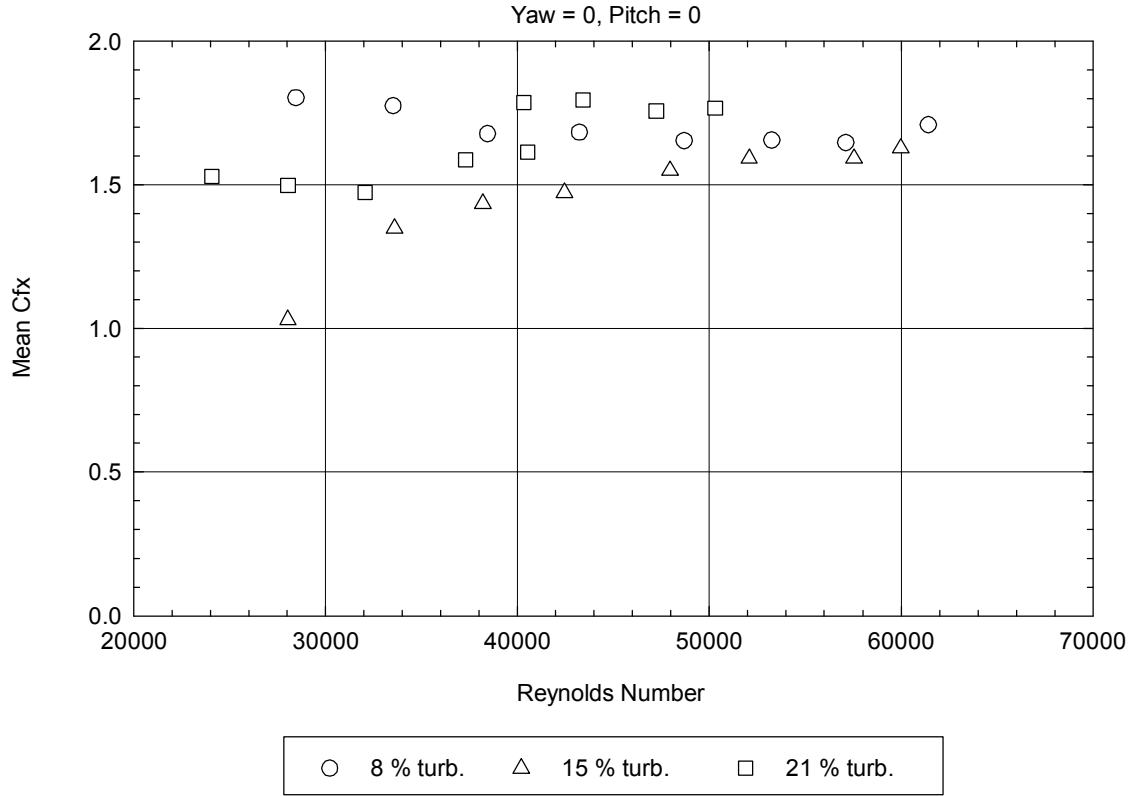


Figure 4-3 Effects of turbulence intensity on horizontal force

4.3 Isolated Solar Collector

4.3.1 Test Results

Drag and Lift Force Tests (Phase 1 data): In practice, the solar collector is used in an array consisting of a number of similar units, and the design wind loads should be determined for such a configuration. However, loads on an isolated collector are informative for characterizing the baseline performance. The isolated solar collector was tested with and without a torque tube (on the back side of the collector concentrator, discussed in Section 2.2.1 and Figure 3-1). Figure 4-4a shows the load coefficients for the isolated solar collector as a function of the pitch angle obtained by the balance measurement. The yaw angle was 0 degrees, and the approach wind is perpendicular to the major axis (y axis) of the solar collector. For each of the collector configurations, two curves are plotted in the figure. The lines represent the mean loads, and the symbols represent the peak maximum and minimum loads. Note that the test configuration relative to the wind were duplicated at pitch angles of +90 and -90 degrees as a check for repeatability. Refer to Section 3.1 for the definition of the overall load coefficients.

When the torque tube increases the load, for example, for C_fz at pitch = -105 degrees, the change in the peak loads is more notable than that of the mean loads. This implies that the torque tube can affect the load fluctuations considerably. The effect of the torque tube is different, however, for the collector in an array field, depending on the location in the field, as discussed in Sections 4.4 and 4.5. Similar plots are presented in Figure 4-4b for data obtained by the pressure model tests. The load coefficients were computed by integrating the measured point pressures over the

exposed area of the solar collector concentrator and by resolving the resulting load into the specified load components.

The effect of the torque tube is more apparent for the vertical force, Cf_z , than for the horizontal force, Cf_x . The torque tube does not necessarily worsen the wind loads, for example, the vertical force component for a range of pitch angles from 45 to 90 degrees is notably reduced with the torque tube. As far as the largest absolute load of the individual load components is concerned, the torque tube did not increase the load values.

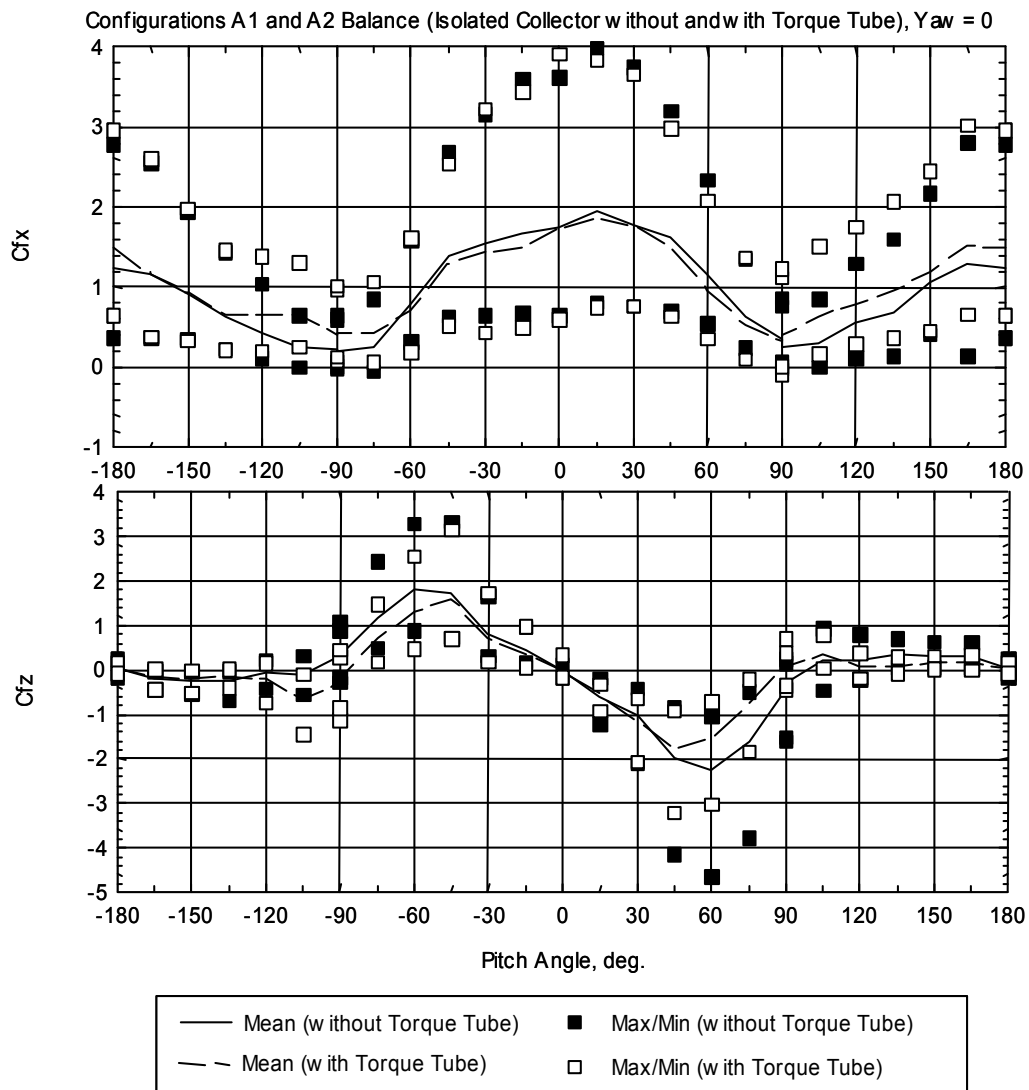


Figure 4-4a Loads on isolated solar collector with and without torque tube, balance study

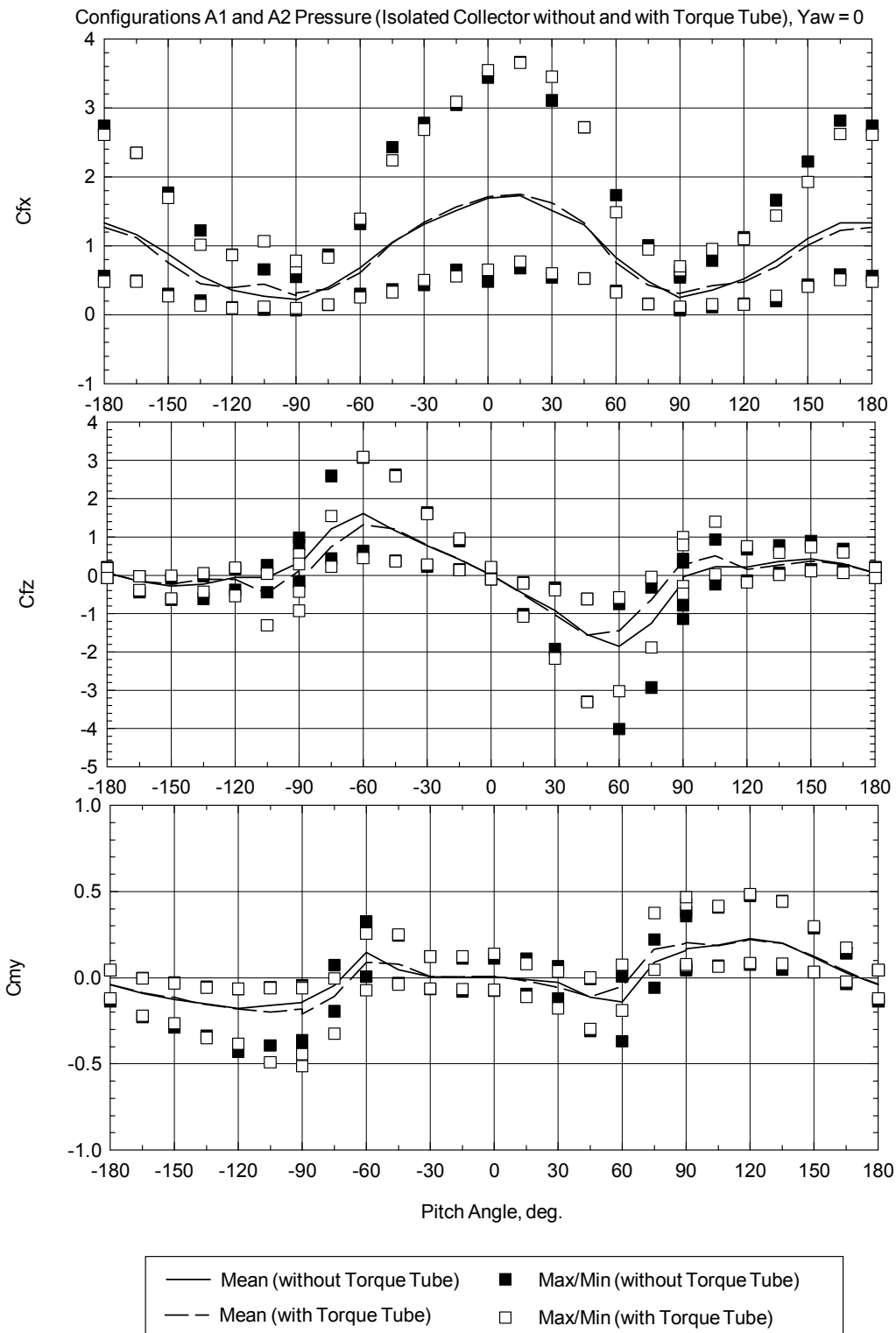


Figure 4-4b Loads on isolated solar collector with and without torque tube, pressure study

Figure 4-5a and Figure 4-5b compare the balance and pressure test results for the isolated solar collector tests. Note that in Figure 4-5a, the balance results from Phase 1 and 4 tests have been combined. To aid comparison between the force components and among the various test configurations shown later, the plots have been produced using consistent scales. Note also that in this and following figures, the balance results are consistently slightly larger than the pressure results. The reason has to do with the discrete nature of the pressure taps; adjustment factors for the pressure results are derived in Section 4-9.

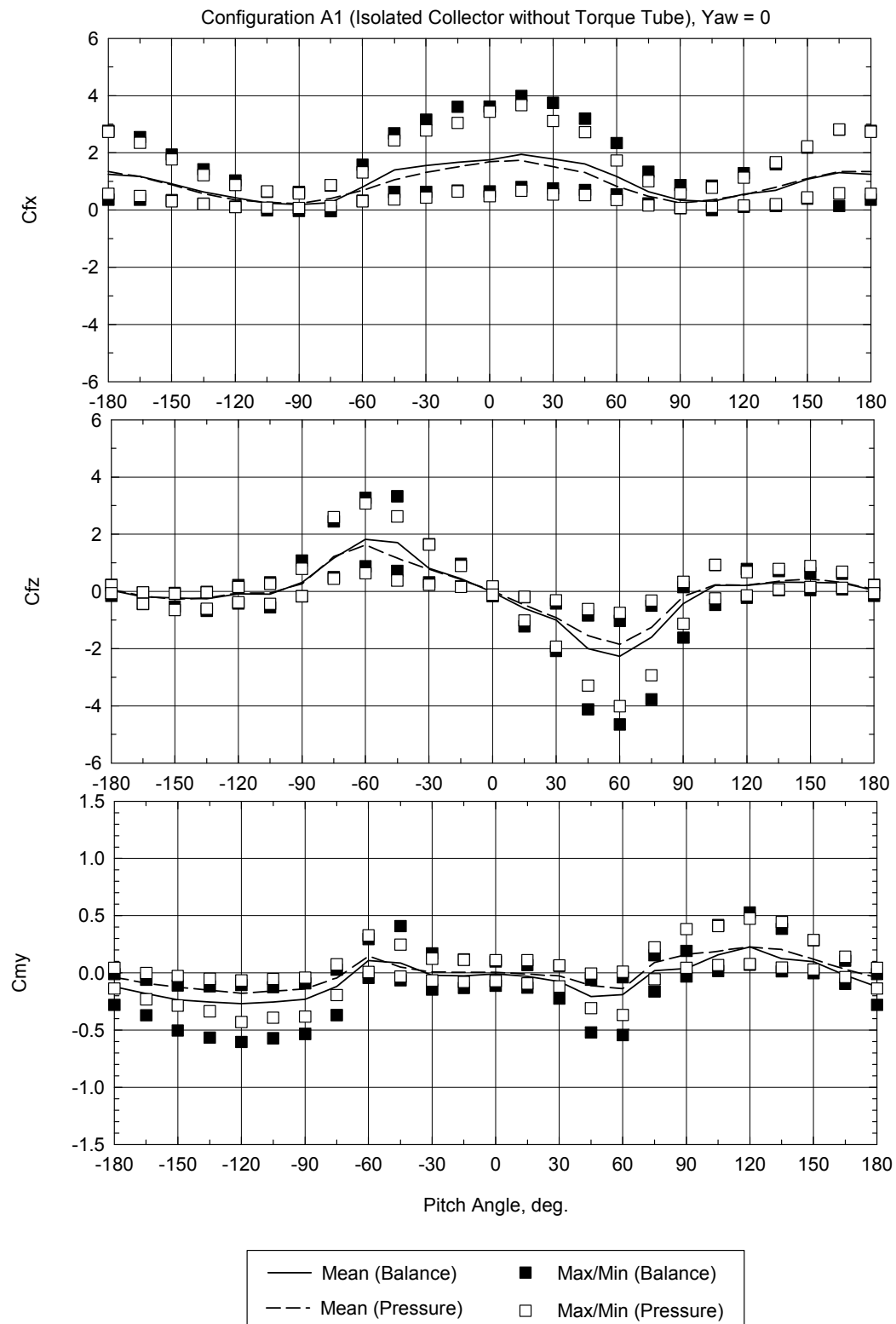


Figure 4-5a Comparisons of balance and pressure results for isolated collector, without torque tube

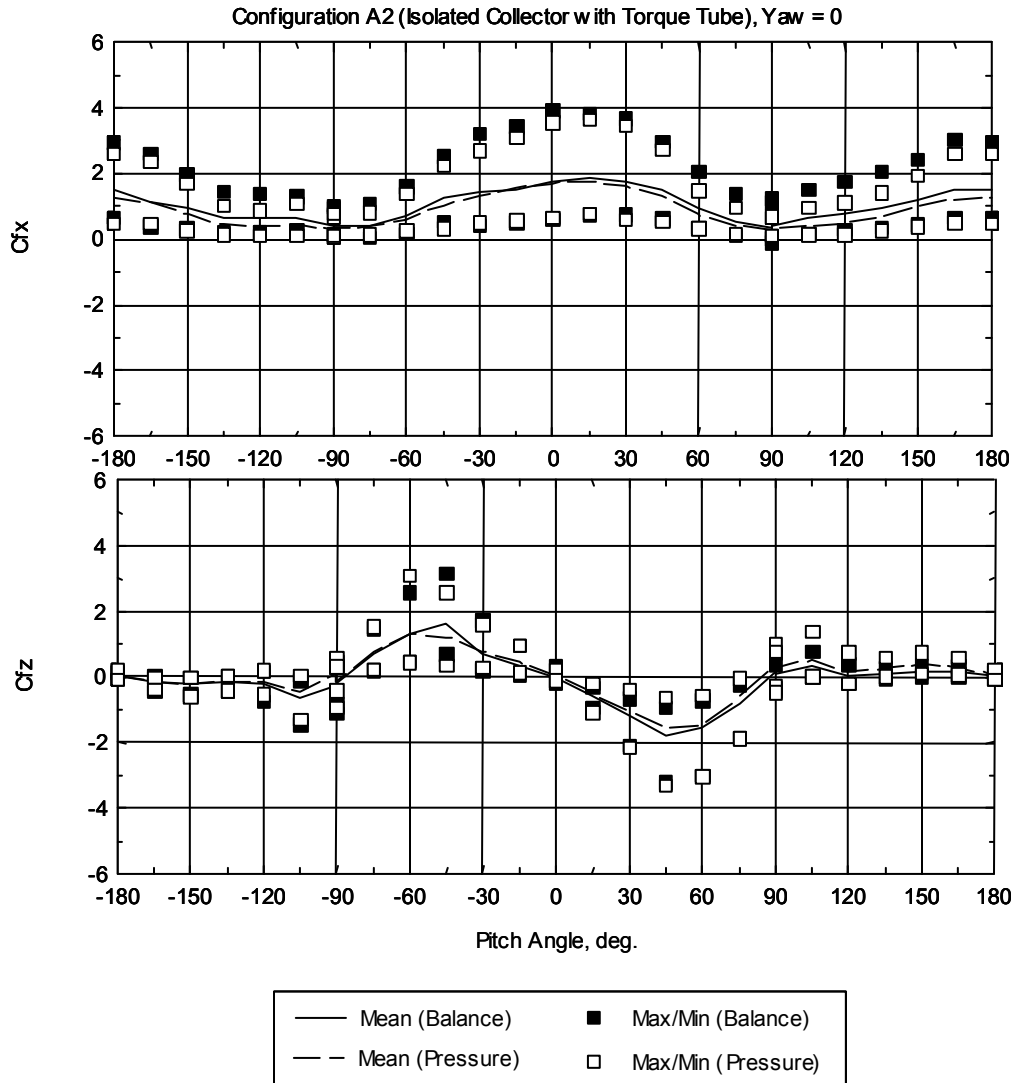
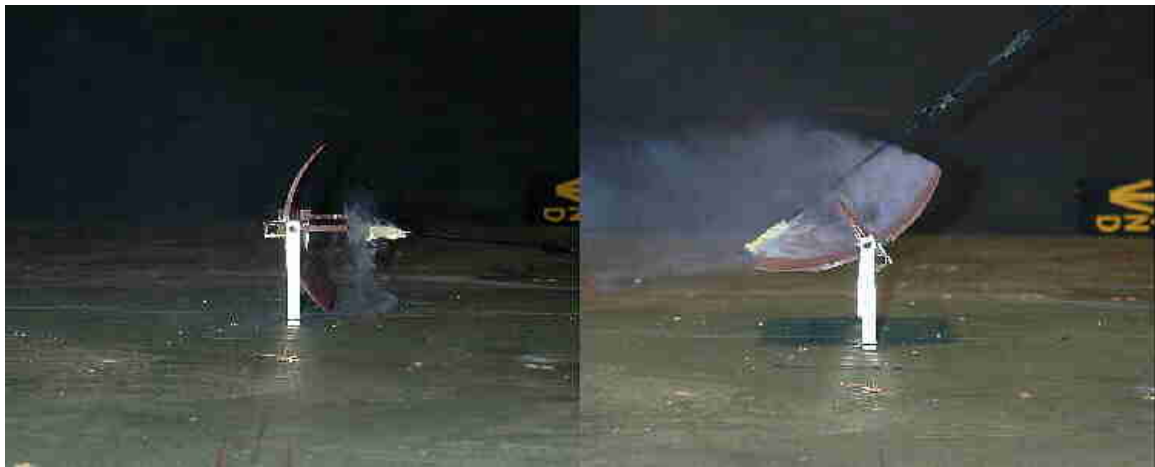


Figure 4-5b Comparisons of balance and pressure results for isolated collector, with torque tube

4.3.2 Flow Visualization

Observing air flow around the model using smoke is helpful for two reasons: in understanding and interpreting mean and fluctuating pressures and in defining zones of separated flow and reattachment, including zones of vortex formation where pressure coefficients may be expected to be high. Titanium dioxide smoke was released from sources on and near the model to make the flow lines visible to the eye and to make it possible to obtain photographic records of the tests. Several photographs showing the flow around the isolated solar collector are given in Figure 4-6. Dramatic differences in the flow characteristics near the center of the concentrator are shown in Figure 4-6(a). The side-by-side photographs depict flow stagnation on the windward face of the concentrator and complete separation on the leeward face. The stagnation at the pitch angle of near 0 degrees is the major contributor to the maximum horizontal drag force (see also Figure 4-4). The flow around the edge of the concentrator is shown in Figure 4-6(b), where an intense streak of flow stream, known as the shear layer, is evident. The shear layer envelops the

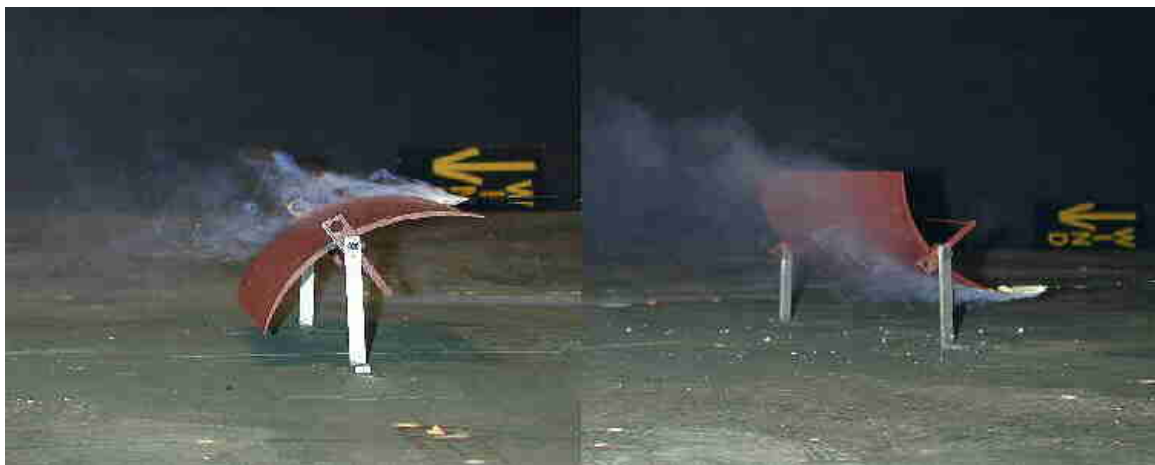
separation zone, and its trajectory varies depending on the pitch angle. For example, at a pitch angle of 0 degrees (i.e., the photograph on the left) the shear layer is much elevated compared to that at a pitch of 120 degrees (on the right), despite the similar height of the top edge of the concentrator. Transition of the flow pattern is shown in Figure 4–6(c). Near the leading edge of the concentrator, the flow seems to follow the curvature of the concentrator and eventually separates from the surface around the center of the concentrator. Before separation, the flow tends to accelerate, creating a zone of high negative pressure on the leeward face of the concentrator. Combined with the near stagnant positive pressure on the windward face, both pitch angles (-60 and +60 degrees) result in a significant vertical force, though of opposite sign.



(a) Flow Stagnation and Separation



(b) Formation of Shear Layer



(c) Flow Transition

Figure 4-6 Flow around isolated solar collector

4.4 Exterior Solar Collectors in Array Field

4.4.1 General Observations

Figure 4-7 through Figure 4-10 show the Phase 2 test data on drag and lift load coefficients for the collectors at the exterior edge of the array field and compare the balance and pressure measurement techniques. Figure 4-11 shows the Phase 4 pitching moment load coefficients for selected collectors at the exterior edge of the array field, also comparing the balance and pressure measurement techniques.

Particular collector positions can be identified by the configuration ID and by referring to Figure 2-11a. At a yaw of 0 degrees, the loads on the collectors in all module positions in the most upwind row are similar for all pitch angles (e.g., see Figure 4-7 and Figure 4-8a). The collector at the edge of the field shows a higher horizontal force at a yaw of 30 degrees (Figure 4-8b) when the collector is near upright, while the vertical force and pitching moment are similar to those at yaw = 0 degrees. Some reduction of the loads is realized for the collectors along the field edge at the row positions 2 and 3 because of upwind shielding (see Figure 4-9 and Figure 4-10).

Figure 4-12 illustrates the variation of the wind loads along the side edge of the array field. The row position is measured from the upwind edge of the field with a position of 0, denoting an isolated collector. The pitch angles were selected separately for individual load components on basis of significance. In general, differences in the loads become insignificant beyond a row position of 3.

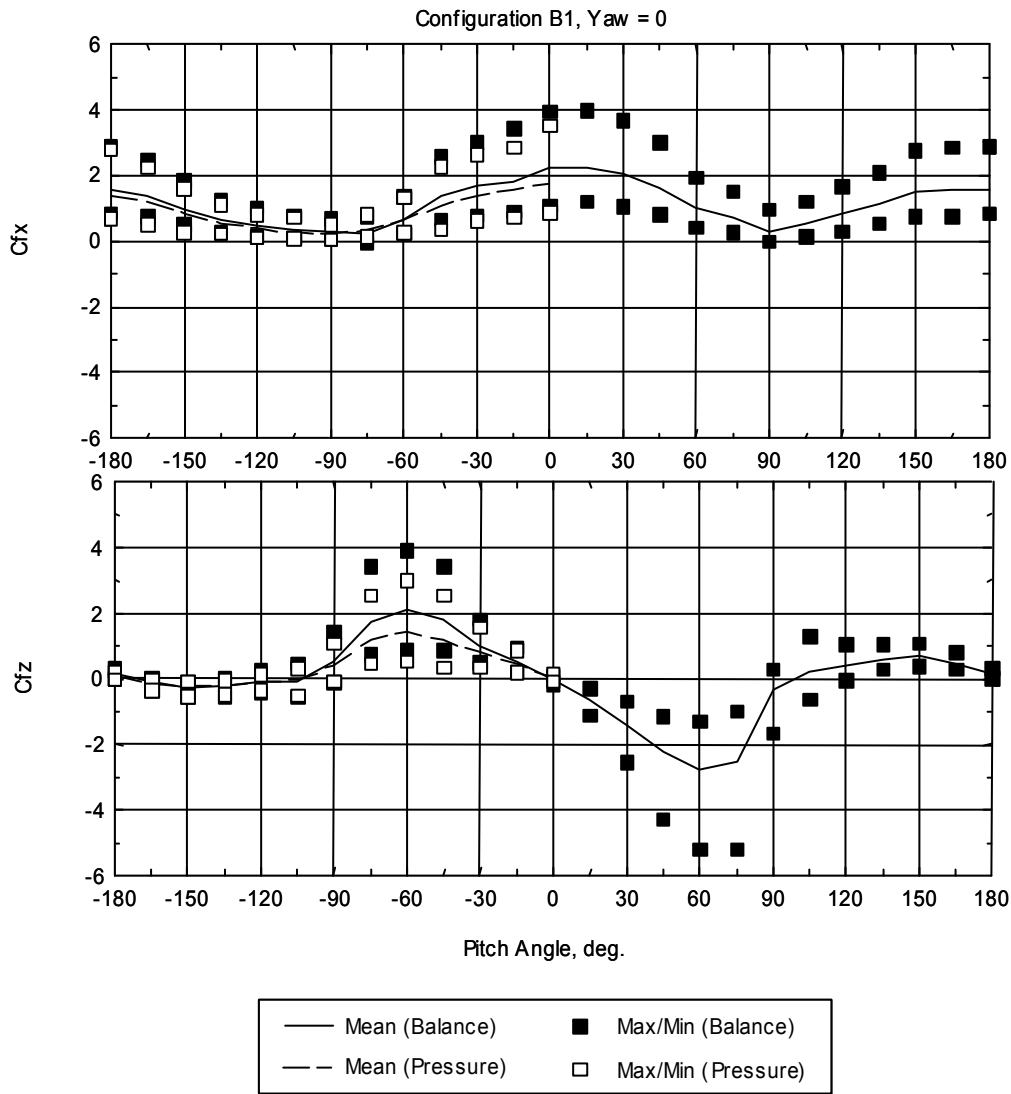


Figure 4-7 Loads on exterior collector for Configuration B1, collector in Row 1 at Module Position 4 (from edge), yaw = 0 degrees

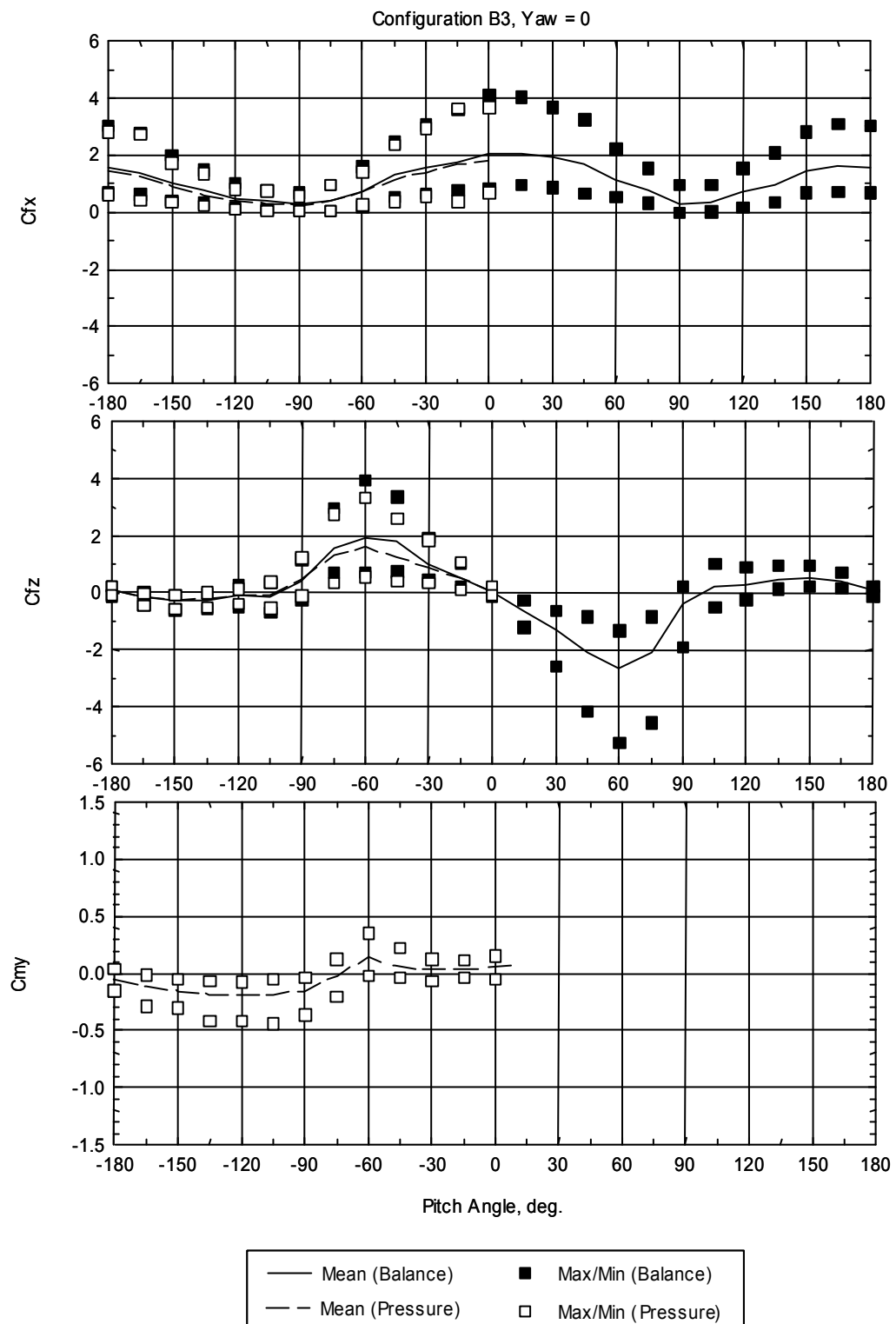


Figure 4-8a Loads on exterior collector for Configuration B3 Collector in Row 1 at Module Position 1 (at edge), yaw = 0 degrees

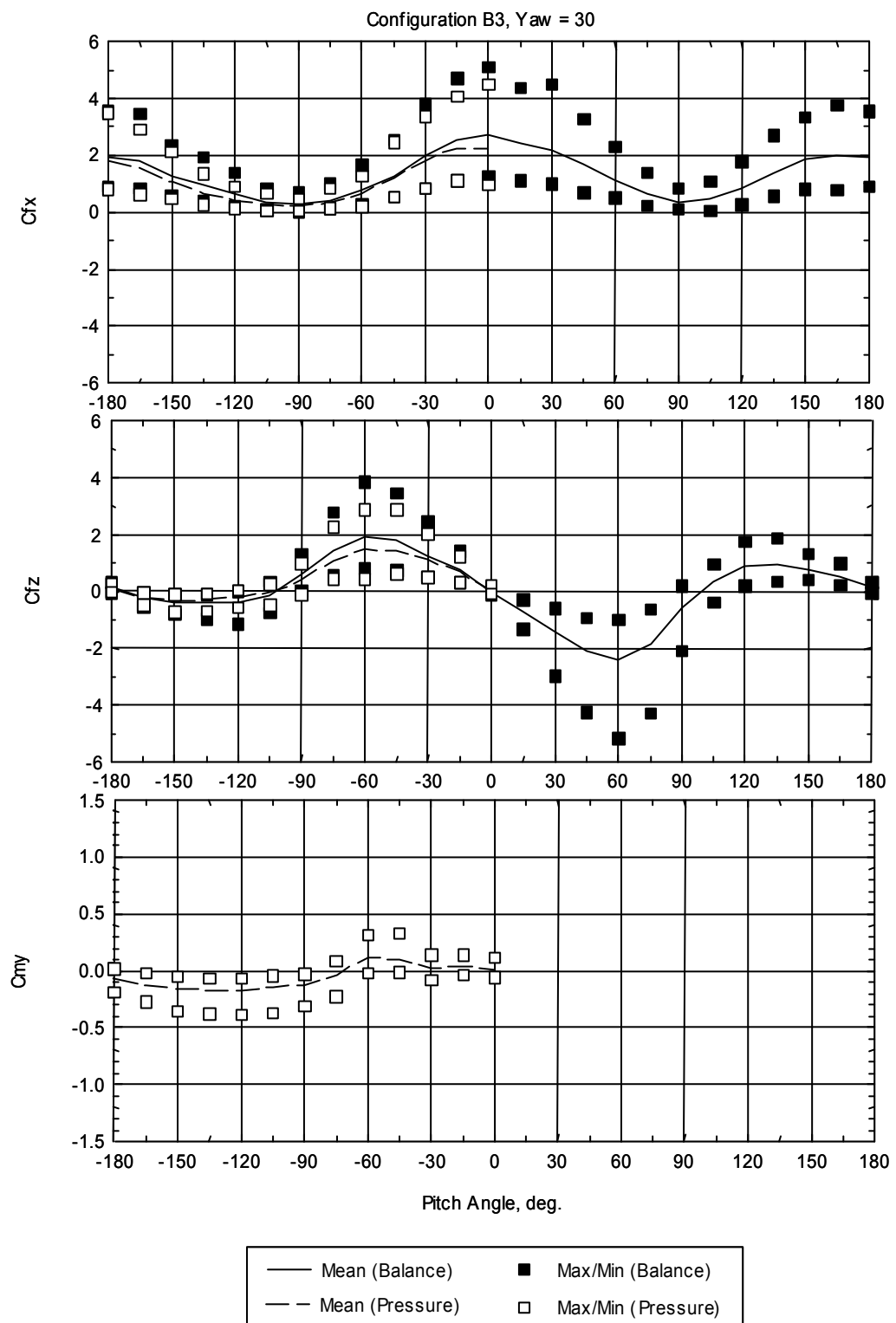


Figure 4-8b Loads on exterior collector for Configuration B3, collector in Row 1 at Module Position 1 (at edge), yaw = 30 degrees

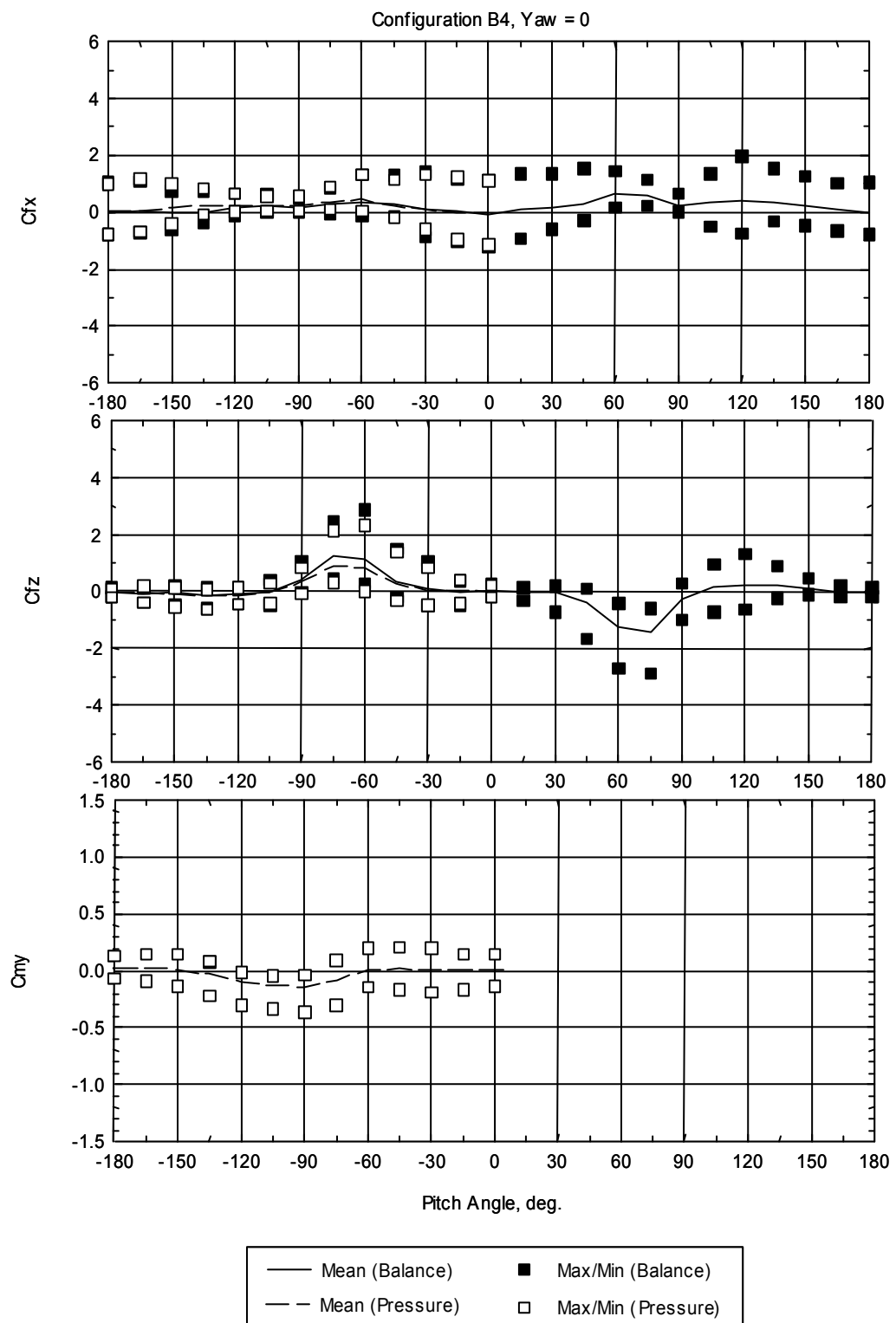


Figure 4-9a Loads on exterior collector for Configuration B4, collector in Row 2 at Module Position 1 (at edge), yaw = 0 degrees

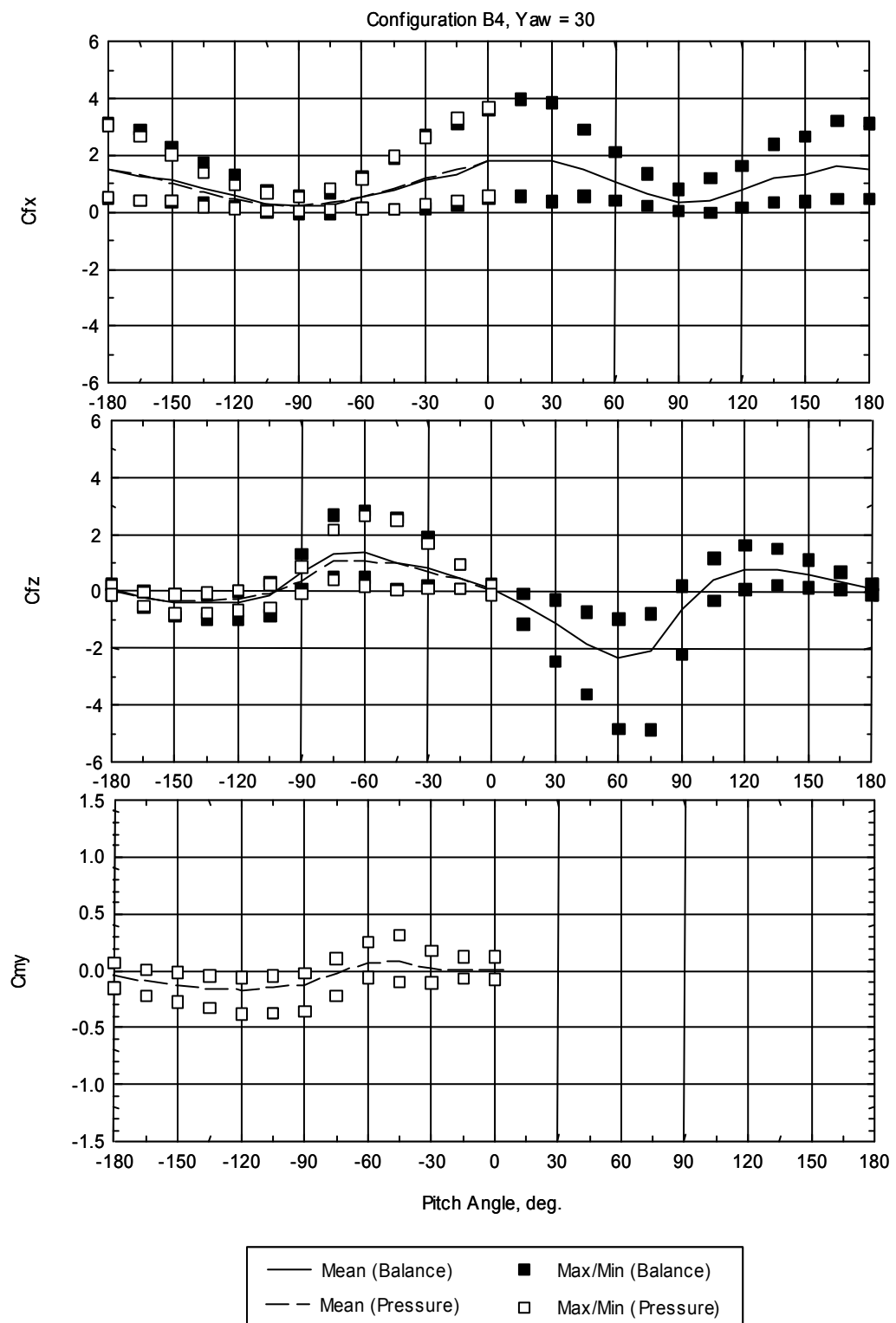


Figure 4-9b Loads on exterior collector for Configuration B4, collector in Row 2 at Module Position 1 (at edge), yaw = 30 degrees

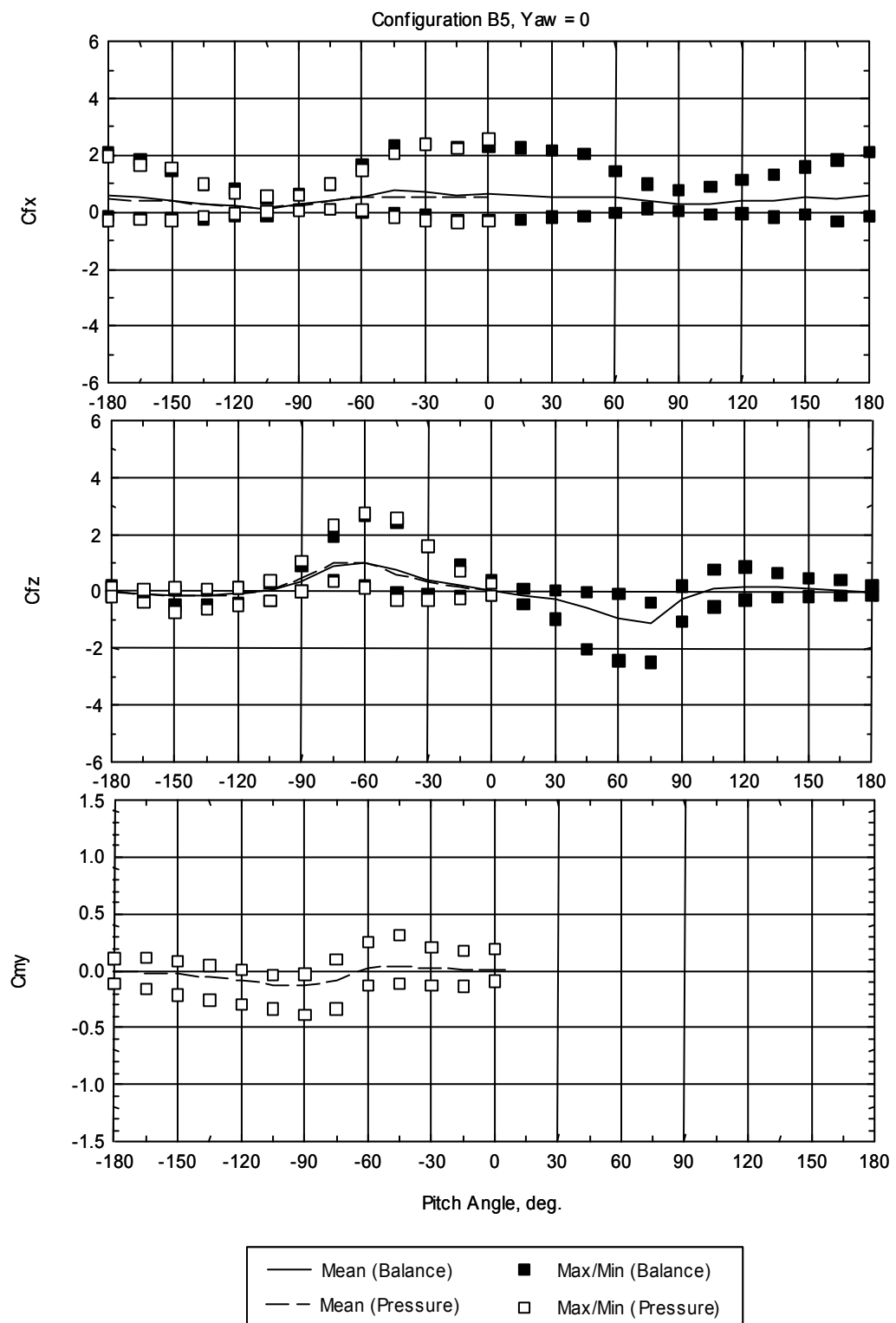


Figure 4-10a Loads on exterior collector for Configuration B5, collector in Row 3 at Module Position 1 (at edge), yaw = 0 degrees

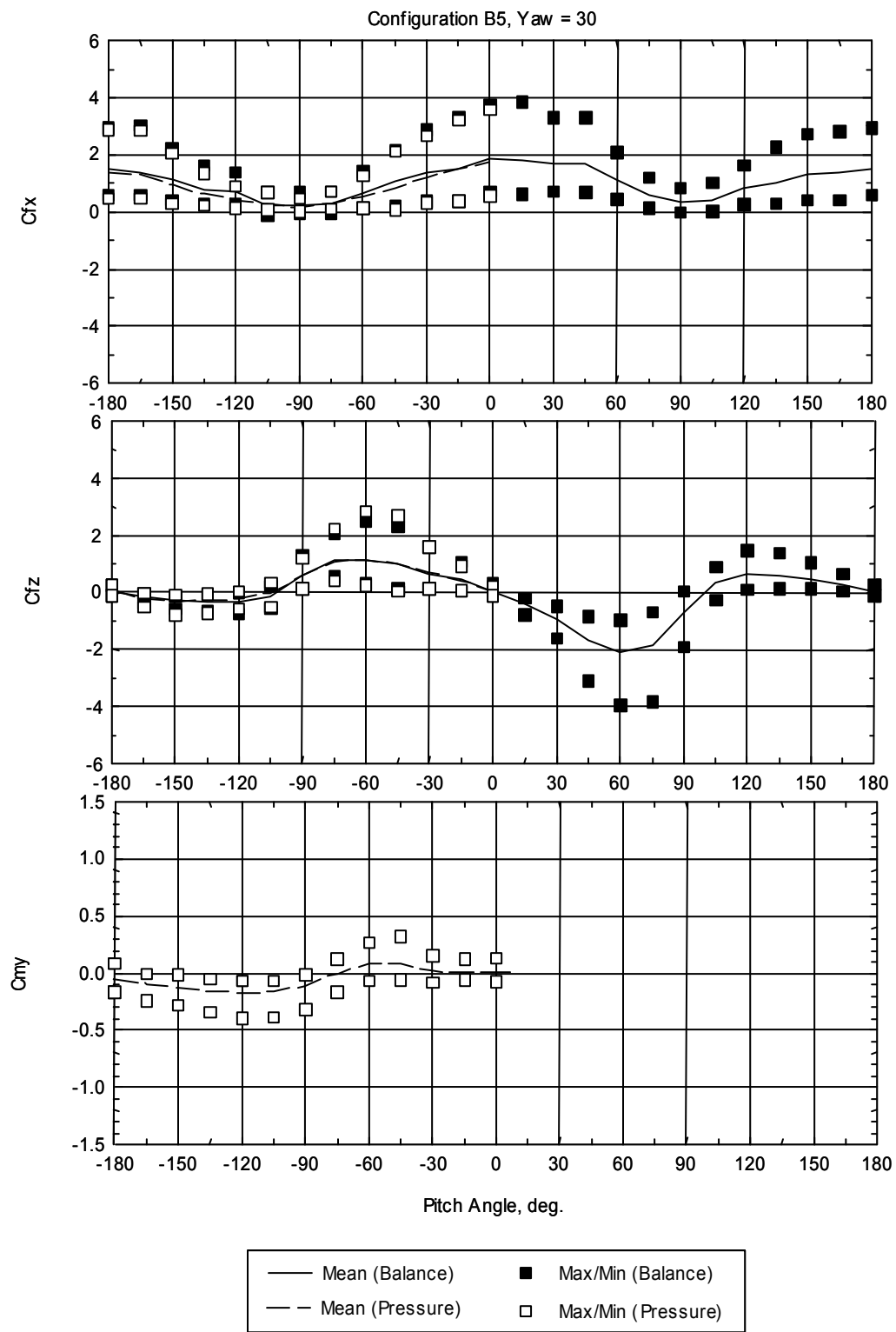


Figure 4-10b Loads on exterior collector for Configuration B5, collector in Row 3 at Module Position 1 (at edge), yaw = 30 degrees

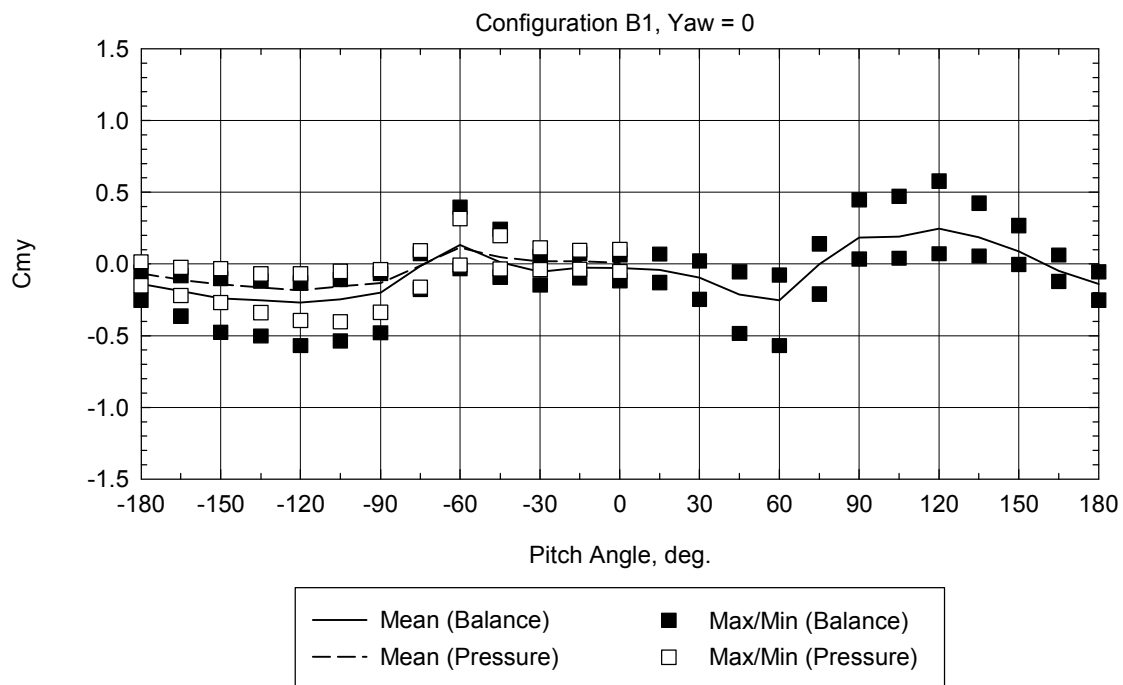
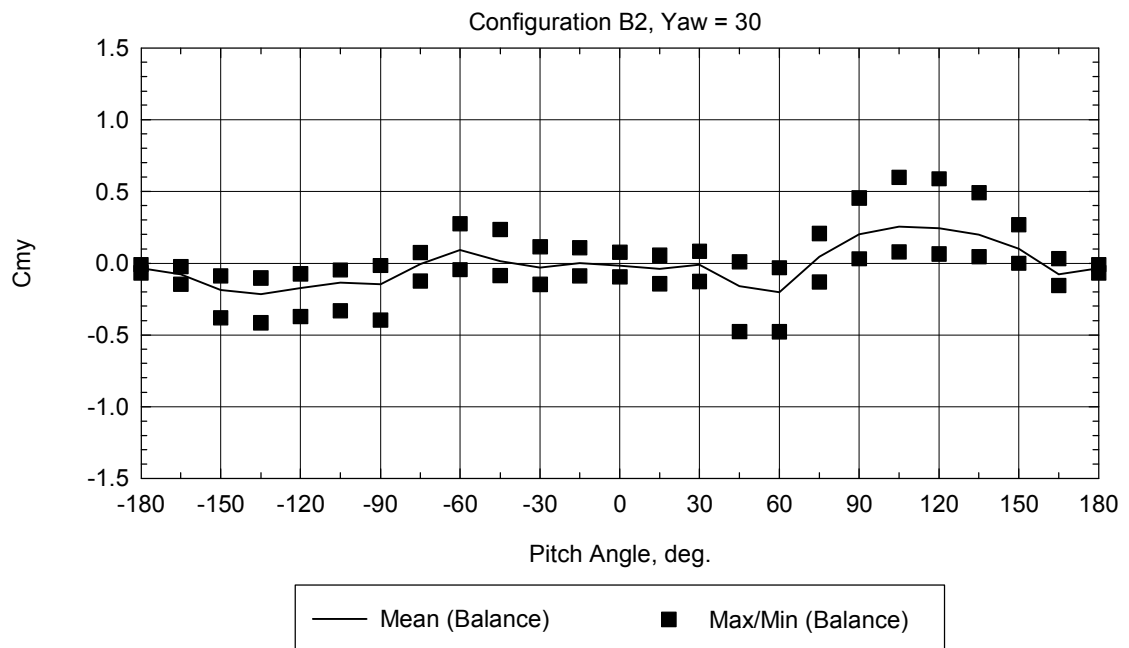
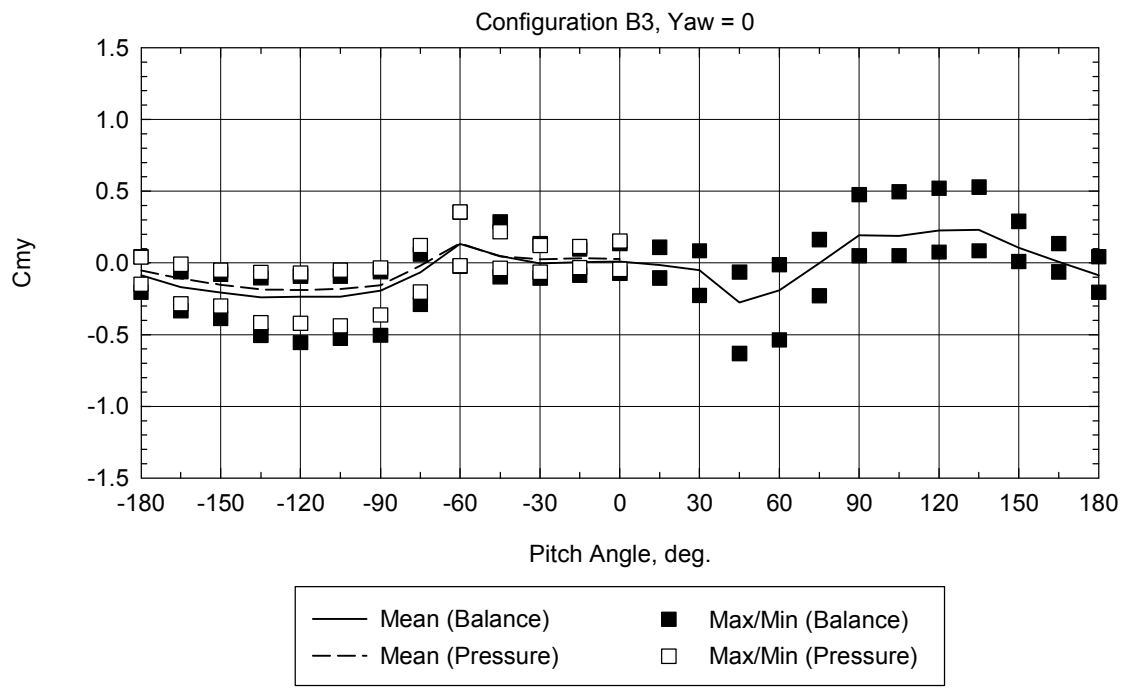


Figure 4-11 Pitching Moment of Exterior Collector
(a) Configuration B1, Yaw = 0 degrees



**Figure 4-11 Pitching Moment of Exterior Collector,
(b) Configuration B2, Yaw = 30 degrees**



**Figure 4-11 Pitching Moment of Exterior Collector,
(c) Configuration B3, Yaw = 0 degrees**

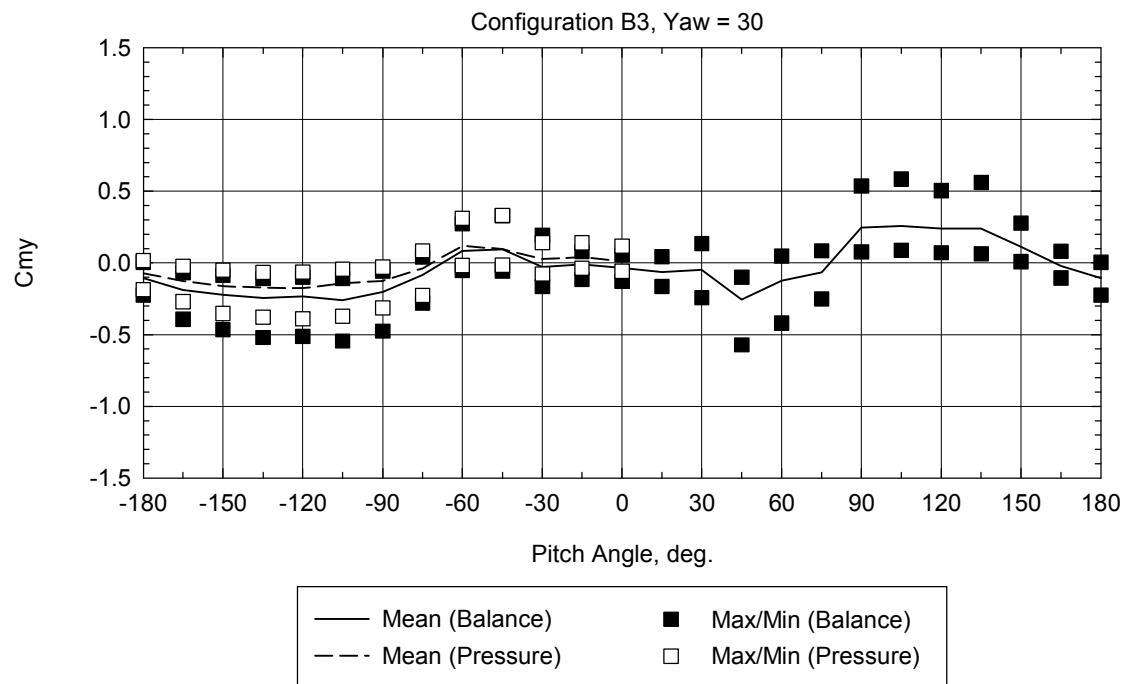


**Figure 4-11 Pitching Moment of Exterior Collector,
(d) Configuration B3, Yaw = 30 degrees**

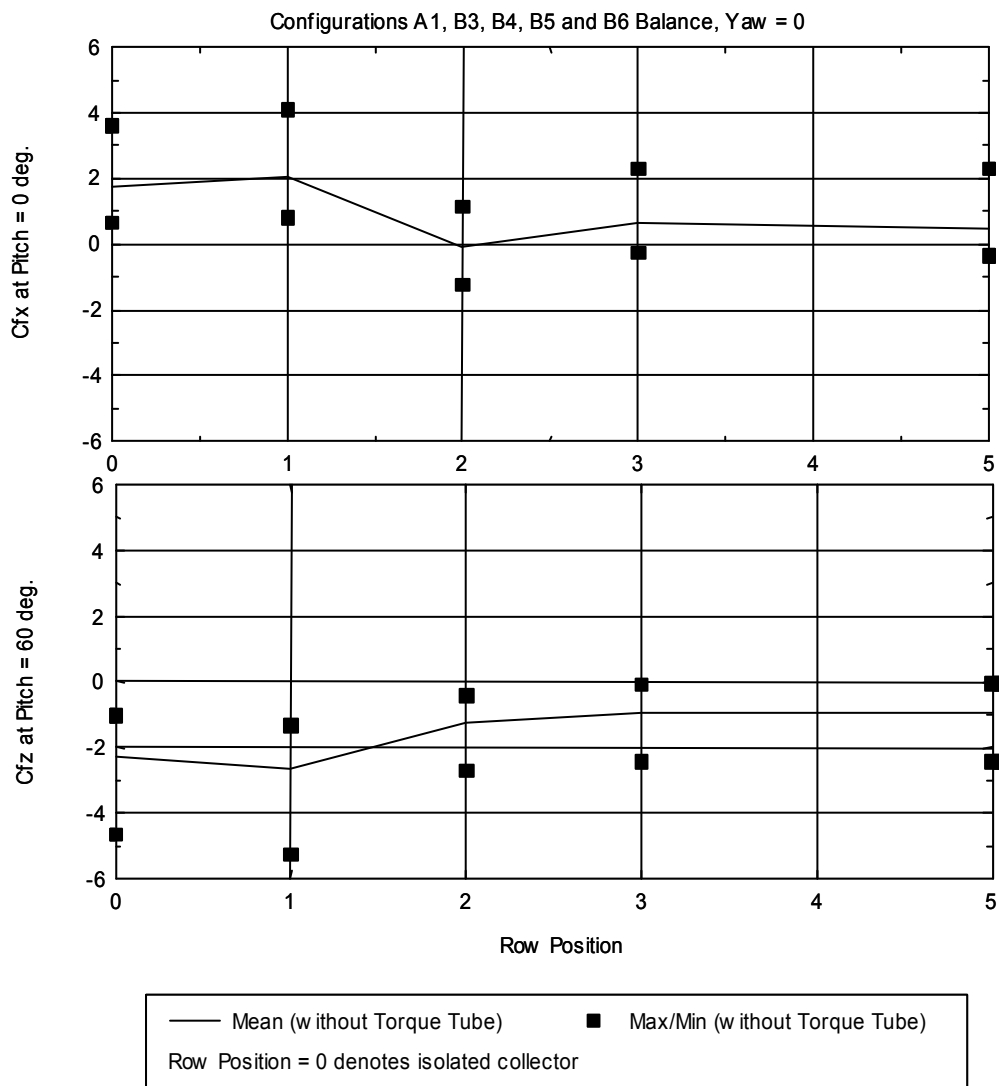


**Figure 4-12a Effect of row position along edge of array field,
yaw = 0 degrees**

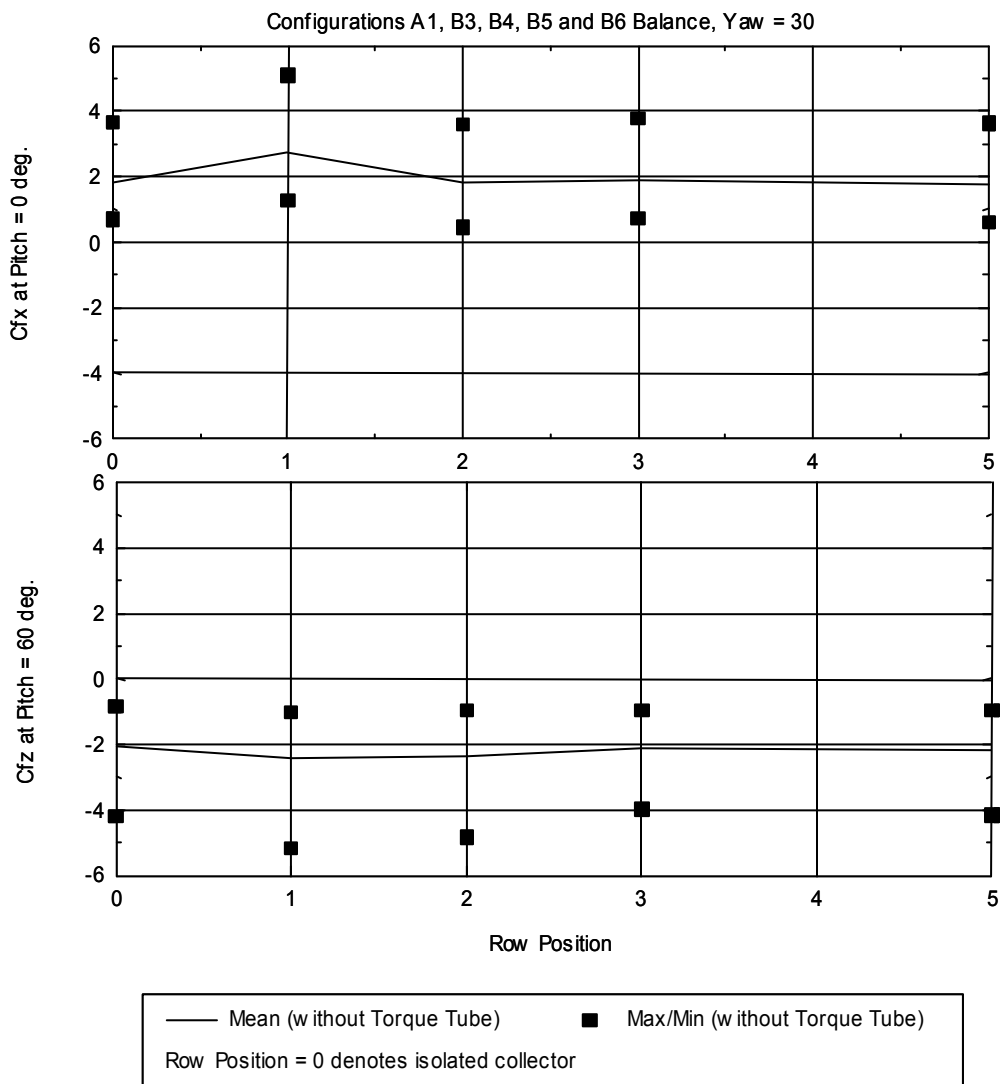


Figure 4-12b Effect of row position along edge of array field, yaw = 30 degrees

General patterns of the wind flow within the array field are shown in Figure 4-13. The flow within the field is highly turbulent as expected. The flow passing over the most upwind row of the collectors tends to reattach to the second row and diffuse gradually downwind.



(a)



(b)

Figure 4-13 General flow patterns within array field

4.4.2 Effects of Wind Protective Fence Barrier and Torque Tube

Drastic reduction of the loads can be seen when a protective fence surrounds the collector field, as shown by comparing Figure 4-14 with Figure 4-8a and Figure 4-8b. The effectiveness of the fence is more pronounced for the vertical force component.

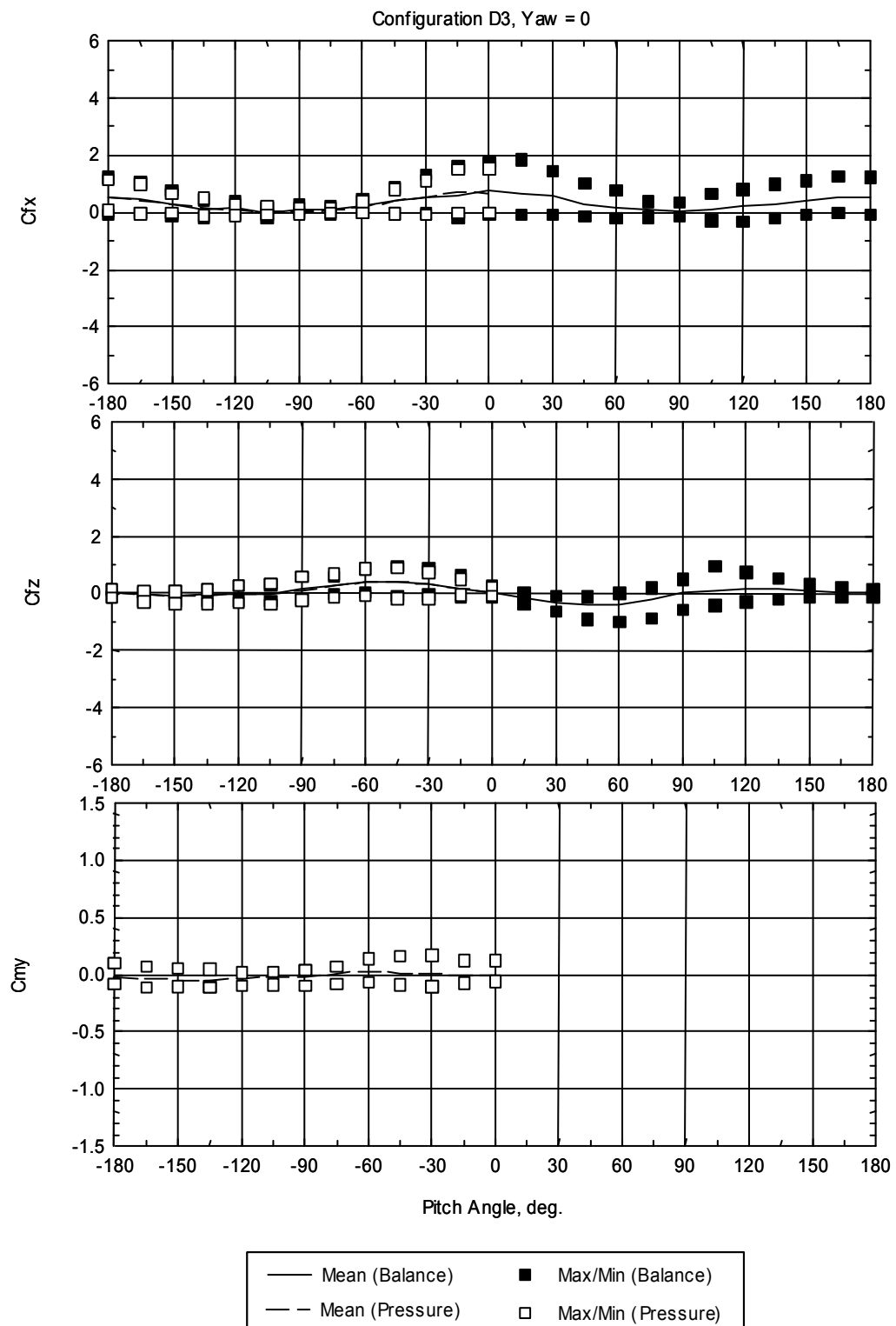


Figure 4-14a Loads on exterior collector with protective fence for Configuration D3, collector in Row 1 at Module Position 1 (at edge), yaw = 0 degrees

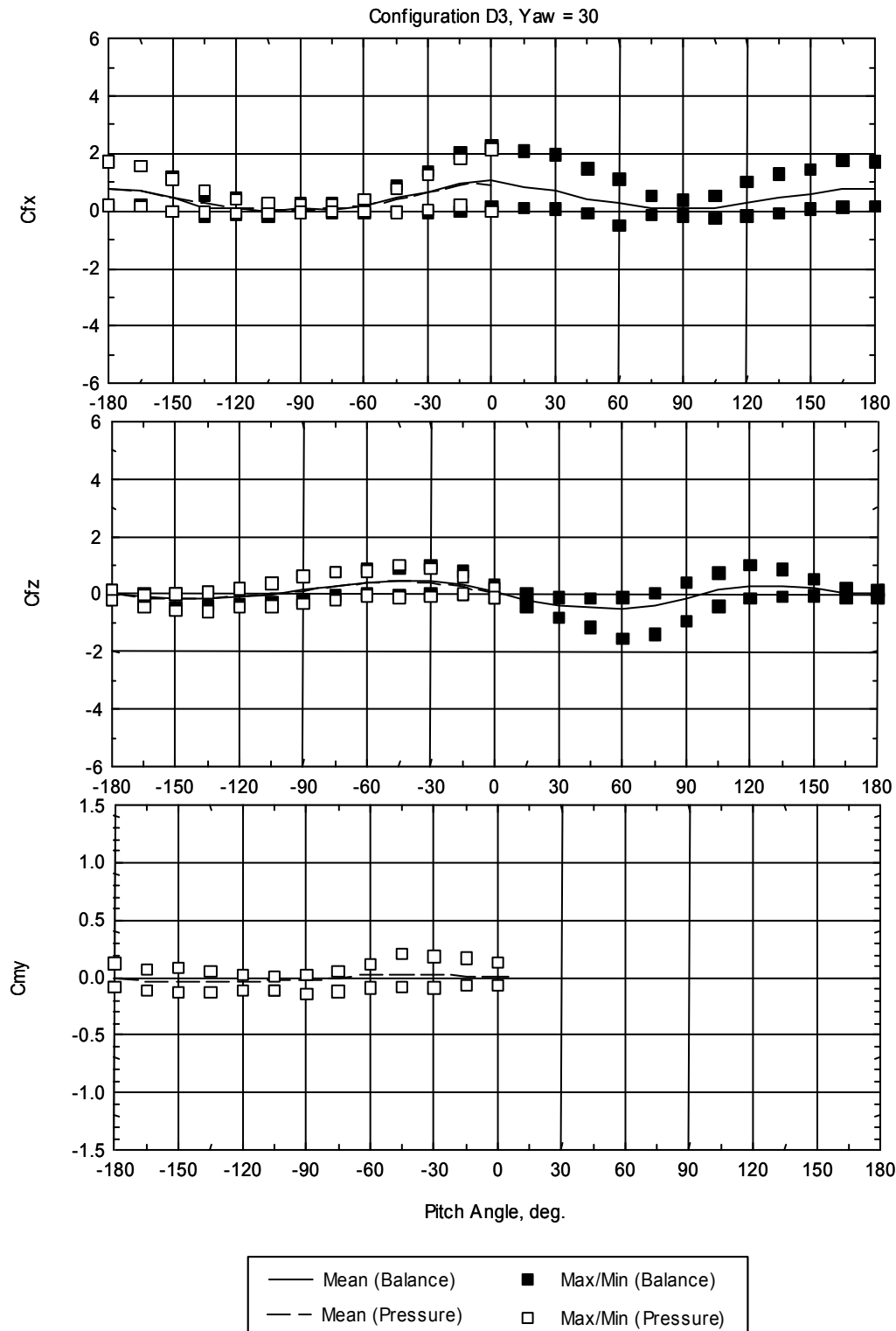


Figure 4-14b Loads on exterior collector with protective fence for Configuration D3, collector in Row 1 at Module Position 1, (at edge), yaw = 30 degrees

The effect of the protective fence is apparent in the photographs shown in Figure 4-15, which compare the wind flows with and without the fence. With the porous protective fence in place, the flow is more diffused.

The effect of the torque tube on the exterior collectors can be seen in Figure 4-16 through Figure 4-18. In general, the influence of the torque tube is small, with the effect being most noticeable on the vertical force, especially at a pitch angle of about 60 degrees.

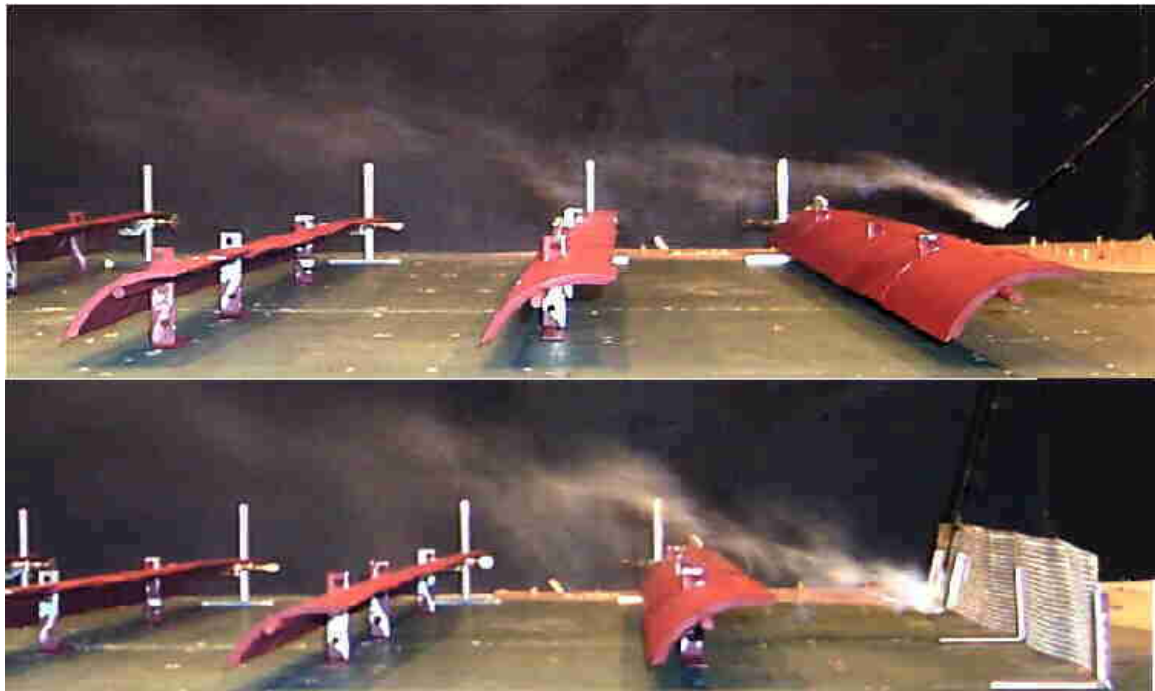


Figure 4-15 Effect of wind protective fence

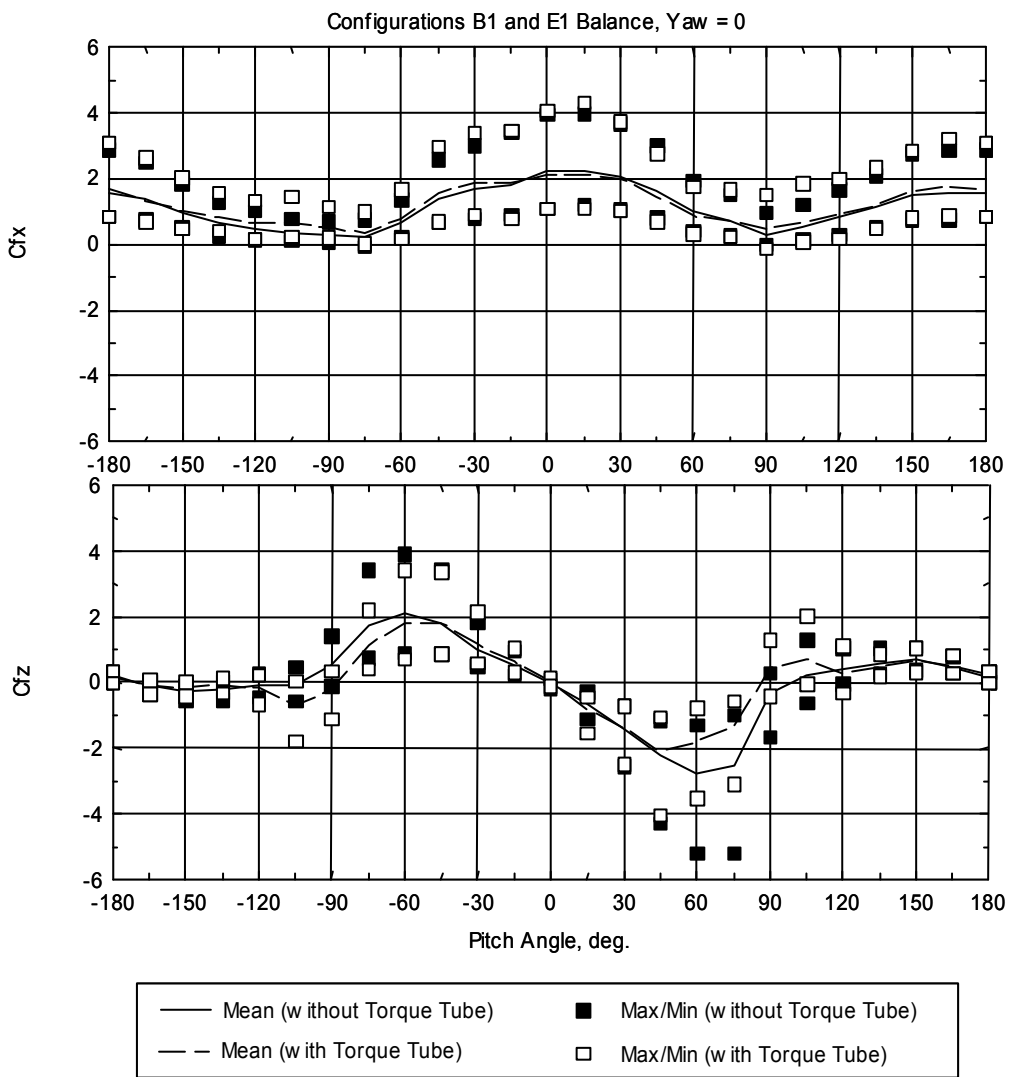


Figure 4-16 Effect of torque tube on collector in array field, Configurations B1 and E1, collector in Row 1 at Module Position 4 (from edge), yaw = 0 degrees

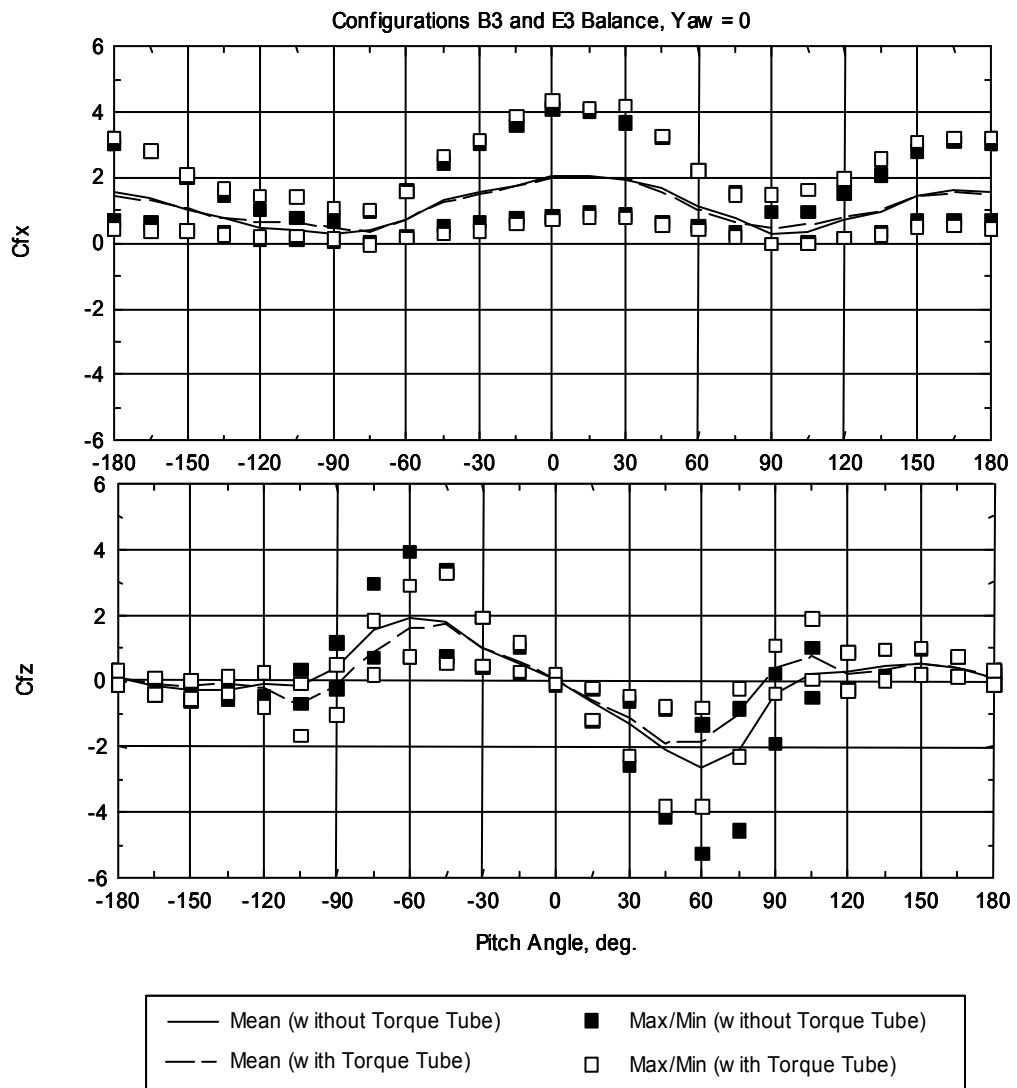


Figure 4-17 Effect of torque tube on collector in array field, Configurations B3 and E3, collector in Row 1 at Module Position 1 (at edge), yaw = 0 degrees

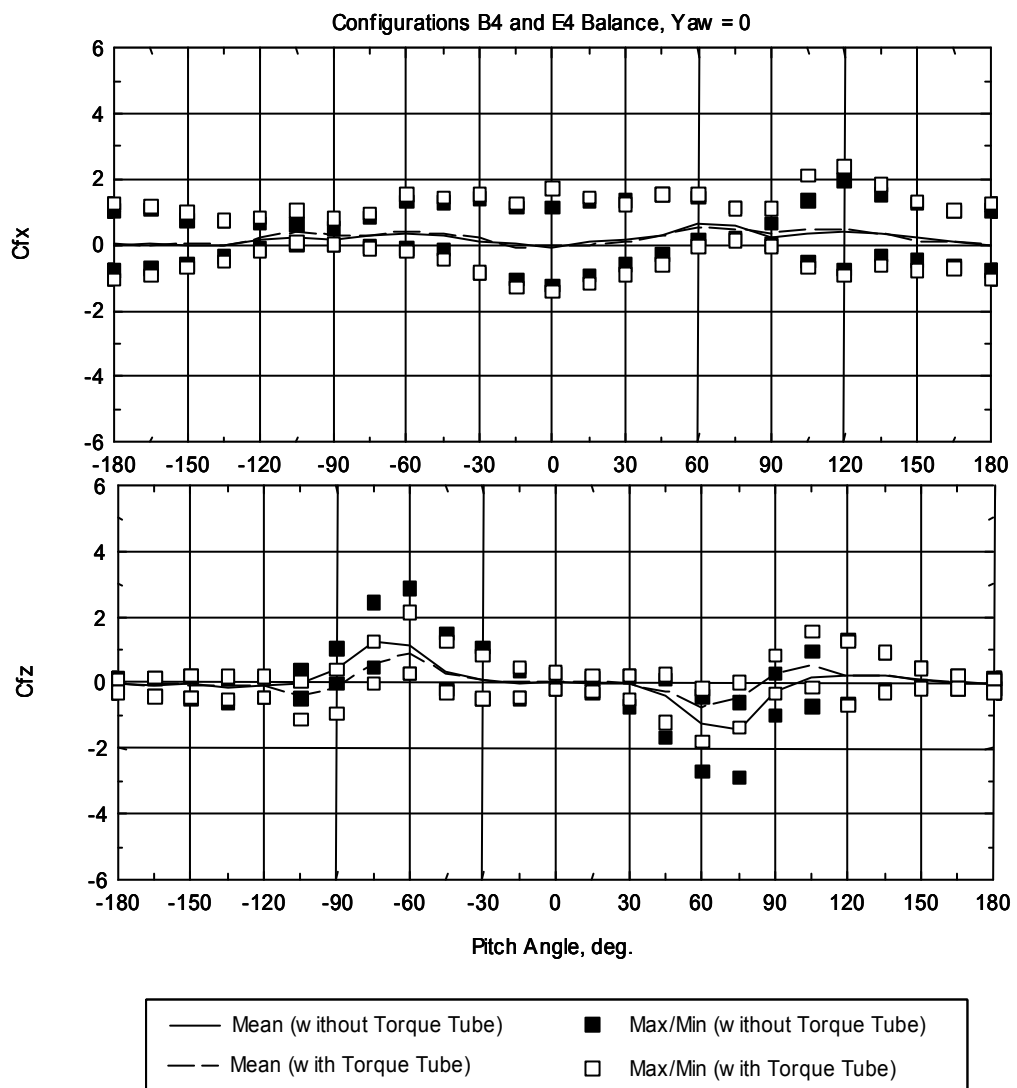


Figure 4-18 Effect of torque tube on collector in array field, Configurations B4 and E4, collector in Row 2 at Module Position 1 (at edge), yaw = 0

4.5 Interior Solar Collectors in Array Field

4.5.1 General Observations

Figure 4-19 through Figure 4-21 show the Phase 3 test data on drag and lift load coefficients, obtained by both the balance and pressure measurements, for the solar collectors located interior of the array field. Figure 4-23 shows the Phase 4 pitching moment load coefficients for selected collectors interior of the array field, also comparing the pressure measurement data where available.

Figure 2-11(b) can be used to identify the positions of the collector within the field. For Configuration C1 (presented in Figure 4-19 a, b, and c), the solar collector of interest is located at the second row from the windward field edge. Agreement between the two test methods (balance and pressure data) is generally good. The largest difference is evident for the peak vertical force component at a yaw angle of 75 degrees, shown in Figure 4-19b. Compared with the collector directly in front of this unit (Configuration B1 in Figure 4-7), considerable reduction of the wind loads is noticed due to shielding.

The wind loads continue to decrease slightly for the collectors located further downwind, (Configurations C3 and C5 in Figure 4-20 and Figure 4-21). Patterns of the vertical force and pitching moment are similar among the interior collectors, while some variations in the horizontal force component can be observed. The effect of the row positions for these interior collectors is illustrated in Figure 4-22.

The pitching moment for the interior solar collectors are shown in Figure 4-23. No Phase 3 pressure data are available for Configuration C2 at a yaw angle of 0 degrees (Figure 4-23a).

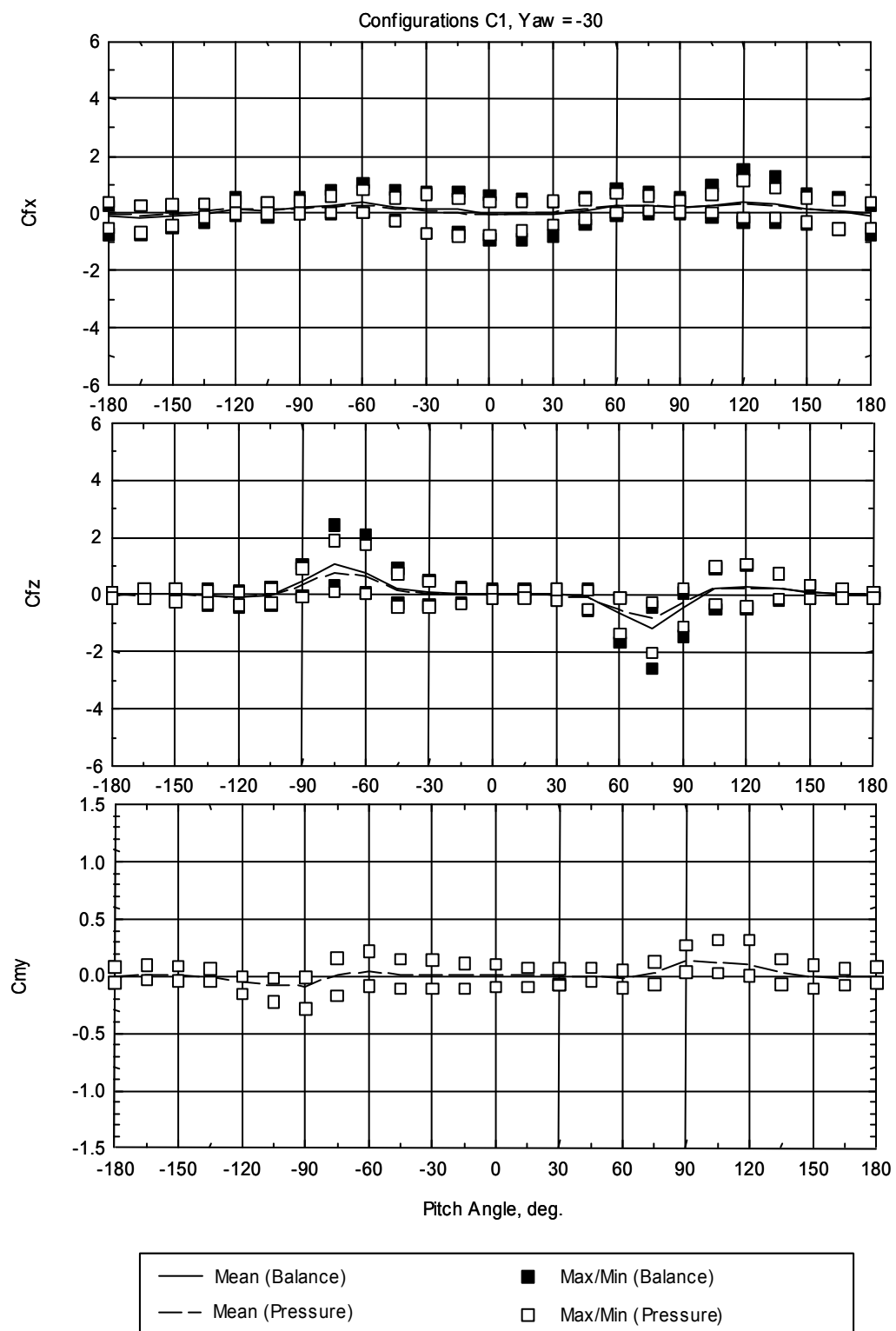


Figure 4-19a Loads on interior collector for Configuration C1, collector in Row 2 at Module Position 4 (from edge), yaw = - 30 degrees

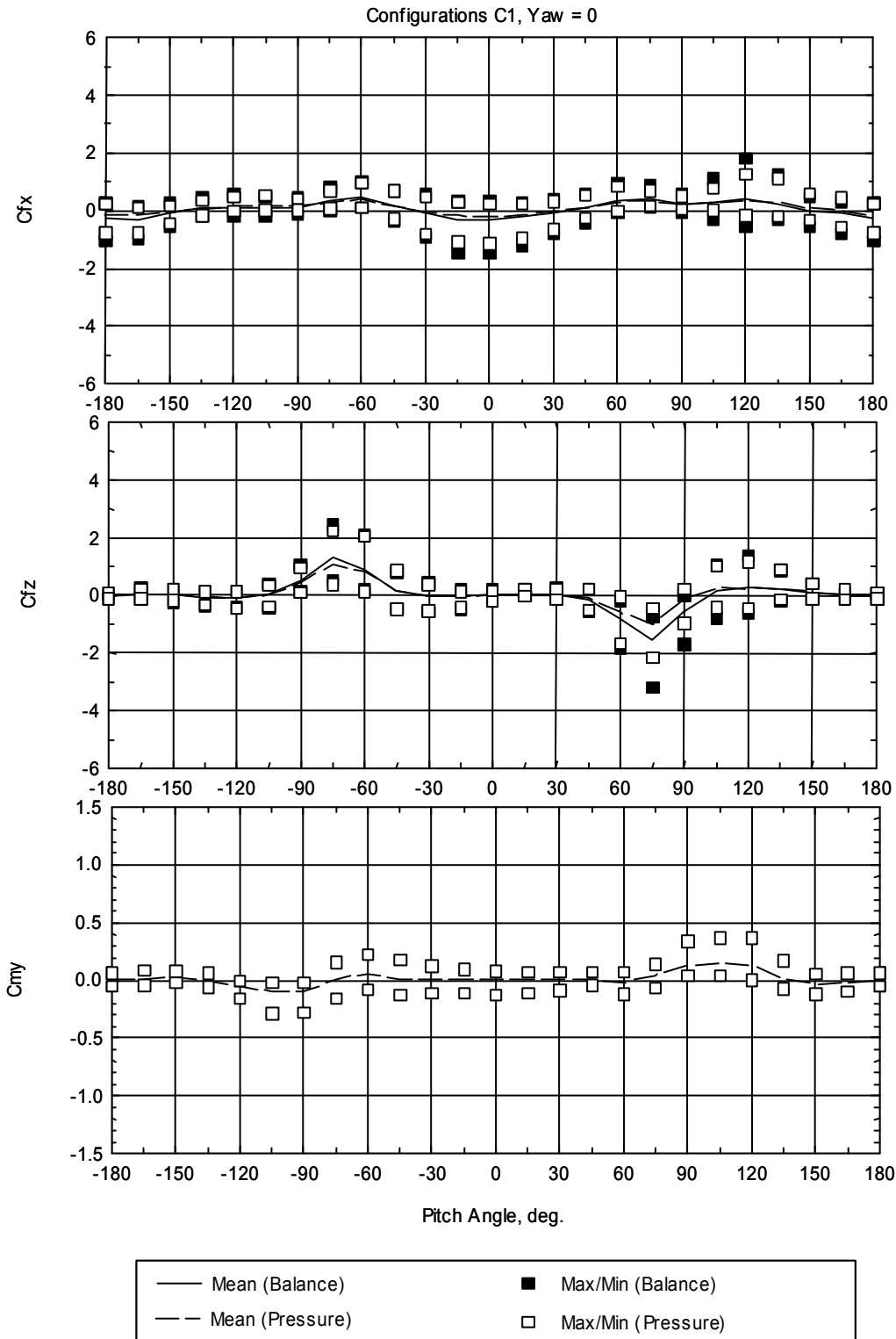


Figure 4-19b Loads on interior collector for Configuration C1, collector in Row 2 at Module Position 4 (from edge), yaw = 0 degrees

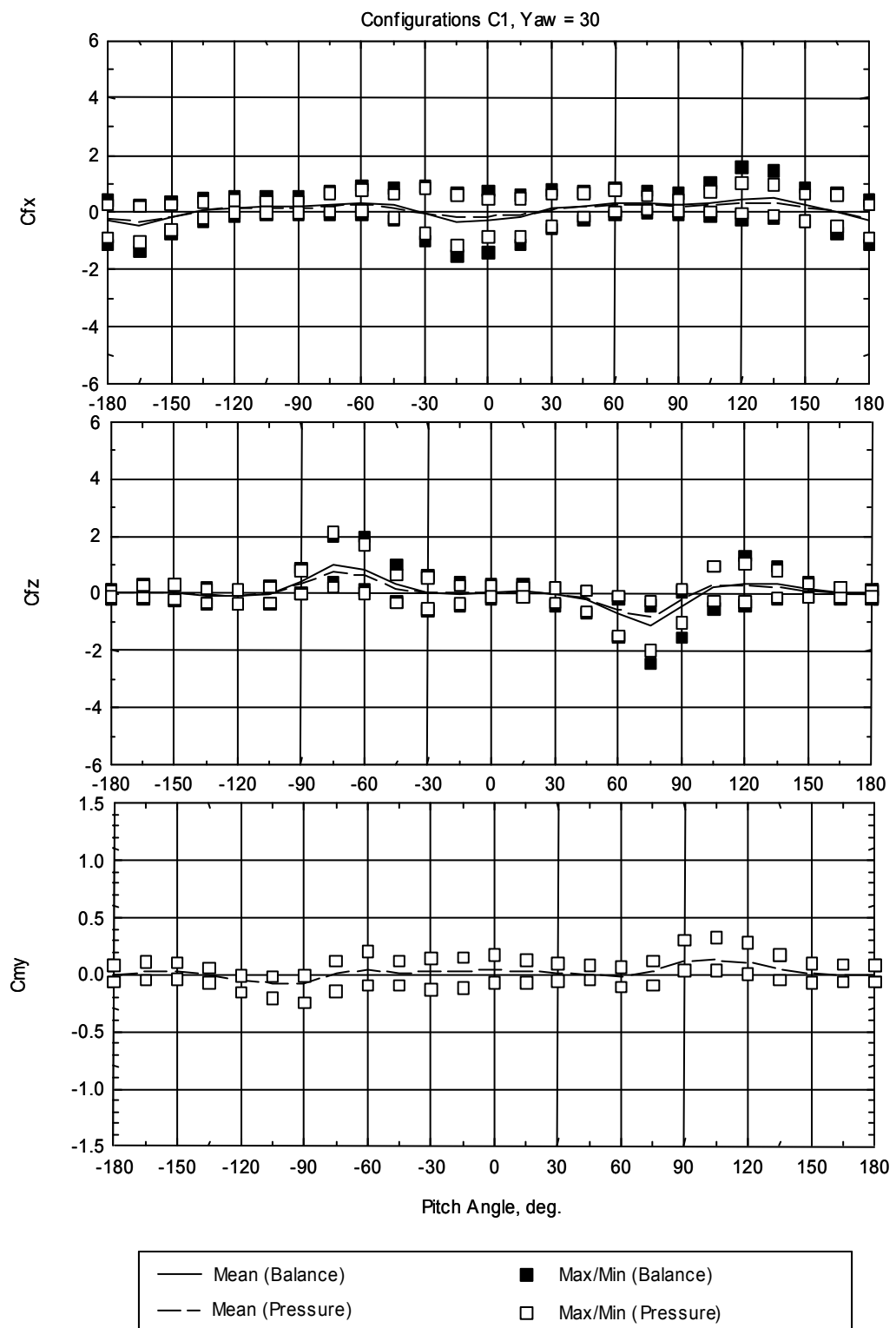


Figure 4-19c Loads on interior collector for Configuration C1, collector in Row 2 at Module Position 4 (from edge), yaw = 30 degrees

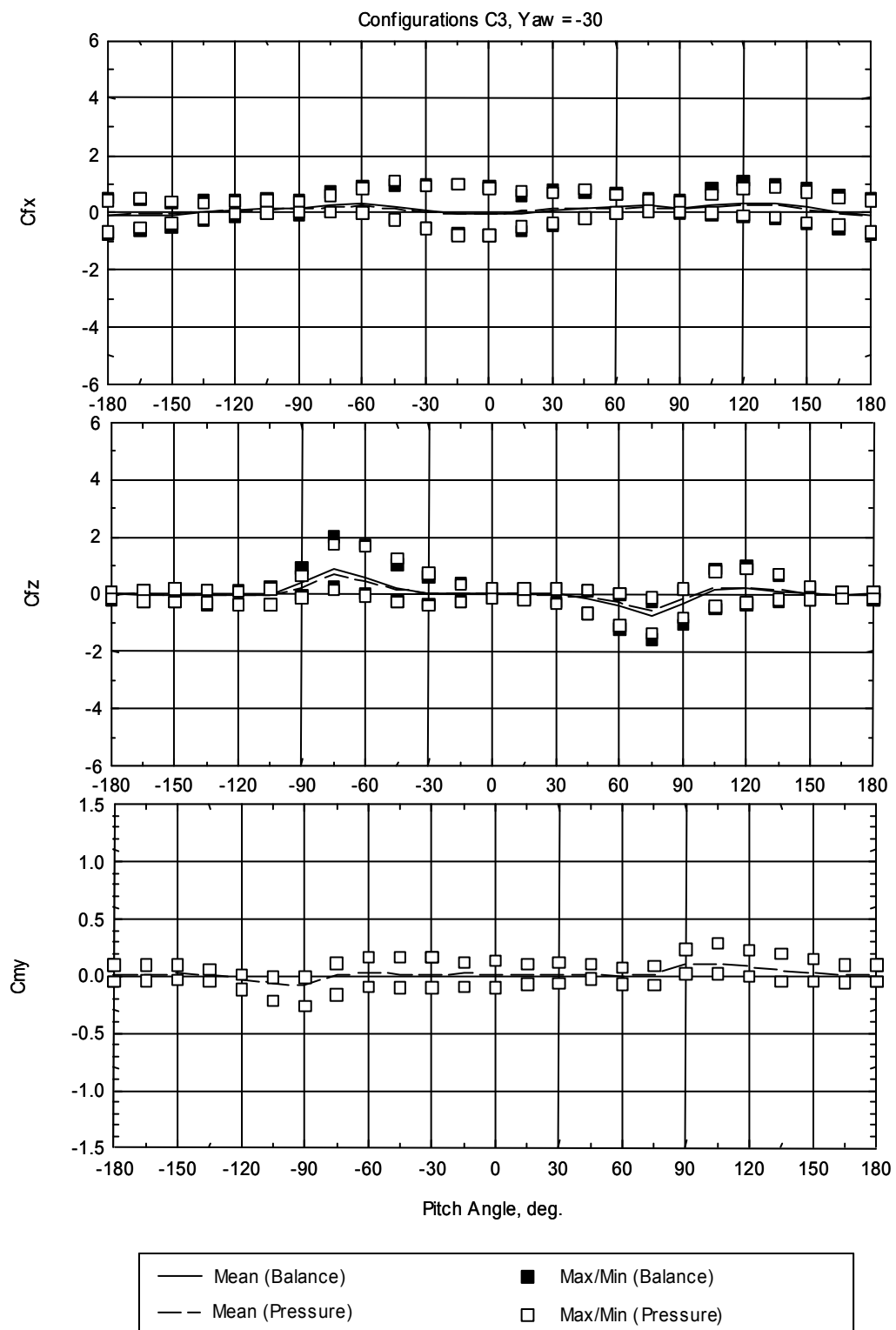


Figure 4-20a Loads on interior collector for Configuration C3, collector in Row 3 at Module Position 4 (from edge), yaw = - 30 degrees

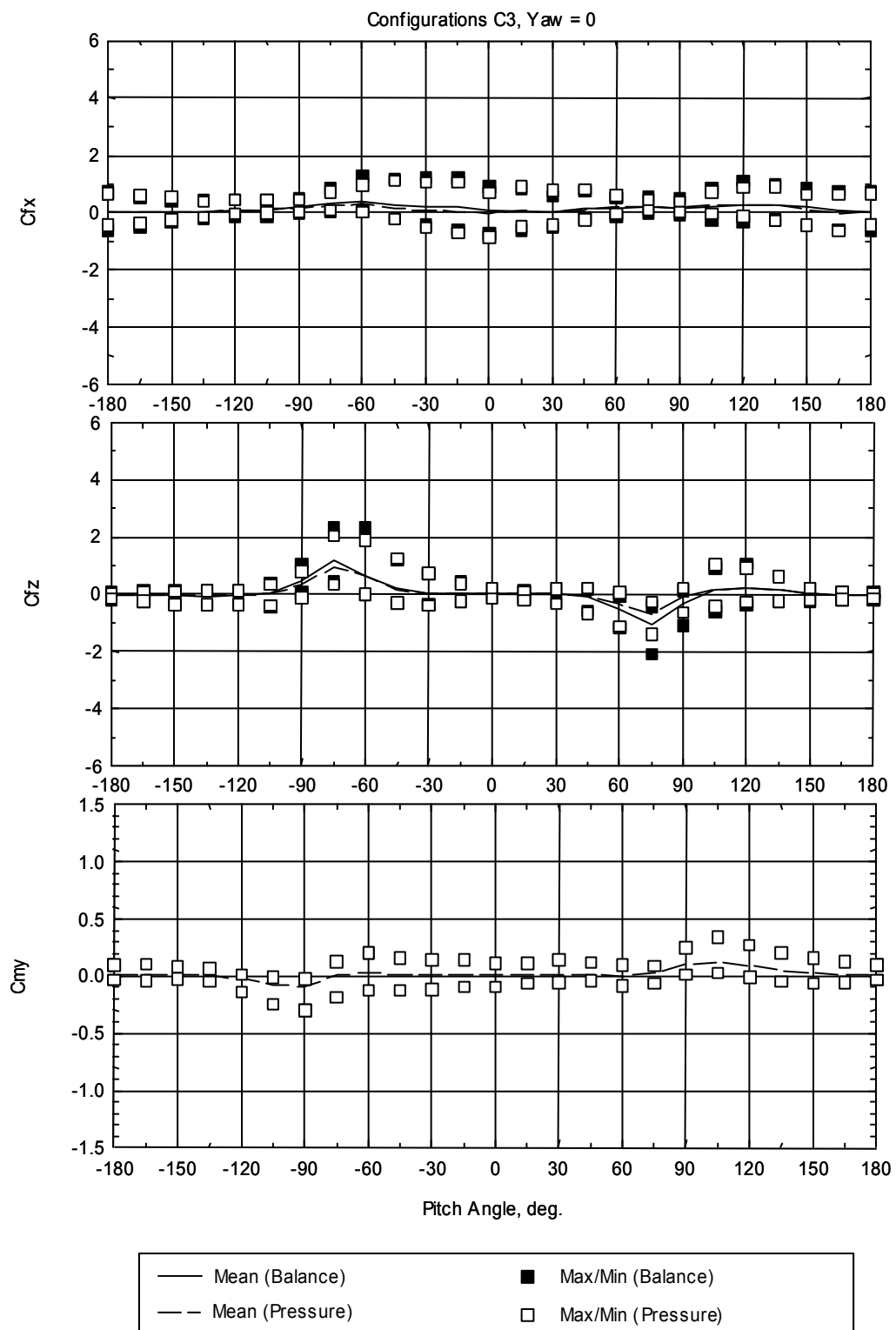


Figure 4-20b Loads on interior collector for Configuration C3, collector in Row 3 at Module Position 4 (from edge), yaw = 0 degrees

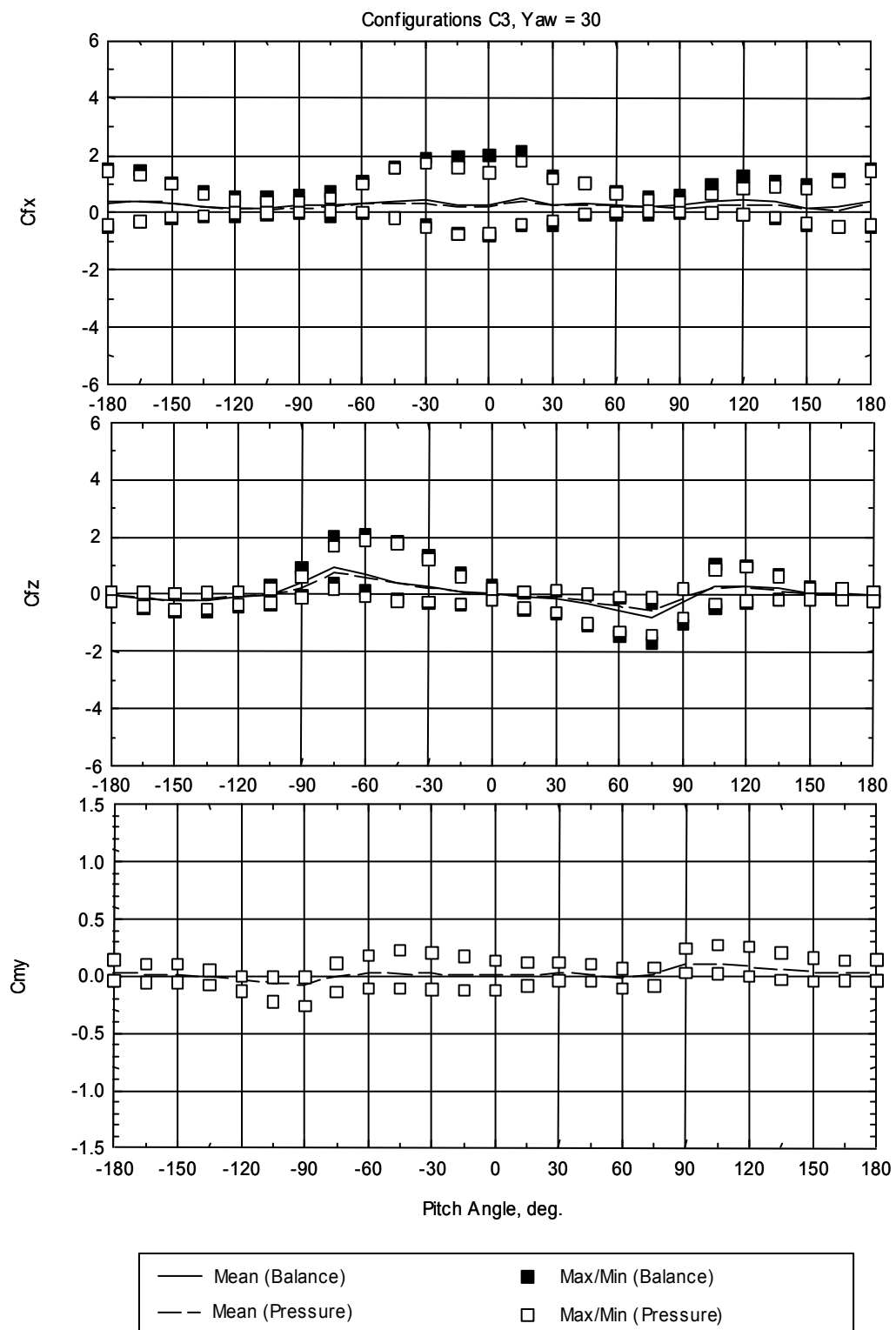


Figure 4-20c Loads on interior collector for Configuration C3, collector in Row 3 at Module Position 4 (from edge), yaw = 30 degrees

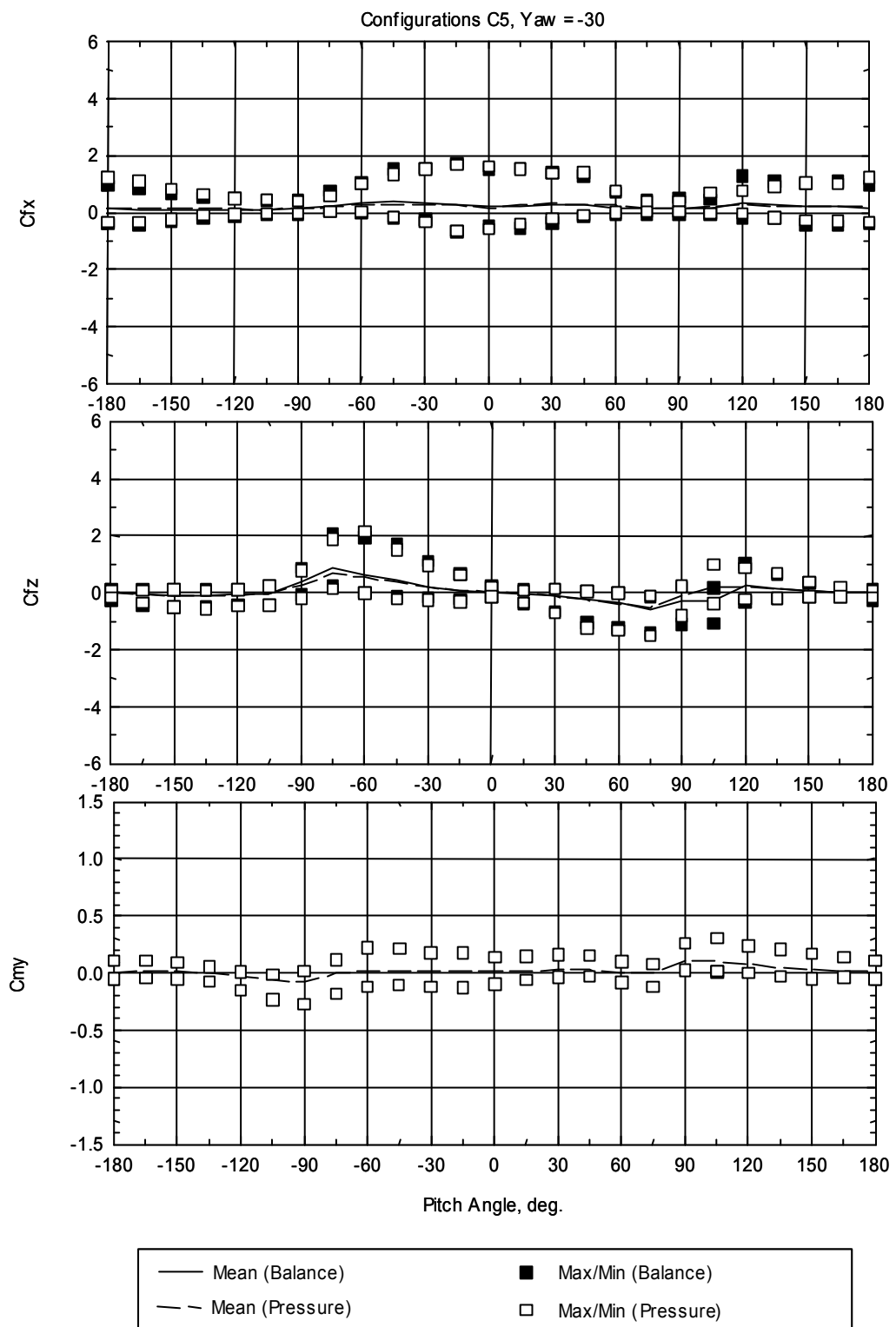


Figure 4-21a Loads on interior collector for Configuration C5, collector in Row 5 at Module Position 4 (from edge), yaw = - 30 degrees

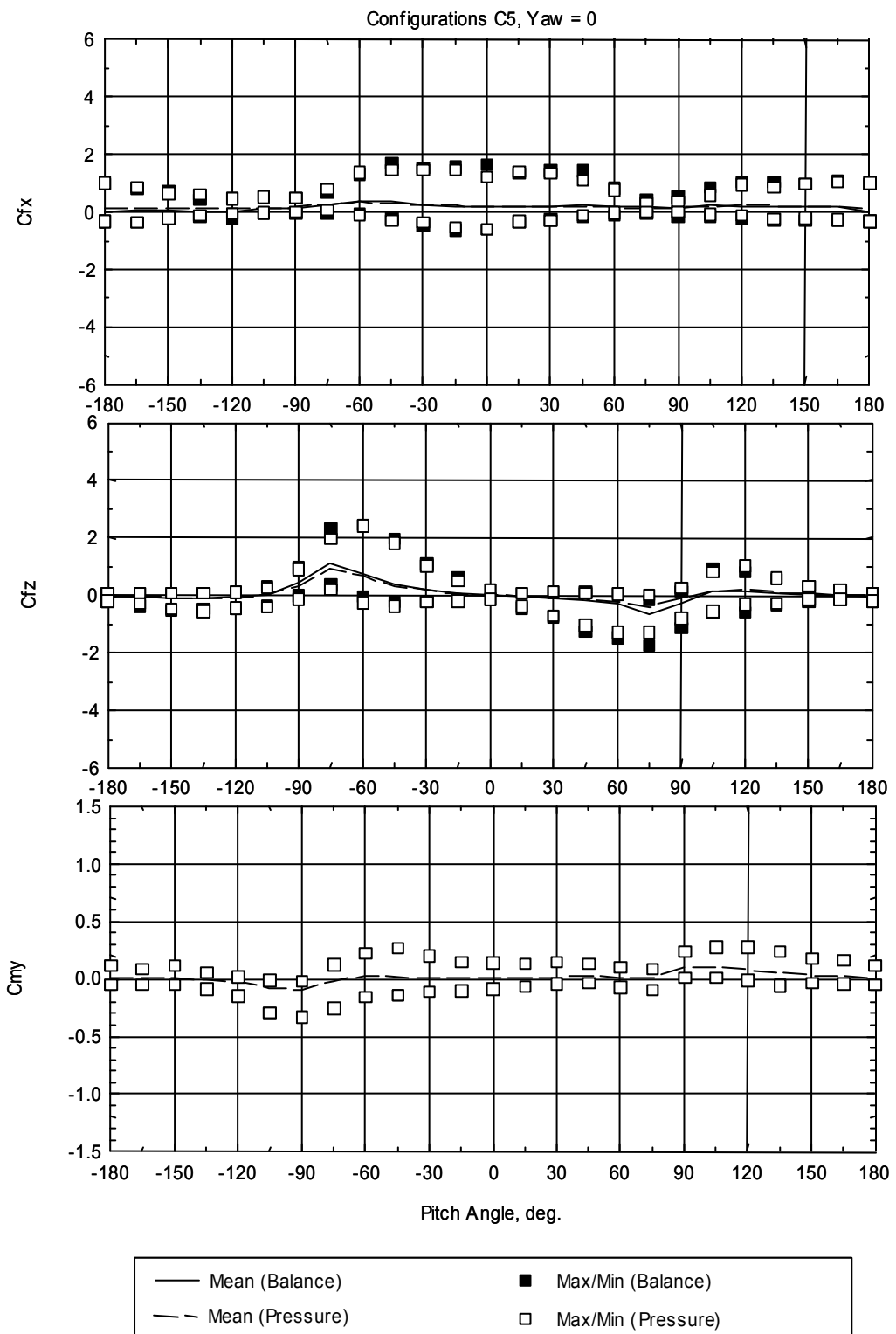


Figure 4-21b Loads on interior collector for Configuration C5, collector in Row 5 at Module Position 4 (from edge), yaw = 0 degrees

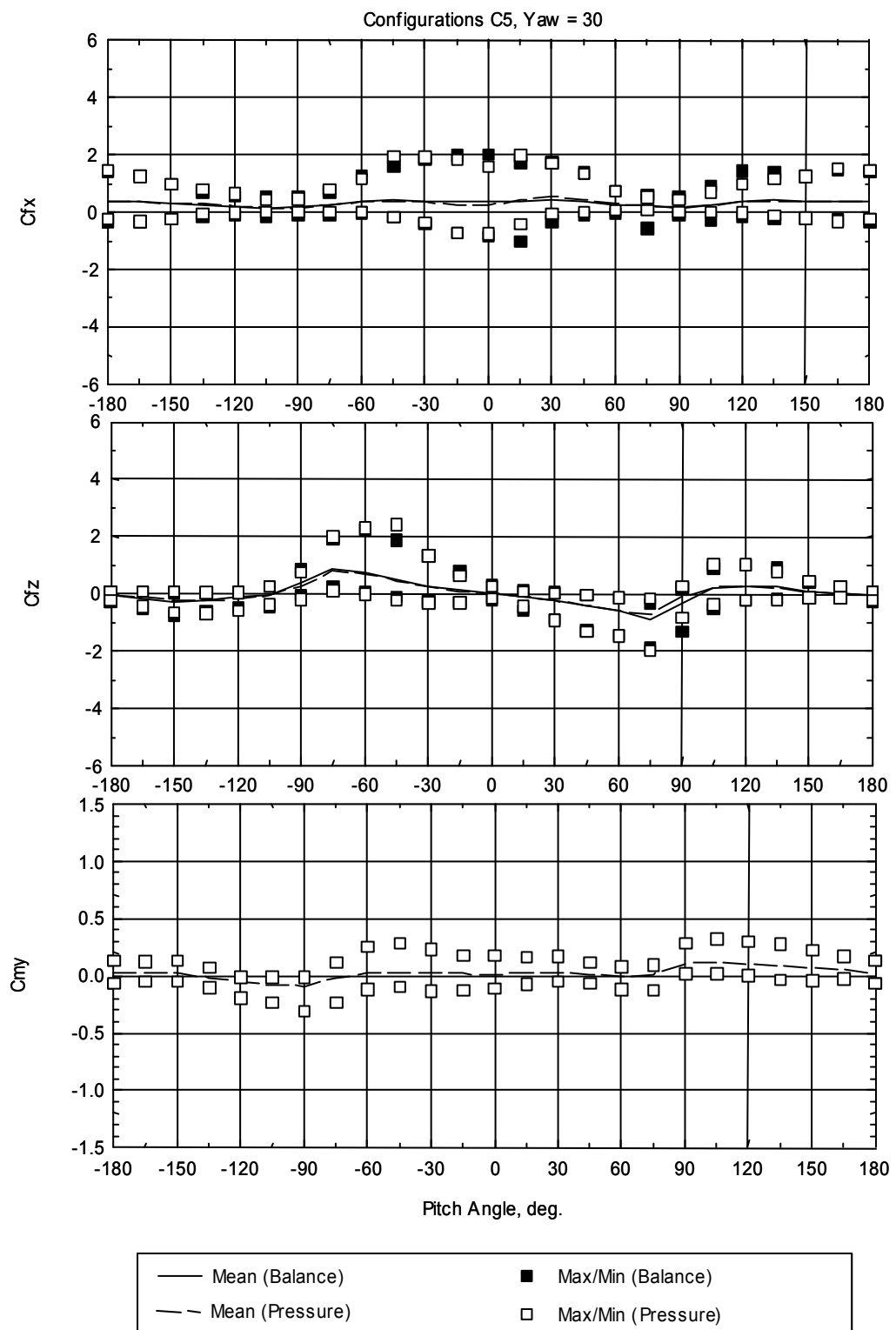


Figure 4-21c Loads on interior collector for Configuration C5, collector in Row 5 at Module Position 4 (from edge), yaw = 30 degrees

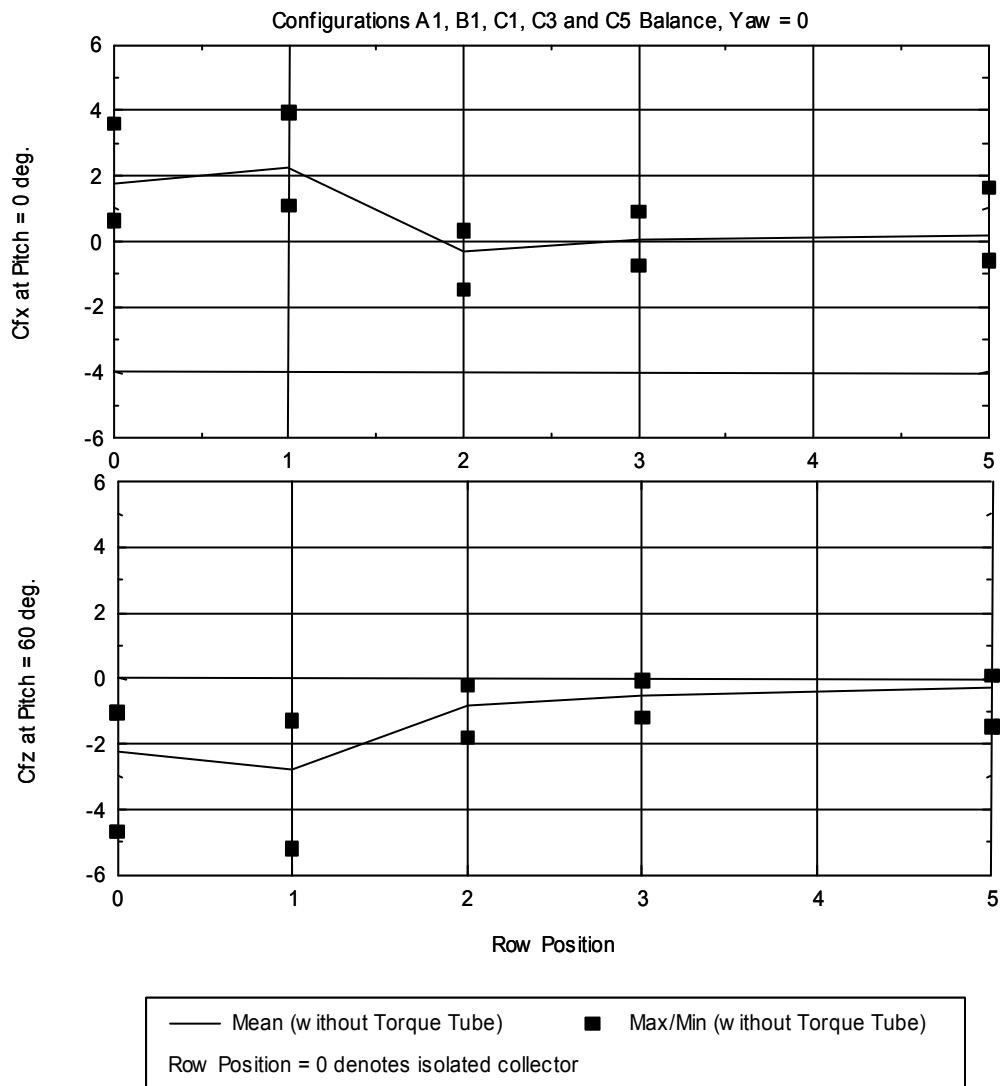
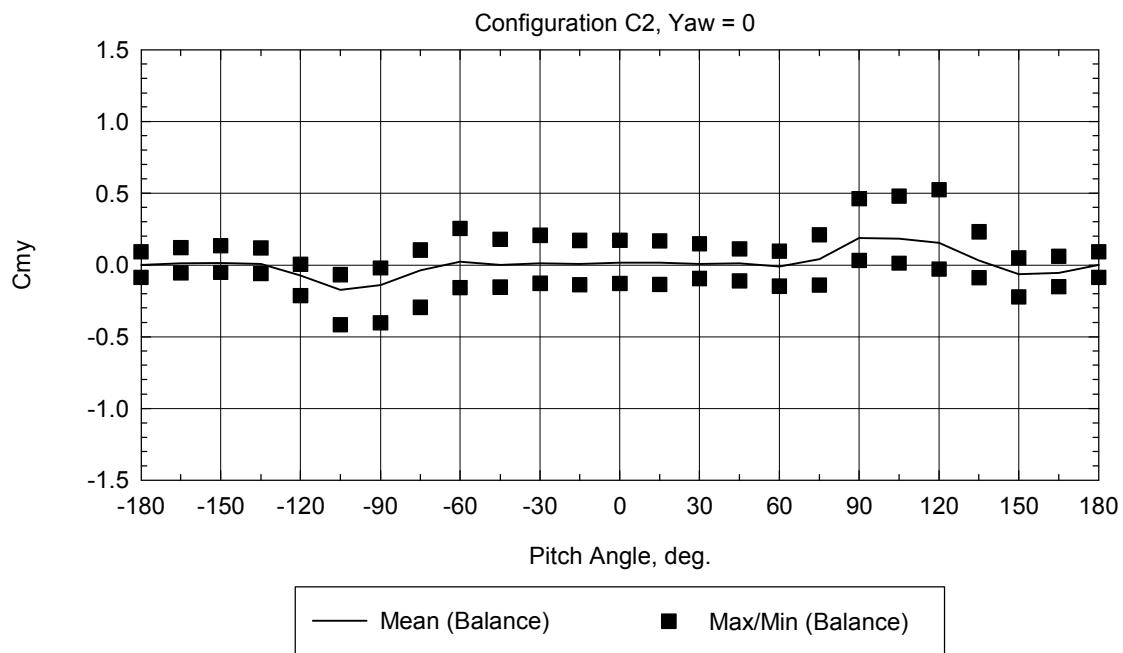
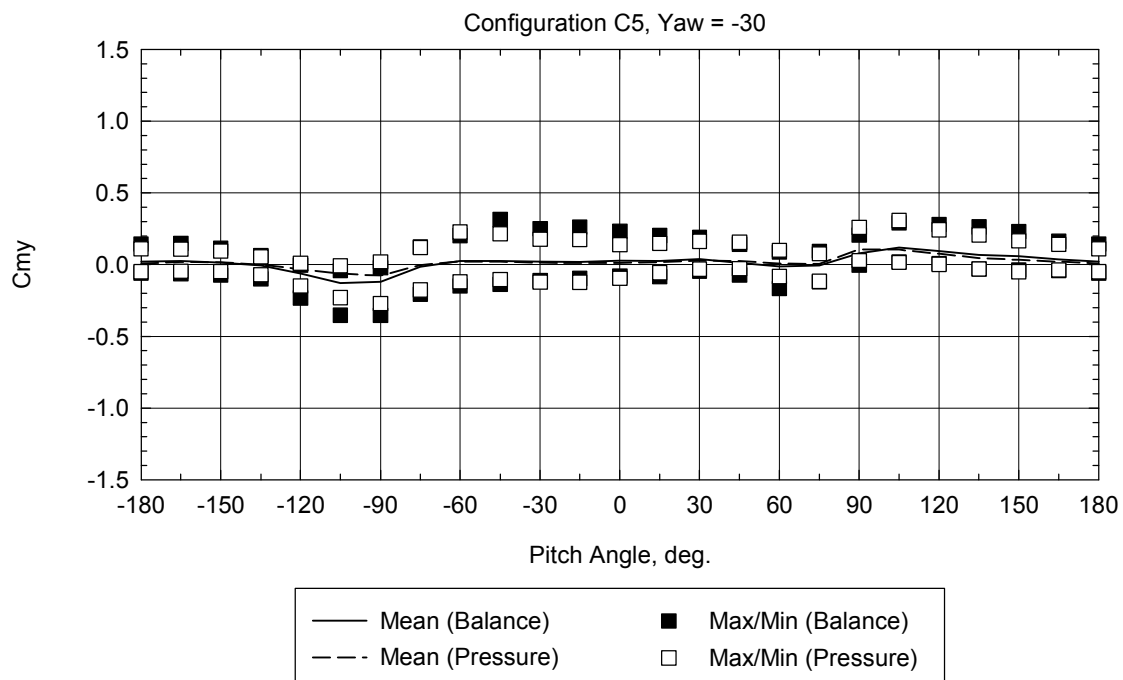


Figure 4-22 Effect of row position at interior of array field, yaw = 0 degrees



**Figure 4-23 Pitching Moment of Interior Collector
(a) Configuration C2, Yaw = 0 degrees**



**Figure 4-23 Pitching Moment of Interior Collector
(b) Configuration C5, Yaw = -30 degrees**

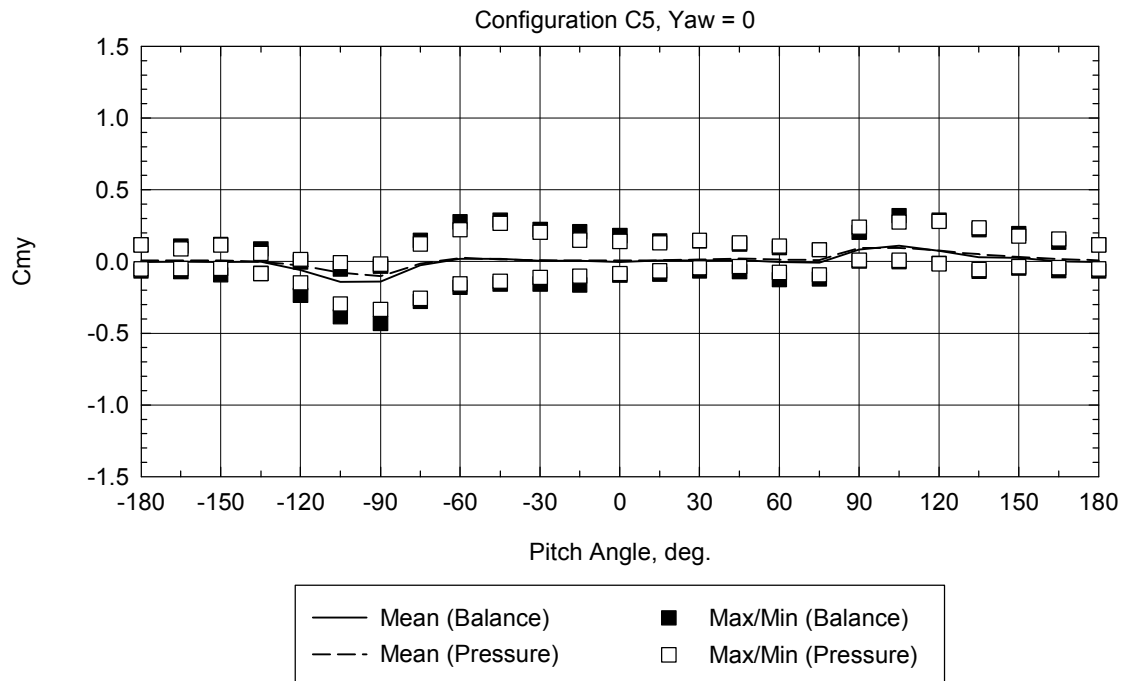


**Figure 4-23 Pitching Moment of Interior Collector
(c) Configuration C5, Yaw = 0 degrees**

A photograph of the flow in the deep interior of the array field is shown in Figure 4-24. At approximately the height of the concentrator pivot axis, the flow is very stagnant.

The Phase 3 balance test results on the interior solar collectors near the side edge of the array field are given in Figure 4-25 through Figure 4-27, for Configurations C2, C4, and C6. In general, the effect of the row position is similar to that for the collectors in the further interior. Some increase in the wind loads is seen, however, compared to the inner collectors.



Figure 4-24 Wind flow within interior of array field

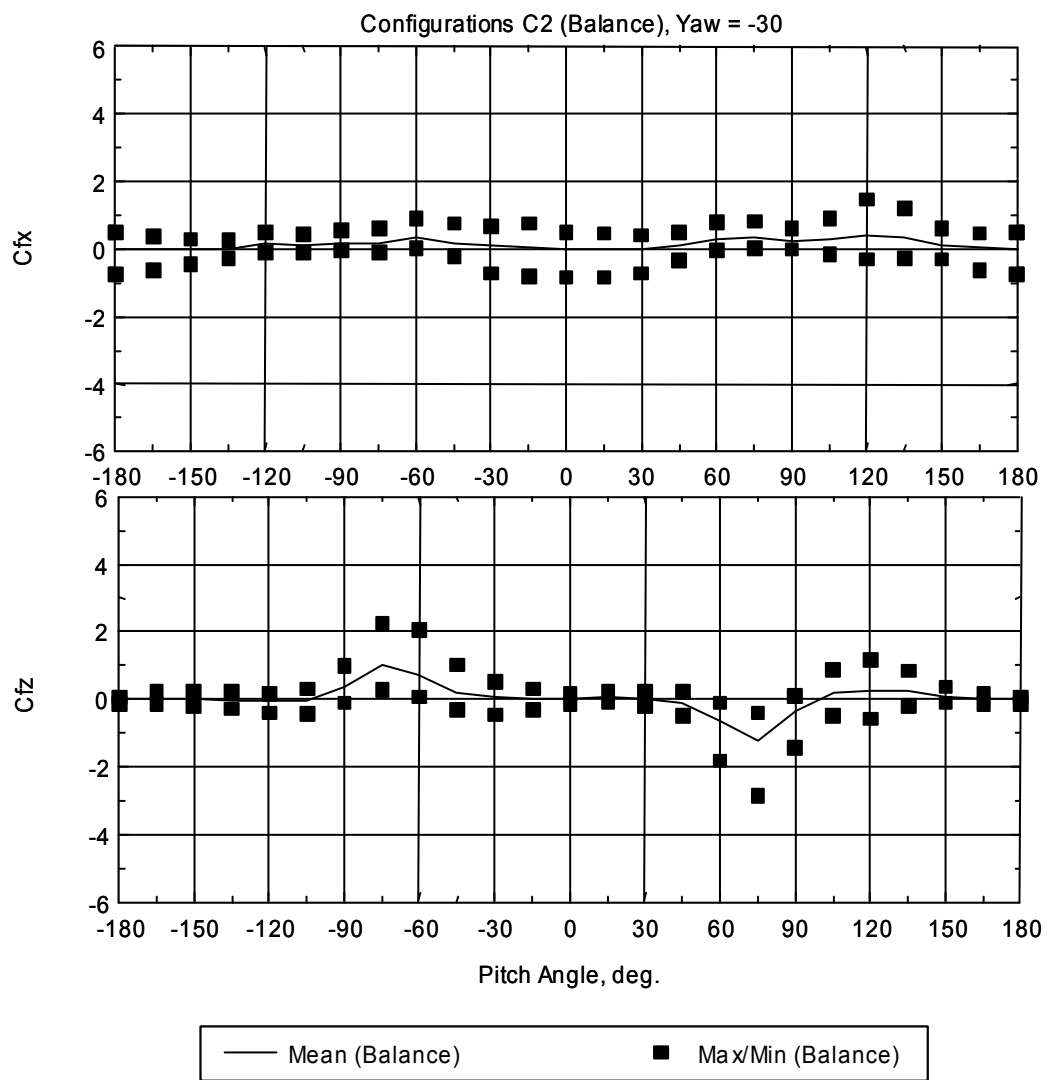


Figure 4-25a Loads on interior collector for Configuration C2, collector in Row 2 at Module Position 2 (from edge), yaw = - 30 degrees

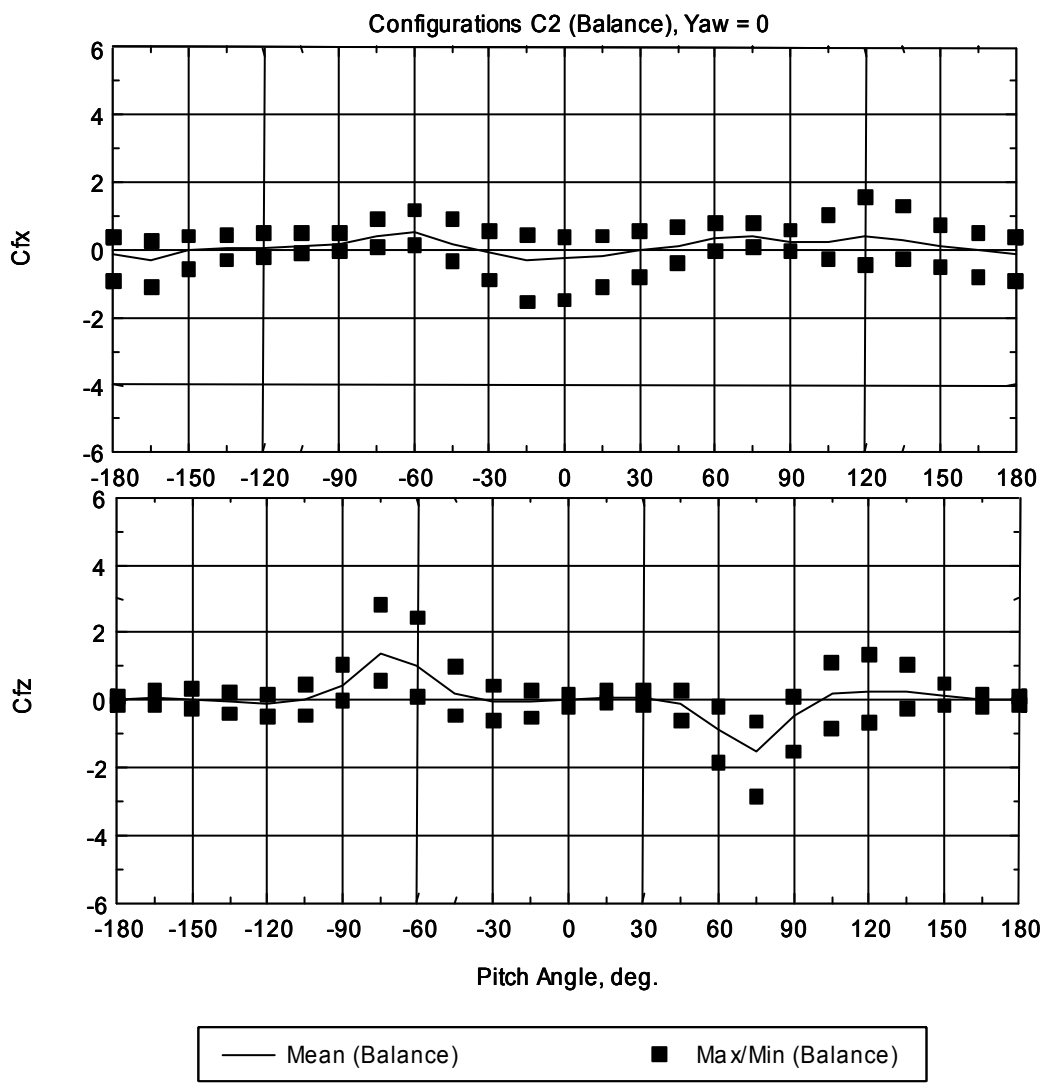


Figure 4-25b Loads on interior collector for Configuration C2, collector in Row 2 at Module Position 2 (from edge), yaw = 0 degrees

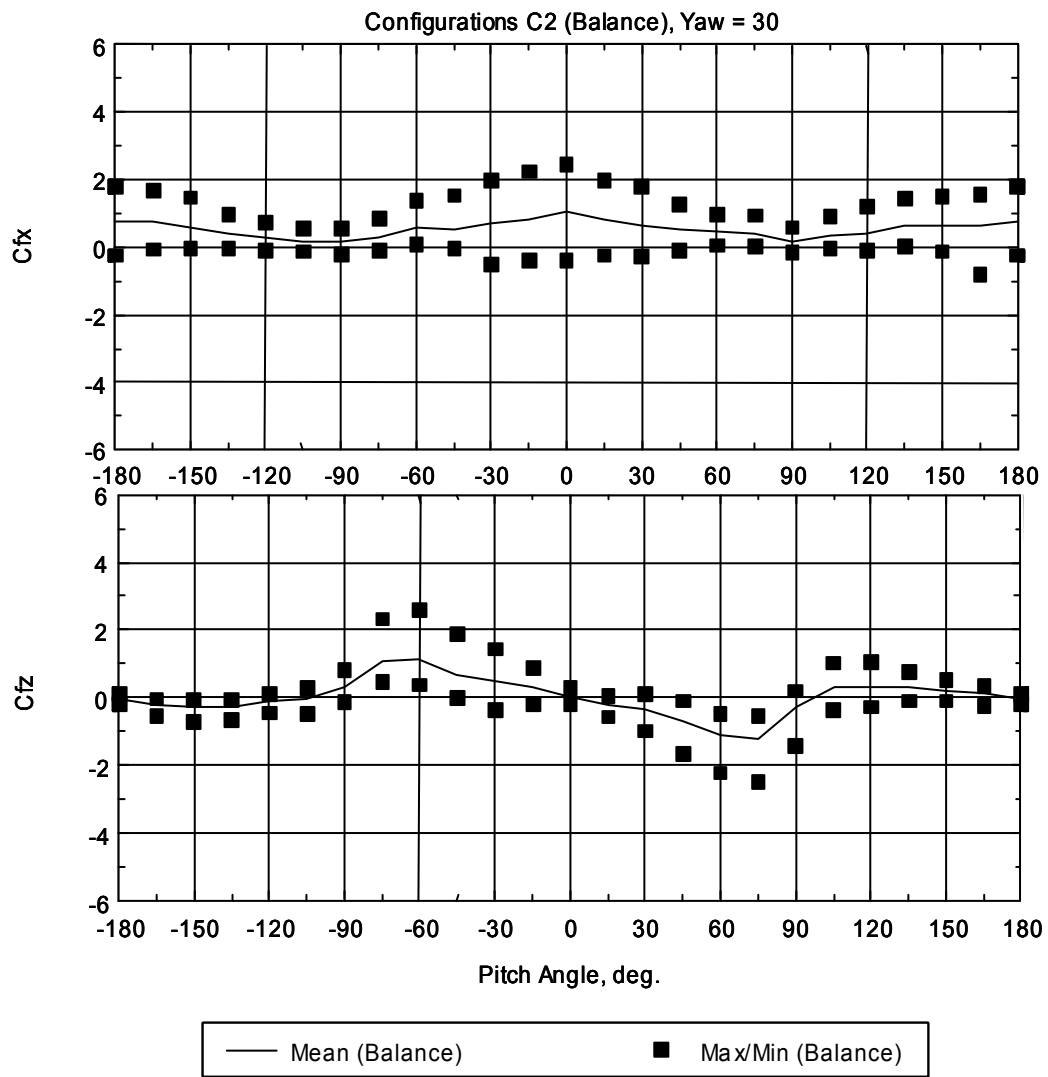


Figure 4-25c Loads on interior collector for Configuration C2, collector in Row 2 at Module Position 2 (from edge), yaw = 30 degrees

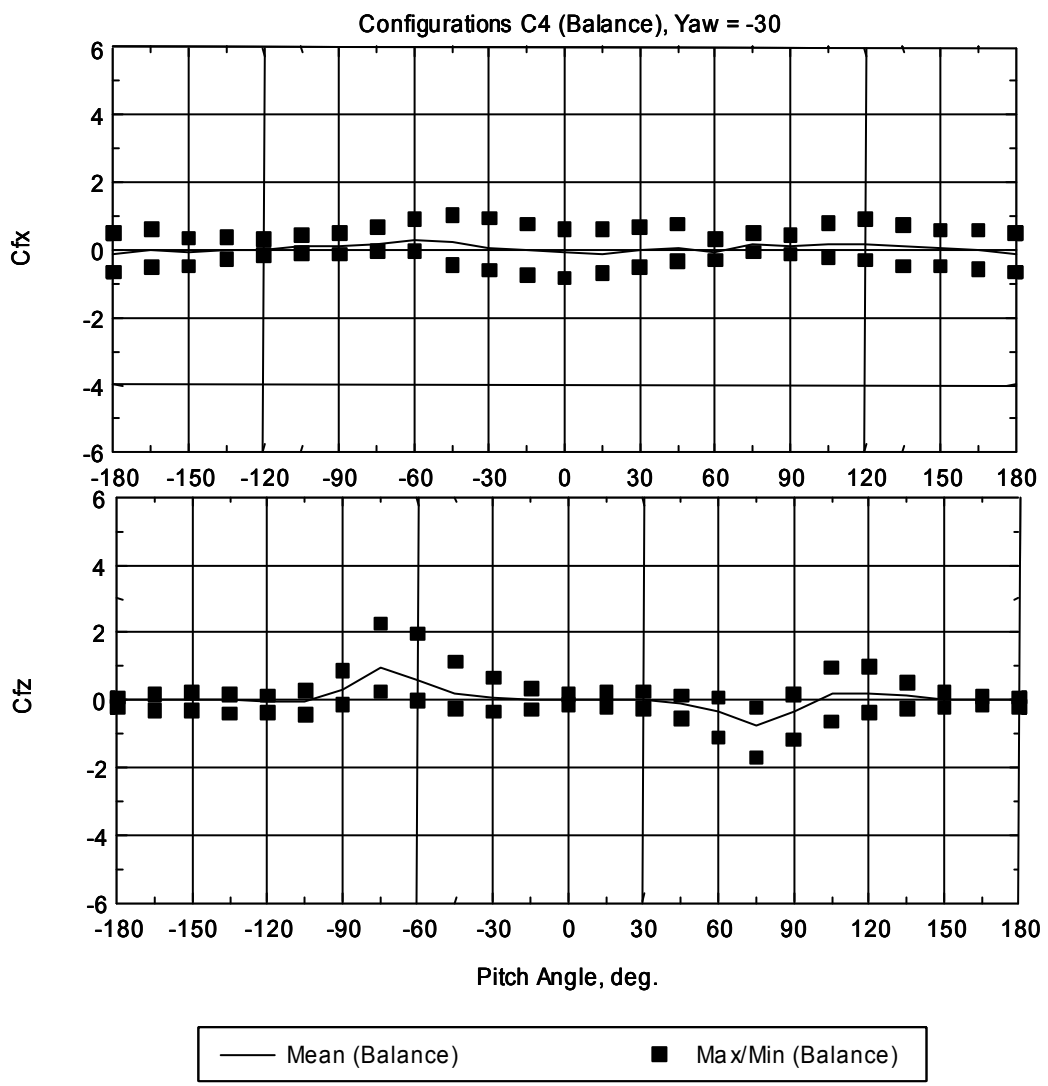


Figure 4-26a Loads on interior collector for Configuration C4, collector in Row 3 at Module Position 2 (from edge), yaw = - 30 degrees

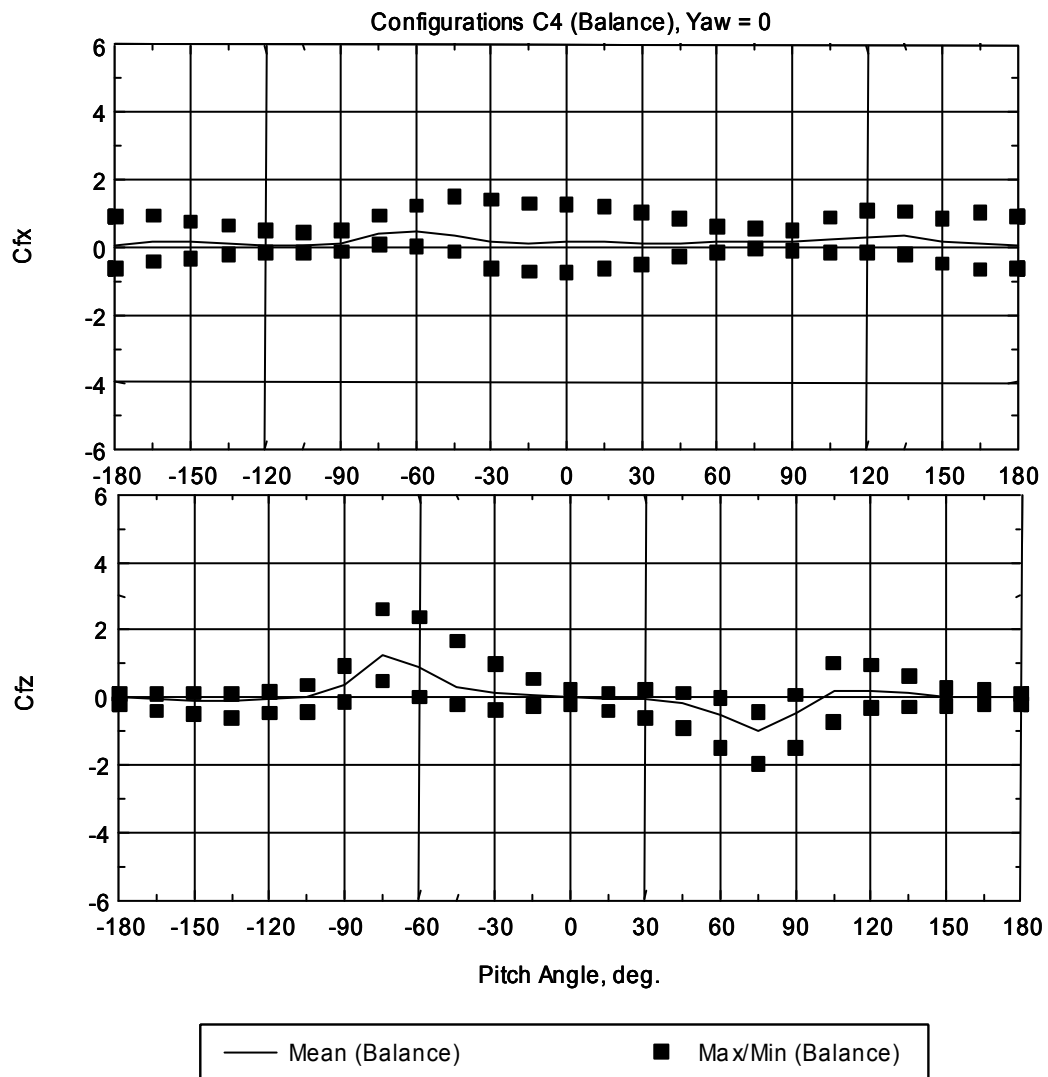


Figure 4-26b Loads on interior collector for Configuration C4, collector in Row 3 at Module Position 2 (from edge), yaw = 0 degrees

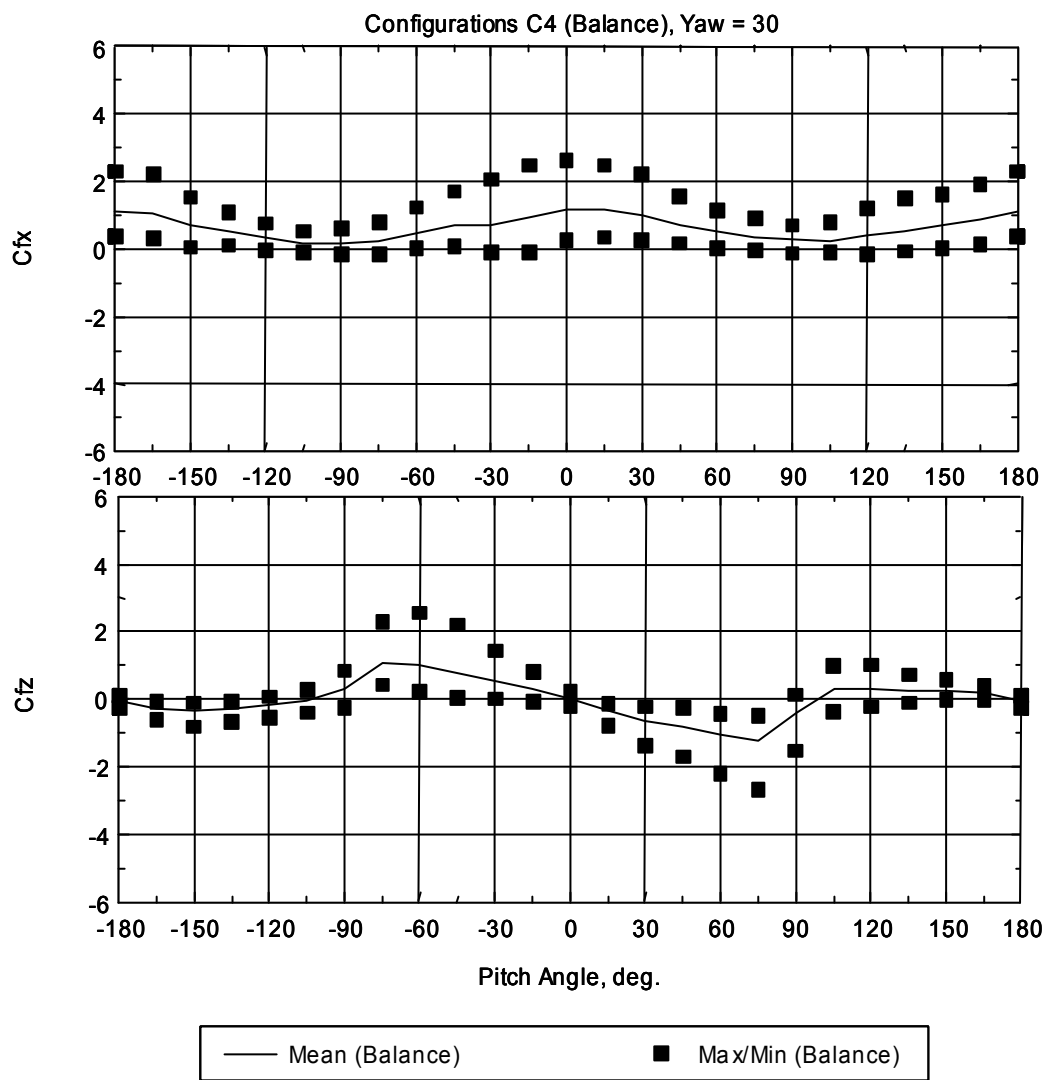
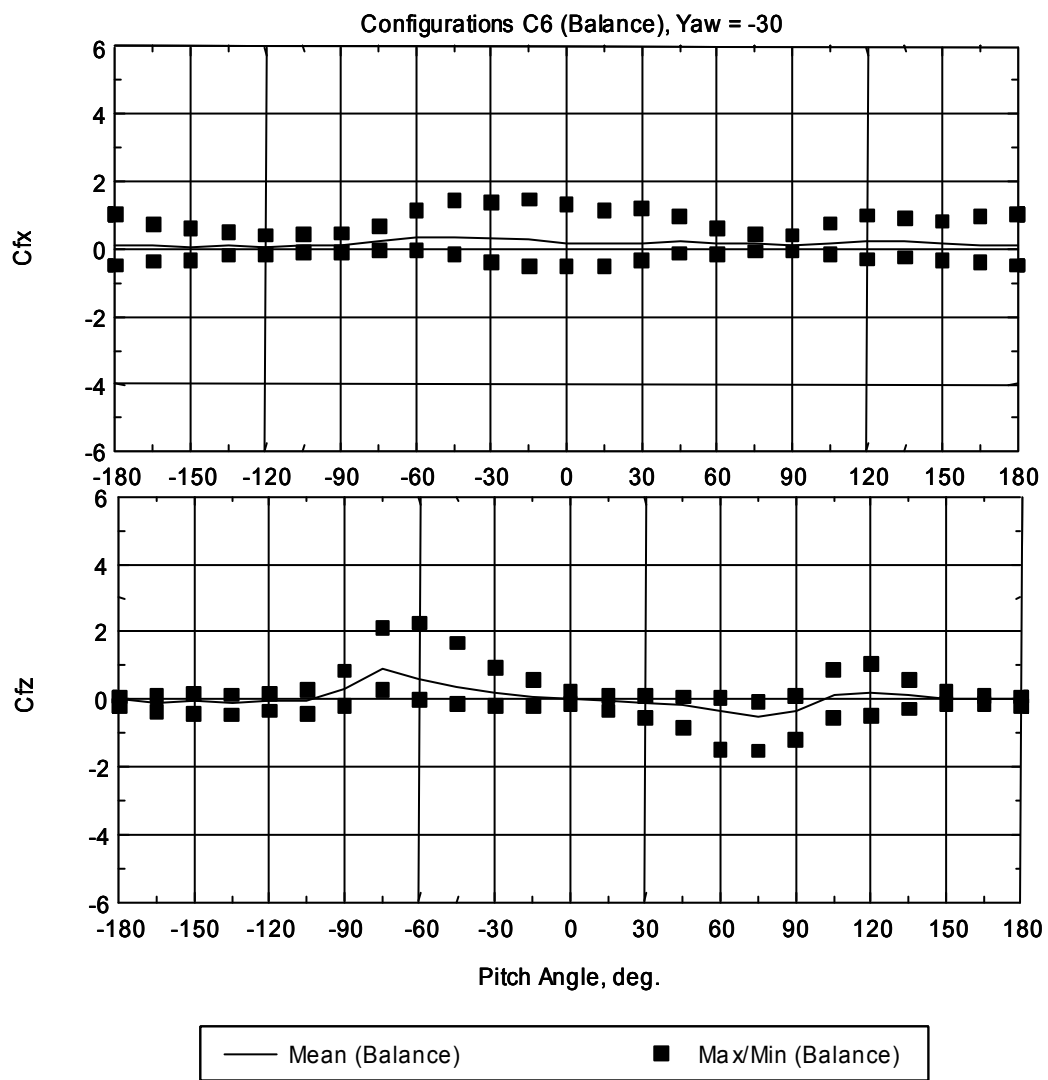


Figure 4-26c Loads on interior collector for Configuration C4, collector in Row 3 at Module Position 2 (from edge), yaw = 30 degrees



**Figure 4-27a Loads on interior collector for Configuration C6,
collector in Row 5 at Module Position 2 (from edge), yaw = - 30 degrees**

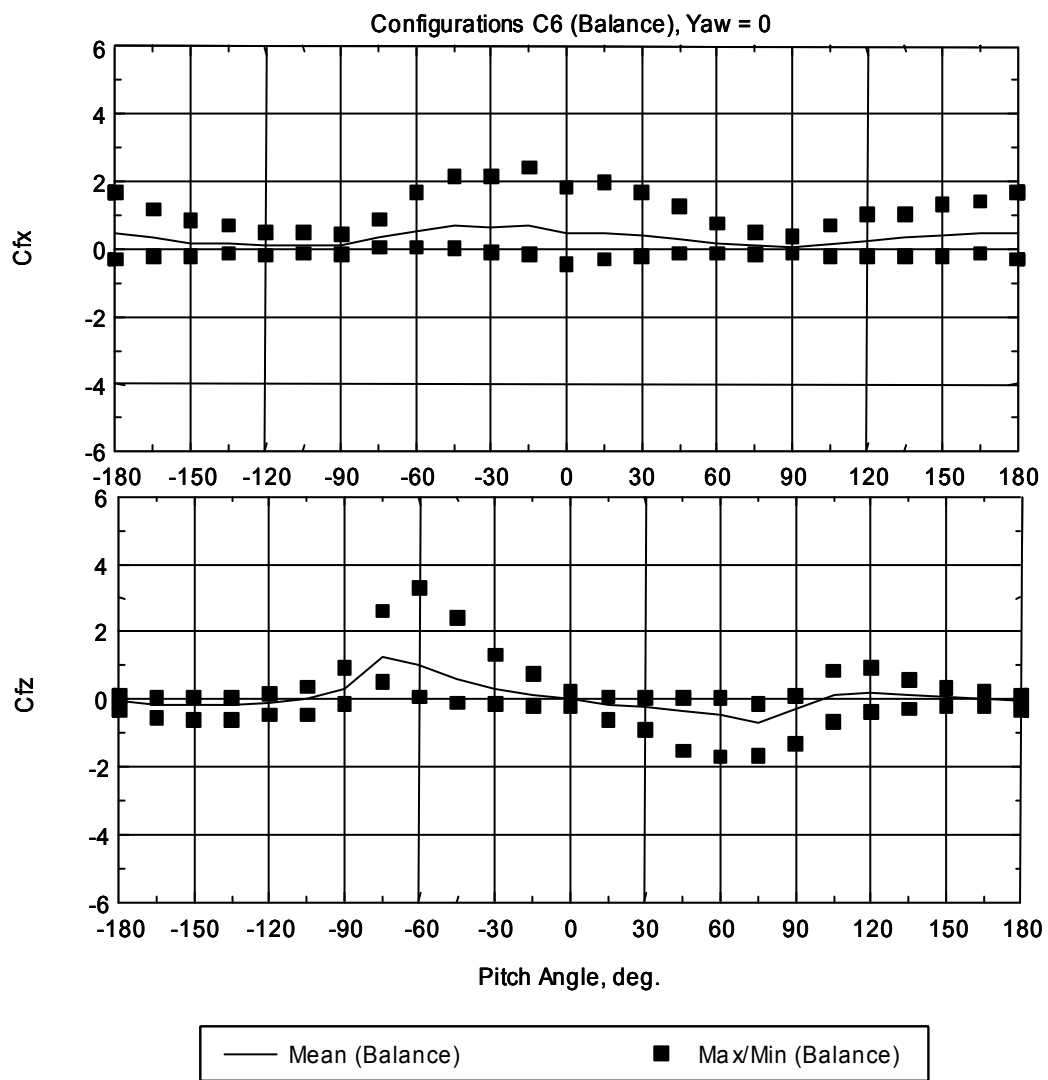


Figure 4-27b Loads on interior collector for Configuration C6, collector in Row 5 at Module Position 2 (from edge), yaw = 0 degrees

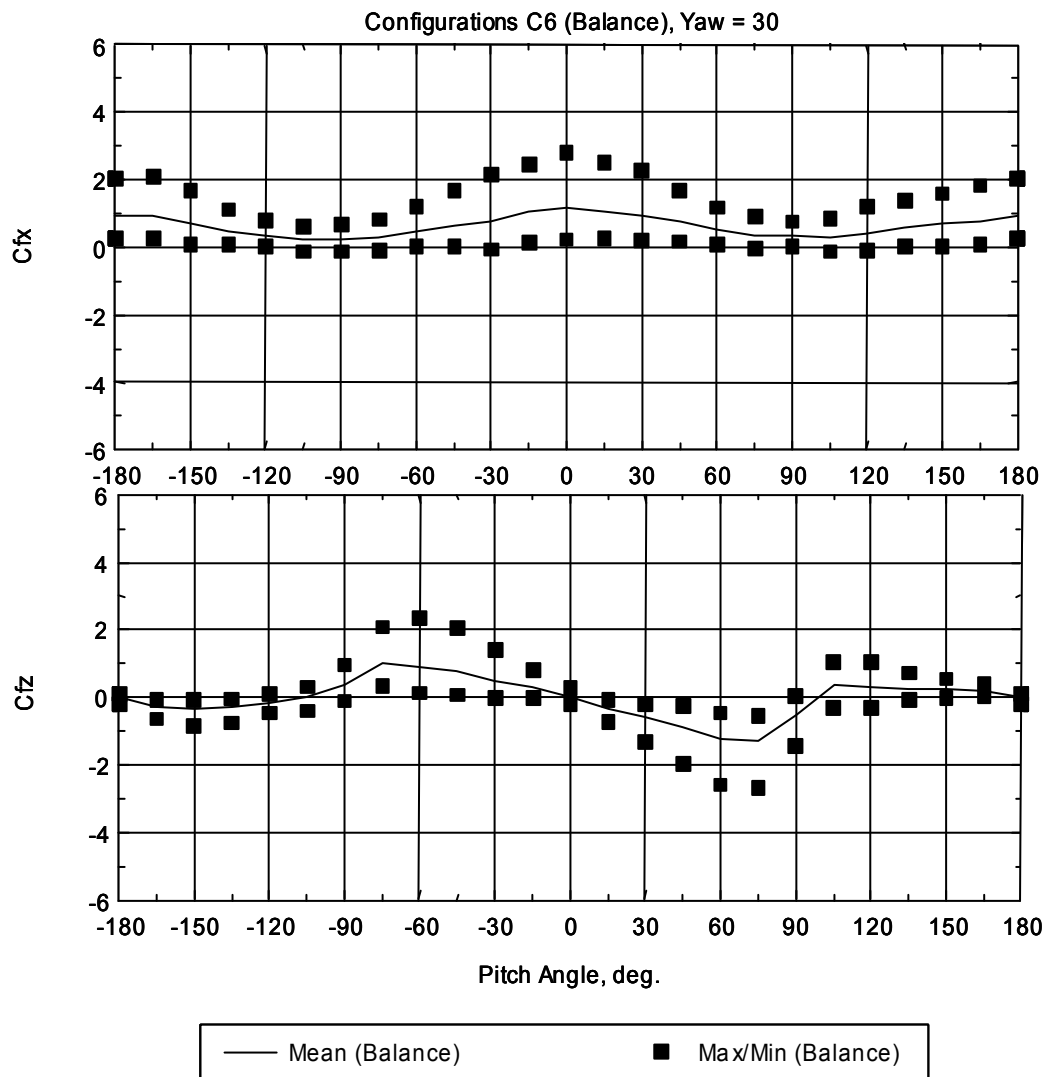
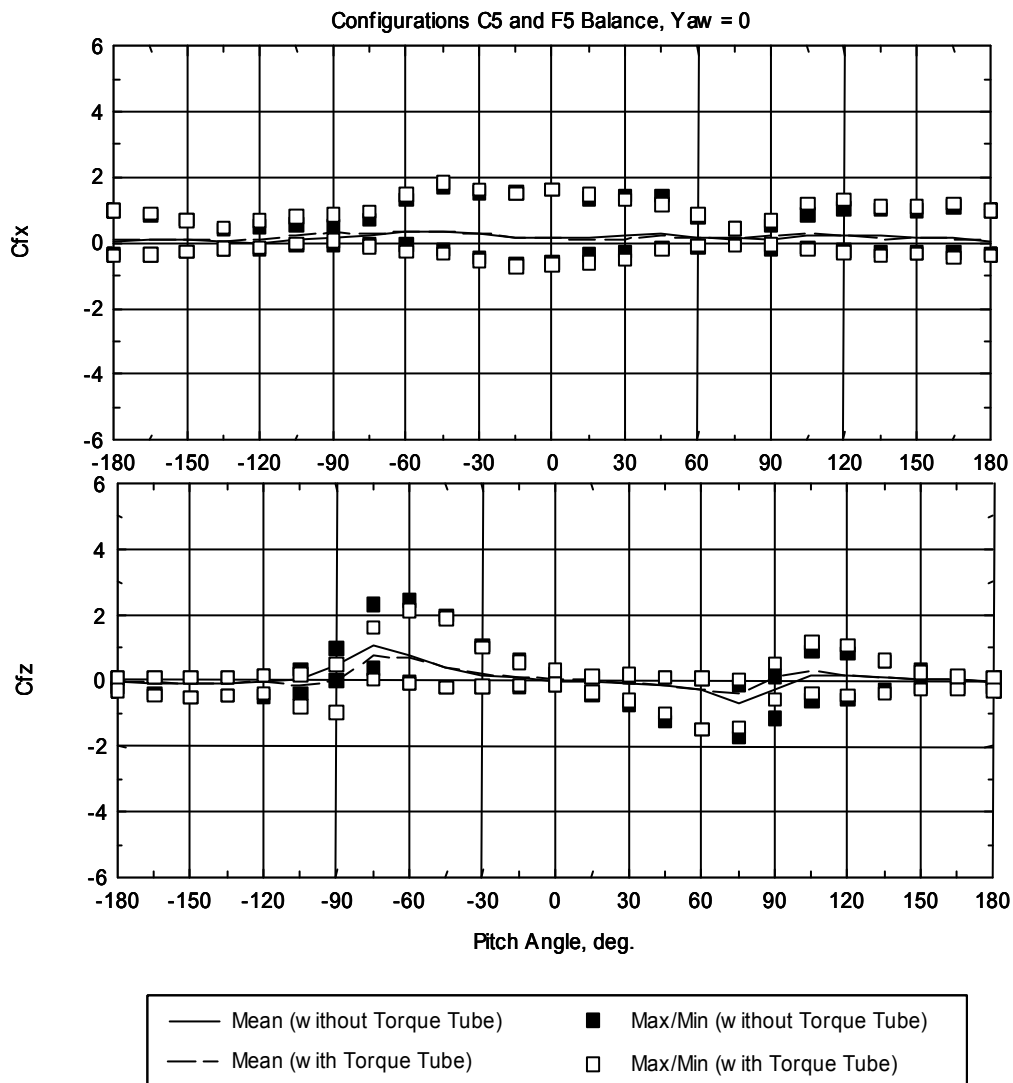


Figure 4-27c Loads on interior collector for Configuration C6, collector in Row 5 at Module Position 2 (from edge), yaw = 30 degrees

4.5.2 Effects of Torque Tube

The effect of the torque tube on the most interior solar collector is shown in Figure 4-28. As far as the structural design loads are concerned, the torque tube caused no significant effect.



**Figure 4-28 Effect of torque tube on collector in array field,
Configurations C5 and F5, yaw = 0 degrees**

4.6 Loads on Deep Interior Solar Collectors

In order to determine wind loads that can be regarded as representative for a majority of the solar collector modules within a large array field, tests were conducted on a collector module at various row and column positions. Pressure distributions over the collector module concentrator were measured, which were then integrated to yield the overall forces and pitch moment. Refer to Section 2.4 for the tested locations of the solar collector module within the array field.

At each row and column combination, the wind-tunnel test was performed for pitch angles of -15, -60, 0, 75 and 105 degrees, at which the Phase 3 wind-tunnel study showed relatively large wind loads. For sake of clarity, however, this section selectively presents the test results based on the significance found for the individual overall load components exerted on the pivotal axis of the collector concentrator. The following discussion deals with the lateral and vertical forces and the pitching moment at particular pitch angles of 0, -60 and 105 degrees, respectively. A complete set of the test results is found in Appendix B.

Variations of the mean and peak loads at different row positions are shown in Figure 4-29 for the 4th column collectors at a yaw angle of 0 degrees. The Phase 3 pressure model test results, where available, are included to show the load pattern on the collectors near the upwind edge of the array field (1st through 4th rows). Note that at the 5th row position, both the Phase 3 and 4 test results are plotted, showing a good repeatability in the mean load measurement, and some scatter in the peaks due to inherent statistical variability. For the lateral force, C_{fx} , at a pitch angle of 0 degrees, the most drastic reduction is realized on the 2nd row collector, and the load tends to recover somewhat for the collectors up to the 5th row. No appreciable change in the lateral force is evident for the collectors further downwind. The vertical force component, C_{fz} , at a pitch angle of -60 degrees shows a similar trend, except that the recovery of the peak load is more vigorous. In fact, the positive peak on the interior collectors is nearly as large as that on the collector at the field edge. The pitching moment component, C_{my} , appears to decrease slowly through the 5th row collector, and becomes independent of the row position downwind.

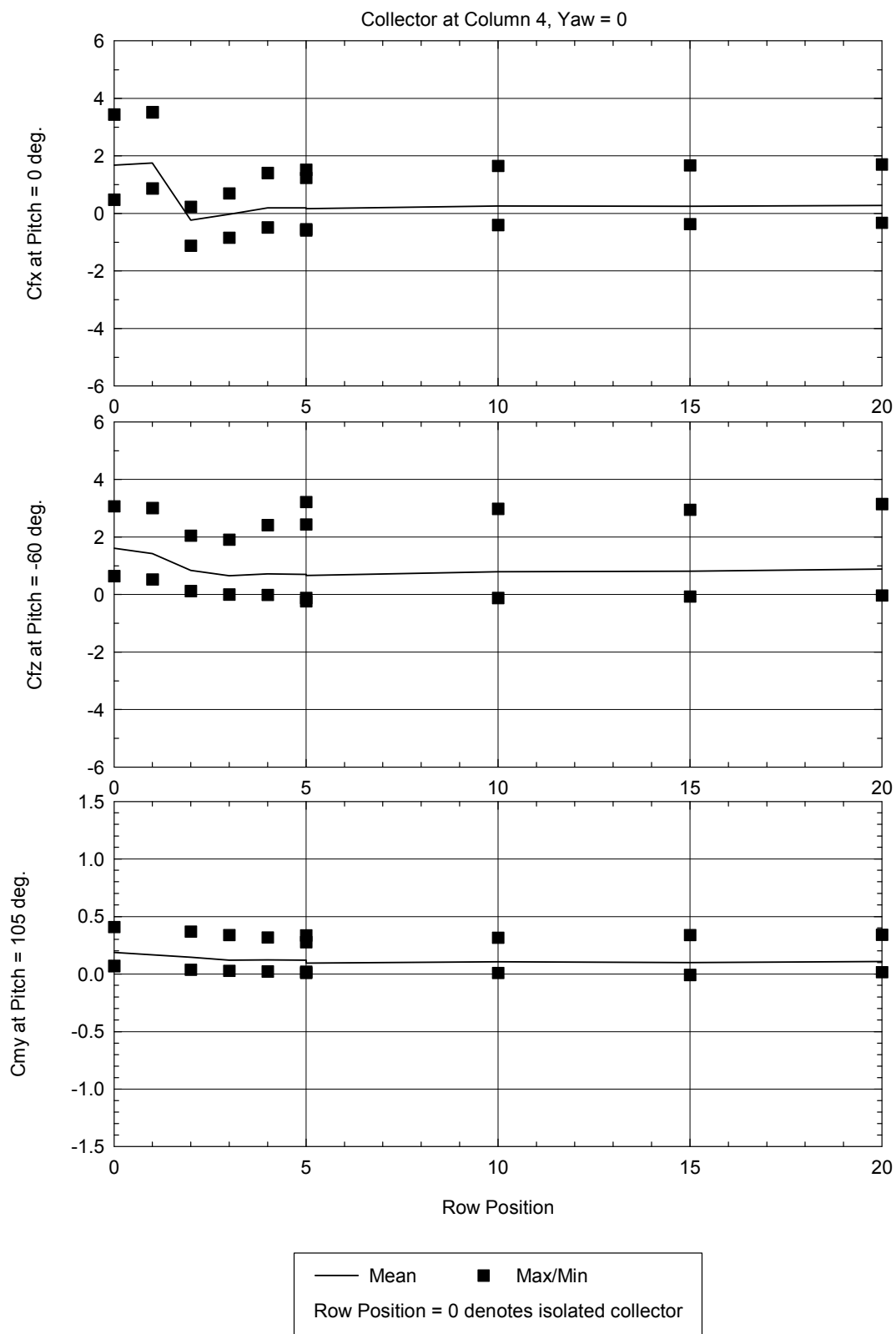


Figure 4-29 Effect of Row Position for Collectors at 4th Column, Yaw = 0 degrees

Some observations can be made here. The change in the overall loads seems to take place through the 5th row from the upwind edge of the array field. The mean loads tend to decrease continually through the 5th row where they reach their minimum, regardless of the pitch angle. The dynamic loads, however, are amplified within the interior of the field in some cases, resulting in negligible reduction in the effective peak design load. This is especially true when the collectors are at near horizontal stow position, i.e., a pitch angle of -60 degrees. The load characteristics are directly related to those of the wind within the array field. This is discussed more in the following section.

Figure 4-30 shows the loads on the interior solar collectors at the 4th column for a yaw of 30 degrees. The general trend of the load variation is similar to that at 0 degree yaw angle. The effect of the row position for the collectors at the 8th and 12th column from the side edge of the array is depicted in Figure 4-31 through Figure 4-33. In all cases, the variation of the loads beyond the 5th row is small. It appears that the loads on the solar collector at the 5th row position are well representative for the entire array field. Comparing Figure 4-30, Figure 4-32, and Figure 4-33, it is noticed that the sensitivity of the loads to the column position is almost negligible in the range tested.

Although it was initially hoped to derive an empirical formula that conveniently describes the design wind loads for the solar collector at an arbitrary location inside a large array field, the wind-tunnel test indicates considerable variations of the exact load pattern depending on the pitch angles and the load component of interest. In addition, the test indicates that the mean and dynamic load components vary differently within the field. While one can produce a set of empirical formulae to accommodate a variety of relevant parameters, it would not probably result in a practical design technique. The wind-tunnel tests performed for the Task 2 study, however, lead us to a rather definitive conclusion. That is, the wind loads on the interior solar collectors are essentially invariant beyond the 5th row and 4th column from the edge of the field. This implies that the loads measured for Configuration C5 represent typical design loads equally applicable to the rest of the interior solar collectors in the array field.

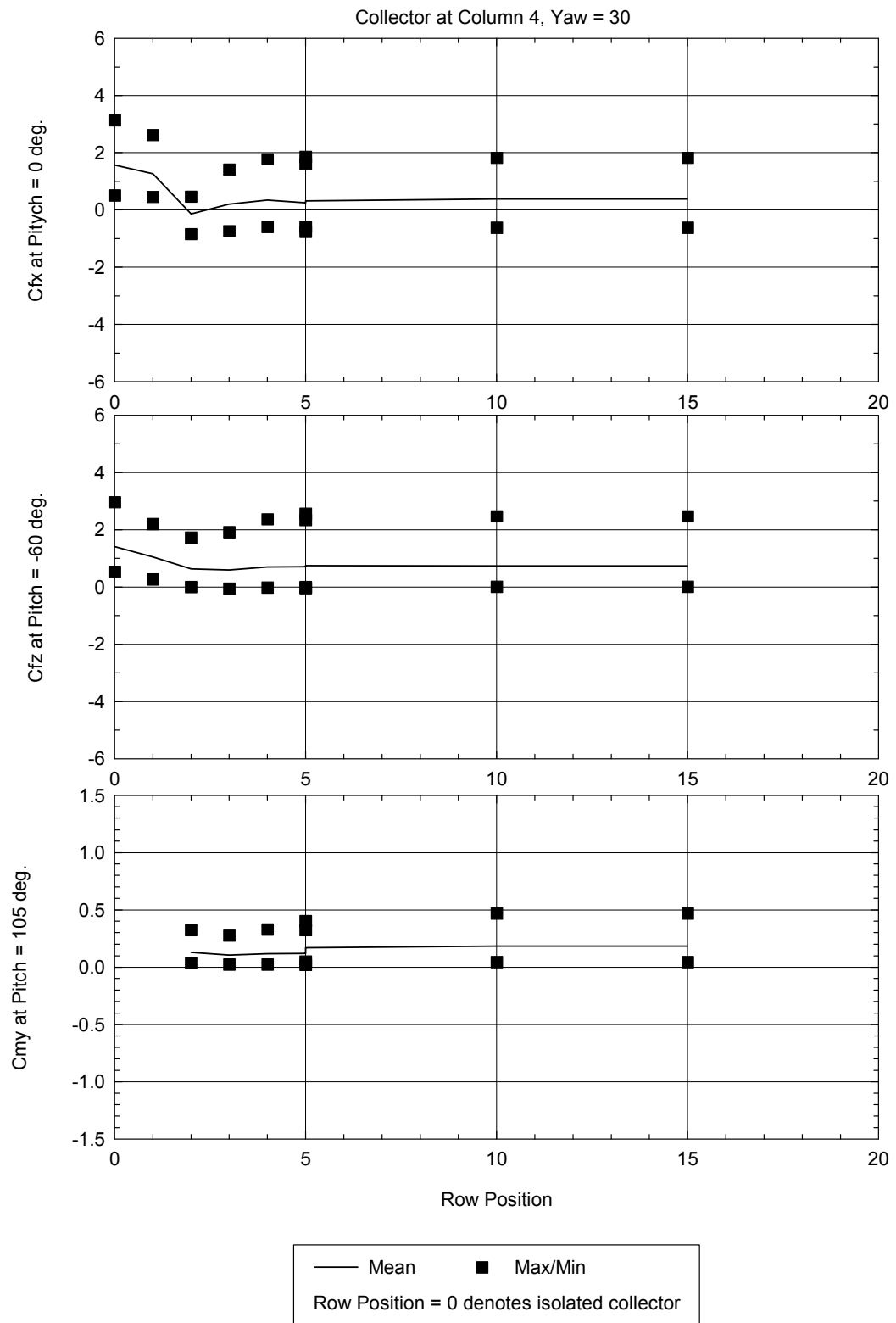


Figure 4-30 Effect of Row Position for Collectors at 4th Column, Yaw = 30 degrees

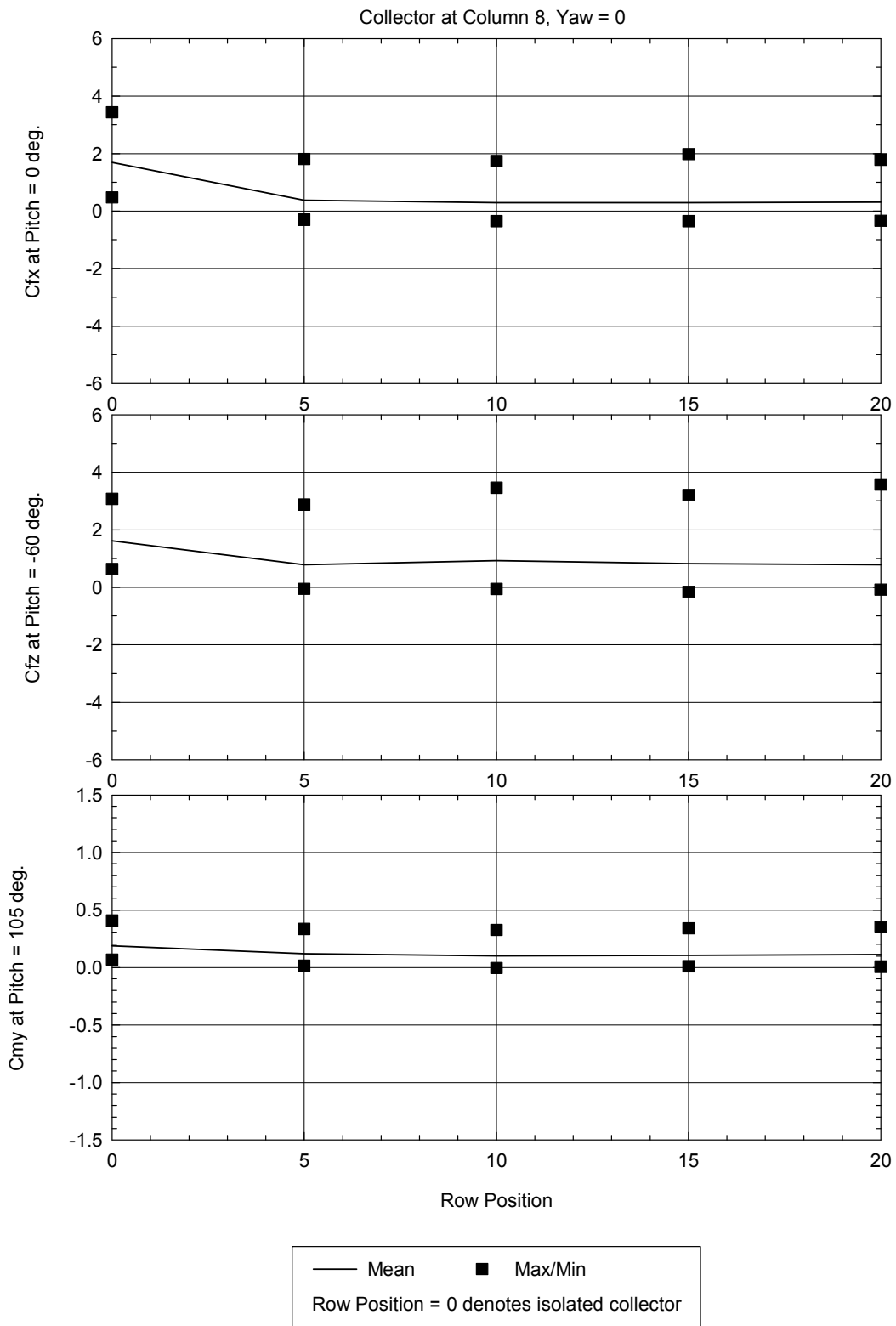


Figure 4-31 Effect of Row Position for Collectors at 8th Column, Yaw = 0 degrees

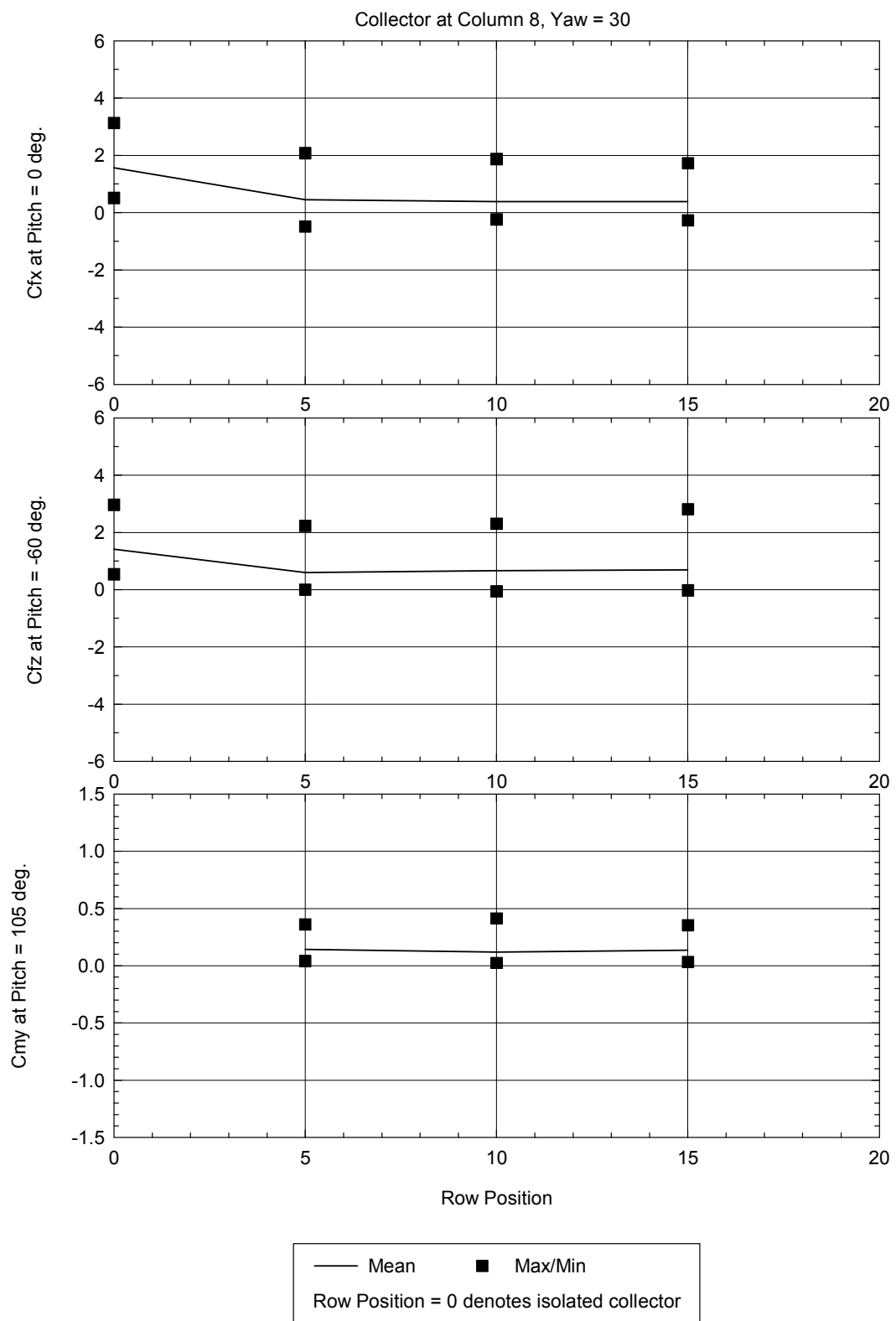
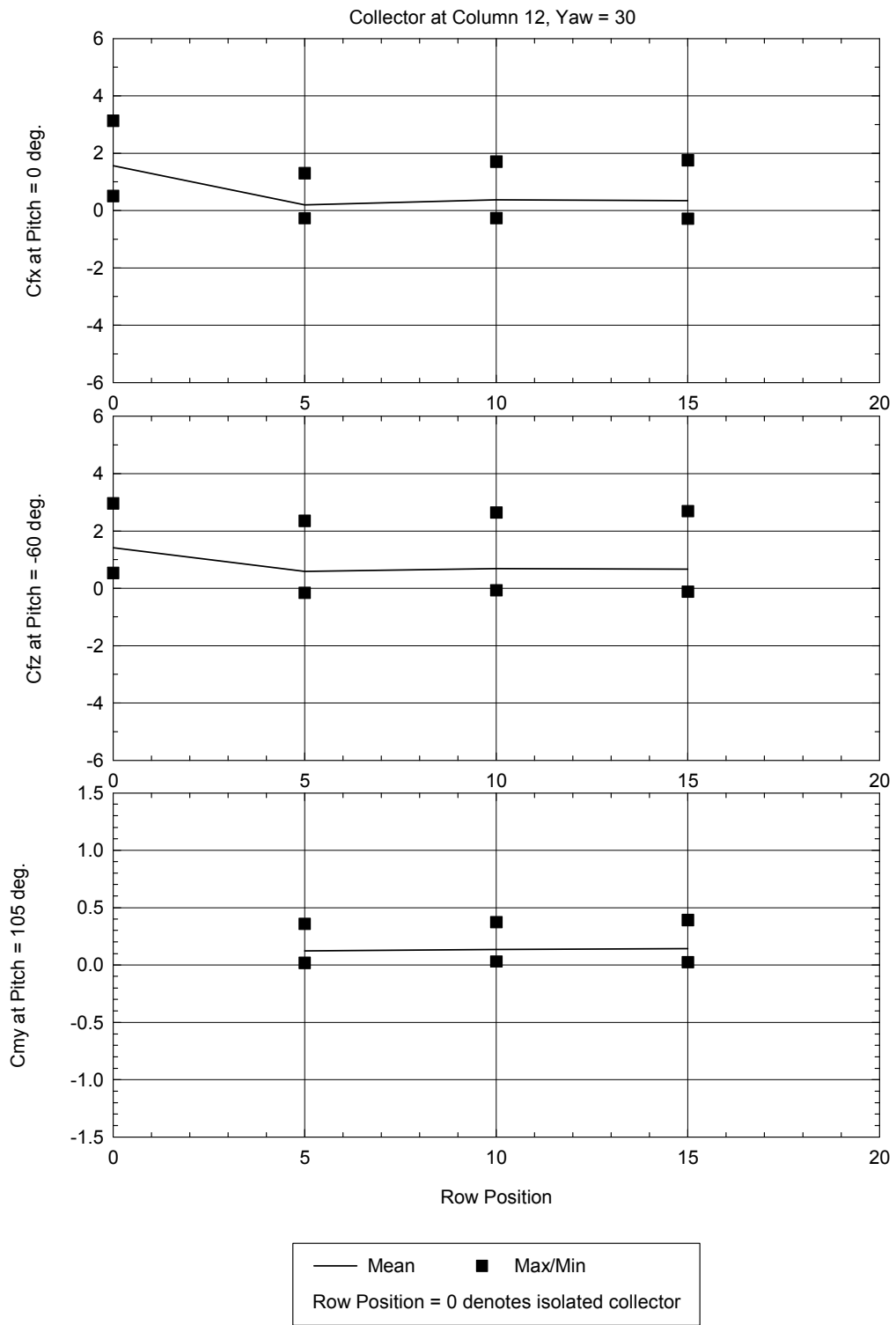


Figure 4-32 Effect of Row Position for Collectors at 8th Column, Yaw = 30 degrees



**Figure 4-33 Effect of Row Position for Collectors at 12th Column,
Yaw = 30 degrees**

4.7 Wind Characteristics Within Array Field

Vertical profiles of the mean wind speed and local turbulence intensity are given in Figure 4-34 (at the top and bottom, respectively) at various row positions within the array field. The undisturbed velocity profiles approaching the array field are also shown at the far left of the figure. All data were taken at a yaw angle of 0 degrees with the collectors rotated at pitch angles of 0 (Figure 4-34 (a)) and -60 (Figure 4-34 (b)) degrees. The mean wind speeds have been normalized relative to the speed at the collector pivot height of the approach wind. The figure clearly shows drastic reduction of the mean wind speed and increased turbulence intensity as the wind initially enters the array field. The shapes of the mean and turbulence intensity profiles seem to become invariant beyond the 5th row position. As expected, the mean wind speed over the collector height is much smaller when the collectors are at upright position (Figure 4-34 (a)) than at near stow position (Figure 4-34 (b)) due to increased blockage. Differences in the shapes of the turbulence intensity between the two collector positions are also noticeable.

The characteristics of the wind speed and turbulence intensity inside the array field are consistent with the resulting wind loads on the solar collectors described above. That is, the reduced mean loads and increased dynamic loads. Little variation of the wind loads beyond the 5th row position is also well explained by the wind profiles.

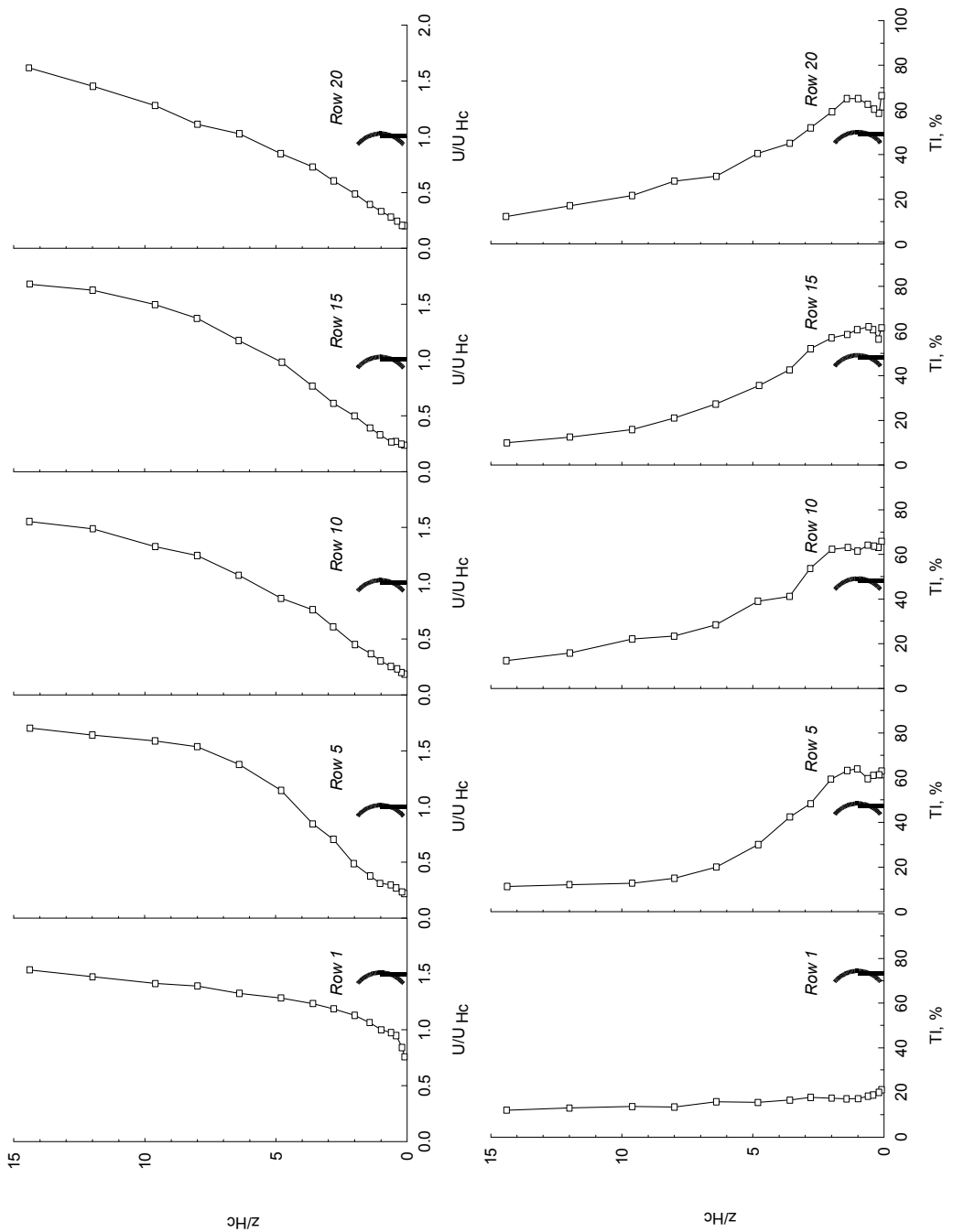


**Figure 4-34 Mean Velocity and Turbulent Profiles Within Array Field
(a) Pitch = 0 deg**

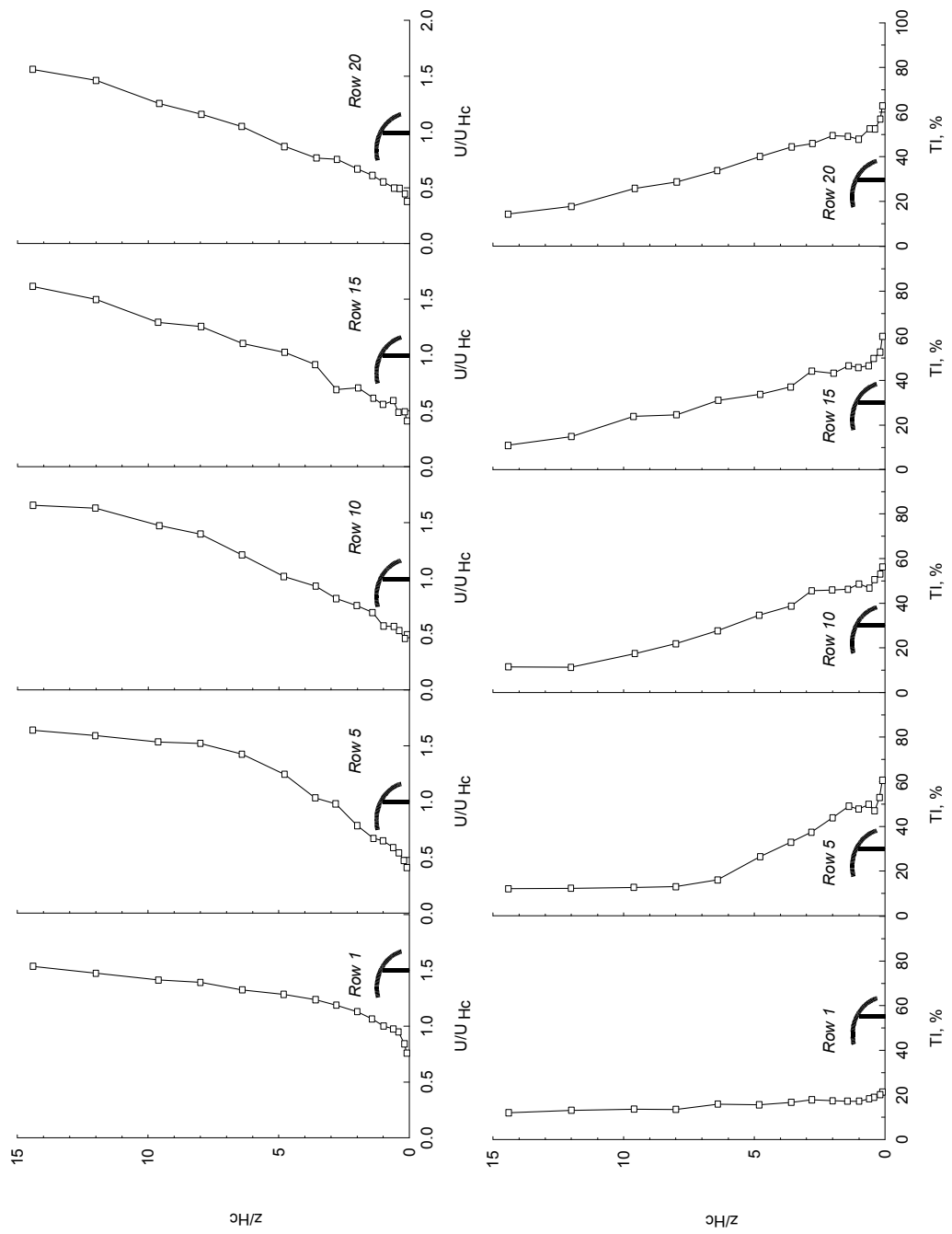


**Figure 4-34 Mean Velocity and Turbulent Profiles Within Array Field
(b) Pitch = -60 deg**

4.8 Summary of Design Load Cases and Combinations

The primary objective of the wind tunnel studies presented in this report was to identify wind loads applicable to designs for strength of the structure, strength of the collector drive mechanism, and deformation analysis of the collector by measurements of overall loads and distributions of local pressures for a number of field positions and collector orientations. For practical design of the collector drive design, appropriate combinations of the primary load components, i.e. forces and pitching moment, must be simultaneously specified, while maximizing the effect of at least one load component. For this reason, several load cases were derived using the pressure distribution data that provide all of the primary load components by integration. It also should be noted that the design loads given in this section have been adjusted to account for the finite resolution of the pressure data as described in Section 4.9. This section summarizes these design loads and demonstrates the use of the data. For an explanation of the method and rationale that was applied in determining the design load cases and combinations, refer to Sections 3.2.2 and 3.2.3.

4.8.1 Structural Strength Design Loads

The load cases were selected from the pressure test data for several groups of similar test configurations, for example, the exterior collectors (Configurations B1 to B6) and interior collectors (Configurations C1 to C6). Each group yielded six load cases, each of which would maximize or minimize one of the three load components of interest. The individual load case tabulates all three load components occurring simultaneously. It should be pointed out that in evaluating structural strength, applying the combination of all three load components is appropriate because each component can affect the net overall stress on the collector.

Table 4-1 summarizes the load cases and load combinations for different groups of the solar collector tests. In the table, Load Case 1 refers to the case where the horizontal force, C_{fx} , resulted in the largest positive peak and Load Case 2 the largest negative peak. The group denoted as *Exterior Collector* includes all of the exterior collector configurations without the torque tube. A much more limited number of runs were made with a torque tube on the back of the collector model, so a complete data set of peak loads with a torque tube was not constructed. The second group includes collector loads with or without the torque tube, to envelop the design loads regardless of the presence of the torque tube. Test configurations with a protective wind fence were also very limited for the balance study. The group, *Exterior Collector With Protective Fence*, consists of Configuration D3 only, the collector at the corner of the array field. Configuration D3 was selected for testing because wind tunnel test experience suggests the corner generally sees high wind loads, and these peaks normally occur at or near yaw angles of 45 degrees. A similar grouping scheme was used for the interior collectors. Only Configuration C5 is shown because it is the most representative configuration for the bulk of a large solar field, as it is well shielded by surrounding collectors. For the interior of the array field, the torque tube has little effect on the design loads, and the load combinations with and without the torque tube are nearly identical to those without the torque tube.

Table 4-1 Summary of Load Cases and Load Combinations

(a) Exterior Collectors

Operational Mode (positoive pitch angles)*

Case	Condition	Conf.	Yaw	Pitch	Cfx	Cfz	Cmy
1	Max Cfx	B3	30	0	5.097	-0.034	---
2	Min Cfx	B4	0	0	-1.242	-0.125	---
3	Max Cfz	B3	30	135	2.527	1.849	---
4	Min Cfz	B3	0	60	2.107	-5.256	---
5	Max Cmy	---	---	---	---	---	---
6	Min Cmy	---	---	---	---	---	---

Stow Mode (negative pitch angles)

Case	Condition	Conf.	Yaw	Pitch	Cfx	Cfz	Cmy
1	Max Cfx	B3	45	-15	5.117	1.550	0.114
2	Min Cfx	B4	0	-15	-1.130	-0.404	-0.065
3	Max Cfz	B3	0	-60	1.647	3.952	0.364
4	Min Cfz	B4	30	-150	2.306	-0.927	-0.232
5	Max Cmy	B3	0	-60	1.410	3.709	0.419
6	Min Cmy	B3	0	-105	0.870	-0.231	-0.517

(b) Exterior Collectors With Protective Fence

Operational Mode (positoive pitch angles)*

Case	Condition	Conf.	Yaw	Pitch	Cfx	Cfz	Cmy
1	Max Cfx	D3	45	15	2.900	-0.374	---
2	Min Cfx	D3	30	60	-0.503	-0.264	---
3	Max Cfz	D3	45	135	1.705	1.030	---
4	Min Cfz	D3	45	60	1.175	-2.281	---
5	Max Cmy	---	---	---	---	---	---
6	Min Cmy	---	---	---	---	---	---

Stow Mode (negative pitch angles)

Case	Condition	Conf.	Yaw	Pitch	Cfx	Cfz	Cmy
1	Max Cfx	D4	30	-15	4.033	1.026	-0.035
2	Min Cfx	D4	-30	-15	-0.852	-0.278	-0.032
3	Max Cfz	D5	30	-60	1.294	2.984	0.246
4	Min Cfz	D4	30	-135	1.481	-1.050	-0.202
5	Max Cmy	D5	30	-45	1.573	2.282	0.332
6	Min Cmy	D5	30	-105	0.849	-0.436	-0.468

(c) Interior Collectors Without Torque Tube

Operational Mode (positoive pitch angles)

Case	Condition	Conf.	Yaw	Pitch	Cfx	Cfz	Cmy
1	Max Cfx	C5	30	15	2.264	-0.429	0.113
2	Min Cfx	C1	0	0	-1.330	-0.148	-0.098
3	Max Cfz	C1	0	120	1.433	1.362	0.370
4	Min Cfz	C1	0	75	0.712	-2.533	0.021
5	Max Cmy	C1	0	120	1.384	1.081	0.436
6	Min Cmy	C1	0	0	-1.228	-0.236	-0.156

Stow Mode (negative pitch angles)

Case	Condition	Conf.	Yaw	Pitch	Cfx	Cfz	Cmy
1	Max Cfx	C7	0	-30	2.569	1.717	0.134
2	Min Cfx	C1	30	-15	-1.374	-0.329	0.025
3	Max Cfz	C5	0	-60	1.404	2.754	0.107
4	Min Cfz	C5	30	-135	0.859	-0.763	-0.045
5	Max Cmy	C5	30	-45	1.929	2.618	0.322
6	Min Cmy	C5	0	-90	0.571	0.303	-0.378

(d) Interior Collectors With Torque Tube

Operational Mode (positoive pitch angles)

Case	Condition	Conf.	Yaw	Pitch	Cfx	Cfz	Cmy
1	Max Cfx	F3	30	0	2.646	0.007	0.005
2	Min Cfx	F3	0	0	-1.195	-0.081	-0.053
3	Max Cfz	F3	0	105	1.108	1.428	0.463
4	Min Cfz	F3	30	60	1.148	-2.155	-0.055
5	Max Cmy	F3	30	105	1.139	1.127	0.535
6	Min Cmy	F3	30	0	0.157	-0.307	-0.203

Stow Mode (negative pitch angles)

Case	Condition	Conf.	Yaw	Pitch	Cfx	Cfz	Cmy
1	Max Cfx	F3	30	-15	2.777	0.823	0.051
2	Min Cfx	F3	0	-15	-1.475	-0.554	-0.102
3	Max Cfz	F3	30	-60	1.478	2.760	0.066
4	Min Cfz	F3	0	-90	0.783	-1.127	-0.518
5	Max Cmy	F3	30	-30	1.477	1.402	0.315
6	Min Cmy	F3	0	-90	0.950	-0.806	-0.629

(e) Interior Collectors - Configuration C5 only

Operational Mode (positoive pitch angles)

Case	Condition	Conf.	Yaw	Pitch	Cfx	Cfz	Cmy
1	Max Cfx	C5	30	15	2.264	-0.429	0.113
2	Min Cfx	C5	30	0	-0.858	-0.106	-0.070
3	Max Cfz	C5	0	120	1.011	1.186	0.187
4	Min Cfz	C5	30	75	0.456	-2.233	-0.091
5	Max Cmy	C5	30	105	0.716	0.550	0.363
6	Min Cmy	C5	30	75	0.244	-1.759	-0.145

Stow Mode (negative pitch angles)

Case	Condition	Conf.	Yaw	Pitch	Cfx	Cfz	Cmy
1	Max Cfx	C5	30	-45	2.209	2.721	0.239
2	Min Cfx	C5	30	-15	-0.819	-0.220	0.000
3	Max Cfz	C5	0	-60	1.404	2.754	0.107
4	Min Cfz	C5	30	-135	0.859	-0.763	-0.045
5	Max Cmy	C5	30	-45	1.929	2.618	0.322
6	Min Cmy	C5	0	-90	0.571	0.303	-0.378

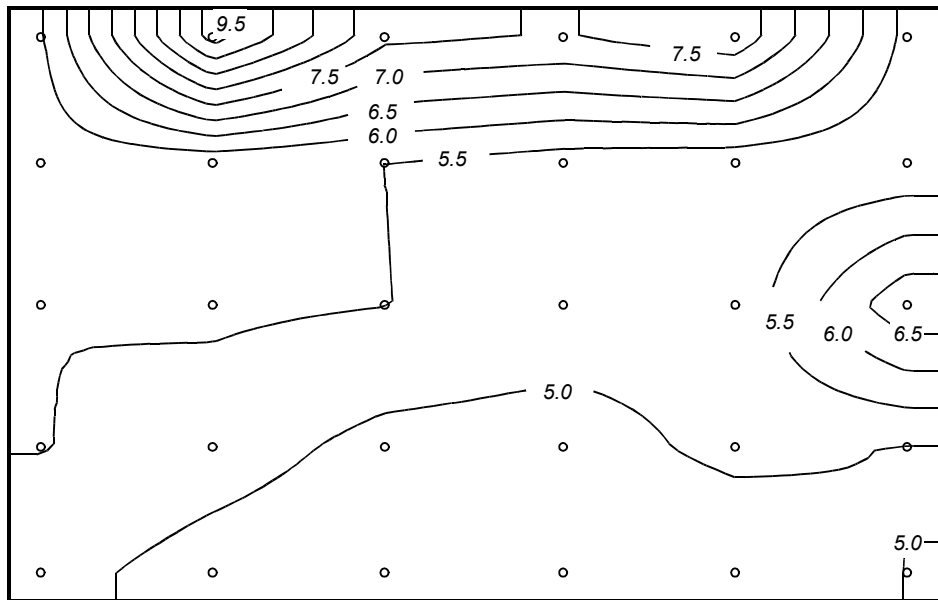
* Data available only by Phase 2 force balance study.

4.8.2 Local Peak Differential Design Pressures

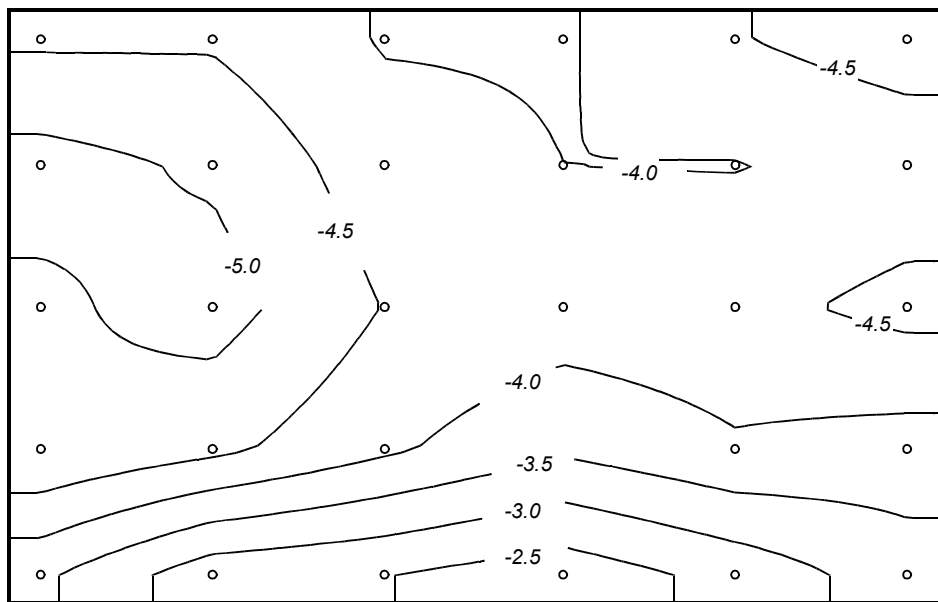
From all the pressure data taken, the largest local differential pressures were extracted irrespective of the yaw or the pitch angle. The results are presented as a contour map in Figure 4-35, looking into the reflective side of the concentrator. The data are applicable to limited surface areas on the collector and are intended to provide a guideline for a mounting scheme for the individual reflector panels, for example. High pressures are typically concentrated around the edges of the collector because of flow separation or vortex formation from the corner (Figure 4-36) where the most wind damage, such as breakage of the reflector panels, is expected to occur. The results are also tabulated in Table 4-2.

The use of the local peak pressures given here for the structural design is inappropriate because these peak pressures do not occur simultaneously for the structural frames to react. The differential pressure distributions suitable for the structural concerns are presented in the next section.

Field Exterior



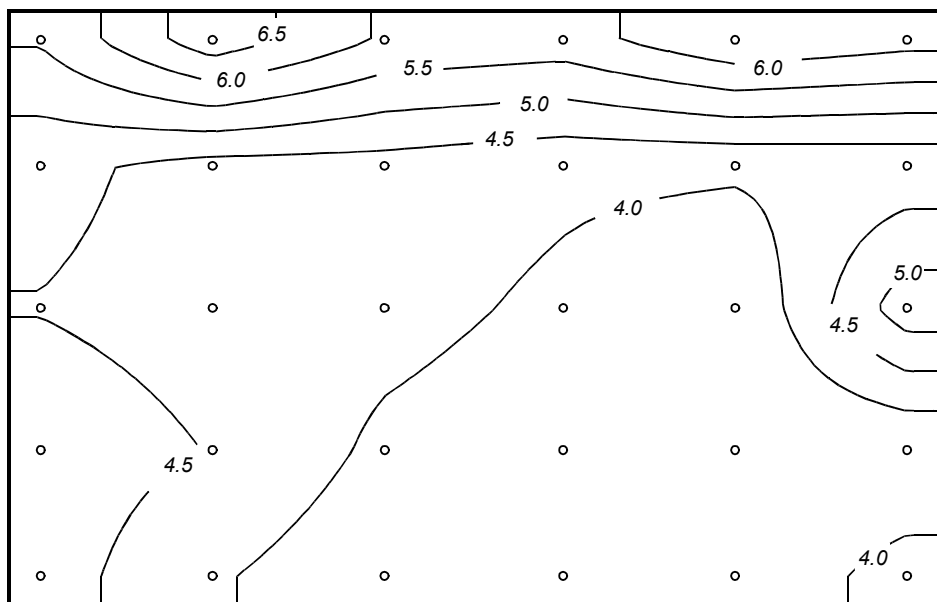
Peak Positive



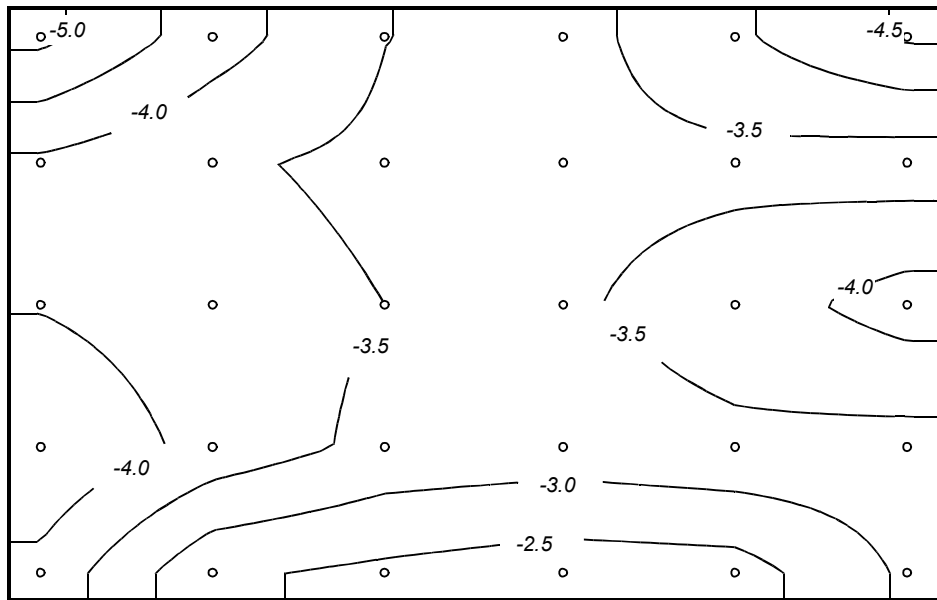
Peak Negative

Figure 4-35a Local peak differential pressure distribution, field exterior

Field Exterior with Protective Fence



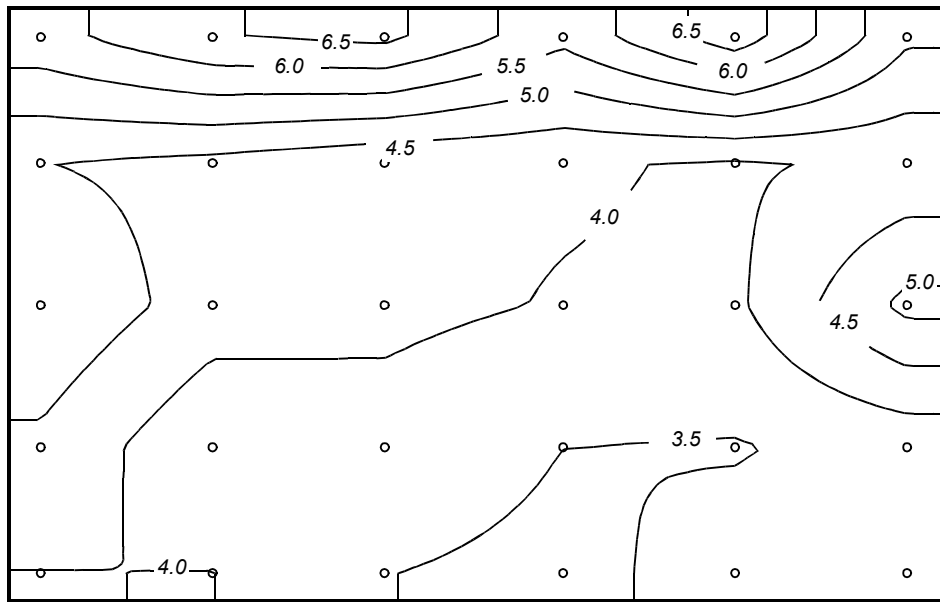
Peak Positive



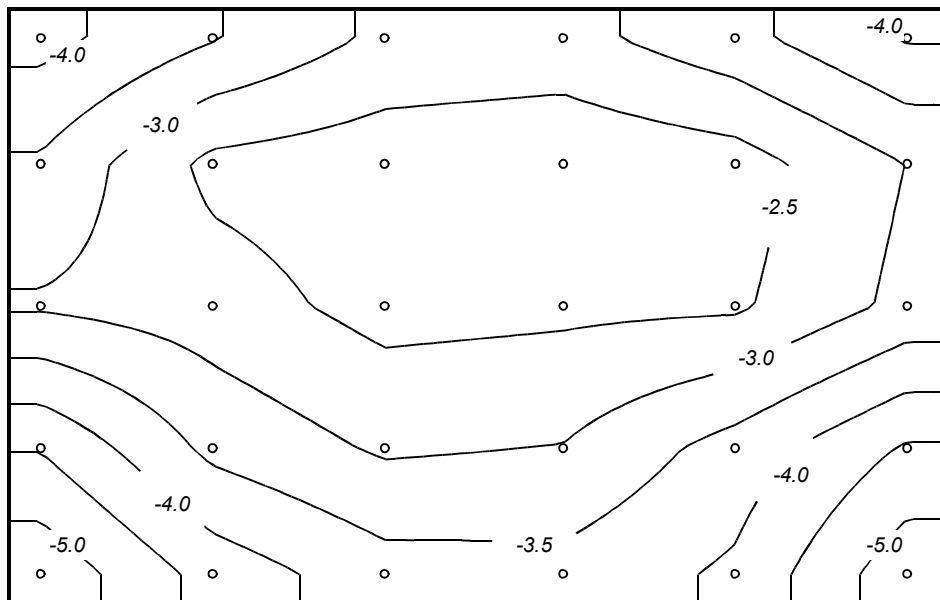
Peak Negative

**Figure 4-35b Local peak differential pressure distribution,
field exterior with protective fence**

Field Interior



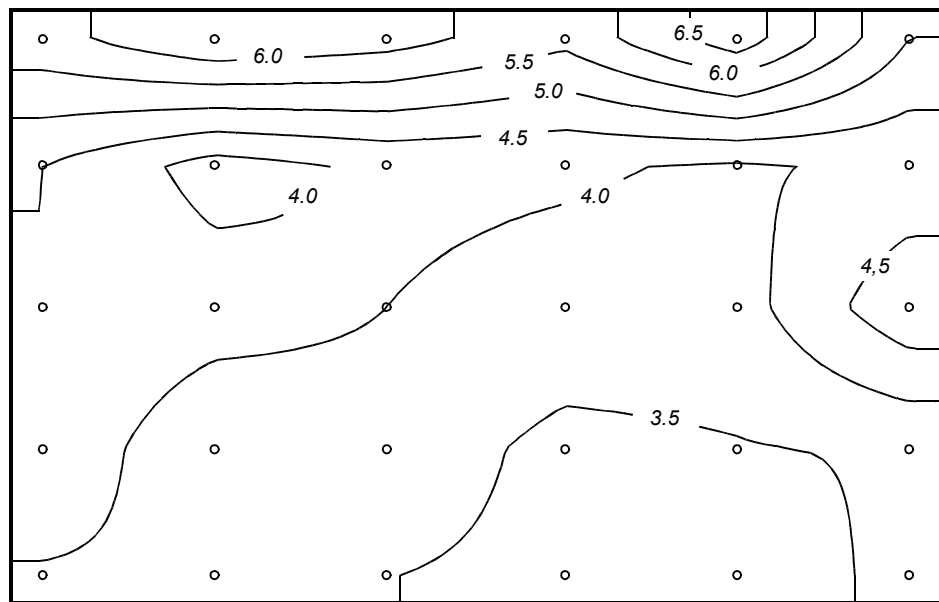
Peak Positive



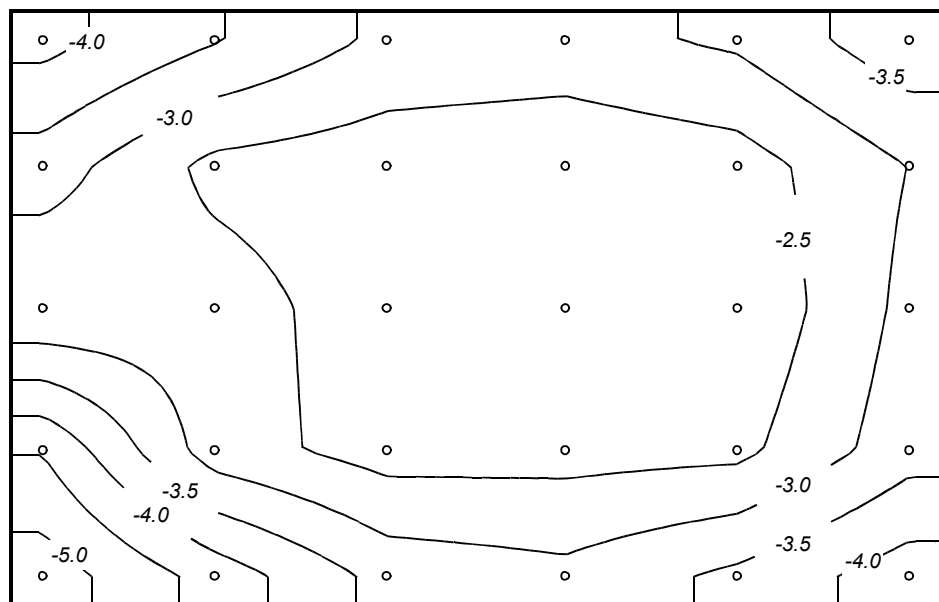
Peak Negative

Figure 4-35c Local peak differential pressure distribution, field interior

Innermost Collector, Configuration C5



Peak Positive



Peak Negative

**Figure 4-35d Local peak differential pressure distribution,
innermost collector, Configuration C5**

Table 4-2 Summary of Peak Local Differential Pressures

Field Exterior										Field Exterior With Protective Fence									
Tap	Max	Conf	Yaw	Pitch	Min	Conf	Yaw	Pitch	Tap	Max	Conf	Yaw	Pitch	Min	Conf	Yaw	Pitch		
5001	5.924	B3	45	-30	-4.419	B4	30	-120	5001	5.550	D4	30	-30	-5.131	D3	45	-90		
5002	9.733	B3	45	-45	-4.440	B3	45	180	5002	6.829	D4	30	-30	-4.232	D4	30	-90		
5003	7.634	B3	45	-45	-3.956	B3	0	-105	5003	5.930	D4	45	-45	-3.507	D5	30	-90		
5004	7.459	B3	0	-60	-3.950	B3	0	-105	5004	5.776	D5	30	-45	-3.305	D4	30	-90		
5005	7.887	B3	0	-60	-4.473	B3	0	-105	5005	6.452	D5	30	-45	-3.918	D4	30	-90		
5006	5.352	B3	30	-45	-4.770	B3	0	-105	5006	6.181	D5	30	-45	-4.567	D4	30	-90		
5007	5.693	B3	45	0	-5.193	B3	45	180	5007	4.638	D4	30	0	-3.908	D4	30	-150		
5008	5.626	B3	45	-15	-4.916	B3	45	180	5008	4.324	D4	30	0	-3.564	D5	30	-150		
5009	5.502	B3	45	-15	-4.220	B3	45	-165	5009	4.300	D5	30	-45	-3.399	D5	30	-150		
5010	5.252	B3	45	-15	-4.001	B3	45	-165	5010	4.112	D5	30	-45	-3.365	D5	30	-165		
5011	5.156	B3	45	-15	-3.982	B3	30	180	5011	4.088	D5	30	-45	-3.378	D5	30	-165		
5012	5.083	B3	30	0	-4.157	B3	0	-165	5012	4.150	D5	30	0	-3.230	D5	30	-165		
5013	5.500	B3	45	-15	-4.901	B3	45	180	5013	4.477	D4	30	0	-3.966	D4	30	-165		
5014	5.592	B3	45	-15	-5.219	B3	45	180	5014	4.313	D4	30	0	-3.711	D4	30	-165		
5015	5.508	B3	45	-15	-4.482	B3	45	180	5015	4.177	D4	30	-30	-3.498	D5	30	-165		
5016	5.286	B3	45	-15	-4.276	B3	30	180	5016	3.888	D4	30	-30	-3.429	D5	30	-165		
5017	5.171	B3	45	-15	-4.344	B3	30	180	5017	3.489	D4	30	-30	-3.738	D4	30	-165		
5018	6.897	B3	45	-15	-4.663	B3	30	180	5018	5.313	D3	45	0	-4.241	D4	30	-165		
5019	5.518	B3	45	0	-4.977	B3	45	180	5019	4.781	D4	30	0	-4.459	D3	45	180		
5020	5.248	B3	45	-15	-4.628	B3	45	180	5020	4.477	D4	30	0	-3.834	D4	30	180		
5021	4.843	B3	45	0	-4.089	B3	45	180	5021	3.894	D4	30	0	-3.358	D4	30	180		
5022	4.762	B3	30	0	-3.587	B3	30	180	5022	3.675	D4	30	0	-3.268	D4	30	180		
5023	5.137	B3	30	0	-3.941	B3	30	180	5023	3.519	D5	30	0	-3.399	D4	30	180		
5024	4.968	B3	30	0	-3.777	B3	0	180	5024	3.501	D5	30	0	-3.295	D4	30	-165		
5025	5.185	B3	45	0	-3.601	B3	45	180	5025	4.740	D4	30	0	-3.848	D3	45	180		
5026	4.773	B3	45	-15	-2.678	B3	45	180	5026	4.056	D4	30	0	-2.578	D4	30	180		
5027	4.599	B3	45	0	-2.522	B3	45	180	5027	3.637	D4	30	0	-2.394	D3	45	180		
5028	4.549	B3	45	-15	-2.193	B4	0	180	5028	3.542	D4	30	0	-2.213	D4	0	180		
5029	4.557	B3	30	0	-2.669	B4	0	180	5029	3.537	D4	30	0	-2.265	D4	30	180		
5030	5.014	B3	45	0	-3.270	B4	30	180	5030	4.240	D4	30	0	-3.080	D4	30	180		

Field Interior										Innermost Interior Collector - Config. C5									
Tap	Max	Conf	Yaw	Pitch	Min	Conf	Yaw	Pitch	Tap	Max	Conf	Yaw	Pitch	Min	Conf	Yaw	Pitch		
5001	5.819	C5	30	30	-4.171	C5	30	-90	5001	5.819	C5	30	30	-4.171	C5	30	-90		
5002	6.465	C5	30	-45	-3.539	C5	30	-90	5002	6.465	C5	30	-45	-3.539	C5	30	-90		
5003	6.628	C7	30	-45	-2.895	C5	0	-90	5003	6.220	C5	30	-45	-2.895	C5	0	-90		
5004	5.639	C5	30	-45	-2.827	C5	0	-90	5004	5.639	C5	30	-45	-2.827	C5	0	-90		
5005	6.818	C5	30	-45	-3.343	C1	330	-90	5005	6.818	C5	30	-45	-3.086	C5	0	-105		
5006	5.084	C7	330	-30	-4.054	C7	330	-90	5006	4.999	C5	30	-45	-3.847	C5	0	-105		
5007	4.505	C5	30	30	-3.435	C7	30	0	5007	4.505	C5	30	30	-3.259	C5	30	-120		
5008	4.361	C3	30	-30	-2.356	C5	30	-120	5008	3.794	C5	30	-45	-2.356	C5	30	-120		
5009	4.101	C5	0	-60	-2.203	C5	30	-120	5009	4.101	C5	0	-60	-2.203	C5	30	-120		
5010	4.058	C5	0	-60	-2.094	C5	30	-120	5010	4.058	C5	0	-60	-2.094	C5	30	-120		
5011	3.941	C5	30	-45	-2.273	C5	30	-120	5011	3.941	C5	30	-45	-2.273	C5	30	-120		
5012	4.109	C5	0	-60	-3.012	C5	330	-120	5012	4.109	C5	0	-60	-3.012	C5	330	-120		
5013	4.935	C7	330	0	-2.943	C1	0	135	5013	4.480	C5	330	45	-2.512	C5	330	-135		
5014	4.256	C5	30	-45	-2.737	C5	30	-135	5014	4.256	C5	30	-45	-2.737	C5	30	-135		
5015	4.118	C7	0	-75	-2.322	C1	0	135	5015	3.999	C5	0	-60	-2.217	C5	30	-135		
5016	3.975	C7	0	-75	-2.393	C1	0	135	5016	3.836	C5	0	-60	-2.011	C5	30	-135		
5017	3.907	C7	0	-75	-2.420	C1	0	135	5017	3.793	C5	0	-60	-2.058	C5	330	-135		
5018	5.144	C7	30	15	-3.139	C5	30	-135	5018	4.888	C5	30	15	-3.139	C5	30	-135		
5019	4.397	C5	30	30	-4.473	C5	30	120	5019	4.397	C5	30	30	-4.473	C5	30	120		
5020	3.569	C7	0	-75	-3.368	C1	0	120	5020	3.560	C5	0	-45	-2.729	C5	30	180		
5021	3.796	C5	30	-45	-2.926	C1	0	120	5021	3.796	C5	30	-45	-2.276	C5	30	-165		
5022	3.498	C7	0	-75	-3.020	C1	0	120	5022	3.349	C5	30	-45	-2.305	C5	30	165		
5023	3.469	C5	0	-75	-3.707	C1	0	120	5023	3.469	C5	0	-75	-2.364	C5	30	165		
5024	3.651	C7	0	-60	-4.563	C1	0	120	5024	3.550	C5	30	-75	-3.285	C5	0	120		
5025	3.995	C1	30	60	-5.377	C7	30	120	5025	3.955	C5	30	60	-5.283	C5	30	105		
5026	4.010	C1	0	75	-4.301	C5	30	120	5026	3.903	C5	30	75	-4.301	C5	30	120		
5027	3.505	C5	30	75	-3.711	C1	0	105	5027	3.505	C5	30	75	-3.329	C5	30	120		
5028	3.383	C5	30	75	-3.671	C7	330	105	5028	3.383	C5	30	75	-3.144	C5	30	120		
5029	3.670	C1	330	75	-4.091	C1	0	105	5029	3.113	C5	30	75	-3.618	C5	30	105		
5030	3.920	C7	330	-30	-5.342	C7	330	105	5030	3.676	C5	330	60	-4.273	C5	330	105		

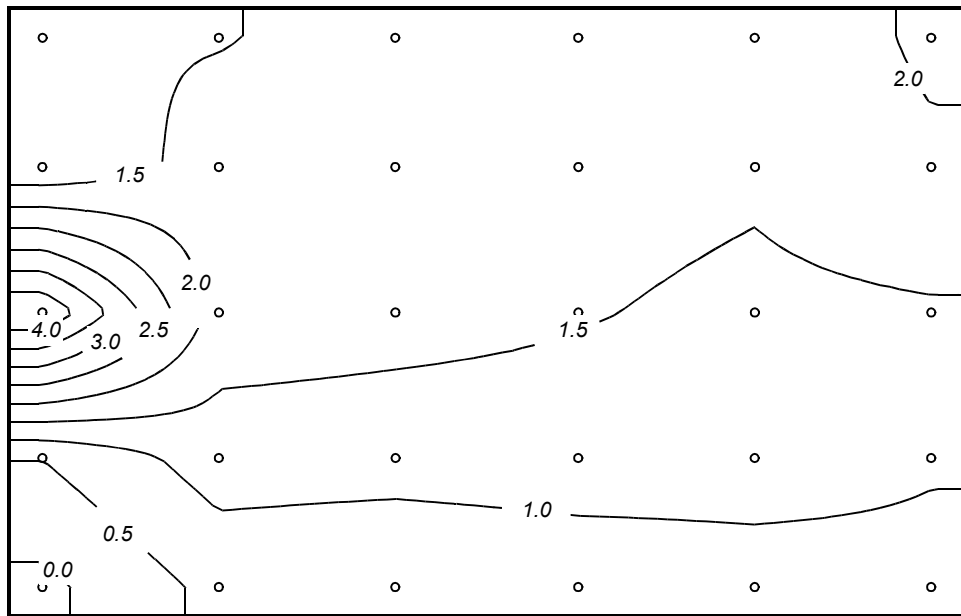


Figure 4-36 Vortex flow forming from corner of collector

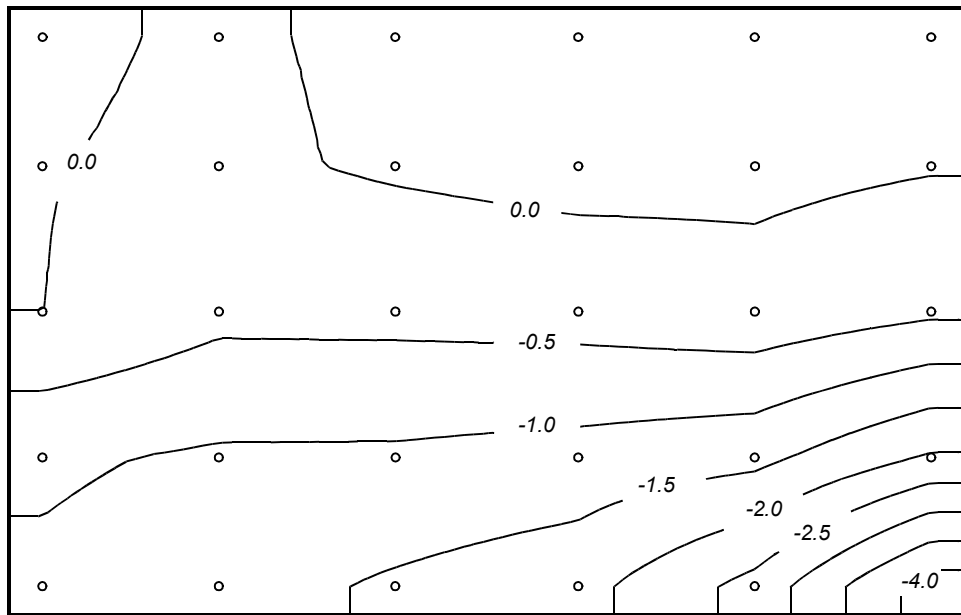
4.8.3 Instantaneous Differential Pressures

Differential pressures over collector reflectors can cause the reflector to deflect, resulting in a loss of efficiency because the reflected sunlight may move out of focus. Severe deflection of the collector can also cause the reflector to break. To assess wind-induced reflector deflection and structural failure, the relationship between the loading condition and the resulting reflector deflection (and mechanical stresses) can be established through structural analysis, for example using finite element modeling. Collector designs vary by manufacturer, and each structure can respond differently to imposed loads. The pressure distribution data in this section are intended to enable this type of structural analysis. A very large number of pressure distributions have been obtained during these tests. Presenting all the pressure distribution results in this report is neither practical nor desirable. Accordingly, this section presents a limited number of the pressure test results, shown as differential pressure distributions realized instantaneously — in essence, a “snapshot” extracted from the pressure time series data.

The results presented here are selected from the data taken for Configuration C5, because it is representative of most of the collectors within the interior of the solar field. Figure 4-37 shows the instantaneous pressure distributions that contained the largest differential pressure at any of the tap locations, for each of the three yaw angles tested. The numerical values of the differential pressures are presented in Table 4-3.

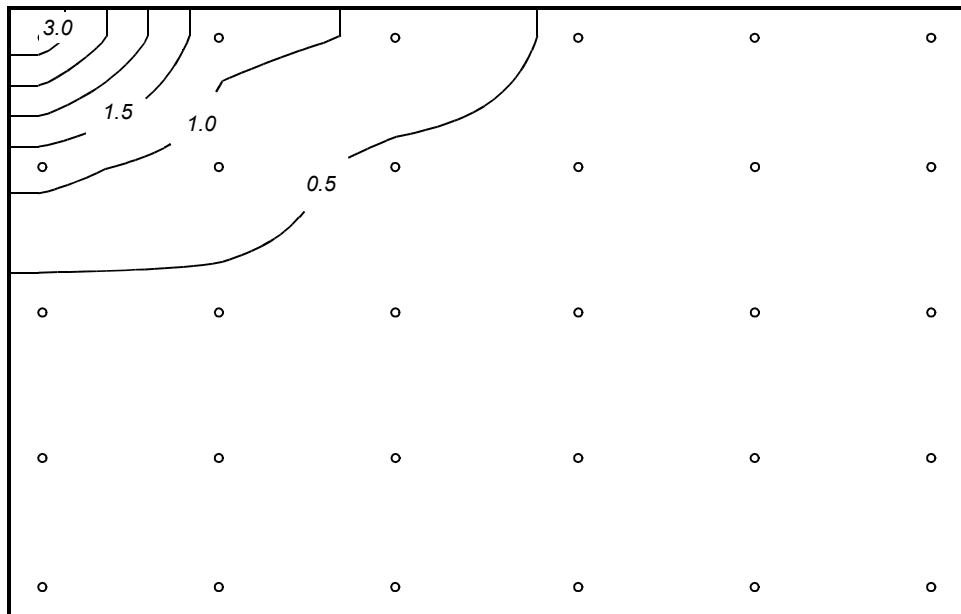


Peak Positive, Yaw = -30, Pitch = 45

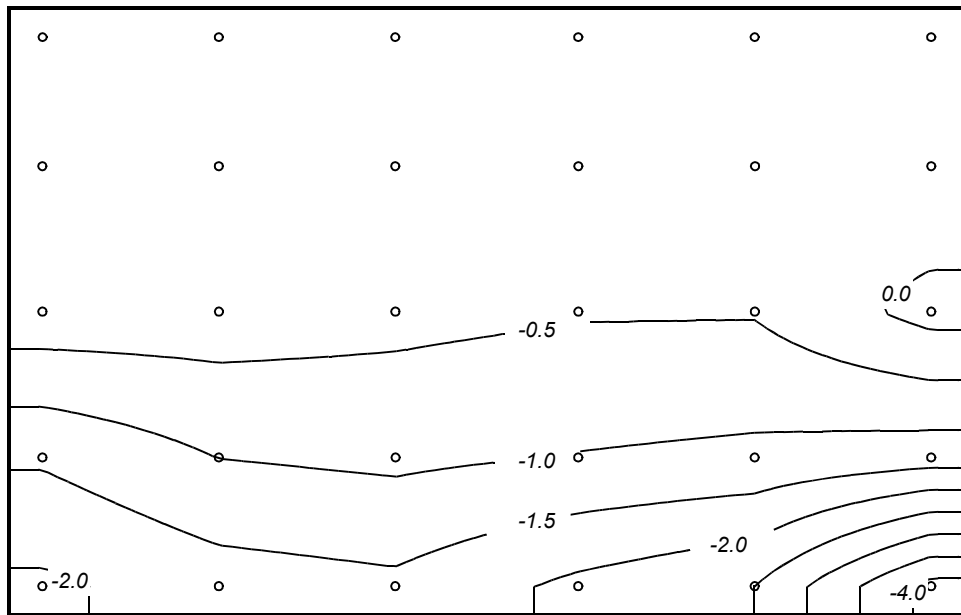


Peak Negative, Yaw = -30, Pitch = 105

Figure 4-37a Instantaneous differential pressure distribution with the largest local peak, yaw = - 30 degrees

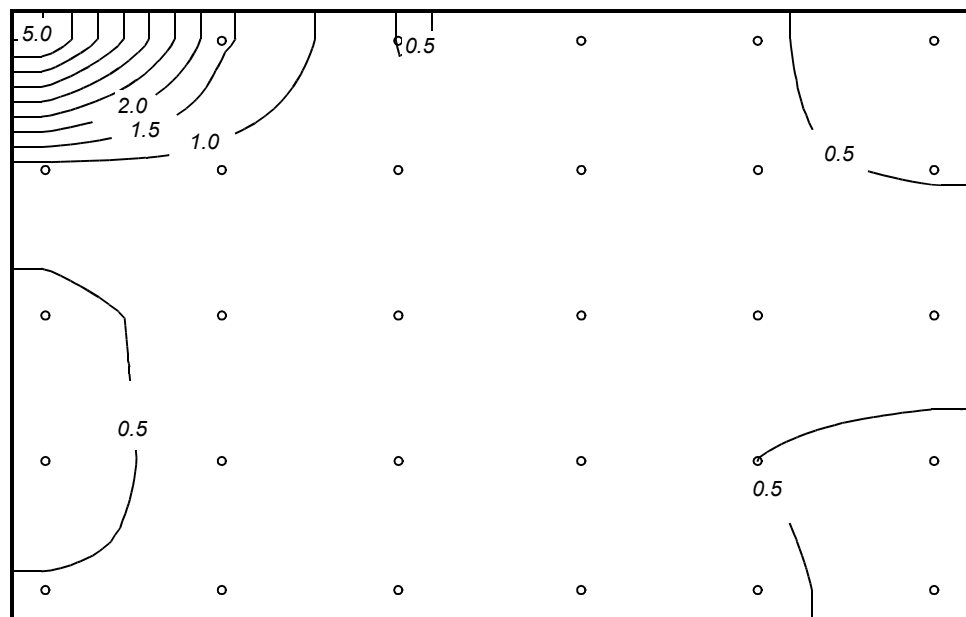


Peak Positive, Yaw = 0, Pitch = 0

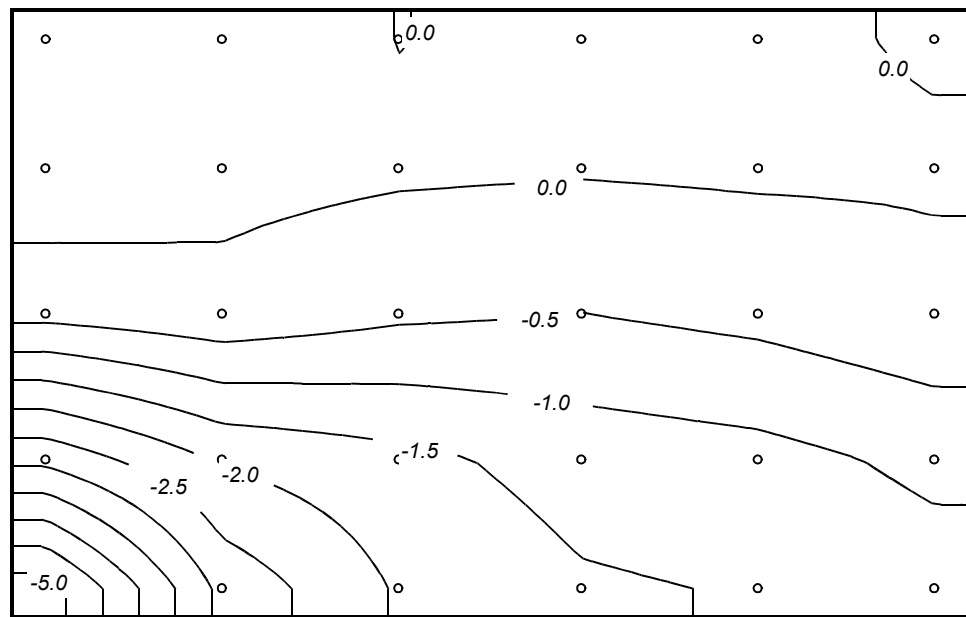


Peak Negative, Yaw = 0, Pitch = 120

Figure 4-37b Instantaneous differential pressure distribution with the largest local peak, yaw = 0 degrees



Peak Positive, Yaw = 30, Pitch = 0



Peak Negative, Yaw = 30, Pitch = 120

Figure 4-37c Instantaneous differential pressure distribution with the largest local peak, yaw = 30 degrees

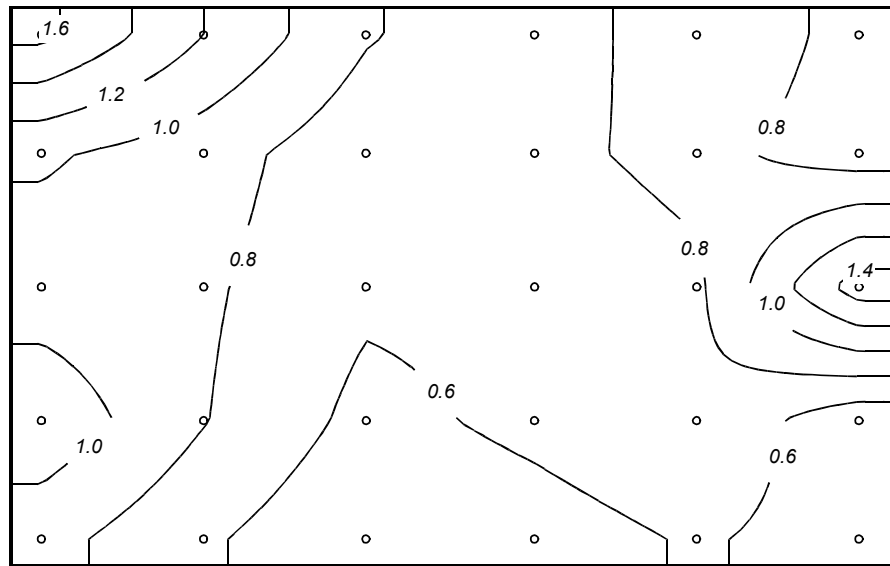
Table 4-3 Selected Summary of Instantaneous Differential Distribution with the Largest Local Peak

Tap	Yaw = -30		Yaw = 0		Yaw = 30	
	Pk Pos	Pk Neg	Pk Pos	Pk Neg	Pk Pos	Pk Neg
	Pitch Angle		Pitch Angle		Pitch Angle	
	45 deg.	105 deg.	0 deg.	120 deg.	0 deg.	120 deg.
5001	1.450	0.070	3.275	-0.041	5.018	0.489
5002	1.473	-0.054	1.146	-0.245	1.586	0.295
5003	1.678	0.077	0.934	-0.197	0.479	-0.009
5004	1.834	0.208	0.374	-0.089	0.594	0.118
5005	1.582	0.263	0.311	-0.117	0.594	0.089
5006	2.103	0.170	0.365	-0.337	0.085	-0.044
5007	1.060	0.016	1.167	-0.399	0.741	0.365
5008	1.709	-0.082	0.725	-0.249	0.815	0.158
5009	1.794	0.056	0.368	-0.127	0.653	0.077
5010	1.683	0.154	0.344	-0.193	0.729	0.042
5011	1.579	0.111	0.340	-0.161	0.560	0.076
5012	1.907	0.029	0.354	-0.447	0.460	0.057
5013	4.480	0.007	0.249	-0.179	0.385	-0.345
5014	1.783	-0.373	0.383	-0.236	0.642	-0.152
5015	1.673	-0.358	0.386	-0.353	0.582	-0.406
5016	1.534	-0.303	0.389	-0.459	0.617	-0.503
5017	1.388	-0.167	0.385	-0.464	0.691	-0.356
5018	1.444	-0.412	0.205	0.182	0.840	-0.117
5019	0.508	-0.925	0.252	-1.438	0.363	-2.874
5020	1.245	-1.071	0.319	-0.992	0.628	-1.937
5021	1.231	-1.080	0.265	-0.894	0.684	-1.639
5022	1.275	-1.185	0.316	-1.023	0.559	-1.298
5023	1.230	-1.359	0.394	-1.109	0.497	-1.168
5024	1.041	-2.059	0.312	-1.270	0.311	-0.883
5025	-0.122	-1.088	0.239	-2.095	0.523	-5.283
5026	0.645	-1.290	0.233	-1.738	0.527	-2.862
5027	0.501	-1.572	0.279	-1.609	0.556	-1.949
5028	0.658	-1.828	0.306	-2.123	0.561	-1.562
5029	0.782	-2.672	0.392	-2.501	0.597	-1.464
5030	0.874	-4.273	0.328	-4.175	0.282	-1.214

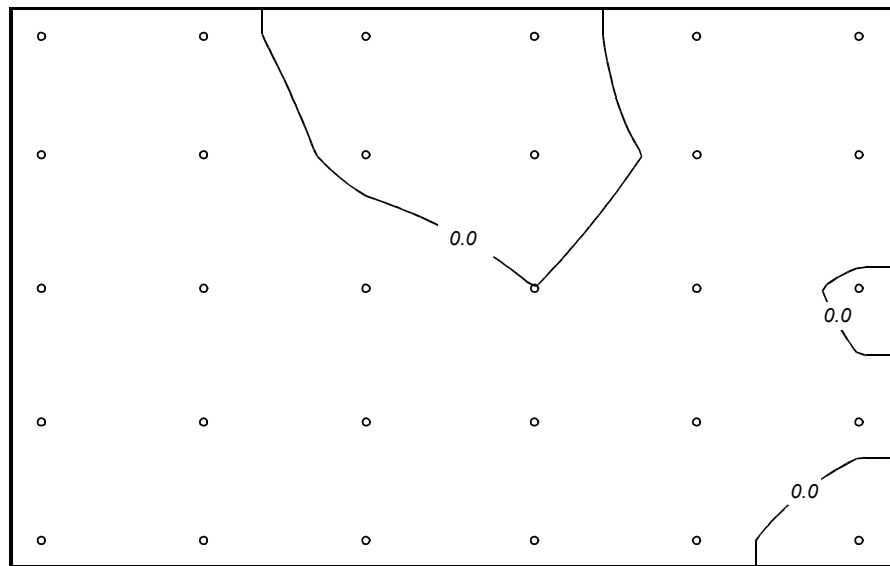
The largest pressure is in bold.

Additional pressure contours are presented in Appendix D for Configurations B1, C1, C3, C5 and D1.

Other pressure distributions of interest to the design engineer are those that, when integrated over the collector surface, result in specific overall load levels. Various load levels may be used to evaluate the deformation of the structure to optimize structural and economical impact due to wind loads. This section presents instantaneous pressure distributions that resulted in the integral loads at the 80th percentile of their peak values. The choice of the load level was somewhat arbitrary, however. Figure 4-38 shows the selected results for positive pitch angles. The corresponding tabulated data are given in Table 4-4.

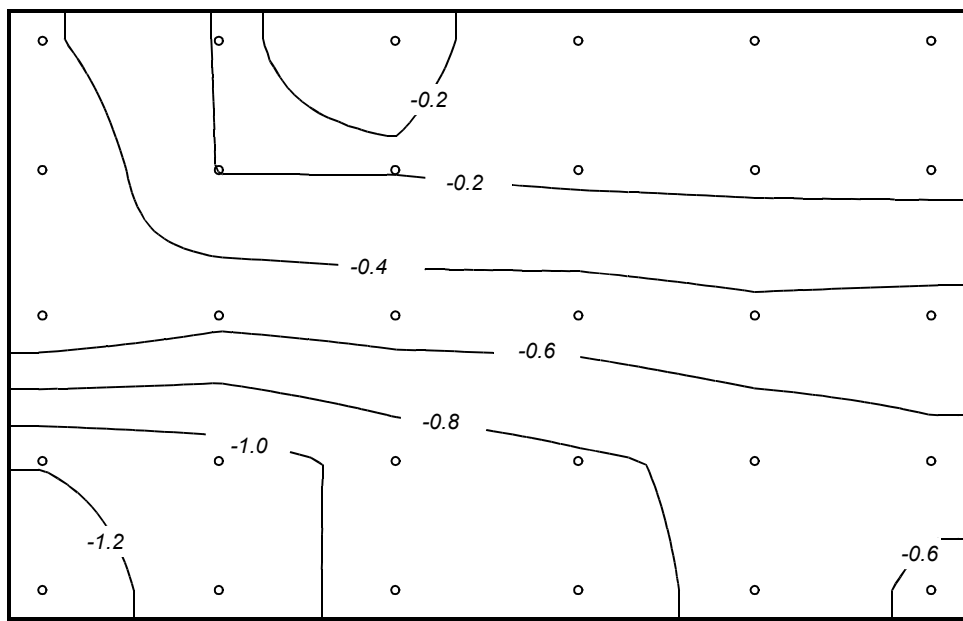


Positive 80th Percentile Level at Yaw = 30 deg., Pitch = 30 deg.

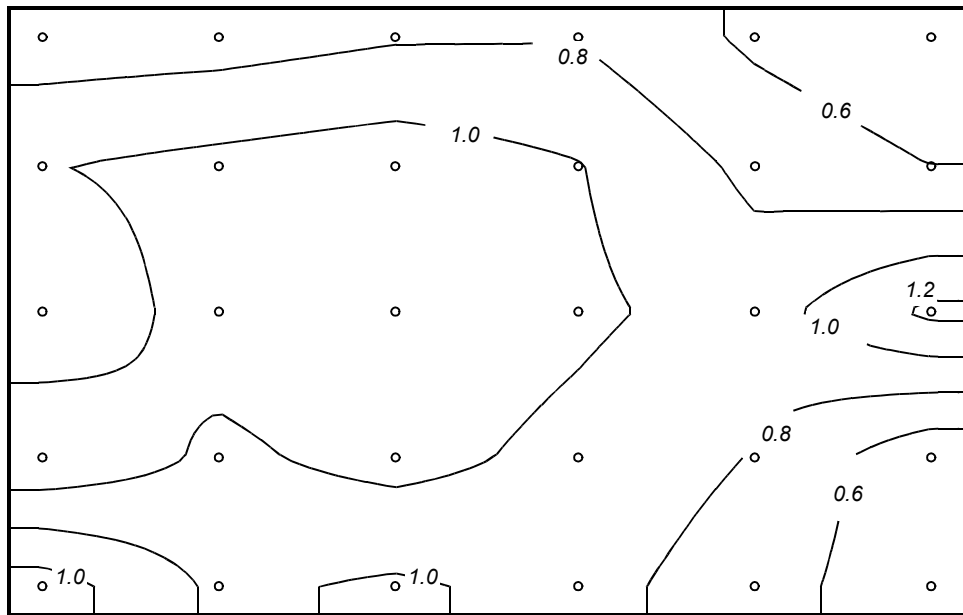


Negative 80th Percentile Level at Yaw = -30 deg., Pitch = 0 deg.

Figure 4-38a Instantaneous differential pressure distribution with horizontal force at 80th percentile level of peak

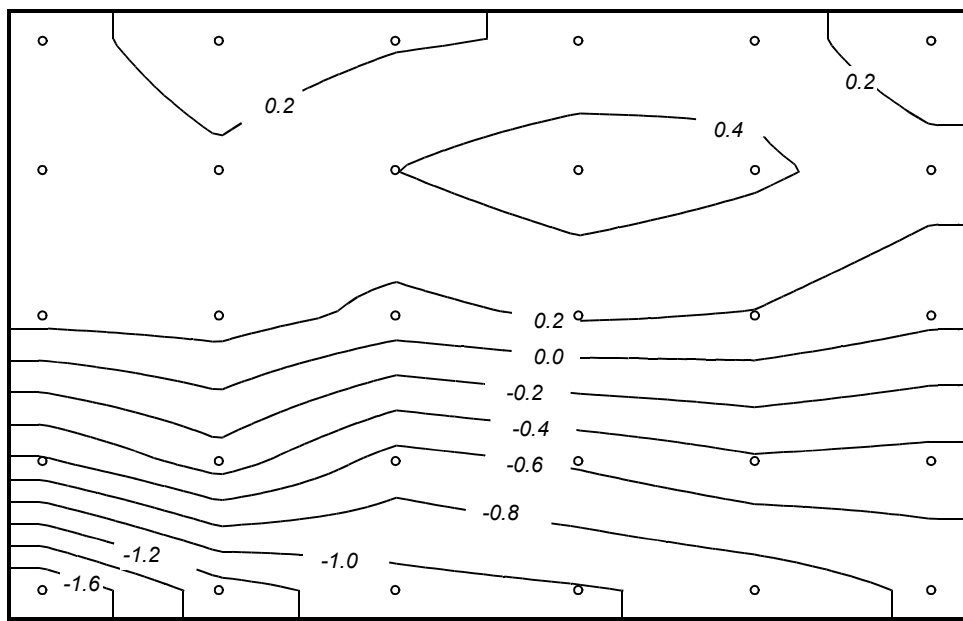


Positive 80th Percentile Level at Yaw = 30 deg., Pitch = 120 deg.

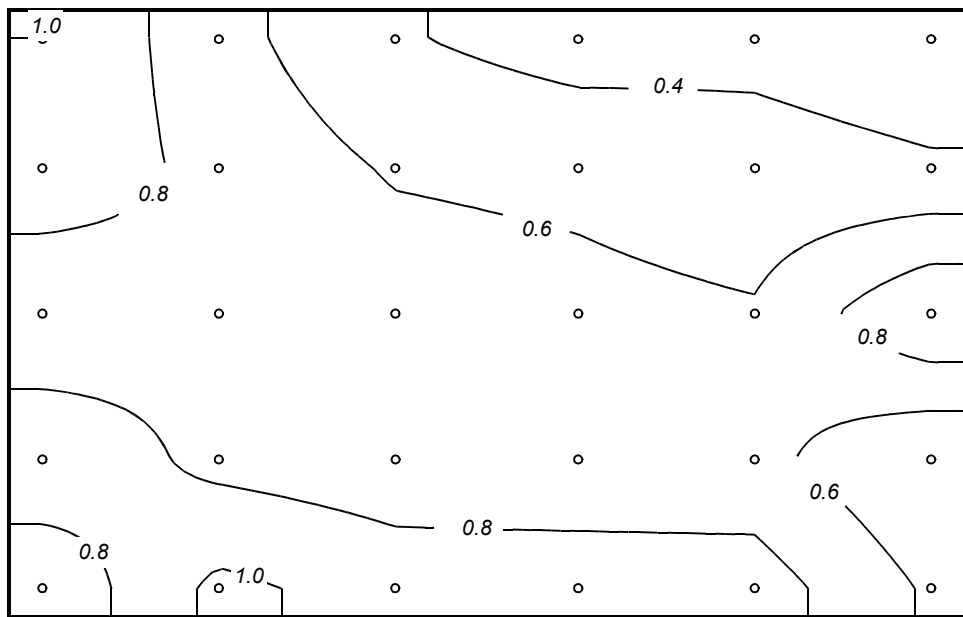


Negative 80th Percentile Level at Yaw = 30 deg., Pitch = 75 deg.

Figure 4-38b Instantaneous differential pressure distribution with vertical force at 80th percentile level of peak



Positive 80th Percentile Level at Yaw = 30 deg., Pitch = 105 deg.



Negative 80th Percentile Level at Yaw = 30 deg., Pitch = 60 deg.

Figure 4-38c Instantaneous differential pressure distribution with pitching moment at 80th percentile level of peak

Table 4-4 Differential Pressure Distributions Resulting in Overall Loads at 80th Percentile of Respective Peaks

Tap	fx		fz		my	
	Yaw 30 Pitch 30	Yaw -30 Pitch 0	Yaw 30 Pitch 120	Yaw 30 Pitch 75	Yaw 30 Pitch 105	Yaw 30 Pitch 60
Pos.	Neg.	Pos.	Neg.	Pos.	Neg.	
5001	1.653	-0.143	-0.434	0.687	0.277	1.004
5002	1.198	-0.036	-0.185	0.711	0.075	0.666
5003	0.817	0.074	-0.235	0.776	0.184	0.418
5004	0.629	0.109	-0.144	0.786	0.217	0.312
5005	0.982	-0.149	-0.029	0.557	0.324	0.354
5006	0.721	-0.145	-0.054	0.412	0.029	0.289
5007	1.027	-0.013	-0.591	0.989	0.366	0.939
5008	0.895	-0.090	-0.194	1.062	0.244	0.741
5009	0.658	0.040	-0.191	1.117	0.397	0.579
5010	0.754	0.076	-0.154	1.013	0.538	0.554
5011	0.856	-0.041	-0.138	0.750	0.438	0.470
5012	0.689	-0.162	-0.134	0.600	0.289	0.419
5013	0.886	-0.186	-0.401	0.844	0.283	0.635
5014	0.835	-0.113	-0.536	1.090	0.312	0.762
5015	0.642	-0.092	-0.502	1.144	0.135	0.712
5016	0.663	-0.001	-0.513	1.045	0.232	0.656
5017	0.759	-0.096	-0.449	0.907	0.193	0.621
5018	1.509	0.028	-0.475	1.252	0.048	1.002
5019	1.146	-0.080	-1.188	1.172	-0.630	0.964
5020	0.810	-0.015	-1.097	0.965	-0.290	0.736
5021	0.535	-0.164	-0.931	1.070	-0.685	0.684
5022	0.653	-0.143	-0.835	0.935	-0.575	0.651
5023	0.775	-0.075	-0.746	0.786	-0.426	0.658
5024	0.452	-0.027	-0.658	0.437	-0.472	0.397
5025	0.873	-0.050	-1.343	0.505	-1.803	0.636
5026	0.630	-0.157	-1.066	0.836	-1.298	1.053
5027	0.428	-0.069	-0.949	0.773	-1.083	0.907
5028	0.514	-0.089	-0.877	0.867	-1.024	0.921
5029	0.624	-0.036	-0.741	0.692	-0.938	0.897
5030	0.520	0.069	-0.559	0.452	-0.761	0.568

4.8.4 Example Calculations of Design Loads

This section demonstrates the use of the current wind-tunnel test results to determine the wind loads required by the designer. First, recall the definition of the load coefficients given in Section 3.1:

$$\text{Horizontal Force, } f_x \quad C_{fx} = \frac{f_x}{qLW} \quad (4.1)$$

$$\text{Vertical Force, } f_z \quad C_{fz} = \frac{f_z}{qLW} \quad (4.2)$$

$$\text{Pitching Moment, } m_y \quad C_{my} = \frac{m_y}{qLW^2} \quad (4.3)$$

and the mean reference dynamic pressure measured at the collector pivot height, H_c , of the solar collector as given by

$$q = \frac{1}{2} \rho U^2. \quad (4.4)$$

Here U is the mean wind speed at the pivot height, and ρ is the density of air. The above equations can be rewritten to obtain the loads as

$$\text{Horizontal Force, } f_x \quad f_x = qLWC_{fx} \quad (4.5)$$

$$\text{Vertical Force, } f_z \quad f_z = qLWC_{fz} \quad (4.6)$$

$$\text{Pitching Moment, } m_y \quad m_y = qLW^2C_{my}. \quad (4.7)$$

For the full-scale loads, the corresponding reference dimensions, L is 25.97 ft and W is 16.40 ft. In addition, the velocity reference elevation, H_c , is 9.35 ft. Note that these reference dimensions must be used consistently between the model and full-scale to properly calculate the loads applicable to the full-scale solar collector. To actually determine the full-scale loads, the design wind pressure, q , or equivalently, the design wind speed, U , must be also specified. An example procedure is described next.

Specifying Design Wind Speed

Several available sources provide wind speed to be used for estimating design wind loads on civil engineering structures and buildings. They include, but are not limited to, the current US standard, ASCE 7-98, and regional wind load codes. Regional wind data are also available from the National Climate Data Center (NCDC), but require considerable data analysis to determine a rational design wind speed. For the example in this section, the wind map provided by ASCE 7-98 (Figure 6-1, pp. 34-38) is used because it is a widely accepted practice.

The ASCE 7-98 specifies design wind speeds as 3-sec gust speeds at an elevation of 33 ft for the entire United States in a form of a wind map. Except for hurricane-prone southern and eastern coastal regions and Alaska, much of the United States plains have been zoned as 90-mph regions. Western states such as California, Oregon, and Washington have been zoned as 85 mph regions. These wind speeds are referred to as the basic wind speed that would result in 50-year recurrence wind loads for structures in open countries. The ASCE-specified wind speeds, however, cannot

be used directly for the present solar collector data because (1) the ASCE wind speeds are given as a 3-second gust speed rather than a mean speed adopted for the wind-tunnel test, and (2) the ASCE wind speeds are referenced at an elevation of 33 ft rather than the collector pivot height of 9.35 ft. Thus, conversion of the ASCE wind speeds is necessary using the procedures explained in ASCE 7-98. Conversion of a 50-year wind load is also explained in ASCE 7-98 for different mean recurrence intervals and is presented here.

Conversion of ASCE Basic Wind Speed

Consider a solar collector site in California for which ASCE 7-98 (Figure 6-1) gives the basic wind speed of $V = 85$ mph. Using Figure C6-1, the corresponding hourly mean wind speed at 33 ft, U_{33} , is obtained as

$$U_{33} = V / 1.53 = 85 / 1.53 = 55.6 \text{ mph hourly mean.}$$

Using values implied by Table 6-4 of ASCE 7-98, the mean wind speed at the collector pivot height, U_{hc} , is given as

$$U_{hc} = U_{33} \left(\frac{9.32}{33} \right)^{1/7} = 55.6 \left(\frac{9.32}{33} \right)^{1/7} = 46.4 \text{ mph hourly mean.}$$

The hourly mean wind speed of 46.4 mph is the design wind speed for the solar collectors in California.

Design Wind Loads

Based on the design wind speed, the corresponding design pressure, q , is calculated by

$$q = \frac{1}{2} \rho U_{hc}^2 = 0.00256(46.4)^2 = 5.51 \text{ psf.}$$

Here, the constant 0.00256 is conveniently used to obtain the reference pressure in psf from the wind speed in mph. As an example, we wish to determine the 50-year peak design loads on the innermost-shielded solar collectors (Configuration C5) when that collector is oriented at a -60 degree pitch angle (a downward-facing stow position). We note from Table 4.1 that the largest peak vertical force, Load Case 3, is produced at this -60 degree pitch angle, at a yaw angle of 0 degrees, so this orientation is of special interest to designers. Table 4.1 shows the peak Cfz is 2.754 and the corresponding Cfx value is 1.404, and the Cmy value is 0.107. Using equations (4.5) – (4.7):

Horizontal Force $f_x = qLWCfx = (5.51)(25.97)(16.40)(1.404) = 3,295 \text{ lbs}$

Vertical Force, $f_z = qLWCfz = (5.51)(25.97)(16.40)(2.754) = 6,463 \text{ lbs}$

Pitching Moment, $m_y = qLW^2Cmy = (5.51)(25.97)(16.40)^2(0.107) = 4,118 \text{ lb-ft.}$

Note that these loads are to be applied simultaneously to the structure because the wind-tunnel results were obtained as a concurrent load combination from the time series data for which the vertical force was maximized.

Comparison to Design Loads Determined by Quasi-Steady Assumption

As pointed out in Section 1.2, the traditional approach to obtaining the structural design loads on solar collectors has been based on the quasi-steady assumption. With this technique, the measured mean load is scaled to follow the gust wind speed to provide the equivalent peak load. The scale factor is known as the gust load factor, and ASCE 7-98 or the model building code IBC

2000 would predict the gust load factor to be 2.34 for a structure in open country. To illustrate this, the next example calculates the load combination using the mean load data for the innermost-shielded solar collectors (Configuration C5) under the quasi-steady assumption. To make a direct comparison with the values calculated just above, we use the same assumptions for pitch angle and yaw angle, -60 degrees and 0 degrees, respectively.

From Appendix B (pg. 8-51) and using the scale factor of 1.13 (see Section 4.9) it can be shown that mean coefficients for a -60 degree pitch angle, with a yaw of 0 degrees, are: $C_{fx} = 0.382$, $C_{fy} = 0.742$, and $C_{my} = 0.027$.

Applying the gust factor, the design loads are calculated as:

$$\text{Horizontal Force } f_x = (2.34)qLWC_{fx} = (2.34)(5.51)(25.97)(16.40)(0.382) = 2,098 \text{ lbs}$$

$$\text{Vertical Force, } f_z = (2.34)qLWC_{fz} = (2.34)(5.51)(25.97)(16.40)(0.742) = 4,075 \text{ lbs}$$

$$\text{Pitching Moment, } my = (2.34)qLW^2C_{my} = (2.34)(5.51)(25.97)(16.40)^2(0.027) = 2,432 \text{ lb-ft.}$$

The quasi-steady approach considerably underestimated the design loads for the interior solar collectors. Not all collector orientations and collector configurations will yield underestimates, but this example is intended to illustrate the differences between these two approaches, as well as the calculation methods. In wind tunnels, measurement of the mean loads is far easier than measuring the peak loads, as done in the current wind-tunnel study, because the design of the wind-tunnel model, as well as necessary instrumentation, need not concern high frequency gust response due to turbulence. However, the estimate of the design load based on the quasi-steady assumption has limited applicability to the realistic structural design, so generally the measured peak coefficients should instead be used.

Design Loads for Other Mean Recurrence Intervals

The above examples demonstrates the use of the wind-tunnel results to determine the design wind loads of the solar collector with the design wind speed provided by ASCE 7-98. The calculated loads are expected to occur at an annual probability of 0.02, or once in 50 years. ASCE 7-98 also tabulates a set of conversion factors to obtain the design loads for other mean recurrence intervals. Table 4-5 is a summary of the conversion factors for most of the United States with the basic wind speed of 85 to 90 mph.

Table 4-5 Design Pressure Conversion Factors for Different Mean Recurrence Intervals

MRI, years	5	10	25	50	100	200	500
Conversion Factor	0.61	0.71	0.86	1	1.14	1.3	1.51

4.9 Adjustment to Pressure Test Data

4.9.1 Adjustment Factor

Although the overall loads calculated by integration of the local pressure data generally agree well with the directly measured balance results, a slight discrepancy is noted primarily due to the degree of the finite resolution of the pressure distributions actually measured. A denser array of pressure tap measurements (were it physically possible) would likely result in better agreement. Before the pressure data can be used the discrepancy needs to be quantified. Figure 4-39 compares the balance and pressure results for the horizontal and vertical force components. The comparisons are made for all of the essential statistical measures for completeness.

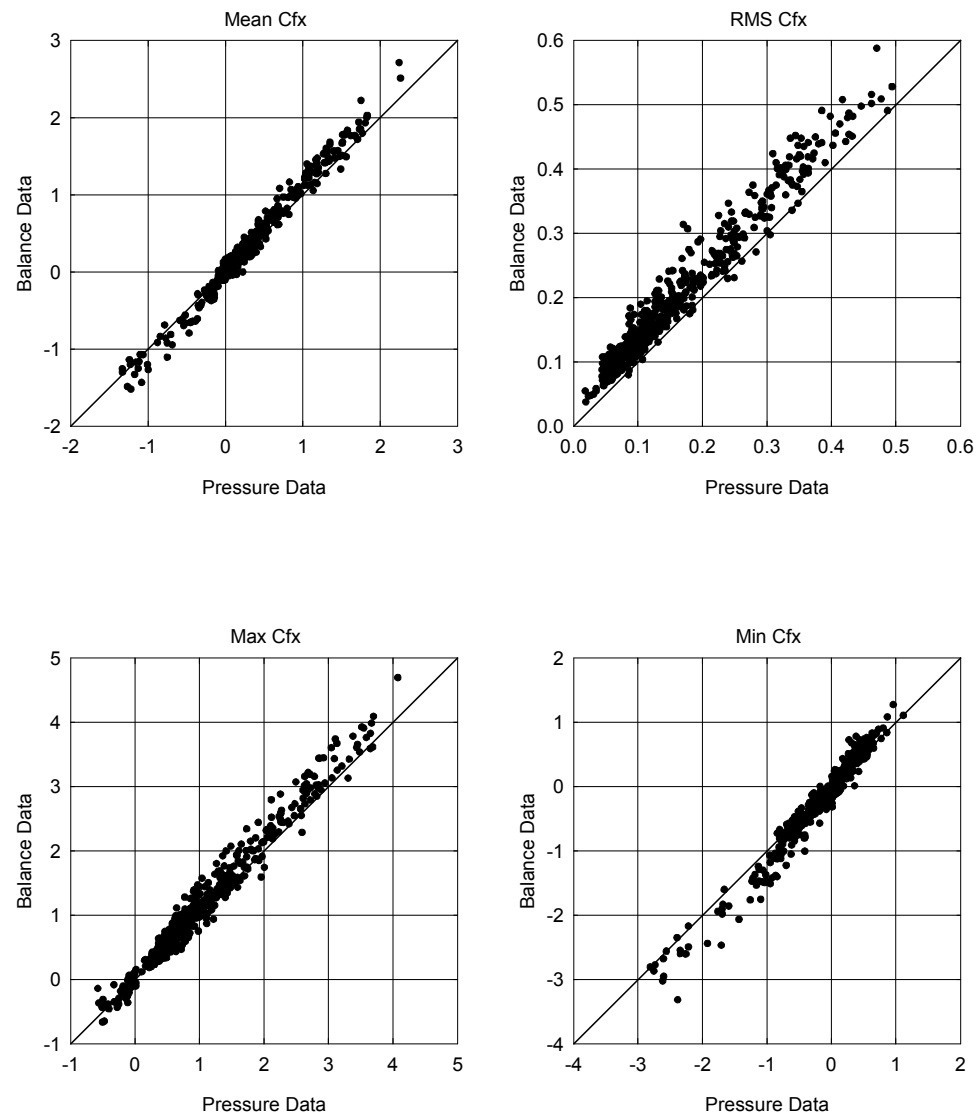
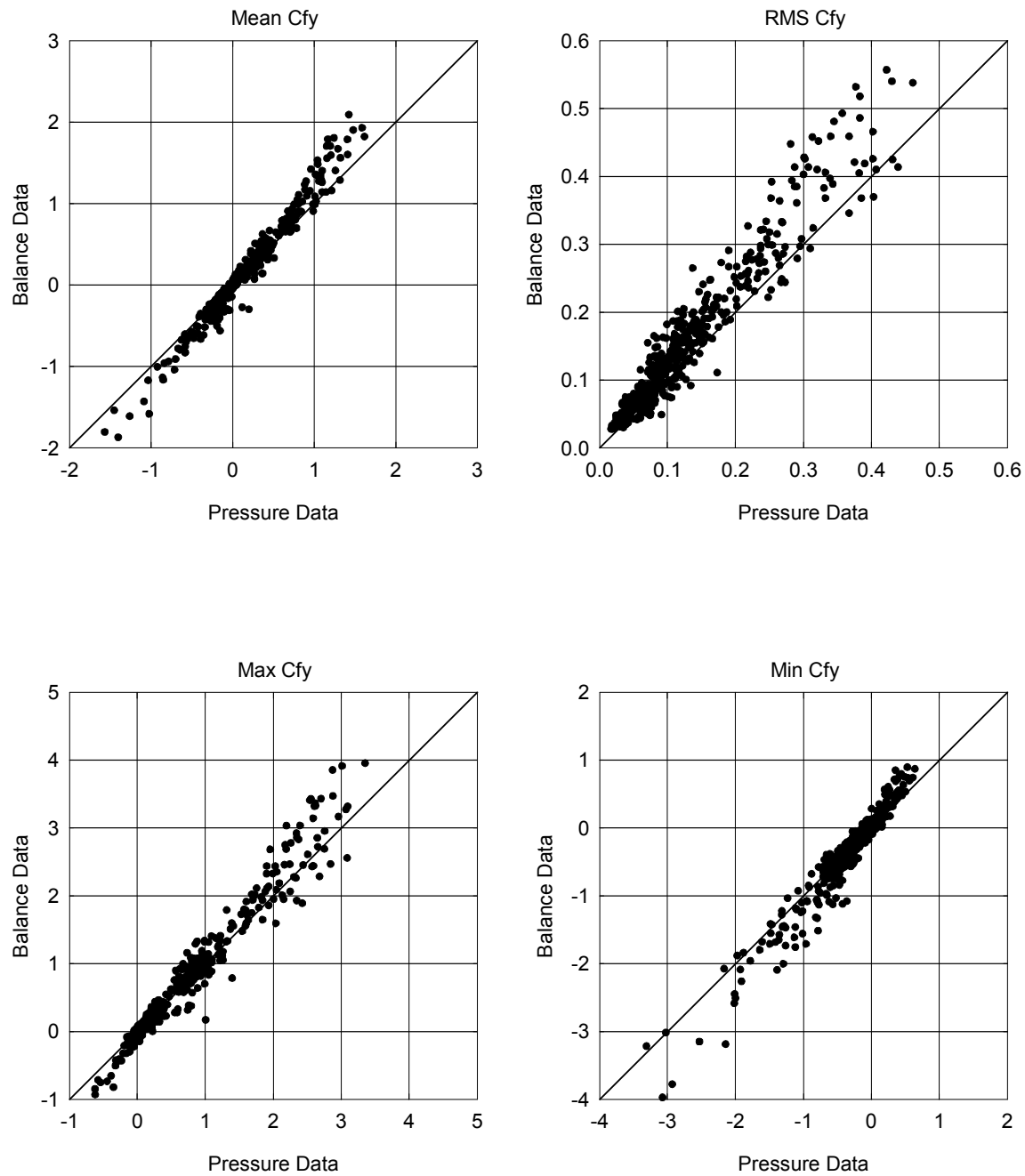
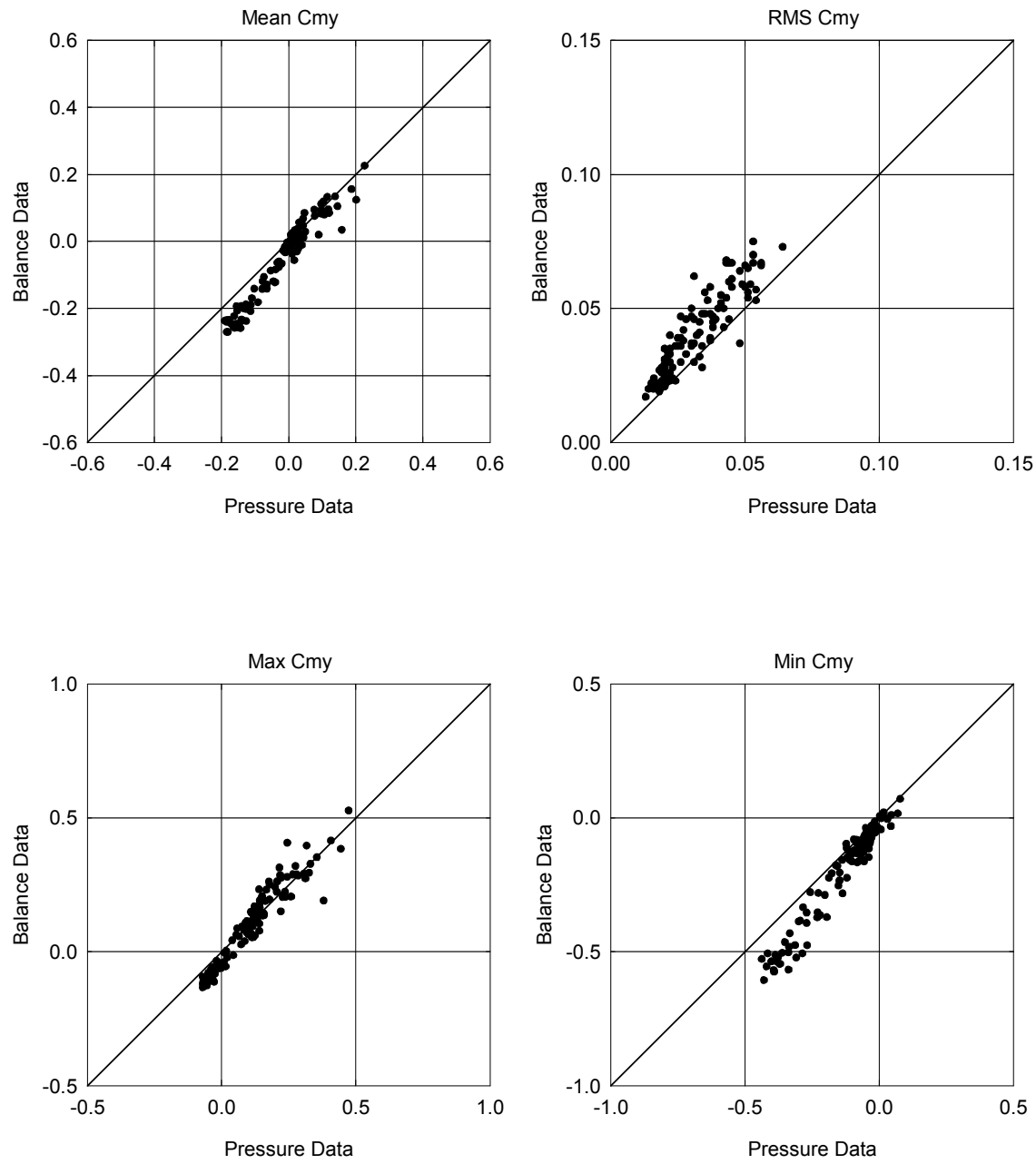


Figure 4-39 Comparison of Balance and Pressure Data, (a) Horizontal Force Component



**Figure 4-39 Comparison of Balance and Pressure Data,
(b) Vertical Force Component**



**Figure 4-39 Comparison of Balance and Pressure Data,
(c) Pitching Moment Component**

As can be seen, the integrated pressure loads tend to consistently underestimate those measured by the force balance for all the force components. That is, the best fit line when drawn would have a slope larger than 1.

By performing statistical linear regression on the data plotted in Figure 4-39c for the pitching moment and Figure 4-39a-b for the force components, scaling factors that would adjust the pressure data to best-match the balance data were calculated as the slopes of the best fit lines. Table 4-6 summarizes the result of the analysis. Note that the separate adjustment factors were estimated for Configuration C5 and all the other configurations. This is because the wind loads for Configuration C5 were practically applicable to the majority of the collector modules in the array field as pointed out earlier, thus warranting a particularly accurate adjustment.

Table 4-6 Adjustment Factors to Be Applied to Pressure Data

All Data Except for C5				
	Mean	RMS	Max	Min
Cfx	1.12	1.20	1.10	1.15
Cfy	1.21	1.21	1.10	1.17
Cmy	1.27	1.26	0.99	1.43
Overall Average	1.18			

C5 Only				
	Mean	RMS	Max	Min
Cfx	1.00	1.15	1.03	1.13
Cfy	1.15	1.12	1.00	1.05
Cmy	1.21	1.27	1.11	1.28
Overall Average	1.13			

The values of the adjustment factors vary little for the different statistical measures and load components. The overall averages indicated in Table 4-6 are appropriate as the adjustment factors to be uniformly applied to the pressure data. These adjustment factors are applicable to any statistical component, including the Mean, RMS, Maximum and Minimum coefficients, as well as the instantaneous load coefficients as described in the next section. As far as the design loads for the structural elements based on the pressure distribution data is concerned, the use of the scale factor is also appropriate. The factor should be applied to the individual local pressures uniformly. The effectiveness of the adjustment factors is demonstrated in the next section.

4.9.2 Effectiveness of the Adjustment Factors to Pressure Data

To verify the effectiveness of the adjustment factors given in Table 4-6, a new set of the integrated load coefficients were computed by applying those factors to the earlier pressure data. Figure 4-40 compares the adjusted pressure data with the original balance data. It appears that the adjusted pressure data correspond well to the balance data for all the load components. The effectiveness of the adjustment factors is also demonstrated in Figure 4-41 and Figure 4-42 that show variations of the load coefficients as a function of pitch angles for isolated and typical interior solar collectors, respectively.

It should be understood that all of the pressure test results given in this report, with an exception of those in Figure 4-41 and Figure 4-42, are not adjusted. These are presented as raw data, including the load summary shown in Appendix B for sake of consistency within the context of the present wind-tunnel study.

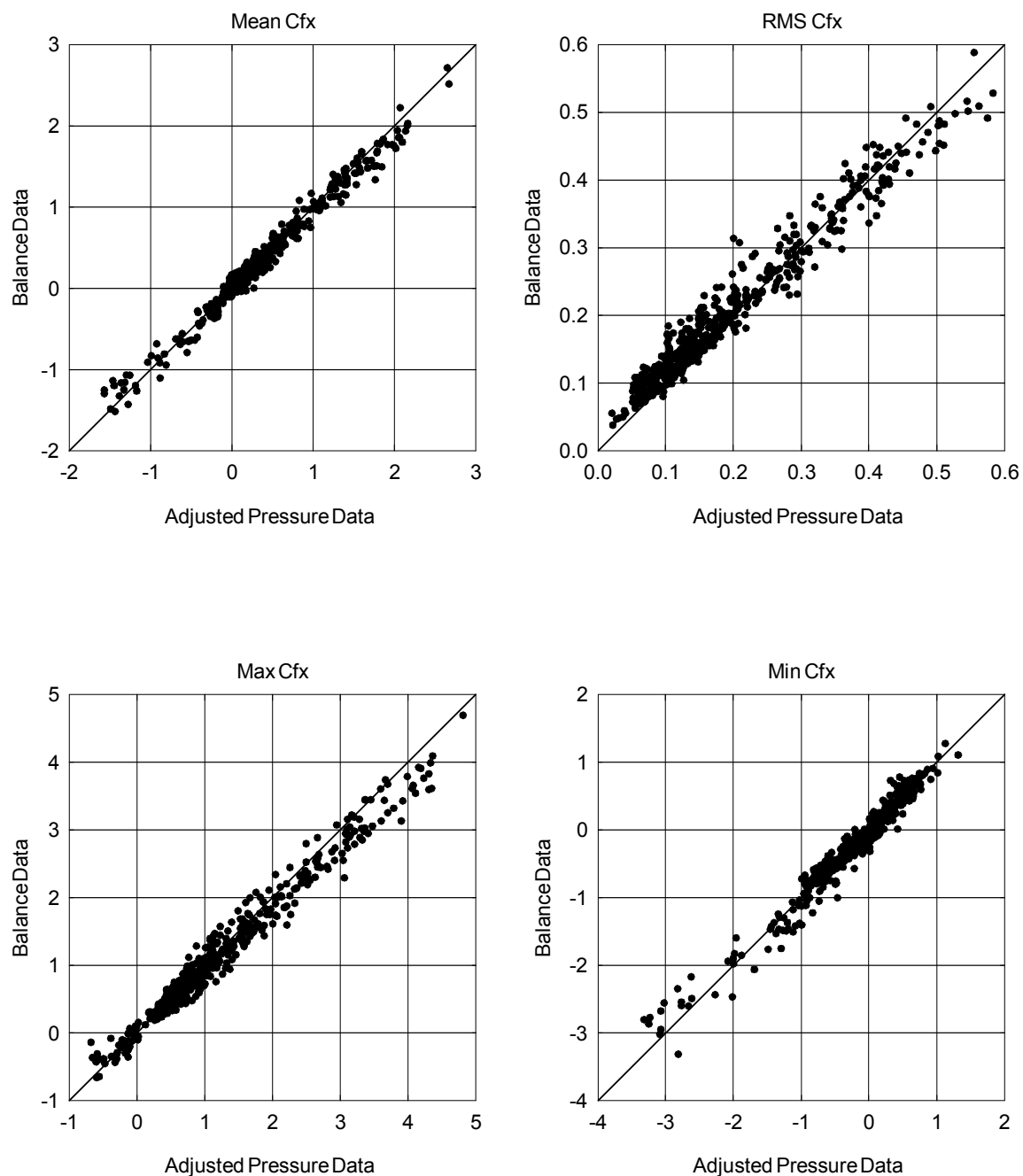


**Figure 4-40 Comparison of Balance and Adjusted Pressure Data,
(a) Horizontal Force Component**

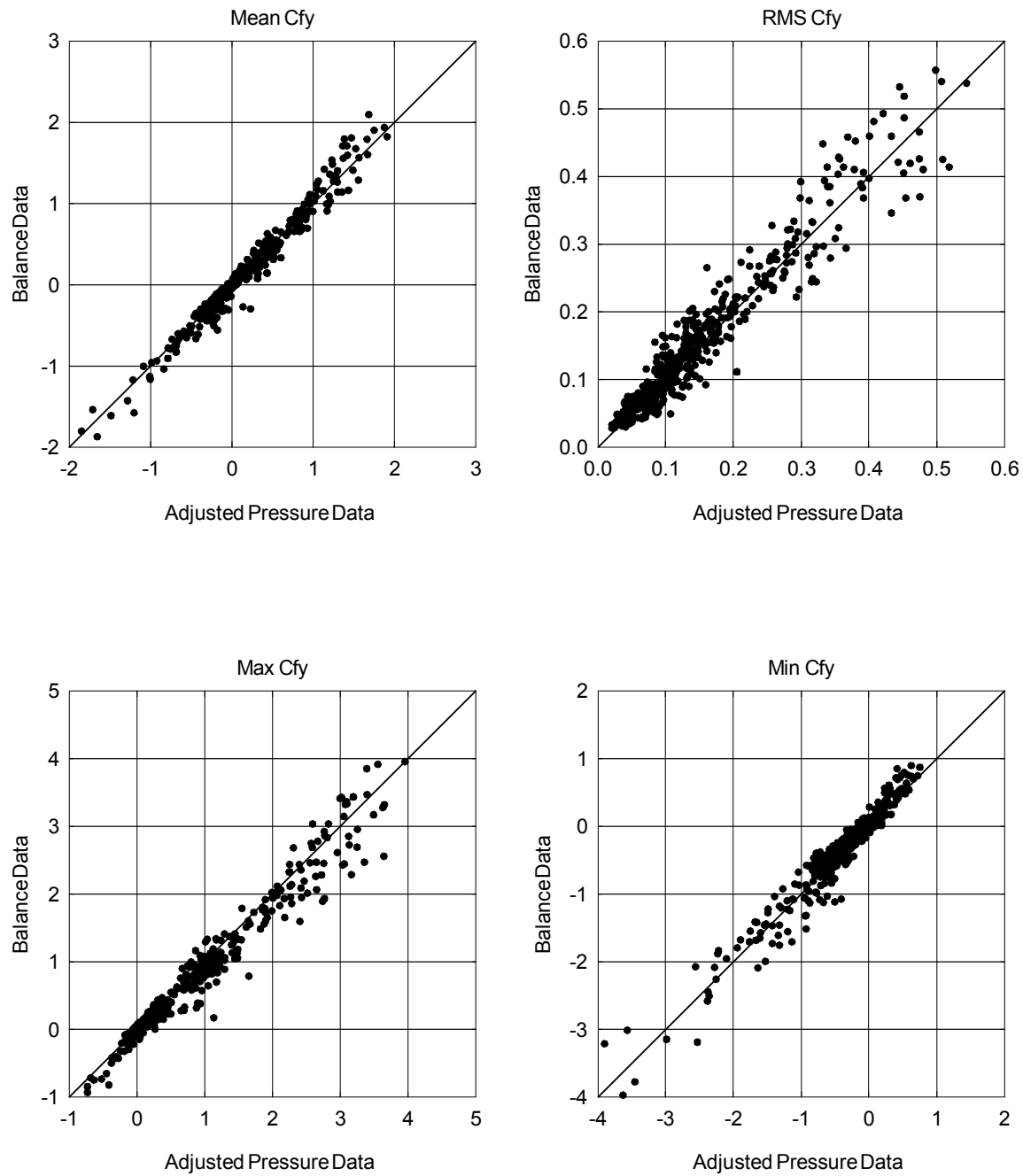


**Figure 4-40 Comparison of Balance and Adjusted Pressure Data,
(b) Vertical Force Component**

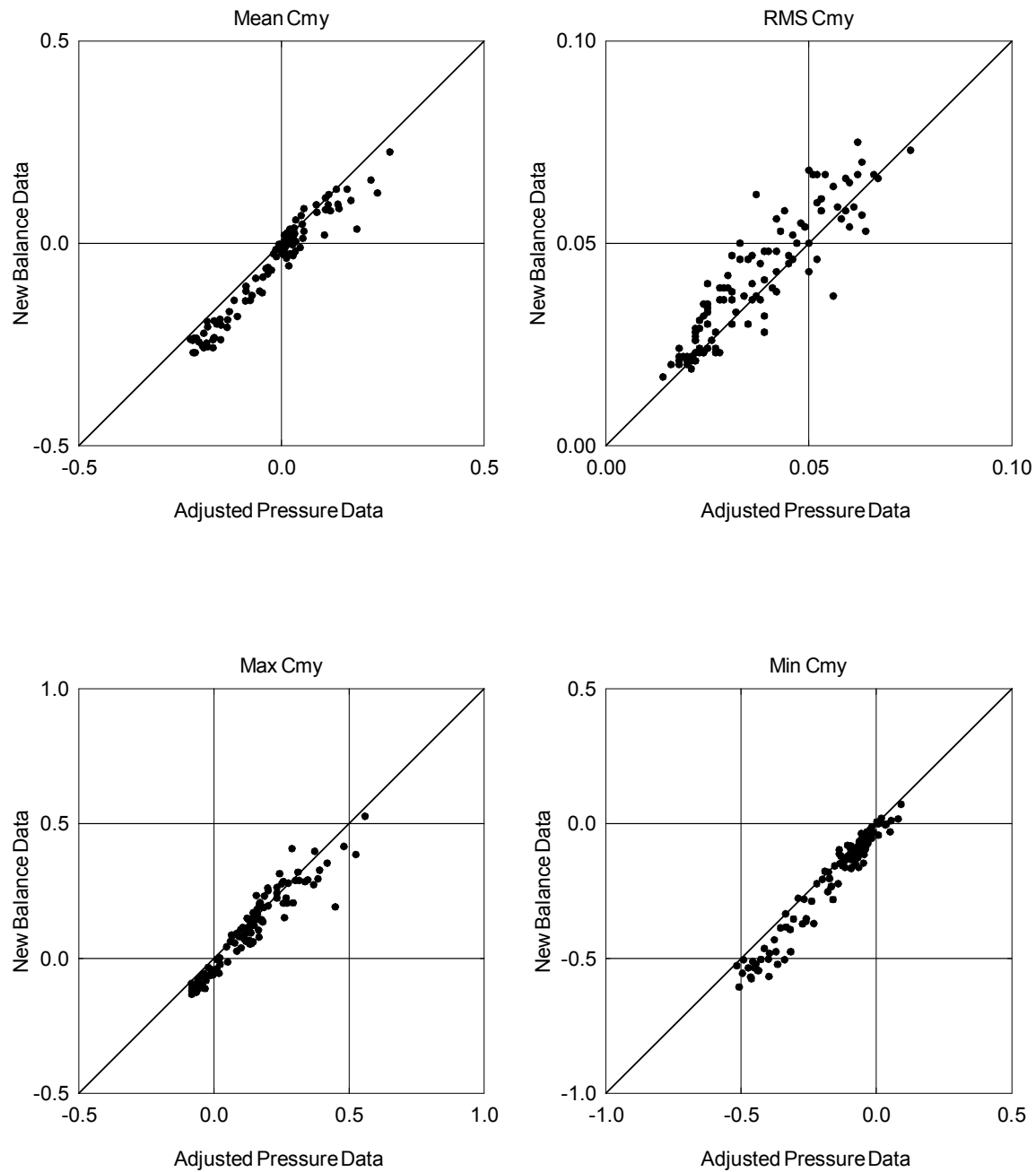


**Figure 4-40 Comparison of Balance and Adjusted Pressure Data,
(c) Pitching Moment Component**

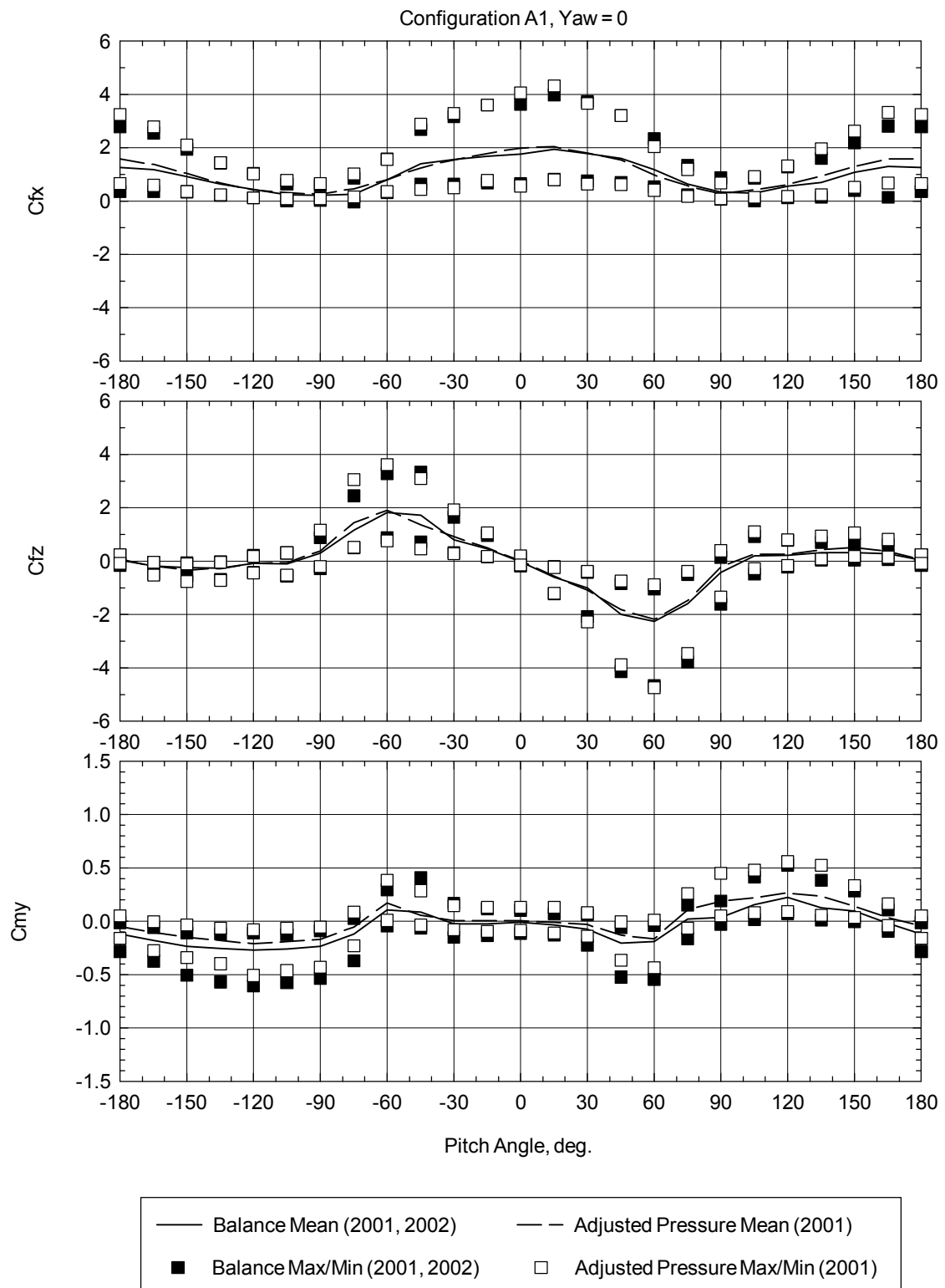


Figure 4-41 Comparison of Balance and Adjusted Pressure Data for Isolated Solar Collector

JAP note: Why blank page?

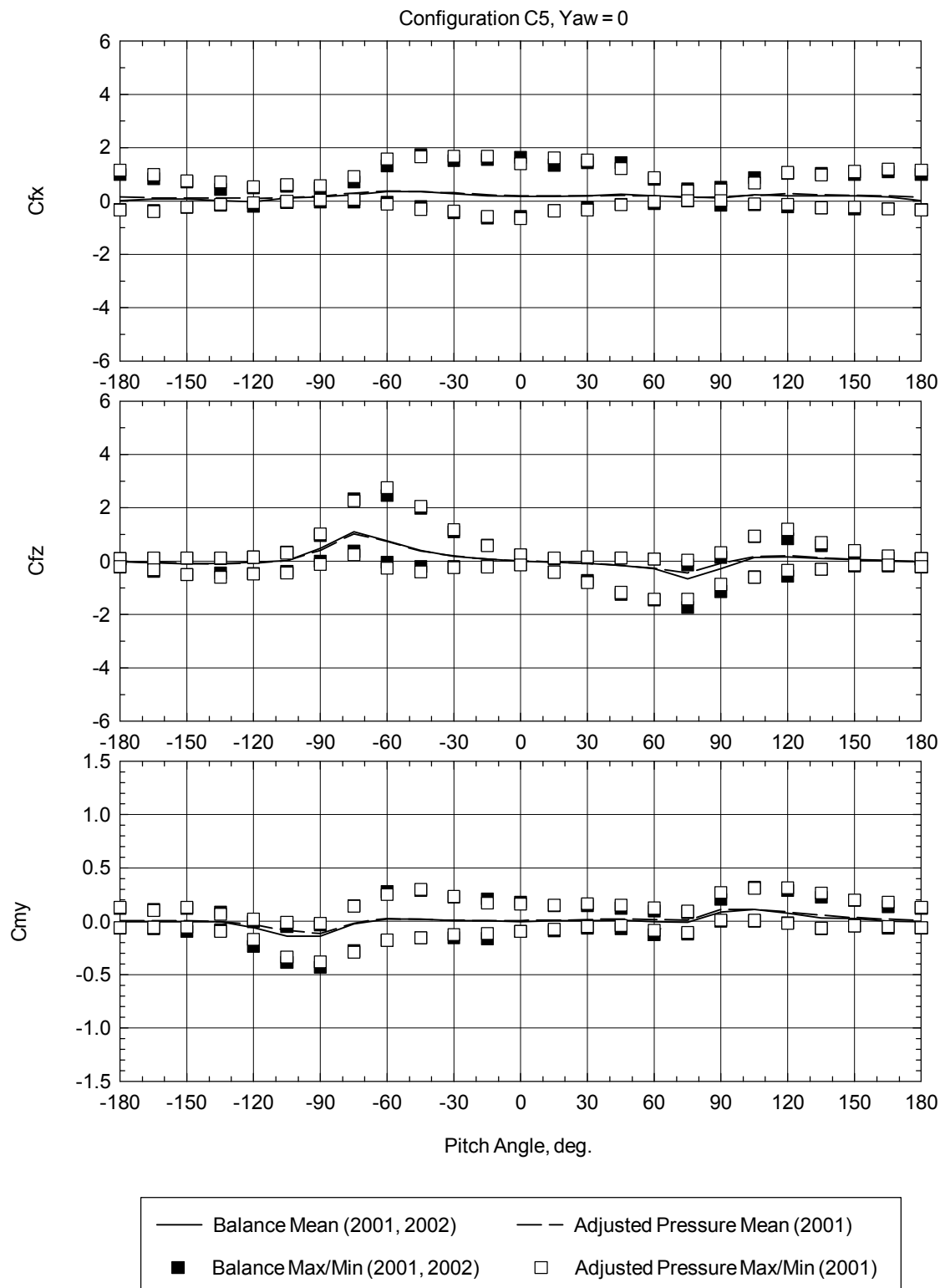


Figure 4-42 Comparison of Balance and Adjusted Pressure Data for Interior Solar Collector

5. CONCLUDING REMARKS

Extensive wind-tunnel tests were conducted on parabolic trough solar collectors to determine practical wind loads applicable to the structural design for stress and deformation, as well as the local component design for the concentrator reflectors. The overall dynamic loads and simultaneous pressure distributions on the concentrator were measured using force balances and a multi-pressure data acquisition system, respectively, in a boundary layer wind tunnel at CPP. Various test configurations were examined, including an isolated collector and solar field collectors at different positions.

Significant test results are presented and discussed in detail. Overall, the wind-tunnel tests produced sufficient data that can be used by designers of the present and future for a variety of design practices.

Several recommendations can be made for future work. The validity of the wind-tunnel data is particularly important. Ultimately, the acceptability of the test results should be based on model-to-full-scale comparison, which requires measurement of wind loads on a full-scale solar collector. Should further wind tunnel prove useful, the pressure test model should attempt to increase the pressure tap installation density to enhance the resolution of discrete pressure distribution data.

6. REFERENCES

- ASCE 7-98 (2000), Minimum Design Loads for Buildings and Other Structures, *Standard ANSI/ASCE 7-98*, American Society of Civil Engineers and American National Standards Institute, New York.
- Cermak, J.E. (1971), "Laboratory Simulation of the Atmospheric Boundary Layer," AIAA Journal, Vol. 9, September.
- Cermak, J.E. (1975), "Applications of Fluid Mechanics to Wind Engineering," A Freeman Scholar Lecture, ASME Journal of Fluids Engineering, Vol. 97, No. 1, March.
- Cermak, J.E. (1976), "Aerodynamics of Buildings," Annual Review of Fluid Mechanics, Vol. 8, pp. 75 – 106.
- Cohen, G.E., D.W. Kearney and G.J. Kolb (1999), Final Report on the Operation and Maintenance Improvement for Concentrating Solar Power Plants, Report SAND99-1290, Sandia National Laboratories.
- Counihan, J. (1975), "Adiabatic Atmospheric Boundary Layers: A Review and Analysis of Data from the Period 1880-1972," Atmos. Environ., Vol. 9, pp. 871 – 905.
- Engineering Science Data Unit [ESDU], (1975), "Characteristics of Atmospheric Turbulence Near the Ground," Item No. 75001, London, U.K.
- Huebner, K.H., E.A. Thornton and T.G. Byrom, (1995), The Finite Element Method for Engineer, Third Edition, A Wiley-Interscience Publication, Jon Wiley & Sons, Inc., New York
- International Code Council, Inc. (2000), International Building Code 2000 (IBC 2000), Falls Church, VA.
- Peterka, J. A. and R.G. Derickson (1992), Wind Load Design Methods for Ground-Based Heliostats and Parabolic Dish Collectors, Report SAND 92-7009, Sandia National Laboratories.
- Peterka, J. A., J. M. Sinou and J. E. Cermak (1980), Mean Wind Forces on Parabolic-Trough Solar Collectors, Report SAND80-7023, Sandia National Laboratories.
- Randall, D.E., D.D. McBride and R.E. Tate (1980), Steady-State Wind Loading on Parabolic-Trough Solar Collectors, Report SAND79-2134, Sandia National Laboratories.
- Randall, D.E., R.E. Tate and D.A Powers (1982), Experimental Results of Pitching Moment Tests on Parabolic-Trough Solar-Collector Array Configurations, Report SAND82-1569, Sandia National Laboratories.

7. APPENDICES

7.1 APPENDIX A - VALIDITY OF FULL-SCALE PREDICTION

Boundary-layer wind-tunnel testing for wind loads on structures has been an accepted practice for many years. The first well-conducted test for a structure using modern understanding of wind/structure interaction was performed for the World Trade center in New York City, conducted in about 1963 at Colorado State University under the direction of Drs. Jack Cermak (a principal of CPP, Inc.) and Alan Davenport. The wind load standard ANSI A58.1-1982 was referenced by most U.S. building codes by the mid 1980's, and permitted properly conducted wind-tunnel tests to be used in lieu of local building code wind load provisions. This capability continues today, with most U.S. building codes referring to some version of ASCE 7, the national wind load standard, which permits wind tunnel testing to replace code provisions. Survey references that discuss wind-tunnel modeling and its validity include Cermak (1971, 1975, 1976).

The basis for acceptance of wind-tunnel testing relied initially on early testing in aeronautical wind tunnels which showed that non-dimensional load coefficients become invariant with increasing Reynolds number. In the final analysis, comparisons of model and full-scale data have provided confidence in the ability of boundary-layer wind tunnels to correctly model full-scale wind loads. There have been a number of model/full-scale comparisons that have shown that the same non-dimensional wind load coefficients are obtained for models and full-scale structures. A few of these are listed below. These references include Meroney (1980) for wind flow similarity over terrain, Dalgiesh et al (1980) for cladding loads on a high-rise building, Cermak and Cochran (1992) for wind-tunnel simulation of a partial height boundary layer, Cochran and Cermak (1993) for cladding and frame pressures on a low rise building, Cheung et al. (1996) for cladding pressures and frame loads on a low-rise building, Cochran, Peterka and Derickson (1999) for wind speed similarity close to the roofs of low-rise buildings, Peterka and Hosoya, et al. (1998) for area-averaged pressures on a low-rise building.

For the current study, parabolic collectors have curved surfaces. Curved shapes such as cylinders are the shapes most sensitive to Reynolds number effects. For example, it is well-known that automobiles and airplanes must be modeled at near-full-scale Reynolds numbers to achieve acceptable accuracy. Both of these vehicle types are typically tested in uniform-flow, aeronautical-type wind tunnels with very low turbulence (typically less than 1 percent). For stationary objects at the surface of the earth, the turbulence intensity is much larger, typically greater than 15-20 percent. The added turbulence decreases the Reynolds number effects by inserting turbulence directly into the boundary layer on the object, increasing the effective Reynolds number of the flow. Several proprietary studies by CPP, Inc. have demonstrated this effect. Reynolds number tests on the solar collector models have shown no significant effect of Reynolds numbers over the range of Reynolds numbers that are permitted at model scale. On the basis of available information, it is likely that Reynolds number effects are not significant for determination of design wind loads on parabolic collectors using properly conducted boundary-layer wind tunnel tests. However, model to full scale comparisons for this geometry would be valuable and should be considered for future funding.

References

- Cermak, J.E. (1971), "Laboratory Simulation of the Atmospheric Boundary Layer," *AIAA Jl.*, Vol. 9, September.
- Cermak, J.E. (1975), "Applications of Fluid Mechanics to Wind Engineering," A Freeman Scholar Lecture, *ASME Journal of Fluids Engineering*, Vol. 97, No. 1, March.
- Cermak, J.E. (1976), "Aerodynamics of Buildings," *Annual Review of Fluid Mechanics*, Vol. 8, pp. 75 B 106.
- Cermak, J. E. and L. S. Cochran (1992), "Physical modeling of the atmospheric boundary layer," *Journal of Wind Engineering and Industrial Aerodynamics*, Vol. 41-44, pp 935-946.
- Cheung, J. C. K., Holmes, J. D., Melbourne, W. H., Lakshmanan, N., and Bowditch, P. (1996), "Pressures on a 1/10 Scale Model of the Texas Tech Building," *Third International Colloquium on Bluff Body Aerodynamics & Applications BBAA*, Blacksburg, Virginia, pp A IX 5 - A IX 8.
- Cochran, L.S. and Cermak, J. E. (1992), "Full- and model-scale cladding pressures on the Texas Tech University experimental building," *Journal of Wind Engineering and Industrial Aerodynamics*, Vol. 41-44, pp 1589-1600.
- Cochran, L. S., Peterka, J., and Derickson, R. (1999), "Roof Surface Wind Speed Distributions on Low-Rise Buildings," *Architectural Science Review*, Vol. 42, pp 151-160.
- Dalgliesh, W.A., J.T. Templin and K.R. Cooper, (1980), "Comparison of Wind Tunnel and Full-Scale Building Surface Pressures with Emphasis on Peaks," The Proceedings of the Fifth International Conference in Wind Engineering, Fort Collins, Colorado, Vol. 1, pp553-565.
- Meroney, R. N. (1980), "Wind-Tunnel Simulation of the Flow Over Hills and Complex Terrain," *Journal of Industrial Aerodynamics*, Vol. 5, pp 297-321.
- Peterka, J. N., Hosoya, N., Dodge, S., Cochran, L., and Cermak, J. E. (1998), "Area-average peak pressures in a gable roof vortex region," *Journal of Wind Engineering and Industrial Aerodynamics*, Vol. 77-78, pp 205-215.

7.2 APPENDIX B - LIST OF OVERALL LOAD DATA

This appendix section presents a list of overall load coefficients (Mean, RMS, Max and Min) measured by the balance and surface integration of the local pressure data. For the integrated pressure loads, the original local pressures as measured were used, and have not been adjusted to account for loss of resolutions due to the finite pressure tap layout on the wind-tunnel model (See Section 4.9).

Phase 1, 2, and 3 Balance Data

Phase 1, 2, and 3 Balance Data

Run	Conf	Uref fps	Cfx			Cfz						
			Yaw	Pitch	Mean	RMS	Max	Min	Mean	RMS	Max	Min
174	A1	10.6	0	0	1.529	0.442	2.927	0.557	0.048	0.091	0.309	-0.215
175	A1	12.3	0	0	1.499	0.463	3.009	0.451	0.049	0.081	0.329	-0.158
176	A1	14.1	0	0	1.473	0.435	3.011	0.499	0.042	0.072	0.313	-0.121
177	A1	16.4	0	0	1.588	0.463	3.295	0.519	0.038	0.069	0.324	-0.112
178	A1	17.8	0	0	1.614	0.472	3.400	0.594	0.032	0.068	0.332	-0.144
179	A1	17.7	0	0	1.788	0.442	3.564	0.748	0.031	0.065	0.328	-0.152
180	A1	19.1	0	0	1.795	0.511	3.546	0.671	0.025	0.069	0.351	-0.131
181	A1	20.7	0	0	1.757	0.499	3.688	0.695	0.021	0.067	0.339	-0.140
182	A1	22.1	0	0	1.767	0.475	3.745	0.525	0.014	0.070	0.513	-0.369
183	A1	10.5	0	-90	-0.133	0.148	0.359	-0.558	1.591	0.162	2.056	1.111
184	A1	12.3	0	-90	-0.097	0.157	0.467	-0.570	0.846	0.181	1.552	0.307
185	A1	14.5	0	-90	-0.079	0.154	0.380	-0.499	0.532	0.158	1.115	-0.003
186	A1	16.3	0	-90	0.003	0.157	0.528	-0.433	0.415	0.165	1.018	-0.145
187	A1	18.1	0	-90	0.033	0.143	0.496	-0.351	0.356	0.155	0.884	-0.146
188	A1	19.7	0	-90	0.069	0.135	0.546	-0.271	0.329	0.162	0.952	-0.171
189	A1	21.2	0	-90	0.113	0.135	0.577	-0.255	0.340	0.176	1.020	-0.239
190	A1	22.5	0	-90	0.120	0.134	0.593	-0.251	0.338	0.176	1.041	-0.194
207	A3	12.5	0	0	1.804	0.332	2.756	1.070	-0.015	0.082	0.192	-0.124
208	A3	14.7	0	0	1.776	0.328	2.896	0.984	-0.006	0.063	0.184	-0.180
209	A3	16.9	0	0	1.678	0.348	2.758	0.818	-0.010	0.053	0.163	-0.137
210	A3	19.0	0	0	1.683	0.342	2.827	0.929	-0.010	0.051	0.193	-0.127
211	A3	21.4	0	0	1.654	0.359	2.949	0.761	-0.008	0.050	0.253	-0.302
212	A3	23.4	0	0	1.656	0.360	3.014	0.859	-0.008	0.048	0.193	-0.126
213	A3	25.1	0	0	1.647	0.371	3.069	0.851	-0.012	0.047	0.189	-0.130
214	A3	27.0	0	0	1.709	0.364	3.042	0.876	-0.010	0.049	0.199	-0.135
215	A3	12.7	0	-90	0.594	0.081	0.834	0.404	-0.053	0.106	0.309	-0.468
216	A3	15.0	0	-90	0.408	0.084	0.673	0.203	0.002	0.128	0.516	-0.366
217	A3	17.0	0	-90	0.291	0.082	0.568	0.089	0.041	0.120	0.514	-0.364
218	A3	19.3	0	-90	0.268	0.076	0.527	0.095	0.082	0.124	0.557	-0.325
219	A3	21.7	0	-90	0.252	0.079	0.545	0.062	0.119	0.127	0.639	-0.287
220	A3	23.7	0	-90	0.256	0.075	0.554	0.022	0.157	0.129	0.656	-0.514
221	A3	25.7	0	-90	0.262	0.073	0.523	0.074	0.170	0.135	0.755	-0.249
222	A3	27.3	0	-90	0.262	0.073	0.554	0.078	0.207	0.136	0.714	-0.233
223	A4	12.6	0	-90	-0.073	0.097	0.204	-0.316	0.099	0.117	0.494	-0.276
224	A4	14.4	0	-90	-0.171	0.089	0.124	-0.384	0.135	0.129	0.568	-0.338
225	A4	16.6	0	-90	-0.175	0.082	0.128	-0.371	0.157	0.124	0.543	-0.241
226	A4	19.3	0	-90	-0.095	0.076	0.184	-0.285	0.181	0.131	0.645	-0.259
227	A4	21.4	0	-90	-0.067	0.077	0.193	-0.239	0.198	0.131	0.747	-0.211
228	A4	23.0	0	-90	-0.013	0.072	0.247	-0.194	0.215	0.133	0.756	-0.213
229	A4	24.8	0	-90	0.046	0.072	0.341	-0.118	0.240	0.140	0.799	-0.194
230	A4	26.6	0	-90	0.057	0.078	0.361	-0.126	0.270	0.143	0.843	-0.182
231	A4	12.3	0	0	1.031	0.349	2.121	0.256	0.903	0.076	1.122	0.710
232	A4	14.8	0	0	1.348	0.341	2.642	0.571	0.349	0.064	0.540	0.193
233	A4	16.8	0	0	1.435	0.374	2.736	0.630	0.192	0.056	0.395	0.032
234	A4	18.6	0	0	1.474	0.360	2.731	0.651	0.123	0.051	0.329	0.007
235	A4	21.1	0	0	1.550	0.355	2.774	0.770	0.081	0.049	0.265	-0.046
236	A4	22.9	0	0	1.592	0.365	3.074	0.760	0.055	0.049	0.256	-0.090
237	A4	25.3	0	0	1.592	0.366	2.880	0.755	0.041	0.047	0.235	-0.084
238	A4	26.3	0	0	1.628	0.398	3.080	0.753	0.031	0.049	0.245	-0.101
239	A2	23.2	0	0	1.720	0.509	3.910	0.598	-0.006	0.065	0.326	-0.174

Phase 1, 2, and 3 Balance Data

Run	Conf	Uref fps	Cfx		Cfz							
			Yaw	Pitch	Mean	RMS	Max	Min	Mean	RMS	Max	Min
240	A2	22.7	0	15	1.851	0.498	3.828	0.745	-0.570	0.101	-0.324	-0.926
241	A2	22.8	0	30	1.765	0.487	3.658	0.762	-1.170	0.249	-0.651	-2.075
242	A2	23.3	0	45	1.482	0.401	2.980	0.632	-1.803	0.425	-0.930	-3.215
243	A2	22.8	0	60	0.971	0.287	2.073	0.346	-1.539	0.410	-0.713	-3.015
244	A2	22.9	0	75	0.531	0.206	1.367	0.096	-0.792	0.280	-0.220	-1.837
245	A2	22.6	0	90	0.321	0.171	1.114	-0.094	0.144	0.150	0.704	-0.443
246	A2	23.1	0	-90	0.406	0.144	0.960	0.080	-0.272	0.201	0.278	-1.119
247	A2	23.0	0	-75	0.423	0.174	1.062	0.062	0.703	0.200	1.480	0.172
248	A2	22.6	0	-60	0.706	0.232	1.616	0.182	1.290	0.346	2.559	0.479
249	A2	22.7	0	-45	1.280	0.330	2.538	0.514	1.594	0.410	3.144	0.689
250	A2	22.7	0	-30	1.434	0.416	3.219	0.426	0.697	0.237	1.722	0.174
251	A2	22.9	0	-15	1.494	0.456	3.435	0.496	0.360	0.142	0.967	0.047
252	A2	23.1	180	-15	-1.159	0.362	-0.386	-2.597	-0.168	0.076	0.008	-0.438
253	A2	23.4	180	-30	-0.919	0.273	-0.328	-1.980	-0.211	0.083	-0.007	-0.522
254	A2	23.2	180	-45	-0.655	0.201	-0.217	-1.462	-0.147	0.061	0.016	-0.403
255	A2	23.2	180	-60	-0.637	0.180	-0.203	-1.381	-0.227	0.125	0.162	-0.737
256	A2	23.4	180	-75	-0.647	0.169	-0.253	-1.298	-0.651	0.209	-0.109	-1.458
257	A2	23.0	180	-90	-0.435	0.145	-0.121	-1.021	-0.199	0.184	0.441	-0.849
258	A2	22.9	180	90	-0.394	0.172	-0.014	-1.225	0.074	0.092	0.378	-0.362
259	A2	22.9	180	75	-0.637	0.195	-0.163	-1.510	0.331	0.111	0.788	0.031
260	A2	23.1	180	60	-0.791	0.229	-0.295	-1.753	0.062	0.077	0.387	-0.207
261	A2	22.7	180	45	-0.943	0.270	-0.365	-2.064	0.081	0.051	0.280	-0.089
262	A2	23.1	180	30	-1.199	0.333	-0.453	-2.438	0.144	0.049	0.319	0.015
263	A2	22.5	180	15	-1.516	0.406	-0.661	-3.019	0.138	0.048	0.330	0.004
264	A2	23.4	180	0	-1.483	0.375	-0.647	-2.950	0.037	0.031	0.140	-0.083
265	A1	22.7	180	0	-1.253	0.425	-0.366	-2.772	0.032	0.052	0.231	-0.159
266	A1	22.9	150	0	-1.137	0.388	-0.311	-2.558	0.061	0.046	0.218	-0.152
267	A1	22.8	120	0	-1.431	0.448	-0.433	-3.314	0.007	0.043	0.171	-0.174
268	A1	22.7	60	0	1.271	0.448	3.045	0.243	0.031	0.048	0.244	-0.108
269	A1	22.7	30	0	1.814	0.480	3.672	0.714	-0.020	0.038	0.146	-0.149
270	A1	22.7	0	0	1.757	0.482	3.609	0.648	-0.027	0.042	0.131	-0.175
271	A1	22.0	0	15	1.941	0.516	3.986	0.805	-0.595	0.162	-0.207	-1.225
272	A1	22.5	30	15	1.686	0.437	3.426	0.565	-0.510	0.137	-0.160	-1.073
273	A1	23.1	60	15	1.220	0.437	2.818	0.192	-0.394	0.142	-0.054	-0.931
274	A1	22.8	120	15	-1.327	0.441	-0.359	-2.869	0.246	0.101	0.628	0.008
275	A1	23.0	150	15	-1.198	0.392	-0.380	-2.676	0.291	0.086	0.622	0.095
276	A1	22.6	180	15	-1.297	0.396	-0.138	-2.803	0.287	0.087	0.612	0.066
277	A1	22.7	180	30	-1.069	0.309	-0.396	-2.171	0.311	0.092	0.643	0.047
278	A1	22.9	150	30	-1.248	0.343	-0.430	-2.491	0.430	0.111	0.817	0.168
279	A1	23.3	120	30	-1.264	0.378	-0.383	-2.602	0.461	0.139	0.952	0.142
280	A1	23.3	60	30	1.069	0.424	2.580	0.124	-0.675	0.275	-0.083	-1.676
281	A1	22.7	30	30	1.682	0.439	3.441	0.727	-0.961	0.258	-0.415	-1.958
282	A1	22.8	0	30	1.780	0.482	3.739	0.762	-1.002	0.274	-0.422	-2.085
283	A1	22.6	0	45	1.604	0.435	3.190	0.696	-2.004	0.557	-0.845	-4.128
284	A1	22.7	30	45	1.455	0.410	3.071	0.581	-1.868	0.532	-0.749	-3.971
285	A1	22.7	60	45	0.664	0.310	1.806	0.000	-0.936	0.403	-0.149	-2.508
286	A1	22.8	120	45	-0.809	0.295	-0.098	-1.830	0.481	0.185	1.143	0.048
287	A1	22.6	150	45	-0.835	0.255	-0.079	-1.856	0.456	0.136	1.079	0.013
288	A1	22.6	180	45	-0.687	0.229	-0.142	-1.599	0.329	0.097	0.708	0.046
289	A1	22.9	180	60	-0.558	0.190	-0.115	-1.290	0.212	0.127	0.782	-0.223

Phase 1, 2, and 3 Balance Data

Run	Conf	Uref fps	Cfx		Cfz							
			Yaw	Pitch	Mean	RMS	Max	Min	Mean	RMS	Max	Min
290	A1	22.4	150	60	-0.627	0.194	-0.181	-1.370	0.456	0.164	1.036	-0.023
291	A1	22.5	120	60	-0.654	0.222	-0.110	-1.490	0.452	0.180	1.166	-0.013
292	A1	22.6	60	60	0.385	0.211	1.155	-0.114	-0.778	0.385	0.006	-2.259
293	A1	22.5	30	60	1.083	0.291	2.106	0.437	-2.034	0.606	-0.819	-4.182
294	A1	22.7	0	60	1.166	0.304	2.342	0.542	-2.267	0.640	-1.033	-4.656
295	A1	22.9	0	75	0.632	0.182	1.336	0.235	-1.610	0.540	-0.503	-3.775
296	A1	22.5	30	75	0.525	0.161	1.081	0.173	-1.429	0.493	-0.431	-3.146
297	A1	22.7	60	75	0.151	0.109	0.594	-0.142	-0.502	0.288	0.197	-1.710
298	A1	22.9	120	75	-0.240	0.125	0.097	-0.761	0.101	0.163	0.761	-0.540
299	A1	22.5	150	75	-0.281	0.136	0.067	-0.809	0.241	0.160	0.897	-0.444
300	A1	22.6	180	75	-0.297	0.118	0.001	-0.848	0.206	0.176	0.927	-0.474
301	A1	22.7	180	90	-0.244	0.116	0.035	-0.756	-0.311	0.241	0.229	-1.515
302	A1	22.8	150	90	-0.274	0.119	0.022	-0.714	-0.502	0.291	0.228	-1.754
303	A1	22.6	120	90	-0.354	0.098	-0.100	-0.755	-0.238	0.226	0.364	-1.327
304	A1	22.8	60	90	0.001	0.090	0.358	-0.242	-0.201	0.215	0.423	-1.084
305	A1	22.2	30	90	0.397	0.124	0.882	0.114	-0.614	0.327	0.106	-1.999
306	A1	22.4	0	90	0.337	0.124	0.866	0.056	-0.430	0.273	0.145	-1.612
307	A1	22.6	0	-90	0.211	0.095	0.588	0.007	0.295	0.167	0.871	-0.278
308	A1	22.6	30	-90	0.264	0.112	0.728	0.025	0.467	0.151	1.030	-0.048
309	A1	22.6	60	-90	0.182	0.098	0.565	-0.079	0.203	0.122	0.758	-0.208
310	A1	22.6	120	-90	-0.086	0.106	0.155	-0.546	0.227	0.149	0.899	-0.219
311	A1	22.3	150	-90	-0.222	0.118	0.037	-0.645	0.512	0.162	1.162	-0.022
312	A1	22.2	180	-90	-0.189	0.107	0.030	-0.639	0.320	0.179	1.076	-0.180
313	A1	22.9	180	-75	-0.235	0.107	0.011	-0.638	-0.106	0.119	0.312	-0.556
314	A1	22.7	150	-75	-0.285	0.121	-0.010	-0.750	-0.131	0.133	0.252	-0.681
315	A1	22.5	120	-75	-0.333	0.121	-0.052	-0.801	-0.097	0.115	0.240	-0.577
316	A1	22.5	60	-75	0.098	0.100	0.510	-0.160	0.498	0.196	1.325	0.010
317	A1	22.6	30	-75	0.391	0.165	1.014	-0.035	1.090	0.286	2.280	0.484
318	A1	22.6	0	-75	0.255	0.145	0.850	-0.048	1.162	0.294	2.444	0.504
319	A1	22.7	0	-60	0.793	0.219	1.584	0.320	1.823	0.426	3.273	0.871
320	A1	22.4	30	-60	0.807	0.223	1.686	0.350	1.603	0.421	3.167	0.741
321	A1	22.8	60	-60	0.425	0.169	1.059	0.027	0.766	0.279	1.860	0.159
322	A1	22.3	120	-60	-0.347	0.184	0.097	-1.049	-0.402	0.155	-0.022	-1.032
323	A1	22.8	150	-60	-0.465	0.162	-0.126	-1.119	-0.274	0.126	0.076	-0.840
324	A1	22.3	180	-60	-0.434	0.151	-0.113	-1.035	-0.084	0.089	0.217	-0.425
325	A1	22.7	180	-45	-0.625	0.203	-0.219	-1.425	-0.263	0.097	-0.020	-0.677
326	A1	21.9	150	-45	-0.661	0.202	-0.215	-1.472	-0.287	0.104	-0.026	-0.719
327	A1	22.8	120	-45	-0.607	0.211	-0.089	-1.422	-0.376	0.135	-0.018	-0.875
328	A1	22.9	60	-45	0.613	0.242	1.612	0.057	0.905	0.308	2.189	0.253
329	A1	22.3	30	-45	1.244	0.333	2.524	0.508	1.673	0.459	3.323	0.635
330	A1	22.4	0	-45	1.402	0.350	2.675	0.634	1.705	0.452	3.328	0.716
331	A1	22.5	0	-30	1.550	0.419	3.159	0.638	0.801	0.219	1.649	0.319
332	A1	22.6	30	-30	1.552	0.406	3.158	0.682	0.851	0.243	1.790	0.328
333	A1	22.6	60	-30	1.017	0.361	2.447	0.207	0.700	0.257	1.764	0.156
334	A1	22.7	120	-30	-0.692	0.275	-0.018	-1.761	-0.330	0.107	-0.085	-0.754
335	A1	22.8	150	-30	-0.856	0.269	-0.289	-1.904	-0.247	0.088	-0.054	-0.600
336	A1	22.8	180	-30	-0.913	0.276	-0.345	-1.942	-0.237	0.085	-0.059	-0.530
337	A1	22.6	180	-15	-1.166	0.358	-0.363	-2.544	-0.190	0.069	-0.040	-0.451
338	A1	22.6	150	-15	-1.070	0.341	-0.347	-2.348	-0.166	0.068	-0.028	-0.420
339	A1	22.4	120	-15	-1.103	0.347	-0.264	-2.465	-0.169	0.074	-0.011	-0.478

Phase 1, 2, and 3 Balance Data

Run	Conf	Uref fps	Cfx		Cfz							
			Mean	RMS	Max	Min	Mean	RMS	Max	Min		
340	A1	22.0	60	-15	1.055	0.452	2.947	0.012	0.526	0.168	1.291	0.130
341	A1	22.8	30	-15	1.510	0.441	3.254	0.513	0.446	0.121	0.896	0.158
342	A1	22.5	0	-15	1.669	0.491	3.604	0.674	0.453	0.132	0.964	0.167
343	C5	21.7	30	-15	0.392	0.382	2.001	-0.714	0.129	0.144	0.772	-0.278
344	C5	21.7	0	-15	0.192	0.269	1.549	-0.643	0.070	0.087	0.599	-0.175
345	C5	21.6	-30	-15	0.261	0.271	1.747	-0.659	0.073	0.093	0.657	-0.222
346	C5	21.7	-30	-30	0.324	0.249	1.560	-0.248	0.206	0.158	1.124	-0.174
347	C5	21.5	0	-30	0.270	0.265	1.524	-0.432	0.172	0.168	1.095	-0.212
348	C5	21.5	30	-30	0.373	0.304	1.852	-0.417	0.250	0.209	1.333	-0.255
349	C5	21.6	30	-45	0.408	0.263	1.594	-0.165	0.520	0.297	1.891	-0.079
350	C5	21.6	0	-45	0.366	0.264	1.737	-0.202	0.407	0.299	1.982	-0.207
351	C5	21.3	-30	-45	0.392	0.230	1.546	-0.160	0.431	0.246	1.727	-0.135
352	C5	22.0	-30	-60	0.317	0.158	1.051	-0.033	0.649	0.287	1.952	0.012
353	C5	21.7	0	-60	0.362	0.215	1.326	-0.053	0.756	0.389	2.454	-0.045
354	C5	21.6	30	-60	0.388	0.186	1.268	-0.022	0.763	0.324	2.262	0.101
355	C5	21.8	30	-75	0.210	0.126	0.711	-0.108	0.877	0.260	1.954	0.279
356	C5	21.7	0	-75	0.243	0.128	0.724	-0.033	1.096	0.300	2.327	0.368
357	C5	21.6	-30	-75	0.234	0.116	0.751	0.023	0.870	0.278	2.060	0.236
358	C5	21.8	-30	-90	0.136	0.077	0.444	-0.068	0.377	0.131	0.883	-0.063
359	C5	22.1	0	-90	0.146	0.080	0.491	-0.052	0.481	0.137	0.972	0.000
360	C5	22.2	30	-90	0.173	0.101	0.546	-0.103	0.382	0.121	0.853	-0.033
361	C5	21.5	30	-105	0.124	0.106	0.552	-0.163	-0.043	0.084	0.259	-0.416
362	C5	21.9	0	-105	0.122	0.088	0.565	-0.063	0.017	0.081	0.340	-0.384
363	C5	22.1	-30	-105	0.111	0.084	0.447	-0.086	-0.033	0.082	0.277	-0.400
364	C5	22.0	-30	-120	0.114	0.087	0.512	-0.105	-0.063	0.073	0.148	-0.412
365	C5	21.4	0	-120	-0.013	0.088	0.493	-0.198	-0.045	0.075	0.165	-0.467
366	C5	22.0	30	-120	0.166	0.107	0.574	-0.121	-0.121	0.077	0.085	-0.472
367	C5	22.1	30	-135	0.210	0.119	0.704	-0.142	-0.228	0.094	0.014	-0.602
368	C5	21.8	0	-135	0.020	0.087	0.437	-0.167	-0.081	0.081	0.107	-0.445
369	C5	21.9	-30	-135	0.085	0.099	0.522	-0.208	-0.103	0.087	0.126	-0.464
370	C5	21.9	-30	-150	0.068	0.131	0.653	-0.317	-0.099	0.093	0.123	-0.505
371	C5	21.6	0	-150	0.068	0.121	0.711	-0.247	-0.090	0.084	0.109	-0.504
372	C5	21.8	30	-150	0.286	0.168	0.999	-0.220	-0.262	0.112	0.045	-0.747
373	C5	22.1	30	-165	0.347	0.234	1.281	-0.345	-0.150	0.090	0.088	-0.490
374	C5	21.5	0	-165	0.078	0.164	0.832	-0.355	-0.061	0.067	0.088	-0.387
375	C5	21.7	-30	-165	0.080	0.175	0.872	-0.467	-0.066	0.076	0.142	-0.431
376	C5	21.7	-30	180	0.133	0.188	0.938	-0.405	-0.012	0.047	0.106	-0.236
377	C5	22.0	0	180	0.011	0.673	0.997	-0.319	-0.017	0.042	0.090	-0.212
378	C5	22.0	30	180	0.403	0.256	1.428	-0.319	-0.058	0.055	0.104	-0.253
379	C5	21.8	30	165	0.402	0.253	1.502	-0.270	0.056	0.051	0.252	-0.124
380	C5	21.4	0	165	0.159	0.181	1.100	-0.283	-0.001	0.037	0.115	-0.169
381	C5	22.0	-30	165	0.186	0.196	1.106	-0.446	0.004	0.041	0.139	-0.168
382	C5	21.8	-30	150	0.226	0.176	1.022	-0.431	0.084	0.065	0.363	-0.143
383	C5	21.8	0	150	0.192	0.163	0.993	-0.300	0.051	0.063	0.308	-0.178
384	C5	21.9	30	150	0.360	0.217	1.271	-0.236	0.103	0.075	0.399	-0.167
385	C5	21.7	30	135	0.417	0.215	1.395	-0.193	0.247	0.137	0.893	-0.153
386	C5	21.8	0	135	0.201	0.158	1.032	-0.258	0.101	0.096	0.582	-0.299
387	C5	22.3	-30	135	0.296	0.162	1.114	-0.170	0.144	0.105	0.639	-0.213
388	C5	22.0	-30	120	0.316	0.168	1.282	-0.214	0.228	0.148	1.044	-0.302
389	C5	22.2	0	120	0.202	0.155	1.041	-0.226	0.159	0.132	0.836	-0.566

Phase 1, 2, and 3 Balance Data

Run	Conf	Uref fps	Cfx			Cfz						
			Mean	RMS	Max	Min	Mean	RMS	Max	Min		
390	C5	22.4	30	120	0.389	0.196	1.441	-0.161	0.252	0.164	1.001	-0.214
391	C5	22.2	30	105	0.224	0.153	0.915	-0.257	0.231	0.179	0.931	-0.513
392	C5	22.5	0	105	0.231	0.127	0.871	-0.143	0.133	0.182	0.917	-0.590
393	C5	22.1	-30	105	0.164	0.080	0.473	-0.056	-0.297	0.175	0.172	-1.078
394	C5	22.6	-30	90	0.168	0.089	0.516	-0.073	-0.258	0.172	0.208	-1.097
395	C5	22.2	0	90	0.124	0.094	0.519	-0.159	-0.292	0.178	0.146	-1.131
396	C5	22.7	30	90	0.148	0.097	0.542	-0.112	-0.326	0.205	0.195	-1.316
397	C5	22.3	30	75	0.229	0.106	0.613	-0.061	-0.908	0.231	-0.323	-1.882
398	C5	22.0	0	75	0.158	0.059	0.458	-0.004	-0.664	0.204	-0.144	-1.734
399	C5	22.5	-30	75	0.149	0.072	0.421	-0.044	-0.612	0.186	-0.135	-1.415
400	C5	22.2	-30	60	0.169	0.112	0.722	-0.101	-0.351	0.178	0.029	-1.221
401	C5	22.3	0	60	0.189	0.120	0.822	-0.105	-0.280	0.200	0.083	-1.469
402	C5	22.6	30	60	0.257	0.117	0.730	-0.070	-0.604	0.189	-0.161	-1.423
403	C5	22.7	30	45	0.367	0.191	1.374	-0.124	-0.390	0.168	-0.042	-1.279
404	C5	22.4	0	45	0.253	0.176	1.443	-0.131	-0.167	0.156	0.115	-1.240
405	C5	22.4	-30	45	0.252	0.187	1.276	-0.149	-0.223	0.154	0.091	-1.035
406	C5	22.2	-30	30	0.246	0.236	1.410	-0.352	-0.106	0.100	0.129	-0.634
407	C5	22.0	0	30	0.202	0.216	1.439	-0.252	-0.079	0.107	0.129	-0.720
408	C5	22.0	30	30	0.430	0.287	1.746	-0.311	-0.245	0.130	0.053	-0.871
409	C5	22.6	30	15	0.384	0.325	1.745	-1.003	-0.107	0.076	0.161	-0.591
410	C5	22.2	0	15	0.178	0.222	1.347	-0.362	-0.043	0.064	0.105	-0.405
411	C5	22.2	-30	15	0.225	0.267	1.552	-0.545	-0.062	0.064	0.103	-0.364
412	C5	22.2	-30	0	0.201	0.257	1.538	-0.471	0.016	0.045	0.262	-0.122
413	C5	22.5	0	0	0.184	0.258	1.640	-0.580	-0.009	0.040	0.220	-0.131
414	C5	22.1	30	0	0.362	0.402	2.006	-0.830	0.010	0.072	0.294	-0.208
415	F5	22.0	0	-165	0.085	0.162	0.887	-0.351	-0.056	0.081	0.114	-0.457
416	F5	21.6	0	-150	0.090	0.125	0.704	-0.256	-0.077	0.088	0.104	-0.508
417	F5	22.7	0	-135	0.053	0.093	0.471	-0.172	-0.080	0.082	0.108	-0.434
418	F5	22.2	0	-120	0.098	0.102	0.669	-0.121	-0.038	0.066	0.162	-0.379
419	F5	22.7	0	-105	0.228	0.127	0.823	-0.013	-0.162	0.135	0.172	-0.784
420	F5	22.1	0	-90	0.326	0.128	0.866	0.069	-0.016	0.199	0.495	-0.948
421	F5	22.7	0	-75	0.267	0.153	0.942	-0.105	0.730	0.223	1.623	0.035
422	F5	22.3	0	-50	0.356	0.235	1.469	-0.254	0.686	0.310	2.137	-0.067
423	F5	22.2	0	-45	0.352	0.264	1.838	-0.318	0.415	0.266	1.920	-0.192
424	F5	22.4	0	-30	0.282	0.265	1.638	-0.527	0.190	0.151	1.019	-0.177
425	F5	22.2	0	-15	0.179	0.276	1.511	-0.706	0.105	0.087	0.549	-0.142
426	F5	22.0	0	0	0.156	0.281	1.622	-0.662	0.035	0.045	0.300	-0.092
427	F5	22.1	0	15	0.109	0.249	1.483	-0.607	-0.007	0.061	0.140	-0.349
428	F5	22.2	0	30	0.138	0.221	1.312	-0.498	-0.064	0.105	0.175	-0.597
429	F5	22.5	0	45	0.196	0.192	1.174	-0.210	-0.164	0.163	0.107	-0.999
430	F5	22.3	0	60	0.169	0.125	0.866	-0.076	-0.291	0.219	0.066	-1.472
431	F5	22.4	0	75	0.119	0.069	0.438	-0.070	-0.400	0.177	0.038	-1.412
432	F5	22.8	0	90	0.208	0.100	0.697	-0.048	0.096	0.136	0.514	-0.574
433	F5	23.2	0	105	0.297	0.166	1.194	-0.190	0.294	0.202	1.176	-0.373
434	F5	22.4	0	120	0.215	0.171	1.321	-0.275	0.166	0.152	1.091	-0.432
435	F5	22.1	0	135	0.126	0.168	1.105	-0.384	0.093	0.103	0.605	-0.369
436	F5	22.4	0	150	0.189	0.179	1.125	-0.322	0.037	0.064	0.266	-0.239
437	F5	22.2	0	165	0.137	0.189	1.211	-0.432	-0.004	0.050	0.159	-0.250
438	F5	22.2	0	180	0.089	0.182	0.990	-0.378	-0.027	0.055	0.085	-0.309
439	E1	22.1	0	180	1.677	0.356	3.078	0.849	0.192	0.052	0.351	-0.034

Phase 1, 2, and 3 Balance Data

Run	Conf	Uref fps	Cfx		Cfz							
			Yaw	Pitch	Mean	RMS	Max	Min	Mean	RMS	Max	Min
440	E1	22.2	0	165	1.762	0.369	3.218	0.873	0.521	0.087	0.843	0.281
441	E1	22.5	0	150	1.610	0.332	2.859	0.813	0.644	0.108	1.061	0.333
442	E1	22.4	0	135	1.178	0.268	2.322	0.478	0.492	0.098	0.869	0.188
443	E1	22.2	0	120	0.899	0.266	2.019	0.185	0.252	0.155	1.104	-0.328
444	E1	22.5	0	105	0.665	0.237	1.837	0.072	0.698	0.280	2.021	-0.050
445	E1	22.2	0	90	0.457	0.234	1.497	-0.130	0.460	0.206	1.278	-0.411
446	E1	22.9	0	75	0.731	0.222	1.673	0.224	-1.393	0.435	-0.562	-3.110
447	E1	22.4	0	60	0.869	0.232	1.768	0.323	-1.793	0.481	-0.773	-3.513
448	E1	22.4	0	45	1.458	0.346	2.752	0.704	-2.103	0.507	-1.041	-4.037
449	E1	22.5	0	30	1.989	0.411	3.732	1.016	-1.368	0.286	-0.703	-2.490
450	E1	22.2	0	15	2.138	0.455	4.320	1.065	-0.823	0.168	-0.437	-1.534
451	E1	22.5	0	0	2.104	0.434	4.080	1.071	0.024	0.038	0.155	-0.098
452	E1	22.4	0	-15	1.855	0.401	3.462	0.793	0.617	0.118	1.064	0.332
453	E1	22.3	0	-30	1.846	0.370	3.405	0.899	1.151	0.248	2.161	0.595
454	E1	22.6	0	-45	1.563	0.350	2.985	0.691	1.798	0.424	3.366	0.875
455	E1	22.6	0	-60	0.769	0.230	1.663	0.160	1.812	0.450	3.417	0.716
456	E1	22.6	0	-75	0.324	0.157	0.973	0.029	1.114	0.279	2.198	0.398
457	E1	23.2	0	-90	0.516	0.145	1.159	0.207	-0.231	0.221	0.360	-1.119
458	E1	22.5	0	-105	0.663	0.185	1.438	0.214	-0.713	0.239	0.032	-1.771
459	E1	22.7	0	-120	0.625	0.179	1.321	0.163	-0.175	0.126	0.220	-0.645
460	E1	22.4	0	-135	0.830	0.187	1.587	0.416	-0.083	0.063	0.127	-0.320
461	E1	22.4	0	-150	1.012	0.248	2.035	0.479	-0.129	0.071	0.030	-0.418
462	E1	22.5	0	-165	1.331	0.308	2.628	0.678	-0.087	0.069	0.066	-0.350
463	B1	22.9	-30	-165	0.965	0.254	2.009	0.410	-0.051	0.056	0.085	-0.251
464	B1	22.6	0	-165	1.378	0.294	2.498	0.742	-0.096	0.061	0.030	-0.345
465	B1	22.4	30	-165	0.994	0.252	1.861	0.359	-0.107	0.053	0.028	-0.324
466	B1	22.6	60	-165	0.418	0.167	1.075	-0.024	-0.033	0.037	0.067	-0.165
467	B1	22.4	60	-150	0.237	0.130	0.754	-0.134	-0.089	0.050	0.044	-0.303
468	B1	22.4	30	-150	0.792	0.181	1.519	0.378	-0.206	0.072	-0.033	-0.488
469	B1	22.3	0	-150	0.986	0.212	1.837	0.510	-0.258	0.076	-0.098	-0.546
470	B1	22.2	-30	-150	0.720	0.203	1.473	0.255	-0.198	0.073	-0.023	-0.479
471	B1	22.9	-30	-135	0.514	0.164	1.153	0.123	-0.175	0.071	0.004	-0.448
472	B1	22.4	0	-135	0.661	0.171	1.288	0.273	-0.224	0.081	0.007	-0.534
473	B1	22.7	30	-135	0.605	0.155	1.216	0.245	-0.203	0.074	-0.017	-0.494
474	B1	22.4	60	-135	0.165	0.111	0.610	-0.121	-0.075	0.052	0.078	-0.300
475	B1	23.1	60	-120	0.100	0.099	0.511	-0.155	-0.057	0.062	0.146	-0.304
476	B1	22.4	30	-120	0.432	0.136	1.008	0.125	-0.119	0.080	0.099	-0.449
477	B1	22.4	0	-120	0.473	0.147	1.028	0.147	-0.094	0.090	0.251	-0.442
478	B1	22.3	-30	-120	0.387	0.139	0.952	0.086	-0.140	0.076	0.128	-0.451
479	B1	23.2	-30	-105	0.197	0.115	0.646	-0.065	-0.114	0.115	0.322	-0.620
480	B1	22.7	0	-105	0.334	0.112	0.780	0.091	-0.096	0.136	0.466	-0.565
481	B1	22.7	30	-105	0.228	0.109	0.635	-0.047	-0.097	0.113	0.318	-0.570
482	B1	22.4	60	-105	0.093	0.094	0.456	-0.163	-0.047	0.094	0.213	-0.472
483	B1	22.3	60	-90	0.040	0.080	0.347	-0.163	0.192	0.109	0.641	-0.212
484	B1	22.2	30	-90	0.160	0.099	0.558	-0.059	0.525	0.164	1.190	0.007
485	B1	22.3	0	-90	0.274	0.101	0.704	0.063	0.545	0.200	1.408	-0.104
486	B1	22.3	-30	-90	0.183	0.116	0.657	-0.052	0.544	0.196	1.341	-0.084
487	B1	22.4	-30	-75	0.197	0.132	0.686	-0.094	1.422	0.414	2.923	0.492
488	B1	22.7	0	-75	0.221	0.139	0.744	-0.077	1.707	0.428	3.411	0.753
489	B1	22.4	30	-75	0.333	0.119	0.785	0.064	1.276	0.364	2.684	0.474

Phase 1, 2, and 3 Balance Data

Run	Conf	Uref fps	Cfx		Cfz							
			Mean	RMS	Max	Min	Mean	RMS	Max	Min		
490	B1	22.3	60	-75	0.074	0.072	0.367	-0.124	0.424	0.179	1.159	-0.007
491	B1	22.8	60	-60	0.142	0.096	0.549	-0.123	0.502	0.215	1.490	0.023
492	B1	22.6	30	-60	0.491	0.159	1.120	0.153	1.484	0.426	3.034	0.562
493	B1	22.2	0	-60	0.654	0.186	1.359	0.221	2.093	0.518	3.915	0.895
494	B1	22.5	-30	-60	0.508	0.175	1.223	0.139	1.555	0.481	3.431	0.526
495	B1	22.3	-30	-45	1.037	0.279	2.138	0.361	1.534	0.414	3.036	0.606
496	B1	22.1	0	-45	1.367	0.319	2.583	0.638	1.792	0.448	3.429	0.851
497	B1	22.2	30	-45	0.965	0.255	2.030	0.416	1.360	0.385	2.832	0.565
498	B1	22.3	60	-45	0.376	0.142	0.954	-0.007	0.486	0.182	1.344	0.078
499	B1	22.3	60	-30	0.617	0.224	1.536	0.054	0.447	0.140	1.098	0.116
500	B1	22.2	30	-30	1.372	0.319	2.796	0.651	0.908	0.201	1.789	0.461
501	B1	22.0	0	-30	1.653	0.375	3.013	0.771	0.993	0.222	1.799	0.502
502	B1	22.3	-30	-30	1.316	0.331	2.632	0.446	0.818	0.201	1.600	0.308
503	B1	22.5	-30	-15	1.476	0.359	2.885	0.656	0.495	0.120	0.954	0.237
504	B1	22.2	0	-15	1.835	0.399	3.438	0.891	0.509	0.116	0.959	0.239
505	B1	22.2	30	-15	1.414	0.348	2.730	0.529	0.402	0.116	0.884	0.125
506	B1	22.5	60	-15	0.673	0.220	1.594	0.088	0.192	0.065	0.466	0.021
507	B1	22.7	60	0	0.681	0.245	1.728	0.084	0.009	0.029	0.124	-0.083
508	B1	22.2	30	0	1.530	0.367	2.930	0.581	-0.015	0.044	0.147	-0.166
509	B1	22.1	0	0	2.224	0.450	3.926	1.084	-0.038	0.038	0.098	-0.162
510	B1	22.1	-30	0	1.575	0.375	2.979	0.727	-0.012	0.043	0.176	-0.122
511	B1	22.4	-30	15	1.580	0.403	3.064	0.678	-0.475	0.120	-0.188	-0.882
512	B1	22.3	0	15	2.217	0.468	3.963	1.193	-0.617	0.129	-0.306	-1.098
513	B1	22.4	30	15	1.688	0.364	3.120	0.806	-0.496	0.103	-0.229	-0.877
514	B1	22.7	60	15	0.697	0.262	1.701	0.089	-0.225	0.080	-0.028	-0.526
515	B1	22.4	60	30	0.568	0.226	1.505	0.015	-0.385	0.165	0.006	-1.078
516	B1	22.0	30	30	1.628	0.358	3.067	0.771	-1.143	0.258	-0.520	-2.206
517	B1	22.3	0	30	2.035	0.430	3.694	1.045	-1.409	0.304	-0.671	-2.557
518	B1	22.3	-30	30	1.558	0.393	3.091	0.679	-1.193	0.292	-0.542	-2.349
519	B1	22.6	-30	45	1.234	0.356	2.584	0.473	-1.779	0.522	-0.692	-3.717
520	B1	22.1	0	45	1.604	0.355	3.016	0.812	-2.236	0.508	-1.140	-4.289
521	B1	22.5	30	45	1.243	0.312	2.433	0.547	-1.767	0.464	-0.747	-3.468
522	B1	22.6	60	45	0.405	0.193	1.177	-0.056	-0.620	0.270	-0.106	-1.672
523	B1	22.7	60	60	0.256	0.136	0.793	-0.109	-0.698	0.317	-0.052	-1.968
524	B1	22.2	30	60	0.919	0.255	2.006	0.366	-2.302	0.673	-0.972	-5.119
525	B1	22.4	0	60	1.000	0.264	1.938	0.418	-2.767	0.712	-1.288	-5.196
526	B1	22.3	-30	60	0.869	0.264	1.895	0.301	-2.303	0.695	-0.843	-4.797
527	B1	22.9	-30	75	0.573	0.179	1.230	0.155	-2.039	0.630	-0.762	-4.236
528	B1	22.4	0	75	0.715	0.212	1.494	0.244	-2.528	0.779	-1.001	-5.205
529	B1	22.5	30	75	0.573	0.168	1.239	0.188	-1.997	0.609	-0.700	-4.309
530	B1	22.2	60	75	0.133	0.102	0.551	-0.111	-0.618	0.312	0.052	-1.949
531	B1	22.7	60	90	0.041	0.078	0.352	-0.193	-0.134	0.194	0.328	-0.945
532	B1	22.8	30	90	0.282	0.111	0.745	0.013	-0.410	0.283	0.222	-1.630
533	B1	22.6	0	90	0.313	0.137	0.947	-0.001	-0.330	0.309	0.299	-1.664
534	B1	22.6	-30	90	0.271	0.125	0.818	-0.020	-0.473	0.314	0.206	-1.856
535	B1	22.5	-30	105	0.357	0.146	0.938	-0.012	0.323	0.193	1.005	-0.300
536	B1	22.6	0	105	0.502	0.148	1.215	0.134	0.236	0.223	1.282	-0.613
537	B1	22.3	30	105	0.274	0.130	0.895	-0.058	0.331	0.185	1.205	-0.279
538	B1	22.5	60	105	0.154	0.088	0.530	-0.106	0.184	0.132	0.754	-0.254
539	B1	22.7	60	120	0.165	0.113	0.719	-0.131	0.179	0.108	0.721	-0.112

Phase 1, 2, and 3 Balance Data

Run	Conf	Uref fps	Cfx		Cfz					
			Yaw	Pitch	Mean	RMS	Max	Min	Mean	RMS
540	B1	22.1	30	120	0.556	0.182	1.295	0.119	0.338	0.143
541	B1	22.4	0	120	0.819	0.218	1.649	0.307	0.377	0.144
542	B1	22.4	-30	120	0.614	0.193	1.396	0.136	0.332	0.138
543	B1	22.2	-30	135	0.915	0.244	1.817	0.334	0.505	0.116
544	B1	22.3	0	135	1.107	0.274	2.104	0.517	0.607	0.129
545	B1	22.2	30	135	0.937	0.230	1.850	0.424	0.492	0.108
546	B1	22.6	60	135	0.314	0.149	0.956	-0.053	0.165	0.081
547	B1	22.7	60	150	0.423	0.190	1.214	-0.020	0.231	0.077
548	B1	22.8	30	150	1.230	0.278	2.308	0.573	0.534	0.104
549	B1	22.5	0	150	1.523	0.328	2.765	0.743	0.673	0.116
550	B1	22.4	-30	150	1.286	0.334	2.499	0.527	0.554	0.120
551	B1	22.6	-30	165	1.266	0.330	2.537	0.493	0.424	0.080
552	B1	22.3	0	165	1.545	0.346	2.866	0.742	0.483	0.080
553	B1	22.3	30	165	1.473	0.309	2.609	0.812	0.391	0.074
554	B1	22.4	60	165	0.600	0.205	1.410	0.095	0.154	0.058
555	B1	22.5	60	180	0.551	0.194	1.291	0.055	0.086	0.031
556	B1	22.3	30	180	1.300	0.274	2.255	0.625	0.144	0.040
557	B1	22.3	0	180	1.568	0.339	2.886	0.837	0.158	0.045
558	B1	22.3	-30	180	1.241	0.315	2.444	0.517	0.100	0.044
559	B3	22.5	-30	-165	0.777	0.243	1.720	0.263	-0.049	0.058
560	B3	22.2	0	-165	1.415	0.360	2.791	0.619	-0.120	0.074
561	B3	22.5	30	-165	1.776	0.420	3.447	0.833	-0.183	0.079
562	B3	22.4	60	-165	1.455	0.442	3.090	0.285	-0.210	0.085
563	B3	22.7	60	-150	1.017	0.333	2.170	0.127	-0.358	0.139
564	B3	22.4	30	-150	1.246	0.293	2.360	0.578	-0.358	0.112
565	B3	22.8	0	-150	1.005	0.266	2.003	0.430	-0.274	0.091
566	B3	22.9	-30	-150	0.575	0.181	1.342	0.156	-0.154	0.064
567	B3	23.0	-30	-135	0.444	0.146	1.041	0.121	-0.130	0.067
568	B3	22.6	0	-135	0.773	0.199	1.487	0.326	-0.258	0.090
569	B3	22.2	30	-135	0.949	0.242	1.924	0.391	-0.420	0.131
570	B3	22.6	60	-135	0.718	0.266	1.632	0.007	-0.489	0.178
571	B3	22.5	60	-120	0.387	0.184	1.065	-0.061	-0.372	0.187
572	B3	22.2	30	-120	0.619	0.176	1.369	0.226	-0.402	0.165
573	B3	22.4	0	-120	0.454	0.144	1.038	0.140	-0.096	0.096
574	B3	22.6	-30	-120	0.333	0.138	0.878	0.022	-0.118	0.082
575	B3	22.8	-30	-105	0.263	0.117	0.688	0.011	-0.109	0.110
576	B3	23.0	0	-105	0.368	0.108	0.793	0.108	-0.121	0.134
577	B3	23.0	30	-105	0.354	0.122	0.822	0.075	-0.164	0.148
578	B3	22.8	60	-105	0.222	0.139	0.758	-0.150	-0.115	0.139
579	B3	22.3	60	-90	0.112	0.098	0.517	-0.138	0.262	0.148
580	B3	22.9	30	-90	0.247	0.110	0.694	0.011	0.579	0.183
581	B3	23.0	0	-90	0.286	0.098	0.679	0.067	0.381	0.191
582	B3	23.0	-30	-90	0.231	0.114	0.679	-0.005	0.412	0.160
583	B3	22.7	-30	-75	0.319	0.134	0.883	0.042	1.291	0.368
584	B3	22.7	0	-75	0.387	0.153	0.958	0.058	1.561	0.383
585	B3	22.2	30	-75	0.430	0.145	0.993	0.120	1.403	0.361
586	B3	22.7	60	-75	0.206	0.105	0.672	-0.044	0.608	0.246
587	B3	22.3	60	-60	0.379	0.177	1.114	-0.025	0.961	0.341
588	B3	22.4	30	-60	0.776	0.224	1.685	0.277	1.904	0.486
589	B3	23.0	0	-60	0.706	0.225	1.595	0.208	1.931	0.538

Phase 1, 2, and 3 Balance Data

Run	Conf	Uref fps	Cfx				Cfz			
			Yaw	Pitch	Mean	RMS	Max	Min	Mean	RMS
590	B3	22.5	-30	-60	0.603	0.190	1.448	0.178	1.405	0.466
591	B3	22.2	-30	-45	0.825	0.265	1.878	0.208	1.171	0.394
592	B3	22.9	0	-45	1.292	0.329	2.463	0.533	1.808	0.458
593	B3	22.7	30	-45	1.289	0.324	2.546	0.529	1.790	0.459
594	B3	22.7	60	-45	0.740	0.245	1.727	0.134	0.954	0.339
595	B3	22.7	60	-30	1.178	0.379	2.731	0.218	0.950	0.308
596	B3	22.5	30	-30	2.002	0.508	3.784	0.839	1.261	0.318
597	B3	22.8	0	-30	1.568	0.403	3.055	0.656	1.026	0.256
598	B3	22.6	-30	-30	1.073	0.326	2.444	0.310	0.648	0.220
599	B3	22.5	-30	-15	1.128	0.347	2.551	0.363	0.391	0.116
600	B3	22.7	0	-15	1.770	0.443	3.592	0.783	0.517	0.128
601	B3	22.3	30	-15	2.512	0.588	4.693	1.106	0.768	0.184
602	B3	21.9	60	-15	1.541	0.513	3.487	0.388	0.552	0.184
603	B3	22.3	60	0	1.708	0.527	3.683	-0.077	0.097	0.060
604	B3	22.1	30	0	2.714	0.630	5.097	1.274	-0.014	0.044
605	B3	22.2	0	0	2.027	0.502	4.091	0.810	-0.002	0.039
606	B3	22.8	-30	0	1.131	0.365	2.850	0.221	0.006	0.035
607	B3	22.6	-30	15	1.147	0.350	2.608	0.341	-0.348	0.110
608	B3	22.3	0	15	2.060	0.497	4.038	0.961	-0.621	0.153
609	B3	22.3	30	15	2.385	0.550	4.374	1.104	-0.699	0.173
610	B3	22.1	60	15	1.601	0.545	3.588	0.269	-0.512	0.178
611	B3	22.2	60	30	1.264	0.491	3.025	0.142	-0.930	0.362
612	B3	21.9	30	30	2.168	0.544	4.493	1.001	-1.403	0.375
613	B3	22.1	0	30	1.901	0.462	3.671	0.873	-1.330	0.320
614	B3	22.2	-30	30	1.145	0.344	2.459	0.348	-0.900	0.258
615	B3	22.0	-30	45	1.090	0.337	2.452	0.433	-1.537	0.479
616	B3	22.2	0	45	1.657	0.417	3.252	0.652	-2.119	0.541
617	B3	22.4	30	45	1.674	0.423	3.285	0.693	-2.131	0.553
618	B3	22.2	60	45	0.890	0.376	2.387	0.089	-1.152	0.491
619	B3	22.5	60	60	0.430	0.209	1.274	-0.107	-0.921	0.436
620	B3	22.1	30	60	1.134	0.305	2.293	0.504	-2.403	0.704
621	B3	22.2	0	60	1.123	0.286	2.208	0.524	-2.648	0.709
622	B3	22.1	-30	60	0.812	0.259	1.765	0.230	-2.095	0.651
623	B3	22.5	-30	75	0.521	0.184	1.240	0.145	-1.791	0.638
624	B3	22.4	0	75	0.763	0.198	1.562	0.324	-2.106	0.674
625	B3	22.2	30	75	0.620	0.185	1.389	0.231	-1.837	0.622
626	B3	22.8	60	75	0.179	0.120	0.674	-0.131	-0.634	0.354
627	B3	22.8	60	90	0.096	0.088	0.426	-0.180	-0.196	0.238
628	B3	22.5	30	90	0.364	0.115	0.840	0.087	-0.561	0.327
629	B3	22.1	0	90	0.307	0.133	0.953	-0.005	-0.379	0.306
630	B3	22.3	-30	90	0.338	0.136	0.938	0.021	-0.460	0.320
631	B3	22.6	-30	105	0.309	0.128	0.887	-0.002	0.240	0.176
632	B3	22.9	0	105	0.356	0.129	0.942	0.025	0.209	0.203
633	B3	22.3	30	105	0.450	0.155	1.071	0.043	0.328	0.181
634	B3	22.2	60	105	0.244	0.135	0.861	-0.114	0.162	0.178
635	B3	22.6	60	120	0.521	0.215	1.318	-0.027	0.521	0.189
636	B3	22.5	30	120	0.843	0.248	1.791	0.266	0.855	0.242
637	B3	22.6	0	120	0.677	0.196	1.535	0.158	0.278	0.149
638	B3	22.8	-30	120	0.463	0.168	1.237	0.063	0.182	0.112
639	B3	22.2	-30	135	0.664	0.216	1.634	0.175	0.326	0.090

Phase 1, 2, and 3 Balance Data

Run	Conf	Uref fps	Cfx		Cfz							
			Mean	RMS	Max	Min	Mean	RMS	Max	Min		
640	B3	22.5	0	135	0.950	0.269	2.076	0.345	0.459	0.122	0.954	0.131
641	B3	22.3	30	135	1.398	0.354	2.710	0.552	0.941	0.240	1.849	0.353
642	B3	22.5	60	135	0.904	0.316	2.049	0.057	0.608	0.204	1.341	0.078
643	B3	22.7	60	150	1.343	0.475	3.119	0.211	0.640	0.184	1.317	0.202
644	B3	22.5	30	150	1.857	0.462	3.349	0.799	0.776	0.176	1.334	0.390
645	B3	22.5	0	150	1.440	0.366	2.815	0.673	0.525	0.118	0.958	0.236
646	B3	22.6	-30	150	0.945	0.271	1.950	0.370	0.309	0.085	0.604	0.099
647	B3	22.6	-30	165	0.974	0.288	2.105	0.339	0.279	0.063	0.522	0.127
648	B3	22.3	0	165	1.629	0.419	3.100	0.712	0.396	0.092	0.722	0.169
649	B3	22.2	30	165	1.976	0.510	3.771	0.784	0.544	0.124	0.988	0.224
650	B3	21.8	60	165	1.658	0.528	3.614	0.401	0.425	0.125	0.927	0.129
651	B3	22.7	60	180	1.621	0.509	3.355	0.263	0.148	0.047	0.333	0.002
652	B3	22.4	30	180	1.931	0.451	3.537	0.910	0.134	0.051	0.304	-0.053
653	B3	22.4	0	180	1.573	0.392	3.023	0.688	0.072	0.046	0.223	-0.106
654	B3	22.3	-30	180	0.985	0.297	2.204	0.386	0.024	0.038	0.153	-0.115
655	E3	22.4	0	-180	1.458	0.420	3.216	0.449	0.114	0.057	0.305	-0.125
656	E3	22.3	0	-165	1.295	0.374	2.819	0.398	-0.103	0.077	0.087	-0.415
657	E3	22.2	0	-150	1.064	0.272	2.110	0.405	-0.173	0.084	0.012	-0.522
658	E3	22.6	0	-135	0.741	0.211	1.657	0.270	-0.074	0.070	0.126	-0.372
659	E3	22.7	0	-120	0.633	0.193	1.459	0.199	-0.222	0.146	0.266	-0.777
660	E3	22.0	0	-105	0.628	0.186	1.401	0.222	-0.706	0.242	-0.085	-1.653
661	E3	22.0	0	-90	0.445	0.154	1.071	0.124	-0.137	0.224	0.499	-1.025
662	E3	22.5	0	-75	0.352	0.168	1.019	-0.042	0.909	0.229	1.830	0.173
663	E3	22.8	0	-60	0.737	0.231	1.566	0.169	1.599	0.399	2.919	0.725
664	E3	23.0	0	-45	1.233	0.359	2.671	0.302	1.709	0.450	3.257	0.524
665	E3	23.4	0	-30	1.488	0.417	3.154	0.404	1.036	0.242	1.950	0.464
666	E3	22.8	0	-15	1.724	0.487	3.896	0.604	0.602	0.137	1.165	0.290
667	E3	22.8	0	0	2.008	0.530	4.350	0.716	0.057	0.040	0.218	-0.068
668	E3	22.8	0	15	2.011	0.500	4.123	0.818	-0.591	0.157	-0.211	-1.184
669	E3	21.9	0	30	1.999	0.520	4.203	0.788	-1.110	0.288	-0.463	-2.266
670	E3	22.2	0	45	1.584	0.437	3.270	0.558	-1.897	0.525	-0.775	-3.812
671	E3	22.6	0	60	1.040	0.285	2.217	0.409	-1.849	0.524	-0.801	-3.826
672	E3	22.7	0	75	0.635	0.197	1.473	0.206	-1.000	0.356	-0.220	-2.308
673	E3	22.3	0	90	0.456	0.197	1.482	-0.001	0.408	0.189	1.072	-0.369
674	E3	22.4	0	105	0.568	0.236	1.628	-0.013	0.732	0.262	1.879	0.039
675	E3	22.9	0	120	0.795	0.257	1.969	0.180	0.196	0.149	0.871	-0.307
676	E3	22.5	0	135	1.000	0.318	2.587	0.250	0.349	0.103	0.950	0.004
677	E3	22.3	0	150	1.436	0.394	3.079	0.502	0.531	0.122	1.018	0.192
678	E3	22.5	0	165	1.536	0.417	3.213	0.544	0.397	0.087	0.726	0.157
679	E4	22.6	0	15	0.001	0.293	1.439	-1.152	0.038	0.053	0.238	-0.243
680	E4	22.9	0	30	0.080	0.248	1.247	-0.909	-0.031	0.087	0.223	-0.504
681	E4	22.4	0	45	0.276	0.236	1.560	-0.579	-0.250	0.192	0.258	-1.212
682	E4	22.5	0	60	0.552	0.208	1.554	-0.034	-0.731	0.240	-0.179	-1.797
683	E4	22.5	0	75	0.480	0.161	1.124	0.123	-0.452	0.210	0.017	-1.358
684	E4	23.0	0	90	0.352	0.164	1.122	-0.053	0.270	0.149	0.818	-0.334
685	E4	22.4	0	105	0.485	0.318	2.123	-0.671	0.531	0.248	1.557	-0.130
686	E4	22.4	0	120	0.474	0.368	2.408	-0.914	0.200	0.252	1.271	-0.673
687	E4	22.6	0	135	0.341	0.307	1.854	-0.633	0.232	0.148	0.918	-0.277
688	E4	22.7	0	150	0.132	0.256	1.316	-0.775	0.099	0.078	0.428	-0.166
689	E4	22.9	0	165	0.085	0.226	1.046	-0.716	0.016	0.050	0.216	-0.177

Phase 1, 2, and 3 Balance Data

Run	Conf	Uref fps	Cfx		Cfz							
			Mean	RMS	Max	Min	Mean	RMS	Max	Min		
690	E4	22.3	0	180	0.016	0.261	1.283	-1.065	-0.053	0.050	0.102	-0.304
691	E4	22.5	0	-165	-0.043	0.262	1.169	-0.922	-0.040	0.075	0.168	-0.413
692	E4	22.5	0	-150	0.037	0.213	0.981	-0.695	-0.065	0.090	0.221	-0.433
693	E4	22.7	0	-135	0.000	0.162	0.762	-0.509	-0.088	0.092	0.180	-0.498
694	E4	22.6	0	-120	0.211	0.139	0.841	-0.192	-0.063	0.088	0.210	-0.433
695	E4	22.7	0	-105	0.398	0.148	1.041	0.070	-0.397	0.176	0.043	-1.119
696	E4	22.5	0	-90	0.309	0.130	0.823	0.022	-0.130	0.180	0.415	-0.915
697	E4	22.3	0	-75	0.312	0.162	0.953	-0.098	0.558	0.183	1.249	-0.030
698	E4	22.4	0	-60	0.416	0.269	1.542	-0.193	0.904	0.287	2.151	0.287
699	E4	22.7	0	-45	0.328	0.245	1.440	-0.439	0.288	0.207	1.248	-0.299
700	E4	23.1	0	-30	0.206	0.269	1.523	-0.827	0.067	0.150	0.827	-0.474
701	E4	22.7	0	-15	-0.077	0.305	1.285	-1.289	0.006	0.101	0.480	-0.451
702	E4	22.4	0	0	-0.040	0.346	1.718	-1.417	0.027	0.060	0.311	-0.213
703	B4	22.8	-30	0	0.020	0.147	0.526	-0.765	0.035	0.037	0.194	-0.101
704	B4	22.1	0	0	-0.098	0.269	1.157	-1.242	0.029	0.057	0.296	-0.205
705	B4	22.0	30	0	1.796	0.528	3.613	0.460	0.094	0.044	0.268	-0.054
706	B4	22.9	60	0	1.338	0.500	3.236	0.207	0.040	0.052	0.250	-0.123
707	B4	22.5	60	-15	1.198	0.452	3.060	0.140	0.505	0.162	1.131	0.152
708	B4	22.6	30	-15	1.333	0.454	3.132	0.236	0.430	0.134	0.949	0.100
709	B4	22.2	0	-15	0.039	0.256	1.155	-1.068	-0.058	0.104	0.383	-0.483
710	B4	22.7	-30	-15	0.133	0.155	0.645	-0.722	0.012	0.056	0.216	-0.307
711	B4	22.6	-30	-30	0.121	0.154	0.671	-0.509	0.096	0.096	0.550	-0.318
712	B4	22.3	0	-30	0.072	0.237	1.407	-0.844	0.090	0.170	1.080	-0.515
713	B4	22.2	30	-30	1.145	0.419	2.732	0.137	0.831	0.277	1.939	0.192
714	B4	22.2	60	-30	1.108	0.377	2.602	0.237	0.780	0.284	1.878	0.169
715	B4	22.8	60	-45	0.649	0.228	1.491	0.067	0.968	0.315	2.160	0.252
716	B4	22.6	30	-45	0.745	0.298	1.914	0.109	0.993	0.419	2.610	0.093
717	B4	22.5	0	-45	0.289	0.198	1.310	-0.143	0.366	0.252	1.511	-0.209
718	B4	23.2	-30	-45	0.186	0.124	0.727	-0.252	0.209	0.150	0.912	-0.364
719	B4	23.1	-30	-60	0.178	0.132	0.795	-0.097	0.670	0.282	1.916	0.054
720	B4	22.9	0	-60	0.330	0.232	1.324	-0.107	1.108	0.406	2.861	0.284
721	B4	23.1	30	-60	0.512	0.182	1.252	0.120	1.350	0.397	2.853	0.493
722	B4	23.2	60	-60	0.555	0.164	1.221	0.152	0.904	0.319	2.270	0.172
723	B4	22.9	60	-75	0.166	0.114	0.596	-0.104	0.657	0.254	1.651	0.074
724	B4	23.3	30	-75	0.195	0.120	0.703	-0.061	1.327	0.332	2.687	0.538
725	B4	22.1	0	-75	0.285	0.147	0.841	-0.049	1.235	0.322	2.459	0.483
726	B4	23.3	-30	-75	0.284	0.116	0.782	0.045	0.901	0.308	2.138	0.253
727	B4	23.3	-30	-90	0.167	0.082	0.478	-0.015	0.292	0.131	0.818	-0.132
728	B4	23.2	0	-90	0.179	0.082	0.500	-0.017	0.400	0.144	1.041	-0.011
729	B4	23.0	30	-90	0.217	0.104	0.607	-0.043	0.626	0.188	1.329	0.107
730	B4	22.6	60	-90	0.156	0.095	0.534	-0.091	0.276	0.142	0.862	-0.194
731	B4	23.0	60	-105	0.189	0.124	0.656	-0.127	-0.088	0.134	0.325	-0.676
732	B4	22.9	30	-105	0.313	0.125	0.785	0.031	-0.151	0.162	0.356	-0.848
733	B4	22.9	0	-105	0.198	0.088	0.627	-0.013	-0.023	0.109	0.392	-0.479
734	B4	22.9	-30	-105	0.106	0.080	0.439	-0.078	-0.057	0.094	0.293	-0.438
735	B4	23.0	-30	-120	0.047	0.073	0.370	-0.150	-0.050	0.071	0.176	-0.374
736	B4	23.3	0	-120	0.160	0.109	0.639	-0.099	-0.100	0.084	0.164	-0.463
737	B4	22.8	30	-120	0.604	0.186	1.315	0.194	-0.373	0.163	0.032	-0.991
738	B4	23.2	60	-120	0.385	0.196	1.169	-0.073	-0.391	0.186	0.103	-1.150
739	B4	23.3	60	-135	0.618	0.239	1.579	0.061	-0.407	0.163	-0.009	-1.027

Phase 1, 2, and 3 Balance Data

Run	Conf	Uref fps	Cfx		Cfz							
			Mean	RMS	Max	Min	Mean	RMS	Max	Min		
740	B4	22.7	30	-135	0.846	0.230	1.767	0.319	-0.425	0.132	-0.116	-0.958
741	B4	23.3	0	-135	0.002	0.148	0.725	-0.356	-0.135	0.094	0.137	-0.591
742	B4	23.1	-30	-135	0.017	0.074	0.340	-0.263	-0.026	0.062	0.214	-0.317
743	B4	22.7	-30	-150	-0.051	0.096	0.265	-0.482	0.014	0.055	0.240	-0.204
744	B4	23.1	0	-150	-0.030	0.181	0.754	-0.573	-0.050	0.090	0.204	-0.480
745	B4	22.8	30	-150	1.123	0.308	2.318	0.388	-0.371	0.123	-0.069	-0.865
746	B4	22.4	60	-150	0.961	0.329	2.345	0.053	-0.370	0.133	-0.014	-0.899
747	B4	23.1	60	-165	1.131	0.399	2.691	0.066	-0.138	0.077	0.068	-0.441
748	B4	23.2	30	-165	1.276	0.391	2.922	0.431	-0.217	0.090	0.013	-0.578
749	B4	22.9	0	-165	0.053	0.231	1.084	-0.733	-0.088	0.067	0.127	-0.385
750	B4	23.2	-30	-165	0.020	0.117	0.395	-0.524	0.002	0.039	0.164	-0.186
751	B4	22.6	-30	180	-0.049	0.126	0.344	-0.658	0.003	0.028	0.112	-0.101
752	B4	22.5	0	180	-0.006	0.230	1.054	-0.763	-0.012	0.039	0.126	-0.169
753	B4	22.3	30	180	1.499	0.416	3.133	0.474	0.070	0.054	0.253	-0.119
754	B4	22.2	60	180	1.511	0.484	3.319	0.402	0.052	0.043	0.208	-0.099
755	B4	22.8	60	165	1.431	0.470	3.058	0.227	0.405	0.105	0.785	0.130
756	B4	22.3	30	165	1.625	0.451	3.221	0.484	0.335	0.108	0.682	0.067
757	B4	22.3	0	165	0.105	0.201	1.024	-0.653	-0.027	0.047	0.173	-0.173
758	B4	22.8	-30	165	0.030	0.122	0.407	-0.576	0.007	0.036	0.109	-0.125
759	B4	22.2	-30	150	0.028	0.111	0.499	-0.396	0.096	0.058	0.318	-0.077
760	B4	22.7	0	150	0.196	0.214	1.263	-0.481	0.117	0.077	0.478	-0.111
761	B4	22.3	30	150	1.306	0.421	2.662	0.377	0.551	0.173	1.107	0.147
762	B4	22.3	60	150	1.231	0.399	2.723	0.313	0.535	0.160	1.150	0.172
763	B4	22.7	60	135	0.852	0.310	1.993	-0.007	0.635	0.198	1.367	0.116
764	B4	21.8	30	135	1.171	0.346	2.392	0.341	0.754	0.228	1.509	0.222
765	B4	22.2	0	135	0.345	0.250	1.536	-0.325	0.222	0.145	0.895	-0.223
766	B4	21.8	-30	135	0.239	0.173	1.283	-0.303	0.174	0.123	0.818	-0.220
767	B4	22.9	-30	120	0.230	0.218	1.319	-0.510	0.178	0.209	1.082	-0.538
768	B4	22.2	0	120	0.387	0.291	1.964	-0.750	0.233	0.232	1.317	-0.617
769	B4	22.4	30	120	0.752	0.234	1.635	0.162	0.731	0.241	1.619	0.073
770	B4	22.4	60	120	0.574	0.211	1.465	0.017	0.499	0.191	1.277	-0.032
771	B4	22.6	60	105	0.231	0.130	0.781	-0.109	0.220	0.174	0.910	-0.401
772	B4	22.3	30	105	0.433	0.166	1.196	0.000	0.410	0.189	1.166	-0.311
773	B4	21.9	0	105	0.318	0.206	1.345	-0.501	0.124	0.212	0.958	-0.736
774	B4	22.2	-30	105	0.258	0.179	1.158	-0.345	0.175	0.194	0.943	-0.567
775	B4	22.1	-30	90	0.160	0.093	0.524	-0.070	-0.232	0.182	0.266	-1.114
776	B4	22.1	0	90	0.245	0.101	0.657	0.012	-0.242	0.171	0.267	-1.004
777	B4	21.8	30	90	0.335	0.115	0.828	0.057	-0.657	0.358	0.197	-2.210
778	B4	21.8	60	90	0.187	0.093	0.574	-0.061	-0.219	0.241	0.508	-1.252
779	B4	22.9	60	75	0.242	0.123	0.753	-0.061	-0.687	0.355	0.103	-2.146
780	B4	21.7	30	75	0.640	0.180	1.347	0.216	-2.126	0.669	-0.780	-4.859
781	B4	22.2	0	75	0.578	0.156	1.148	0.224	-1.440	0.391	-0.601	-2.882
782	B4	21.8	-30	75	0.311	0.116	0.736	0.043	-1.106	0.366	-0.328	-2.392
783	B4	22.0	-30	60	0.263	0.122	0.852	-0.096	-0.587	0.224	-0.026	-1.621
784	B4	22.7	0	60	0.651	0.204	1.458	0.175	-1.219	0.377	-0.401	-2.713
785	B4	22.4	30	60	1.062	0.295	2.119	0.415	-2.331	0.680	-0.956	-4.819
786	B4	21.6	60	60	0.478	0.227	1.392	-0.049	-1.013	0.475	-0.062	-2.931
787	B4	22.1	60	45	0.863	0.359	2.178	0.017	-1.090	0.467	-0.049	-2.844
788	B4	22.3	30	45	1.488	0.393	2.905	0.563	-1.827	0.488	-0.732	-3.622
789	B4	22.5	0	45	0.306	0.226	1.530	-0.297	-0.409	0.251	0.115	-1.646

Phase 1, 2, and 3 Balance Data

Run	Conf	Uref fps	Cfx		Cfz					
			Yaw	Pitch	Mean	RMS	Max	Min	Mean	RMS
790	B4	22.5	-30	45	0.143	0.099	0.635	-0.237	-0.105	0.092
791	B4	22.5	-30	30	0.099	0.127	0.549	-0.540	-0.016	0.058
792	B4	22.2	0	30	0.158	0.217	1.347	-0.611	-0.058	0.115
793	B4	21.9	30	30	1.798	0.519	3.861	0.381	-1.150	0.348
794	B4	21.7	60	30	1.219	0.478	2.998	0.102	-0.924	0.352
795	B4	22.4	60	15	1.368	0.475	3.147	0.160	-0.375	0.159
796	B4	22.2	30	15	1.840	0.501	3.969	0.561	-0.471	0.158
797	B4	22.0	0	15	0.104	0.242	1.355	-0.921	-0.032	0.055
798	B4	22.5	-30	15	0.029	0.130	0.477	-0.720	0.027	0.037
799	B5	22.8	-30	-165	-0.071	0.129	0.418	-0.563	0.013	0.030
800	B5	22.3	0	-165	0.520	0.337	1.827	-0.204	-0.100	0.053
801	B5	22.3	30	-165	1.416	0.384	3.029	0.610	-0.170	0.051
802	B5	22.7	60	-165	1.167	0.396	2.586	0.216	-0.158	0.042
803	B5	22.9	60	-150	0.900	0.316	1.949	0.108	-0.305	0.081
804	B5	22.3	30	-150	1.106	0.299	2.213	0.408	-0.300	0.074
805	B5	22.8	0	-150	0.393	0.267	1.436	-0.209	-0.148	0.076
806	B5	22.8	-30	-150	0.014	0.099	0.418	-0.334	-0.007	0.042
807	B5	22.8	-30	-135	0.001	0.087	0.341	-0.291	-0.016	0.049
808	B5	22.2	0	-135	0.260	0.205	0.966	-0.223	-0.152	0.080
809	B5	23.1	30	-135	0.782	0.226	1.638	0.246	-0.331	0.086
810	B5	21.9	60	-135	0.645	0.274	1.744	-0.081	-0.395	0.129
811	B5	22.7	60	-120	0.367	0.191	1.182	-0.124	-0.319	0.131
812	B5	23.0	30	-120	0.675	0.174	1.396	0.250	-0.329	0.106
813	B5	22.3	0	-120	0.226	0.147	0.805	-0.095	-0.073	0.066
814	B5	23.0	-30	-120	0.148	0.072	0.496	-0.061	-0.030	0.044
815	B5	22.7	-30	-105	0.158	0.070	0.464	-0.017	-0.016	0.060
816	B5	22.7	0	-105	0.126	0.091	0.484	-0.092	0.010	0.078
817	B5	22.9	30	-105	0.238	0.136	0.693	-0.119	-0.143	0.118
818	B5	22.7	60	-105	0.175	0.129	0.669	-0.153	-0.065	0.097
819	B5	23.1	60	-90	0.118	0.095	0.471	-0.158	0.262	0.113
820	B5	22.4	30	-90	0.226	0.123	0.700	-0.090	0.605	0.155
821	B5	22.6	0	-90	0.292	0.087	0.644	0.099	0.340	0.126
822	B5	23.1	-30	-90	0.261	0.084	0.574	0.061	0.217	0.090
823	B5	23.3	-30	-75	0.267	0.115	0.766	0.026	0.653	0.222
824	B5	22.6	0	-75	0.400	0.150	0.994	0.088	0.907	0.244
825	B5	23.1	30	-75	0.291	0.124	0.732	-0.028	1.144	0.244
826	B5	23.0	60	-75	0.195	0.109	0.590	-0.099	0.556	0.197
827	B5	23.1	60	-60	0.515	0.173	1.221	0.092	0.839	0.273
828	B5	22.6	30	-60	0.644	0.209	1.406	0.154	1.144	0.370
829	B5	22.8	0	-60	0.556	0.286	1.668	0.020	1.027	0.414
830	B5	22.7	-30	-60	0.451	0.146	1.149	0.121	0.518	0.233
831	B5	22.9	-30	-45	0.320	0.163	1.223	-0.067	0.207	0.161
832	B5	21.8	0	-45	0.788	0.371	2.332	0.004	0.791	0.405
833	B5	22.7	30	-45	1.067	0.325	2.188	0.211	0.989	0.368
834	B5	22.7	60	-45	0.702	0.254	1.834	0.110	0.828	0.282
835	B5	22.8	60	-30	1.119	0.358	2.705	0.262	0.667	0.246
836	B5	22.9	30	-30	1.351	0.397	2.889	0.382	0.664	0.239
837	B5	22.6	0	-30	0.704	0.373	2.418	-0.097	0.390	0.250
838	B5	22.3	-30	-30	0.129	0.185	1.139	-0.435	0.060	0.111
839	B5	22.4	-30	-15	0.100	0.196	0.934	-0.630	0.032	0.074

Phase 1, 2, and 3 Balance Data

Run	Conf	Uref fps	Uref		Cfx				Cfz			
			Yaw	Pitch	Mean	RMS	Max	Min	Mean	RMS	Max	Min
840	B5	22.5	0	-15	0.613	0.422	2.297	-0.285	0.212	0.159	0.929	-0.145
841	B5	22.7	30	-15	1.510	0.470	3.318	0.368	0.437	0.160	1.078	0.046
842	B5	22.4	60	-15	1.332	0.453	3.055	0.302	0.470	0.185	1.196	0.043
843	B5	23.1	60	0	1.334	0.464	3.232	0.222	0.075	0.068	0.349	-0.106
844	B5	22.5	30	0	1.851	0.491	3.764	0.724	0.029	0.063	0.305	-0.122
845	B5	22.3	0	0	0.623	0.410	2.290	-0.270	0.040	0.070	0.376	-0.147
846	B5	21.8	-30	0	0.124	0.183	0.871	-0.585	0.028	0.045	0.217	-0.115
847	B5	22.8	-30	15	0.050	0.146	0.617	-0.506	0.023	0.038	0.168	-0.084
848	B5	22.9	0	15	0.575	0.426	2.253	-0.241	-0.116	0.080	0.091	-0.437
849	B5	22.3	30	15	1.777	0.514	3.870	0.633	-0.424	0.091	-0.209	-0.775
850	B5	22.6	60	15	1.408	0.557	3.421	0.281	-0.342	0.105	-0.081	-0.723
851	B5	23.2	60	30	1.279	0.479	3.091	0.220	-0.737	0.235	-0.181	-1.592
852	B5	22.8	30	30	1.695	0.450	3.304	0.729	-0.914	0.197	-0.472	-1.607
853	B5	22.8	0	30	0.548	0.355	2.189	-0.163	-0.248	0.162	0.037	-0.965
854	B5	22.4	-30	30	0.110	0.130	0.840	-0.360	0.021	0.042	0.152	-0.156
855	B5	22.6	-30	45	0.204	0.125	0.872	-0.201	-0.074	0.064	0.091	-0.410
856	B5	22.1	0	45	0.508	0.341	2.057	-0.143	-0.560	0.322	-0.022	-2.042
857	B5	22.4	30	45	1.683	0.448	3.314	0.669	-1.701	0.390	-0.827	-3.097
858	B5	22.5	60	45	0.902	0.398	2.453	0.061	-0.939	0.366	-0.173	-2.368
859	B5	22.9	60	60	0.486	0.210	1.282	-0.035	-0.841	0.333	-0.094	-2.053
860	B5	22.9	30	60	1.111	0.284	2.107	0.453	-2.103	0.509	-0.959	-3.955
861	B5	22.5	0	60	0.547	0.229	1.451	-0.008	-0.927	0.374	-0.080	-2.427
862	B5	22.6	-30	60	0.224	0.082	0.637	-0.035	-0.217	0.101	0.061	-0.761
863	B5	22.7	-30	75	0.202	0.076	0.487	0.006	-0.437	0.139	-0.060	-1.046
864	B5	22.8	0	75	0.437	0.147	0.995	0.133	-1.144	0.379	-0.389	-2.485
865	B5	22.7	30	75	0.576	0.182	1.215	0.139	-1.866	0.538	-0.684	-3.811
866	B5	23.4	60	75	0.258	0.134	0.761	-0.101	-0.617	0.306	0.101	-1.740
867	B5	23.2	60	90	0.083	0.091	0.455	-0.169	-0.197	0.179	0.285	-1.020
868	B5	22.8	30	90	0.366	0.131	0.852	-0.002	-0.702	0.315	0.035	-1.889
869	B5	22.8	0	90	0.295	0.108	0.774	0.056	-0.274	0.178	0.176	-1.044
870	B5	22.7	-30	90	0.247	0.081	0.545	0.032	-0.188	0.115	0.187	-0.656
871	B5	23.2	-30	105	0.289	0.122	0.853	-0.064	0.127	0.139	0.706	-0.357
872	B5	22.7	0	105	0.300	0.136	0.897	-0.084	0.110	0.156	0.779	-0.519
873	B5	22.8	30	105	0.414	0.158	1.018	0.019	0.333	0.152	0.889	-0.257
874	B5	23.3	60	105	0.218	0.134	0.729	-0.132	0.194	0.139	0.726	-0.341
875	B5	23.5	60	120	0.486	0.213	1.298	-0.048	0.449	0.172	1.148	-0.006
876	B5	22.7	30	120	0.796	0.218	1.630	0.254	0.622	0.200	1.456	0.098
877	B5	22.5	0	120	0.407	0.179	1.164	-0.057	0.159	0.146	0.848	-0.302
878	B5	22.8	-30	120	0.349	0.160	1.233	-0.070	0.133	0.157	0.915	-0.364
879	B5	22.8	-30	135	0.298	0.134	0.998	-0.137	0.099	0.091	0.587	-0.193
880	B5	22.4	0	135	0.391	0.221	1.334	-0.156	0.155	0.118	0.655	-0.195
881	B5	22.4	30	135	1.032	0.331	2.253	0.287	0.610	0.215	1.380	0.137
882	B5	22.9	60	135	0.828	0.297	1.947	0.106	0.558	0.184	1.272	0.122
883	B5	22.9	60	150	1.096	0.384	2.422	0.114	0.482	0.160	1.036	0.093
884	B5	23.1	30	150	1.325	0.398	2.732	0.435	0.472	0.159	1.050	0.137
885	B5	22.7	0	150	0.538	0.259	1.615	-0.074	0.084	0.090	0.472	-0.178
886	B5	22.1	-30	150	0.337	0.131	0.979	-0.115	0.041	0.056	0.279	-0.161
887	B5	23.0	-30	165	0.094	0.114	0.576	-0.373	-0.005	0.032	0.093	-0.120
888	B5	22.2	0	165	0.482	0.342	1.852	-0.317	0.043	0.080	0.390	-0.156
889	B5	23.2	30	165	1.355	0.404	2.802	0.421	0.277	0.101	0.648	0.040

Phase 1, 2, and 3 Balance Data

Run	Conf	Uref fps	Cfx		Cfz							
			Mean	RMS	Max	Min	Mean	RMS	Max	Min		
890	B5	22.9	60	165	1.315	0.429	2.802	0.224	0.293	0.109	0.709	0.031
891	B5	22.7	60	180	1.381	0.441	2.891	0.300	0.081	0.054	0.306	-0.052
892	B5	23.0	30	180	1.478	0.394	2.946	0.599	0.064	0.053	0.296	-0.100
893	B5	22.3	0	180	0.575	0.336	2.125	-0.129	-0.005	0.052	0.226	-0.148
894	B5	21.9	-30	180	0.053	0.132	0.550	-0.445	0.004	0.028	0.074	-0.102
895	B6	22.9	-30	-180	0.118	0.184	1.022	-0.426	-0.007	0.027	0.073	-0.111
896	B6	22.6	0	-180	0.463	0.299	1.926	-0.126	-0.018	0.049	0.205	-0.176
897	B6	23.2	30	-180	1.396	0.391	2.795	0.565	0.059	0.057	0.274	-0.105
898	B6	22.9	60	-180	1.403	0.463	3.360	0.368	0.085	0.065	0.393	-0.069
899	B6	23.6	60	-165	1.218	0.385	2.693	0.215	-0.150	0.042	0.007	-0.285
900	B6	22.9	30	-165	1.357	0.375	2.855	0.514	-0.155	0.047	-0.030	-0.334
901	B6	22.7	0	-165	0.368	0.265	1.450	-0.204	-0.095	0.050	0.042	-0.296
902	B6	22.9	-30	-165	0.115	0.162	0.855	-0.333	-0.052	0.042	0.081	-0.216
903	B6	22.4	-30	-150	0.072	0.130	0.645	-0.289	-0.073	0.061	0.097	-0.334
904	B6	22.8	0	-150	0.350	0.231	1.345	-0.108	-0.153	0.072	0.024	-0.466
905	B6	23.2	30	-150	0.998	0.283	2.066	0.338	-0.288	0.070	-0.103	-0.545
906	B6	23.3	60	-150	0.873	0.305	2.061	0.109	-0.308	0.082	-0.048	-0.616
907	B6	23.7	60	-135	0.605	0.233	1.521	-0.005	-0.357	0.112	-0.034	-0.765
908	B6	23.2	30	-135	0.807	0.228	1.722	0.306	-0.328	0.089	-0.088	-0.681
909	B6	22.7	0	-135	0.268	0.190	1.143	-0.091	-0.148	0.078	0.046	-0.521
910	B6	23.0	-30	-135	0.085	0.099	0.510	-0.217	-0.084	0.057	0.102	-0.318
911	B6	23.0	-30	-120	0.077	0.087	0.487	-0.161	-0.042	0.052	0.151	-0.269
912	B6	22.8	0	-120	0.163	0.125	0.708	-0.099	-0.066	0.064	0.185	-0.340
913	B6	23.0	30	-120	0.566	0.175	1.282	0.168	-0.345	0.118	-0.018	-0.779
914	B6	23.2	60	-120	0.323	0.169	0.978	-0.124	-0.296	0.125	0.098	-0.775
915	B6	23.1	60	-105	0.200	0.123	0.710	-0.091	-0.046	0.101	0.298	-0.435
916	B6	23.2	30	-105	0.364	0.123	0.790	0.046	-0.131	0.119	0.264	-0.536
917	B6	22.6	0	-105	0.169	0.098	0.600	-0.033	-0.003	0.078	0.271	-0.322
918	B6	23.1	-30	-105	0.128	0.079	0.451	-0.073	-0.027	0.063	0.230	-0.294
919	B6	23.1	-30	-90	0.194	0.083	0.560	-0.015	0.208	0.093	0.600	-0.144
920	B6	23.0	0	-90	0.195	0.088	0.559	-0.009	0.268	0.112	0.845	-0.047
921	B6	23.4	30	-90	0.183	0.103	0.518	-0.067	0.592	0.154	1.273	0.157
922	B6	23.7	60	-90	0.144	0.089	0.515	-0.078	0.259	0.125	0.879	-0.098
923	B6	23.6	60	-75	0.184	0.102	0.578	-0.083	0.571	0.216	1.620	0.115
924	B6	23.3	30	-75	0.260	0.120	0.725	-0.029	1.143	0.292	2.208	0.493
925	B6	23.2	0	-75	0.456	0.157	1.130	0.143	0.894	0.268	1.967	0.326
926	B6	23.0	-30	-75	0.279	0.107	0.700	0.041	0.626	0.201	1.569	0.156
927	B6	23.0	-30	-60	0.216	0.124	0.794	-0.061	0.442	0.208	1.462	-0.179
928	B6	23.5	0	-60	0.510	0.250	1.458	0.033	0.983	0.411	2.596	0.139
929	B6	23.1	30	-60	0.452	0.171	1.067	0.049	1.170	0.373	2.419	0.334
930	B6	23.3	60	-60	0.342	0.132	0.853	0.019	0.735	0.257	1.832	0.193
931	B6	23.5	60	-45	0.743	0.237	1.689	0.139	0.827	0.279	1.891	0.183
932	B6	23.4	30	-45	0.884	0.292	2.041	0.171	1.008	0.357	2.385	0.159
933	B6	23.0	0	-45	0.655	0.362	2.068	-0.025	0.748	0.422	2.435	-0.029
934	B6	22.8	-30	-45	0.326	0.185	1.225	-0.120	0.284	0.188	1.270	-0.110
935	B6	23.1	-30	-30	0.337	0.232	1.465	-0.242	0.173	0.151	0.949	-0.168
936	B6	22.7	0	-30	0.529	0.365	2.104	-0.296	0.369	0.264	1.470	-0.179
937	B6	23.3	30	-30	1.281	0.370	2.654	0.095	0.727	0.244	1.651	0.103
938	B6	23.6	60	-30	1.000	0.334	2.330	0.209	0.690	0.250	1.637	0.117
939	B6	23.5	60	-15	1.226	0.434	3.103	0.236	0.428	0.169	1.290	-0.182

Phase 1, 2, and 3 Balance Data

Run	Conf	Uref fps	Cfx		Cfz							
			Mean	RMS	Max	Min	Mean	RMS	Max	Min		
940	B6	23.4	30	-15	1.548	0.483	3.392	0.482	0.413	0.156	1.029	0.066
941	B6	22.6	0	-15	0.486	0.355	2.121	-0.278	0.132	0.133	0.761	-0.161
942	B6	22.3	-30	-15	0.310	0.271	1.564	-0.400	0.063	0.103	0.641	-0.202
943	B6	22.5	-30	0	0.204	0.247	1.390	-0.453	0.006	0.050	0.297	-0.148
944	B6	22.4	0	0	0.470	0.386	2.306	-0.351	0.019	0.069	0.388	-0.149
945	B6	23.0	30	0	1.729	0.503	3.637	0.594	0.054	0.066	0.339	-0.116
946	B6	23.3	60	0	1.392	0.474	3.216	0.236	0.088	0.078	0.448	-0.107
947	B6	23.7	60	15	1.414	0.478	3.381	0.249	-0.311	0.088	-0.027	-0.675
948	B6	23.2	30	15	1.789	0.468	3.566	0.638	-0.374	0.077	-0.150	-0.646
949	B6	22.5	0	15	0.554	0.378	2.369	-0.174	-0.096	0.065	0.085	-0.385
950	B6	22.3	-30	15	0.156	0.213	1.288	-0.446	-0.024	0.038	0.132	-0.187
951	B6	22.4	-30	30	0.153	0.188	1.058	-0.364	-0.044	0.049	0.107	-0.242
952	B6	22.7	0	30	0.535	0.363	2.195	-0.197	-0.246	0.147	0.027	-0.876
953	B6	23.4	30	30	1.752	0.468	3.541	0.704	-0.840	0.181	-0.378	-1.475
954	B6	23.5	60	30	1.289	0.455	3.085	0.154	-0.666	0.204	-0.123	-1.397
955	B6	23.5	60	45	0.913	0.354	2.173	0.099	-0.947	0.347	-0.153	-2.195
956	B6	23.2	30	45	1.641	0.417	3.205	0.623	-1.707	0.394	-0.653	-3.173
957	B6	22.6	0	45	0.565	0.338	2.020	-0.125	-0.606	0.335	0.035	-1.957
958	B6	22.8	-30	45	0.242	0.159	1.102	-0.195	-0.132	0.091	0.079	-0.633
959	B6	22.9	-30	60	0.192	0.105	0.742	-0.073	-0.234	0.117	0.061	-0.893
960	B6	23.2	0	60	0.522	0.266	1.470	-0.053	-0.919	0.415	-0.041	-2.438
961	B6	23.3	30	60	1.201	0.298	2.328	0.481	-2.205	0.513	-0.965	-4.156
962	B6	23.5	60	60	0.506	0.226	1.382	-0.010	-0.858	0.357	-0.069	-2.253
963	B6	23.5	60	75	0.249	0.122	0.720	-0.067	-0.605	0.282	0.135	-1.645
964	B6	23.7	30	75	0.585	0.159	1.157	0.206	-1.812	0.487	-0.654	-3.459
965	B6	23.5	0	75	0.440	0.163	1.027	0.082	-1.090	0.419	-0.174	-2.577
966	B6	22.9	-30	75	0.151	0.075	0.413	-0.053	-0.344	0.120	0.003	-0.944
967	B6	23.3	-30	90	0.174	0.081	0.485	-0.065	-0.234	0.122	0.131	-0.752
968	B6	23.6	0	90	0.213	0.107	0.650	-0.019	-0.342	0.202	0.084	-1.270
969	B6	23.5	30	90	0.336	0.105	0.756	0.071	-0.808	0.303	-0.069	-2.053
970	B6	23.7	60	90	0.137	0.083	0.474	-0.096	-0.244	0.188	0.295	-0.989
971	B6	23.4	60	105	0.241	0.134	0.807	-0.153	0.208	0.146	0.812	-0.319
972	B6	23.3	30	105	0.493	0.155	1.090	0.105	0.351	0.159	0.978	-0.218
973	B6	23.4	0	105	0.268	0.126	0.827	-0.082	0.103	0.143	0.679	-0.418
974	B6	23.0	-30	105	0.282	0.117	0.846	-0.078	0.117	0.136	0.748	-0.422
975	B6	22.9	-30	120	0.290	0.128	0.896	-0.093	0.145	0.122	0.703	-0.298
976	B6	22.6	0	120	0.271	0.177	1.092	-0.145	0.148	0.136	0.795	-0.266
977	B6	22.9	30	120	0.766	0.236	1.611	0.204	0.616	0.215	1.410	0.050
978	B6	23.4	60	120	0.511	0.215	1.414	-0.034	0.474	0.177	1.238	-0.011
979	B6	23.5	60	135	0.808	0.283	1.941	0.116	0.546	0.174	1.266	0.088
980	B6	23.1	30	135	1.099	0.317	2.236	0.345	0.605	0.203	1.343	0.143
981	B6	23.1	0	135	0.393	0.213	1.383	-0.118	0.123	0.108	0.662	-0.224
982	B6	22.8	-30	135	0.299	0.133	0.933	-0.134	0.097	0.081	0.463	-0.202
983	B6	22.8	-30	150	0.220	0.146	0.873	-0.224	0.035	0.051	0.262	-0.132
984	B6	22.9	0	150	0.399	0.275	1.620	-0.211	0.105	0.099	0.552	-0.136
985	B6	23.2	30	150	1.221	0.371	2.529	0.438	0.461	0.152	1.010	0.136
986	B6	23.4	60	150	1.173	0.408	2.568	0.175	0.495	0.172	1.094	0.091
987	B6	23.6	60	165	1.313	0.424	2.797	-0.040	0.337	0.120	0.934	0.006
988	B6	23.0	30	165	1.435	0.425	3.108	0.541	0.300	0.117	0.810	0.065
989	B6	22.4	0	165	0.543	0.292	1.749	-0.094	0.057	0.079	0.407	-0.134

Phase 1, 2, and 3 Balance Data

Run	Conf	Uref fps	Cfx		Cfz					
			Yaw	Pitch	Mean	RMS	Max	Min	Mean	RMS
990	B6	22.3	-30	165	0.239	0.177	1.031	-0.348	0.005	0.040
1001	D3	23.3	330	165	0.302	0.121	0.846	-0.125	0.034	0.029
1002	D3	23.2	0	165	0.536	0.165	1.281	0.006	0.052	0.039
1003	D3	22.8	30	165	0.771	0.233	1.765	0.141	0.044	0.047
1004	D3	23.1	45	165	1.162	0.342	2.376	0.352	0.011	0.046
1005	D3	23.2	45	150	1.001	0.288	2.104	0.292	0.320	0.105
1006	D3	23.3	30	150	0.614	0.191	1.440	0.082	0.213	0.078
1007	D3	23.8	0	150	0.426	0.144	1.101	-0.085	0.122	0.056
1008	D3	23.6	330	150	0.282	0.117	0.899	-0.152	0.078	0.047
1009	D3	23.3	330	135	0.242	0.118	0.825	-0.174	0.081	0.078
1010	D3	23.1	0	135	0.282	0.143	0.993	-0.218	0.127	0.087
1011	D3	23.2	30	135	0.441	0.175	1.305	-0.064	0.273	0.119
1012	D3	23.1	45	135	0.741	0.247	1.785	0.096	0.388	0.152
1013	D3	23.6	45	120	0.422	0.174	1.219	-0.094	0.293	0.169
1014	D3	23.3	30	120	0.311	0.147	1.017	-0.154	0.291	0.145
1015	D3	23.4	0	120	0.197	0.124	0.815	-0.317	0.126	0.119
1016	D3	23.4	330	120	0.139	0.106	0.816	-0.249	0.074	0.109
1017	D3	23.5	330	105	0.085	0.078	0.458	-0.199	0.073	0.123
1018	D3	23.3	0	105	0.077	0.097	0.648	-0.300	0.108	0.146
1019	D3	23.5	30	105	0.102	0.101	0.535	-0.254	0.159	0.145
1020	D3	23.2	45	105	0.157	0.116	0.601	-0.233	-0.091	0.221
1021	D3	23.3	45	90	0.088	0.083	0.440	-0.185	-0.540	0.299
1022	D3	23.5	30	90	0.082	0.071	0.390	-0.174	-0.130	0.171
1023	D3	23.3	0	90	0.032	0.057	0.360	-0.142	-0.001	0.119
1024	D3	23.5	330	90	0.063	0.053	0.317	-0.124	-0.001	0.109
1025	D3	23.4	330	75	0.076	0.063	0.325	-0.134	-0.142	0.109
1026	D3	23.3	0	75	0.071	0.065	0.391	-0.172	-0.224	0.127
1027	D3	23.8	30	75	0.119	0.092	0.544	-0.136	-0.382	0.184
1028	D3	23.5	45	75	0.284	0.120	0.726	-0.147	-0.885	0.342
1029	D3	23.4	45	60	0.573	0.217	1.403	0.046	-0.954	0.340
1030	D3	23.1	30	60	0.294	0.159	1.106	-0.503	-0.494	0.181
1031	D3	22.9	0	60	0.184	0.115	0.792	-0.216	-0.377	0.127
1032	D3	23.1	330	60	0.133	0.091	0.596	-0.165	-0.202	0.098
1033	D3	23.1	330	45	0.237	0.114	0.856	-0.124	-0.212	0.082
1034	D3	23.1	0	45	0.314	0.142	1.035	-0.115	-0.395	0.103
1035	D3	23.1	30	45	0.428	0.202	1.480	-0.061	-0.472	0.136
1036	D3	23.0	45	45	0.807	0.288	1.860	0.107	-0.806	0.241
1037	D3	23.1	45	30	1.115	0.346	2.433	0.310	-0.529	0.137
1038	D3	22.7	30	30	0.731	0.264	1.962	0.085	-0.366	0.094
1039	D3	22.7	0	30	0.567	0.194	1.466	-0.060	-0.315	0.077
1040	D3	23.4	330	30	0.330	0.136	0.981	-0.120	-0.167	0.060
1041	D3	23.2	330	15	0.402	0.154	1.018	-0.124	-0.098	0.041
1042	D3	23.0	0	15	0.644	0.221	1.836	-0.065	-0.180	0.049
1043	D3	22.8	30	15	0.857	0.263	2.098	0.101	-0.206	0.057
1044	D3	22.3	45	15	1.331	0.396	2.900	0.367	-0.272	0.072
1045	D3	23.3	45	0	1.159	0.340	2.654	0.301	0.133	0.075
1046	D3	22.6	30	0	1.078	0.292	2.267	0.161	0.070	0.067
1047	D3	22.8	0	0	0.765	0.230	1.763	-0.056	0.005	0.048
1048	D3	22.3	330	0	0.456	0.171	1.191	-0.123	0.000	0.037
1049	D3	23.0	330	-15	0.358	0.165	1.177	-0.212	0.086	0.062

Phase 1, 2, and 3 Balance Data

Run	Conf	Uref fps	Cfx		Cfz							
			Mean	RMS	Max	Min	Mean	RMS	Max	Min		
1050	D3	22.8	0	-15	0.618	0.221	1.609	-0.211	0.171	0.081	0.626	-0.110
1051	D3	22.8	30	-15	0.957	0.268	2.027	0.009	0.315	0.112	0.813	-0.036
1052	D3	22.7	45	-15	1.048	0.290	2.273	0.226	0.400	0.133	0.941	0.033
1053	D3	23.0	45	-30	0.860	0.224	1.932	0.176	0.479	0.163	1.247	0.007
1054	D3	22.4	30	-30	0.642	0.201	1.397	-0.043	0.427	0.136	1.008	0.002
1055	D3	22.8	0	-30	0.534	0.171	1.321	-0.051	0.304	0.109	0.867	-0.046
1056	D3	22.7	330	-30	0.311	0.140	0.870	-0.186	0.175	0.086	0.581	-0.163
1057	D3	22.7	330	-45	0.260	0.100	0.688	-0.114	0.223	0.092	0.633	-0.128
1058	D3	22.7	0	-45	0.399	0.115	0.874	-0.043	0.386	0.118	0.940	-0.071
1059	D3	22.8	30	-45	0.454	0.116	0.899	0.008	0.448	0.121	0.933	-0.029
1060	D3	22.9	45	-45	0.660	0.159	1.354	0.244	0.487	0.156	1.123	0.024
1061	D3	23.1	45	-60	0.329	0.119	0.806	0.026	0.449	0.142	1.034	-0.002
1062	D3	22.9	30	-60	0.149	0.068	0.427	-0.072	0.400	0.105	0.891	0.032
1063	D3	22.9	0	-60	0.194	0.064	0.442	-0.016	0.396	0.097	0.865	0.042
1064	D3	22.2	330	-60	0.161	0.063	0.387	-0.067	0.243	0.086	0.663	-0.166
1065	D3	22.6	330	-75	0.108	0.045	0.255	-0.025	0.160	0.066	0.525	-0.106
1066	D3	22.9	0	-75	0.092	0.038	0.212	-0.025	0.246	0.070	0.578	-0.030
1067	D3	22.9	30	-75	0.055	0.048	0.258	-0.088	0.270	0.096	0.780	-0.051
1068	D3	22.4	45	-75	0.155	0.088	0.489	-0.049	0.305	0.129	0.810	-0.103
1069	D3	22.7	45	-90	0.048	0.082	0.347	-0.152	0.182	0.135	0.692	-0.329
1070	D3	23.2	30	-90	0.098	0.047	0.253	-0.046	0.173	0.095	0.644	-0.184
1071	D3	22.5	0	-90	0.133	0.055	0.298	-0.020	0.131	0.076	0.594	-0.211
1072	D3	22.9	330	-90	0.110	0.042	0.236	-0.033	0.089	0.061	0.434	-0.161
1073	D3	23.1	330	-105	0.150	0.051	0.316	-0.027	-0.020	0.062	0.352	-0.231
1074	D3	22.5	0	-105	-0.006	0.050	0.186	-0.178	-0.026	0.069	0.327	-0.255
1075	D3	22.9	30	-105	-0.021	0.055	0.203	-0.204	-0.010	0.081	0.397	-0.301
1076	D3	22.6	45	-105	0.101	0.103	0.560	-0.156	-0.091	0.117	0.290	-0.605
1077	D3	23.1	45	-120	0.166	0.122	0.667	-0.126	-0.215	0.102	0.063	-0.587
1078	D3	22.9	30	-120	0.134	0.077	0.467	-0.123	-0.083	0.064	0.185	-0.336
1079	D3	22.9	0	-120	0.155	0.063	0.388	-0.088	-0.024	0.055	0.282	-0.229
1080	D3	22.8	330	-120	0.167	0.064	0.376	-0.066	-0.017	0.050	0.242	-0.182
1081	D3	23.2	330	-135	0.158	0.070	0.438	-0.088	-0.025	0.040	0.156	-0.195
1082	D3	23.1	0	-135	0.127	0.080	0.448	-0.180	-0.049	0.043	0.149	-0.234
1083	D3	23.0	30	-135	0.129	0.097	0.541	-0.195	-0.128	0.060	0.081	-0.383
1084	D3	23.1	45	-135	0.337	0.160	1.031	-0.037	-0.297	0.106	-0.021	-0.676
1085	D3	23.3	45	-150	0.686	0.227	1.551	0.152	-0.306	0.089	-0.082	-0.573
1086	D3	22.9	30	-150	0.461	0.152	1.173	0.008	-0.153	0.060	-0.001	-0.460
1087	D3	23.1	0	-150	0.309	0.111	0.768	-0.125	-0.066	0.037	0.073	-0.248
1088	D3	23.0	330	-150	0.239	0.087	0.602	-0.102	-0.033	0.030	0.096	-0.158
1089	D3	23.2	330	-165	0.233	0.105	0.673	-0.177	-0.017	0.027	0.069	-0.158
1090	D3	22.9	0	-165	0.469	0.138	1.043	-0.003	-0.036	0.035	0.060	-0.227
1091	D3	22.8	30	-165	0.717	0.196	1.589	0.199	-0.094	0.046	0.004	-0.290
1092	D3	22.8	45	-165	0.987	0.295	2.140	0.267	-0.203	0.059	-0.039	-0.422
1093	D3	23.0	45	-180	1.211	0.332	2.392	0.420	-0.025	0.043	0.131	-0.153
1094	D3	22.8	30	-180	0.763	0.218	1.737	0.186	0.029	0.044	0.158	-0.137
1095	D3	22.9	0	-180	0.499	0.169	1.239	-0.062	0.049	0.036	0.162	-0.118
1096	D3	22.4	45	-180	0.366	0.125	0.857	-0.099	0.021	0.030	0.099	-0.096
1097	B2	22.9	-30	180	1.170	0.300	2.250	0.440	0.049	0.043	0.202	-0.089
1098	B2	22.7	0	180	1.840	0.363	3.102	0.965	0.089	0.045	0.242	-0.073
1099	B2	23.1	30	180	1.584	0.346	2.921	0.693	0.187	0.044	0.332	0.034

Phase 1, 2, and 3 Balance Data

Run	Conf	Uref fps	Cfx		Cfz							
			Mean	RMS	Max	Min	Mean	RMS	Max	Min		
1100	B2	23.1	60	180	0.755	0.259	1.863	0.130	0.052	0.041	0.204	-0.071
1101	B2	22.8	60	-165	0.662	0.247	1.582	0.100	-0.066	0.046	0.050	-0.254
1102	B2	22.4	30	-165	1.549	0.305	2.652	0.789	-0.151	0.059	-0.011	-0.381
1103	B2	22.9	0	-165	1.549	0.318	2.838	0.889	-0.168	0.067	-0.016	-0.426
1104	B2	23.0	-30	-165	0.946	0.262	1.886	0.340	-0.126	0.058	0.011	-0.360
1105	B2	22.9	-30	-150	0.697	0.217	1.494	0.183	-0.172	0.065	-0.026	-0.416
1106	B2	22.8	0	-150	0.945	0.224	1.798	0.412	-0.215	0.071	-0.034	-0.500
1107	B2	22.8	30	-150	1.042	0.256	1.935	0.448	-0.237	0.077	-0.063	-0.533
1108	B2	22.8	60	-150	0.569	0.204	1.351	0.064	-0.145	0.069	0.019	-0.441
1109	B2	22.5	60	-135	0.339	0.138	0.878	-0.024	-0.159	0.068	0.039	-0.442
1110	B2	22.7	30	-135	0.598	0.180	1.277	0.092	-0.214	0.075	-0.014	-0.508
1111	B2	23.0	0	-135	0.677	0.165	1.267	0.259	-0.204	0.077	0.012	-0.495
1112	B2	22.7	-30	-135	0.536	0.156	1.178	0.165	-0.171	0.067	0.030	-0.447
1113	B2	23.3	-30	-120	0.360	0.128	0.829	0.022	-0.113	0.078	0.148	-0.434
1114	B2	22.6	0	-120	0.477	0.138	1.004	0.115	-0.081	0.092	0.274	-0.443
1115	B2	22.7	30	-120	0.403	0.142	0.945	0.014	-0.112	0.087	0.179	-0.473
1116	B2	22.5	60	-120	0.223	0.108	0.647	-0.083	-0.073	0.061	0.157	-0.350
1117	B2	22.8	60	-105	0.226	0.097	0.585	-0.061	-0.096	0.094	0.171	-0.533
1118	B2	23.1	30	-105	0.254	0.121	0.705	-0.072	-0.089	0.109	0.312	-0.580
1119	B2	23.0	0	-105	0.316	0.105	0.738	0.067	-0.084	0.128	0.456	-0.591
1120	B2	22.5	-30	-105	0.306	0.110	0.782	0.022	-0.114	0.107	0.267	-0.522
1121	B2	22.9	-30	-90	0.278	0.109	0.678	0.022	0.414	0.158	1.025	-0.184
1122	B2	22.8	0	-90	0.233	0.099	0.620	-0.022	0.400	0.190	1.104	-0.280
1123	B2	23.0	30	-90	0.327	0.119	0.821	-0.003	0.425	0.151	1.002	-0.139
1124	B2	22.5	60	-90	0.190	0.092	0.552	-0.064	0.154	0.115	0.673	-0.239
1125	B2	22.6	60	-75	0.204	0.095	0.586	-0.059	0.484	0.206	1.418	-0.003
1126	B2	22.8	30	-75	0.496	0.146	1.044	0.124	1.268	0.370	2.688	0.513
1127	B2	22.6	0	-75	0.633	0.143	1.136	0.325	1.576	0.405	3.153	0.677
1128	B2	22.8	-30	-75	0.426	0.132	0.904	0.130	1.270	0.394	2.687	0.412
1129	B2	22.5	-30	-60	0.877	0.202	1.639	0.411	1.486	0.472	3.270	0.481
1130	B2	22.6	0	-60	1.197	0.205	1.925	0.673	1.740	0.494	3.444	0.558
1131	B2	22.6	30	-60	0.721	0.203	1.493	0.192	1.593	0.438	3.204	0.597
1132	B2	23.2	60	-60	0.271	0.133	0.819	-0.066	0.659	0.256	1.678	0.045
1133	B2	23.1	60	-45	0.591	0.206	1.394	0.075	0.697	0.261	1.718	0.117
1134	B2	22.6	30	-45	1.425	0.315	2.741	0.681	1.480	0.409	3.180	0.612
1135	B2	22.8	0	-45	1.617	0.328	2.871	0.808	1.467	0.390	2.931	0.565
1136	B2	22.5	-30	-45	1.063	0.309	2.289	0.412	1.181	0.395	2.672	0.386
1137	B2	22.6	-30	-30	1.062	0.299	2.229	0.321	0.706	0.183	1.455	0.262
1138	B2	22.9	0	-30	1.497	0.339	2.756	0.578	0.885	0.199	1.594	0.385
1139	B2	22.2	30	-30	1.803	0.424	3.512	0.784	1.088	0.253	2.106	0.489
1140	B2	22.4	60	-30	0.790	0.285	1.949	0.072	0.572	0.185	1.300	0.083
1141	B2	22.8	60	-15	1.005	0.339	2.196	0.169	0.367	0.106	0.693	0.072
1142	B2	22.3	30	-15	2.171	0.446	4.033	1.057	0.523	0.123	1.035	0.210
1143	B2	22.5	0	-15	1.919	0.419	3.450	0.981	0.493	0.124	0.957	0.207
1144	B2	22.8	-30	-15	1.290	0.354	2.617	0.451	0.359	0.114	0.816	0.092
1145	B2	22.7	-30	0	1.358	0.383	2.923	0.388	0.025	0.040	0.208	-0.090
1146	B2	22.3	0	0	2.001	0.442	3.593	0.915	0.022	0.042	0.198	-0.097
1147	B2	22.5	30	0	2.154	0.442	3.757	1.121	0.007	0.043	0.188	-0.116
1148	B2	22.7	60	0	1.092	0.358	2.621	0.271	0.067	0.047	0.227	-0.077
1149	B2	22.8	60	15	0.951	0.313	2.210	0.198	-0.339	0.113	-0.063	-0.794

Phase 1, 2, and 3 Balance Data

Run	Conf	Uref fps	Cfx		Cfz							
			Mean	RMS	Max	Min	Mean	RMS	Max	Min		
1150	B2	22.8	30	15	1.947	0.460	3.704	0.893	-0.698	0.159	-0.339	-1.293
1151	B2	22.8	0	15	2.001	0.463	3.830	1.007	-0.711	0.155	-0.348	-1.301
1152	B2	22.8	-30	15	1.399	0.395	2.869	0.546	-0.524	0.144	-0.198	-1.051
1153	B2	23.1	-30	30	1.287	0.359	2.731	0.428	-1.039	0.280	-0.355	-2.178
1154	B2	22.8	0	30	1.841	0.442	3.753	0.841	-1.354	0.313	-0.644	-2.684
1155	B2	22.8	30	30	1.608	0.408	3.284	0.667	-1.183	0.282	-0.540	-2.445
1156	B2	22.6	60	30	0.846	0.298	1.997	-0.133	-0.638	0.222	-0.092	-1.470
1157	B2	22.8	60	45	0.586	0.241	1.488	0.030	-0.859	0.340	-0.121	-2.163
1158	B2	22.6	30	45	1.238	0.355	2.747	0.399	-1.877	0.501	-0.713	-3.950
1159	B2	23.1	0	45	1.439	0.373	2.878	0.614	-2.110	0.519	-0.958	-4.150
1160	B2	22.6	-30	45	1.190	0.349	2.515	0.463	-1.710	0.523	-0.660	-3.648
1161	B2	22.6	-30	60	0.835	0.274	1.826	0.223	-2.232	0.682	-0.845	-4.732
1162	B2	22.8	0	60	1.050	0.260	1.977	0.474	-2.735	0.670	-1.340	-5.212
1163	B2	23.0	30	60	0.912	0.265	1.851	0.245	-2.309	0.630	-0.927	-4.563
1164	B2	23.1	60	60	0.383	0.169	1.055	-0.027	-0.856	0.395	-0.092	-2.480
1165	B2	22.7	60	75	0.153	0.114	0.564	-0.180	-0.572	0.304	0.082	-1.817
1166	B2	23.0	30	75	0.486	0.173	1.152	0.044	-1.818	0.584	-0.644	-4.008
1167	B2	22.7	0	75	0.610	0.185	1.251	0.157	-2.275	0.692	-0.901	-4.744
1168	B2	23.0	-30	75	0.514	0.177	1.226	0.117	-1.934	0.633	-0.650	-4.345
1169	B2	22.8	-30	90	0.285	0.117	0.760	-0.018	-0.528	0.314	0.155	-1.942
1170	B2	22.8	0	90	0.279	0.128	0.821	-0.038	-0.440	0.319	0.187	-2.230
1171	B2	23.1	30	90	0.324	0.136	0.852	-0.058	-0.491	0.323	0.224	-1.855
1172	B2	22.9	60	90	0.170	0.089	0.501	-0.099	-0.210	0.195	0.306	-0.958
1173	B2	22.8	60	105	0.178	0.123	0.679	-0.188	0.180	0.143	0.765	-0.379
1174	B2	23.2	30	105	0.367	0.154	1.025	-0.072	0.362	0.192	1.122	-0.416
1175	B2	23.1	0	105	0.391	0.140	0.942	0.024	0.220	0.215	1.153	-0.543
1176	B2	22.8	-30	105	0.374	0.139	0.919	0.014	0.270	0.193	1.084	-0.412
1177	B2	22.7	-30	120	0.528	0.186	1.229	0.075	0.283	0.125	0.809	-0.143
1178	B2	22.9	0	120	0.671	0.198	1.443	0.170	0.330	0.138	0.961	-0.159
1179	B2	22.8	30	120	0.679	0.195	1.411	0.115	0.448	0.149	1.031	0.012
1180	B2	23.4	60	120	0.394	0.158	1.065	-0.018	0.324	0.142	0.908	-0.024
1181	B2	22.8	60	135	0.517	0.204	1.288	-0.025	0.362	0.130	0.852	0.063
1182	B2	22.5	30	135	1.028	0.268	2.085	0.368	0.566	0.133	1.130	0.219
1183	B2	23.0	0	135	0.946	0.265	2.014	0.315	0.462	0.121	0.942	0.130
1184	B2	22.4	-30	135	0.821	0.244	1.755	0.257	0.371	0.106	0.771	0.080
1185	B2	22.9	-30	150	0.975	0.281	2.031	0.353	0.388	0.096	0.749	0.154
1186	B2	22.6	0	150	1.365	0.328	2.596	0.630	0.533	0.114	0.947	0.244
1187	B2	22.8	30	150	1.399	0.320	2.601	0.643	0.560	0.116	1.004	0.266
1188	B2	22.8	60	150	0.715	0.240	1.624	0.090	0.297	0.100	0.687	0.050
1189	B2	22.9	60	165	0.765	0.280	1.930	0.161	0.178	0.073	0.513	0.010
1190	B2	22.8	30	165	1.474	0.340	2.824	0.656	0.334	0.077	0.630	0.132
1191	B2	22.4	0	165	1.497	0.391	3.051	0.641	0.334	0.077	0.632	0.119
1192	B2	22.6	-30	165	1.173	0.299	2.238	0.449	0.237	0.063	0.478	0.056
1193	C4	22.2	-30	180	-0.105	0.145	0.509	-0.645	-0.011	0.037	0.073	-0.171
1194	C4	22.8	0	180	0.043	0.200	0.898	-0.631	-0.025	0.043	0.107	-0.202
1195	C4	22.3	30	180	1.132	0.301	2.301	0.373	-0.039	0.049	0.099	-0.229
1196	C4	22.4	30	165	0.879	0.267	1.939	0.140	0.166	0.062	0.414	-0.005
1197	C4	22.5	0	165	0.107	0.212	1.029	-0.668	-0.003	0.056	0.215	-0.194
1198	C4	22.1	-30	165	-0.043	0.144	0.589	-0.584	-0.014	0.040	0.106	-0.165
1199	C4	22.4	-30	150	0.062	0.139	0.608	-0.476	0.017	0.056	0.213	-0.212

Phase 1, 2, and 3 Balance Data

Run	Conf	Uref fps	Cfx			Cfz						
			Mean	RMS	Max	Min	Mean	RMS	Max	Min		
1200	C4	22.1	0	150	0.133	0.173	0.872	-0.489	0.031	0.068	0.302	-0.236
1201	C4	22.2	30	150	0.681	0.248	1.613	0.017	0.237	0.089	0.578	0.006
1202	C4	22.3	30	135	0.538	0.226	1.520	-0.062	0.244	0.116	0.727	-0.096
1203	C4	22.2	0	135	0.339	0.161	1.060	-0.225	0.128	0.107	0.615	-0.287
1204	C4	22.5	-30	135	0.105	0.149	0.725	-0.469	0.097	0.098	0.512	-0.250
1205	C4	22.6	-30	120	0.167	0.168	0.908	-0.301	0.197	0.179	1.002	-0.370
1206	C4	22.3	0	120	0.301	0.163	1.083	-0.142	0.214	0.173	0.953	-0.321
1207	C4	22.9	30	120	0.391	0.183	1.227	-0.147	0.277	0.163	1.029	-0.216
1208	C4	22.6	30	105	0.235	0.120	0.810	-0.090	0.281	0.180	0.968	-0.361
1209	C4	22.4	0	105	0.227	0.144	0.880	-0.158	0.165	0.217	1.012	-0.735
1210	C4	22.6	-30	105	0.163	0.135	0.807	-0.205	0.169	0.189	0.950	-0.632
1211	C4	22.8	-30	90	0.087	0.083	0.429	-0.135	-0.355	0.190	0.175	-1.160
1212	C4	22.6	0	90	0.163	0.095	0.522	-0.094	-0.443	0.223	0.083	-1.469
1213	C4	22.5	30	90	0.256	0.123	0.700	-0.115	-0.429	0.236	0.137	-1.510
1214	C4	22.7	30	75	0.371	0.139	0.899	-0.032	-1.253	0.367	-0.498	-2.663
1215	C4	22.2	0	75	0.184	0.091	0.555	-0.052	-0.997	0.235	-0.414	-1.979
1216	C4	22.6	-30	75	0.177	0.087	0.517	-0.058	-0.793	0.241	-0.210	-1.716
1217	C4	22.8	-30	60	-0.068	0.089	0.336	-0.314	-0.330	0.160	0.068	-1.107
1218	C4	22.4	0	60	0.176	0.109	0.624	-0.172	-0.546	0.200	0.004	-1.490
1219	C4	22.5	30	60	0.525	0.177	1.154	0.038	-1.062	0.311	-0.408	-2.207
1220	C4	22.6	30	45	0.729	0.218	1.584	0.178	-0.801	0.233	-0.233	-1.687
1221	C4	23.0	0	45	0.110	0.145	0.847	-0.278	-0.139	0.132	0.141	-0.913
1222	C4	23.0	-30	45	0.033	0.125	0.777	-0.326	-0.116	0.101	0.135	-0.551
1223	C4	22.5	-30	30	-0.003	0.143	0.662	-0.492	0.032	0.067	0.242	-0.247
1224	C4	22.4	0	30	0.090	0.199	1.042	-0.515	-0.061	0.103	0.198	-0.599
1225	C4	22.8	30	30	0.985	0.285	2.191	0.274	-0.618	0.167	-0.208	-1.387
1226	C4	22.6	30	15	1.166	0.323	2.484	0.346	-0.370	0.099	-0.123	-0.763
1227	C4	22.2	0	15	0.145	0.240	1.223	-0.611	-0.037	0.068	0.134	-0.386
1228	C4	22.5	-30	15	-0.102	0.169	0.623	-0.678	0.022	0.052	0.217	-0.174
1229	C4	22.6	-30	0	-0.076	0.181	0.622	-0.818	0.014	0.042	0.177	-0.125
1230	C4	22.6	0	0	0.150	0.268	1.283	-0.730	0.000	0.050	0.242	-0.176
1231	C4	22.7	30	0	1.185	0.355	2.644	0.272	-0.016	0.053	0.209	-0.185
1232	C4	22.5	30	-15	0.926	0.371	2.476	-0.075	0.293	0.124	0.824	-0.063
1233	C4	22.4	0	-15	0.100	0.266	1.312	-0.722	0.050	0.094	0.543	-0.258
1234	C4	22.1	-30	-15	0.004	0.203	0.778	-0.732	0.007	0.073	0.352	-0.267
1235	C4	22.7	-30	-30	0.054	0.205	0.931	-0.589	0.071	0.129	0.663	-0.340
1236	C4	22.3	0	-30	0.185	0.266	1.420	-0.636	0.148	0.171	0.999	-0.372
1237	C4	23.0	30	-30	0.703	0.314	2.050	-0.081	0.530	0.210	1.436	0.016
1238	C4	21.8	30	-45	0.683	0.242	1.719	0.102	0.776	0.312	2.203	0.043
1239	C4	22.3	0	-45	0.359	0.222	1.506	-0.109	0.310	0.255	1.661	-0.208
1240	C4	22.5	-30	-45	0.227	0.169	1.042	-0.434	0.201	0.177	1.129	-0.237
1241	C4	22.6	30	-60	0.455	0.192	1.247	0.001	1.003	0.362	2.562	0.221
1242	C4	22.7	0	-60	0.447	0.190	1.239	0.042	0.887	0.385	2.380	0.016
1243	C4	22.3	-30	-60	0.275	0.139	0.926	-0.028	0.609	0.277	1.971	-0.023
1244	C4	22.8	30	-75	0.246	0.141	0.791	-0.142	1.082	0.278	2.280	0.419
1245	C4	22.6	0	-75	0.394	0.132	0.951	0.104	1.277	0.345	2.612	0.500
1246	C4	22.6	-30	-75	0.194	0.119	0.672	-0.050	0.952	0.315	2.258	0.244
1247	C4	22.5	-30	-90	0.109	0.091	0.491	-0.115	0.306	0.136	0.893	-0.148
1248	C4	22.3	0	-90	0.106	0.092	0.513	-0.120	0.370	0.139	0.943	-0.124
1249	C4	22.6	30	-90	0.181	0.122	0.625	-0.142	0.292	0.138	0.835	-0.234

Phase 1, 2, and 3 Balance Data

Run	Conf	Uref fps	Cfx		Cfz							
			Mean	RMS	Max	Min	Mean	RMS	Max	Min		
1250	C4	22.5	30	-105	0.196	0.092	0.531	-0.067	-0.035	0.092	0.287	-0.384
1251	C4	22.7	0	-105	0.022	0.081	0.427	-0.158	-0.012	0.099	0.364	-0.430
1252	C4	22.3	-30	-105	0.107	0.075	0.432	-0.069	-0.034	0.090	0.285	-0.420
1253	C4	22.6	-30	-120	0.018	0.068	0.326	-0.172	-0.049	0.063	0.136	-0.350
1254	C4	22.8	0	-120	0.063	0.081	0.512	-0.151	-0.062	0.075	0.169	-0.447
1255	C4	22.4	30	-120	0.323	0.129	0.784	-0.043	-0.152	0.082	0.090	-0.527
1256	C4	22.9	30	-135	0.513	0.153	1.107	0.127	-0.297	0.100	-0.075	-0.685
1257	C4	22.7	0	-135	0.093	0.120	0.656	-0.221	-0.121	0.093	0.116	-0.581
1258	C4	22.4	-30	-135	-0.026	0.084	0.394	-0.270	-0.031	0.071	0.184	-0.394
1259	C4	22.8	-30	-150	-0.087	0.108	0.348	-0.471	-0.013	0.067	0.198	-0.295
1260	C4	22.2	0	-150	0.138	0.156	0.760	-0.325	-0.108	0.086	0.135	-0.470
1261	C4	22.4	30	-150	0.677	0.232	1.538	0.049	-0.364	0.116	-0.100	-0.807
1262	C4	22.6	30	-165	1.086	0.297	2.190	0.309	-0.266	0.092	-0.056	-0.602
1263	C4	22.2	0	-165	0.135	0.198	0.960	-0.420	-0.068	0.066	0.106	-0.387
1264	C4	22.4	-30	-165	-0.007	0.137	0.636	-0.491	-0.013	0.055	0.156	-0.294
1265	C2	22.1	-30	-165	-0.033	0.139	0.383	-0.631	0.024	0.044	0.228	-0.144
1266	C2	22.6	0	-165	-0.301	0.181	0.254	-1.111	0.045	0.057	0.301	-0.146
1267	C2	22.9	30	-165	0.779	0.273	1.706	-0.054	-0.254	0.080	-0.036	-0.553
1268	C2	22.5	30	-150	0.602	0.217	1.468	-0.031	-0.312	0.100	-0.062	-0.720
1269	C2	22.3	0	-150	-0.032	0.132	0.403	-0.561	0.029	0.071	0.328	-0.226
1270	C2	22.6	-30	-150	-0.042	0.105	0.293	-0.442	0.005	0.057	0.235	-0.217
1271	C2	22.5	-30	-135	-0.007	0.074	0.259	-0.280	-0.044	0.063	0.198	-0.292
1272	C2	22.5	0	-135	0.068	0.094	0.448	-0.285	-0.058	0.074	0.207	-0.386
1273	C2	22.2	30	-135	0.396	0.160	0.986	-0.020	-0.281	0.092	-0.082	-0.663
1274	C2	22.4	30	-120	0.281	0.122	0.746	-0.066	-0.111	0.075	0.128	-0.463
1275	C2	22.4	0	-120	0.060	0.091	0.496	-0.199	-0.095	0.083	0.171	-0.488
1276	C2	22.3	-30	-120	0.129	0.076	0.488	-0.089	-0.073	0.071	0.162	-0.390
1277	C2	22.9	-30	-105	0.097	0.078	0.461	-0.103	-0.041	0.094	0.312	-0.417
1278	C2	22.2	0	-105	0.122	0.088	0.522	-0.106	-0.029	0.113	0.464	-0.441
1279	C2	22.5	30	-105	0.175	0.106	0.570	-0.122	-0.080	0.096	0.265	-0.476
1280	C2	22.8	30	-90	0.141	0.118	0.561	-0.210	0.315	0.135	0.812	-0.132
1281	C2	22.4	0	-90	0.151	0.085	0.516	-0.043	0.420	0.145	1.038	-0.017
1282	C2	22.0	-30	-90	0.185	0.097	0.553	-0.039	0.377	0.156	0.994	-0.108
1283	C2	22.9	-30	-75	0.188	0.110	0.632	-0.066	1.007	0.312	2.224	0.281
1284	C2	22.3	0	-75	0.383	0.131	0.912	0.101	1.380	0.364	2.819	0.574
1285	C2	22.5	30	-75	0.287	0.149	0.874	-0.103	1.103	0.308	2.330	0.442
1286	C2	22.6	30	-60	0.577	0.206	1.390	0.094	1.110	0.365	2.592	0.376
1287	C2	22.5	0	-60	0.534	0.159	1.184	0.156	1.006	0.356	2.445	0.120
1288	C2	22.7	-30	-60	0.320	0.136	0.928	0.030	0.731	0.299	2.039	0.071
1289	C2	23.0	-30	-45	0.164	0.126	0.753	-0.212	0.217	0.157	1.015	-0.307
1290	C2	22.4	0	-45	0.161	0.150	0.892	-0.331	0.191	0.179	0.976	-0.447
1291	C2	22.9	30	-45	0.509	0.221	1.538	-0.011	0.648	0.284	1.882	-0.004
1292	C2	22.4	30	-30	0.695	0.349	1.969	-0.497	0.488	0.254	1.432	-0.371
1293	C2	23.1	0	-30	-0.064	0.198	0.553	-0.896	-0.039	0.132	0.429	-0.606
1294	C2	22.3	-30	-30	0.113	0.175	0.681	-0.723	0.063	0.109	0.506	-0.452
1295	C2	22.7	-30	-15	0.056	0.186	0.760	-0.808	0.021	0.068	0.312	-0.313
1296	C2	22.7	0	-15	-0.284	0.254	0.450	-1.548	-0.043	0.095	0.252	-0.518
1297	C2	22.6	30	-15	0.830	0.393	2.260	-0.372	0.276	0.146	0.896	-0.194
1298	C2	22.6	30	0	1.064	0.397	2.445	-0.377	0.016	0.058	0.294	-0.182
1299	C2	22.8	0	0	-0.256	0.242	0.377	-1.486	0.020	0.048	0.189	-0.193

Phase 1, 2, and 3 Balance Data

Run	Conf	Uref fps	Cfx		Cfz					
			Yaw	Pitch	Mean	RMS	Max	Min	Mean	RMS
1300	C2	22.7	-30	0	-0.033	0.163	0.504	-0.821	0.017	0.040
1301	C2	22.7	-30	15	-0.041	0.149	0.472	-0.846	0.045	0.043
1302	C2	23.0	0	15	-0.178	0.193	0.418	-1.082	0.067	0.046
1303	C2	22.9	30	15	0.789	0.352	1.970	-0.240	-0.224	0.103
1304	C2	22.7	30	30	0.655	0.316	1.806	-0.264	-0.356	0.173
1305	C2	22.5	0	30	-0.035	0.158	0.572	-0.803	0.051	0.059
1306	C2	22.4	-30	30	-0.023	0.142	0.426	-0.725	0.009	0.057
1307	C2	22.7	-30	45	0.077	0.109	0.515	-0.326	-0.087	0.096
1308	C2	22.4	0	45	0.110	0.120	0.667	-0.386	-0.111	0.105
1309	C2	22.5	30	45	0.533	0.209	1.275	-0.064	-0.712	0.246
1310	C2	22.7	30	60	0.461	0.150	0.998	0.067	-1.133	0.273
1311	C2	23.0	0	60	0.320	0.123	0.813	-0.043	-0.857	0.244
1312	C2	23.1	-30	60	0.273	0.117	0.802	-0.017	-0.640	0.237
1313	C2	22.8	-30	75	0.319	0.122	0.837	0.035	-1.210	0.396
1314	C2	22.7	0	75	0.383	0.120	0.819	0.075	-1.511	0.361
1315	C2	22.5	30	75	0.420	0.133	0.945	0.040	-1.219	0.330
1316	C2	23.2	30	90	0.166	0.114	0.605	-0.171	-0.290	0.200
1317	C2	22.6	0	90	0.202	0.095	0.584	-0.036	-0.446	0.246
1318	C2	22.8	-30	90	0.226	0.094	0.615	-0.008	-0.366	0.216
1319	C2	23.0	-30	105	0.251	0.144	0.912	-0.159	0.171	0.189
1320	C2	22.9	0	105	0.240	0.180	1.050	-0.248	0.164	0.248
1321	C2	22.6	30	105	0.349	0.140	0.912	-0.051	0.300	0.186
1322	C2	22.8	30	120	0.405	0.183	1.225	-0.095	0.282	0.180
1323	C2	22.7	0	120	0.384	0.282	1.576	-0.429	0.267	0.276
1324	C2	22.8	-30	120	0.394	0.232	1.473	-0.305	0.226	0.228
1325	C2	22.7	-30	135	0.308	0.187	1.215	-0.257	0.229	0.142
1326	C2	22.4	0	135	0.277	0.215	1.305	-0.280	0.248	0.168
1327	C2	22.3	30	135	0.620	0.212	1.456	0.034	0.274	0.124
1328	C2	22.4	30	150	0.648	0.236	1.517	-0.131	0.197	0.086
1329	C2	22.4	0	150	0.097	0.152	0.731	-0.491	0.111	0.085
1330	C2	23.0	-30	150	0.115	0.121	0.611	-0.296	0.094	0.069
1331	C2	22.6	-30	165	0.066	0.140	0.478	-0.615	0.020	0.046
1332	C2	22.6	0	165	-0.020	0.157	0.508	-0.803	0.004	0.049
1333	C2	22.8	30	165	0.628	0.293	1.563	-0.800	0.119	0.066
1334	C2	22.8	30	180	0.776	0.307	1.813	-0.240	-0.033	0.043
1335	C2	22.9	0	180	-0.128	0.177	0.391	-0.919	-0.019	0.034
1336	C2	22.6	-30	180	-0.038	0.137	0.487	-0.748	-0.006	0.031
1337	C6	22.7	-30	180	0.104	0.204	1.040	-0.473	-0.027	0.040
1338	C6	21.8	0	180	0.461	0.274	1.660	-0.303	-0.071	0.060
1339	C6	22.3	30	180	0.965	0.290	2.027	0.253	-0.025	0.044
1340	C6	22.5	30	-165	0.965	0.283	2.118	0.261	-0.269	0.093
1341	C6	22.3	0	-165	0.325	0.200	1.183	-0.203	-0.142	0.086
1342	C6	22.4	-30	-165	0.088	0.170	0.740	-0.353	-0.095	0.072
1343	C6	22.4	-30	-150	0.056	0.134	0.644	-0.324	-0.069	0.084
1344	C6	22.8	0	-150	0.190	0.159	0.862	-0.212	-0.166	0.099
1345	C6	22.9	30	-150	0.697	0.224	1.670	0.110	-0.336	0.113
1346	C6	23.0	30	-135	0.481	0.160	1.119	0.081	-0.287	0.103
1347	C6	22.3	0	-135	0.137	0.111	0.703	-0.130	-0.161	0.089
1348	C6	22.5	-30	-135	0.086	0.091	0.514	-0.186	-0.097	0.078
1349	C6	23.1	-30	-120	0.058	0.074	0.400	-0.143	-0.048	0.066

Phase 1, 2, and 3 Balance Data

Run	Conf	Uref fps	Cfx		Cfz							
			Mean	RMS	Max	Min	Mean	RMS	Max	Min		
1350	C6	22.6	0	-120	0.079	0.096	0.504	-0.187	-0.095	0.080	0.177	-0.454
1351	C6	22.7	30	-120	0.347	0.121	0.792	0.018	-0.143	0.078	0.108	-0.458
1352	C6	23.1	30	-105	0.200	0.108	0.616	-0.136	-0.019	0.090	0.310	-0.391
1353	C6	22.5	0	-105	0.083	0.093	0.515	-0.112	0.005	0.098	0.364	-0.440
1354	C6	23.0	-30	-105	0.101	0.077	0.461	-0.072	-0.032	0.083	0.295	-0.407
1355	C6	22.7	-30	-90	0.111	0.088	0.475	-0.105	0.322	0.134	0.831	-0.196
1356	C6	22.8	0	-90	0.085	0.092	0.468	-0.149	0.319	0.141	0.918	-0.131
1357	C6	22.5	30	-90	0.213	0.117	0.681	-0.127	0.365	0.139	0.951	-0.088
1358	C6	23.1	30	-75	0.298	0.140	0.823	-0.082	1.032	0.281	2.095	0.362
1359	C6	22.5	0	-75	0.366	0.133	0.885	0.074	1.279	0.339	2.634	0.508
1360	C6	22.6	-30	-75	0.226	0.113	0.671	-0.014	0.900	0.285	2.103	0.269
1361	C6	22.6	-30	-60	0.327	0.157	1.152	-0.017	0.605	0.299	2.247	-0.026
1362	C6	22.6	0	-60	0.543	0.235	1.667	0.064	1.030	0.482	3.308	0.071
1363	C6	22.8	30	-60	0.441	0.182	1.201	0.007	0.889	0.340	2.332	0.135
1364	C6	22.9	30	-45	0.640	0.252	1.694	0.028	0.763	0.305	2.068	0.084
1365	C6	22.7	0	-45	0.684	0.299	2.166	0.042	0.621	0.353	2.424	-0.101
1366	C6	22.3	-30	-45	0.327	0.215	1.446	-0.148	0.366	0.242	1.665	-0.121
1367	C6	22.6	-30	-30	0.297	0.243	1.386	-0.372	0.179	0.152	0.913	-0.197
1368	C6	22.3	0	-30	0.649	0.323	2.171	-0.089	0.305	0.211	1.315	-0.150
1369	C6	22.4	30	-30	0.743	0.326	2.170	-0.055	0.493	0.205	1.428	0.009
1370	C6	23.0	30	-15	1.046	0.367	2.459	0.139	0.282	0.118	0.801	-0.008
1371	C6	22.0	0	-15	0.712	0.374	2.419	-0.143	0.124	0.122	0.738	-0.201
1372	C6	22.0	-30	-15	0.264	0.292	1.486	-0.495	0.066	0.099	0.562	-0.198
1373	C6	22.3	-30	0	0.197	0.265	1.325	-0.503	0.001	0.049	0.235	-0.148
1374	C6	22.7	0	0	0.443	0.337	1.828	-0.434	-0.009	0.055	0.229	-0.212
1375	C6	22.5	30	0	1.185	0.374	2.798	0.242	0.007	0.055	0.254	-0.203
1376	C6	22.7	30	15	1.075	0.332	2.494	0.256	-0.319	0.099	-0.073	-0.726
1377	C6	22.3	0	15	0.455	0.328	1.959	-0.295	-0.135	0.094	0.081	-0.608
1378	C6	22.3	-30	15	0.174	0.228	1.177	-0.508	-0.060	0.062	0.127	-0.338
1379	C6	22.3	-30	30	0.169	0.202	1.206	-0.334	-0.088	0.093	0.122	-0.555
1380	C6	22.8	0	30	0.395	0.263	1.678	-0.197	-0.224	0.139	0.049	-0.903
1381	C6	22.4	30	30	0.944	0.293	2.264	0.205	-0.562	0.162	-0.193	-1.294
1382	C6	23.1	30	45	0.756	0.237	1.687	0.172	-0.888	0.266	-0.258	-1.957
1383	C6	22.8	0	45	0.295	0.205	1.265	-0.131	-0.363	0.226	0.050	-1.506
1384	C6	22.7	-30	45	0.240	0.149	0.963	-0.132	-0.193	0.132	0.082	-0.841
1385	C6	22.5	-30	60	0.141	0.103	0.630	-0.156	-0.358	0.190	0.043	-1.470
1386	C6	22.5	0	60	0.161	0.123	0.775	-0.133	-0.442	0.251	0.053	-1.708
1387	C6	22.4	30	60	0.548	0.175	1.181	0.077	-1.233	0.353	-0.451	-2.587
1388	C6	22.7	30	75	0.373	0.136	0.898	-0.015	-1.283	0.372	-0.532	-2.662
1389	C6	22.6	0	75	0.101	0.093	0.484	-0.155	-0.696	0.223	-0.128	-1.683
1390	C6	22.7	-30	75	0.146	0.068	0.429	-0.055	-0.558	0.202	-0.080	-1.509
1391	C6	22.5	-30	90	0.109	0.070	0.407	-0.063	-0.329	0.178	0.123	-1.194
1392	C6	22.8	0	90	0.060	0.070	0.382	-0.121	-0.303	0.182	0.133	-1.292
1393	C6	22.8	30	90	0.319	0.114	0.763	0.002	-0.516	0.233	0.049	-1.415
1394	C6	22.7	30	105	0.283	0.132	0.859	-0.123	0.349	0.184	1.040	-0.305
1395	C6	22.6	0	105	0.148	0.120	0.701	-0.201	0.144	0.183	0.852	-0.652
1396	C6	22.7	-30	105	0.190	0.122	0.773	-0.168	0.145	0.184	0.862	-0.561
1397	C6	22.5	-30	120	0.223	0.155	1.010	-0.286	0.182	0.167	1.038	-0.472
1398	C6	22.5	0	120	0.233	0.156	1.037	-0.224	0.173	0.161	0.919	-0.366
1399	C6	22.5	30	120	0.427	0.185	1.205	-0.072	0.278	0.164	1.071	-0.309

Phase 1, 2, and 3 Balance Data

Run	Conf	Uref fps	Cfx		Cfz							
			Mean	RMS	Max	Min	Mean	RMS	Max	Min		
1400	C6	22.9	30	135	0.582	0.211	1.401	0.005	0.264	0.111	0.722	-0.052
1401	C6	22.6	0	135	0.311	0.155	1.021	-0.204	0.119	0.105	0.564	-0.287
1402	C6	22.5	-30	135	0.217	0.148	0.925	-0.241	0.105	0.098	0.575	-0.269
1403	C6	22.7	-30	150	0.148	0.151	0.832	-0.349	0.030	0.050	0.231	-0.151
1404	C6	22.5	0	150	0.430	0.204	1.343	-0.219	0.065	0.073	0.344	-0.189
1405	C6	22.5	30	150	0.687	0.252	1.594	0.013	0.241	0.082	0.545	-0.009
1406	C6	22.4	30	165	0.781	0.270	1.832	0.104	0.163	0.060	0.397	0.011
1407	C6	22.5	0	165	0.470	0.217	1.422	-0.108	0.015	0.057	0.226	-0.175
1408	C6	22.5	-30	165	0.088	0.168	0.989	-0.400	-0.006	0.038	0.127	-0.141
1409	C1	22.5	-30	-165	-0.147	0.152	0.285	-0.748	0.031	0.043	0.191	-0.147
1410	C1	22.8	0	-165	-0.317	0.150	0.119	-0.992	0.049	0.050	0.261	-0.111
1411	C1	22.9	30	-165	-0.438	0.224	0.256	-1.369	0.049	0.067	0.312	-0.196
1412	C1	22.0	30	-150	-0.136	0.158	0.369	-0.725	0.020	0.083	0.300	-0.273
1413	C1	23.3	0	-150	-0.074	0.115	0.311	-0.568	0.008	0.060	0.245	-0.243
1414	C1	22.7	-30	-150	-0.092	0.105	0.237	-0.497	0.009	0.056	0.206	-0.188
1415	C1	22.7	-30	-135	-0.014	0.079	0.333	-0.300	-0.040	0.063	0.181	-0.356
1416	C1	22.5	0	-135	0.087	0.090	0.441	-0.209	-0.070	0.068	0.156	-0.361
1417	C1	22.7	30	-135	0.096	0.108	0.500	-0.293	-0.091	0.071	0.178	-0.377
1418	C1	22.7	30	-120	0.148	0.102	0.547	-0.150	-0.077	0.064	0.112	-0.383
1419	C1	22.7	0	-120	0.114	0.099	0.560	-0.154	-0.073	0.075	0.163	-0.408
1420	C1	22.4	-30	-120	0.136	0.082	0.546	-0.085	-0.076	0.068	0.143	-0.408
1421	C1	22.9	-30	-105	0.057	0.083	0.377	-0.160	-0.037	0.083	0.290	-0.376
1422	C1	22.2	0	-105	0.068	0.089	0.485	-0.164	-0.002	0.105	0.406	-0.455
1423	C1	23.2	30	-105	0.193	0.093	0.553	-0.084	-0.021	0.082	0.280	-0.357
1424	C1	22.9	30	-90	0.204	0.100	0.565	-0.082	0.420	0.126	0.901	-0.003
1425	C1	23.0	0	-90	0.113	0.092	0.445	-0.121	0.547	0.155	1.098	0.134
1426	C1	21.5	-30	-90	0.218	0.092	0.586	-0.015	0.429	0.155	1.070	-0.026
1427	C1	22.4	-30	-75	0.273	0.123	0.825	0.005	1.049	0.321	2.438	0.353
1428	C1	22.4	0	-75	0.317	0.126	0.814	0.020	1.275	0.315	2.466	0.530
1429	C1	21.9	30	-75	0.224	0.125	0.707	-0.111	0.991	0.261	2.012	0.370
1430	C1	22.1	30	-60	0.320	0.143	0.941	-0.069	0.801	0.267	2.001	0.132
1431	C1	22.4	0	-60	0.450	0.140	1.007	0.090	0.903	0.296	2.088	0.192
1432	C1	22.1	-30	-60	0.388	0.140	1.069	0.048	0.757	0.283	2.113	0.078
1433	C1	22.1	-30	-45	0.217	0.144	0.799	-0.239	0.222	0.158	0.918	-0.308
1434	C1	21.8	0	-45	0.158	0.135	0.692	-0.355	0.152	0.155	0.810	-0.444
1435	C1	21.8	30	-45	0.246	0.174	0.829	-0.285	0.312	0.187	0.999	-0.303
1436	C1	22.3	30	-30	-0.025	0.261	0.921	-1.004	0.012	0.161	0.606	-0.607
1437	C1	22.0	0	-30	-0.091	0.196	0.553	-0.942	-0.033	0.123	0.428	-0.581
1438	C1	21.8	-30	-30	0.115	0.187	0.740	-0.689	0.070	0.109	0.514	-0.374
1439	C1	21.7	-30	-15	0.165	0.197	0.771	-0.670	0.022	0.069	0.285	-0.267
1440	C1	22.1	0	-15	-0.318	0.237	0.334	-1.481	-0.057	0.081	0.188	-0.468
1441	C1	22.1	30	-15	-0.371	0.328	0.688	-1.532	-0.021	0.118	0.380	-0.417
1442	C1	21.8	30	0	-0.291	0.314	0.747	-1.402	0.069	0.075	0.335	-0.179
1443	C1	21.8	0	0	-0.305	0.233	0.320	-1.470	0.019	0.042	0.176	-0.184
1444	C1	21.8	-30	0	-0.016	0.191	0.644	-0.893	0.034	0.045	0.224	-0.130
1445	C1	21.8	-30	15	-0.064	0.175	0.475	-0.911	0.037	0.040	0.188	-0.083
1446	C1	22.0	0	15	-0.205	0.192	0.312	-1.182	0.054	0.036	0.211	-0.024
1447	C1	22.0	30	15	-0.184	0.242	0.602	-1.125	0.096	0.064	0.360	-0.102
1448	C1	22.2	30	30	0.138	0.182	0.779	-0.566	-0.051	0.088	0.216	-0.413
1449	C1	22.5	0	30	-0.068	0.143	0.405	-0.797	0.038	0.052	0.257	-0.124

Phase 1, 2, and 3 Balance Data

Run	Conf	Uref fps	Cfx		Cfz							
			Yaw	Pitch	Mean	RMS	Max	Min	Mean	RMS	Max	Min
1450	C1	22.4	-30	30	-0.048	0.142	0.372	-0.787	-0.004	0.056	0.213	-0.192
1451	C1	21.8	-30	45	0.089	0.116	0.591	-0.379	-0.125	0.095	0.202	-0.531
1452	C1	21.9	0	45	0.123	0.124	0.592	-0.426	-0.152	0.111	0.237	-0.576
1453	C1	22.1	30	45	0.184	0.139	0.719	-0.278	-0.206	0.108	0.117	-0.686
1454	C1	22.1	30	60	0.331	0.134	0.859	-0.093	-0.696	0.193	-0.168	-1.550
1455	C1	22.0	0	60	0.338	0.135	0.938	-0.063	-0.827	0.222	-0.213	-1.799
1456	C1	22.2	-30	60	0.272	0.127	0.855	-0.101	-0.654	0.219	-0.071	-1.648
1457	C1	22.0	-30	75	0.292	0.113	0.740	0.016	-1.165	0.368	-0.418	-2.582
1458	C1	21.9	0	75	0.412	0.125	0.895	0.117	-1.580	0.392	-0.732	-3.186
1459	C1	22.2	30	75	0.332	0.123	0.773	-0.034	-1.134	0.334	-0.407	-2.446
1460	C1	22.1	30	90	0.249	0.112	0.687	-0.079	-0.448	0.230	0.081	-1.557
1461	C1	22.6	0	90	0.194	0.103	0.611	-0.060	-0.561	0.265	0.005	-1.710
1462	C1	22.5	-30	90	0.203	0.086	0.537	-0.021	-0.444	0.219	0.058	-1.459
1463	C1	22.3	-30	105	0.271	0.159	0.971	-0.160	0.195	0.188	0.926	-0.517
1464	C1	21.9	0	105	0.261	0.190	1.096	-0.317	0.159	0.248	1.058	-0.773
1465	C1	22.4	30	105	0.331	0.166	1.025	-0.131	0.242	0.197	0.941	-0.519
1466	C1	22.6	30	120	0.443	0.226	1.575	-0.252	0.308	0.221	1.317	-0.408
1467	C1	22.3	0	120	0.392	0.307	1.805	-0.570	0.286	0.267	1.376	-0.608
1468	C1	22.0	-30	120	0.414	0.241	1.508	-0.319	0.250	0.211	1.064	-0.468
1469	C1	22.3	-30	135	0.327	0.194	1.267	-0.291	0.223	0.131	0.751	-0.203
1470	C1	21.8	0	135	0.202	0.191	1.249	-0.312	0.227	0.141	0.885	-0.181
1471	C1	21.9	30	135	0.512	0.202	1.471	-0.166	0.303	0.146	0.962	-0.197
1472	C1	21.9	30	150	0.248	0.164	0.888	-0.309	0.128	0.081	0.412	-0.126
1473	C1	21.8	0	150	-0.041	0.135	0.463	-0.553	0.092	0.072	0.402	-0.128
1474	C1	21.8	-30	150	0.145	0.138	0.676	-0.376	0.094	0.067	0.347	-0.109
1475	C1	22.1	-30	165	0.092	0.148	0.577	-0.544	0.030	0.041	0.166	-0.121
1476	C1	22.0	0	165	-0.080	0.142	0.332	-0.791	-0.005	0.039	0.112	-0.151
1477	C1	22.1	30	165	0.025	0.189	0.660	-0.750	0.024	0.057	0.212	-0.189
1478	C1	22.1	30	180	-0.313	0.209	0.427	-1.113	-0.005	0.047	0.149	-0.195
1479	C1	21.9	0	180	-0.245	0.173	0.258	-1.056	-0.011	0.033	0.106	-0.122
1480	C1	22.0	-30	180	-0.104	0.145	0.287	-0.738	-0.008	0.029	0.095	-0.125
1481	C3	22.1	-30	-180	-0.112	0.156	0.508	-0.723	-0.003	0.035	0.107	-0.161
1482	C3	22.2	0	-180	0.023	0.159	0.736	-0.600	-0.033	0.037	0.056	-0.199
1483	C3	22.1	30	-180	0.380	0.303	1.521	-0.514	-0.056	0.051	0.097	-0.234
1484	C3	22.2	30	-165	0.415	0.275	1.480	-0.354	-0.176	0.093	0.090	-0.502
1485	C3	22.1	0	-165	0.035	0.125	0.534	-0.466	-0.038	0.050	0.121	-0.264
1486	C3	21.7	-30	-165	-0.102	0.145	0.476	-0.615	-0.014	0.058	0.157	-0.265
1487	C3	22.5	-30	-150	-0.106	0.115	0.336	-0.530	-0.008	0.066	0.207	-0.277
1488	C3	22.7	0	-150	0.000	0.096	0.430	-0.350	-0.044	0.057	0.133	-0.330
1489	C3	22.1	30	-150	0.314	0.188	1.036	-0.206	-0.233	0.104	0.026	-0.617
1490	C3	22.4	30	-135	0.215	0.114	0.720	-0.136	-0.187	0.085	0.048	-0.610
1491	C3	22.4	0	-135	0.029	0.084	0.461	-0.218	-0.059	0.067	0.132	-0.385
1492	C3	22.3	-30	-135	0.007	0.085	0.408	-0.271	-0.046	0.069	0.170	-0.343
1493	C3	22.5	-30	-120	0.077	0.079	0.416	-0.140	-0.052	0.065	0.148	-0.336
1494	C3	22.7	0	-120	0.077	0.076	0.451	-0.119	-0.045	0.062	0.141	-0.335
1495	C3	22.4	30	-120	0.157	0.105	0.578	-0.143	-0.100	0.067	0.086	-0.423
1496	C3	22.5	30	-105	0.158	0.090	0.560	-0.092	-0.013	0.079	0.312	-0.357
1497	C3	22.5	0	-105	0.058	0.078	0.420	-0.132	-0.003	0.092	0.369	-0.405
1498	C3	22.6	-30	-105	0.146	0.070	0.486	-0.048	-0.035	0.080	0.291	-0.374
1499	C3	22.9	-30	-90	0.136	0.083	0.452	-0.085	0.385	0.139	0.916	-0.031

Phase 1, 2, and 3 Balance Data

Run	Conf	Uref fps	Cfx		Cfz							
			Mean	RMS	Max	Min	Mean	RMS	Max	Min		
1500	C3	22.9	0	-90	0.178	0.085	0.525	-0.031	0.491	0.145	1.089	0.064
1501	C3	22.2	30	-90	0.241	0.108	0.620	-0.049	0.421	0.133	0.928	-0.022
1502	C3	22.5	30	-75	0.250	0.122	0.730	-0.113	0.937	0.253	2.022	0.389
1503	C3	22.6	0	-75	0.321	0.121	0.865	0.063	1.157	0.294	2.353	0.422
1504	C3	22.5	-30	-75	0.267	0.107	0.725	0.030	0.896	0.272	2.020	0.247
1505	C3	22.5	-30	-60	0.304	0.132	0.951	0.008	0.550	0.236	1.750	0.031
1506	C3	22.0	0	-60	0.410	0.181	1.318	0.049	0.655	0.333	2.326	-0.017
1507	C3	22.6	30	-60	0.351	0.174	1.122	-0.039	0.719	0.298	2.116	0.122
1508	C3	22.5	30	-45	0.405	0.241	1.563	-0.153	0.400	0.269	1.825	-0.159
1509	C3	21.8	0	-45	0.266	0.184	1.184	-0.223	0.178	0.191	1.180	-0.323
1510	C3	22.3	-30	-45	0.189	0.155	0.955	-0.220	0.186	0.163	1.053	-0.219
1511	C3	22.4	-30	-30	0.098	0.201	0.984	-0.531	0.037	0.117	0.614	-0.325
1512	C3	22.0	0	-30	0.203	0.224	1.235	-0.441	0.056	0.138	0.725	-0.369
1513	C3	21.8	30	-30	0.460	0.327	1.907	-0.384	0.274	0.232	1.347	-0.303
1514	C3	22.2	30	-15	0.290	0.383	1.939	-0.739	0.082	0.147	0.737	-0.350
1515	C3	21.7	0	-15	0.185	0.235	1.213	-0.586	0.015	0.080	0.435	-0.274
1516	C3	22.0	-30	-15	-0.019	0.231	1.023	-0.749	0.007	0.076	0.413	-0.248
1517	C3	21.9	-30	0	-0.030	0.207	0.902	-0.802	0.021	0.044	0.227	-0.133
1518	C3	22.3	0	0	0.054	0.200	0.911	-0.724	0.000	0.038	0.215	-0.132
1519	C3	22.1	30	0	0.291	0.401	2.000	-0.828	0.009	0.072	0.334	-0.209
1520	C3	22.3	30	15	0.497	0.364	2.153	-0.434	-0.124	0.093	0.082	-0.581
1521	C3	21.8	0	15	0.043	0.179	0.833	-0.613	0.010	0.041	0.167	-0.151
1522	C3	22.4	-30	15	-0.026	0.167	0.612	-0.642	0.022	0.050	0.221	-0.131
1523	C3	21.9	-30	30	0.071	0.149	0.784	-0.443	0.016	0.065	0.206	-0.265
1524	C3	22.2	0	30	0.036	0.140	0.593	-0.536	0.009	0.057	0.221	-0.217
1525	C3	22.3	30	30	0.254	0.229	1.267	-0.421	-0.155	0.108	0.116	-0.682
1526	C3	22.1	30	45	0.326	0.157	1.060	-0.105	-0.349	0.146	-0.011	-1.102
1527	C3	22.4	0	45	0.156	0.104	0.753	-0.182	-0.062	0.085	0.188	-0.397
1528	C3	22.5	-30	45	0.164	0.114	0.734	-0.167	-0.132	0.100	0.130	-0.675
1529	C3	22.6	-30	60	0.194	0.088	0.654	-0.058	-0.366	0.156	0.008	-1.202
1530	C3	22.6	0	60	0.148	0.094	0.518	-0.135	-0.516	0.170	-0.052	-1.184
1531	C3	22.0	30	60	0.246	0.113	0.726	-0.103	-0.592	0.171	-0.135	-1.446
1532	C3	22.3	30	75	0.210	0.095	0.534	-0.071	-0.831	0.204	-0.295	-1.683
1533	C3	22.2	0	75	0.197	0.082	0.535	-0.018	-1.041	0.247	-0.430	-2.090
1534	C3	22.7	-30	75	0.238	0.071	0.518	0.034	-0.752	0.206	-0.221	-1.573
1535	C3	22.3	-30	90	0.161	0.078	0.474	-0.050	-0.313	0.174	0.158	-1.061
1536	C3	22.8	0	90	0.145	0.088	0.497	-0.083	-0.326	0.182	0.132	-1.087
1537	C3	22.3	30	90	0.265	0.108	0.637	-0.046	-0.295	0.187	0.154	-1.058
1538	C3	22.6	30	105	0.357	0.139	0.991	-0.045	0.263	0.189	1.037	-0.493
1539	C3	22.4	0	105	0.184	0.150	0.838	-0.249	0.163	0.207	0.934	-0.588
1540	C3	22.7	-30	105	0.295	0.135	0.901	-0.067	0.175	0.184	0.880	-0.489
1541	C3	22.4	-30	120	0.309	0.164	1.106	-0.153	0.181	0.168	0.983	-0.348
1542	C3	22.5	0	120	0.240	0.171	1.116	-0.294	0.193	0.174	1.080	-0.384
1543	C3	22.2	30	120	0.428	0.180	1.259	-0.107	0.288	0.183	1.020	-0.321
1544	C3	22.6	30	135	0.370	0.176	1.122	-0.177	0.201	0.126	0.717	-0.173
1545	C3	22.4	0	135	0.265	0.158	0.996	-0.254	0.150	0.112	0.663	-0.261
1546	C3	22.5	-30	135	0.321	0.150	1.012	-0.231	0.121	0.111	0.677	-0.242
1547	C3	22.5	-30	150	0.175	0.148	0.833	-0.391	0.022	0.056	0.222	-0.178
1548	C3	22.3	0	150	0.182	0.151	0.855	-0.456	0.007	0.059	0.215	-0.248
1549	C3	22.2	30	150	0.139	0.199	0.956	-0.462	0.027	0.066	0.291	-0.190

Phase 1, 2, and 3 Balance Data

Run	Conf	Uref fps	Yaw	Pitch	Cfx				Cfz			
					Mean	RMS	Max	Min	Mean	RMS	Max	Min
1550	C3	22.1	30	165	0.205	0.238	1.166	-0.510	-0.001	0.044	0.191	-0.145
1551	C3	22.3	0	165	0.088	0.164	0.770	-0.567	-0.042	0.038	0.083	-0.210
1552	C3	21.9	-30	165	0.009	0.149	0.619	-0.559	-0.027	0.037	0.101	-0.152

Phase 4 Balance Data

Phase 4 Balance Data

Run	Conf	Uref fps	Uref		Cmy			
			Yaw	Pitch	Mean	RMS	Max	Min
4	A1	25.1	0	180	-0.122	0.034	-0.013	-0.282
5	A1	25.3	0	-165	-0.181	0.046	-0.061	-0.372
6	A1	25.5	0	-150	-0.238	0.056	-0.112	-0.506
7	A1	25.4	0	-135	-0.256	0.067	-0.119	-0.567
8	A1	25.6	0	-120	-0.270	0.075	-0.109	-0.606
9	A1	25.7	0	-105	-0.258	0.065	-0.126	-0.574
10	A1	25.4	0	-90	-0.233	0.067	-0.092	-0.535
11	A1	25.8	0	-75	-0.119	0.053	0.027	-0.371
12	A1	24.9	0	-60	0.105	0.046	0.295	-0.044
13	A1	25.1	0	-45	0.085	0.062	0.407	-0.064
14	A1	25.5	0	-30	-0.025	0.035	0.169	-0.149
15	A1	25.1	0	-15	-0.027	0.024	0.115	-0.133
16	A1	25.2	0	0	-0.014	0.001	-0.010	-0.016
17	A1	25.3	0	15	-0.033	0.023	0.068	-0.130
18	A1	25.7	0	30	-0.076	0.033	0.058	-0.224
19	A1	25.0	0	45	-0.002	0.002	0.004	-0.008
20	A1	25.2	0	60	-0.092	0.040	-0.044	-0.230
21	A1	24.9	0	75	0.020	0.036	0.151	-0.163
22	A1	25.4	0	90	0.035	0.037	0.191	-0.031
23	A1	25.0	0	105	0.156	0.057	0.415	0.016
24	A1	24.9	0	120	0.001	0.001	0.005	-0.002
25	A1	25.2	0	135	0.124	0.067	0.384	0.011
26	A1	24.8	0	150	0.096	0.045	0.284	-0.003
27	A1	25.4	0	165	-0.020	0.023	0.105	-0.096
28	B1	25.0	0	165	-0.050	0.023	0.062	-0.122
29	B1	24.9	0	150	-0.067	0.003	-0.054	-0.072
30	B1	25.1	0	135	0.186	0.059	0.423	0.055
31	B1	24.6	0	120	0.246	0.078	0.577	0.072
32	B1	25.4	0	105	0.192	0.063	0.472	0.040
33	B1	24.8	0	90	0.184	0.064	0.446	0.034
34	B1	25.1	0	75	-0.002	0.039	0.140	-0.210
35	B1	25.1	0	60	-0.254	0.072	-0.078	-0.569
36	B1	24.8	0	45	-0.213	0.057	-0.055	-0.484
37	B1	25.1	0	30	-0.096	0.036	0.021	-0.247
38	B1	25.0	0	15	-0.043	0.022	0.068	-0.130
39	B1	25.1	0	0	-0.028	0.023	0.064	-0.116
40	B1	25.0	0	-15	-0.027	0.021	0.072	-0.097
41	B1	25.5	0	-30	-0.056	0.022	0.053	-0.147
42	B1	25.1	0	-45	0.012	0.036	0.242	-0.092
43	B1	24.9	0	-60	0.133	0.061	0.396	-0.033
44	B1	24.9	0	-75	-0.016	0.032	0.072	-0.177
45	B1	25.2	0	-90	-0.200	0.060	-0.067	-0.481
46	B1	25.2	0	-105	-0.246	0.064	-0.109	-0.536
47	B1	25.4	0	-120	-0.270	0.066	-0.133	-0.568
48	B1	24.9	0	-135	-0.253	0.055	-0.119	-0.502
49	B1	24.8	0	-150	-0.239	0.047	-0.102	-0.476
50	B1	25.1	0	-165	-0.189	0.036	-0.082	-0.363
51	B1	25.1	0	-180	-0.141	0.027	-0.055	-0.253
52	B1	25.0	0	-150	0.089	0.041	0.268	-0.004
53	C5	23.7	0	-165	-0.003	0.021	0.107	-0.071

Phase 4 Balance Data

Run	Conf	Uref fps	Cmy					
			Yaw	Pitch	Mean	RMS	Max	Min
54	C5	24.1	-30	-165	0.024	0.026	0.149	-0.063
55	C5	24.0	-30	-150	0.014	0.024	0.115	-0.074
56	C5	24.1	0	-150	-0.005	0.020	0.119	-0.094
57	C5	24.1	0	-135	-0.003	0.017	0.087	-0.083
58	C5	24.8	-30	-135	-0.007	0.020	0.064	-0.100
59	C5	25.0	-30	-120	-0.063	0.029	-0.004	-0.233
60	C5	24.7	0	-120	-0.060	0.029	-0.003	-0.235
61	C5	24.9	0	-105	-0.142	0.052	-0.052	-0.384
62	C5	24.9	-30	-105	-0.129	0.046	-0.042	-0.353
63	C5	25.2	-30	-90	-0.119	0.048	-0.022	-0.354
64	C5	24.4	0	-90	-0.141	0.054	-0.034	-0.431
65	C5	25.0	0	-75	-0.027	0.056	0.147	-0.278
66	C5	24.7	-30	-75	-0.017	0.043	0.124	-0.207
67	C5	24.8	-30	-60	0.023	0.040	0.204	-0.149
68	C5	24.3	0	-60	0.018	0.048	0.277	-0.180
69	C5	23.3	0	-45	0.018	0.048	0.289	-0.157
70	C5	24.4	-30	-45	0.024	0.050	0.314	-0.138
71	C5	24.3	-30	-30	0.021	0.042	0.251	-0.112
72	C5	23.3	0	-30	0.005	0.039	0.224	-0.156
73	C5	22.9	0	-15	0.004	0.032	0.208	-0.163
74	C5	24.7	-30	-15	0.017	0.039	0.262	-0.097
75	C5	25.4	-30	0	0.026	0.040	0.233	-0.081
76	C5	23.8	0	0	-0.004	0.026	0.181	-0.095
77	C5	23.9	0	15	0.006	0.022	0.143	-0.089
78	C5	24.9	-30	15	0.025	0.035	0.203	-0.084
79	C5	24.8	-30	30	0.038	0.030	0.190	-0.047
80	C5	24.0	0	30	0.007	0.022	0.145	-0.067
81	C5	24.5	0	45	0.009	0.019	0.122	-0.071
82	C5	25.1	-30	45	0.012	0.021	0.143	-0.073
83	C5	25.5	-30	60	-0.014	0.021	0.086	-0.167
84	C5	24.9	0	60	-0.004	0.021	0.096	-0.127
85	C5	25.2	0	75	-0.008	0.022	0.082	-0.122
86	C5	25.4	-30	75	-0.006	0.021	0.093	-0.121
87	C5	25.5	-30	90	0.080	0.028	0.206	-0.004
88	C5	24.9	0	90	0.083	0.030	0.205	0.002
89	C5	25.0	0	105	0.112	0.045	0.320	-0.002
90	C5	25.3	-30	105	0.120	0.038	0.292	0.020
91	C5	24.9	-30	120	0.095	0.037	0.280	0.006
92	C5	24.8	0	120	0.076	0.039	0.289	-0.014
93	C5	24.2	0	135	0.029	0.036	0.224	-0.068
94	C5	24.5	-30	135	0.068	0.038	0.263	-0.031
95	C5	24.6	-30	150	0.053	0.035	0.217	-0.044
96	C5	23.9	0	150	0.018	0.033	0.198	-0.057
97	C5	23.8	0	150	0.024	0.033	0.195	-0.047
98	C5	24.6	-30	150	0.057	0.036	0.231	-0.038
99	C5	24.5	-30	165	0.035	0.031	0.164	-0.042
100	C5	23.4	0	165	0.001	0.023	0.137	-0.064
101	C5	23.8	0	180	-0.004	0.020	0.118	-0.067
102	C5	24.3	-30	180	0.020	0.028	0.145	-0.059
103	A1	25.5	0	0	-0.010	0.024	0.098	-0.114

Phase 4 Balance Data

Run	Conf	Uref fps			Cmy			
			Yaw	Pitch	Mean	RMS	Max	Min
104	A1	25.7	0	45	-0.208	0.058	-0.060	-0.522
105	A1	25.4	0	60	-0.192	0.070	-0.039	-0.545
106	A1	25.5	0	120	0.226	0.073	0.527	0.070
107	B3	25.1	0	165	0.007	0.028	0.135	-0.063
108	B3	24.9	30	150	0.114	0.040	0.278	0.008
109	B3	25.1	0	150	0.108	0.042	0.290	0.010
110	B3	25.2	30	165	-0.022	0.025	0.080	-0.106
111	B3	25.2	30	135	0.240	0.073	0.560	0.064
112	B3	25.4	0	135	0.231	0.067	0.527	0.085
113	B3	25.6	0	120	0.227	0.068	0.519	0.075
114	B3	24.8	30	120	0.211	0.064	0.457	0.067
115	B3	25.3	30	105	0.257	0.078	0.584	0.088
116	B3	25.2	0	105	0.189	0.059	0.496	0.051
117	B3	25.1	0	90	0.193	0.062	0.476	0.050
118	B3	25.4	30	90	0.248	0.069	0.536	0.077
119	B3	25.3	30	75	-0.066	0.040	0.085	-0.251
120	B3	25.3	0	75	-0.002	0.043	0.164	-0.228
121	B3	25.6	0	60	-0.191	0.068	-0.014	-0.537
122	B3	25.7	30	60	-0.124	0.060	0.047	-0.419
123	B3	25.9	30	45	-0.443	0.074	-0.257	-0.834
124	B3	25.5	0	45	-0.277	0.078	-0.064	-0.633
125	B3	25.5	0	30	-0.051	0.031	0.085	-0.227
126	B3	25.1	30	30	-0.082	0.035	0.054	-0.212
127	B3	25.2	30	15	0.027	0.025	0.146	-0.075
128	B3	25.4	0	15	-0.016	0.026	0.110	-0.106
129	B3	25.3	0	0	0.009	0.024	0.135	-0.073
130	B3	25.4	30	0	-0.037	0.023	0.055	-0.128
131	B3	25.3	30	-15	-0.011	0.026	0.078	-0.115
132	B3	25.7	0	-15	0.004	0.023	0.095	-0.086
133	B3	25.0	0	-30	-0.004	0.028	0.136	-0.106
134	B3	25.3	30	-30	-0.030	0.039	0.193	-0.164
135	B3	25.4	30	-45	0.095	0.054	0.328	-0.056
136	B3	25.3	0	-45	0.047	0.047	0.286	-0.096
137	B3	25.0	0	-60	0.134	0.053	0.353	-0.024
138	B3	25.7	30	-60	0.085	0.043	0.273	-0.053
139	B3	26.0	30	-75	-0.084	0.047	0.039	-0.281
140	B3	25.6	0	-75	-0.066	0.050	0.060	-0.288
141	B3	25.4	0	-90	-0.193	0.058	-0.062	-0.504
142	B3	25.4	30	-90	-0.202	0.068	-0.056	-0.475
143	B3	25.3	30	-105	-0.259	0.067	-0.109	-0.545
144	B3	25.5	0	-105	-0.235	0.066	-0.094	-0.527
145	B3	26.8	0	-120	-0.237	0.067	-0.093	-0.555
146	B3	26.1	30	-120	-0.234	0.059	-0.100	-0.512
147	B3	26.7	30	-135	-0.244	0.058	-0.108	-0.520
148	B3	26.6	0	-135	-0.240	0.059	-0.104	-0.506
149	B3	27.0	0	-150	-0.207	0.046	-0.079	-0.387
150	B3	26.2	30	-150	-0.223	0.050	-0.087	-0.464
151	B3	26.2	30	-165	-0.188	0.041	-0.068	-0.393
152	B3	26.5	0	-165	-0.169	0.037	-0.062	-0.334
153	B3	26.0	0	180	-0.087	0.028	0.043	-0.204

Phase 4 Balance Data

Run	Conf	Uref fps			Cmy			
			Yaw	Pitch	Mean	RMS	Max	Min
154	B3	26.5	30	180	-0.106	0.030	0.003	-0.224
155	B2	25.2	30	165	-0.078	0.023	0.031	-0.157
156	B2	25.1	30	150	0.101	0.039	0.269	0.000
157	B2	24.9	30	135	0.199	0.070	0.490	0.046
158	B2	25.3	30	120	0.243	0.080	0.588	0.065
159	B2	25.5	30	105	0.254	0.076	0.598	0.079
160	B2	25.6	30	90	0.202	0.061	0.454	0.030
161	B2	25.5	30	75	0.045	0.034	0.208	-0.132
162	B2	25.1	30	60	-0.203	0.066	-0.033	-0.478
163	B2	25.0	30	45	-0.161	0.060	0.009	-0.477
164	B2	25.3	30	30	-0.011	0.024	0.084	-0.128
165	B2	25.0	30	15	-0.042	0.021	0.055	-0.144
166	B2	25.1	30	0	-0.019	0.020	0.077	-0.097
167	B2	25.6	30	-15	0.002	0.023	0.107	-0.090
168	B2	25.5	30	-30	-0.031	0.027	0.114	-0.149
169	B2	25.7	30	-45	0.014	0.039	0.236	-0.087
170	B2	25.1	30	-60	0.092	0.044	0.275	-0.046
171	B2	25.7	30	-75	-0.005	0.027	0.074	-0.126
172	B2	25.6	30	-90	-0.148	0.061	-0.016	-0.396
173	B2	25.4	30	-105	-0.137	0.041	-0.047	-0.333
174	B2	25.4	30	-120	-0.174	0.045	-0.075	-0.372
175	B2	25.8	30	-135	-0.216	0.047	-0.105	-0.415
176	B2	25.4	30	-150	-0.189	0.041	-0.090	-0.380
177	B2	25.0	30	-165	-0.022	0.004	-0.009	-0.040
178	B2	25.2	30	180	-0.018	0.003	-0.006	-0.032
179	B2	25.5	30	180	-0.037	0.007	-0.010	-0.068
180	B2	25.4	30	-165	-0.079	0.016	-0.024	-0.147
181	B3	25.2	30	45	-0.043	0.013	-0.007	-0.101
182	B3	25.0	30	120	0.240	0.066	0.504	0.072
183	B3	25.8	30	45	-0.257	0.059	-0.100	-0.571
184	B3	24.8	30	30	-0.049	0.050	0.136	-0.242
185	B3	25.3	30	15	-0.064	0.027	0.043	-0.164
186	C2	25.4	0	165	-0.056	0.026	0.061	-0.153
187	C2	25.2	0	150	-0.066	0.032	0.050	-0.223
188	C2	25.3	0	135	0.031	0.041	0.231	-0.090
189	C2	25.0	0	120	0.156	0.072	0.523	-0.028
190	C2	25.5	0	105	0.183	0.070	0.479	0.013
191	C2	25.1	0	90	0.188	0.061	0.462	0.032
192	C2	25.4	0	75	0.041	0.039	0.210	-0.141
193	C2	25.1	0	60	-0.012	0.027	0.097	-0.148
194	C2	25.3	0	45	0.011	0.025	0.113	-0.112
195	C2	24.9	0	30	0.008	0.023	0.148	-0.095
196	C2	24.7	0	15	0.017	0.026	0.169	-0.136
197	C2	25.1	0	0	0.017	0.030	0.173	-0.130
198	C2	25.3	0	-15	0.008	0.031	0.172	-0.139
199	C2	24.9	0	-30	0.013	0.034	0.207	-0.128
200	C2	25.6	0	-45	0.001	0.037	0.179	-0.155
201	C2	25.5	0	-60	0.024	0.046	0.256	-0.159
202	C2	25.5	0	-75	-0.039	0.052	0.105	-0.295
203	C2	26.0	0	-90	-1.277	0.048	-1.169	-1.510
204	C2	25.4	0	-90	-0.140	0.049	-0.020	-0.403
205	C2	25.5	0	-105	-0.174	0.050	-0.069	-0.416
206	C2	25.4	0	-120	-0.075	0.024	0.005	-0.214
207	C2	25.5	0	-135	0.008	0.020	0.120	-0.061
208	C2	25.4	0	-150	0.015	0.022	0.135	-0.052
209	C2	25.6	0	-165	0.012	0.020	0.121	-0.055
210	C2	24.8	0	180	0.001	0.019	0.093	-0.087

Phase 1, 2, and 3 Integrated Pressure Data

Phase 1, 2, and 3 Integrated Pressure Data

Run	Conf	Uref fps	Cfx			Cfz				Cmy						
			Mean	RMS	Max	Min	Mean	RMS	Max	Min	Mean	RMS	Max	Min		
1	A1	24.8	0	0	1.683	0.433	3.436	0.479	0.005	0.031	0.165	-0.113	0.004	0.021	0.109	-0.074
2	A1	24.9	30	0	1.567	0.425	3.129	0.510	0.009	0.029	0.172	-0.084	0.006	0.019	0.114	-0.056
3	A1	24.8	60	0	1.179	0.353	2.657	0.340	0.013	0.024	0.147	-0.072	0.009	0.016	0.097	-0.047
4	A1	24.9	120	0	-1.083	0.336	-0.279	-2.385	0.050	0.025	0.165	-0.044	0.033	0.017	0.109	-0.029
5	A1	24.6	150	0	-1.242	0.326	-0.500	-2.562	0.060	0.032	0.229	-0.084	0.040	0.021	0.152	-0.056
6	A1	24.6	180	0	-1.334	0.373	-0.562	-2.737	0.061	0.032	0.207	-0.065	0.040	0.021	0.137	-0.043
7	A1	24.1	180	15	-1.331	0.359	-0.579	-2.811	0.311	0.083	0.684	0.127	-0.029	0.024	0.037	-0.140
8	A1	24.8	150	15	-1.229	0.324	-0.421	-2.607	0.298	0.079	0.632	0.114	-0.020	0.020	0.036	-0.124
9	A1	24.7	120	15	-1.173	0.364	-0.116	-2.755	0.290	0.089	0.695	0.025	-0.016	0.018	0.045	-0.100
10	A1	24.6	60	15	1.078	0.348	2.607	0.117	-0.309	0.104	-0.037	-0.778	-0.013	0.017	0.071	-0.097
11	A1	24.7	30	15	1.514	0.402	3.321	0.572	-0.421	0.112	-0.148	-0.953	-0.010	0.019	0.101	-0.103
12	A1	24.7	0	15	1.724	0.462	3.666	0.670	-0.479	0.131	-0.195	-1.015	-0.011	0.022	0.110	-0.094
13	A1	24.6	0	30	1.513	0.398	3.105	0.542	-0.924	0.242	-0.319	-1.931	-0.029	0.022	0.065	-0.121
14	A1	24.6	30	30	1.350	0.380	2.848	0.439	-0.838	0.234	-0.278	-1.782	-0.033	0.021	0.055	-0.127
15	A1	24.8	60	30	0.921	0.309	2.257	0.234	-0.628	0.215	-0.156	-1.608	-0.055	0.028	0.047	-0.192
16	A1	24.8	120	30	-0.997	0.338	-0.255	-2.256	0.426	0.147	1.000	0.113	-0.086	0.033	0.005	-0.217
17	A1	25.1	150	30	-1.128	0.293	-0.513	-2.217	0.467	0.117	0.933	0.208	-0.106	0.036	-0.031	-0.273
18	A1	24.9	180	30	-1.102	0.280	-0.433	-2.221	0.431	0.107	0.888	0.157	-0.118	0.038	-0.031	-0.285
19	A1	24.7	180	45	-0.785	0.200	-0.196	-1.661	0.356	0.093	0.787	0.067	-0.201	0.056	-0.045	-0.444
20	A1	24.8	150	45	-0.844	0.203	-0.330	-1.593	0.445	0.109	0.879	0.153	-0.187	0.051	-0.055	-0.395
21	A1	24.7	120	45	-0.708	0.227	-0.188	-1.684	0.428	0.138	1.044	0.092	-0.131	0.045	-0.024	-0.321
22	A1	24.9	60	45	0.649	0.240	1.629	0.115	-0.785	0.300	-0.127	-2.002	-0.064	0.035	0.033	-0.211
23	A1	24.5	30	45	1.167	0.314	2.492	0.475	-1.404	0.377	-0.543	-3.076	-0.111	0.037	-0.002	-0.312
24	A1	24.3	0	45	1.302	0.357	2.715	0.525	-1.545	0.422	-0.624	-3.295	-0.114	0.037	-0.007	-0.310
25	A1	24.4	0	60	0.826	0.228	1.730	0.345	-1.857	0.537	-0.751	-4.018	-0.141	0.053	0.008	-0.369
26	A1	24.6	30	60	0.701	0.197	1.647	0.172	-1.510	0.451	-0.353	-3.618	-0.098	0.044	0.031	-0.309
27	A1	25.0	60	60	0.350	0.132	0.903	0.054	-0.667	0.290	-0.055	-1.914	-0.020	0.029	0.062	-0.167
28	A1	24.6	120	60	-0.458	0.149	-0.054	-1.035	0.377	0.134	0.954	-0.084	-0.138	0.046	-0.020	-0.307
29	A1	24.5	150	60	-0.588	0.147	-0.226	-1.188	0.416	0.126	1.057	0.052	-0.199	0.056	-0.080	-0.419
30	A1	24.4	180	60	-0.519	0.141	-0.156	-1.121	0.215	0.087	0.673	-0.134	-0.226	0.064	-0.077	-0.473
31	A1	24.4	180	75	-0.354	0.101	-0.108	-0.782	0.228	0.133	0.931	-0.243	-0.187	0.054	-0.068	-0.407
32	A1	24.6	150	75	-0.360	0.094	-0.094	-0.759	0.343	0.127	0.927	-0.192	-0.171	0.046	-0.056	-0.370
33	A1	24.8	120	75	-0.246	0.094	-0.005	-0.688	0.179	0.122	0.826	-0.280	-0.127	0.047	-0.006	-0.347
34	A1	24.7	60	75	0.180	0.069	0.487	0.010	-0.442	0.222	0.130	-1.495	0.039	0.019	0.131	-0.062
35	A1	24.7	30	75	0.400	0.107	0.833	0.143	-1.088	0.357	-0.235	-2.532	0.069	0.027	0.195	-0.106
36	A1	24.6	0	75	0.478	0.138	1.007	0.158	-1.262	0.430	-0.324	-2.931	0.089	0.030	0.220	-0.057
37	A1	24.9	0	90	0.238	0.072	0.575	0.065	-0.182	0.179	0.327	-1.135	0.158	0.048	0.380	0.043
38	A1	24.4	30	90	0.271	0.072	0.581	0.090	-0.356	0.218	0.208	-1.297	0.179	0.048	0.385	0.059
39	A1	24.9	60	90	0.128	0.048	0.362	-0.001	-0.140	0.155	0.319	-0.946	0.085	0.032	0.240	-0.001
40	A1	24.7	120	90	-0.152	0.058	0.010	-0.416	-0.135	0.159	0.387	-0.798	-0.100	0.038	0.006	-0.275
41	A1	25.0	150	90	-0.260	0.068	-0.095	-0.530	-0.191	0.190	0.388	-1.121	-0.172	0.045	-0.063	-0.351
42	A1	24.7	180	90	-0.252	0.071	-0.079	-0.539	-0.038	0.152	0.421	-0.786	-0.167	0.047	-0.052	-0.357
43	A1	24.7	180	-15	-1.159	0.306	-0.496	-2.348	-0.166	0.059	-0.033	-0.438	0.092	0.028	0.231	0.002
44	A1	25.0	150	-15	-1.066	0.295	-0.327	-2.396	-0.147	0.056	-0.015	-0.419	0.089	0.028	0.216	0.002
45	A1	25.1	120	-15	-0.752	0.240	-0.126	-1.710	-0.115	0.046	0.022	-0.322	0.056	0.022	0.160	-0.012
46	A1	25.3	60	-15	1.135	0.344	2.604	0.356	0.348	0.110	0.853	0.087	0.028	0.025	0.170	-0.050
47	A1	24.4	30	-15	1.507	0.385	3.133	0.486	0.420	0.112	0.887	0.133	0.010	0.019	0.113	-0.067
48	A1	24.2	0	-15	1.508	0.385	3.043	0.647	0.408	0.111	0.895	0.155	0.002	0.020	0.112	-0.081
49	A1	24.6	0	-30	1.311	0.335	2.780	0.429	0.766	0.201	1.631	0.232	0.005	0.020	0.122	-0.067
50	A1	24.3	30	-30	1.295	0.334	2.631	0.310	0.773	0.201	1.592	0.182	0.014	0.020	0.130	-0.053

Phase 1, 2, and 3 Integrated Pressure Data

Run	Conf	Uref		Yaw	Pitch	Cfx			Cfz			Cmy				
		fps	Mean			RMS	Max	Min	Mean	RMS	Max	Min	Mean	RMS	Max	Min
51	A1	24.6	60	-30	0.975	0.300	2.262	0.165	0.673	0.215	1.569	0.091	0.063	0.035	0.230	-0.041
52	A1	24.7	120	-30	-0.540	0.179	-0.047	-1.261	-0.201	0.075	0.014	-0.506	0.063	0.027	0.185	-0.005
53	A1	24.7	150	-30	-0.774	0.227	-0.249	-1.699	-0.249	0.086	-0.058	-0.612	0.113	0.034	0.268	0.033
54	A1	24.6	180	-30	-0.878	0.244	-0.302	-1.765	-0.285	0.092	-0.082	-0.647	0.127	0.035	0.287	0.028
55	A1	24.3	180	-45	-0.562	0.163	-0.203	-1.219	-0.233	0.085	-0.031	-0.610	0.154	0.043	0.338	0.054
56	A1	25.0	150	-45	-0.514	0.154	-0.129	-1.235	-0.232	0.083	-0.022	-0.604	0.132	0.040	0.339	0.034
57	A1	24.9	120	-45	-0.364	0.129	-0.037	-0.924	-0.219	0.085	0.011	-0.607	0.068	0.027	0.190	0.004
58	A1	24.9	60	-45	0.672	0.235	1.697	0.117	0.806	0.297	2.088	0.077	0.063	0.036	0.235	-0.041
59	A1	24.8	30	-45	1.068	0.267	2.113	0.403	1.290	0.340	2.602	0.468	0.104	0.045	0.284	-0.013
60	A1	24.4	0	-45	1.053	0.293	2.431	0.369	1.153	0.322	2.621	0.382	0.047	0.031	0.244	-0.032
61	A1	24.2	0	-60	0.680	0.167	1.316	0.304	1.616	0.402	3.069	0.638	0.145	0.044	0.326	0.006
62	A1	24.6	30	-60	0.631	0.169	1.317	0.227	1.410	0.375	2.956	0.532	0.105	0.039	0.274	-0.042
63	A1	24.8	60	-60	0.373	0.143	0.951	0.062	0.701	0.291	1.932	0.059	0.019	0.030	0.172	-0.093
64	A1	24.8	120	-60	-0.226	0.088	-0.022	-0.627	-0.158	0.071	0.031	-0.522	0.077	0.032	0.220	0.005
65	A1	24.5	150	-60	-0.340	0.103	-0.071	-0.788	-0.140	0.073	0.093	-0.470	0.149	0.045	0.365	0.044
66	A1	24.3	180	-60	-0.350	0.110	-0.106	-0.869	-0.061	0.060	0.156	-0.380	0.181	0.053	0.430	0.067
67	A1	24.5	180	-75	-0.269	0.087	-0.075	-0.654	-0.054	0.080	0.263	-0.438	0.162	0.051	0.392	0.055
68	A1	24.6	150	-75	-0.233	0.076	-0.058	-0.584	-0.072	0.074	0.196	-0.472	0.137	0.041	0.331	0.046
69	A1	24.5	120	-75	-0.145	0.061	0.015	-0.420	-0.051	0.060	0.193	-0.400	0.084	0.034	0.225	0.007
70	A1	24.7	60	-75	0.160	0.069	0.471	0.015	0.383	0.182	1.305	-0.054	-0.037	0.023	0.032	-0.136
71	A1	24.6	30	-75	0.352	0.110	0.881	0.128	1.010	0.270	2.303	0.395	-0.052	0.035	0.063	-0.216
72	A1	24.5	0	-75	0.397	0.118	0.869	0.136	1.212	0.310	2.589	0.442	-0.046	0.036	0.072	-0.196
73	A1	24.6	0	-90	0.216	0.067	0.551	0.072	0.330	0.128	0.985	-0.174	-0.143	0.044	-0.048	-0.364
74	A1	24.7	30	-90	0.212	0.070	0.525	0.063	0.330	0.108	0.802	-0.113	-0.140	0.046	-0.041	-0.347
75	A1	24.8	60	-90	0.099	0.045	0.365	0.003	0.105	0.079	0.541	-0.174	-0.066	0.030	-0.002	-0.242
76	A1	24.6	120	-90	-0.097	0.054	0.015	-0.391	0.093	0.085	0.563	-0.255	0.064	0.036	0.258	-0.010
77	A1	24.8	150	-90	-0.200	0.069	-0.020	-0.530	0.275	0.098	0.730	-0.108	0.132	0.045	0.351	0.013
78	A1	24.8	180	-90	-0.213	0.069	-0.066	-0.579	0.262	0.119	0.794	-0.172	0.141	0.045	0.383	0.044
79	A2	24.0	0	-90	0.276	0.088	0.669	0.078	0.116	0.115	0.548	-0.425	-0.183	0.058	-0.052	-0.443
80	A2	23.9	0	-75	0.370	0.105	0.831	0.143	0.736	0.187	1.543	0.225	-0.110	0.046	-0.005	-0.326
81	A2	24.1	0	-60	0.607	0.172	1.388	0.248	1.316	0.367	3.085	0.451	0.088	0.032	0.256	-0.073
82	A2	23.9	0	-45	1.038	0.272	2.233	0.328	1.204	0.320	2.585	0.357	0.077	0.034	0.251	-0.039
83	A2	23.8	0	-30	1.340	0.346	2.683	0.503	0.783	0.207	1.602	0.274	0.005	0.021	0.121	-0.064
84	A2	24.3	0	-15	1.560	0.406	3.088	0.553	0.426	0.118	0.949	0.130	0.005	0.020	0.123	-0.068
85	A2	23.8	0	0	1.707	0.477	3.546	0.652	0.011	0.033	0.209	-0.108	0.007	0.022	0.138	-0.072
86	A2	24.2	0	15	1.747	0.446	3.651	0.770	-0.502	0.127	-0.209	-1.078	-0.022	0.022	0.079	-0.111
87	A2	23.8	0	30	1.620	0.427	3.448	0.599	-1.035	0.268	-0.386	-2.170	-0.057	0.024	0.035	-0.178
88	A2	23.9	0	45	1.328	0.364	2.717	0.523	-1.568	0.431	-0.621	-3.311	-0.113	0.038	0.000	-0.298
89	A2	24.1	0	60	0.750	0.193	1.486	0.326	-1.454	0.407	-0.580	-3.024	-0.051	0.033	0.076	-0.190
90	A2	23.5	0	75	0.428	0.126	0.949	0.155	-0.643	0.263	-0.050	-1.881	0.163	0.045	0.375	0.045
91	A2	24.1	0	90	0.302	0.086	0.643	0.101	0.360	0.134	0.988	-0.283	0.200	0.057	0.425	0.067
92	A2	25.0	180	90	-0.306	0.086	-0.116	-0.704	0.267	0.134	0.791	-0.480	-0.203	0.057	-0.077	-0.465
93	A2	24.9	180	75	-0.423	0.114	-0.150	-0.949	0.508	0.173	1.395	0.024	-0.184	0.051	-0.064	-0.415
94	A2	24.8	180	60	-0.470	0.133	-0.147	-1.097	0.150	0.096	0.756	-0.191	-0.219	0.063	-0.083	-0.484
95	A2	24.5	180	45	-0.687	0.182	-0.275	-1.434	0.264	0.075	0.584	0.015	-0.198	0.058	-0.080	-0.441
96	A2	25.0	180	30	-1.008	0.245	-0.405	-1.924	0.368	0.091	0.738	0.105	-0.122	0.037	-0.032	-0.297
97	A2	25.1	180	15	-1.221	0.329	-0.505	-2.620	0.271	0.074	0.594	0.068	-0.036	0.023	0.022	-0.172
98	A2	24.8	180	0	-1.268	0.340	-0.477	-2.603	0.060	0.030	0.182	-0.067	0.040	0.020	0.121	-0.044
99	A2	24.8	180	-15	-1.116	0.305	-0.477	-2.344	-0.161	0.059	-0.030	-0.387	0.088	0.026	0.222	0.005
100	A2	25.0	180	-30	-0.753	0.215	-0.264	-1.694	-0.232	0.082	-0.018	-0.599	0.116	0.032	0.265	0.034

Phase 1, 2, and 3 Integrated Pressure Data

Run	Conf	Uref fps	Cfx		Cfz				Cmy							
			Mean	RMS	Max	Min	Mean	RMS	Max	Min	Mean	RMS	Max			
101	A2	24.3	180	-45	-0.450	0.136	-0.134	-1.012	-0.113	0.060	0.050	-0.427	0.158	0.044	0.350	0.059
102	A2	24.1	180	-60	-0.387	0.110	-0.093	-0.866	-0.119	0.095	0.203	-0.543	0.183	0.050	0.385	0.066
103	A2	24.0	180	-75	-0.440	0.131	-0.117	-1.064	-0.474	0.172	0.032	-1.310	0.200	0.058	0.490	0.060
104	A2	24.2	180	-90	-0.319	0.100	-0.093	-0.779	-0.149	0.142	0.300	-0.928	0.211	0.066	0.516	0.061
105	D1	24.8	0	180	0.553	0.120	1.071	0.118	0.055	0.026	0.121	-0.112	-0.037	0.017	0.074	-0.080
106	D1	24.6	30	180	0.417	0.110	0.859	0.001	0.044	0.021	0.108	-0.080	-0.029	0.014	0.053	-0.071
107	D1	24.9	45	180	0.311	0.115	0.824	-0.142	0.030	0.021	0.100	-0.071	-0.020	0.014	0.047	-0.066
108	D1	24.3	-30	180	0.392	0.108	0.878	-0.011	0.034	0.021	0.103	-0.092	-0.023	0.014	0.061	-0.068
109	B1	24.8	-30	180	1.031	0.234	1.910	0.453	0.068	0.025	0.173	-0.035	-0.045	0.017	0.023	-0.114
110	B1	25.1	45	180	0.857	0.209	1.787	0.321	0.067	0.023	0.169	-0.028	-0.044	0.015	0.019	-0.112
111	B1	24.4	30	180	1.114	0.241	2.162	0.460	0.084	0.025	0.181	-0.014	-0.055	0.017	0.009	-0.120
112	B1	24.3	0	180	1.393	0.292	2.785	0.697	0.099	0.028	0.230	-0.023	-0.065	0.018	0.015	-0.152
113	B1	25.1	45	-165	0.721	0.187	1.642	0.208	-0.083	0.035	0.032	-0.289	-0.070	0.020	-0.004	-0.156
114	B1	24.6	30	-165	0.922	0.211	1.854	0.396	-0.103	0.042	0.018	-0.319	-0.092	0.021	-0.020	-0.186
115	B1	24.5	0	-165	1.179	0.257	2.250	0.508	-0.139	0.048	-0.034	-0.347	-0.113	0.024	-0.025	-0.221
116	B1	24.6	-30	-165	0.879	0.227	1.808	0.329	-0.107	0.044	0.007	-0.309	-0.082	0.022	-0.001	-0.182
117	D1	24.4	-30	-165	0.304	0.093	0.714	-0.038	-0.034	0.025	0.049	-0.196	-0.030	0.014	0.053	-0.080
118	D1	24.8	0	-165	0.452	0.102	1.006	0.077	-0.044	0.029	0.043	-0.269	-0.049	0.018	0.064	-0.110
119	D1	24.4	30	-165	0.311	0.107	0.765	-0.080	-0.027	0.027	0.075	-0.185	-0.036	0.015	0.043	-0.085
120	D1	24.5	45	-165	0.166	0.130	0.719	-0.341	-0.010	0.032	0.108	-0.168	-0.022	0.015	0.040	-0.068
121	D1	24.8	45	-150	0.128	0.096	0.581	-0.323	-0.028	0.048	0.184	-0.246	-0.026	0.014	0.045	-0.080
122	D1	24.2	30	-150	0.237	0.076	0.585	-0.089	-0.068	0.035	0.106	-0.257	-0.039	0.014	0.038	-0.096
123	D1	24.3	0	-150	0.305	0.073	0.628	-0.025	-0.080	0.034	0.054	-0.297	-0.055	0.016	0.026	-0.108
124	D1	24.4	-30	-150	0.209	0.071	0.528	-0.068	-0.060	0.033	0.072	-0.249	-0.035	0.014	0.036	-0.082
125	B1	24.6	-30	-150	0.647	0.170	1.436	0.152	-0.181	0.059	-0.025	-0.448	-0.111	0.031	-0.012	-0.256
126	B1	24.7	0	-150	0.840	0.187	1.598	0.261	-0.236	0.066	-0.076	-0.535	-0.143	0.030	-0.034	-0.269
127	B1	24.3	30	-150	0.730	0.171	1.559	0.307	-0.212	0.064	-0.044	-0.507	-0.120	0.027	-0.045	-0.269
128	B1	25.2	45	-150	0.562	0.143	1.142	0.125	-0.168	0.052	-0.012	-0.374	-0.090	0.024	-0.018	-0.206
129	B1	24.9	45	-135	0.359	0.093	0.717	0.114	-0.144	0.051	0.002	-0.365	-0.101	0.026	-0.025	-0.203
130	B1	25.0	30	-135	0.466	0.114	0.918	0.190	-0.180	0.056	-0.023	-0.420	-0.134	0.033	-0.050	-0.287
131	B1	24.8	0	-135	0.549	0.136	1.122	0.238	-0.194	0.061	-0.038	-0.474	-0.166	0.041	-0.070	-0.339
132	B1	24.6	-30	-135	0.446	0.121	0.982	0.163	-0.155	0.056	0.009	-0.375	-0.136	0.038	-0.043	-0.317
133	D1	24.6	-30	-135	0.120	0.051	0.379	-0.074	-0.043	0.038	0.126	-0.255	-0.036	0.012	0.024	-0.087
134	D1	24.6	0	-135	0.172	0.053	0.393	-0.037	-0.058	0.039	0.125	-0.243	-0.053	0.014	0.017	-0.109
135	D1	24.3	30	-135	0.138	0.055	0.369	-0.088	-0.057	0.042	0.144	-0.266	-0.038	0.013	0.031	-0.089
136	D1	24.6	45	-135	0.088	0.060	0.323	-0.139	-0.035	0.050	0.167	-0.237	-0.025	0.012	0.033	-0.066
137	D1	24.4	45	-120	0.044	0.039	0.289	-0.112	-0.016	0.052	0.258	-0.323	-0.020	0.010	0.026	-0.071
138	D1	24.1	30	-120	0.071	0.040	0.263	-0.113	-0.027	0.051	0.255	-0.250	-0.032	0.011	0.028	-0.085
139	D1	24.8	0	-120	0.086	0.043	0.291	-0.097	-0.023	0.052	0.274	-0.306	-0.042	0.012	0.020	-0.093
140	D1	24.6	-30	-120	0.061	0.037	0.225	-0.091	-0.018	0.048	0.240	-0.240	-0.029	0.010	0.018	-0.079
141	B1	25.5	-30	-120	0.288	0.083	0.617	0.072	-0.075	0.048	0.098	-0.314	-0.140	0.039	-0.046	-0.299
142	B1	24.9	0	-120	0.372	0.102	0.823	0.116	-0.085	0.056	0.135	-0.356	-0.185	0.050	-0.070	-0.394
143	B1	25.3	30	-120	0.308	0.084	0.695	0.097	-0.103	0.050	0.057	-0.357	-0.143	0.038	-0.052	-0.300
144	B1	25.4	45	-120	0.230	0.073	0.543	0.054	-0.093	0.046	0.059	-0.325	-0.101	0.031	-0.029	-0.237
145	B1	25.6	45	-105	0.141	0.056	0.399	0.004	-0.028	0.061	0.167	-0.335	-0.085	0.029	-0.019	-0.209
146	B1	24.9	30	-105	0.208	0.067	0.529	0.030	-0.065	0.072	0.216	-0.434	-0.122	0.035	-0.031	-0.290
147	B1	25.4	0	-105	0.260	0.082	0.715	0.072	-0.054	0.081	0.311	-0.489	-0.157	0.048	-0.053	-0.402
148	B1	25.3	-30	-105	0.205	0.070	0.525	0.036	-0.062	0.072	0.224	-0.466	-0.120	0.038	-0.038	-0.290
149	D1	24.1	-30	-105	0.032	0.025	0.172	-0.080	-0.004	0.061	0.315	-0.291	-0.020	0.010	0.021	-0.077
150	D1	24.3	0	-105	0.048	0.028	0.180	-0.070	-0.016	0.061	0.316	-0.285	-0.028	0.011	0.015	-0.079

Phase 1, 2, and 3 Integrated Pressure Data

Run	Conf	Uref		Mean	Cfx			Mean	Cfz			Cmy				
		fps	Yaw		Pitch	Mean	RMS	Max	Min	Mean	RMS	Max	Min	Mean	RMS	Max
151	D1	25.2	30	-105	0.030	0.023	0.185	-0.074	0.000	0.055	0.323	-0.292	-0.019	0.008	0.018	-0.076
152	D1	24.7	45	-105	0.016	0.023	0.150	-0.071	0.023	0.056	0.302	-0.248	-0.014	0.009	0.019	-0.061
153	D1	24.6	45	-90	0.011	0.014	0.111	-0.057	0.071	0.059	0.478	-0.248	-0.008	0.009	0.038	-0.074
154	D1	24.6	30	-90	0.020	0.013	0.109	-0.041	0.085	0.057	0.374	-0.206	-0.014	0.009	0.027	-0.072
155	D1	24.3	0	-90	0.034	0.015	0.119	-0.030	0.108	0.064	0.508	-0.184	-0.022	0.010	0.020	-0.079
156	D1	24.7	-30	-90	0.024	0.014	0.103	-0.052	0.091	0.059	0.459	-0.188	-0.016	0.009	0.034	-0.068
157	B1	25.1	-30	-90	0.163	0.060	0.433	0.027	0.354	0.123	0.985	-0.066	-0.108	0.039	-0.018	-0.287
158	B1	25.1	0	-90	0.203	0.067	0.508	0.061	0.411	0.138	1.090	-0.064	-0.135	0.044	-0.040	-0.336
159	B1	24.9	30	-90	0.153	0.058	0.422	0.024	0.392	0.114	0.950	-0.025	-0.101	0.038	-0.016	-0.279
160	B1	25.7	45	-90	0.102	0.047	0.343	-0.002	0.281	0.091	0.796	-0.051	-0.067	0.031	0.001	-0.227
161	B1	25.2	45	-75	0.162	0.069	0.501	0.002	0.566	0.198	1.589	0.097	-0.007	0.022	0.076	-0.108
162	B1	24.9	30	-75	0.253	0.094	0.646	0.069	0.901	0.265	1.954	0.251	-0.007	0.027	0.082	-0.126
163	B1	25.2	0	-75	0.340	0.108	0.812	0.118	1.197	0.301	2.538	0.488	-0.012	0.033	0.093	-0.162
164	B1	24.8	-30	-75	0.266	0.100	0.759	0.046	0.960	0.287	2.339	0.261	-0.006	0.031	0.114	-0.142
165	D1	24.5	-30	-75	0.046	0.016	0.122	-0.018	0.201	0.067	0.562	-0.124	0.005	0.010	0.057	-0.059
166	D1	24.5	0	-75	0.069	0.018	0.170	-0.001	0.307	0.077	0.728	-0.072	0.008	0.011	0.080	-0.060
167	D1	24.7	30	-75	0.043	0.015	0.120	-0.033	0.195	0.069	0.541	-0.155	0.006	0.010	0.068	-0.057
168	D1	24.6	45	-75	0.028	0.015	0.103	-0.034	0.128	0.063	0.442	-0.188	0.004	0.010	0.054	-0.056
169	D1	24.5	45	-60	0.091	0.040	0.259	-0.085	0.186	0.084	0.503	-0.238	0.010	0.013	0.077	-0.062
170	D1	24.4	30	-60	0.132	0.041	0.336	-0.025	0.284	0.088	0.725	-0.078	0.018	0.013	0.112	-0.046
171	D1	24.5	0	-60	0.207	0.046	0.406	0.040	0.438	0.095	0.831	0.040	0.026	0.013	0.107	-0.057
172	D1	24.5	-30	-60	0.137	0.043	0.388	-0.034	0.303	0.091	0.801	-0.194	0.022	0.014	0.117	-0.078
173	B1	24.7	-30	-60	0.487	0.146	1.179	0.099	1.156	0.345	2.703	0.242	0.103	0.038	0.270	-0.007
174	B1	24.7	0	-60	0.622	0.158	1.314	0.264	1.425	0.383	3.012	0.528	0.115	0.045	0.316	-0.009
175	B1	24.5	30	-60	0.441	0.128	0.966	0.130	1.044	0.302	2.194	0.266	0.093	0.035	0.244	-0.017
176	B1	24.9	45	-60	0.287	0.101	0.888	0.078	0.669	0.235	2.052	0.156	0.057	0.028	0.212	-0.034
177	B1	24.7	45	-45	0.489	0.165	1.324	-0.018	0.603	0.221	1.739	-0.099	0.053	0.033	0.230	-0.048
178	B1	24.7	30	-45	0.811	0.228	1.909	0.193	1.016	0.287	2.370	0.192	0.096	0.043	0.308	-0.019
179	B1	24.6	0	-45	1.074	0.248	2.255	0.354	1.168	0.281	2.554	0.352	0.044	0.026	0.198	-0.035
180	B1	24.3	-30	-45	0.888	0.254	1.986	0.212	1.040	0.307	2.393	0.247	0.071	0.039	0.253	-0.027
181	D1	23.9	-30	-45	0.317	0.094	0.688	-0.071	0.351	0.101	0.739	-0.103	0.016	0.017	0.114	-0.061
182	D1	23.8	0	-45	0.460	0.100	0.833	0.013	0.482	0.106	0.956	-0.033	0.010	0.016	0.132	-0.064
183	D1	23.8	30	-45	0.335	0.092	0.766	-0.049	0.385	0.103	0.827	-0.059	0.023	0.018	0.141	-0.062
184	D1	24.0	45	-45	0.203	0.080	0.502	-0.093	0.225	0.092	0.574	-0.143	0.011	0.016	0.106	-0.054
185	D1	24.0	45	-30	0.310	0.129	0.866	-0.163	0.195	0.082	0.607	-0.175	0.009	0.015	0.129	-0.065
186	D1	23.8	30	-30	0.522	0.134	1.160	-0.016	0.308	0.082	0.811	-0.057	0.004	0.018	0.152	-0.058
187	D1	23.4	0	-30	0.679	0.149	1.282	0.129	0.388	0.087	0.832	0.039	-0.002	0.016	0.132	-0.065
188	D1	24.1	-30	-30	0.448	0.127	0.908	-0.049	0.271	0.077	0.588	-0.064	0.007	0.014	0.110	-0.049
189	B1	24.6	-30	-30	1.072	0.266	2.271	0.437	0.663	0.165	1.390	0.262	0.025	0.015	0.101	-0.026
190	B1	24.6	0	-30	1.350	0.278	2.626	0.630	0.807	0.172	1.569	0.361	0.016	0.015	0.113	-0.040
191	B1	24.6	30	-30	1.102	0.245	2.112	0.372	0.678	0.151	1.312	0.239	0.024	0.020	0.148	-0.046
192	B1	24.6	45	-30	0.781	0.218	1.894	0.215	0.523	0.155	1.258	0.128	0.041	0.027	0.176	-0.027
193	B1	25.4	45	-15	0.864	0.259	1.963	0.186	0.257	0.083	0.647	0.063	0.016	0.018	0.127	-0.033
194	B1	24.4	30	-15	1.177	0.291	2.476	0.436	0.342	0.093	0.749	0.120	0.017	0.021	0.127	-0.049
195	B1	24.5	0	-15	1.578	0.329	2.857	0.730	0.451	0.102	0.875	0.190	0.018	0.017	0.095	-0.038
196	B1	24.9	-30	-15	1.186	0.281	2.254	0.471	0.359	0.092	0.722	0.135	0.026	0.018	0.116	-0.030
197	D1	24.0	-30	-15	0.550	0.156	1.257	0.023	0.154	0.046	0.465	-0.035	0.004	0.014	0.139	-0.045
198	D1	24.7	0	-15	0.765	0.166	1.456	0.142	0.192	0.045	0.433	-0.001	-0.008	0.013	0.089	-0.060
199	D1	24.7	30	-15	0.519	0.150	1.077	-0.049	0.136	0.042	0.335	-0.045	-0.002	0.014	0.101	-0.045
200	D1	24.6	45	-15	0.334	0.149	0.902	-0.175	0.109	0.043	0.293	-0.111	0.013	0.014	0.095	-0.049

Phase 1, 2, and 3 Integrated Pressure Data

Run	Conf	Uref		Cfx				Cfz				Cmy				
		fps		Mean	RMS	Max	Min	Mean	RMS	Max	Min	Mean	RMS	Max	Min	
201	D1	24.6	45	0	0.333	0.150	0.945	-0.191	0.012	0.023	0.169	-0.068	0.008	0.015	0.112	-0.045
202	D1	24.9	30	0	0.489	0.152	1.166	-0.100	-0.017	0.019	0.114	-0.078	-0.011	0.012	0.076	-0.052
203	D1	24.4	0	0	0.823	0.169	1.526	0.196	-0.021	0.018	0.156	-0.081	-0.014	0.012	0.103	-0.053
204	D1	24.1	-30	0	0.540	0.153	1.162	-0.053	-0.011	0.018	0.131	-0.068	-0.007	0.012	0.086	-0.045
205	B1	24.7	-30	0	1.308	0.314	2.836	0.271	0.006	0.027	0.130	-0.079	0.004	0.018	0.086	-0.052
206	B1	24.9	0	0	1.752	0.375	3.516	0.866	0.007	0.029	0.152	-0.081	0.004	0.019	0.101	-0.053
207	B1	24.6	30	0	1.266	0.303	2.618	0.454	-0.002	0.030	0.131	-0.105	-0.002	0.020	0.086	-0.070
208	B1	24.8	45	0	0.956	0.253	1.892	0.293	-0.010	0.023	0.102	-0.081	-0.006	0.015	0.067	-0.053
209	C1	24.4	30	0	-0.143	0.170	0.460	-0.844	0.062	0.044	0.256	-0.106	0.041	0.029	0.169	-0.070
210	C1	23.9	0	0	-0.226	0.172	0.228	-1.127	0.007	0.030	0.121	-0.200	0.005	0.020	0.080	-0.132
211	C1	24.1	-30	0	-0.042	0.138	0.376	-0.757	0.025	0.029	0.162	-0.137	0.016	0.019	0.107	-0.091
212	C1	23.9	-30	15	-0.005	0.117	0.394	-0.619	0.015	0.030	0.155	-0.107	0.009	0.016	0.076	-0.093
213	C1	24.4	0	15	-0.147	0.134	0.236	-0.950	0.042	0.025	0.190	-0.025	0.002	0.017	0.068	-0.113
214	C1	24.2	30	15	-0.095	0.154	0.491	-0.843	0.064	0.044	0.244	-0.104	0.024	0.024	0.128	-0.074
215	C1	24.2	30	30	0.092	0.129	0.648	-0.470	-0.032	0.072	0.209	-0.329	0.012	0.016	0.096	-0.057
216	C1	24.2	0	30	-0.042	0.102	0.321	-0.653	0.034	0.043	0.239	-0.153	0.006	0.014	0.067	-0.089
217	C1	24.4	-30	30	0.043	0.095	0.414	-0.409	-0.019	0.045	0.173	-0.203	0.003	0.012	0.065	-0.076
218	C1	24.7	-30	45	0.132	0.077	0.480	-0.182	-0.130	0.079	0.143	-0.486	0.001	0.013	0.071	-0.051
219	C1	24.3	0	45	0.110	0.086	0.530	-0.255	-0.094	0.081	0.218	-0.496	0.008	0.013	0.074	-0.045
220	C1	24.3	30	45	0.181	0.090	0.662	-0.140	-0.182	0.086	0.103	-0.623	0.000	0.015	0.079	-0.053
221	C1	24.3	30	60	0.290	0.086	0.779	0.041	-0.572	0.166	-0.068	-1.484	-0.023	0.019	0.066	-0.105
222	C1	24.8	0	60	0.303	0.093	0.839	0.008	-0.582	0.175	-0.053	-1.645	-0.019	0.020	0.068	-0.121
223	C1	24.9	-30	60	0.279	0.088	0.694	0.035	-0.545	0.173	-0.107	-1.364	-0.020	0.018	0.050	-0.102
224	C1	24.7	-30	75	0.268	0.077	0.605	0.093	-0.852	0.252	-0.280	-2.020	0.026	0.022	0.128	-0.074
225	C1	24.9	0	75	0.341	0.081	0.692	0.162	-1.023	0.253	-0.446	-2.147	0.043	0.022	0.140	-0.065
226	C1	24.8	30	75	0.265	0.071	0.594	0.097	-0.860	0.245	-0.265	-2.014	0.022	0.021	0.122	-0.090
227	C1	25.4	30	90	0.183	0.055	0.452	0.057	-0.217	0.146	0.154	-1.015	0.121	0.036	0.299	0.038
228	C1	24.9	0	90	0.192	0.057	0.509	0.063	-0.153	0.137	0.222	-0.964	0.127	0.038	0.337	0.042
229	C1	24.7	-30	90	0.188	0.052	0.415	0.054	-0.262	0.156	0.214	-1.122	0.125	0.034	0.274	0.036
230	C1	25.1	-30	105	0.251	0.086	0.672	0.017	0.237	0.140	0.975	-0.311	0.119	0.037	0.315	0.026
231	C1	24.8	0	105	0.295	0.104	0.772	0.011	0.251	0.163	1.013	-0.428	0.145	0.045	0.367	0.037
232	C1	24.8	30	105	0.271	0.089	0.740	0.039	0.271	0.136	0.970	-0.262	0.127	0.039	0.322	0.037
233	C1	25.0	30	120	0.335	0.146	1.037	-0.058	0.269	0.173	1.046	-0.308	0.103	0.035	0.280	0.007
234	C1	24.8	0	120	0.364	0.177	1.261	-0.184	0.251	0.190	1.154	-0.449	0.125	0.047	0.369	-0.001
235	C1	24.5	-30	120	0.314	0.148	1.135	-0.137	0.235	0.168	1.096	-0.425	0.102	0.038	0.317	0.009
236	C1	24.7	-30	135	0.255	0.126	0.887	-0.140	0.195	0.103	0.733	-0.132	0.028	0.025	0.153	-0.075
237	C1	24.7	0	135	0.278	0.157	1.120	-0.191	0.241	0.125	0.888	-0.148	0.017	0.030	0.173	-0.072
238	C1	24.7	30	135	0.337	0.130	0.969	-0.106	0.234	0.108	0.809	-0.143	0.048	0.024	0.172	-0.046
239	C1	24.4	30	150	0.172	0.111	0.639	-0.316	0.084	0.063	0.350	-0.129	0.009	0.019	0.099	-0.068
240	C1	24.5	0	150	0.093	0.105	0.610	-0.324	0.117	0.067	0.420	-0.097	-0.036	0.021	0.060	-0.121
241	C1	24.5	-30	150	0.103	0.098	0.545	-0.314	0.085	0.060	0.361	-0.134	-0.014	0.022	0.093	-0.105
242	C1	24.3	-30	165	0.054	0.114	0.473	-0.546	0.032	0.037	0.184	-0.113	-0.011	0.016	0.069	-0.079
243	C1	24.5	0	165	-0.010	0.111	0.440	-0.568	0.029	0.038	0.207	-0.138	-0.020	0.016	0.062	-0.098
244	C1	24.2	30	165	0.047	0.131	0.603	-0.484	0.014	0.043	0.188	-0.142	-0.001	0.017	0.086	-0.066
245	C1	24.3	30	180	-0.241	0.152	0.265	-0.884	-0.005	0.027	0.100	-0.127	0.003	0.018	0.084	-0.066
246	C1	24.0	0	180	-0.151	0.116	0.213	-0.783	-0.004	0.018	0.079	-0.098	0.003	0.012	0.065	-0.052
247	C1	23.8	-30	180	-0.009	0.111	0.376	-0.517	0.002	0.021	0.083	-0.122	-0.001	0.014	0.081	-0.055
248	C1	24.2	-30	-15	-0.004	0.157	0.522	-0.804	0.012	0.058	0.240	-0.319	0.009	0.020	0.112	-0.108
249	C1	24.2	0	-15	-0.184	0.173	0.305	-1.076	-0.033	0.061	0.151	-0.399	0.010	0.019	0.092	-0.112
250	C1	24.5	30	-15	-0.184	0.225	0.598	-1.164	-0.002	0.077	0.271	-0.362	0.030	0.030	0.152	-0.114

Phase 1, 2, and 3 Integrated Pressure Data

Run	Conf	Uref fps	Cfx		Cfz				Cmy							
			Mean	RMS	Max	Min	Mean	RMS	Max	Min	Mean	RMS	Max			
251	C1	24.4	30	-30	-0.043	0.168	0.860	-0.741	0.016	0.108	0.553	-0.518	0.023	0.026	0.143	-0.132
252	C1	24.2	0	-30	-0.070	0.149	0.465	-0.816	-0.018	0.095	0.389	-0.536	0.013	0.022	0.121	-0.113
253	C1	24.5	-30	-30	0.076	0.147	0.685	-0.687	0.058	0.097	0.464	-0.430	0.008	0.022	0.140	-0.110
254	C1	24.3	-30	-45	0.134	0.098	0.562	-0.278	0.153	0.113	0.734	-0.423	0.009	0.023	0.154	-0.105
255	C1	23.9	0	-45	0.150	0.117	0.692	-0.308	0.162	0.135	0.876	-0.474	0.006	0.028	0.180	-0.129
256	C1	24.5	30	-45	0.135	0.094	0.635	-0.191	0.159	0.108	0.672	-0.314	0.011	0.023	0.117	-0.095
257	C1	24.7	30	-60	0.288	0.091	0.778	0.053	0.625	0.202	1.715	-0.004	0.042	0.031	0.201	-0.096
258	C1	24.8	0	-60	0.392	0.124	0.953	0.102	0.841	0.273	2.045	0.121	0.054	0.037	0.224	-0.083
259	C1	24.7	-30	-60	0.291	0.106	0.816	0.038	0.629	0.236	1.753	0.043	0.041	0.033	0.219	-0.080
260	C1	25.0	-30	-75	0.204	0.084	0.601	0.036	0.794	0.237	1.903	0.113	0.006	0.034	0.159	-0.166
261	C1	24.9	0	-75	0.267	0.091	0.704	0.077	1.057	0.261	2.241	0.379	0.011	0.037	0.151	-0.152
262	C1	24.8	30	-75	0.187	0.074	0.661	0.044	0.755	0.219	2.130	0.228	0.010	0.031	0.123	-0.149
263	C1	24.8	30	-90	0.122	0.048	0.368	0.009	0.341	0.098	0.785	-0.018	-0.081	0.032	-0.006	-0.243
264	C1	25.3	0	-90	0.151	0.051	0.428	0.029	0.454	0.121	0.964	0.093	-0.100	0.034	-0.019	-0.283
265	C1	25.0	-30	-90	0.137	0.056	0.425	0.011	0.325	0.119	0.930	-0.071	-0.091	0.037	-0.007	-0.281
266	C1	24.8	-30	-105	0.135	0.054	0.397	0.010	-0.028	0.063	0.219	-0.309	-0.082	0.028	-0.022	-0.219
267	C1	25.2	0	-105	0.159	0.061	0.527	0.014	-0.004	0.077	0.342	-0.394	-0.101	0.033	-0.024	-0.285
268	C1	25.1	30	-105	0.120	0.047	0.386	0.008	-0.010	0.059	0.218	-0.328	-0.075	0.024	-0.017	-0.205
269	C1	24.9	30	-120	0.125	0.052	0.442	-0.012	-0.066	0.054	0.118	-0.365	-0.050	0.016	-0.005	-0.154
270	C1	24.9	0	-120	0.149	0.058	0.488	-0.008	-0.072	0.062	0.141	-0.436	-0.061	0.018	-0.005	-0.154
271	C1	24.8	-30	-120	0.126	0.053	0.440	-0.009	-0.072	0.052	0.117	-0.353	-0.049	0.017	-0.003	-0.152
272	C1	24.5	-30	-135	0.064	0.056	0.338	-0.125	-0.052	0.051	0.131	-0.297	-0.006	0.013	0.064	-0.052
273	C1	24.8	0	-135	0.061	0.055	0.357	-0.154	-0.045	0.051	0.150	-0.325	-0.008	0.013	0.065	-0.062
274	C1	24.6	30	-135	0.074	0.064	0.353	-0.175	-0.063	0.057	0.145	-0.331	-0.005	0.014	0.060	-0.071
275	C1	24.8	30	-150	-0.164	0.111	0.272	-0.613	0.058	0.064	0.302	-0.184	0.021	0.017	0.110	-0.040
276	C1	24.5	0	-150	-0.070	0.072	0.158	-0.441	0.016	0.043	0.203	-0.162	0.014	0.012	0.080	-0.022
277	C1	24.2	-30	-150	-0.011	0.085	0.302	-0.421	-0.007	0.049	0.232	-0.222	0.008	0.014	0.088	-0.039
278	C1	24.6	-30	-165	-0.099	0.106	0.277	-0.667	0.008	0.034	0.188	-0.155	0.012	0.014	0.101	-0.034
279	C1	24.4	0	-165	-0.181	0.103	0.104	-0.761	0.028	0.031	0.209	-0.108	0.013	0.012	0.088	-0.040
280	C1	24.4	30	-165	-0.348	0.167	0.219	-1.021	0.063	0.049	0.286	-0.129	0.019	0.020	0.114	-0.048
281	C3	24.2	30	-165	0.399	0.237	1.314	-0.325	-0.130	0.061	0.065	-0.405	0.015	0.021	0.107	-0.057
282	C3	24.0	0	-165	0.022	0.108	0.615	-0.365	-0.024	0.037	0.086	-0.243	0.012	0.015	0.103	-0.037
283	C3	23.7	-30	-165	-0.046	0.119	0.506	-0.532	0.001	0.039	0.137	-0.231	0.008	0.015	0.097	-0.044
284	C3	23.9	-30	-150	-0.027	0.092	0.387	-0.365	-0.015	0.057	0.175	-0.273	0.018	0.014	0.095	-0.031
285	C3	24.3	0	-150	0.028	0.077	0.547	-0.239	-0.038	0.049	0.113	-0.348	0.013	0.014	0.084	-0.025
286	C3	24.3	30	-150	0.331	0.157	0.998	-0.135	-0.215	0.083	0.043	-0.553	0.013	0.021	0.104	-0.058
287	C3	24.4	30	-135	0.197	0.091	0.626	-0.088	-0.177	0.076	0.063	-0.517	-0.009	0.016	0.052	-0.077
288	C3	24.2	0	-135	0.036	0.056	0.399	-0.162	-0.046	0.054	0.127	-0.362	0.004	0.011	0.066	-0.052
289	C3	24.5	-30	-135	0.028	0.064	0.316	-0.170	-0.044	0.058	0.140	-0.309	0.007	0.012	0.061	-0.046
290	C3	24.1	-30	-120	0.077	0.050	0.388	-0.050	-0.054	0.052	0.103	-0.351	-0.027	0.015	0.012	-0.112
291	C3	24.3	0	-120	0.066	0.048	0.456	-0.053	-0.033	0.052	0.130	-0.378	-0.027	0.014	0.013	-0.140
292	C3	24.5	30	-120	0.114	0.053	0.413	-0.025	-0.079	0.053	0.098	-0.360	-0.039	0.016	0.004	-0.133
293	C3	25.1	30	-105	0.095	0.048	0.394	-0.014	0.002	0.055	0.204	-0.290	-0.061	0.025	-0.010	-0.219
294	C3	24.7	0	-105	0.119	0.057	0.444	-0.014	0.008	0.071	0.338	-0.383	-0.078	0.032	-0.012	-0.246
295	C3	24.5	-30	-105	0.099	0.050	0.412	-0.012	-0.018	0.060	0.204	-0.345	-0.060	0.026	-0.010	-0.213
296	C3	25.1	-30	-90	0.127	0.051	0.400	0.017	0.223	0.091	0.658	-0.121	-0.084	0.034	-0.011	-0.265
297	C3	24.7	0	-90	0.148	0.053	0.448	0.036	0.317	0.107	0.786	-0.093	-0.098	0.035	-0.024	-0.296
298	C3	25.0	30	-90	0.124	0.049	0.398	0.019	0.224	0.082	0.625	-0.124	-0.082	0.032	-0.013	-0.264
299	C3	24.8	30	-75	0.203	0.074	0.527	0.051	0.733	0.208	1.682	0.212	-0.004	0.032	0.113	-0.139
300	C3	24.7	0	-75	0.247	0.092	0.713	0.077	0.949	0.237	2.050	0.368	0.005	0.039	0.127	-0.184

Phase 1, 2, and 3 Integrated Pressure Data

Run	Conf	Uref		Cfx				Cfz				Cmy				
		fps		Mean	RMS	Max	Min	Mean	RMS	Max	Min	Mean	RMS	Max	Min	
301	C3	24.5	-30	-75	0.178	0.083	0.605	0.032	0.694	0.235	1.727	0.160	0.005	0.034	0.113	-0.163
302	C3	24.4	-30	-60	0.226	0.114	0.836	-0.014	0.461	0.219	1.681	-0.049	0.023	0.027	0.161	-0.095
303	C3	24.2	0	-60	0.319	0.143	0.990	0.046	0.649	0.268	1.901	-0.005	0.032	0.032	0.208	-0.124
304	C3	24.5	30	-60	0.310	0.126	0.999	0.024	0.596	0.237	1.910	-0.061	0.019	0.032	0.182	-0.110
305	C3	23.9	30	-45	0.329	0.232	1.550	-0.170	0.370	0.265	1.786	-0.228	0.019	0.033	0.230	-0.107
306	C3	24.1	0	-45	0.133	0.148	1.125	-0.226	0.148	0.161	1.258	-0.301	0.007	0.025	0.158	-0.124
307	C3	24.1	-30	-45	0.130	0.144	1.103	-0.235	0.162	0.161	1.257	-0.286	0.015	0.023	0.162	-0.102
308	C3	23.3	-30	-30	0.033	0.184	0.953	-0.551	0.043	0.117	0.732	-0.388	0.014	0.023	0.163	-0.099
309	C3	22.7	0	-30	0.065	0.174	1.064	-0.516	0.048	0.114	0.756	-0.387	0.006	0.023	0.143	-0.114
310	C3	23.1	30	-30	0.352	0.290	1.731	-0.513	0.232	0.192	1.213	-0.281	0.017	0.033	0.206	-0.117
311	C3	22.5	30	-15	0.172	0.336	1.572	-0.780	0.066	0.114	0.602	-0.312	0.013	0.031	0.171	-0.129
312	C3	22.5	0	-15	0.035	0.197	1.058	-0.696	0.020	0.068	0.379	-0.250	0.007	0.021	0.141	-0.093
313	C3	22.2	-30	-15	-0.047	0.201	1.005	-0.805	0.016	0.062	0.367	-0.287	0.018	0.022	0.119	-0.093
314	C3	22.6	-30	0	-0.079	0.173	0.849	-0.804	0.024	0.033	0.201	-0.152	0.016	0.022	0.133	-0.100
315	C3	22.5	0	0	-0.025	0.167	0.698	-0.844	0.009	0.026	0.174	-0.143	0.006	0.017	0.115	-0.095
316	C3	22.6	30	0	0.207	0.316	1.411	-0.736	0.012	0.041	0.202	-0.193	0.008	0.027	0.134	-0.127
317	C3	22.8	30	15	0.416	0.272	1.790	-0.398	-0.094	0.067	0.108	-0.483	0.012	0.023	0.120	-0.083
318	C3	22.6	0	15	0.060	0.146	0.918	-0.479	-0.005	0.031	0.111	-0.184	0.007	0.016	0.114	-0.060
319	C3	22.9	-30	15	0.057	0.140	0.763	-0.498	-0.003	0.042	0.205	-0.184	0.008	0.020	0.109	-0.070
320	C3	22.5	-30	30	0.112	0.121	0.694	-0.375	-0.044	0.057	0.191	-0.327	0.012	0.017	0.119	-0.060
321	C3	22.7	0	30	0.024	0.126	0.775	-0.434	0.005	0.052	0.194	-0.314	0.011	0.018	0.138	-0.055
322	C3	23.2	30	30	0.253	0.195	1.186	-0.276	-0.105	0.095	0.143	-0.633	0.024	0.020	0.121	-0.039
323	C3	23.5	30	45	0.267	0.119	1.032	-0.042	-0.246	0.110	0.011	-1.026	0.010	0.016	0.107	-0.046
324	C3	23.4	0	45	0.100	0.107	0.808	-0.245	-0.063	0.082	0.216	-0.662	0.017	0.016	0.123	-0.038
325	C3	23.0	-30	45	0.139	0.104	0.812	-0.170	-0.110	0.087	0.146	-0.681	0.014	0.014	0.107	-0.026
326	C3	23.8	-30	60	0.163	0.070	0.648	-0.008	-0.285	0.125	0.023	-1.100	-0.001	0.015	0.073	-0.071
327	C3	23.8	0	60	0.192	0.078	0.615	-0.048	-0.340	0.144	0.072	-1.116	-0.003	0.020	0.096	-0.087
328	C3	24.0	30	60	0.222	0.072	0.651	0.022	-0.428	0.141	-0.061	-1.288	-0.015	0.017	0.062	-0.103
329	C3	24.4	30	75	0.180	0.049	0.421	0.051	-0.584	0.165	-0.110	-1.414	0.015	0.017	0.078	-0.086
330	C3	24.1	0	75	0.223	0.051	0.430	0.086	-0.713	0.162	-0.276	-1.390	0.020	0.017	0.092	-0.060
331	C3	24.5	-30	75	0.176	0.048	0.406	0.063	-0.581	0.169	-0.119	-1.355	0.013	0.016	0.089	-0.076
332	C3	23.9	-30	90	0.152	0.044	0.353	0.031	-0.169	0.123	0.188	-0.807	0.100	0.029	0.234	0.021
333	C3	24.1	0	90	0.152	0.044	0.381	0.018	-0.099	0.099	0.236	-0.621	0.100	0.029	0.252	0.012
334	C3	24.2	30	90	0.146	0.045	0.363	0.035	-0.145	0.114	0.211	-0.802	0.097	0.030	0.240	0.023
335	C3	24.6	30	105	0.221	0.080	0.629	-0.015	0.214	0.142	0.862	-0.315	0.105	0.034	0.274	0.022
336	C3	23.8	0	105	0.228	0.090	0.717	-0.030	0.155	0.156	1.035	-0.431	0.119	0.040	0.339	0.027
337	C3	23.8	-30	105	0.209	0.084	0.637	-0.011	0.187	0.148	0.790	-0.398	0.101	0.036	0.287	0.018
338	C3	23.3	-30	120	0.256	0.114	0.852	-0.104	0.205	0.142	0.893	-0.295	0.079	0.028	0.227	-0.001
339	C3	23.6	0	120	0.274	0.122	0.878	-0.112	0.203	0.140	0.908	-0.262	0.090	0.033	0.272	0.000
340	C3	23.7	30	120	0.291	0.114	0.858	-0.065	0.250	0.143	0.958	-0.224	0.084	0.029	0.255	-0.002
341	C3	23.6	30	135	0.245	0.125	0.911	-0.164	0.125	0.089	0.631	-0.197	0.056	0.031	0.208	-0.031
342	C3	23.4	0	135	0.274	0.126	0.913	-0.283	0.165	0.095	0.627	-0.235	0.051	0.027	0.207	-0.051
343	C3	22.9	-30	135	0.248	0.118	0.881	-0.153	0.145	0.095	0.711	-0.174	0.048	0.024	0.194	-0.048
344	C3	23.1	-30	150	0.088	0.114	0.710	-0.351	0.015	0.049	0.298	-0.168	0.020	0.019	0.154	-0.051
345	C3	23.2	0	150	0.083	0.117	0.643	-0.415	0.017	0.053	0.235	-0.209	0.018	0.020	0.155	-0.059
346	C3	23.7	30	150	0.115	0.134	0.807	-0.367	0.013	0.051	0.234	-0.180	0.031	0.026	0.159	-0.052
347	C3	23.7	30	165	0.079	0.184	1.051	-0.470	-0.030	0.042	0.193	-0.196	0.033	0.023	0.135	-0.038
348	C3	23.3	0	165	-0.020	0.133	0.631	-0.655	-0.020	0.030	0.112	-0.177	0.009	0.017	0.128	-0.057
349	C3	23.6	-30	165	-0.031	0.116	0.523	-0.444	-0.017	0.028	0.089	-0.139	0.006	0.016	0.100	-0.056
350	C3	23.3	-30	180	-0.107	0.126	0.410	-0.681	-0.014	0.023	0.072	-0.150	0.009	0.015	0.099	-0.047

Phase 1, 2, and 3 Integrated Pressure Data

Run	Conf	Uref fps	Uref		Cfx			Cfz			Cmy					
			Yaw	Pitch	Mean	RMS	Max	Min	Mean	RMS	Max	Min	Mean	RMS	Max	Min
351	C3	23.5	0	180	0.000	0.125	0.653	-0.453	-0.018	0.022	0.047	-0.151	0.012	0.015	0.100	-0.031
352	C3	23.7	30	180	0.318	0.249	1.454	-0.419	-0.042	0.033	0.068	-0.216	0.028	0.022	0.143	-0.045
353	C7	22.5	30	180	0.299	0.214	1.309	-0.317	-0.048	0.036	0.074	-0.216	0.032	0.024	0.143	-0.049
354	C7	21.9	0	180	0.134	0.144	0.865	-0.305	-0.013	0.024	0.057	-0.166	0.009	0.016	0.110	-0.037
355	C7	21.8	-30	180	0.110	0.214	1.184	-0.417	-0.027	0.029	0.069	-0.176	0.018	0.019	0.117	-0.046
356	C7	22.0	-30	165	0.161	0.174	0.923	-0.425	0.008	0.037	0.189	-0.131	0.022	0.020	0.126	-0.034
357	C7	22.0	0	165	0.145	0.153	0.957	-0.298	0.013	0.033	0.194	-0.115	0.016	0.020	0.119	-0.035
358	C7	22.4	30	165	0.381	0.226	1.370	-0.238	0.019	0.047	0.260	-0.142	0.053	0.025	0.172	-0.022
359	C7	22.4	30	150	0.276	0.183	1.172	-0.238	0.058	0.069	0.400	-0.170	0.058	0.032	0.228	-0.026
360	C7	22.0	0	150	0.145	0.138	0.895	-0.342	0.036	0.055	0.293	-0.189	0.027	0.026	0.161	-0.038
361	C7	22.2	-30	150	0.145	0.141	0.914	-0.266	0.033	0.056	0.328	-0.151	0.029	0.023	0.175	-0.032
362	C7	22.7	-30	135	0.222	0.113	0.768	-0.138	0.126	0.084	0.580	-0.170	0.045	0.025	0.183	-0.024
363	C7	22.3	0	135	0.224	0.122	0.841	-0.272	0.121	0.088	0.629	-0.252	0.048	0.031	0.222	-0.041
364	C7	22.3	30	135	0.313	0.141	0.899	-0.192	0.167	0.107	0.695	-0.193	0.069	0.034	0.228	-0.029
365	C7	22.3	30	120	0.312	0.129	0.976	-0.146	0.260	0.165	1.090	-0.299	0.093	0.033	0.263	-0.010
366	C7	22.0	0	120	0.256	0.122	0.987	-0.129	0.185	0.142	1.062	-0.382	0.086	0.035	0.291	-0.005
367	C7	22.3	-30	120	0.251	0.111	0.831	-0.097	0.199	0.140	0.959	-0.307	0.078	0.028	0.224	0.005
368	C7	22.3	-30	105	0.232	0.090	0.697	0.002	0.214	0.162	1.023	-0.355	0.111	0.039	0.316	0.029
369	C7	22.7	0	105	0.235	0.090	0.711	-0.054	0.161	0.157	0.990	-0.505	0.123	0.040	0.316	0.022
370	C7	22.7	30	105	0.256	0.092	0.676	-0.013	0.272	0.162	1.062	-0.314	0.117	0.040	0.327	0.022
371	C7	22.8	30	90	0.155	0.045	0.361	0.019	-0.090	0.121	0.277	-0.840	0.103	0.030	0.239	0.012
372	C7	22.6	0	90	0.145	0.042	0.354	0.024	-0.043	0.100	0.341	-0.600	0.096	0.027	0.234	0.016
373	C7	22.8	-30	90	0.144	0.044	0.363	0.022	-0.118	0.129	0.294	-1.073	0.095	0.029	0.240	0.015
374	C7	22.7	-30	75	0.144	0.041	0.368	0.046	-0.490	0.159	-0.052	-1.426	0.008	0.018	0.080	-0.103
375	C7	22.8	0	75	0.167	0.037	0.363	0.063	-0.532	0.134	-0.130	-1.256	0.016	0.015	0.090	-0.068
376	C7	22.9	30	75	0.181	0.047	0.422	0.068	-0.599	0.177	-0.161	-1.513	0.013	0.017	0.087	-0.092
377	C7	22.9	30	60	0.214	0.074	0.733	0.032	-0.389	0.139	-0.070	-1.375	-0.006	0.015	0.058	-0.111
378	C7	22.6	0	60	0.144	0.089	0.756	-0.087	-0.225	0.155	0.159	-1.452	0.008	0.019	0.123	-0.081
379	C7	22.9	-30	60	0.180	0.085	0.690	-0.014	-0.285	0.147	0.035	-1.204	0.009	0.015	0.095	-0.055
380	C7	22.2	-30	45	0.244	0.146	1.237	-0.119	-0.199	0.126	0.097	-1.072	0.021	0.016	0.125	-0.026
381	C7	22.2	0	45	0.148	0.143	0.966	-0.198	-0.107	0.118	0.151	-0.847	0.019	0.018	0.134	-0.036
382	C7	22.6	30	45	0.366	0.154	1.261	-0.021	-0.330	0.139	0.012	-1.214	0.017	0.018	0.108	-0.046
383	C7	22.8	30	30	0.462	0.217	1.575	-0.216	-0.214	0.108	0.114	-0.770	0.030	0.024	0.161	-0.042
384	C7	22.0	0	30	0.144	0.169	1.284	-0.307	-0.063	0.081	0.120	-0.658	0.012	0.018	0.127	-0.050
385	C7	22.4	-30	30	0.257	0.202	1.299	-0.290	-0.119	0.100	0.137	-0.637	0.017	0.020	0.119	-0.046
386	C7	22.3	-30	15	0.277	0.256	1.417	-0.457	-0.050	0.061	0.127	-0.375	0.015	0.024	0.161	-0.076
387	C7	22.3	0	15	0.150	0.186	1.230	-0.416	-0.030	0.045	0.089	-0.285	0.007	0.018	0.143	-0.054
388	C7	22.5	30	15	0.398	0.273	1.600	-0.328	-0.076	0.060	0.088	-0.394	0.019	0.028	0.164	-0.076
389	C7	22.4	30	0	0.351	0.304	1.767	-0.590	0.000	0.047	0.279	-0.185	0.000	0.031	0.184	-0.122
390	C7	22.5	0	0	0.193	0.204	1.401	-0.491	0.005	0.027	0.189	-0.124	0.003	0.018	0.125	-0.082
391	C7	22.1	-30	0	0.258	0.293	1.683	-0.565	0.005	0.038	0.206	-0.157	0.003	0.025	0.136	-0.104
392	C7	22.5	-30	-15	0.384	0.313	1.677	-0.519	0.111	0.100	0.573	-0.236	0.005	0.028	0.168	-0.107
393	C7	22.5	0	-15	0.242	0.225	1.458	-0.452	0.070	0.073	0.505	-0.238	0.003	0.021	0.156	-0.106
394	C7	22.8	30	-15	0.334	0.306	1.828	-0.535	0.096	0.106	0.586	-0.284	0.004	0.031	0.172	-0.130
395	C7	22.4	30	-30	0.507	0.305	1.901	-0.236	0.327	0.207	1.330	-0.258	0.019	0.037	0.219	-0.117
396	C7	22.3	0	-30	0.302	0.263	2.177	-0.396	0.191	0.173	1.489	-0.262	0.009	0.028	0.212	-0.109
397	C7	22.6	-30	-30	0.404	0.272	1.682	-0.237	0.257	0.181	1.245	-0.195	0.014	0.031	0.217	-0.094
398	C7	22.4	-30	-45	0.338	0.193	1.316	-0.059	0.374	0.221	1.599	-0.116	0.017	0.033	0.240	-0.126
399	C7	22.4	0	-45	0.330	0.236	1.614	-0.181	0.371	0.275	1.856	-0.215	0.019	0.036	0.244	-0.136
400	C7	22.5	30	-45	0.407	0.244	1.771	-0.142	0.473	0.291	2.106	-0.254	0.031	0.040	0.274	-0.110

Phase 1, 2, and 3 Integrated Pressure Data

Run	Conf	Uref fps	Uref		Cfx			Cfz			Cmy					
			Yaw	Pitch	Mean	RMS	Max	Min	Mean	RMS	Max	Min	Mean	RMS	Max	Min
401	C7	22.5	30	-60	0.353	0.159	1.175	0.026	0.704	0.318	2.358	-0.026	0.031	0.037	0.207	-0.122
402	C7	22.6	0	-60	0.354	0.175	1.205	0.005	0.725	0.349	2.413	-0.016	0.037	0.038	0.245	-0.113
403	C7	23.1	-30	-60	0.296	0.141	1.058	0.021	0.599	0.276	2.103	-0.015	0.028	0.035	0.235	-0.120
404	C7	22.9	-30	-75	0.204	0.090	0.716	0.029	0.801	0.244	2.041	0.173	0.007	0.039	0.130	-0.181
405	C7	22.7	0	-75	0.258	0.104	0.835	0.003	1.017	0.259	2.272	0.210	0.010	0.045	0.151	-0.198
406	C7	22.9	30	-75	0.241	0.094	0.783	0.068	0.831	0.239	1.973	0.225	-0.012	0.039	0.111	-0.229
407	C7	22.9	30	-90	0.119	0.051	0.371	0.006	0.376	0.110	0.921	-0.005	-0.079	0.034	-0.004	-0.245
408	C7	23.0	0	-90	0.128	0.053	0.433	0.016	0.514	0.135	1.168	0.065	-0.085	0.035	-0.010	-0.286
409	C7	23.0	-30	-90	0.112	0.056	0.384	-0.007	0.391	0.141	1.072	-0.040	-0.074	0.037	0.004	-0.254
410	C7	22.6	-30	-105	0.097	0.057	0.434	-0.009	-0.021	0.062	0.183	-0.413	-0.059	0.029	-0.007	-0.219
411	C7	23.0	0	-105	0.103	0.059	0.498	-0.026	0.012	0.067	0.317	-0.345	-0.068	0.033	-0.006	-0.282
412	C7	22.7	30	-105	0.121	0.055	0.487	0.010	-0.024	0.060	0.247	-0.398	-0.073	0.029	-0.018	-0.261
413	C7	22.7	30	-120	0.164	0.062	0.484	-0.010	-0.128	0.061	0.077	-0.429	-0.052	0.019	-0.006	-0.154
414	C7	22.6	0	-120	0.058	0.051	0.325	-0.086	-0.036	0.055	0.169	-0.298	-0.021	0.014	0.019	-0.100
415	C7	22.8	-30	-120	0.092	0.059	0.426	-0.057	-0.077	0.060	0.116	-0.416	-0.027	0.017	0.013	-0.122
416	C7	22.9	-30	-135	0.111	0.089	0.618	-0.134	-0.116	0.078	0.096	-0.529	0.002	0.013	0.059	-0.066
417	C7	22.8	0	-135	0.068	0.064	0.422	-0.123	-0.067	0.062	0.118	-0.381	-0.001	0.011	0.064	-0.049
418	C7	22.9	30	-135	0.246	0.095	0.676	-0.007	-0.222	0.087	0.011	-0.606	-0.011	0.016	0.068	-0.082
419	C7	22.6	30	-150	0.230	0.141	0.796	-0.251	-0.168	0.088	0.108	-0.598	0.020	0.022	0.143	-0.055
420	C7	22.3	0	-150	0.099	0.096	0.635	-0.220	-0.069	0.064	0.108	-0.452	0.007	0.016	0.092	-0.043
421	C7	22.4	-30	-150	0.123	0.135	0.812	-0.253	-0.101	0.080	0.108	-0.473	0.017	0.017	0.105	-0.040
422	C7	22.4	-30	-165	0.048	0.175	0.821	-0.467	-0.048	0.055	0.106	-0.305	0.022	0.020	0.113	-0.042
423	C7	22.3	0	-165	0.099	0.119	0.690	-0.350	-0.034	0.043	0.105	-0.272	0.005	0.017	0.105	-0.044
424	C7	22.5	30	-165	0.200	0.196	1.020	-0.357	-0.094	0.065	0.110	-0.389	0.026	0.023	0.140	-0.048
425	D3	22.7	45	180	1.023	0.266	2.103	0.281	-0.019	0.033	0.091	-0.169	0.012	0.022	0.112	-0.060
426	D3	22.5	30	180	0.752	0.197	1.731	0.199	0.020	0.039	0.126	-0.182	-0.013	0.026	0.121	-0.084
427	D3	22.8	0	180	0.518	0.134	1.152	0.069	0.038	0.030	0.125	-0.147	-0.025	0.020	0.097	-0.082
428	D3	22.6	-30	180	0.260	0.100	0.719	-0.136	0.024	0.023	0.086	-0.117	-0.016	0.015	0.078	-0.057
429	D3	22.6	-30	-165	0.189	0.090	0.593	-0.179	-0.019	0.028	0.075	-0.200	-0.021	0.015	0.071	-0.065
430	D3	22.7	0	-165	0.421	0.120	0.977	-0.027	-0.049	0.039	0.084	-0.294	-0.041	0.021	0.073	-0.108
431	D3	22.7	30	-165	0.668	0.166	1.586	0.170	-0.126	0.057	-0.009	-0.453	-0.034	0.025	0.074	-0.112
432	D3	22.7	45	-165	0.915	0.254	1.995	0.270	-0.219	0.073	-0.017	-0.533	-0.017	0.021	0.068	-0.096
433	D3	22.7	45	-150	0.622	0.185	1.377	0.181	-0.311	0.106	-0.056	-0.712	-0.028	0.021	0.059	-0.117
434	D3	22.6	30	-150	0.447	0.124	1.135	0.004	-0.184	0.075	-0.002	-0.578	-0.043	0.024	0.083	-0.128
435	D3	22.7	0	-150	0.280	0.081	0.654	-0.011	-0.079	0.042	0.076	-0.342	-0.047	0.018	0.055	-0.103
436	D3	22.5	-30	-150	0.133	0.067	0.439	-0.148	-0.031	0.034	0.112	-0.301	-0.026	0.014	0.072	-0.077
437	D3	22.5	-30	-135	0.087	0.056	0.321	-0.140	-0.027	0.043	0.198	-0.231	-0.028	0.014	0.041	-0.078
438	D3	22.6	0	-135	0.163	0.063	0.491	-0.111	-0.063	0.050	0.160	-0.349	-0.047	0.016	0.048	-0.116
439	D3	22.6	30	-135	0.243	0.085	0.732	-0.025	-0.156	0.076	0.076	-0.607	-0.041	0.020	0.059	-0.126
440	D3	22.6	45	-135	0.387	0.136	1.120	0.012	-0.312	0.121	0.043	-0.882	-0.035	0.021	0.067	-0.142
441	D3	22.2	45	-120	0.201	0.096	0.659	-0.019	-0.195	0.111	0.104	-0.752	-0.051	0.023	0.012	-0.159
442	D3	22.7	30	-120	0.110	0.054	0.418	-0.065	-0.080	0.070	0.196	-0.463	-0.037	0.015	0.027	-0.115
443	D3	22.6	0	-120	0.079	0.047	0.312	-0.107	-0.018	0.060	0.268	-0.328	-0.039	0.013	0.022	-0.095
444	D3	22.8	-30	-120	0.045	0.039	0.225	-0.096	-0.005	0.051	0.240	-0.261	-0.024	0.010	0.024	-0.068
445	D3	22.2	-30	-105	0.028	0.026	0.162	-0.093	0.007	0.062	0.436	-0.257	-0.019	0.010	0.022	-0.068
446	D3	22.7	0	-105	0.048	0.031	0.217	-0.085	-0.015	0.072	0.357	-0.382	-0.028	0.012	0.025	-0.090
447	D3	22.6	30	-105	0.047	0.035	0.253	-0.070	0.003	0.080	0.370	-0.408	-0.031	0.014	0.012	-0.109
448	D3	22.6	45	-105	0.111	0.067	0.442	-0.040	-0.049	0.099	0.284	-0.561	-0.063	0.030	0.003	-0.211
449	D3	22.7	45	-90	0.091	0.051	0.352	-0.049	0.079	0.114	0.583	-0.412	-0.060	0.034	0.032	-0.233
450	D3	22.6	30	-90	0.040	0.023	0.214	-0.042	0.121	0.091	0.603	-0.317	-0.027	0.015	0.028	-0.141

Phase 1, 2, and 3 Integrated Pressure Data

Run	Conf	Uref fps	Uref		Cfx			Cfz			Cmy					
			Yaw	Pitch	Mean	RMS	Max	Min	Mean	RMS	Max	Min	Mean	RMS	Max	Min
451	D3	23.0	0	-90	0.035	0.018	0.145	-0.060	0.104	0.075	0.576	-0.219	-0.023	0.012	0.040	-0.096
452	D3	22.2	-30	-90	0.022	0.015	0.128	-0.060	0.091	0.062	0.556	-0.204	-0.014	0.010	0.040	-0.084
453	D3	22.8	-30	-75	0.038	0.016	0.131	-0.032	0.187	0.073	0.583	-0.182	0.008	0.011	0.067	-0.065
454	D3	22.6	0	-75	0.066	0.019	0.161	-0.019	0.281	0.082	0.680	-0.138	0.006	0.013	0.072	-0.077
455	D3	22.7	30	-75	0.083	0.026	0.232	-0.005	0.273	0.097	0.772	-0.199	-0.006	0.017	0.057	-0.122
456	D3	22.4	45	-75	0.133	0.053	0.402	0.012	0.255	0.115	0.714	-0.245	-0.042	0.036	0.045	-0.206
457	D3	22.4	45	-60	0.252	0.089	0.733	0.019	0.424	0.137	1.053	-0.080	-0.004	0.035	0.113	-0.165
458	D3	22.5	30	-60	0.180	0.050	0.406	0.006	0.388	0.112	0.808	-0.051	0.025	0.019	0.112	-0.089
459	D3	22.3	0	-60	0.176	0.046	0.385	0.006	0.387	0.100	0.849	-0.087	0.027	0.017	0.142	-0.066
460	D3	22.5	-30	-60	0.123	0.045	0.375	-0.057	0.265	0.092	0.804	-0.197	0.017	0.015	0.125	-0.079
461	D3	22.7	-30	-45	0.241	0.089	0.592	-0.097	0.254	0.094	0.696	-0.145	0.006	0.017	0.131	-0.064
462	D3	22.4	0	-45	0.368	0.099	0.813	-0.053	0.390	0.110	0.914	-0.174	0.010	0.021	0.164	-0.092
463	D3	22.3	30	-45	0.378	0.103	0.775	-0.056	0.440	0.122	1.001	-0.103	0.029	0.024	0.205	-0.083
464	D3	22.2	45	-45	0.427	0.142	1.205	0.046	0.491	0.153	1.248	0.004	0.030	0.032	0.161	-0.109
465	D3	22.5	45	-30	0.679	0.201	1.578	0.114	0.478	0.147	1.181	-0.015	0.049	0.035	0.233	-0.085
466	D3	22.6	30	-30	0.634	0.160	1.283	0.033	0.397	0.109	0.898	-0.084	0.018	0.027	0.183	-0.093
467	D3	22.6	0	-30	0.552	0.146	1.113	-0.064	0.323	0.094	0.749	-0.174	0.002	0.023	0.173	-0.107
468	D3	22.6	-30	-30	0.335	0.129	1.074	-0.224	0.195	0.080	0.683	-0.193	0.001	0.017	0.136	-0.066
469	D3	22.4	-30	-15	0.388	0.142	1.036	-0.416	0.101	0.043	0.384	-0.167	-0.002	0.014	0.132	-0.068
470	D3	22.4	0	-15	0.690	0.185	1.515	-0.010	0.178	0.058	0.495	-0.058	-0.004	0.019	0.122	-0.075
471	D3	22.6	30	-15	0.909	0.218	1.796	0.187	0.260	0.071	0.612	0.006	0.011	0.022	0.171	-0.069
472	D3	23.0	45	-15	0.918	0.247	2.089	0.228	0.300	0.092	0.706	-0.013	0.035	0.031	0.198	-0.086
473	D3	23.0	45	0	1.158	0.307	2.564	0.319	0.034	0.038	0.258	-0.081	0.023	0.025	0.170	-0.054
474	D3	23.1	30	0	0.935	0.236	2.165	0.006	0.005	0.034	0.204	-0.105	0.004	0.022	0.135	-0.069
475	D3	23.0	0	0	0.681	0.186	1.531	0.008	-0.010	0.025	0.191	-0.086	-0.007	0.016	0.126	-0.057
476	D3	22.7	-30	0	0.357	0.145	0.971	-0.136	-0.003	0.019	0.153	-0.061	-0.002	0.013	0.101	-0.040
477	B3	22.3	-30	0	1.105	0.354	2.814	0.304	0.038	0.030	0.225	-0.052	0.025	0.020	0.149	-0.034
478	B3	22.8	0	0	1.832	0.462	3.696	0.671	0.039	0.034	0.231	-0.070	0.026	0.023	0.153	-0.046
479	B3	22.9	30	0	2.245	0.504	4.477	0.956	0.016	0.031	0.178	-0.089	0.010	0.021	0.118	-0.059
480	B3	22.7	45	0	2.290	0.500	4.319	1.077	0.022	0.033	0.170	-0.102	0.014	0.022	0.113	-0.068
481	B3	22.6	45	-15	2.205	0.498	4.337	0.911	0.670	0.156	1.327	0.244	0.050	0.029	0.197	-0.032
482	B3	22.8	30	-15	2.262	0.470	4.075	1.114	0.667	0.140	1.222	0.315	0.039	0.022	0.140	-0.039
483	B3	22.5	0	-15	1.668	0.422	3.647	0.382	0.493	0.130	1.093	0.113	0.030	0.020	0.116	-0.034
484	B3	22.3	-30	-15	1.058	0.348	2.576	0.282	0.328	0.112	0.849	0.088	0.029	0.017	0.122	-0.023
485	B3	22.6	-30	-30	0.937	0.299	2.296	0.210	0.586	0.184	1.411	0.128	0.026	0.015	0.121	-0.026
486	B3	22.6	0	-30	1.412	0.356	2.943	0.579	0.855	0.217	1.840	0.340	0.023	0.019	0.122	-0.067
487	B3	22.8	30	-30	1.826	0.417	3.378	0.858	1.097	0.250	2.027	0.502	0.024	0.025	0.142	-0.078
488	B3	22.5	45	-30	1.644	0.389	3.378	0.631	1.048	0.245	2.128	0.406	0.056	0.041	0.266	-0.065
489	B3	23.0	45	-45	1.026	0.275	2.224	0.416	1.287	0.352	2.832	0.502	0.122	0.047	0.346	-0.008
490	B3	22.6	30	-45	1.201	0.296	2.468	0.537	1.409	0.367	2.878	0.609	0.097	0.051	0.331	-0.016
491	B3	22.5	0	-45	1.150	0.290	2.371	0.396	1.242	0.313	2.616	0.406	0.043	0.026	0.218	-0.040
492	B3	22.9	-30	-45	0.797	0.253	1.870	0.198	0.887	0.283	2.175	0.230	0.042	0.026	0.223	-0.034
493	B3	22.8	-30	-60	0.524	0.164	1.303	0.120	1.261	0.402	3.094	0.343	0.117	0.047	0.340	-0.025
494	B3	22.8	0	-60	0.676	0.188	1.405	0.250	1.587	0.461	3.349	0.556	0.138	0.054	0.355	-0.021
495	B3	23.4	30	-60	0.644	0.165	1.288	0.187	1.478	0.383	2.871	0.438	0.120	0.042	0.312	-0.020
496	B3	22.9	45	-60	0.569	0.170	1.321	0.200	1.231	0.371	2.843	0.374	0.081	0.039	0.273	-0.076
497	B3	22.6	45	-75	0.289	0.099	0.721	0.076	0.835	0.261	1.964	0.177	-0.042	0.032	0.075	-0.177
498	B3	22.8	30	-75	0.355	0.114	0.838	0.121	1.098	0.290	2.259	0.427	-0.039	0.038	0.085	-0.227
499	B3	22.4	0	-75	0.387	0.119	0.944	0.062	1.323	0.330	2.755	0.337	-0.021	0.040	0.123	-0.203
500	B3	23.0	-30	-75	0.292	0.114	0.780	0.011	1.087	0.332	2.654	0.368	-0.001	0.034	0.136	-0.143

Phase 1, 2, and 3 Integrated Pressure Data

Run	Conf	Uref		Cfx				Cfz				Cmy				
		fps	Yaw	Pitch	Mean	RMS	Max	Min	Mean	RMS	Max	Min	Mean	RMS	Max	Min
501	B3	22.7	-30	-90	0.192	0.071	0.555	0.033	0.427	0.147	1.217	-0.066	-0.127	0.047	-0.022	-0.367
502	B3	23.0	0	-90	0.236	0.075	0.548	0.056	0.437	0.154	1.232	-0.093	-0.156	0.050	-0.037	-0.362
503	B3	23.0	30	-90	0.192	0.064	0.475	0.046	0.403	0.125	0.988	-0.116	-0.127	0.043	-0.031	-0.314
504	B3	23.1	45	-90	0.148	0.057	0.409	0.011	0.296	0.112	0.856	-0.094	-0.098	0.038	-0.007	-0.271
505	B3	23.0	45	-105	0.196	0.073	0.547	0.014	-0.052	0.076	0.226	-0.431	-0.116	0.039	-0.020	-0.300
506	B3	23.0	30	-105	0.240	0.081	0.650	0.051	-0.058	0.082	0.252	-0.479	-0.144	0.044	-0.044	-0.372
507	B3	22.7	0	-105	0.304	0.096	0.747	0.064	-0.065	0.101	0.371	-0.528	-0.183	0.056	-0.051	-0.438
508	B3	23.0	-30	-105	0.232	0.083	0.620	0.020	-0.059	0.090	0.275	-0.560	-0.138	0.044	-0.040	-0.337
509	B3	22.7	-30	-120	0.304	0.103	0.808	0.069	-0.072	0.058	0.121	-0.371	-0.151	0.048	-0.036	-0.386
510	B3	23.0	0	-120	0.373	0.108	0.828	0.113	-0.070	0.062	0.160	-0.378	-0.191	0.053	-0.071	-0.420
511	B3	22.6	30	-120	0.420	0.115	0.907	0.139	-0.188	0.080	0.051	-0.570	-0.178	0.049	-0.065	-0.388
512	B3	22.9	45	-120	0.367	0.108	0.867	0.088	-0.221	0.081	0.035	-0.670	-0.137	0.042	-0.045	-0.337
513	B3	22.9	45	-135	0.619	0.163	1.311	0.246	-0.324	0.094	-0.088	-0.721	-0.138	0.040	-0.047	-0.327
514	B3	22.5	30	-135	0.666	0.169	1.357	0.262	-0.296	0.088	-0.077	-0.667	-0.173	0.045	-0.068	-0.378
515	B3	22.6	0	-135	0.594	0.171	1.359	0.226	-0.197	0.076	-0.004	-0.507	-0.185	0.052	-0.067	-0.416
516	B3	22.6	-30	-135	0.380	0.128	0.989	0.059	-0.109	0.061	0.091	-0.415	-0.127	0.041	-0.020	-0.334
517	B3	22.6	-30	-150	0.513	0.156	1.200	0.157	-0.132	0.057	-0.005	-0.400	-0.094	0.028	-0.023	-0.216
518	B3	22.7	0	-150	0.899	0.223	1.720	0.366	-0.250	0.078	-0.068	-0.582	-0.154	0.039	-0.051	-0.301
519	B3	22.6	30	-150	1.061	0.265	2.133	0.477	-0.328	0.093	-0.122	-0.700	-0.163	0.042	-0.051	-0.352
520	B3	22.9	45	-150	0.997	0.244	1.979	0.426	-0.337	0.092	-0.108	-0.712	-0.136	0.036	-0.042	-0.307
521	B3	22.3	45	-165	1.524	0.356	3.197	0.686	-0.205	0.064	-0.050	-0.515	-0.130	0.032	-0.041	-0.287
522	B3	22.7	30	-165	1.542	0.352	2.920	0.630	-0.212	0.064	-0.046	-0.483	-0.128	0.033	-0.025	-0.271
523	B3	22.3	0	-165	1.275	0.329	2.718	0.414	-0.170	0.063	-0.017	-0.452	-0.110	0.031	-0.011	-0.284
524	B3	22.4	-30	-165	0.717	0.222	1.746	0.059	-0.091	0.044	0.039	-0.321	-0.065	0.023	0.015	-0.172
525	B3	22.7	-30	180	0.855	0.244	1.868	0.307	0.052	0.026	0.172	-0.060	-0.035	0.017	0.040	-0.114
526	B3	22.2	0	180	1.453	0.357	2.809	0.626	0.082	0.034	0.224	-0.060	-0.054	0.023	0.039	-0.148
527	B3	22.9	30	180	1.807	0.432	3.482	0.802	0.113	0.040	0.283	-0.026	-0.074	0.026	0.017	-0.188
528	B3	22.6	45	180	1.778	0.415	3.389	0.810	0.107	0.035	0.278	-0.020	-0.070	0.023	0.014	-0.184
529	B4	22.7	45	180	1.384	0.386	3.097	0.359	0.087	0.033	0.243	-0.028	-0.057	0.022	0.019	-0.161
530	B4	22.6	30	180	1.476	0.371	3.053	0.528	0.068	0.038	0.223	-0.102	-0.045	0.025	0.067	-0.148
531	B4	22.6	0	180	0.017	0.239	0.976	-0.765	-0.025	0.031	0.097	-0.200	0.016	0.020	0.132	-0.064
532	B4	22.5	-30	180	-0.091	0.107	0.251	-0.620	-0.002	0.017	0.081	-0.115	0.002	0.012	0.076	-0.054
533	B4	22.4	-30	-165	-0.089	0.100	0.262	-0.607	0.016	0.031	0.181	-0.133	0.005	0.014	0.081	-0.046
534	B4	22.4	0	-165	0.053	0.249	1.186	-0.674	-0.052	0.067	0.172	-0.389	0.024	0.026	0.151	-0.087
535	B4	22.8	30	-165	1.296	0.319	2.665	0.411	-0.204	0.067	-0.026	-0.497	-0.091	0.030	0.009	-0.221
536	B4	22.8	45	-165	1.188	0.335	2.585	0.385	-0.167	0.061	-0.020	-0.430	-0.097	0.030	-0.005	-0.235
537	B4	22.7	45	-150	0.921	0.248	1.883	0.272	-0.322	0.099	-0.064	-0.745	-0.120	0.033	-0.021	-0.262
538	B4	22.5	30	-150	1.021	0.253	2.034	0.428	-0.363	0.102	-0.126	-0.786	-0.130	0.036	-0.016	-0.274
539	B4	22.6	0	-150	0.145	0.185	0.982	-0.407	-0.100	0.086	0.158	-0.534	0.010	0.032	0.148	-0.134
540	B4	22.8	-30	-150	-0.007	0.075	0.322	-0.433	-0.007	0.044	0.214	-0.260	0.007	0.014	0.096	-0.033
541	B4	22.4	-30	-135	0.061	0.060	0.486	-0.137	-0.049	0.056	0.126	-0.430	-0.006	0.014	0.063	-0.065
542	B4	22.7	0	-135	0.224	0.133	0.849	-0.083	-0.154	0.089	0.074	-0.610	-0.033	0.036	0.082	-0.217
543	B4	22.7	30	-135	0.678	0.175	1.383	0.202	-0.335	0.098	-0.046	-0.755	-0.160	0.042	-0.040	-0.328
544	B4	22.7	45	-135	0.640	0.162	1.319	0.203	-0.352	0.100	-0.056	-0.769	-0.135	0.037	-0.040	-0.302
545	B4	22.8	45	-120	0.406	0.118	0.976	0.132	-0.286	0.098	-0.038	-0.779	-0.138	0.042	-0.041	-0.364
546	B4	22.9	30	-120	0.435	0.126	0.953	0.144	-0.235	0.093	0.046	-0.655	-0.171	0.050	-0.055	-0.377
547	B4	23.0	0	-120	0.240	0.089	0.667	0.012	-0.114	0.070	0.130	-0.441	-0.100	0.037	-0.012	-0.302
548	B4	22.5	-30	-120	0.125	0.056	0.457	-0.053	-0.057	0.056	0.134	-0.390	-0.053	0.018	0.001	-0.158
549	B4	22.4	-30	-105	0.157	0.063	0.504	0.012	-0.048	0.072	0.247	-0.461	-0.092	0.032	-0.015	-0.259
550	B4	22.8	0	-105	0.209	0.070	0.577	0.039	-0.035	0.080	0.269	-0.406	-0.128	0.041	-0.043	-0.335

Phase 1, 2, and 3 Integrated Pressure Data

Run	Conf	Uref fps	Uref		Cfx				Cfz				Cmy			
			Yaw	Pitch	Mean	RMS	Max	Min	Mean	RMS	Max	Min	Mean	RMS	Max	Min
551	B4	22.6	30	-105	0.244	0.082	0.698	0.052	-0.059	0.084	0.256	-0.560	-0.146	0.044	-0.045	-0.370
552	B4	22.7	45	-105	0.199	0.071	0.517	0.041	-0.052	0.072	0.211	-0.428	-0.118	0.038	-0.030	-0.296
553	B4	22.7	45	-90	0.151	0.061	0.411	0.015	0.244	0.109	0.770	-0.176	-0.100	0.040	-0.010	-0.272
554	B4	22.6	30	-90	0.189	0.067	0.538	0.039	0.367	0.119	0.877	-0.080	-0.125	0.044	-0.026	-0.356
555	B4	22.9	0	-90	0.217	0.068	0.549	0.055	0.319	0.118	0.843	-0.086	-0.144	0.045	-0.036	-0.363
556	B4	22.6	-30	-90	0.169	0.062	0.497	0.027	0.241	0.112	0.818	-0.231	-0.112	0.041	-0.018	-0.328
557	B4	22.4	-30	-75	0.238	0.100	0.728	0.043	0.710	0.246	1.931	0.175	-0.030	0.040	0.106	-0.244
558	B4	22.5	0	-75	0.357	0.114	0.894	0.113	0.884	0.241	2.162	0.300	-0.077	0.049	0.095	-0.302
559	B4	22.6	30	-75	0.318	0.101	0.837	0.091	1.053	0.269	2.189	0.417	-0.023	0.037	0.108	-0.222
560	B4	22.9	45	-75	0.266	0.089	0.645	0.041	0.778	0.244	1.719	0.079	-0.037	0.037	0.090	-0.181
561	B4	22.9	45	-60	0.540	0.147	1.169	0.188	1.140	0.308	2.468	0.373	0.068	0.034	0.230	-0.074
562	B4	22.9	30	-60	0.505	0.151	1.174	0.134	1.078	0.339	2.647	0.197	0.067	0.037	0.257	-0.058
563	B4	22.7	0	-60	0.452	0.199	1.322	0.044	0.810	0.332	2.345	0.003	0.009	0.042	0.203	-0.146
564	B4	22.7	-30	-60	0.223	0.107	0.799	-0.003	0.453	0.216	1.600	-0.139	0.022	0.032	0.184	-0.125
565	B4	22.7	-30	-45	0.121	0.096	0.746	-0.212	0.147	0.114	0.851	-0.299	0.012	0.023	0.135	-0.115
566	B4	22.4	0	-45	0.224	0.166	1.152	-0.197	0.254	0.198	1.367	-0.327	0.014	0.036	0.212	-0.163
567	B4	22.8	30	-45	0.819	0.305	1.970	0.096	0.985	0.390	2.504	0.033	0.078	0.051	0.318	-0.101
568	B4	22.7	45	-45	0.904	0.258	1.961	0.315	1.111	0.326	2.384	0.339	0.097	0.042	0.283	-0.029
569	B4	22.4	45	-30	1.253	0.347	2.534	0.430	0.793	0.234	1.783	0.241	0.040	0.039	0.243	-0.069
570	B4	22.5	30	-30	1.185	0.364	2.633	0.298	0.707	0.224	1.697	0.115	0.013	0.028	0.181	-0.106
571	B4	22.5	0	-30	0.091	0.221	1.319	-0.575	0.055	0.151	0.829	-0.475	0.001	0.037	0.200	-0.185
572	B4	22.6	-30	-30	0.054	0.125	0.544	-0.565	0.043	0.081	0.422	-0.387	0.007	0.019	0.129	-0.085
573	B4	22.5	-30	-15	0.019	0.139	0.504	-0.706	0.014	0.049	0.234	-0.277	0.005	0.016	0.096	-0.091
574	B4	22.9	0	-15	-0.036	0.239	1.236	-0.958	-0.011	0.090	0.393	-0.424	-0.001	0.031	0.144	-0.161
575	B4	22.4	30	-15	1.491	0.427	3.302	0.423	0.416	0.123	0.940	0.097	0.011	0.022	0.121	-0.065
576	B4	22.7	45	-15	1.535	0.424	3.198	0.464	0.437	0.126	0.947	0.114	0.016	0.021	0.145	-0.052
577	B4	22.6	45	0	1.681	0.441	3.562	0.642	0.016	0.029	0.190	-0.131	0.011	0.019	0.125	-0.087
578	B4	22.4	30	0	1.771	0.494	3.683	0.546	0.018	0.036	0.194	-0.114	0.012	0.024	0.128	-0.075
579	B4	23.0	0	0	-0.006	0.249	1.130	-1.133	0.009	0.040	0.223	-0.205	0.006	0.027	0.148	-0.136
580	B4	22.7	-30	0	0.009	0.129	0.453	-0.777	0.005	0.024	0.140	-0.146	0.003	0.016	0.092	-0.096
581	D4	22.8	-30	0	0.028	0.128	0.632	-0.607	0.009	0.023	0.160	-0.133	0.006	0.015	0.106	-0.088
582	D4	22.2	0	0	0.112	0.223	1.191	-0.587	0.015	0.035	0.249	-0.138	0.010	0.023	0.165	-0.091
583	D4	22.2	30	0	1.317	0.504	3.374	0.299	0.028	0.040	0.258	-0.130	0.019	0.026	0.170	-0.086
584	D4	22.4	45	0	0.848	0.383	2.664	0.019	0.025	0.042	0.245	-0.132	0.016	0.028	0.162	-0.087
585	D4	22.7	45	-15	0.681	0.348	2.733	-0.083	0.204	0.107	0.809	-0.083	0.014	0.028	0.176	-0.097
586	D4	22.6	30	-15	1.050	0.437	2.896	0.038	0.290	0.121	0.794	-0.044	0.006	0.028	0.141	-0.114
587	D4	22.6	0	-15	0.081	0.218	1.594	-0.555	0.029	0.079	0.511	-0.260	0.005	0.025	0.181	-0.115
588	D4	22.2	-30	-15	0.041	0.134	0.653	-0.612	0.015	0.049	0.289	-0.296	0.003	0.016	0.125	-0.112
589	D4	22.0	-30	-30	0.070	0.127	0.827	-0.499	0.045	0.084	0.598	-0.362	0.003	0.019	0.145	-0.093
590	D4	22.8	0	-30	0.086	0.163	0.900	-0.496	0.055	0.112	0.663	-0.387	0.003	0.025	0.129	-0.139
591	D4	22.5	30	-30	0.785	0.352	2.317	-0.031	0.516	0.241	1.635	-0.091	0.036	0.042	0.261	-0.100
592	D4	22.6	45	-30	0.570	0.297	1.976	-0.173	0.365	0.199	1.382	-0.187	0.021	0.034	0.207	-0.090
593	D4	22.4	45	-45	0.398	0.228	1.699	-0.030	0.470	0.285	2.160	-0.121	0.034	0.039	0.267	-0.079
594	D4	22.5	30	-45	0.563	0.273	1.769	0.004	0.670	0.331	2.146	-0.055	0.050	0.044	0.254	-0.106
595	D4	22.2	0	-45	0.073	0.104	0.627	-0.250	0.080	0.119	0.777	-0.324	0.003	0.023	0.139	-0.126
596	D4	22.3	-30	-45	0.049	0.088	0.583	-0.368	0.060	0.093	0.595	-0.440	0.005	0.018	0.120	-0.101
597	D4	22.2	-30	-60	0.045	0.047	0.336	-0.159	0.095	0.095	0.583	-0.385	0.006	0.017	0.109	-0.111
598	D4	22.6	0	-60	0.088	0.069	0.601	-0.071	0.168	0.126	0.987	-0.257	0.005	0.021	0.112	-0.122
599	D4	22.5	30	-60	0.403	0.193	1.358	-0.097	0.688	0.313	2.333	-0.119	-0.004	0.037	0.194	-0.164
600	D4	22.5	45	-60	0.255	0.142	1.197	-0.030	0.515	0.261	2.077	-0.059	0.024	0.030	0.191	-0.127

Phase 1, 2, and 3 Integrated Pressure Data

Run	Conf	Uref fps	Uref		Cfx			Cfz			Cmy					
			Yaw	Pitch	Mean	RMS	Max	Min	Mean	RMS	Max	Min	Mean	RMS	Max	Min
601	D4	22.3	45	-75	0.150	0.087	0.601	0.001	0.428	0.191	1.509	-0.082	-0.022	0.040	0.089	-0.210
602	D4	22.1	30	-75	0.241	0.114	0.803	0.033	0.473	0.196	1.552	-0.007	-0.073	0.052	0.058	-0.323
603	D4	22.5	0	-75	0.064	0.036	0.354	-0.020	0.189	0.099	0.733	-0.202	-0.008	0.023	0.058	-0.185
604	D4	22.4	-30	-75	0.036	0.029	0.261	-0.046	0.118	0.092	0.697	-0.327	-0.003	0.019	0.064	-0.140
605	D4	22.3	-30	-90	0.024	0.030	0.228	-0.048	0.082	0.082	0.464	-0.294	-0.016	0.020	0.032	-0.151
606	D4	22.7	0	-90	0.039	0.036	0.300	-0.041	0.115	0.090	0.578	-0.396	-0.026	0.024	0.027	-0.199
607	D4	22.5	30	-90	0.162	0.080	0.526	-0.010	0.134	0.116	0.722	-0.366	-0.107	0.053	0.007	-0.348
608	D4	22.3	45	-90	0.099	0.067	0.492	-0.040	0.179	0.116	0.748	-0.327	-0.066	0.044	0.026	-0.326
609	D4	22.7	45	-105	0.141	0.090	0.614	-0.032	-0.056	0.101	0.285	-0.594	-0.080	0.046	0.005	-0.323
610	D4	22.7	30	-105	0.212	0.106	0.673	-0.020	-0.069	0.109	0.341	-0.643	-0.124	0.054	-0.011	-0.363
611	D4	22.7	0	-105	0.042	0.050	0.475	-0.061	0.027	0.084	0.376	-0.449	-0.032	0.024	0.023	-0.251
612	D4	22.6	-30	-105	0.022	0.037	0.298	-0.071	0.028	0.066	0.309	-0.296	-0.019	0.017	0.016	-0.151
613	D4	22.2	-30	-120	0.021	0.048	0.339	-0.148	0.001	0.057	0.264	-0.324	-0.012	0.013	0.036	-0.112
614	D4	22.6	0	-120	0.050	0.057	0.419	-0.155	-0.017	0.064	0.227	-0.387	-0.023	0.016	0.046	-0.137
615	D4	22.8	30	-120	0.311	0.130	0.816	0.018	-0.204	0.102	0.085	-0.606	-0.111	0.047	-0.014	-0.306
616	D4	22.3	45	-120	0.220	0.116	0.807	-0.037	-0.126	0.094	0.138	-0.577	-0.085	0.044	0.003	-0.318
617	D4	22.6	45	-135	0.359	0.173	1.087	0.025	-0.208	0.113	0.045	-0.696	-0.071	0.040	0.010	-0.249
618	D4	22.3	30	-135	0.559	0.207	1.339	0.099	-0.376	0.133	-0.030	-0.890	-0.086	0.043	0.033	-0.269
619	D4	22.5	0	-135	0.076	0.086	0.612	-0.180	-0.063	0.074	0.144	-0.505	-0.006	0.017	0.087	-0.097
620	D4	22.5	-30	-135	0.021	0.064	0.390	-0.250	-0.018	0.057	0.212	-0.344	-0.001	0.012	0.069	-0.058
621	D4	22.2	-30	-150	0.011	0.089	0.439	-0.394	-0.014	0.050	0.214	-0.279	0.004	0.015	0.095	-0.043
622	D4	22.3	0	-150	0.102	0.130	0.813	-0.253	-0.074	0.078	0.133	-0.522	0.008	0.019	0.108	-0.059
623	D4	22.7	30	-150	0.872	0.298	2.001	0.133	-0.408	0.132	-0.072	-0.879	-0.055	0.036	0.054	-0.206
624	D4	22.5	45	-150	0.567	0.255	1.645	0.072	-0.233	0.112	-0.001	-0.738	-0.054	0.035	0.041	-0.233
625	D4	22.2	45	-165	0.705	0.308	2.145	0.006	-0.131	0.070	0.032	-0.450	-0.037	0.032	0.052	-0.182
626	D4	22.3	30	-165	1.108	0.395	2.607	0.237	-0.246	0.084	-0.042	-0.611	-0.033	0.034	0.068	-0.186
627	D4	22.5	0	-165	0.061	0.160	0.903	-0.479	-0.046	0.055	0.100	-0.392	0.019	0.020	0.136	-0.037
628	D4	22.3	-30	-165	-0.031	0.104	0.398	-0.522	0.003	0.035	0.148	-0.210	0.003	0.016	0.111	-0.043
629	D4	22.4	-30	180	-0.029	0.116	0.547	-0.559	-0.004	0.021	0.069	-0.136	0.003	0.014	0.090	-0.046
630	D4	22.5	0	180	0.089	0.171	0.933	-0.539	-0.026	0.031	0.056	-0.192	0.017	0.020	0.127	-0.037
631	D4	22.4	30	180	1.177	0.402	2.699	0.177	-0.009	0.040	0.170	-0.184	0.006	0.027	0.122	-0.113
632	D4	22.6	45	180	0.753	0.328	2.151	0.048	0.009	0.038	0.176	-0.142	-0.006	0.025	0.094	-0.116
633	B5	22.7	-30	0	-0.027	0.140	0.633	-0.577	0.018	0.028	0.162	-0.101	0.012	0.019	0.107	-0.067
634	B5	23.1	0	0	0.529	0.390	2.590	-0.317	0.020	0.040	0.291	-0.142	0.013	0.027	0.193	-0.094
635	B5	22.6	30	0	1.733	0.487	3.584	0.564	0.014	0.034	0.201	-0.113	0.009	0.023	0.133	-0.074
636	B5	23.1	45	0	1.686	0.422	3.485	0.626	0.011	0.028	0.151	-0.105	0.007	0.018	0.100	-0.070
637	B5	23.2	45	-15	1.619	0.402	3.286	0.666	0.461	0.117	0.982	0.182	0.018	0.019	0.126	-0.058
638	B5	22.9	30	-15	1.483	0.413	3.207	0.379	0.416	0.120	0.930	0.084	0.012	0.021	0.129	-0.057
639	B5	22.8	0	-15	0.517	0.350	2.227	-0.357	0.155	0.109	0.703	-0.237	0.010	0.031	0.176	-0.136
640	B5	22.4	-30	-15	-0.018	0.166	0.880	-0.678	0.016	0.055	0.340	-0.269	0.013	0.020	0.108	-0.080
641	B5	22.4	-30	-30	0.032	0.154	0.947	-0.456	0.045	0.097	0.733	-0.296	0.015	0.021	0.143	-0.092
642	B5	22.5	0	-30	0.543	0.347	2.385	-0.275	0.352	0.232	1.588	-0.274	0.022	0.039	0.209	-0.130
643	B5	23.1	30	-30	1.200	0.355	2.653	0.328	0.716	0.215	1.603	0.159	0.013	0.025	0.160	-0.079
644	B5	23.0	45	-30	1.269	0.344	2.875	0.372	0.802	0.234	1.841	0.184	0.040	0.039	0.249	-0.071
645	B5	23.0	45	-45	0.927	0.248	1.975	0.378	1.144	0.321	2.461	0.405	0.101	0.045	0.295	-0.035
646	B5	23.1	30	-45	0.848	0.304	2.131	0.071	1.007	0.385	2.678	0.063	0.074	0.049	0.320	-0.059
647	B5	22.6	0	-45	0.518	0.308	2.047	-0.179	0.605	0.382	2.569	-0.279	0.041	0.051	0.314	-0.111
648	B5	22.7	-30	-45	0.154	0.146	0.943	-0.169	0.191	0.166	1.188	-0.241	0.017	0.025	0.165	-0.090
649	B5	22.8	-30	-60	0.242	0.128	0.973	0.019	0.505	0.252	1.843	-0.031	0.029	0.030	0.184	-0.100
650	B5	23.1	0	-60	0.543	0.248	1.469	0.071	1.024	0.439	2.749	0.137	0.028	0.043	0.252	-0.131

Phase 1, 2, and 3 Integrated Pressure Data

Run	Conf	Uref fps	Uref		Cfx			Cfz			Cmy					
			Yaw	Pitch	Mean	RMS	Max	Min	Mean	RMS	Max	Min	Mean	RMS	Max	Min
651	B5	23.0	30	-60	0.530	0.174	1.272	0.134	1.145	0.403	2.841	0.259	0.075	0.044	0.269	-0.068
652	B5	23.1	45	-60	0.551	0.144	1.218	0.218	1.208	0.319	2.680	0.428	0.084	0.036	0.269	-0.035
653	B5	23.1	45	-75	0.262	0.087	0.628	0.077	0.857	0.251	1.902	0.234	-0.021	0.038	0.114	-0.168
654	B5	22.7	30	-75	0.294	0.099	0.730	0.089	1.098	0.267	2.245	0.403	0.000	0.038	0.121	-0.164
655	B5	22.7	0	-75	0.391	0.133	0.979	0.096	0.987	0.273	2.343	0.348	-0.081	0.057	0.102	-0.331
656	B5	23.2	-30	-75	0.210	0.094	0.776	0.036	0.704	0.248	2.036	0.132	-0.013	0.038	0.113	-0.216
657	B5	23.1	-30	-90	0.137	0.058	0.451	0.013	0.291	0.114	0.806	-0.132	-0.091	0.038	-0.009	-0.298
658	B5	22.9	0	-90	0.209	0.074	0.590	0.042	0.435	0.139	1.089	0.007	-0.138	0.049	-0.028	-0.391
659	B5	22.9	30	-90	0.163	0.057	0.479	0.026	0.565	0.141	1.199	0.122	-0.108	0.038	-0.017	-0.317
660	B5	23.1	45	-90	0.140	0.055	0.391	0.019	0.389	0.132	1.162	-0.054	-0.093	0.036	-0.013	-0.259
661	B5	23.0	45	-105	0.203	0.074	0.648	-0.034	-0.001	0.077	0.308	-0.454	-0.130	0.039	-0.014	-0.356
662	B5	23.0	30	-105	0.263	0.088	0.700	0.068	-0.009	0.088	0.358	-0.502	-0.166	0.047	-0.064	-0.390
663	B5	23.0	0	-105	0.180	0.076	0.561	0.019	0.041	0.081	0.385	-0.328	-0.122	0.044	-0.034	-0.333
664	B5	22.9	-30	-105	0.107	0.054	0.366	-0.027	0.018	0.066	0.265	-0.326	-0.072	0.027	-0.008	-0.198
665	B5	22.8	-30	-120	0.067	0.059	0.455	-0.089	-0.037	0.060	0.178	-0.392	-0.026	0.017	0.015	-0.152
666	B5	22.8	0	-120	0.198	0.114	0.683	-0.044	-0.093	0.081	0.148	-0.484	-0.083	0.048	0.009	-0.290
667	B5	22.8	30	-120	0.427	0.121	0.911	0.125	-0.208	0.090	0.064	-0.576	-0.176	0.048	-0.063	-0.392
668	B5	22.8	45	-120	0.395	0.117	0.888	0.126	-0.256	0.092	0.009	-0.709	-0.141	0.043	-0.045	-0.340
669	B5	22.9	45	-135	0.570	0.164	1.349	0.173	-0.299	0.098	-0.051	-0.744	-0.127	0.038	-0.030	-0.297
670	B5	22.8	30	-135	0.617	0.167	1.349	0.221	-0.283	0.091	-0.046	-0.706	-0.156	0.042	-0.047	-0.346
671	B5	22.5	0	-135	0.276	0.155	0.994	-0.117	-0.158	0.093	0.113	-0.623	-0.055	0.044	0.045	-0.257
672	B5	22.5	-30	-135	0.014	0.066	0.377	-0.219	-0.022	0.060	0.200	-0.335	0.004	0.012	0.061	-0.050
673	B5	22.2	-30	-150	-0.028	0.092	0.439	-0.466	0.002	0.055	0.229	-0.296	0.008	0.014	0.084	-0.036
674	B5	22.8	0	-150	0.370	0.246	1.589	-0.289	-0.161	0.101	0.131	-0.694	-0.030	0.040	0.080	-0.212
675	B5	22.7	30	-150	0.940	0.263	2.051	0.303	-0.325	0.106	-0.077	-0.779	-0.125	0.035	-0.014	-0.278
676	B5	22.7	45	-150	0.868	0.261	1.937	0.273	-0.297	0.102	-0.070	-0.725	-0.117	0.037	-0.011	-0.282
677	B5	22.6	45	-165	1.219	0.349	2.755	0.341	-0.171	0.064	-0.016	-0.513	-0.100	0.031	-0.006	-0.243
678	B5	22.8	30	-165	1.295	0.351	2.845	0.469	-0.197	0.070	-0.026	-0.499	-0.096	0.031	-0.003	-0.244
679	B5	22.8	0	-165	0.429	0.293	1.671	-0.243	-0.091	0.064	0.084	-0.381	-0.015	0.032	0.116	-0.159
680	B5	22.9	-30	-165	-0.053	0.112	0.374	-0.618	0.004	0.035	0.178	-0.156	0.006	0.013	0.076	-0.038
681	B5	22.2	-30	-180	-0.031	0.117	0.473	-0.525	-0.004	0.019	0.063	-0.122	0.002	0.013	0.081	-0.042
682	B5	22.7	0	180	0.438	0.339	1.966	-0.308	0.001	0.039	0.168	-0.166	-0.001	0.026	0.110	-0.111
683	B5	22.7	30	180	1.410	0.364	2.885	0.472	0.074	0.038	0.247	-0.127	-0.049	0.025	0.084	-0.164
684	B5	22.4	45	180	1.359	0.380	2.913	0.409	0.095	0.034	0.269	-0.041	-0.063	0.022	0.027	-0.178
685	D5	22.9	45	180	0.574	0.199	1.540	0.070	0.012	0.030	0.147	-0.117	-0.008	0.020	0.077	-0.097
686	D5	22.7	30	180	1.028	0.400	2.654	0.042	0.018	0.050	0.242	-0.143	-0.012	0.033	0.095	-0.160
687	D5	22.6	0	180	0.322	0.235	1.420	-0.207	-0.014	0.030	0.084	-0.184	0.009	0.020	0.122	-0.056
688	D5	22.3	-30	180	-0.002	0.122	0.612	-0.455	-0.003	0.020	0.068	-0.135	0.002	0.014	0.090	-0.045
689	D5	22.3	-30	-165	-0.021	0.122	0.584	-0.600	-0.003	0.039	0.154	-0.191	0.006	0.014	0.075	-0.044
690	D5	22.4	0	-165	0.285	0.219	1.542	-0.256	-0.078	0.063	0.054	-0.431	0.001	0.020	0.095	-0.079
691	D5	22.2	30	-165	1.015	0.398	2.662	0.013	-0.195	0.083	0.020	-0.544	-0.050	0.041	0.095	-0.249
692	D5	22.7	45	-165	0.530	0.186	1.484	0.030	-0.099	0.051	0.040	-0.351	-0.028	0.021	0.055	-0.156
693	D5	23.0	45	-150	0.399	0.147	1.224	0.007	-0.164	0.073	0.059	-0.575	-0.038	0.021	0.036	-0.171
694	D5	22.4	30	-150	0.801	0.318	2.086	0.061	-0.329	0.134	-0.001	-0.850	-0.076	0.045	0.058	-0.265
695	D5	22.5	0	-150	0.204	0.166	1.102	-0.205	-0.113	0.090	0.101	-0.610	-0.003	0.020	0.093	-0.118
696	D5	22.5	-30	-150	0.010	0.099	0.565	-0.385	-0.016	0.059	0.195	-0.351	0.006	0.013	0.078	-0.038
697	D5	22.7	-30	-135	0.035	0.079	0.466	-0.221	-0.040	0.069	0.191	-0.357	0.003	0.012	0.059	-0.064
698	D5	22.1	0	-135	0.140	0.123	0.770	-0.131	-0.105	0.097	0.119	-0.638	-0.017	0.021	0.052	-0.135
699	D5	23.0	30	-135	0.526	0.220	1.365	0.020	-0.294	0.129	0.022	-0.803	-0.109	0.054	0.022	-0.335
700	D5	22.6	45	-135	0.256	0.108	0.908	-0.026	-0.148	0.078	0.077	-0.602	-0.051	0.025	0.034	-0.226

Phase 1, 2, and 3 Integrated Pressure Data

Run	Conf	Uref		Cfx			Cfz			Cmy						
		fps	Yaw	Pitch	Mean	RMS	Max	Min	Mean	RMS	Max	Min	Mean	RMS	Max	Min
701	D5	22.8	45	-120	0.154	0.073	0.647	-0.018	-0.092	0.076	0.128	-0.562	-0.058	0.026	0.009	-0.225
702	D5	23.1	30	-120	0.326	0.139	0.946	0.034	-0.179	0.102	0.102	-0.637	-0.128	0.055	-0.015	-0.379
703	D5	22.7	0	-120	0.091	0.092	0.644	-0.113	-0.056	0.085	0.174	-0.540	-0.034	0.029	0.027	-0.213
704	D5	22.4	-30	-120	0.055	0.065	0.460	-0.115	-0.037	0.064	0.190	-0.382	-0.019	0.019	0.025	-0.153
705	D5	22.5	-30	-105	0.053	0.051	0.342	-0.052	0.011	0.064	0.357	-0.347	-0.036	0.026	0.014	-0.183
706	D5	22.7	0	-105	0.065	0.065	0.470	-0.082	0.014	0.075	0.337	-0.431	-0.044	0.034	0.017	-0.243
707	D5	23.0	30	-105	0.220	0.110	0.737	-0.015	-0.077	0.116	0.266	-0.696	-0.128	0.058	-0.010	-0.397
708	D5	23.1	45	-105	0.092	0.051	0.429	-0.028	-0.024	0.079	0.284	-0.484	-0.055	0.025	0.002	-0.233
709	D5	22.9	45	-90	0.066	0.040	0.344	-0.007	0.165	0.093	0.563	-0.433	-0.044	0.026	0.005	-0.228
710	D5	22.5	30	-90	0.173	0.082	0.566	-0.005	0.149	0.134	0.799	-0.443	-0.114	0.054	0.004	-0.374
711	D5	22.8	0	-90	0.072	0.056	0.421	-0.021	0.086	0.090	0.559	-0.314	-0.047	0.037	0.014	-0.279
712	D5	22.6	-30	-90	0.053	0.045	0.374	-0.025	0.081	0.075	0.399	-0.292	-0.035	0.030	0.016	-0.247
713	D5	22.9	-30	-75	0.069	0.049	0.441	-0.018	0.212	0.114	0.850	-0.140	-0.008	0.026	0.070	-0.193
714	D5	22.4	0	-75	0.107	0.074	0.567	-0.009	0.239	0.144	1.108	-0.164	-0.027	0.034	0.055	-0.240
715	D5	23.1	30	-75	0.233	0.111	0.793	-0.017	0.640	0.259	1.856	-0.050	-0.039	0.044	0.101	-0.278
716	D5	22.9	45	-75	0.103	0.041	0.363	0.007	0.418	0.158	1.288	-0.053	0.005	0.025	0.112	-0.134
717	D5	22.6	45	-60	0.208	0.075	0.782	-0.020	0.426	0.153	1.455	-0.056	0.022	0.021	0.128	-0.101
718	D5	22.8	30	-60	0.378	0.177	1.151	-0.051	0.772	0.374	2.529	-0.253	0.039	0.042	0.281	-0.129
719	D5	23.0	0	-60	0.170	0.117	0.874	-0.032	0.296	0.199	1.439	-0.139	0.000	0.025	0.125	-0.154
720	D5	22.7	-30	-60	0.096	0.075	0.560	-0.085	0.195	0.134	0.927	-0.236	0.009	0.020	0.095	-0.102
721	D5	22.3	-30	-45	0.091	0.116	0.794	-0.289	0.119	0.126	0.895	-0.262	0.013	0.020	0.135	-0.095
722	D5	22.6	0	-45	0.224	0.180	1.181	-0.160	0.247	0.208	1.433	-0.267	0.011	0.029	0.199	-0.108
723	D5	22.4	30	-45	0.538	0.273	2.001	-0.064	0.650	0.347	2.398	-0.166	0.052	0.049	0.281	-0.085
724	D5	22.7	45	-45	0.300	0.120	0.884	-0.076	0.340	0.149	1.130	-0.165	0.019	0.026	0.171	-0.090
725	D5	23.1	45	-30	0.398	0.181	1.316	-0.071	0.252	0.130	0.943	-0.103	0.013	0.027	0.172	-0.073
726	D5	23.1	30	-30	0.716	0.401	2.388	-0.211	0.452	0.254	1.455	-0.248	0.022	0.036	0.214	-0.103
727	D5	22.8	0	-30	0.316	0.254	1.644	-0.268	0.208	0.173	1.153	-0.224	0.014	0.030	0.205	-0.107
728	D5	22.7	-30	-30	0.047	0.136	0.829	-0.424	0.047	0.086	0.564	-0.310	0.011	0.018	0.121	-0.091
729	D5	22.8	-30	-15	0.029	0.157	0.819	-0.562	0.025	0.052	0.351	-0.225	0.011	0.017	0.118	-0.064
730	D5	23.0	0	-15	0.421	0.292	1.793	-0.256	0.127	0.092	0.583	-0.139	0.009	0.025	0.174	-0.080
731	D5	22.8	30	-15	0.960	0.446	2.795	-0.078	0.275	0.130	0.810	-0.056	0.012	0.030	0.176	-0.092
732	D5	23.1	45	-15	0.567	0.222	1.687	-0.077	0.173	0.083	0.628	-0.087	0.013	0.026	0.191	-0.062
733	D5	22.9	45	0	0.675	0.226	1.959	-0.020	0.020	0.038	0.245	-0.084	0.013	0.025	0.162	-0.056
734	D5	23.1	30	0	1.133	0.480	3.194	-0.064	0.028	0.043	0.251	-0.134	0.018	0.029	0.166	-0.088
735	D5	23.0	0	0	0.405	0.295	2.022	-0.285	0.017	0.031	0.209	-0.107	0.011	0.021	0.139	-0.071
736	D5	22.8	-30	0	0.004	0.152	0.937	-0.616	0.018	0.025	0.154	-0.111	0.012	0.017	0.102	-0.073
737	F3	20.0	-30	180	-0.159	0.151	0.491	-0.740	-0.024	0.033	0.081	-0.197	0.016	0.022	0.130	-0.054
738	F3	20.2	0	180	-0.030	0.150	0.709	-0.655	-0.030	0.034	0.053	-0.232	0.020	0.023	0.154	-0.035
739	F3	20.1	30	180	0.537	0.305	1.880	-0.340	-0.053	0.045	0.102	-0.298	0.035	0.030	0.197	-0.068
740	F3	20.3	30	165	0.166	0.207	1.048	-0.526	-0.031	0.044	0.179	-0.197	0.048	0.032	0.212	-0.056
741	F3	20.3	0	165	-0.020	0.163	0.760	-0.827	-0.031	0.043	0.116	-0.252	0.016	0.025	0.164	-0.061
742	F3	20.1	-30	165	-0.027	0.147	0.687	-0.592	-0.034	0.036	0.139	-0.191	0.017	0.025	0.158	-0.049
743	F3	20.3	-30	150	0.107	0.145	0.833	-0.378	0.016	0.064	0.318	-0.222	0.027	0.026	0.186	-0.052
744	F3	19.9	0	150	0.114	0.144	0.797	-0.609	0.033	0.068	0.328	-0.267	0.019	0.027	0.205	-0.081
745	F3	20.4	30	150	0.224	0.185	1.123	-0.345	0.035	0.066	0.328	-0.191	0.054	0.036	0.227	-0.050
746	F3	20.0	30	135	0.348	0.153	1.113	-0.150	0.207	0.114	0.750	-0.211	0.066	0.040	0.279	-0.060
747	F3	19.9	0	135	0.282	0.141	0.948	-0.235	0.189	0.116	0.741	-0.230	0.044	0.031	0.227	-0.054
748	F3	20.4	-30	135	0.254	0.139	0.993	-0.271	0.147	0.114	0.756	-0.320	0.050	0.032	0.253	-0.070
749	F3	20.1	-30	120	0.307	0.142	1.100	-0.104	0.240	0.180	1.321	-0.406	0.096	0.037	0.346	-0.001
750	F3	20.3	0	120	0.300	0.139	0.979	-0.159	0.226	0.175	1.175	-0.349	0.097	0.037	0.296	-0.020

Phase 1, 2, and 3 Integrated Pressure Data

Run	Conf	Uref fps	Cfx		Cfz				Cmy							
			Mean	RMS	Max	Min	Mean	RMS	Max	Min	Mean	RMS	Max			
751	F3	20.4	30	120	0.395	0.149	1.125	-0.043	0.334	0.186	1.273	-0.239	0.116	0.043	0.346	0.001
752	F3	20.4	30	105	0.364	0.115	0.999	0.060	0.374	0.182	1.314	-0.214	0.169	0.052	0.453	0.037
753	F3	20.3	0	105	0.358	0.129	0.939	0.051	0.397	0.238	1.491	-0.304	0.161	0.053	0.409	0.035
754	F3	20.3	-30	105	0.350	0.122	1.008	0.046	0.366	0.198	1.430	-0.329	0.161	0.053	0.448	0.047
755	F3	20.1	-30	90	0.295	0.078	0.623	0.106	0.047	0.156	0.625	-0.718	0.195	0.052	0.412	0.070
756	F3	20.6	0	90	0.279	0.078	0.604	0.098	0.335	0.134	0.949	-0.317	0.185	0.051	0.400	0.065
757	F3	20.2	30	90	0.290	0.075	0.597	0.088	0.063	0.148	0.631	-0.691	0.192	0.050	0.395	0.059
758	F3	20.2	30	75	0.275	0.068	0.615	0.106	-0.704	0.207	-0.164	-1.719	0.055	0.026	0.163	-0.057
759	F3	20.1	0	75	0.292	0.069	0.605	0.120	-0.619	0.172	-0.153	-1.373	0.081	0.030	0.202	-0.054
760	F3	20.5	-30	75	0.235	0.063	0.517	0.088	-0.599	0.192	-0.099	-1.504	0.047	0.025	0.156	-0.081
761	F3	20.1	-30	60	0.214	0.088	0.784	-0.011	-0.387	0.163	0.009	-1.500	-0.005	0.019	0.100	-0.098
762	F3	19.6	0	60	0.291	0.099	0.829	0.005	-0.539	0.189	-0.008	-1.590	-0.011	0.021	0.091	-0.122
763	F3	20.1	30	60	0.338	0.107	0.979	0.082	-0.637	0.203	-0.142	-1.827	-0.017	0.023	0.079	-0.133
764	F3	20.1	30	45	0.430	0.177	1.408	-0.045	-0.428	0.183	0.023	-1.396	0.001	0.021	0.103	-0.106
765	F3	20.4	0	45	0.086	0.112	0.930	-0.258	-0.057	0.094	0.209	-0.785	0.014	0.017	0.117	-0.044
766	F3	20.6	-30	45	0.168	0.113	0.897	-0.153	-0.141	0.100	0.119	-0.750	0.012	0.015	0.109	-0.038
767	F3	19.7	-30	30	0.031	0.151	1.086	-0.534	0.015	0.071	0.251	-0.495	0.019	0.022	0.177	-0.072
768	F3	20.4	0	30	0.002	0.151	0.888	-0.549	0.016	0.062	0.247	-0.342	0.010	0.021	0.132	-0.070
769	F3	19.9	30	30	0.311	0.252	1.591	-0.425	-0.149	0.127	0.202	-0.835	0.018	0.026	0.163	-0.085
770	F3	19.8	30	15	0.553	0.377	2.175	-0.673	-0.134	0.095	0.147	-0.594	0.009	0.029	0.154	-0.122
771	F3	20.3	0	15	-0.041	0.188	0.855	-0.867	0.023	0.040	0.204	-0.194	0.008	0.022	0.148	-0.118
772	F3	20.3	-30	15	-0.056	0.183	0.732	-0.786	0.039	0.052	0.237	-0.165	0.015	0.026	0.125	-0.072
773	F3	20.0	-30	0	-0.071	0.210	0.734	-0.869	0.017	0.045	0.215	-0.158	0.011	0.030	0.142	-0.104
774	F3	20.1	0	0	-0.025	0.230	1.202	-1.013	0.008	0.033	0.249	-0.190	0.005	0.022	0.165	-0.126
775	F3	20.4	30	0	0.461	0.410	2.243	-0.763	-0.007	0.051	0.235	-0.260	-0.005	0.034	0.156	-0.172
776	F3	20.1	30	-15	0.445	0.417	2.353	-0.941	0.125	0.144	0.767	-0.442	0.004	0.040	0.227	-0.160
777	F3	19.8	0	-15	0.031	0.248	1.214	-1.250	0.019	0.086	0.506	-0.483	0.007	0.026	0.214	-0.118
778	F3	19.8	-30	-15	-0.078	0.248	1.067	-1.024	-0.003	0.080	0.387	-0.375	0.012	0.030	0.139	-0.118
779	F3	20.5	-30	-30	0.001	0.205	1.232	-0.605	0.024	0.129	0.893	-0.396	0.013	0.027	0.163	-0.113
780	F3	19.9	0	-30	0.044	0.209	1.125	-0.737	0.036	0.137	0.759	-0.567	0.006	0.029	0.174	-0.164
781	F3	20.3	30	-30	0.438	0.355	2.143	-0.480	0.289	0.243	1.471	-0.295	0.021	0.042	0.267	-0.124
782	F3	19.9	30	-45	0.430	0.279	1.717	-0.272	0.475	0.319	1.985	-0.260	0.021	0.043	0.234	-0.184
783	F3	20.1	0	-45	0.131	0.172	1.139	-0.433	0.146	0.186	1.220	-0.547	0.007	0.033	0.180	-0.174
784	F3	20.3	-30	-45	0.150	0.167	1.139	-0.256	0.181	0.186	1.418	-0.310	0.015	0.030	0.214	-0.148
785	F3	20.0	-30	-60	0.320	0.147	1.018	0.011	0.606	0.255	1.771	-0.051	0.017	0.037	0.187	-0.189
786	F3	20.6	0	-60	0.338	0.151	1.240	0.033	0.647	0.267	2.250	-0.011	0.020	0.041	0.183	-0.204
787	F3	20.3	30	-60	0.443	0.185	1.353	0.056	0.809	0.311	2.339	0.109	0.014	0.043	0.195	-0.185
788	F3	20.2	30	-75	0.327	0.111	0.800	0.085	0.920	0.235	2.061	0.212	-0.051	0.056	0.096	-0.316
789	F3	20.3	0	-75	0.312	0.114	0.919	0.061	0.869	0.249	2.150	0.109	-0.050	0.065	0.130	-0.359
790	F3	20.3	-30	-75	0.296	0.109	0.828	0.094	0.842	0.237	1.916	0.150	-0.045	0.058	0.107	-0.328
791	F3	20.7	-30	-90	0.245	0.085	0.661	0.043	0.023	0.145	0.480	-0.816	-0.162	0.057	-0.029	-0.437
792	F3	20.4	0	-90	0.299	0.101	0.805	0.074	-0.075	0.158	0.356	-0.955	-0.198	0.067	-0.049	-0.533
793	F3	20.7	30	-90	0.249	0.079	0.655	0.054	0.056	0.136	0.495	-0.564	-0.165	0.052	-0.035	-0.434
794	F3	20.3	30	-105	0.191	0.070	0.537	0.046	-0.121	0.094	0.161	-0.553	-0.101	0.034	-0.028	-0.271
795	F3	20.3	0	-105	0.239	0.091	0.780	0.044	-0.200	0.123	0.218	-0.857	-0.119	0.043	-0.029	-0.365
796	F3	20.6	-30	-105	0.164	0.071	0.591	0.009	-0.083	0.098	0.252	-0.655	-0.090	0.034	-0.022	-0.281
797	F3	20.0	-30	-120	0.062	0.053	0.368	-0.103	-0.009	0.060	0.240	-0.301	-0.033	0.018	0.012	-0.132
798	F3	20.1	0	-120	0.086	0.060	0.454	-0.088	-0.014	0.064	0.283	-0.347	-0.045	0.020	0.011	-0.171
799	F3	20.1	30	-120	0.134	0.062	0.519	-0.037	-0.066	0.061	0.169	-0.440	-0.055	0.021	0.001	-0.169
800	F3	19.9	30	-135	0.289	0.130	0.973	-0.131	-0.263	0.111	0.069	-0.842	-0.012	0.022	0.089	-0.127

Phase 1, 2, and 3 Integrated Pressure Data

Run	Conf	Uref fps	Uref		Cfx			Cfz			Cmy					
			Yaw	Pitch	Mean	RMS	Max	Min	Mean	RMS	Max	Min	Mean	RMS	Max	Min
801	F3	20.2	0	-135	0.050	0.076	0.415	-0.198	-0.065	0.073	0.151	-0.428	0.007	0.016	0.100	-0.046
802	F3	20.3	-30	-135	-0.001	0.084	0.451	-0.291	-0.021	0.078	0.254	-0.443	0.010	0.015	0.080	-0.061
803	F3	19.6	-30	-150	-0.067	0.120	0.460	-0.539	0.010	0.069	0.245	-0.318	0.017	0.020	0.123	-0.048
804	F3	20.2	0	-150	0.026	0.099	0.528	-0.310	-0.043	0.061	0.152	-0.395	0.016	0.019	0.109	-0.047
805	F3	19.6	30	-150	0.385	0.204	1.248	-0.256	-0.240	0.106	0.098	-0.668	0.010	0.026	0.146	-0.091
806	F3	20.2	30	-165	0.681	0.306	1.998	-0.318	-0.187	0.080	0.096	-0.524	0.003	0.029	0.177	-0.097
807	F3	20.1	0	-165	0.032	0.135	0.730	-0.531	-0.030	0.045	0.123	-0.304	0.014	0.022	0.140	-0.057
808	F3	20.1	-30	-165	-0.054	0.159	0.654	-0.692	0.006	0.049	0.190	-0.243	0.006	0.024	0.143	-0.058
809	F7	21.8	-30	-165	0.127	0.173	0.901	-0.329	-0.061	0.055	0.100	-0.299	0.018	0.022	0.116	-0.051
810	F7	21.8	0	-165	0.108	0.129	0.914	-0.338	-0.039	0.047	0.082	-0.295	0.006	0.019	0.102	-0.050
811	F7	22.2	30	-165	0.286	0.216	1.152	-0.507	-0.123	0.068	0.133	-0.404	0.030	0.028	0.158	-0.058
812	F7	22.3	30	-150	0.257	0.155	0.890	-0.278	-0.182	0.084	0.128	-0.493	0.019	0.024	0.120	-0.064
813	F7	22.3	0	-150	0.083	0.098	0.707	-0.190	-0.058	0.060	0.099	-0.406	0.005	0.016	0.103	-0.048
814	F7	22.0	-30	-150	0.089	0.130	0.713	-0.319	-0.081	0.074	0.158	-0.417	0.017	0.017	0.087	-0.048
815	F7	22.6	-30	-135	0.124	0.093	0.616	-0.113	-0.128	0.080	0.115	-0.555	0.002	0.014	0.075	-0.060
816	F7	22.1	0	-135	0.082	0.076	0.515	-0.109	-0.078	0.070	0.103	-0.493	-0.002	0.012	0.057	-0.059
817	F7	22.1	30	-135	0.279	0.107	0.722	-0.064	-0.242	0.094	0.085	-0.635	-0.017	0.018	0.067	-0.098
818	F7	22.9	30	-120	0.140	0.054	0.444	-0.012	-0.085	0.052	0.114	-0.367	-0.052	0.018	-0.002	-0.147
819	F7	22.4	0	-120	0.062	0.053	0.359	-0.067	-0.024	0.050	0.160	-0.270	-0.028	0.018	0.014	-0.125
820	F7	22.3	-30	-120	0.078	0.055	0.402	-0.090	-0.047	0.052	0.181	-0.319	-0.029	0.018	0.014	-0.139
821	F7	22.7	-30	-105	0.123	0.064	0.518	-0.014	-0.046	0.083	0.245	-0.526	-0.071	0.030	-0.012	-0.257
822	F7	22.5	0	-105	0.165	0.077	0.556	0.022	-0.106	0.094	0.183	-0.564	-0.087	0.037	-0.020	-0.264
823	F7	22.5	30	-105	0.152	0.067	0.620	0.009	-0.054	0.085	0.226	-0.651	-0.088	0.033	-0.022	-0.296
824	F7	22.3	30	-90	0.193	0.066	0.526	0.039	0.078	0.132	0.570	-0.514	-0.128	0.044	-0.026	-0.348
825	F7	22.7	0	-90	0.236	0.084	0.620	0.058	-0.058	0.133	0.344	-0.736	-0.156	0.055	-0.038	-0.410
826	F7	22.4	-30	-90	0.185	0.071	0.508	0.002	0.017	0.126	0.438	-0.630	-0.123	0.047	-0.002	-0.336
827	F7	22.7	-30	-75	0.224	0.087	0.672	0.071	0.557	0.168	1.324	0.095	-0.048	0.049	0.073	-0.287
828	F7	22.5	0	-75	0.256	0.092	0.690	0.060	0.589	0.178	1.398	-0.013	-0.063	0.056	0.076	-0.322
829	F7	22.7	30	-75	0.262	0.088	0.696	0.071	0.598	0.161	1.321	0.015	-0.065	0.049	0.059	-0.305
830	F7	22.1	30	-60	0.362	0.153	1.036	-0.014	0.662	0.261	1.887	-0.052	0.012	0.036	0.151	-0.156
831	F7	22.4	0	-60	0.291	0.149	1.062	-0.002	0.522	0.251	1.970	-0.075	0.006	0.036	0.151	-0.149
832	F7	22.3	-30	-60	0.267	0.131	1.023	-0.009	0.490	0.214	1.788	-0.021	0.009	0.034	0.164	-0.146
833	F7	22.2	-30	-45	0.321	0.218	1.511	-0.125	0.360	0.241	1.727	-0.177	0.019	0.031	0.187	-0.136
834	F7	22.0	0	-45	0.306	0.221	1.607	-0.151	0.336	0.246	1.831	-0.190	0.014	0.032	0.246	-0.125
835	F7	22.2	30	-45	0.433	0.248	1.504	-0.063	0.511	0.290	1.807	-0.116	0.037	0.037	0.228	-0.101
836	F7	22.3	30	-30	0.495	0.327	2.309	-0.447	0.342	0.224	1.597	-0.299	0.032	0.037	0.247	-0.102
837	F7	22.4	0	-30	0.275	0.224	1.449	-0.385	0.181	0.147	0.977	-0.279	0.013	0.026	0.175	-0.108
838	F7	22.0	-30	-30	0.385	0.294	1.834	-0.451	0.258	0.194	1.243	-0.366	0.020	0.032	0.185	-0.122
839	F7	22.0	-30	-15	0.415	0.363	2.078	-0.522	0.140	0.126	0.746	-0.187	0.019	0.033	0.208	-0.086
840	F7	21.7	0	-15	0.261	0.239	1.529	-0.476	0.086	0.079	0.549	-0.149	0.010	0.022	0.154	-0.085
841	F7	22.1	30	-15	0.340	0.369	2.038	-0.712	0.124	0.127	0.760	-0.306	0.021	0.034	0.204	-0.134
842	F7	22.1	30	0	0.256	0.353	1.862	-0.897	0.029	0.048	0.268	-0.162	0.019	0.032	0.177	-0.107
843	F7	22.2	0	0	0.214	0.219	1.445	-0.390	0.011	0.027	0.182	-0.106	0.007	0.018	0.120	-0.070
844	F7	21.9	-30	0	0.324	0.336	1.843	-0.549	0.021	0.040	0.281	-0.146	0.014	0.026	0.186	-0.097
845	C5	22.0	-30	0	0.143	0.261	1.625	-0.575	0.019	0.034	0.210	-0.143	0.012	0.022	0.139	-0.095
846	C5	21.5	0	0	0.164	0.224	1.236	-0.591	0.010	0.030	0.213	-0.129	0.006	0.020	0.141	-0.085
847	C5	22.3	30	0	0.247	0.321	1.609	-0.759	0.016	0.044	0.264	-0.165	0.011	0.029	0.175	-0.109
848	C5	21.8	30	-15	0.244	0.333	1.835	-0.725	0.087	0.114	0.631	-0.300	0.014	0.030	0.179	-0.124
849	C5	21.7	0	-15	0.207	0.222	1.478	-0.524	0.063	0.068	0.516	-0.188	0.005	0.021	0.150	-0.102
850	C5	21.9	-30	-15	0.246	0.283	1.692	-0.642	0.082	0.090	0.635	-0.303	0.010	0.025	0.176	-0.123

Phase 1, 2, and 3 Integrated Pressure Data

Run	Conf	Uref fps	Uref		Cfx			Cfz			Cmy					
			Yaw	Pitch	Mean	RMS	Max	Min	Mean	RMS	Max	Min	Mean	RMS	Max	Min
851	C5	21.6	-30	-30	0.288	0.234	1.534	-0.339	0.186	0.150	0.954	-0.240	0.011	0.027	0.178	-0.122
852	C5	21.5	0	-30	0.266	0.231	1.488	-0.342	0.167	0.151	1.041	-0.222	0.007	0.026	0.205	-0.111
853	C5	22.1	30	-30	0.355	0.300	1.920	-0.355	0.238	0.202	1.325	-0.301	0.019	0.034	0.233	-0.133
854	C5	22.0	30	-45	0.385	0.247	1.955	-0.152	0.449	0.295	2.424	-0.192	0.030	0.040	0.285	-0.098
855	C5	21.6	0	-45	0.303	0.221	1.469	-0.277	0.331	0.254	1.823	-0.357	0.013	0.034	0.266	-0.138
856	C5	22.0	-30	-45	0.304	0.193	1.348	-0.138	0.343	0.218	1.525	-0.232	0.018	0.030	0.215	-0.105
857	C5	22.5	-30	-60	0.270	0.133	1.021	0.023	0.532	0.259	2.149	0.010	0.021	0.032	0.227	-0.120
858	C5	22.4	0	-60	0.338	0.185	1.402	-0.104	0.657	0.343	2.437	-0.237	0.024	0.037	0.222	-0.157
859	C5	22.2	30	-60	0.357	0.166	1.170	0.016	0.707	0.314	2.331	-0.007	0.029	0.036	0.251	-0.120
860	C5	22.2	30	-75	0.255	0.104	0.807	0.029	0.797	0.244	2.004	0.130	-0.027	0.043	0.114	-0.236
861	C5	22.3	0	-75	0.269	0.111	0.810	0.059	0.908	0.248	1.992	0.213	-0.017	0.051	0.123	-0.257
862	C5	22.8	-30	-75	0.193	0.085	0.598	0.044	0.699	0.231	1.877	0.134	-0.004	0.038	0.119	-0.177
863	C5	22.6	-30	-90	0.118	0.053	0.410	-0.031	0.251	0.108	0.801	-0.197	-0.078	0.035	0.020	-0.271
864	C5	22.8	0	-90	0.156	0.066	0.506	0.029	0.356	0.120	0.903	-0.112	-0.103	0.043	-0.019	-0.334
865	C5	22.3	30	-90	0.142	0.062	0.467	0.018	0.287	0.101	0.768	-0.173	-0.094	0.041	-0.012	-0.309
866	C5	22.2	30	-105	0.141	0.061	0.450	0.001	-0.044	0.067	0.285	-0.374	-0.083	0.032	-0.017	-0.237
867	C5	22.2	0	-105	0.122	0.072	0.541	-0.013	0.008	0.068	0.276	-0.390	-0.079	0.041	-0.008	-0.295
868	C5	22.4	-30	-105	0.111	0.061	0.454	-0.015	-0.035	0.067	0.248	-0.419	-0.065	0.031	-0.009	-0.230
869	C5	22.4	-30	-120	0.122	0.073	0.484	-0.046	-0.108	0.074	0.104	-0.466	-0.034	0.020	0.010	-0.148
870	C5	22.2	0	-120	0.091	0.071	0.480	-0.055	-0.069	0.071	0.128	-0.424	-0.029	0.020	0.016	-0.149
871	C5	22.4	30	-120	0.199	0.076	0.635	-0.001	-0.161	0.076	0.078	-0.595	-0.061	0.022	-0.008	-0.190
872	C5	21.9	30	-135	0.287	0.110	0.794	-0.045	-0.246	0.096	0.062	-0.675	-0.019	0.020	0.070	-0.101
873	C5	22.0	0	-135	0.104	0.086	0.632	-0.115	-0.093	0.078	0.100	-0.538	-0.005	0.013	0.057	-0.084
874	C5	22.3	-30	-135	0.141	0.093	0.645	-0.081	-0.139	0.083	0.089	-0.551	-0.001	0.014	0.054	-0.071
875	C5	22.2	-30	-150	0.122	0.131	0.826	-0.237	-0.095	0.079	0.112	-0.498	0.014	0.016	0.094	-0.049
876	C5	22.4	0	-150	0.106	0.110	0.664	-0.205	-0.072	0.070	0.107	-0.443	0.006	0.016	0.115	-0.049
877	C5	22.2	30	-150	0.279	0.160	1.001	-0.232	-0.201	0.094	0.104	-0.634	0.023	0.024	0.130	-0.055
878	C5	22.4	30	-165	0.357	0.214	1.262	-0.325	-0.128	0.066	0.096	-0.429	0.021	0.023	0.122	-0.051
879	C5	21.9	0	-165	0.103	0.142	0.876	-0.353	-0.038	0.048	0.099	-0.289	0.006	0.016	0.088	-0.050
880	C5	22.1	-30	-165	0.126	0.180	1.110	-0.326	-0.060	0.060	0.084	-0.362	0.017	0.019	0.108	-0.047
881	C5	21.8	-30	-180	0.178	0.184	1.215	-0.311	-0.009	0.030	0.075	-0.169	0.006	0.020	0.112	-0.050
882	C5	21.8	0	-180	0.134	0.166	1.027	-0.304	-0.010	0.026	0.079	-0.177	0.006	0.017	0.117	-0.052
883	C5	22.4	30	-180	0.380	0.224	1.476	-0.243	-0.028	0.037	0.097	-0.194	0.018	0.024	0.128	-0.064
884	C5	22.3	30	-165	0.370	0.219	1.525	-0.338	0.027	0.045	0.275	-0.135	0.046	0.025	0.166	-0.029
885	C5	22.0	0	-165	0.170	0.157	1.057	-0.261	0.022	0.033	0.173	-0.125	0.015	0.021	0.158	-0.043
886	C5	22.2	-30	-165	0.187	0.165	0.999	-0.307	0.021	0.035	0.207	-0.116	0.019	0.020	0.142	-0.038
887	C5	22.2	-30	-150	0.205	0.153	1.049	-0.282	0.064	0.060	0.393	-0.123	0.031	0.025	0.166	-0.050
888	C5	21.9	0	-150	0.190	0.143	0.978	-0.196	0.059	0.054	0.341	-0.127	0.029	0.028	0.178	-0.037
889	C5	22.2	30	-150	0.345	0.185	1.257	-0.216	0.090	0.067	0.442	-0.136	0.063	0.033	0.221	-0.040
890	C5	22.4	30	-135	0.353	0.152	1.158	-0.114	0.184	0.109	0.773	-0.193	0.079	0.037	0.277	-0.034
891	C5	22.0	0	-135	0.206	0.124	0.869	-0.226	0.102	0.087	0.607	-0.272	0.049	0.034	0.236	-0.056
892	C5	22.2	-30	-135	0.224	0.121	0.911	-0.158	0.133	0.090	0.708	-0.184	0.043	0.027	0.207	-0.031
893	C5	22.4	-30	-120	0.259	0.110	0.771	-0.026	0.220	0.131	0.866	-0.213	0.076	0.030	0.244	0.001
894	C5	22.4	0	-120	0.239	0.114	0.943	-0.105	0.180	0.132	1.049	-0.306	0.077	0.037	0.279	-0.017
895	C5	22.2	30	-120	0.343	0.132	0.998	-0.024	0.282	0.151	1.031	-0.204	0.104	0.038	0.300	0.002
896	C5	22.1	30	105	0.247	0.093	0.707	0.008	0.231	0.158	1.045	-0.349	0.118	0.041	0.321	0.019
897	C5	22.3	0	105	0.188	0.080	0.598	-0.093	0.142	0.151	0.825	-0.539	0.096	0.033	0.275	0.007
898	C5	22.2	-30	105	0.216	0.085	0.715	-0.011	0.200	0.148	1.003	-0.364	0.104	0.037	0.307	0.016
899	C5	22.7	-30	90	0.161	0.052	0.391	0.044	-0.133	0.133	0.243	-0.793	0.106	0.034	0.259	0.029
900	C5	22.8	0	90	0.146	0.047	0.362	0.014	-0.072	0.115	0.281	-0.774	0.096	0.031	0.239	0.009

Phase 1, 2, and 3 Integrated Pressure Data

Run	Conf	Uref fps	Cfx		Cfz			Cmy								
			Mean	RMS	Max	Min	Mean	RMS	Max	Min	Mean	RMS	Max	Min		
901	C5	23.0	30	90	0.159	0.051	0.429	0.024	-0.115	0.124	0.267	-0.819	0.105	0.034	0.284	0.016
902	C5	22.5	30	75	0.204	0.056	0.536	0.071	-0.700	0.228	-0.166	-1.976	0.011	0.022	0.097	-0.129
903	C5	23.0	0	75	0.117	0.035	0.328	0.018	-0.392	0.153	0.028	-1.263	0.007	0.017	0.082	-0.094
904	C5	22.7	-30	75	0.140	0.045	0.374	0.042	-0.512	0.185	-0.080	-1.485	0.002	0.020	0.075	-0.116
905	C5	22.6	-30	60	0.238	0.101	0.776	0.008	-0.394	0.175	-0.011	-1.319	0.006	0.018	0.099	-0.083
906	C5	22.4	0	60	0.160	0.106	0.775	-0.025	-0.241	0.179	0.071	-1.263	0.012	0.018	0.108	-0.076
907	C5	22.4	30	60	0.310	0.099	0.752	0.080	-0.586	0.192	-0.127	-1.468	-0.017	0.020	0.077	-0.119
908	C5	22.6	30	45	0.441	0.165	1.352	0.021	-0.413	0.155	-0.035	-1.321	0.013	0.020	0.120	-0.069
909	C5	22.1	0	45	0.182	0.159	1.083	-0.124	-0.141	0.133	0.110	-1.035	0.019	0.018	0.132	-0.035
910	C5	22.2	-30	45	0.291	0.175	1.397	-0.079	-0.242	0.151	0.061	-1.235	0.023	0.020	0.157	-0.029
911	C5	22.3	-30	30	0.309	0.215	1.369	-0.208	-0.131	0.102	0.138	-0.709	0.027	0.022	0.164	-0.033
912	C5	22.3	0	30	0.169	0.181	1.351	-0.298	-0.075	0.088	0.146	-0.711	0.013	0.019	0.147	-0.044
913	C5	22.3	30	30	0.523	0.249	1.734	-0.055	-0.250	0.125	0.027	-0.914	0.030	0.028	0.168	-0.055
914	C5	22.3	30	15	0.412	0.282	2.003	-0.414	-0.080	0.062	0.096	-0.432	0.020	0.028	0.160	-0.079
915	C5	22.0	0	15	0.174	0.196	1.428	-0.332	-0.034	0.047	0.099	-0.364	0.008	0.018	0.132	-0.066
916	C5	22.4	-30	15	0.243	0.229	1.530	-0.403	-0.039	0.052	0.095	-0.349	0.016	0.022	0.149	-0.056

Phase 4 Integrated Pressure Data

Phase 4 Integrated Pressure Data

Run	Conf	Uref fps	Cfx				Cfz				Cmy					
			Yaw	Pitch	Mean	RMS	Max	Min	Mean	RMS	Max	Min	Mean	RMS	Max	Min
1	I1	25.7	0	105	0.229	0.088	0.702	-0.040	0.164	0.146	0.856	-0.453	0.118	0.038	0.336	0.020
2	I1	25.4	0	75	0.143	0.037	0.361	0.035	-0.444	0.142	-0.037	-1.150	0.015	0.017	0.102	-0.081
3	I1	25.3	0	0	0.199	0.230	1.517	-0.554	0.009	0.029	0.228	-0.142	0.006	0.019	0.151	-0.094
4	I1	25.2	0	-15	0.259	0.246	1.635	-0.352	0.081	0.082	0.525	-0.177	0.007	0.024	0.167	-0.087
5	I1	25.2	0	-60	0.350	0.195	1.585	-0.014	0.702	0.376	3.220	-0.122	0.032	0.041	0.315	-0.133
6	I4	25.6	0	0	0.277	0.271	1.704	-0.329	0.011	0.030	0.206	-0.113	0.007	0.020	0.136	-0.075
7	I4	25.9	0	-15	0.383	0.315	1.991	-0.297	0.112	0.098	0.677	-0.192	0.006	0.024	0.170	-0.105
8	I4	25.6	0	-60	0.438	0.227	1.454	-0.032	0.892	0.451	3.145	-0.034	0.044	0.047	0.329	-0.137
9	I4	25.5	0	105	0.211	0.092	0.753	0.010	0.161	0.139	0.994	-0.409	0.107	0.043	0.340	0.014
10	I4	25.4	0	75	0.115	0.052	0.442	0.009	-0.393	0.194	-0.010	-1.612	0.006	0.021	0.103	-0.097
11	I3	25.4	0	75	0.117	0.054	0.522	0.004	-0.397	0.207	0.054	-1.625	0.007	0.023	0.147	-0.142
12	I3	25.8	0	105	0.196	0.092	0.714	-0.095	0.150	0.145	0.930	-0.490	0.099	0.043	0.339	-0.008
13	I3	25.5	0	-60	0.403	0.219	1.478	-0.022	0.813	0.433	2.940	-0.072	0.038	0.049	0.314	-0.149
14	I3	25.9	0	-15	0.364	0.313	1.992	-0.425	0.109	0.101	0.694	-0.267	0.007	0.026	0.193	-0.113
15	I3	26.1	0	0	0.254	0.269	1.674	-0.371	0.010	0.030	0.230	-0.113	0.007	0.020	0.152	-0.075
16	I2	25.2	0	0	0.260	0.275	1.654	-0.404	0.010	0.031	0.207	-0.132	0.007	0.021	0.137	-0.087
17	I2	25.3	0	-15	0.324	0.300	1.947	-0.497	0.097	0.096	0.683	-0.221	0.007	0.026	0.199	-0.118
18	I2	25.4	0	-60	0.392	0.215	1.438	-0.050	0.791	0.424	2.977	-0.118	0.037	0.045	0.306	-0.153
19	I2	25.3	0	75	0.112	0.054	0.452	-0.002	-0.380	0.196	0.090	-1.550	0.007	0.022	0.110	-0.102
20	I2	25.4	0	105	0.199	0.089	0.665	-0.039	0.133	0.143	0.862	-0.503	0.104	0.042	0.314	0.008
21	I1	25.5	30	105	0.338	0.103	0.838	0.071	0.268	0.143	0.896	-0.252	0.170	0.049	0.404	0.049
22	I1	25.4	30	75	0.220	0.052	0.430	0.079	-0.617	0.164	-0.210	-1.467	0.035	0.020	0.121	-0.062
23	I1	25.5	30	-60	0.367	0.184	1.271	-0.021	0.739	0.347	2.558	-0.044	0.034	0.042	0.243	-0.138
24	I1	25.4	30	-15	0.322	0.319	1.901	-0.625	0.119	0.115	0.741	-0.275	0.021	0.033	0.206	-0.117
25	I1	25.3	30	0	0.323	0.307	1.853	-0.585	0.020	0.046	0.292	-0.170	0.013	0.031	0.193	-0.113
26	I2	25.1	30	0	0.388	0.322	1.823	-0.619	0.024	0.050	0.275	-0.181	0.016	0.033	0.182	-0.120
27	I2	25.1	30	-15	0.337	0.327	1.993	-0.617	0.126	0.118	0.759	-0.235	0.023	0.035	0.208	-0.115
28	I2	25.2	30	-60	0.363	0.187	1.286	-0.015	0.735	0.359	2.469	0.005	0.035	0.041	0.267	-0.126
29	I2	25.1	30	75	0.230	0.052	0.466	0.084	-0.664	0.166	-0.182	-1.653	0.033	0.020	0.123	-0.090
30	I2	25.3	30	105	0.368	0.114	0.957	0.049	0.301	0.156	1.117	-0.227	0.184	0.055	0.467	0.044
31	I8	25.5	0	105	0.220	0.094	0.708	-0.037	0.158	0.130	0.817	-0.387	0.113	0.046	0.350	0.008
32	I8	25.7	0	75	0.122	0.054	0.421	-0.010	-0.414	0.197	0.040	-1.640	0.007	0.021	0.103	-0.128
33	I8	25.8	0	-60	0.394	0.246	1.738	-0.027	0.779	0.491	3.575	-0.085	0.032	0.048	0.365	-0.186
34	I8	26.1	0	-15	0.345	0.292	1.864	-0.367	0.102	0.092	0.583	-0.155	0.006	0.024	0.143	-0.089
35	I8	25.9	0	0	0.306	0.290	1.790	-0.340	0.010	0.030	0.214	-0.106	0.006	0.020	0.142	-0.070
36	I7	26.4	0	0	0.291	0.267	1.979	-0.357	0.009	0.029	0.255	-0.109	0.006	0.019	0.169	-0.072
37	I7	26.3	0	-15	0.383	0.314	1.840	-0.335	0.112	0.099	0.621	-0.169	0.006	0.024	0.171	-0.103
38	I7	25.6	0	-60	0.412	0.239	1.502	-0.056	0.826	0.484	3.206	-0.162	0.037	0.049	0.325	-0.162
39	I7	25.9	0	75	0.127	0.054	0.457	0.016	-0.439	0.197	-0.049	-1.687	0.006	0.022	0.121	-0.129
40	I7	26.2	0	105	0.207	0.091	0.685	-0.030	0.153	0.139	0.892	-0.425	0.106	0.043	0.342	0.011
41	I6	25.6	0	105	0.201	0.085	0.727	-0.051	0.150	0.137	0.927	-0.366	0.102	0.040	0.326	-0.004
42	I6	25.4	0	75	0.123	0.052	0.437	0.019	-0.402	0.198	-0.040	-1.607	0.010	0.021	0.104	-0.133
43	I6	25.4	0	-60	0.449	0.257	1.652	-0.007	0.923	0.535	3.457	-0.061	0.048	0.055	0.363	-0.146
44	I6	25.3	0	-15	0.385	0.307	2.016	-0.297	0.114	0.098	0.632	-0.129	0.007	0.024	0.162	-0.101
45	I6	25.5	0	0	0.290	0.250	1.736	-0.353	0.009	0.029	0.200	-0.102	0.006	0.019	0.132	-0.067
46	I5	25.1	0	0	0.282	0.230	1.598	-0.289	0.021	0.030	0.218	-0.100	0.014	0.020	0.144	-0.066
47	I5	25.2	0	75	0.201	0.043	0.420	0.070	-0.626	0.150	-0.104	-1.405	0.021	0.020	0.097	-0.096
48	I5	25.0	0	105	0.237	0.088	0.734	-0.035	0.192	0.147	0.986	-0.419	0.119	0.038	0.336	0.017
49	I5	25.0	0	-15	0.366	0.269	1.979	-0.417	0.112	0.089	0.717	-0.241	0.009	0.025	0.236	-0.119
50	I5	25.0	0	-60	0.389	0.205	1.532	-0.031	0.778	0.397	2.870	-0.058	0.035	0.042	0.286	-0.138

Phase 4 Integrated Pressure Data

Run	Conf	Uref fps		Yaw	Pitch	Cfx			Cfz			Cmy					
		Mean	RMS			Max	Min	Mean	RMS	Max	Min	Mean	RMS	Max	Min		
51	I5	24.9	0	0	0	0.373	0.261	1.813	-0.303	0.007	0.029	0.221	-0.120	0.004	0.019	0.146	-0.079
52	I11	25.4	30	-60	0	0.322	0.189	1.296	-0.078	0.664	0.376	2.686	-0.118	0.035	0.041	0.283	-0.129
53	I11	25.2	30	-15	0	0.361	0.288	1.755	-0.364	0.119	0.102	0.644	-0.149	0.014	0.028	0.173	-0.084
54	I11	25.2	30	75	0	0.127	0.046	0.410	0.019	-0.472	0.198	-0.023	-1.607	0.000	0.020	0.086	-0.135
55	I11	25.5	30	105	0	0.275	0.099	0.761	0.018	0.202	0.142	0.886	-0.351	0.141	0.049	0.391	0.023
56	I11	25.3	30	0	0	0.346	0.269	1.754	-0.287	0.021	0.039	0.228	-0.092	0.014	0.026	0.151	-0.061
57	I10	24.7	30	0	0	0.372	0.270	1.709	-0.260	0.024	0.040	0.272	-0.104	0.016	0.027	0.180	-0.069
58	I10	24.7	30	-15	0	0.412	0.308	1.944	-0.342	0.135	0.104	0.690	-0.166	0.016	0.027	0.177	-0.094
59	I10	25.2	30	-60	0	0.341	0.205	1.292	-0.073	0.681	0.388	2.636	-0.078	0.030	0.041	0.278	-0.146
60	I10	25.1	30	75	0	0.123	0.044	0.367	0.008	-0.471	0.191	0.082	-1.642	-0.002	0.019	0.075	-0.122
61	I10	25.3	30	105	0	0.264	0.097	0.761	0.011	0.197	0.137	0.994	-0.343	0.135	0.049	0.373	0.029
62	I9	25.5	30	105	0	0.247	0.089	0.771	-0.003	0.190	0.141	0.955	-0.383	0.125	0.041	0.358	0.018
63	I9	25.7	30	75	0	0.138	0.036	0.333	0.031	-0.449	0.143	-0.036	-1.286	0.011	0.018	0.085	-0.105
64	I9	25.1	30	-60	0	0.301	0.186	1.215	-0.073	0.585	0.351	2.342	-0.161	0.021	0.038	0.243	-0.144
65	I9	25.1	30	-15	0	0.221	0.208	1.265	-0.343	0.073	0.077	0.565	-0.188	0.009	0.023	0.197	-0.084
66	I9	25.1	30	0	0	0.194	0.204	1.299	-0.270	0.008	0.030	0.227	-0.091	0.006	0.020	0.150	-0.060
67	I7	25.3	30	0	0	0.389	0.271	1.720	-0.272	0.025	0.042	0.235	-0.099	0.017	0.028	0.155	-0.065
68	I7	25.4	30	-15	0	0.380	0.287	1.972	-0.338	0.126	0.104	0.710	-0.162	0.016	0.028	0.185	-0.098
69	I7	25.4	30	-60	0	0.347	0.205	1.336	-0.024	0.684	0.381	2.803	-0.028	0.028	0.039	0.250	-0.130
70	I7	25.6	30	75	0	0.120	0.040	0.384	0.014	-0.452	0.163	0.001	-1.341	-0.001	0.019	0.086	-0.111
71	I7	25.4	30	105	0	0.261	0.094	0.703	0.006	0.187	0.129	0.837	-0.336	0.135	0.047	0.352	0.032
72	I6	25.1	30	105	0	0.232	0.097	0.799	-0.005	0.165	0.152	0.930	-0.405	0.120	0.045	0.413	0.023
73	I6	25.4	30	75	0	0.133	0.043	0.385	0.021	-0.490	0.180	-0.065	-1.634	0.001	0.020	0.072	-0.130
74	I6	25.4	30	-60	0	0.330	0.183	1.289	-0.044	0.664	0.348	2.298	-0.061	0.031	0.039	0.242	-0.133
75	I6	25.3	30	-15	0	0.425	0.298	1.896	-0.243	0.144	0.110	0.680	-0.131	0.019	0.030	0.183	-0.075
76	I6	25.1	30	0	0	0.392	0.286	1.872	-0.238	0.029	0.045	0.259	-0.102	0.019	0.030	0.171	-0.067
77	I5	25.3	30	0	0	0.451	0.297	2.071	-0.490	0.030	0.043	0.246	-0.105	0.020	0.029	0.163	-0.069
78	I5	25.3	30	-15	0	0.420	0.272	1.730	-0.385	0.140	0.100	0.652	-0.152	0.017	0.028	0.183	-0.076
79	I5	25.3	30	-60	0	0.308	0.174	1.164	-0.025	0.598	0.320	2.227	-0.010	0.022	0.035	0.186	-0.123
80	I5	25.5	30	75	0	0.138	0.038	0.342	0.034	-0.493	0.169	-0.053	-1.510	0.004	0.019	0.077	-0.104
81	I5	25.6	30	105	0	0.273	0.094	0.758	0.021	0.194	0.136	0.948	-0.397	0.141	0.045	0.359	0.041

7.3 APPENDIX C - WIND CHARACTERISTICS SIMULATED IN A WIND TUNNEL

This section describes some of the primary parameters associated with winds in a thermally neutral atmospheric boundary layer that are commonly simulated in a wind tunnel for proper measurement of wind loads on a scaled model. These parameters specify mean, or time-averaged, and turbulence characteristics of winds which can then be related to the surface roughness of the field site.

C.1 Mean Wind Speed Characteristics

C.1.1. Power Law

Historically, the expression, which describes the mean wind profile over the height of the atmospheric boundary layer, is the power law proposed by Hellman (1916). The power law is given by

$$U(z) = U_R \left(\frac{z}{z_R} \right)^\alpha \quad (\text{C.1})$$

where U is the mean wind speed, z is the height above the ground, and α is the power-law exponent dependent on roughness of terrain and averaging time of measurements. The height z_R is the reference height, commonly 10 meters or 33 ft, and U_R represents the wind speed at the reference height.

The power-law exponent is obtained by a linear regression of wind data measured at different heights on a log-log basis as illustrated in Figure C-1(a). Recommended values of power-law exponent are tabulated in Table C-1.

Table C-1 Recommended values of power-law exponent

	Davenport (1965)	ASCE A58.1 (1982)
Coastal Areas	-	1/10 (0.10)
Open Terrain	0.16	1/7 (0.14)
Suburban Terrain	0.28	1/4.5 (0.22)
Center of Large City	0.4	1/3 (0.33)

C.1.2. Logarithmic Law

Another commonly used expression, particularly in micrometeorological practice, is the logarithmic law that was developed from the similarity theory of a boundary layer flow over a flat plate. Because it has an approximate theoretical basis, meteorologists regard the logarithmic law as a more suitable representation of strong wind profiles than the power law in the lower atmosphere, say up to 50 meters. It is given by

$$U(z) = \frac{u_*}{k} \ln \left(\frac{z}{z_o} \right) \quad (\text{C.2})$$

in which u_* is the shear velocity, z_o is the aerodynamic roughness length, and k is the von Karman's constant, approximately 0.4. The shear velocity may be interpreted as a fluid velocity which would cause a normal stress (i.e., dynamic pressure) equivalent to one half, in magnitude, of the shear stress occurring

over a solid surface, and the roughness length as a height at which the fluid velocity in Equation 6.2 vanishes due to friction.

The roughness length, z_o , is obtained by a regression on a linear-log basis as shown in Figure C-1(b). Values of z_o corresponding to different types of surface roughness have been reported from various sources, however considerable scatter exists from experiment to experiment. The variability is generally attributed to local flow inhomogeneities that cannot be easily accounted for, and to some extent, the fact that the estimate of z_o is extremely susceptible to accuracy involving wind speed measurements due to extrapolation in the regression technique.

Typical roughness lengths for various types of terrain are given in Table C-2.

Table C-2 Typical surface roughness lengths, Simiu et al. (1996)

Type of Surface	z_o (cm)
Sand	0.01-0.1
Snow surface	0.1-0.6
Mown grass (~0.01 m)	0.1-1
Low grass, steppe	1-4
Fallow field	2-3
High grass	4-10
Palmetto	10-30
Pine forest	90-100
Sparsely built-up suburbs	20-40
Densely built-up suburbs	80-120
Center of large cities	200-300

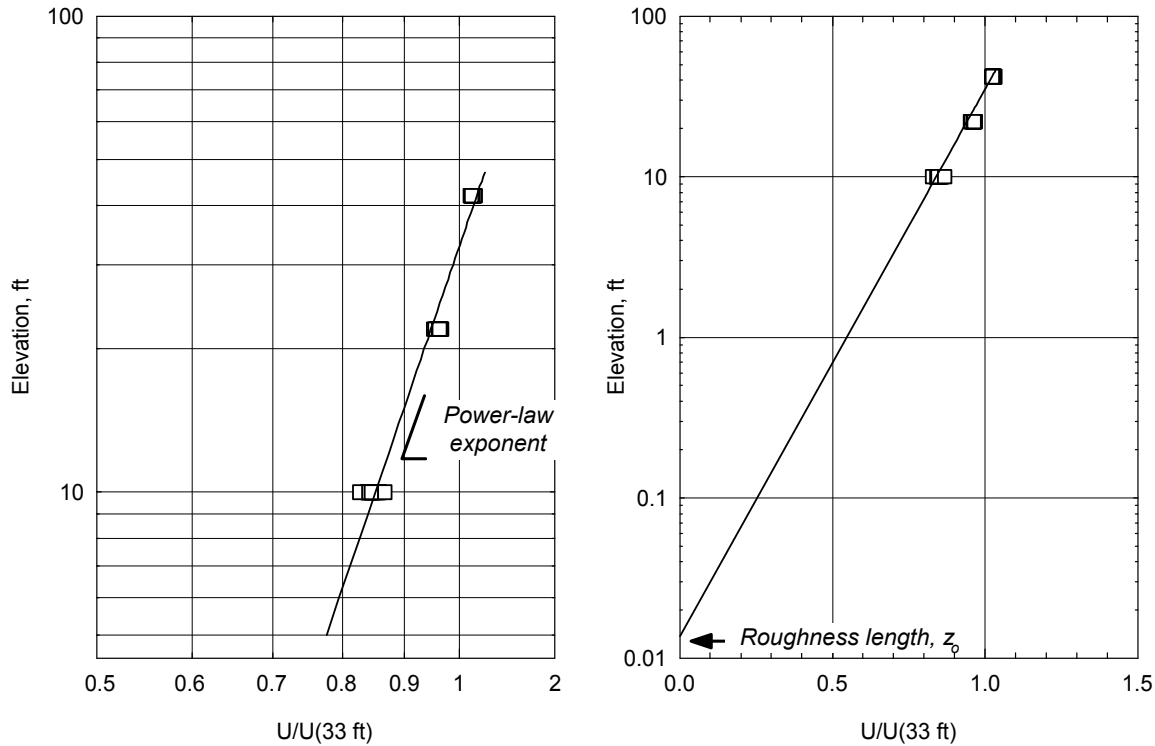


Figure C-1 Regression of wind speed data

C.2. Turbulence Characteristics

C.2.1. Local Turbulence Intensity

Of all the statistical measures of atmospheric turbulence, the turbulence (gustiness) intensity is the simplest parameter. It is defined for the longitudinal component as

$$I_u(z) = \frac{\sigma_u(z)}{U(z)} \quad (\text{C.3})$$

where I_u is the local turbulence intensity and $\sigma_u(z)$ is the standard deviation of the velocity fluctuations in the longitudinal direction at height z . Vertical and lateral turbulence intensity may be similarly defined.

Turbulence intensity can be estimated using several different available empirical equations. Lumley and Panofsky (1964) suggests

$$I_u(z) = \frac{Ck}{\ln\left(\frac{z}{z_o}\right)} \quad (\text{C.4})$$

where C is the constant that varies approximately from 2.0 to 2.5 depending on the roughness length z_o , see Simiu and Scanlan (1996). For a lower surface layer below a height of 100 m, Snyder (1981)

proposed the following formula.

$$I_u(z) = \alpha \frac{\ln\left(\frac{30}{z_o}\right)}{\ln\left(\frac{z}{z_o}\right)} \quad (C.5)$$

in which the heights are measured in full-scale meters, and α is the power-law exponent.

When a mean wind speed is relatively high, say above 20 mph, lateral turbulence intensity may be approximated by the standard deviation of wind direction fluctuations. It can be shown that

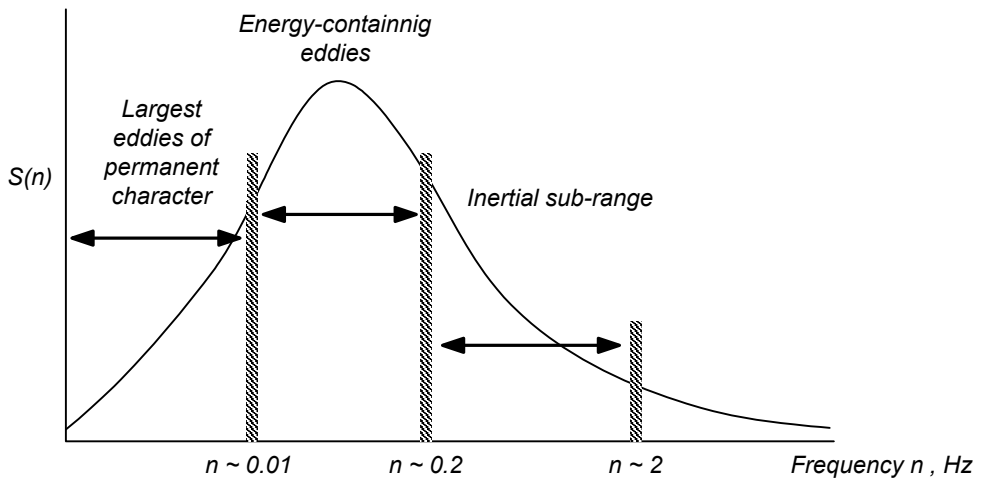
$$I_v(z) = \frac{\pi\sigma_\theta(z)}{180} \quad (C.6)$$

Here, I_v is the lateral turbulence intensity and σ_θ is the standard deviation of wind direction fluctuations measured in degrees. The magnitude of lateral turbulence intensity is somewhat smaller than longitudinal component. For example, empirical equations for velocity power spectral densities proposed by Kaimal (1972), described below, imply that that

$$\frac{I_v(z)}{I_u(z)} = 0.63 \quad (C.7)$$

C.2.2 . Power Spectral Density

Velocity fluctuations of atmospheric turbulence are a random process, and turbulence can be regarded as a combination of fluid motions by eddies of various sizes, each associated with a unique periodicity. Contributions by these eddies to the total turbulence kinetic energy are conveniently described by a power spectral density function. Power spectral densities of atmospheric turbulence are known to depend on the measurement height, and commonly characterized by several distinct regions as illustrated in Figure C-2 after Hinze (1975). Referring to the Figure, the inertial sub-range of turbulence is often considered to be of particular significance as far as wind loads on civil engineering structures are concerned. This is because structural natural frequencies typically fall in the inertial sub-range and the resulting quasi-steady or resonance excitation is controlled by characteristics of this spectral range.



Note: Frequency values are nominal, and vary depending on wind speed and height.

Figure C-2 A form of atmospheric turbulence spectrum, Hinze (1975)

Techniques to obtain a power spectrum density are readily available in a number of sources such as the one by Bendat and Piersol (1971), which involve a Fourier transform of velocity time series. A description of those techniques is beyond the scope of this report, and is omitted here. There are also several empirical equations for longitudinal atmospheric turbulence developed from field measurements. One of the earliest models was proposed by Davenport (1965), and subsequently adopted in the National Building Code of Canada (1980), which is given by

$$\frac{nS(n)}{u_*^2} = 4.0 \frac{x^2}{(1+x^2)^{4/3}} \quad (\text{C.8})$$

where S is the power spectral density, n is the frequency in Hz, and x is defined as

$$x = \frac{1200n}{U(10)} \quad (\text{C.9})$$

in which $U(10)$ is the mean wind speed in meters per second at $z = 10$ m. It should be noted that Davenport's model does not account for the dependence of spectra on height. A more elaborate model was suggested by Kaimal (1972) as

$$\frac{nS(z,n)}{u_*^2} = \frac{200f}{(1+50f)^{5/3}} \quad (\text{C.10})$$

in which f is typically known as the reduced frequency defined by

$$f = \frac{nz}{U(z)}. \quad (\text{C.11})$$

Kaimal also proposed a model for the lateral turbulence spectrum as follows.

$$\frac{nS_v(z, n)}{u_*^2} = \frac{15f}{(1+9.5f)^{5/3}}. \quad (\text{C.12})$$

To illustrate some of the noteworthy properties of a power spectral density, consider time series of wind velocity fluctuations $u(t)$. Then

$$\sigma_u^2 = \int_0^\infty S(n)dn \quad (\text{C.13})$$

and

$$R_u(\tau) = \lim_{T \rightarrow \infty} \frac{1}{2T} \int_{-T}^T u(t)u(t+\tau)dt = \int_0^\infty S(n)\cos(2\pi n\tau)dn \quad (\text{C.14})$$

where $R_u(\tau)$ is the auto-covariance function of the original velocity time series. Applying the spectral property in Equation (C.13) to the Kaimal's longitudinal and lateral spectrum models above, it can be shown that

$$\sigma_u^2 = 6u_*^2 \quad (\text{C.15})$$

for the longitudinal turbulence, and

$$\sigma_v^2 = \frac{45}{19}u_*^2 \quad (\text{C.16})$$

for the lateral turbulence. Equations (I.15) and (I.16) yield

$$\frac{I_v(z)}{I_u(z)} = \frac{\sigma_v/U(z)}{\sigma_u/U(z)} = 0.63 \quad (\text{C.17})$$

as mentioned in the previous section.

C.2.3. Integral Length Scale

Integral scales of turbulence represent the average size of turbulence eddies in three orthogonal directions associated with the longitudinal, lateral and vertical components of fluctuating velocity, i.e. a total of 9 scales to be considered. The most frequently evaluated length scale for characterization of winds and load effects on standing structures is the longitudinal length scale associated with the longitudinal turbulence. Formally, the longitudinal integral length scale is defined as

$$L_{ux} = \frac{1}{\sigma_u^2} \int_0^\infty R_{u1u2}(x)dx \quad (\text{C.18})$$

where $R_{u1u2}(x)$ is the cross-covariance of the longitudinal turbulence components $u1$ and $u2$ measured at two separate points in space with the longitudinal distance of x . However, a simplified approximation to

the above equation is widely accepted based on the Taylor's frozen field hypothesis (1938) that states that;

...the sequence of changes in the fluid velocity at the fixed point are simply due to the passage of an unchanging pattern of turbulent motion over the point,

and given by

$$L_{ux} = \frac{U}{\sigma_u^2} \int_0^\infty R_u(\tau) d\tau . \quad (\text{C.19})$$

This approximation allows the longitudinal length scale to be obtained by a temporal auto-covariance of the turbulence that can be calculated using Equation (C.14).

Among several empirical expressions for longitudinal length scale, the model proposed by Counihan (1975) has been widely recognized. The model takes the following expression.

$$L_{ux} = Cz^m \quad (\text{C.20})$$

where C and m are constants dependent on the surface roughness length, z_o , and all lengths are measured in meters. A model suggested by ESDU (1975) is also often referenced, which is essentially a variation of Counihan's model for which

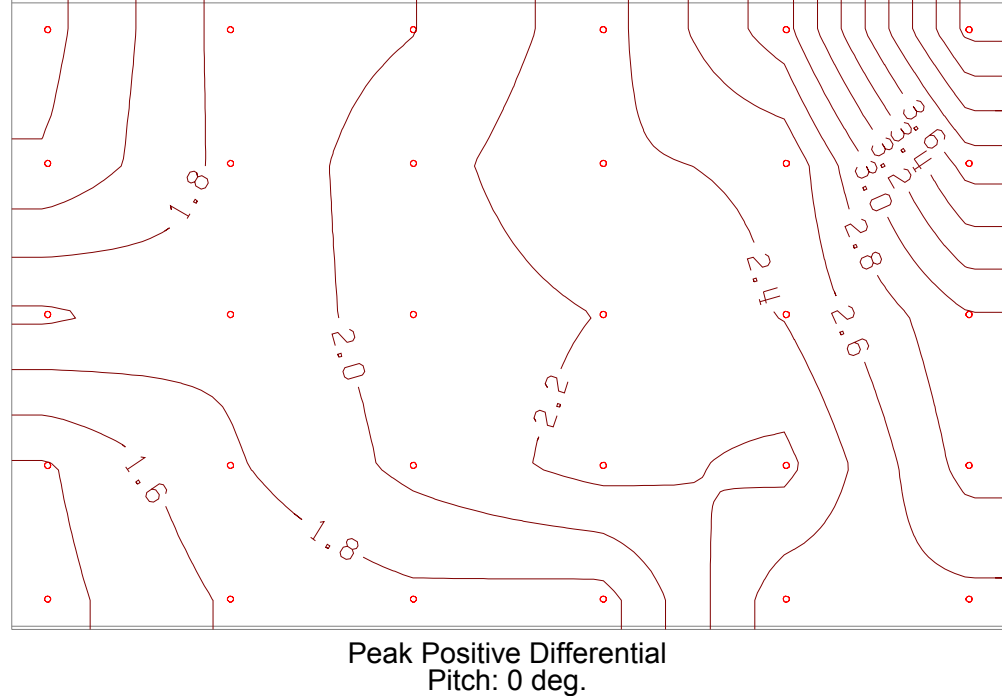
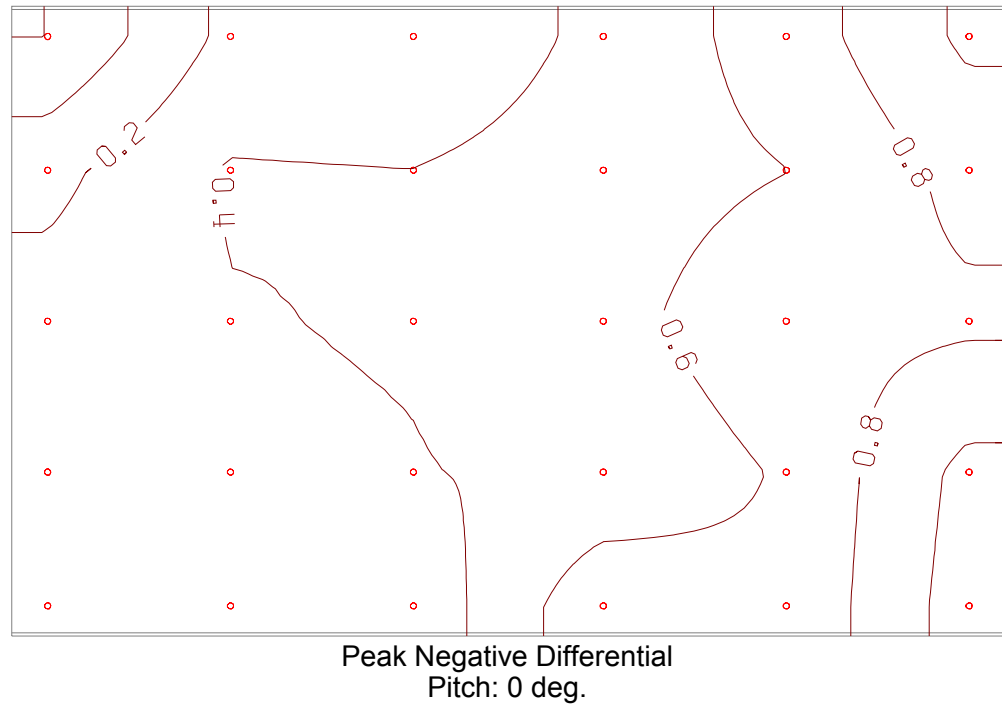
$$C = 25z_o^{-0.063}, \text{ and } m = 0.35 . \quad (\text{C.21})$$

References

- American National Standard A58.1-1982, Minimum Design Loads for Buildings and Other Structures*, American National Standard Institute, Inc., New York, 1982.
- J. S. D. Bendat and A.G. Piersol, *Random Data: Analysis and Measurement Procedures*, A Wiley-Interscience Publication, John Wiley & Sons, Inc., New York, 1971.
- J. Counihan, "Adiabatic Atmospheric Boundary Layers: A Review and Analysis of Data from the Period 1880-1972," *Atmos. Environ.*, 9 (1975), 871-905.
- A. G. Davenport, "The Relationship of Wind Structure to Wind Loading," in *Proceedings of the Symposium on Wind Effects on Buildings and Structures*, Vol. 1, National Physical Laboratory, Teddington, U.K., Her Majesty's Stationery Office, London, 1965, pp.53-102.
- A. G. Davenport, "The Spectrum of Horizontal Gustiness Near the Ground in High Winds," *J. Royal Meteorol. Soc.*, 87 (1961) 194-211.
- ESDU, "Characteristics of Atmospheric Turbulence Near the Ground," Item No. 75001, Engineering Science Data Unit, London, U.K., 1975.
- National Building Code of Canada 1980*, National Research Council of Canada, Associate Committee of the National Building Code, NRCC No. 17724, Ottawa, Canada, 1980.
- G. Hellman, "Über die Bewegung der Luft in den untersten Schichten der Atmosphäre," *Meteoro. Z.*, 34 (1916) 273.
- J. O. Hinze, *Turbulence*, 2nd ed., McGraw-Hill Book Company, New York, 1975.
- J. C. Kaimal et al., "Spectral Characteristics of Surface-Layer Turbulence," *J. Royal Meteorol. Soc.*, 98 (1972) 563-589.
- J. L. Lumley and H. A. Panofsky, *The Structure of Atmospheric Turbulence*, John Wiley & Sons, Inc., New York, 1964.
- E. Simiu and R. H. Scanlan, *Wind Effects on Structures*, 3rd ed., A Wiley-Interscience Publication, John Wiley & Sons, Inc., New York, 1996.
- D. H. Slade, editor, *Meteorology and Atomic Energy 1968*, Technical Information Center, U.S. Department of Energy, 1968.
- W. H. Snyder, "Guideline for Fluid Modeling of Atmospheric Diffusion," Report No. EPA600/8-81-009, USEPA, Environmental Services Research Laboratory, Office of Research and development, Research Triangle Park, New Jersey, 1981.
- Taylor, G. I., "The Spectrum of Turbulence," *Proceedings of the Royal Soc.*, A164 (1938), 476-490.

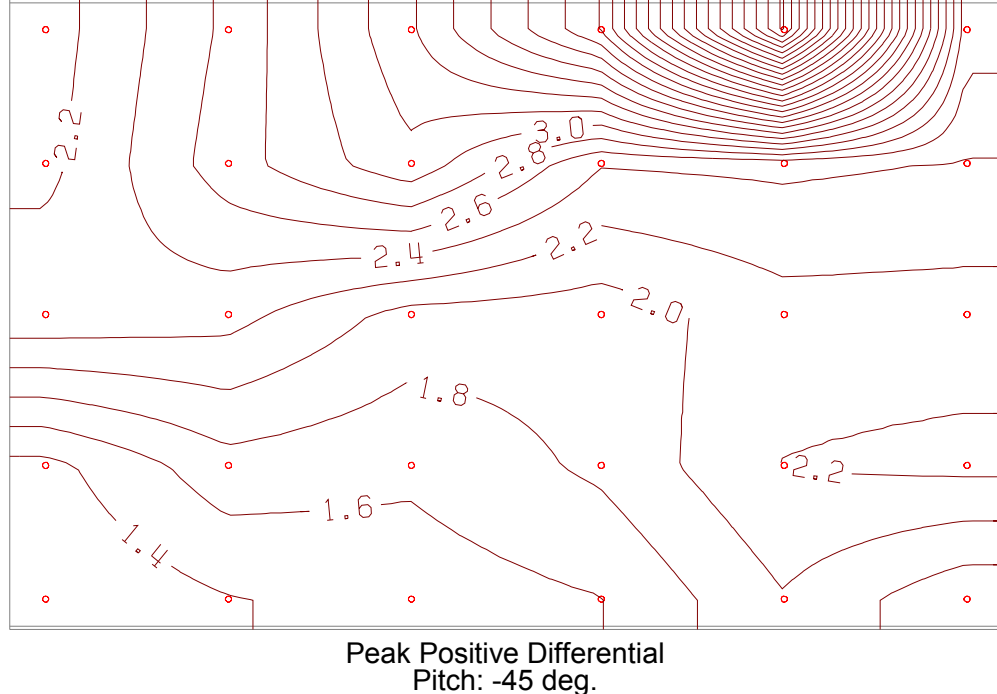
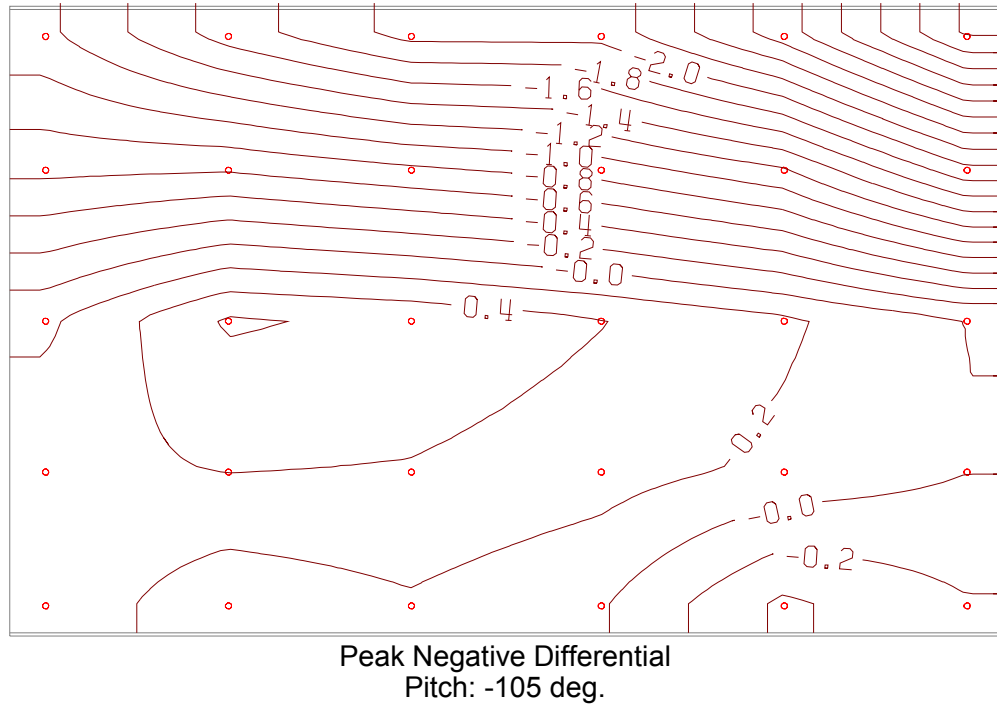
**7.4 APPENDIX D - INSTANTANEOUS DIFFERENTIAL PRESSURE CONTOURS
FOR SELECTED TEST CONFIGURATIONS**

Operational Mode, Yaw: -30 deg.



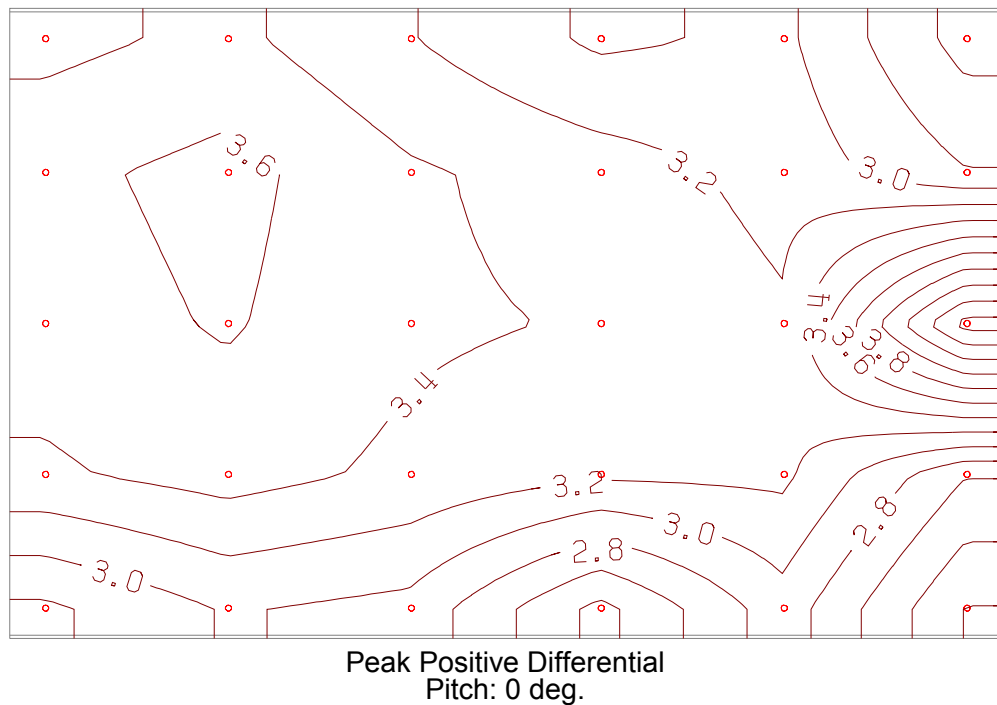
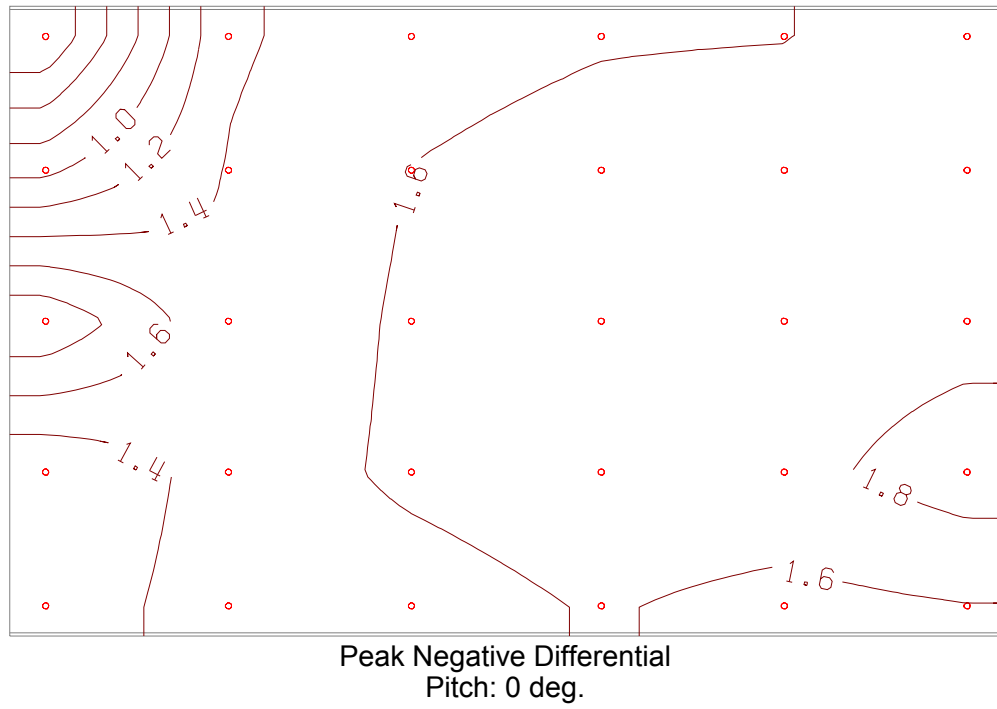
Configuration B1

Stowed Mode, Yaw: -30 deg.



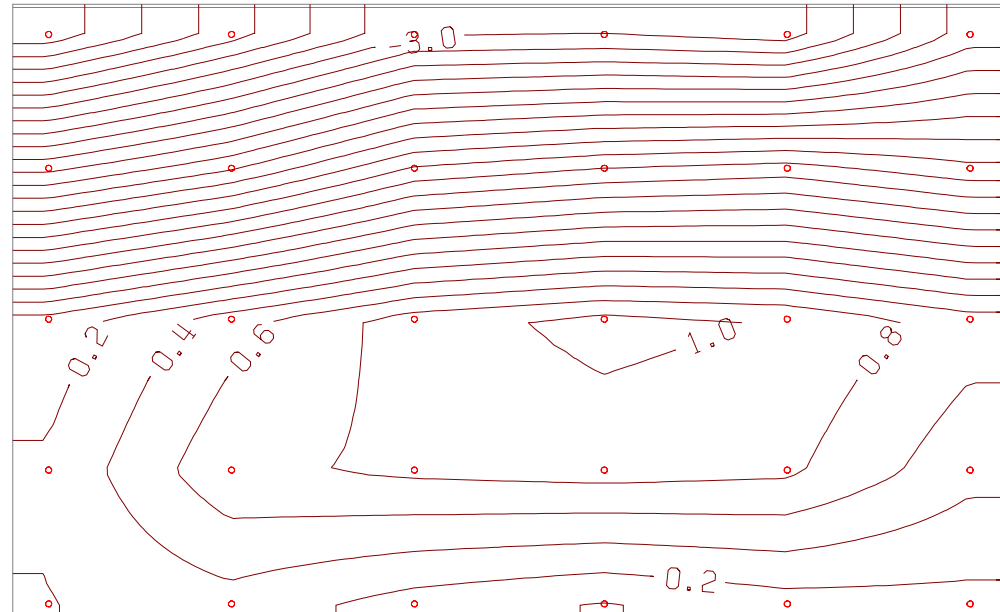
Configuration B1 (continued)

Operational Mode, Yaw: 0 deg.

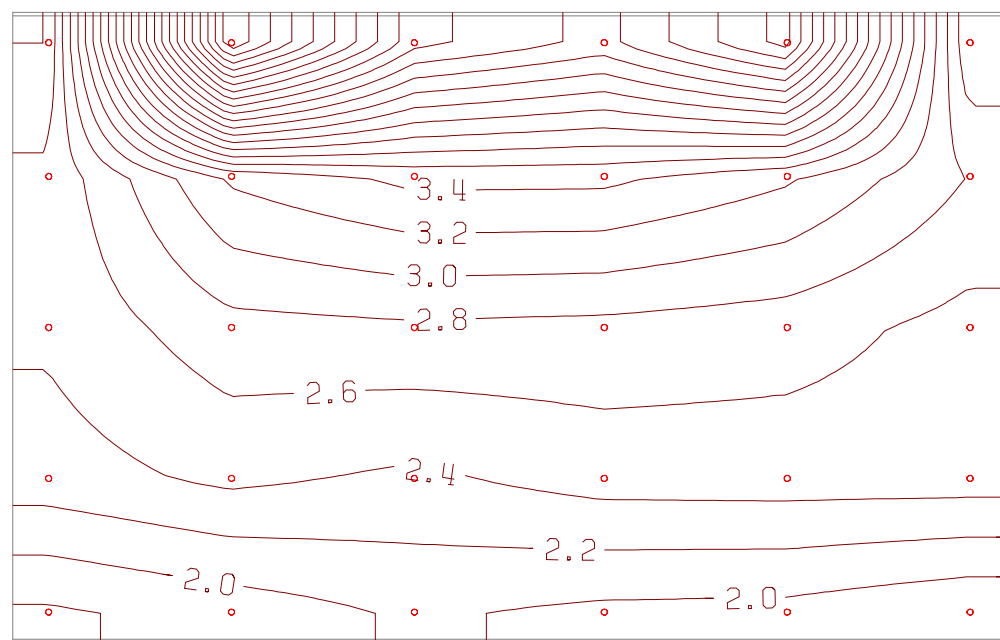


Configuration B1 (continued)

Stowed Mode, Yaw: 0 deg.



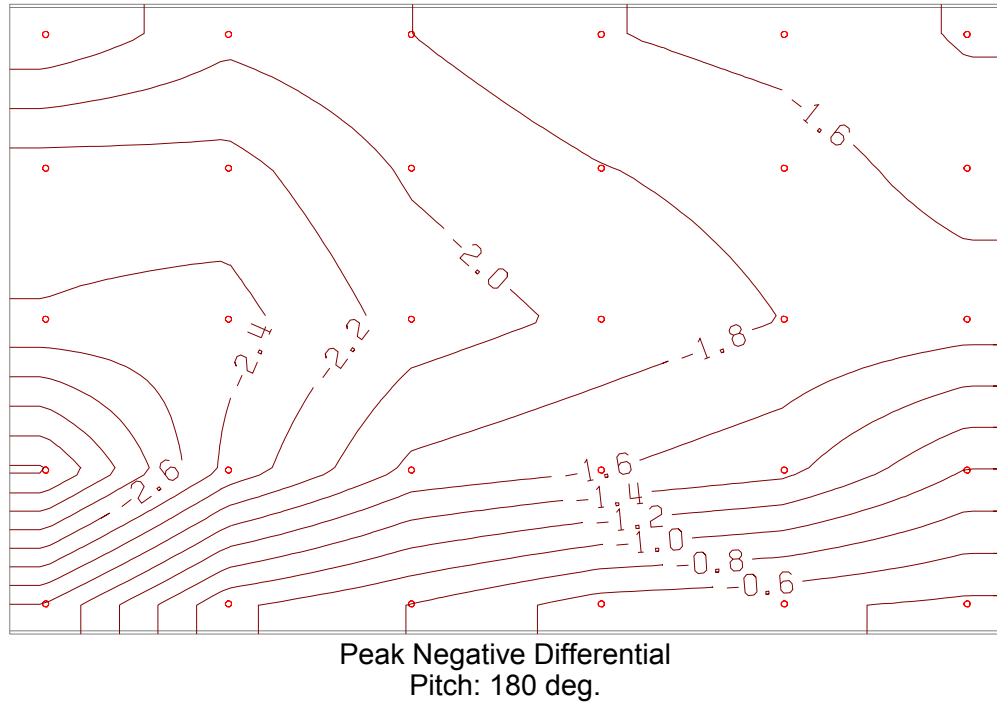
Peak Negative Differential
Pitch: -105 deg.



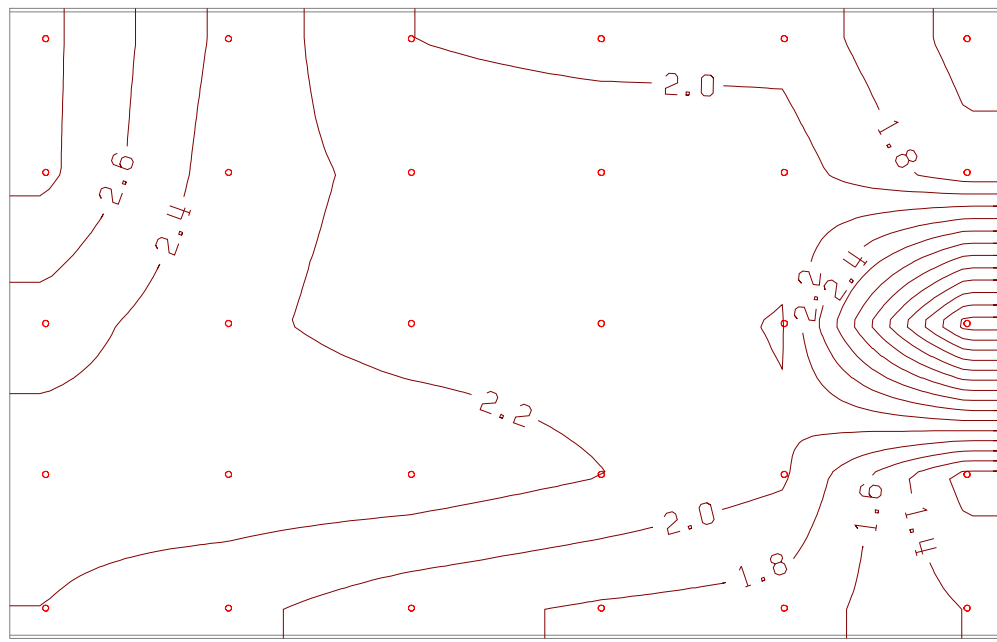
Peak Positive Differential
Pitch: -60 deg.

Configuration B1 (continued)

Operational Mode, Yaw: 30 deg.



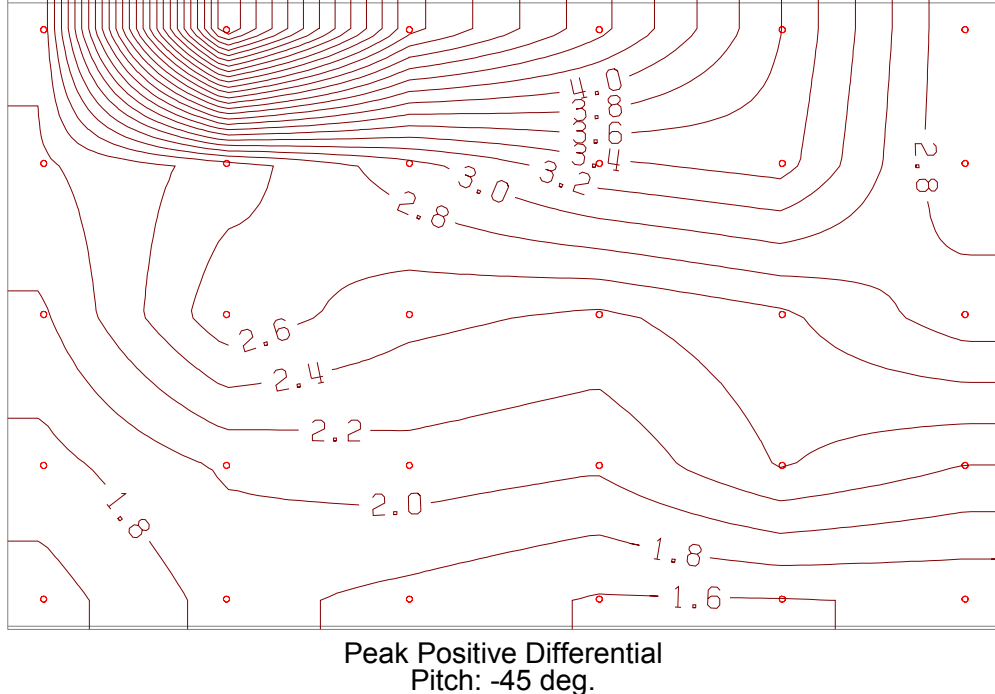
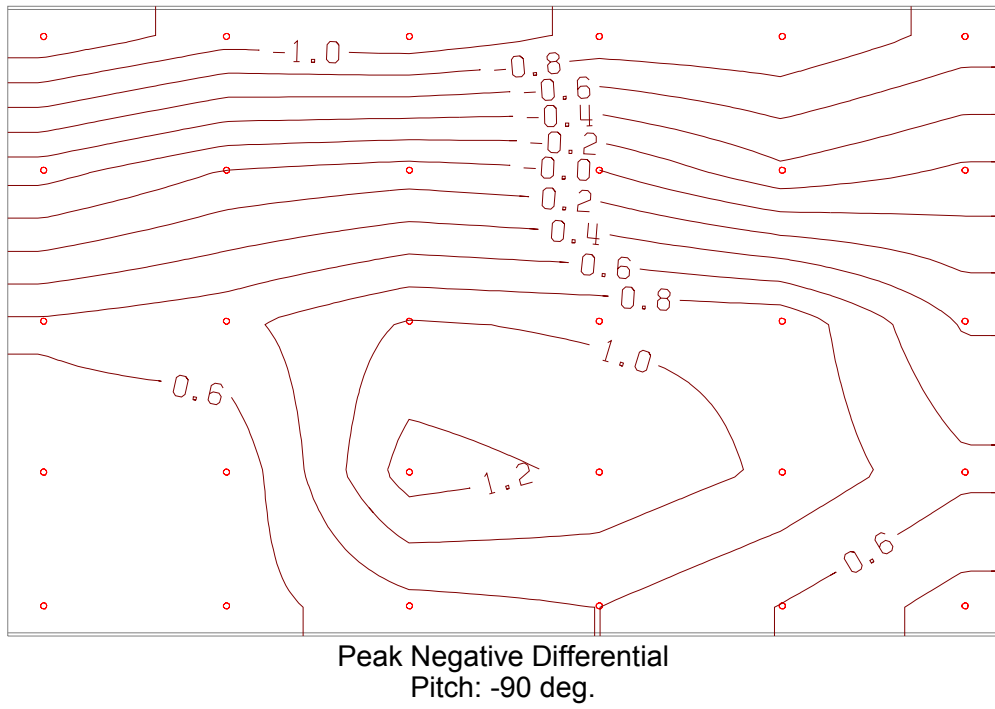
Peak Negative Differential
Pitch: 180 deg.



Peak Positive Differential
Pitch: 0 deg.

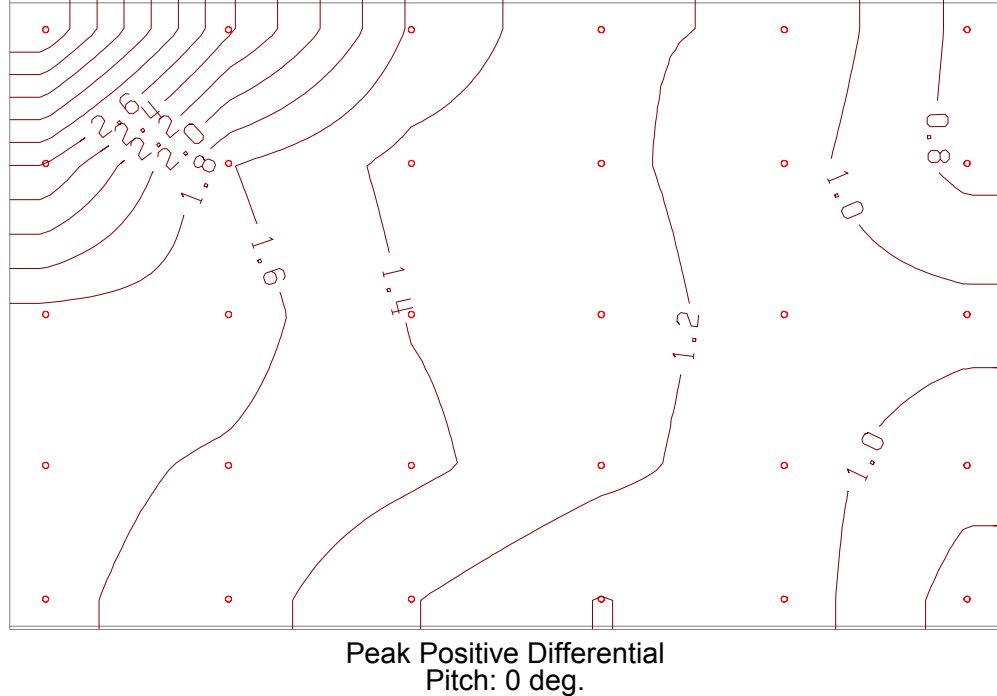
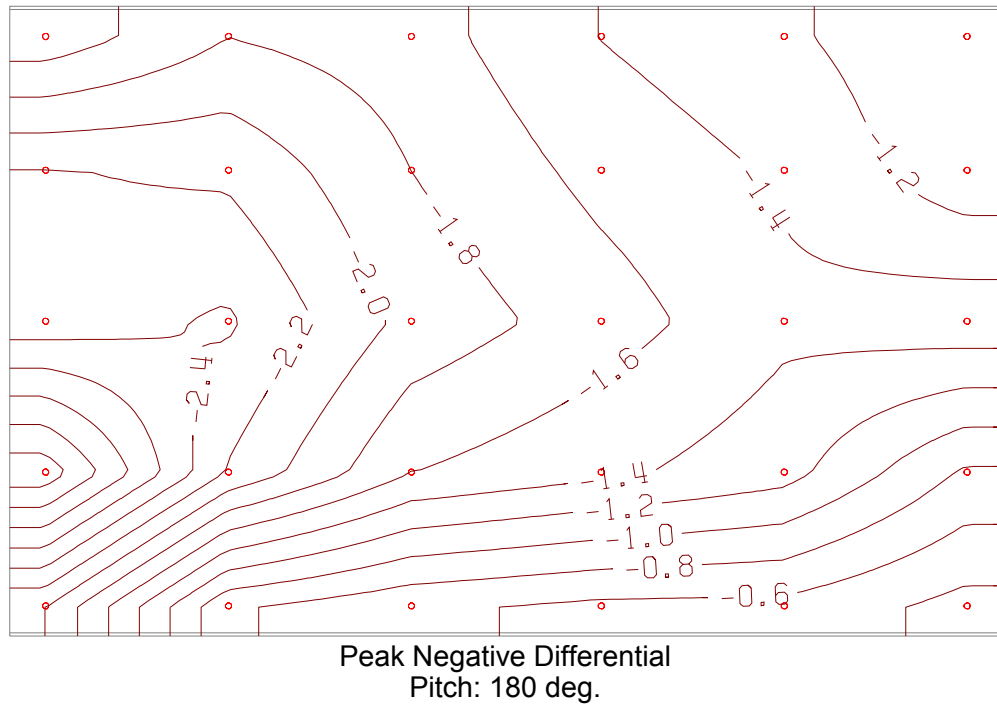
Configuration B1 (continued)

Stowed Mode, Yaw: 30 deg.



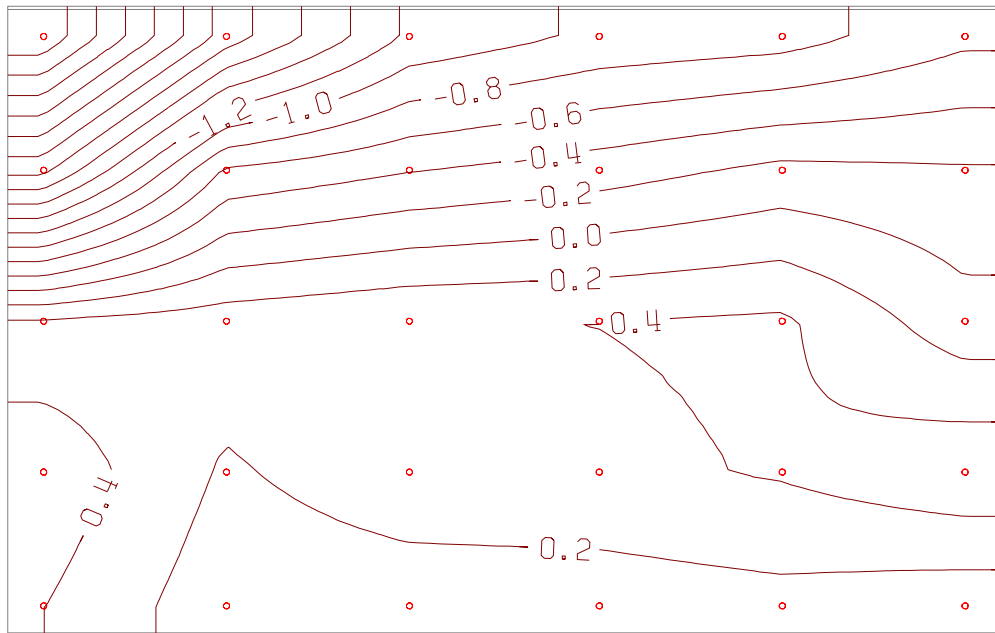
Configuration B1 (continued)

Operational Mode, Yaw: 45 deg.

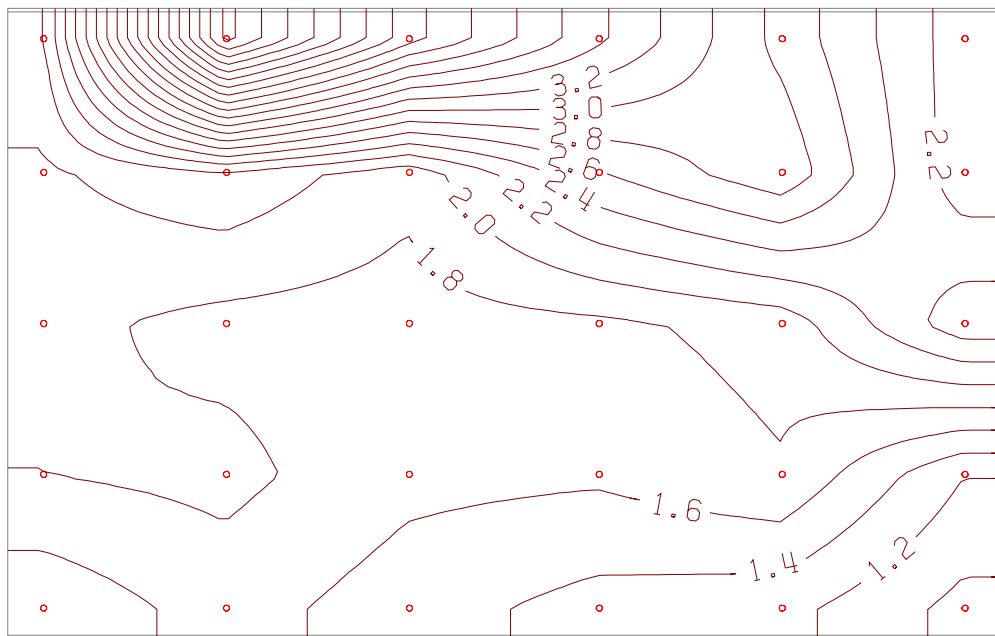


Configuration B1 (continued)

Stowed Mode, Yaw: 45 deg.



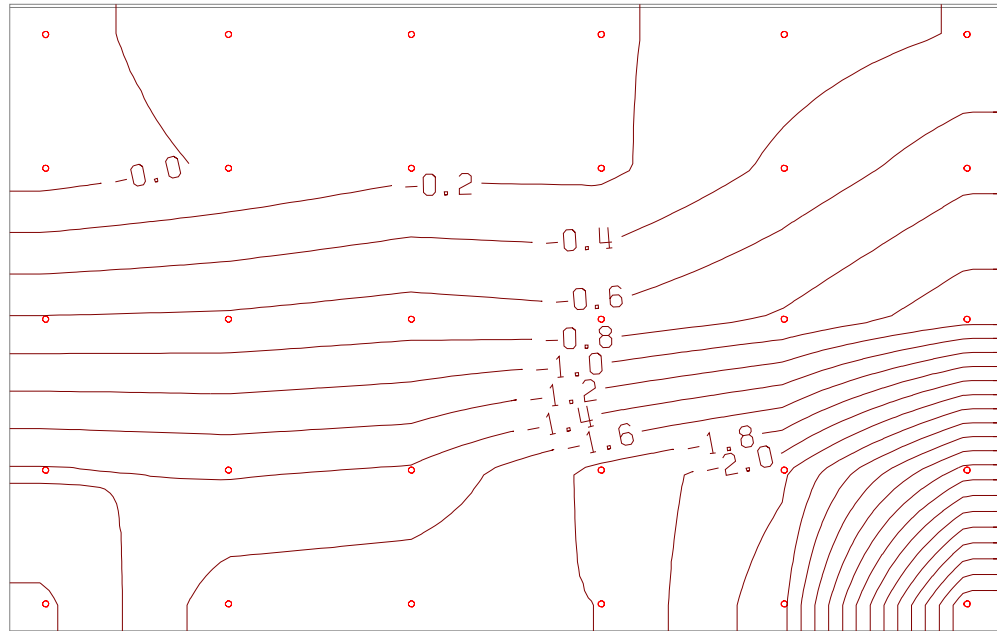
Peak Negative Differential
Pitch: -105 deg.



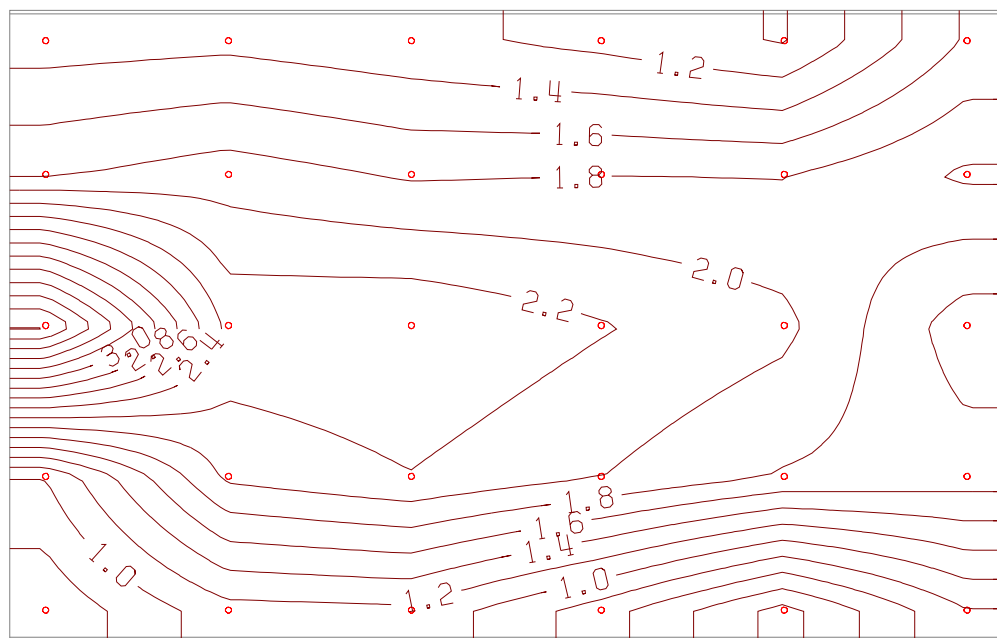
Peak Positive Differential
Pitch: -45 deg.

Configuration B1 (continued)

Operational Mode, Yaw: -30 deg.



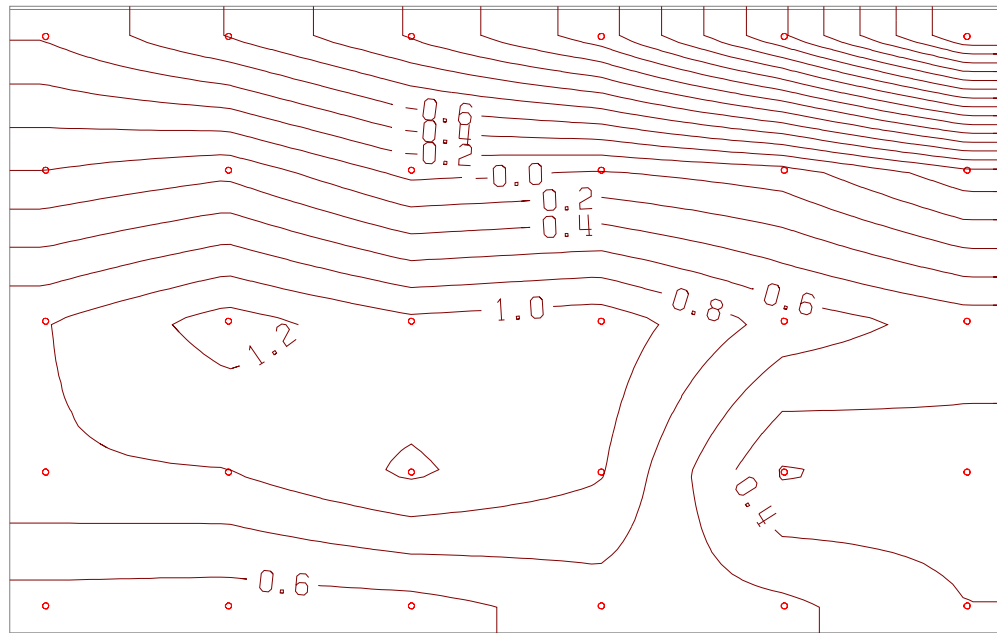
Peak Negative Differential
Pitch: 120 deg.



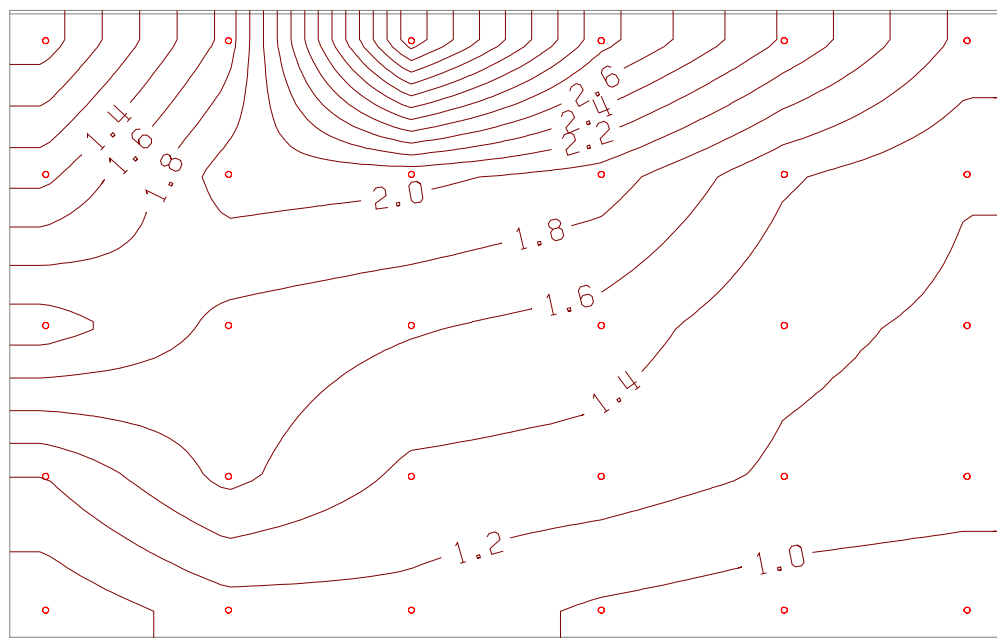
Peak Positive Differential
Pitch: 75 deg.

Configuration C1

Stowed Mode, Yaw: -30 deg.



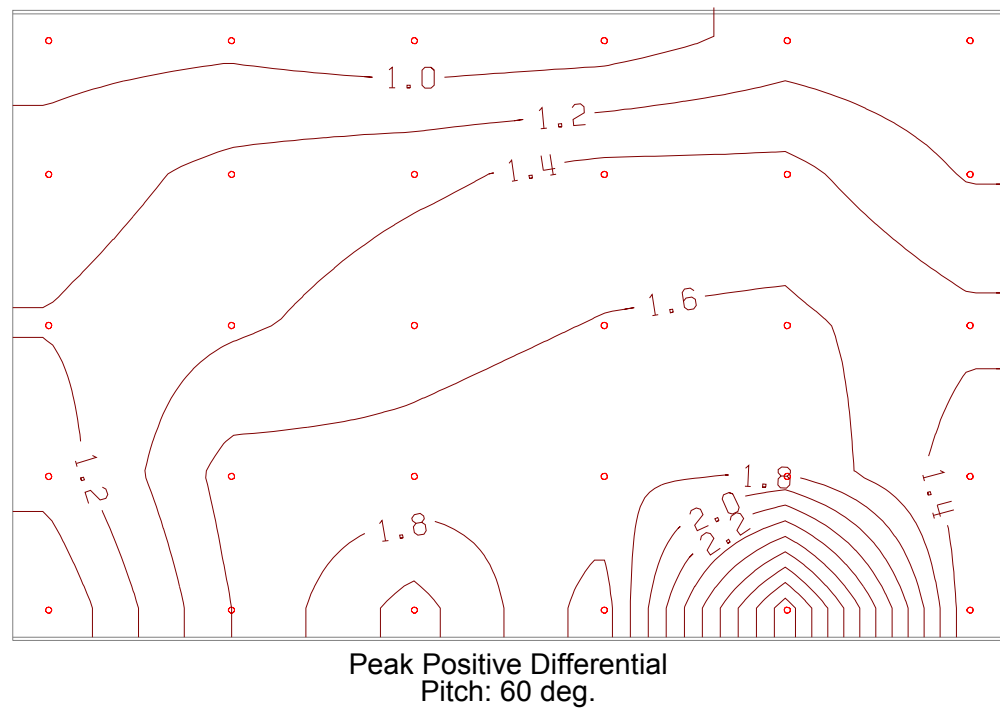
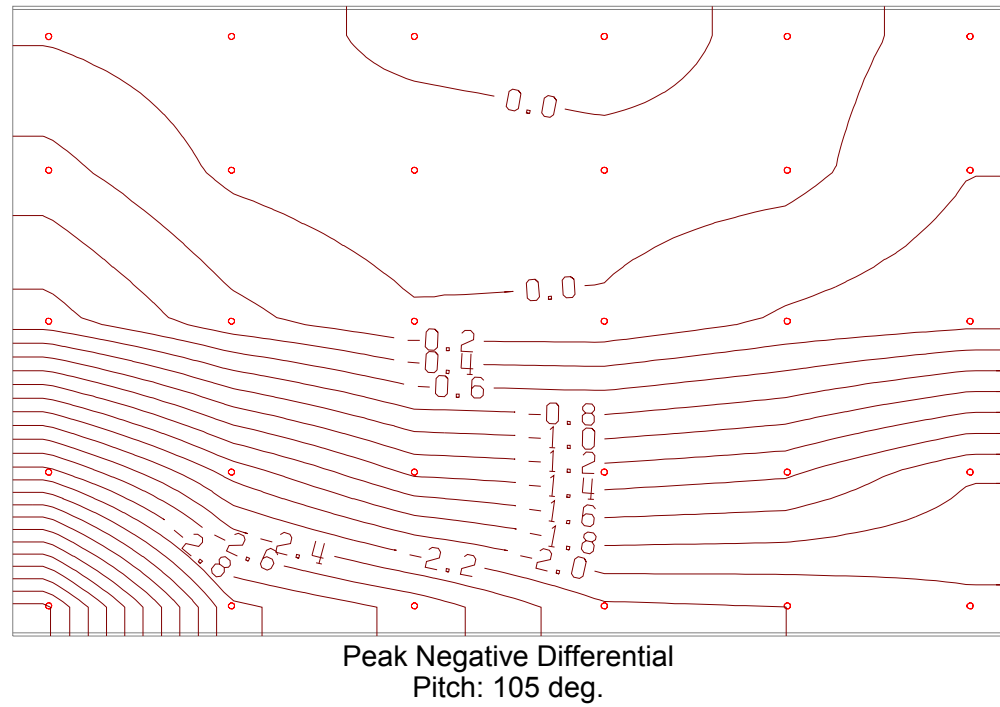
Peak Negative Differential
Pitch: -90 deg.



Peak Positive Differential
Pitch: -60 deg.

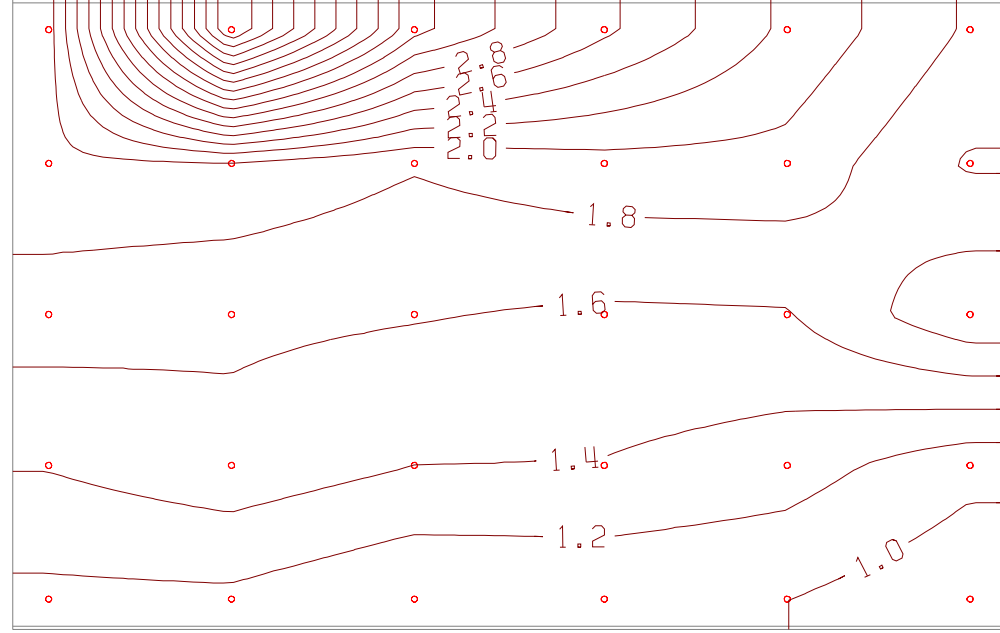
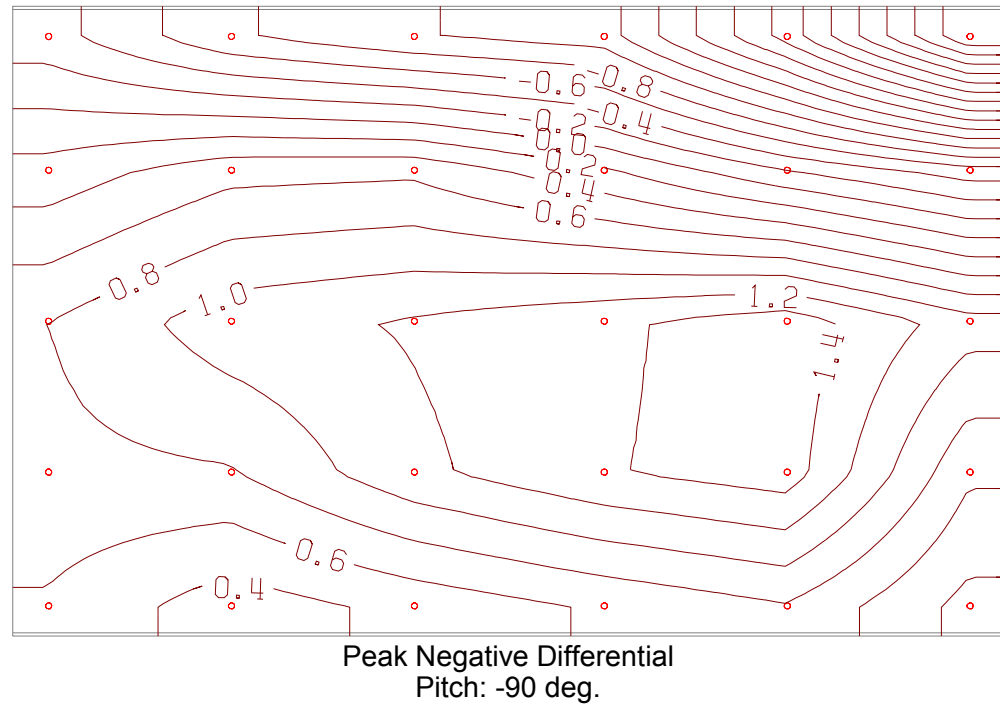
Configuration C1 (continued)

Operational Mode, Yaw: 0 deg.



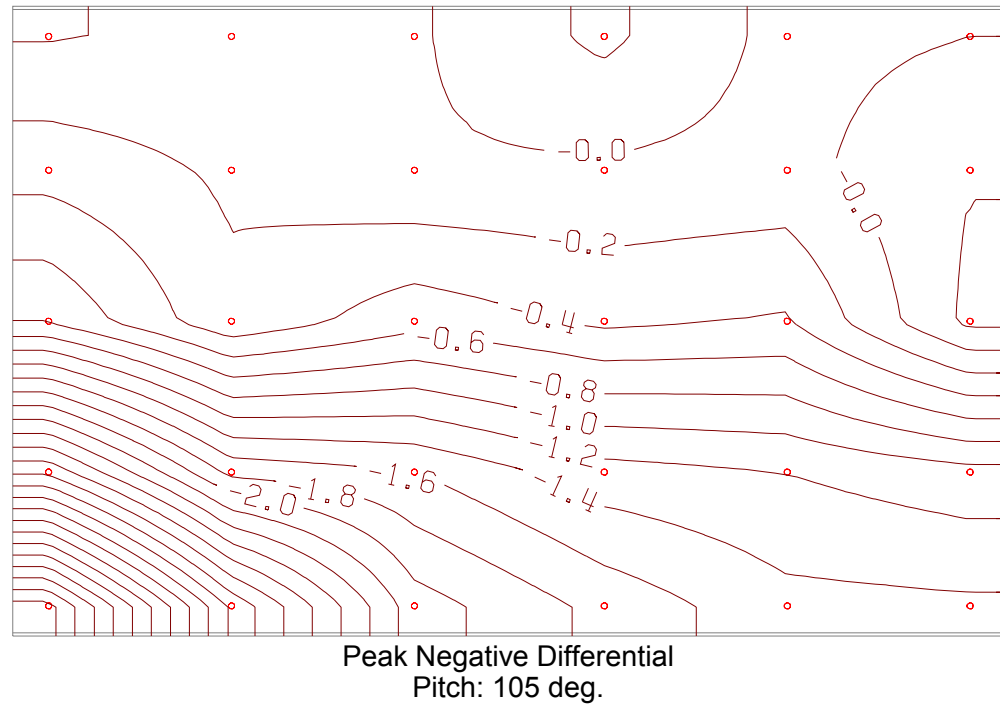
Configuration C1 (continued)

Stowed Mode, Yaw: 0 deg.

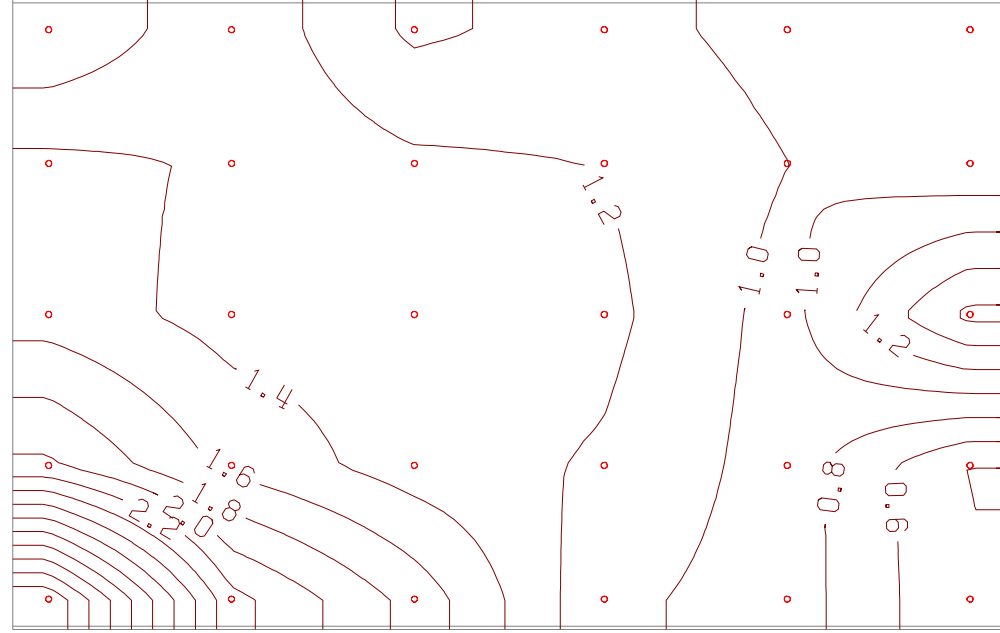


Configuration C1 (continued)

Operational Mode, Yaw: 30 deg.



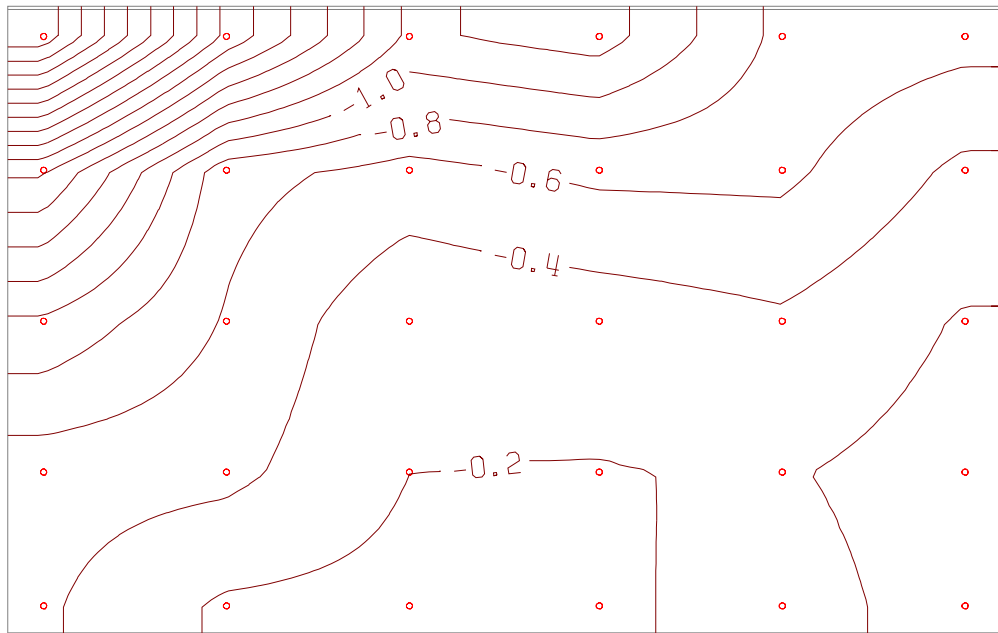
Peak Negative Differential
Pitch: 105 deg.



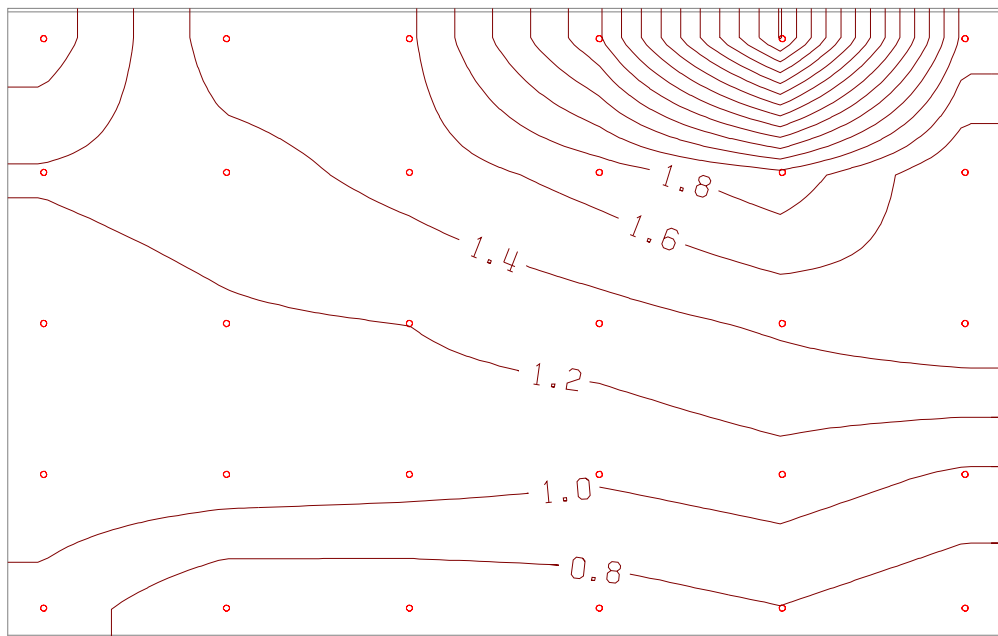
Peak Positive Differential
Pitch: 60 deg.

Configuration C1 (continued)

Stowed Mode, Yaw: 30 deg.



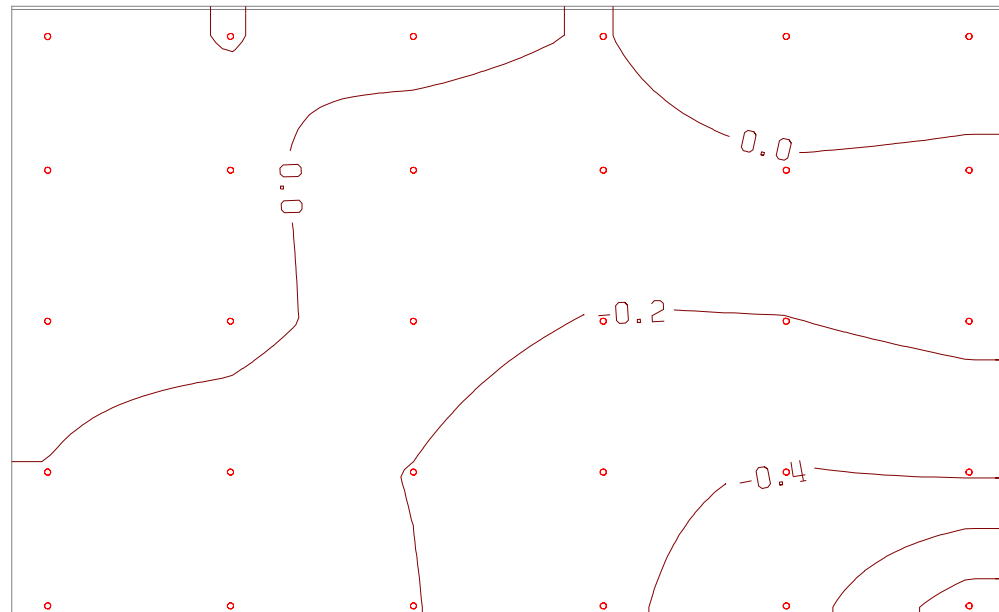
Peak Negative Differential
Pitch: -30 deg.



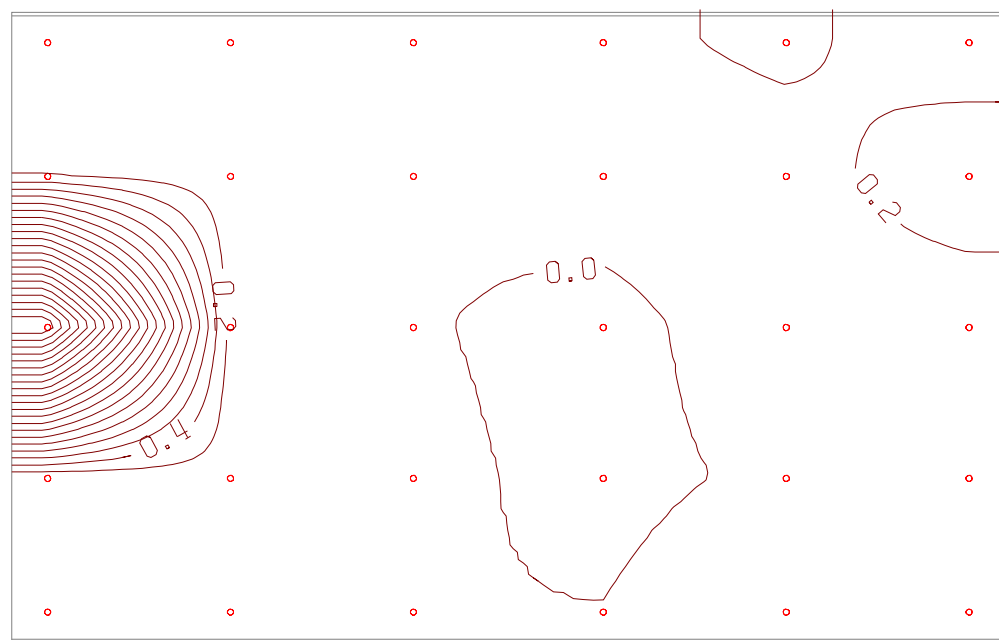
Peak Positive Differential
Pitch: -60 deg.

Configuration C1 (continued)

Operational Mode, Yaw: -30 deg.



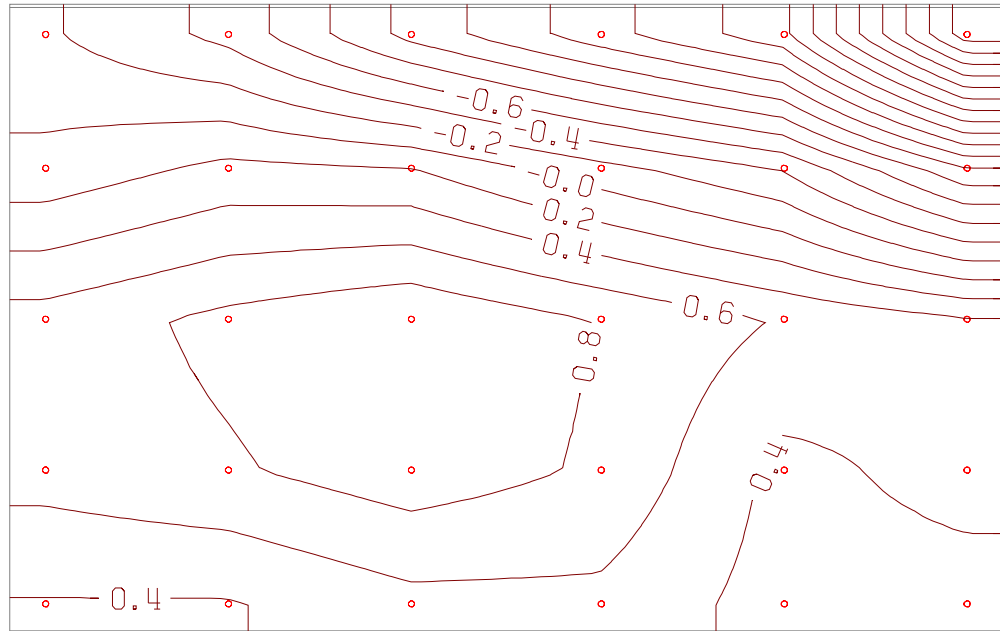
Peak Negative Differential
Pitch: 105 deg.



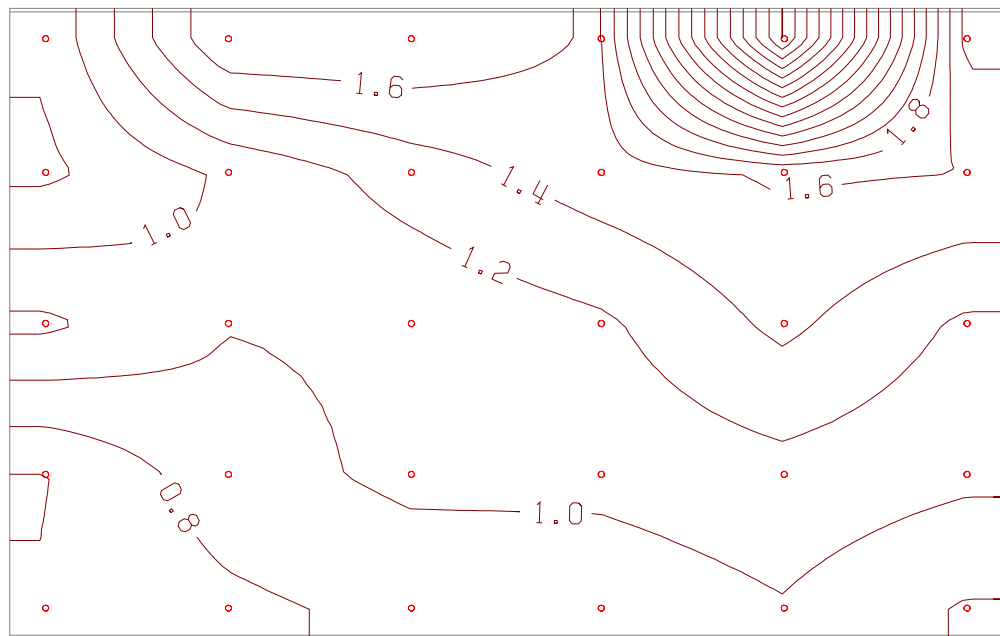
Peak Positive Differential
Pitch: 30 deg.

Configuration C3

Stowed Mode, Yaw: -30 deg.



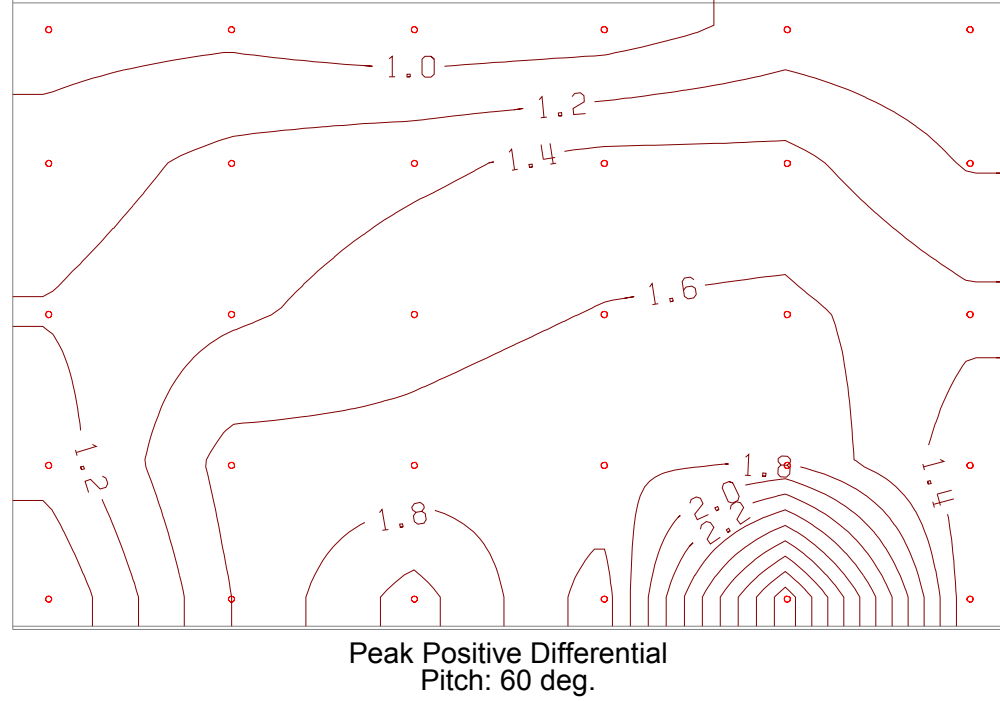
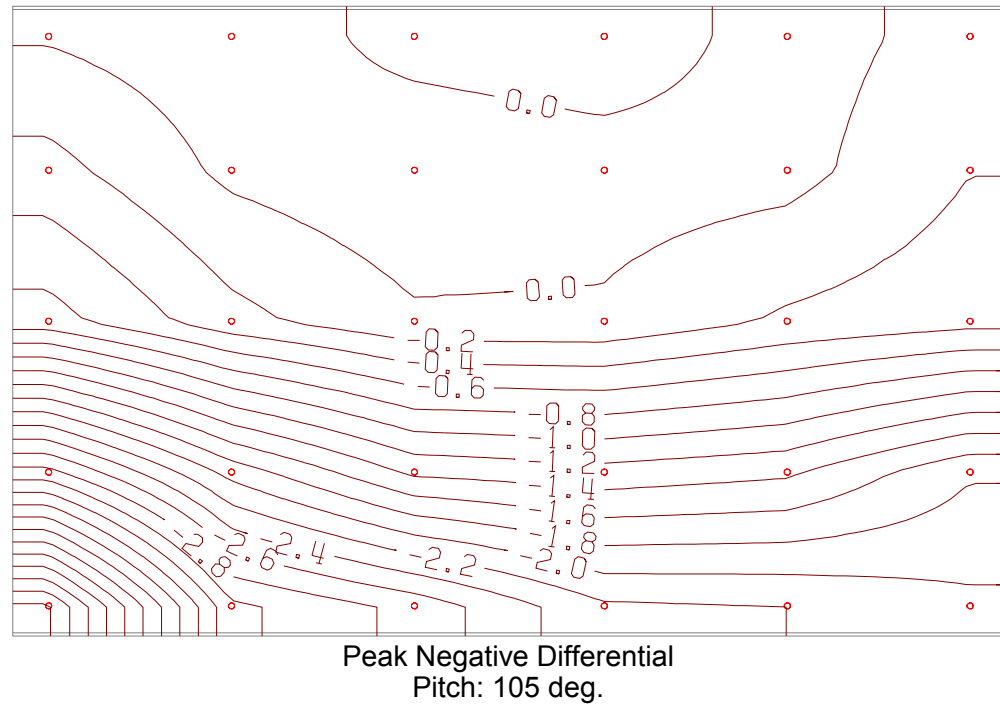
Peak Negative Differential
Pitch: -90 deg.



Peak Positive Differential
Pitch: -45 deg.

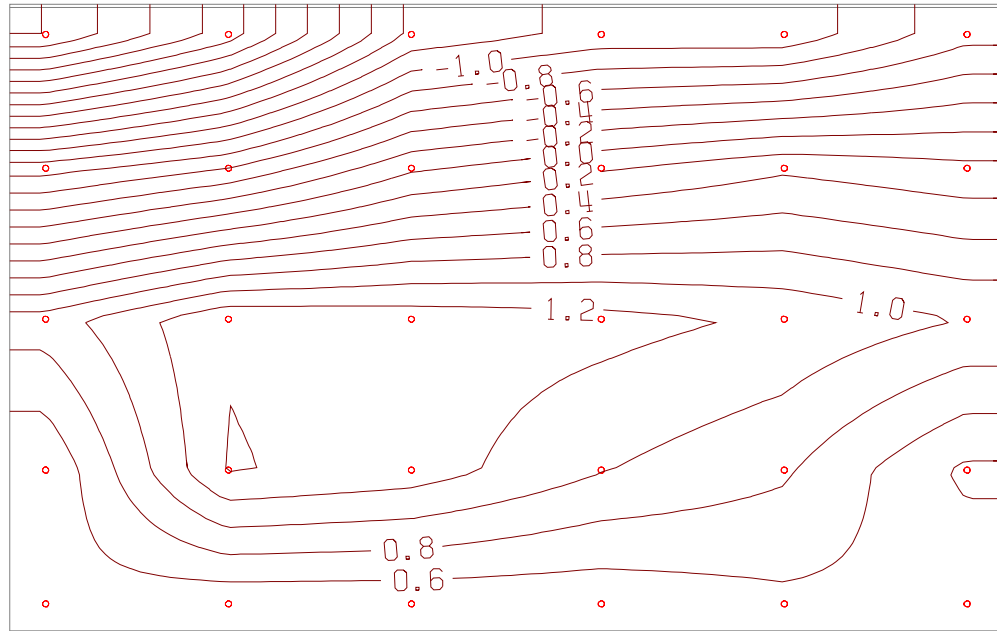
Configuration C3 (continued)

Operational Mode, Yaw: 0 deg.

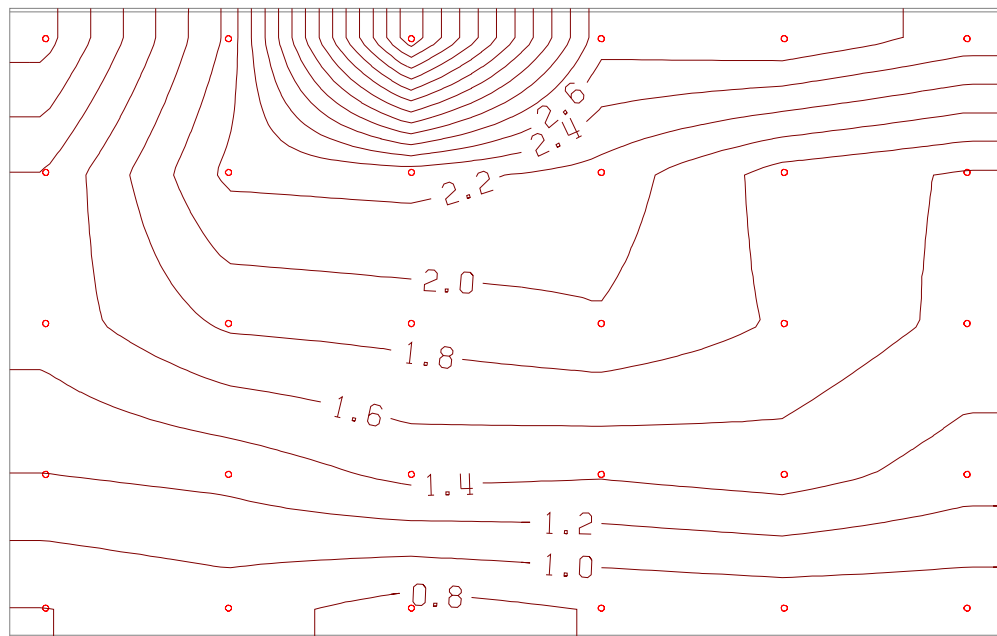


Configuration C3 (continued)

Stowed Mode, Yaw: 0 deg.



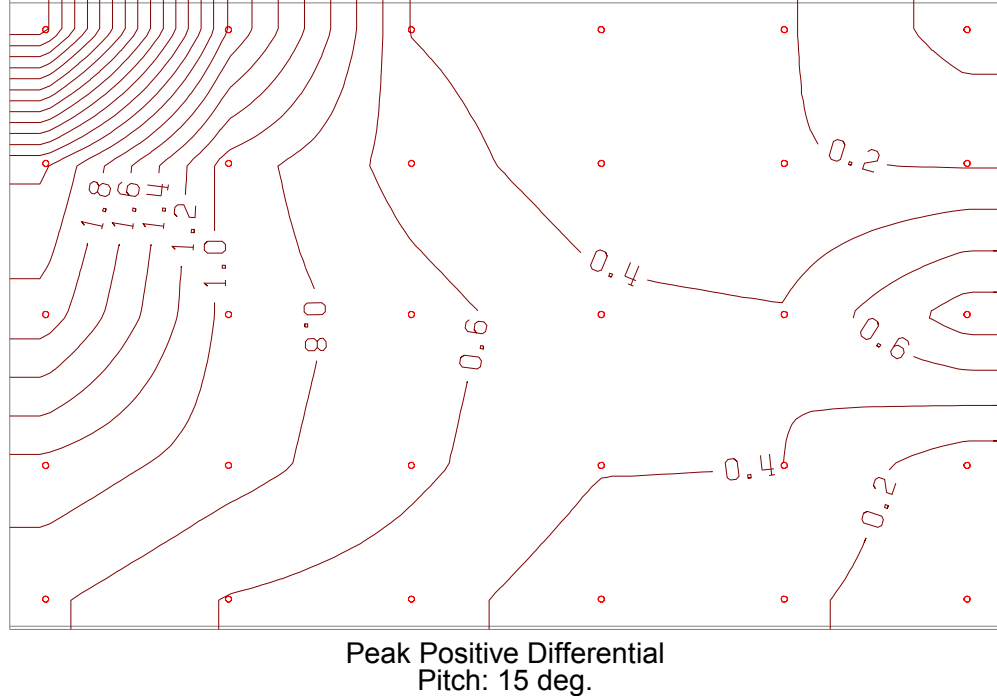
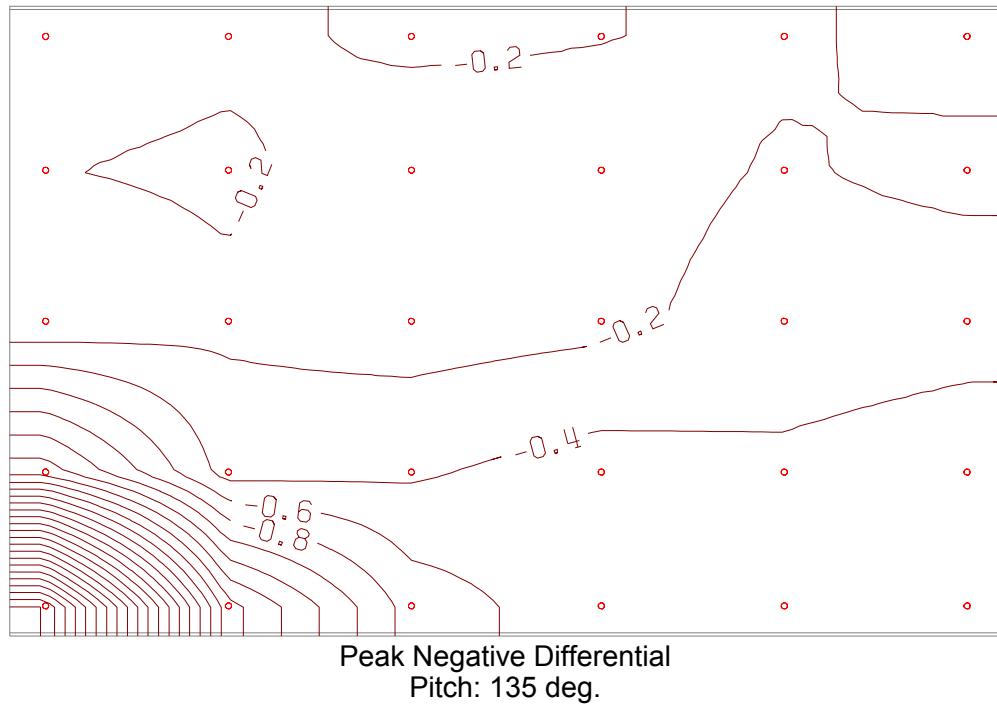
Peak Negative Differential
Pitch: -90 deg.



Peak Positive Differential
Pitch: -60 deg.

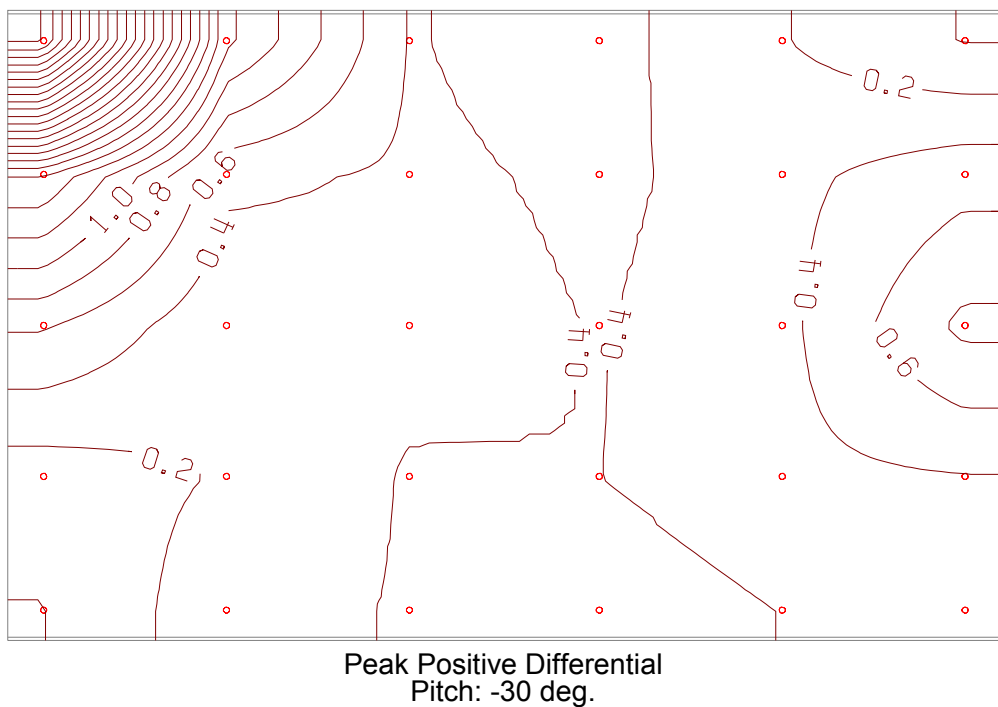
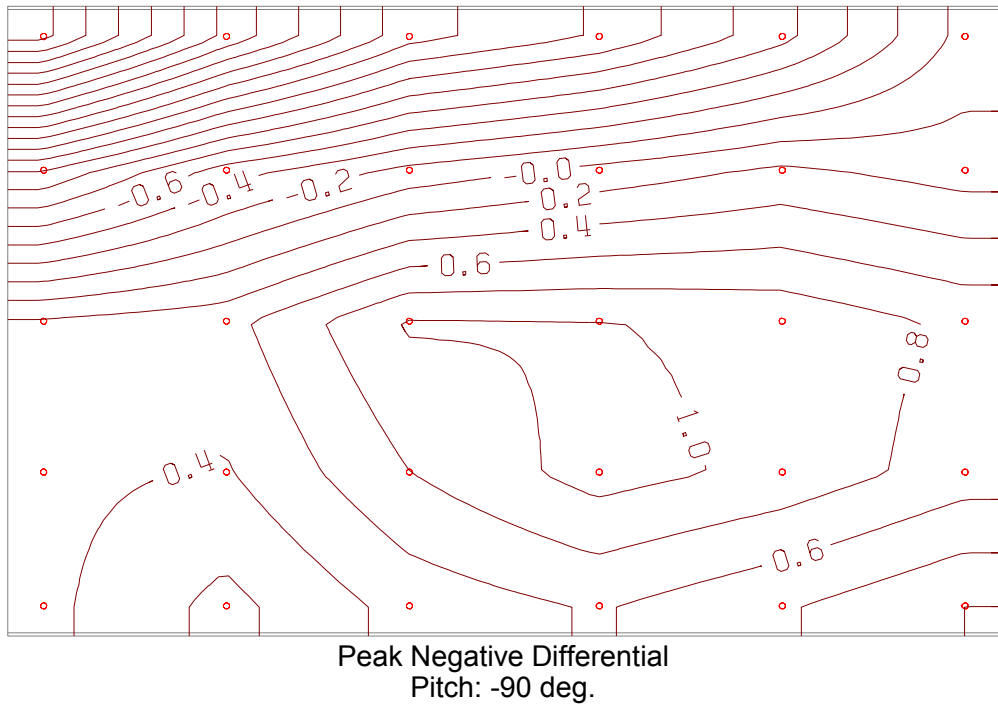
Configuration C3 (continued)

Operational Mode, Yaw: 30 deg.



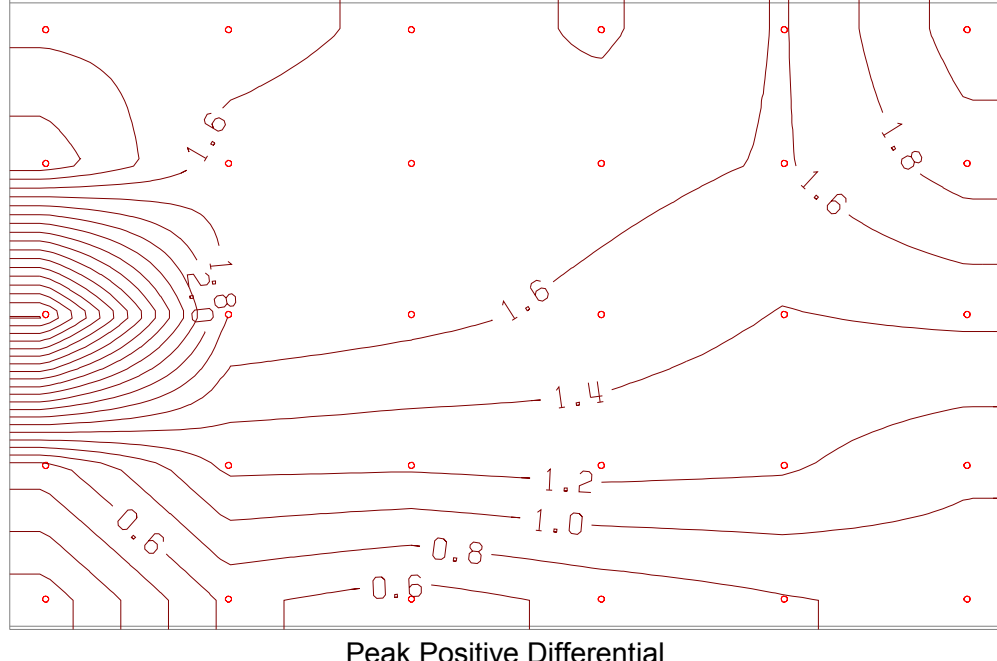
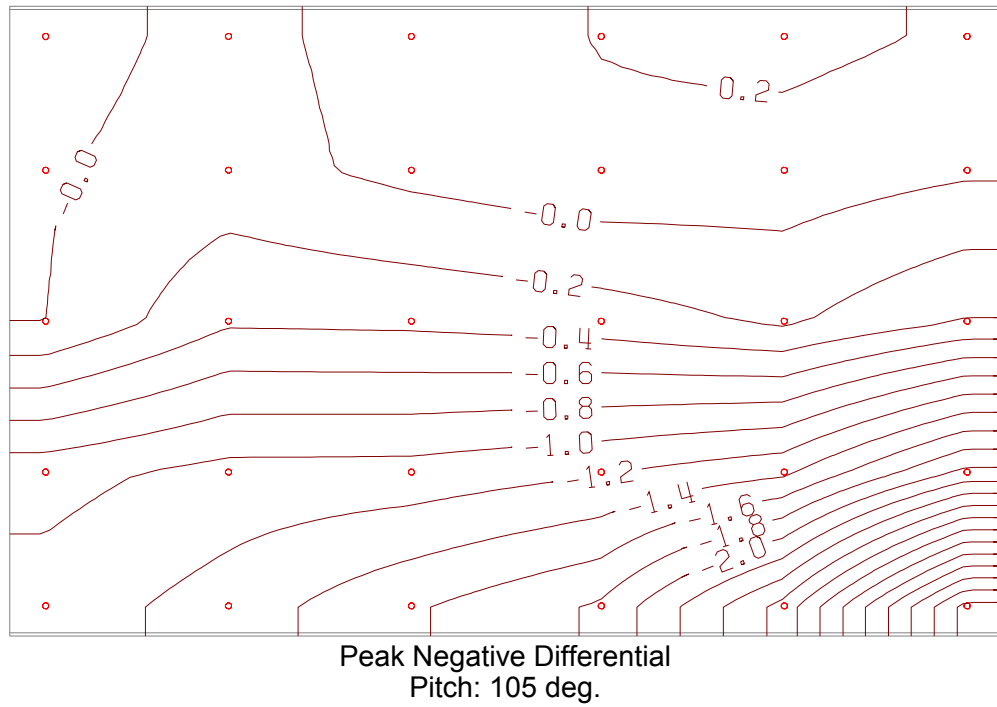
Configuration B3 (continued)

Stowed Mode, Yaw: 30 deg.



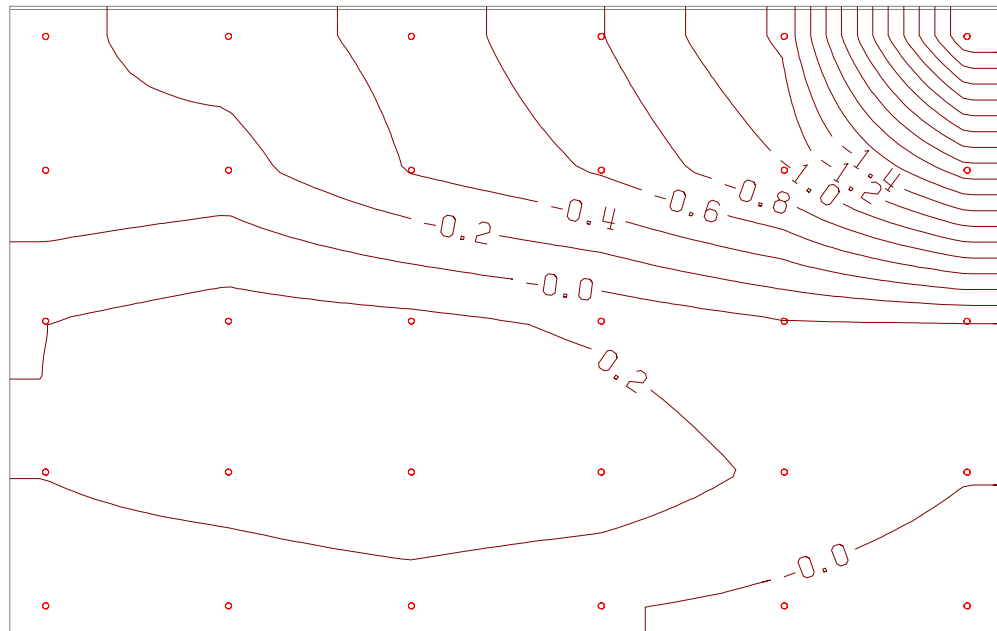
Configuration C3 (continued)

Operational Mode, Yaw: -30 deg.

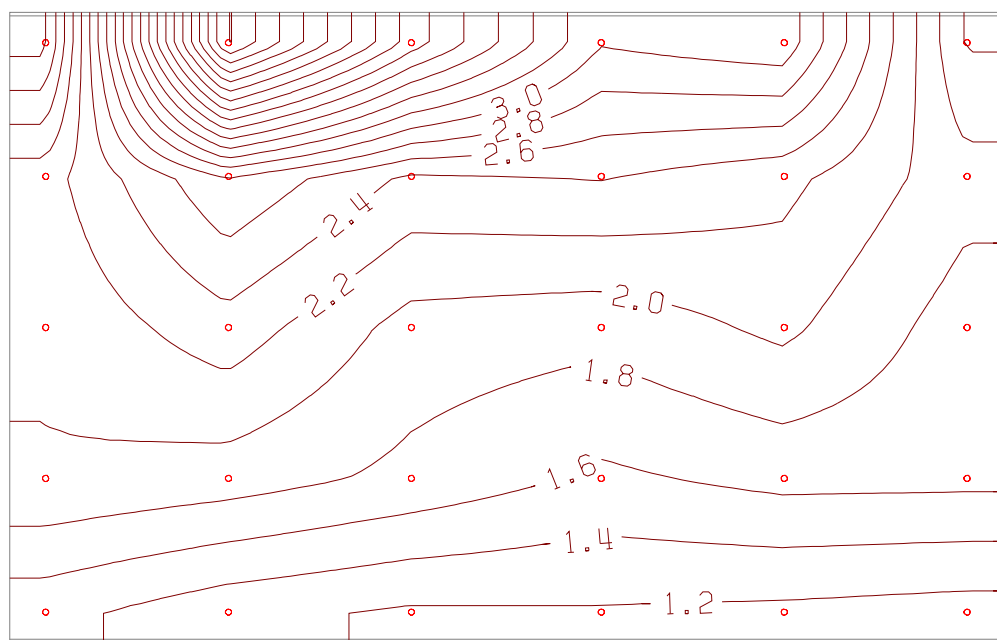


Configuration C5

Stowed Mode, Yaw: -30 deg.



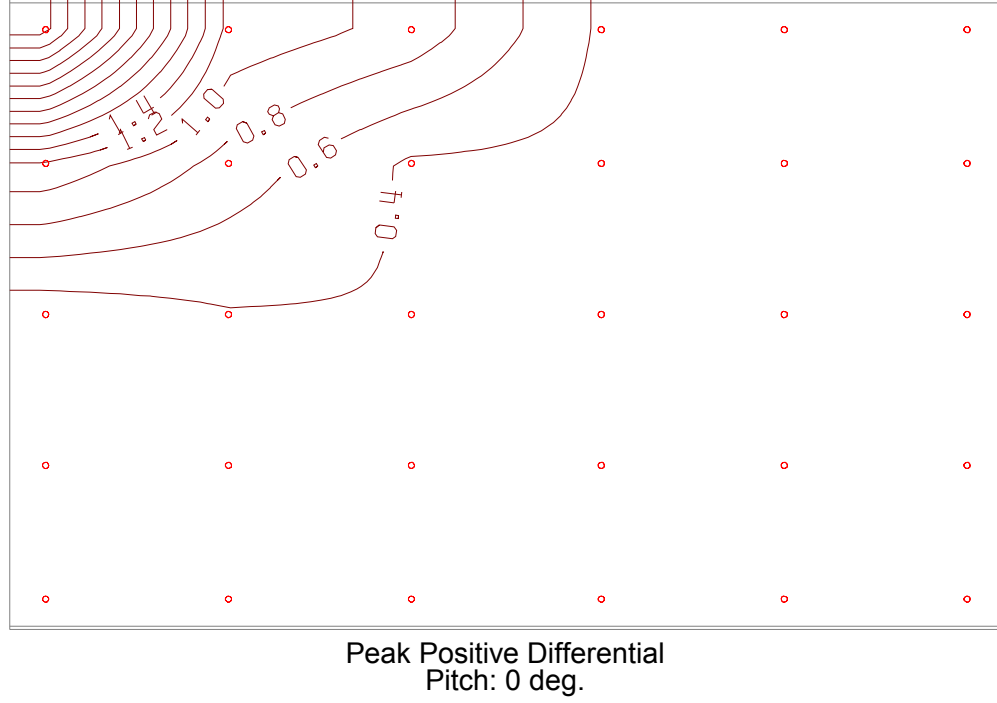
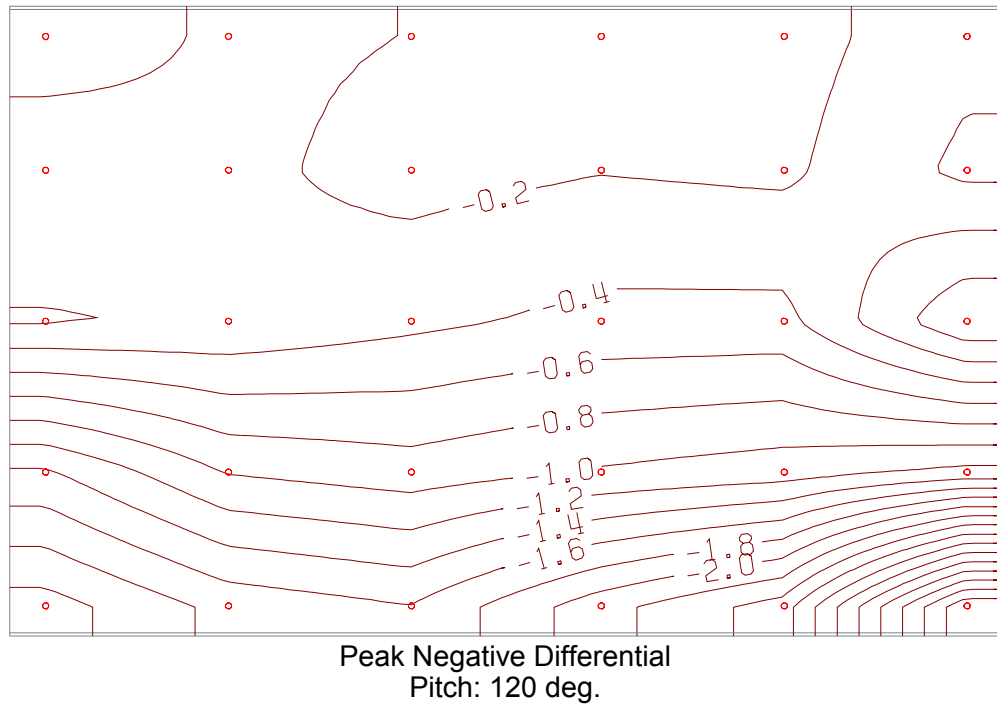
Peak Negative Differential
Pitch: -105 deg.



Peak Positive Differential
Pitch: -60 deg.

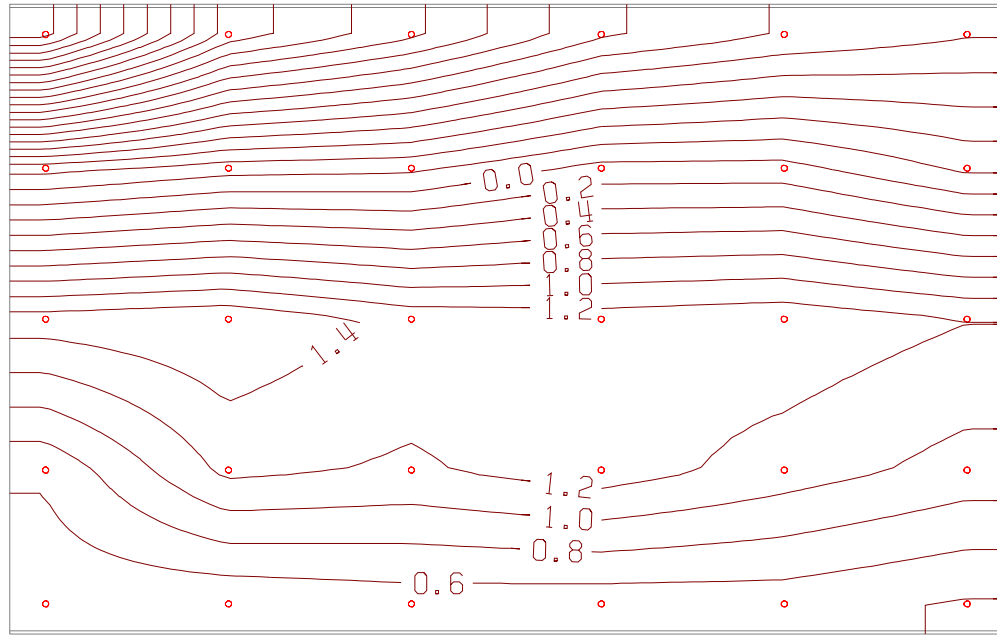
Configuration C5 (continued)

Operational Mode, Yaw: 0 deg.

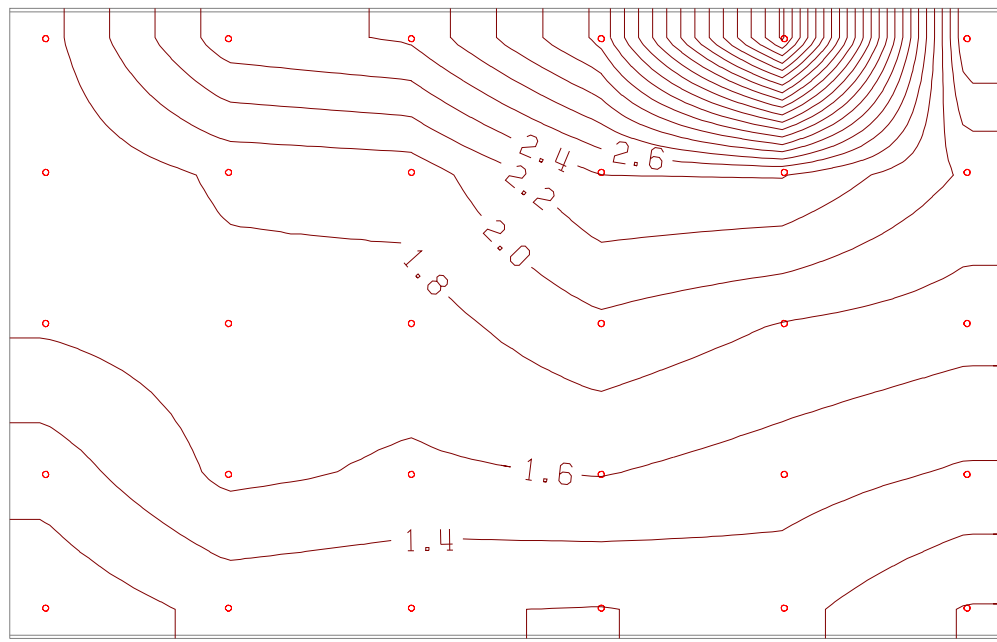


Configuration C5 (continued)

Stowed Mode, Yaw: 0 deg.



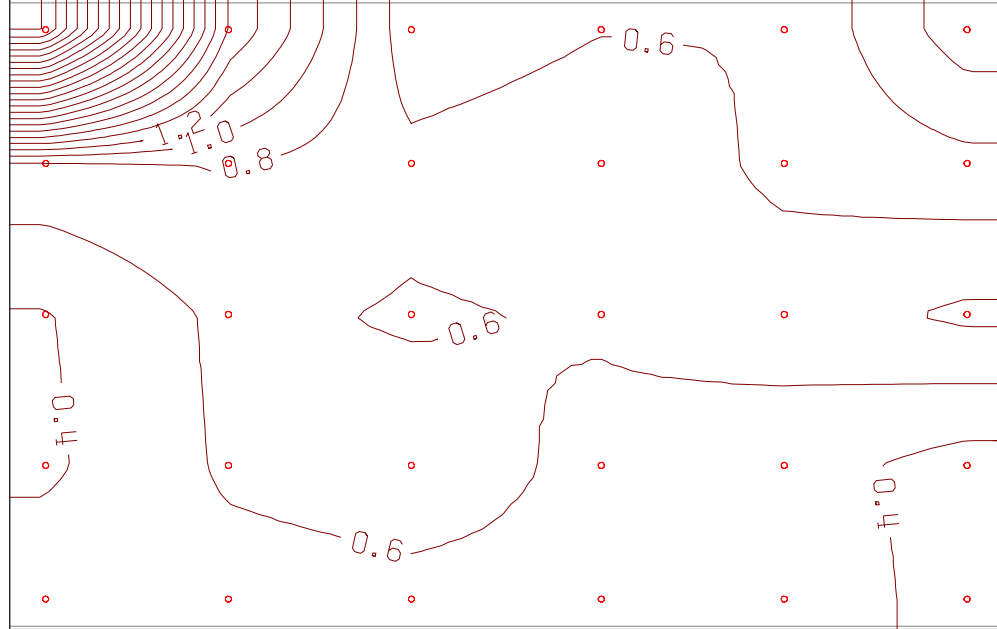
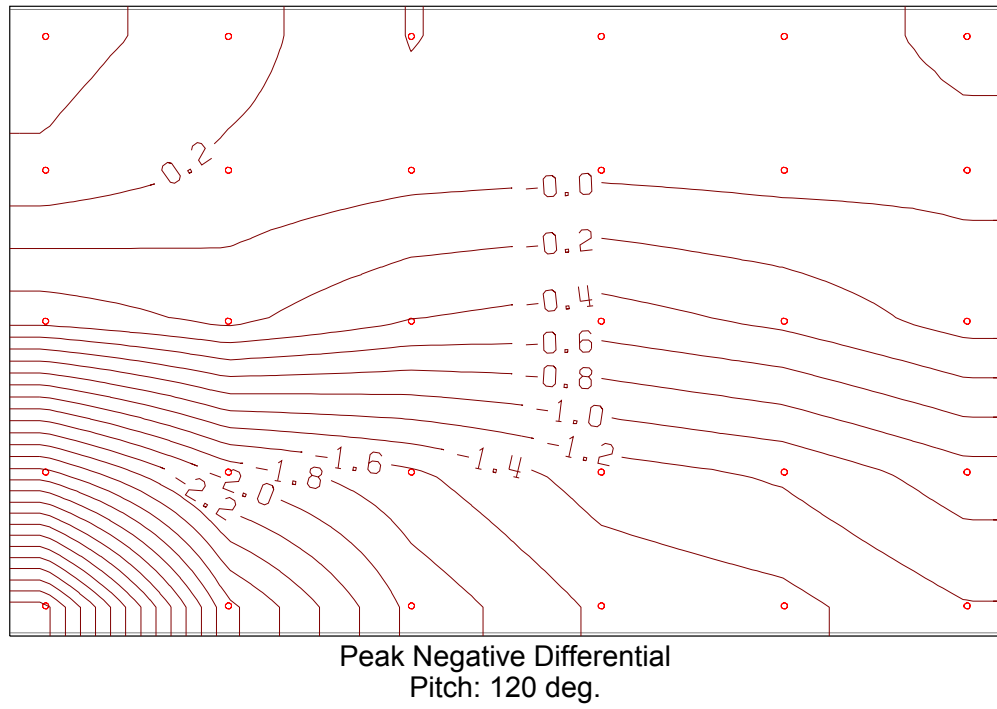
Peak Negative Differential
Pitch: -90 deg.



Peak Positive Differential
Pitch: -45 deg.

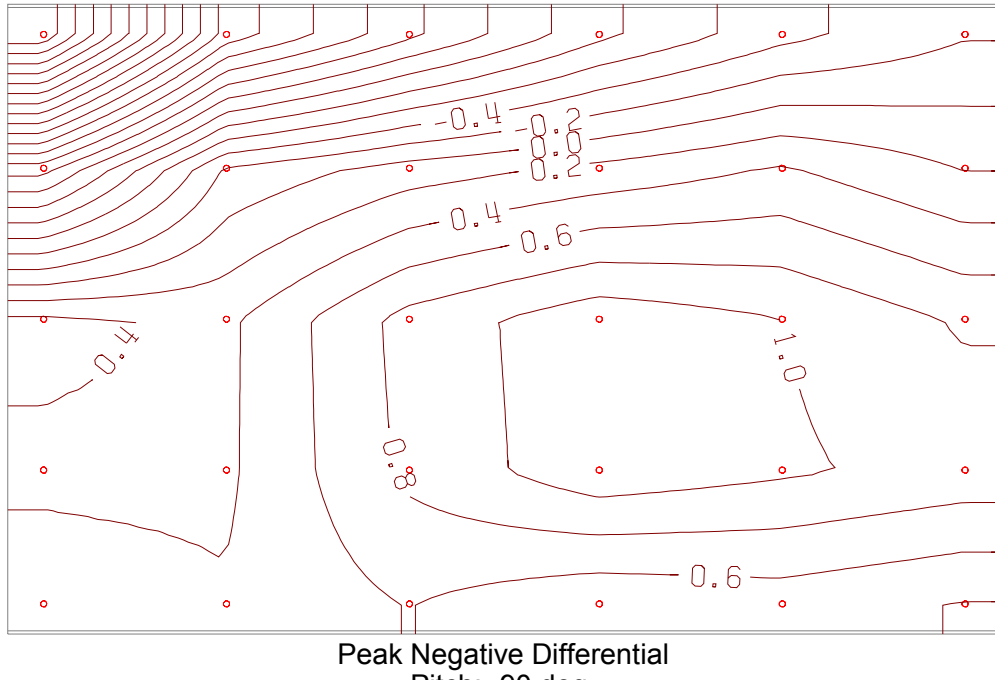
Configuration C5 (continued)

Operational Mode, Yaw: 30 deg.

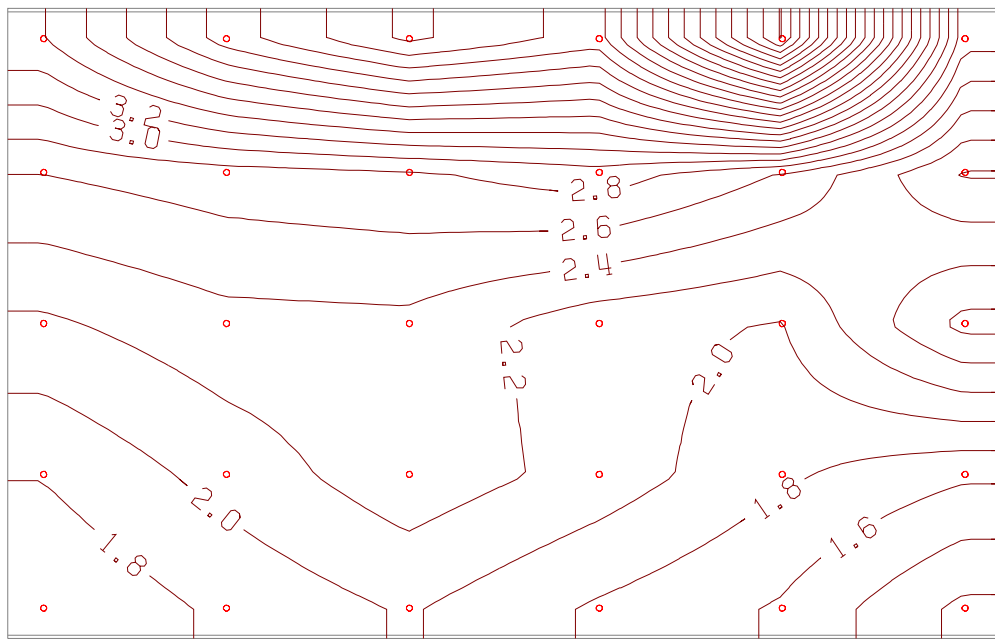


Configuration C5 (continued)

Stowed Mode, Yaw: 30 deg.



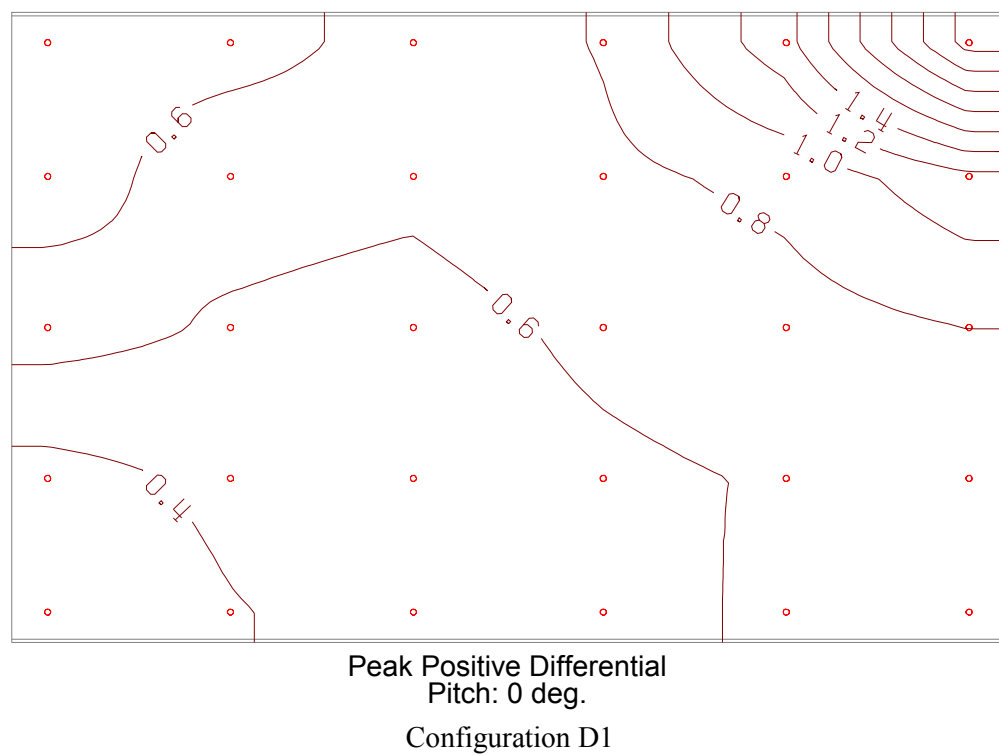
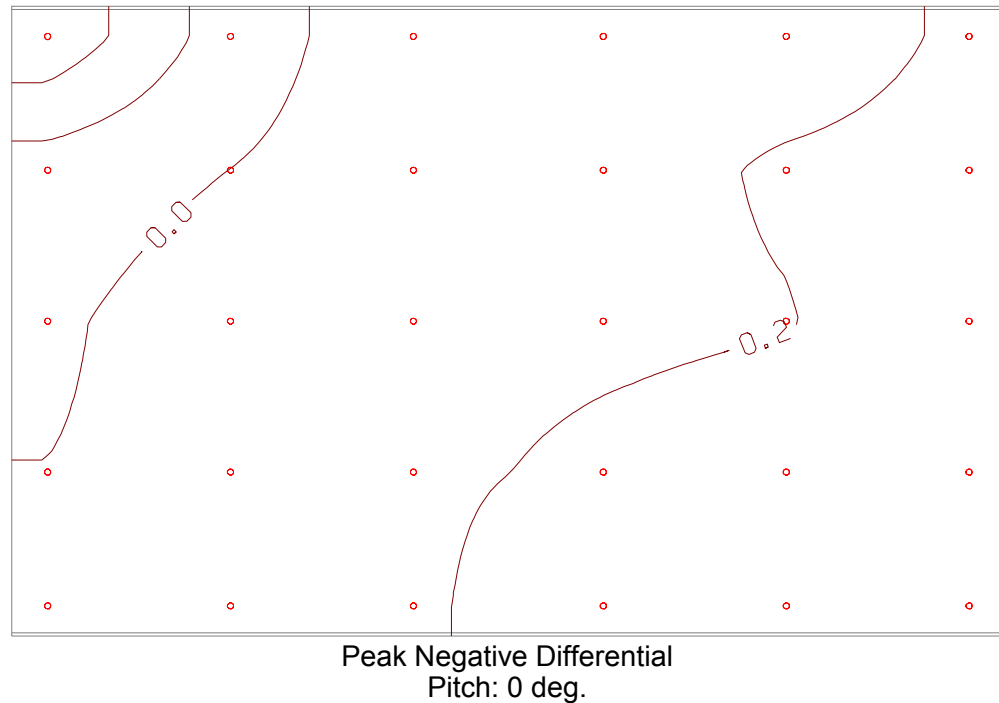
Peak Negative Differential
Pitch: -90 deg.



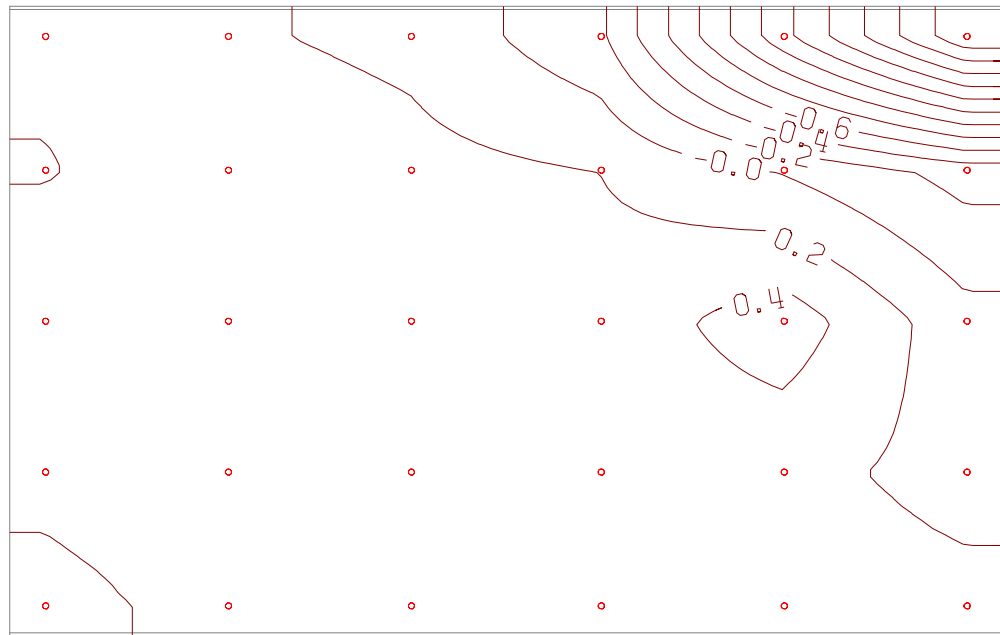
Peak Positive Differential
Pitch: -45 deg.

Configuration C5 (continued)

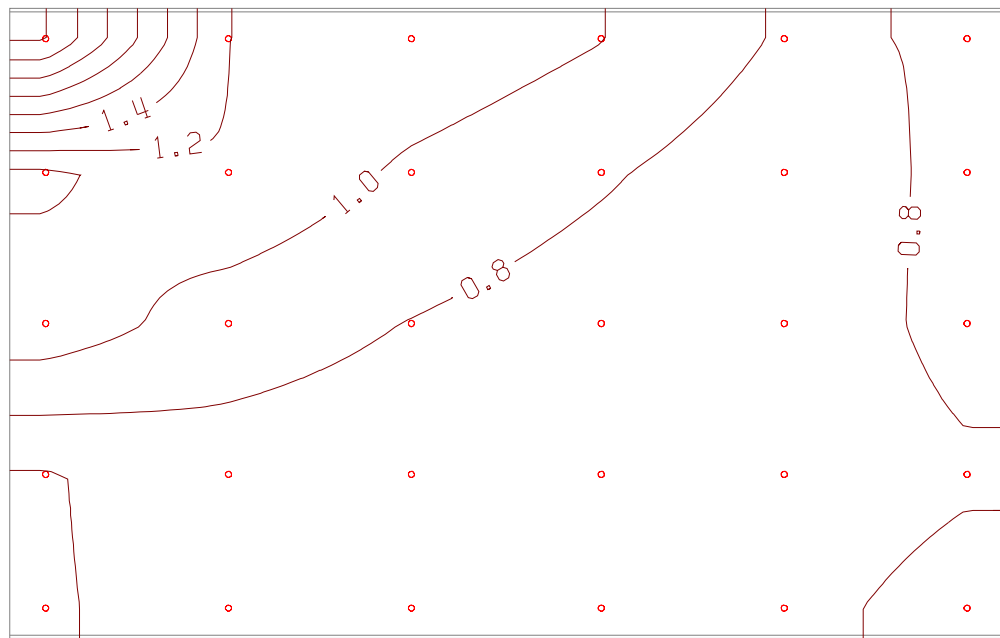
Operational Mode, Yaw: -30 deg.



Stowed Mode, Yaw: -30 deg.



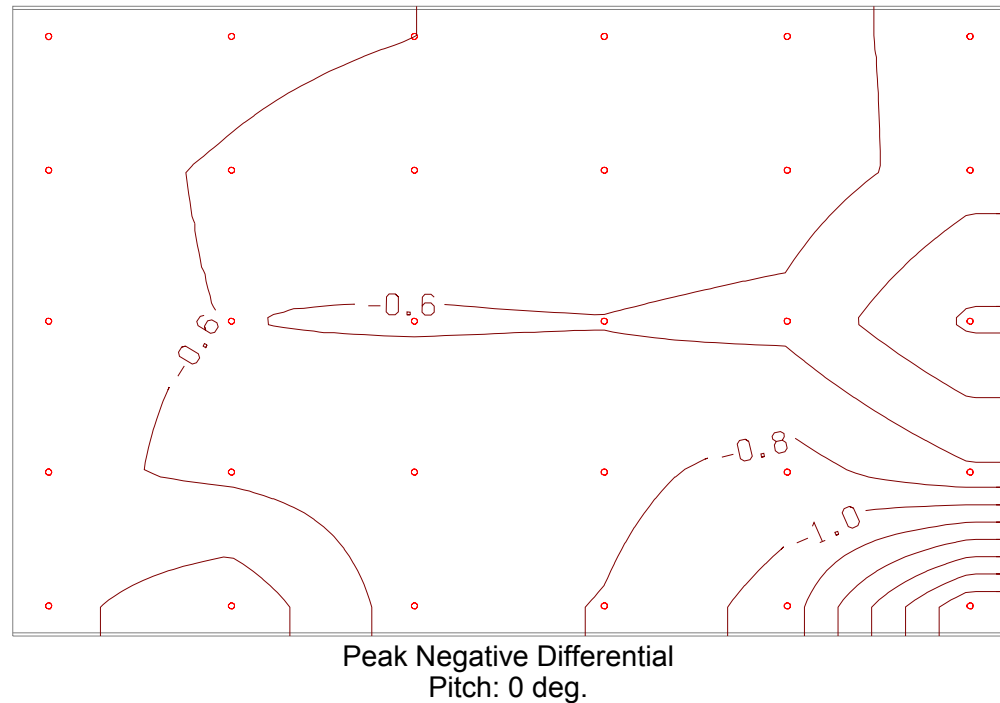
Peak Negative Differential
Pitch: -105 deg.



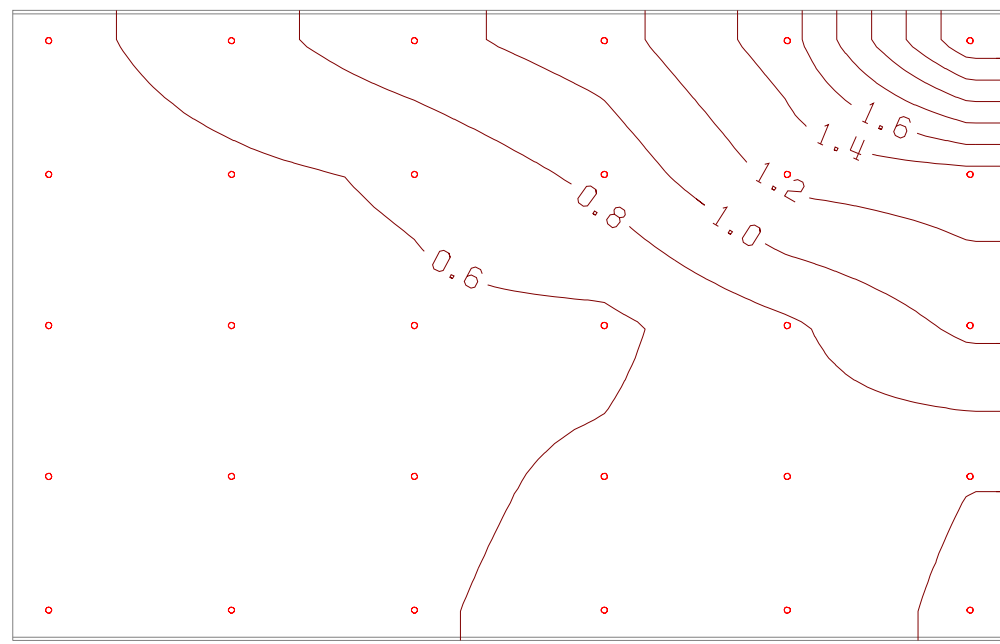
Peak Positive Differential
Pitch: -45 deg.

Configuration D1 (continued)

Operational Mode, Yaw: 0 deg.



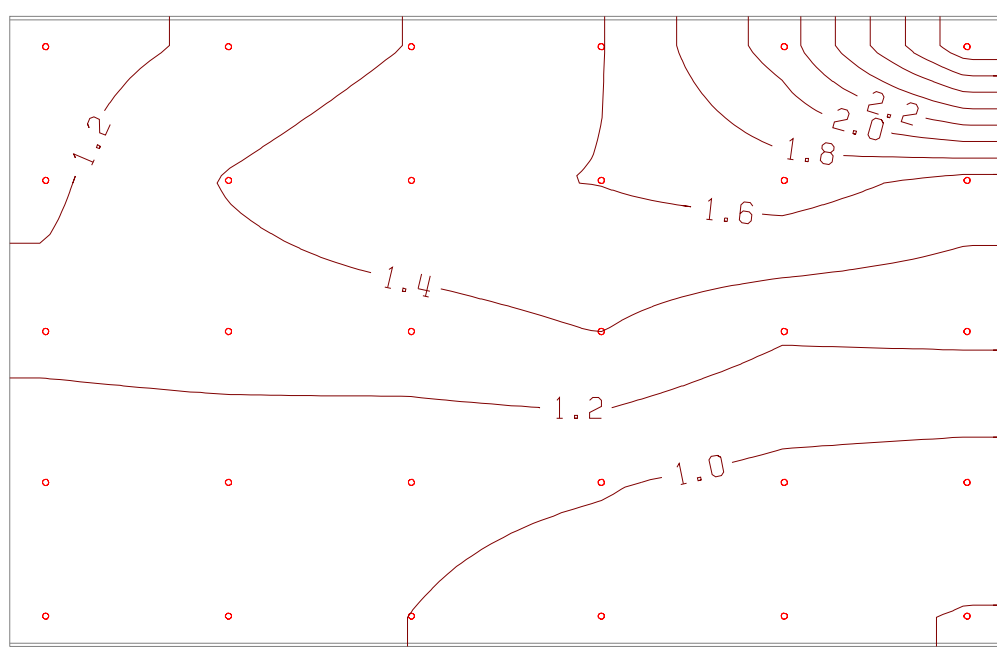
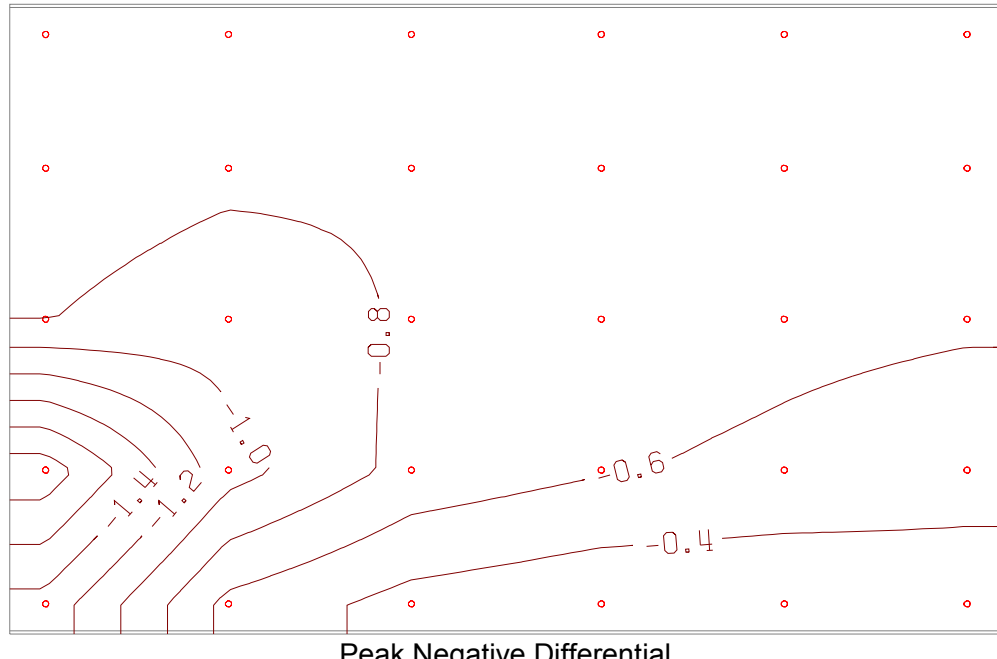
Peak Negative Differential
Pitch: 0 deg.



Peak Positive Differential
Pitch: 0 deg.

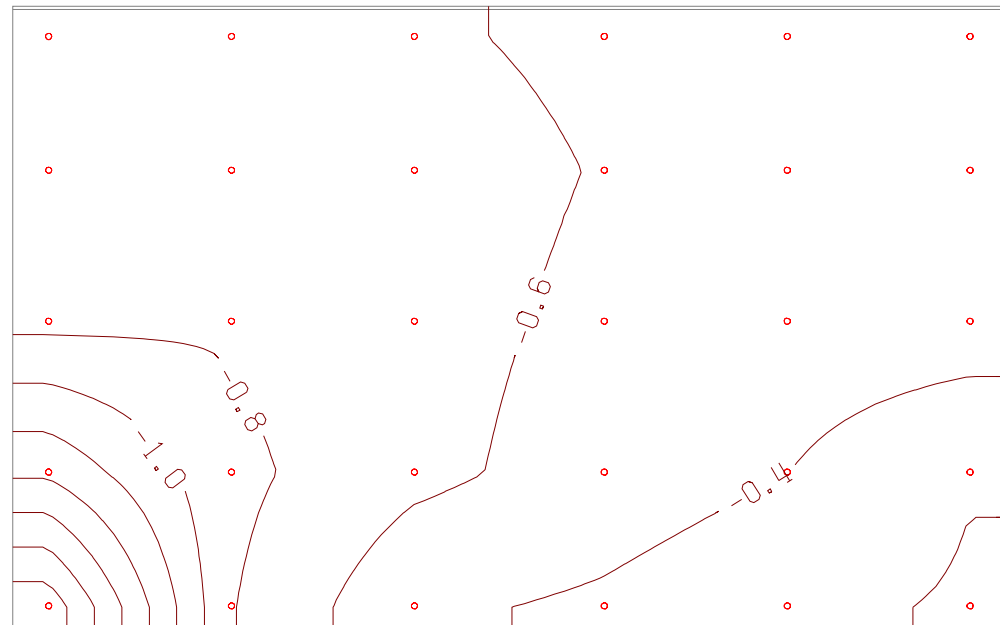
Configuration D1 (continued)

Stowed Mode, Yaw: 0 deg.

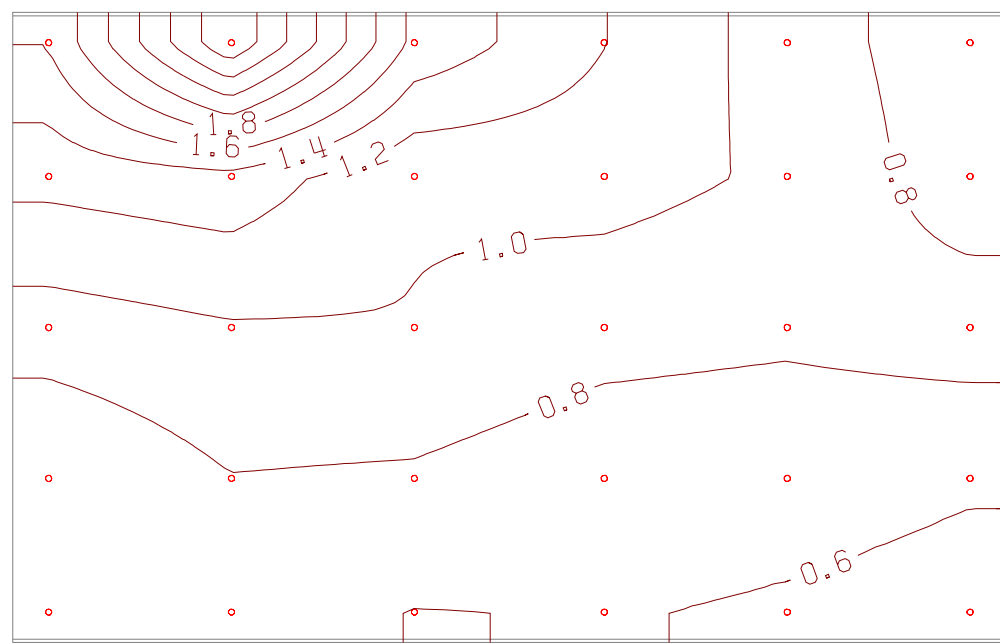


Configuration D1 (continued)

Operational Mode, Yaw: 30 deg.



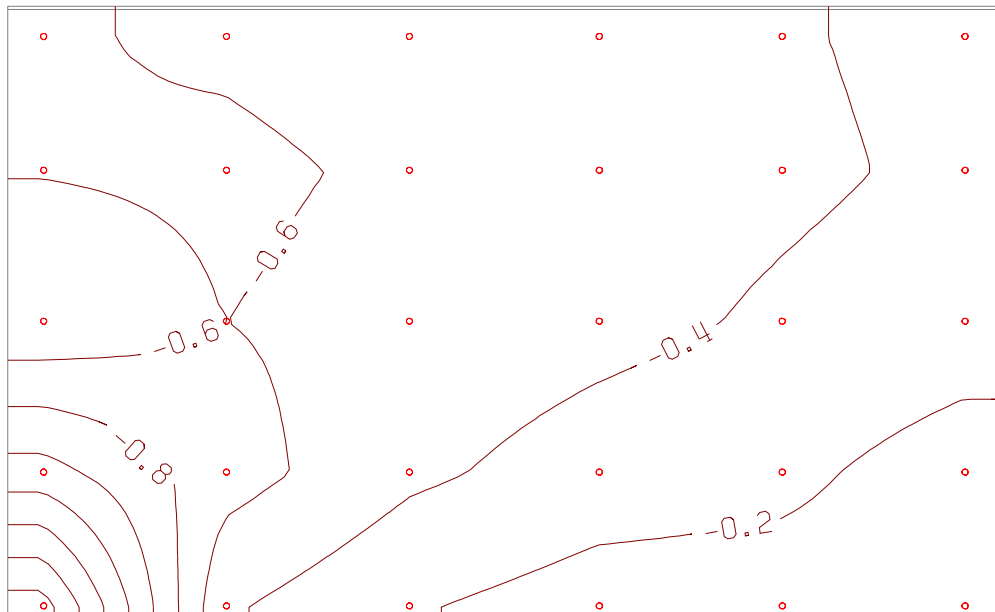
Peak Negative Differential
Pitch: 180 deg.



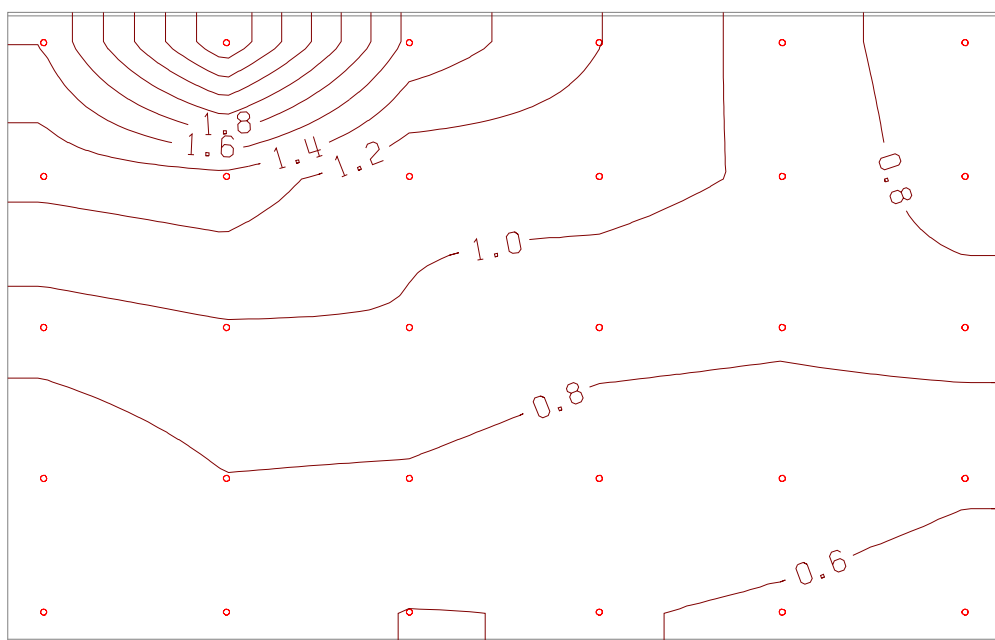
Peak Positive Differential
Pitch: 0 deg.

Configuration D1 (continued)

Stowed Mode, Yaw: 30 deg.



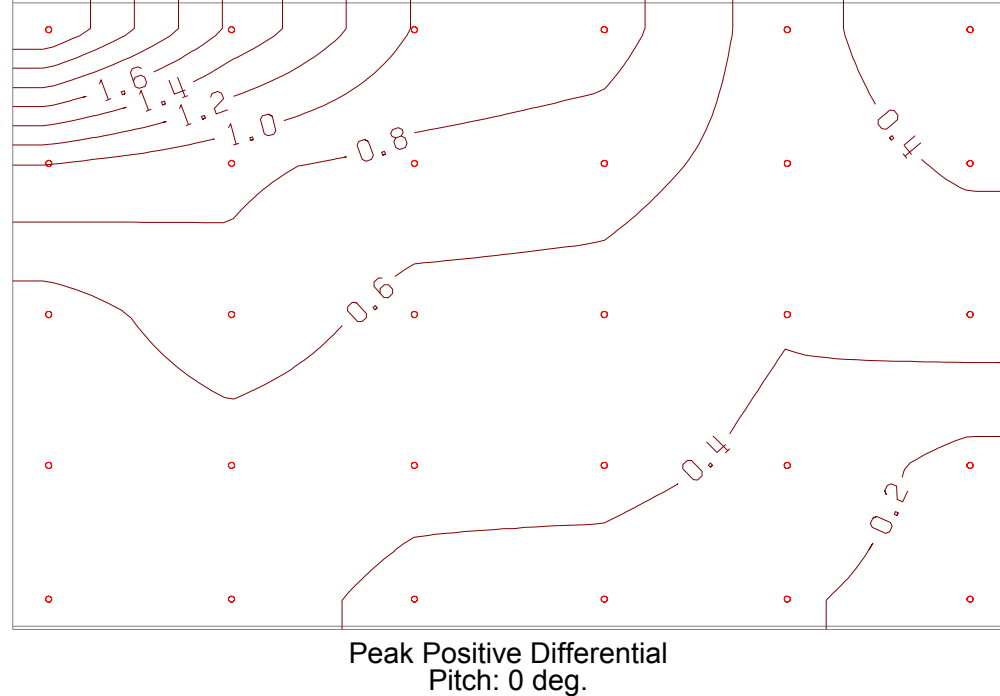
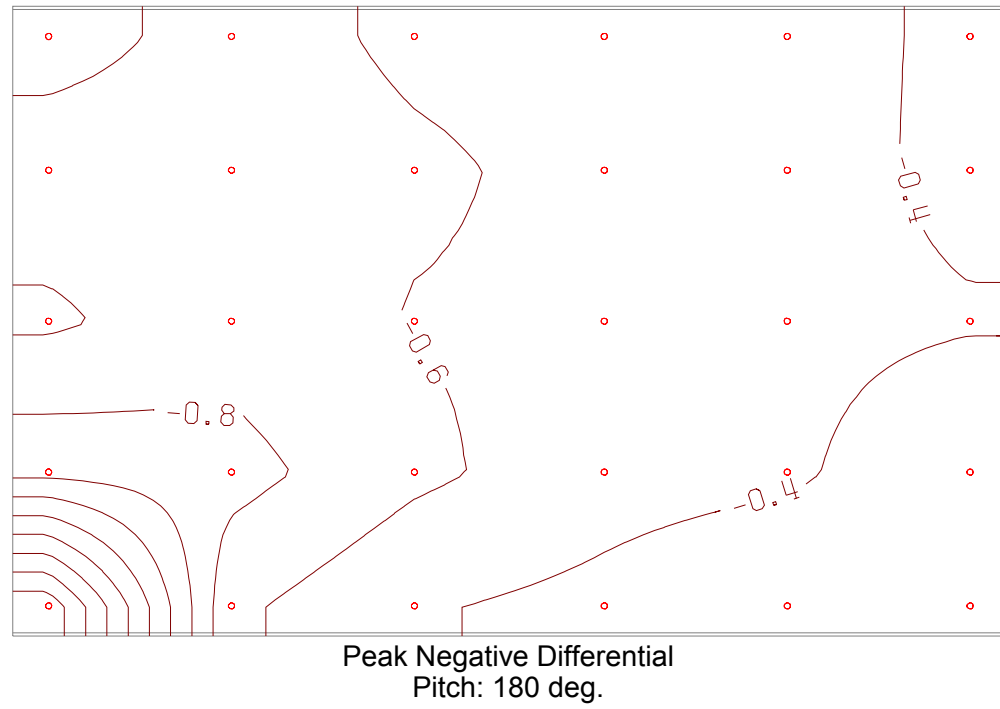
Peak Negative Differential
Pitch: -90 deg.



Peak Positive Differential
Pitch: -45 deg.

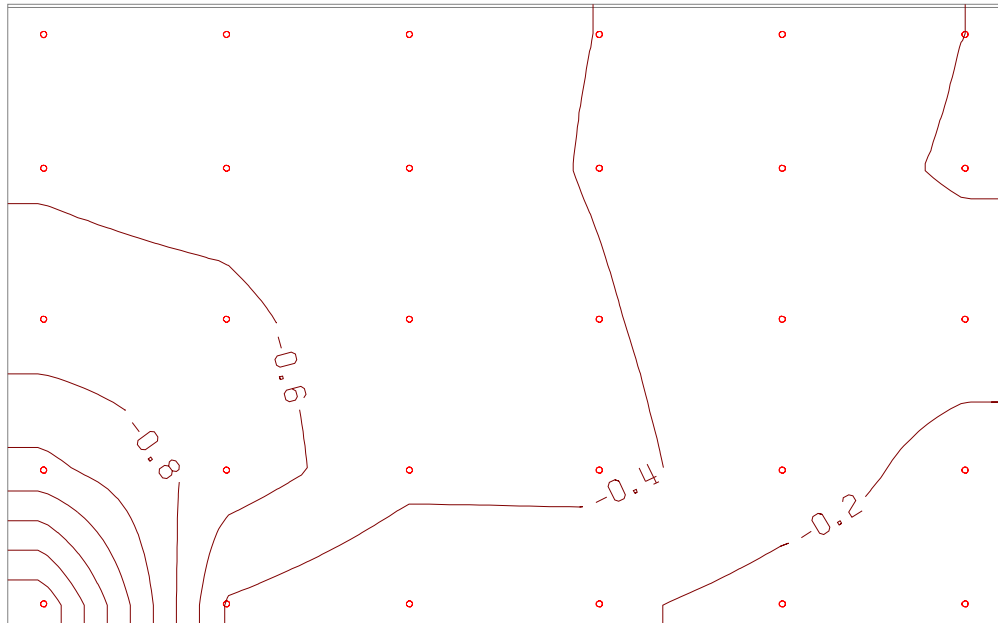
Configuration D1 (continued)

Operational Mode, Yaw: 45 deg.

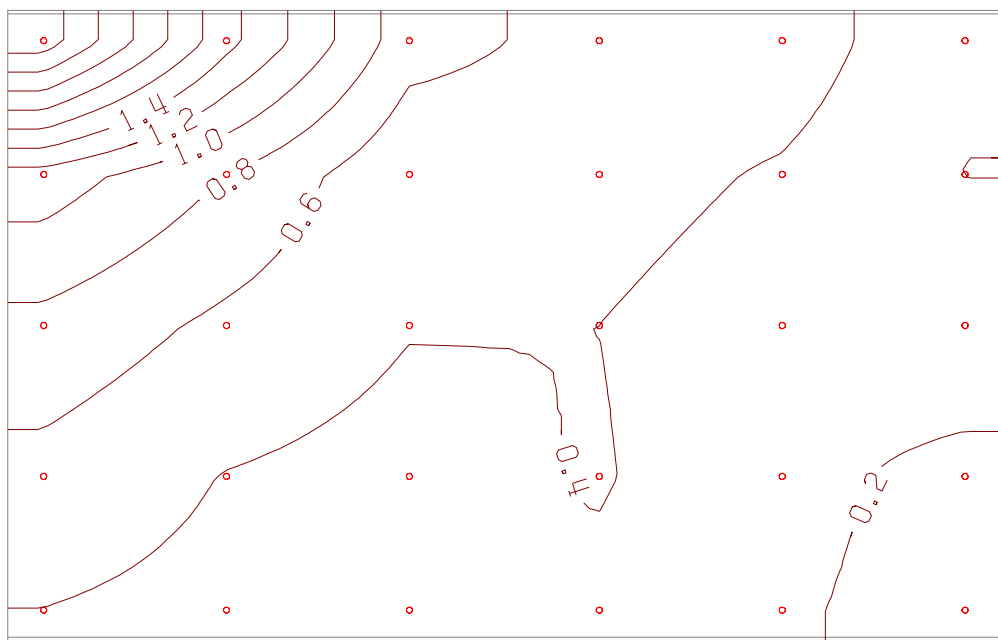


Configuration D1 (continued)

Stowed Mode, Yaw: 45 deg.



Peak Negative Differential
Pitch: -105 deg.



Peak Positive Differential
Pitch: -45 deg.

Configuration D1 (continued)

7.5 APPENDIX E - TIME SERIES OF LOCAL PRESSURES

A set of CD-ROMs provided to NREL as backup to this report contains the time series of local pressure coefficients measured on the model of the solar collector concentrator. The pressure values have been adjusted to approximate the directly measured force and moment balance loads when integrated. The weight factors for pressure integrations are provided in a spreadsheet file (INTEGRATE.XLS), also found on the CD-ROM.

Data Filename Convention

The following data file naming convention is used.

cccP-rrr.DAT

where

- ccc : Test configuration, I1 – I11.
- rrr : Run number.

Data File Format and Contents

The data are stored in printable ASCII format. Each data file contains a brief header followed by series of instantaneous local pressure coefficients. A typical data file might look like this (description of the data lines in parentheses):

Run	1	(Unique run number)
Config	I1	(Test configuration ID)
Yaw (deg.)	.0	(Yaw angle)
Pitch (deg.)	105.0	(Pitch angle)
Uref (fps)	25.69	(Reference wind speed at pivot height)
Qref (psf)	.6270	(Reference pressure at pivot height)
Sample Rate (Hz)	500.0	(Number of samples per second per channel)
No. Samples	8192	(Number of samples per segment block)
No. Segments	4	(Number of segment blocks)
(Blank line)		
130	129	128 (Pressure Tap Number)
(Blank line)		
-.2027	-.1248	-.3266 (1st data point)
-.4157	-.4448	-.5087 (2nd data point)
-.3385	-.3933	-.3903
.	.	.
.	.	.
.	.	.
.	.	.
-.8503	-.9533	-.9259
-1.5147	-1.0938	-1.1680 (8192nd data point of 1st segment)
(Blank line separating segment blocks)		
-.0989	-.1662	-.1522
-.4142	-.3249	-.4434
-.2717	-.3196	-.3241
.	.	.
.	.	.
.	.	.
(End of File)		

REPORT DOCUMENTATION PAGE

*Form Approved
OMB No. 0704-0188*

The public reporting burden for this collection of information is estimated to average 1 hour per response, including the time for reviewing instructions, searching existing data sources, gathering and maintaining the data needed, and completing and reviewing the collection of information. Send comments regarding this burden estimate or any other aspect of this collection of information, including suggestions for reducing the burden, to Department of Defense, Executive Services and Communications Directorate (0704-0188). Respondents should be aware that notwithstanding any other provision of law, no person shall be subject to any penalty for failing to comply with a collection of information if it does not display a currently valid OMB control number.

PLEASE DO NOT RETURN YOUR FORM TO THE ABOVE ORGANIZATION.

1. REPORT DATE (DD-MM-YYYY) May 2008			2. REPORT TYPE Subcontract Report		3. DATES COVERED (From - To) March 2001- August 2003	
4. TITLE AND SUBTITLE Wind Tunnel Tests of Parabolic Trough Solar Collectors			5a. CONTRACT NUMBER DE-AC36-99-GO10337			
			5b. GRANT NUMBER			
			5c. PROGRAM ELEMENT NUMBER			
6. AUTHOR(S) N. Hosoya, J.A. Peterka, R.C. Gee, D. Kearney			5d. PROJECT NUMBER NREL/SR-550-32282			
			5e. TASK NUMBER CP085002			
			5f. WORK UNIT NUMBER			
7. PERFORMING ORGANIZATION NAME(S) AND ADDRESS(ES) Cermak Peterka Petersen, Inc., Fort Collins, Colorado Solaragenix Energy, LLC, Raleigh, North Carolina Kearney & Associates, Vashon, Washington			8. PERFORMING ORGANIZATION REPORT NUMBER NAA-2-32439-01			
9. SPONSORING/MONITORING AGENCY NAME(S) AND ADDRESS(ES) National Renewable Energy Laboratory 1617 Cole Blvd. Golden, CO 80401-3393			10. SPONSOR/MONITOR'S ACRONYM(S) NREL			
			11. SPONSORING/MONITORING AGENCY REPORT NUMBER NREL/SR-550-32282			
12. DISTRIBUTION AVAILABILITY STATEMENT National Technical Information Service U.S. Department of Commerce 5285 Port Royal Road Springfield, VA 22161						
13. SUPPLEMENTARY NOTES NREL Technical Monitor: Mary Jane Hale						
14. ABSTRACT (Maximum 200 Words) Extensive wind-tunnel tests were conducted on parabolic trough solar collectors to determine practical wind loads applicable to the structural design for stress and deformation, as well as the local component design for the concentrator reflectors. The overall dynamic loads and simultaneous pressure distributions on the concentrator were measured using force balances and a multi-pressure data acquisition system, respectively, in a boundary layer wind tunnel at Cermak Peterka Petersen. Various test configurations were examined, including an isolated collector and solar field collectors at different positions. Significant test results are presented and discussed in detail. Overall, the wind-tunnel tests produced sufficient data that can be used by designers of the present and future for a variety of design practices. Several recommendations are made for future work. The validity of the wind-tunnel data is particularly important. Ultimately, the acceptability of the test results should be based on model-to-full-scale comparison, which requires measurement of wind loads on a full-scale solar collector. Should further wind tunnel study prove useful, the pressure test model should attempt to increase the pressure tap installation density to enhance the resolution of discrete pressure distribution data.						
15. SUBJECT TERMS Concentrating solar power; parabolic trough; solar collectors; wind tunnel; wind load; structural design; stress; deformation						
16. SECURITY CLASSIFICATION OF:			17. LIMITATION OF ABSTRACT UL			
a. REPORT Unclassified			18. NUMBER OF PAGES 1			
19a. NAME OF RESPONSIBLE PERSON 						
19b. TELEPHONE NUMBER (Include area code) 						